Synthesis of organophosphores complexes of di -and trivalent lanthanides and their application in catalysis.

Florian Jaroschik

THÈSE

Présentée pour obtenir le titre de

DOCTEUR DE L'ÉCOLE POLYTECHNIQUE

Spécialité CHIMIE

Par

Florian Jaroschik

Synthèse et réactivité de nouveaux complexes organophosphorés de lanthanides divalents et trivalents et leur application en catalyse

Acknowledgements

The work presented in this thesis was mainly carried out in the laboratory « Hétéroéléments et Coordination » at the Ecole Polytechnique and involved many people to whom I would like to express my deep gratitude.

First of all, I thank my supervisor Dr. François Nief for his precious help and guidance over the last three years. As I was starting from zero in the field of lanthanide chemistry he patiently shared his knowledge and skills with me. I also appreciated the liberty he gave me to carry out my own research in different fields of organolanthanide chemistry.

I am grateful to Professor Pascal Le Floch who welcomed me in his laboratory, provided the resources for my rather expensive chemistry and allowed me to participate in a number of national and international conferences.

I thank Dr. Louis Ricard and Dr. Xavier-Frédéric Le Goff for their outstanding work which provided me with so much and good X-ray crystallographic data. I am also grateful to Evelyne Pousson at the Université de Bourgogne, Dijon, for the elemental analyses of my compounds.

I thank Dr. Guy Lavigne, Professor Marc Visseaux, Professor Regis Réau and Dr. Florence Hélion for accepting to be part of my jury and judging this manuscript.

Several national and international collaborations allowed me to explore new chemistry and encounter different working environments:

I express my solemn gratitude to Dr. Zhaomin Hou and all the members of the Organometallic Chemistry Laboratory at RIKEN for the wonderful time in Japan. Arigato gosaimasu.

I thank Professor Geoff Cloke for welcoming me in his laboratory in Brighton.

I thank Dr. Jean-Pierre Majoral and Grégory Franc at the LCC in Toulouse for giving me the possibility to do some dendrimer chemistry again.

I am very grateful to Dr. Thibault Cantat and Dr. Nicolas Mézailles for the time spent together doing carbene chemistry and many other things.

I thank Aurélien Momin for his interest and enthusiasm while working with me.

I thank all the present and ancient members of the laboratory for their kind support and help, especially for all the conversations, discussions and good laughs during their visits in “my” glovebox.

Finally, I would like to thank my family for their love and their support through all these years. Very special thanks to Emilie for her patience, her love and her encouragement which provided me with the necessary strength to bring this work to completion.

Table of Contents

List of abbreviations

CN	coordination number
conv.	conversion observed by NMR
COT	cyclooctatetraenyl
Cp	cyclopentadienyl
Ct	centroid
DME	dimethoxyethane
Et	ethyl
HMPA	hexamethylphosphoramide
iPrOH	isopropanol
isol.	isolated yield
Ln	lanthanide
Me	methyl
NHC	N-heterocyclic carbene
NHE	normal hydrogen electrode
OTf	triflate
Ph	phenyl
py	pyridine
r.t.	room temperature
tBu	tert-butyl
TBS	tert-butyldimethylsilyl
THF	tetrahydrofuran
TMEDA	tetramethylethylenediamine
TMS	trimethylsilyl
TMSI	iodotrimethylsilane
tol	toluene
χ	electronegativity
η	hapticity

List of ligands

Cp	C_5H_5
Cp*	C_5Me_5
Cp’	$C_5H_4(TMS)$
Cp’’	$C_5H_3(TMS)_2$
Cp’’’	$C_5H_2(TMS)_3$
Cp^{tt}	$C_5H_3(tBu)_2$
Cp^{ttt}	$C_5H_2(tBu)_3$
Cp^{4i}	$C_5H(iPr)_4$
Cp*’	$C_5Me_4(TMS)$
Dmp	$PC_4H_2Me_2$
Tmp	PC_4Me_4
Dpp	$PC_4H_2Ph_2$
Htp	$PC_4H_2(tBu)_2$
Hsp	$PC_4H_2(TMS)_2$
Dtp	$PC_4Me_2(tBu)_2$
Dsp	$PC_4Me_2(TMS)_2$
Dsas	$AsC_4Me_2(TMS)_2$
SPCPS	$[Ph_2P(S)]_2C^{2-}$

INTRODUCTION

Introduction to the Organometallic Chemistry of the Lanthanides

The organometallic chemistry of the lanthanides has experienced a tremendous development over the past 30 years.[1-4] Although the first lanthanidocene complexes were synthesized in 1954 by Wilkinson and Birmingham,[5] the breakthrough of this now well-established field of organometallic chemistry only started in the late 1970s. One main reason for this delay in development is the high oxophilicity of organolanthanide complexes, which makes these compounds highly sensitive to air and moisture. With the access to more sophisticated handling techniques, e.g. use of glove boxes and special vacuum lines and the progress in X-ray analysis, the synthesis and characterization of a large number of new complexes has become possible.

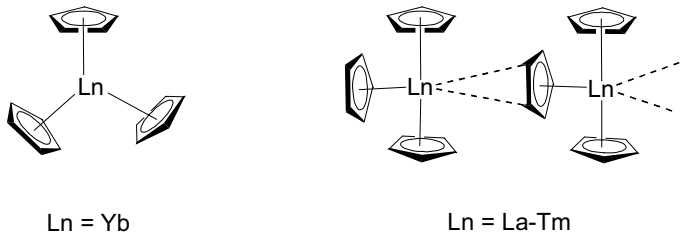

Figure 1. The first lanthanidocene complexes.

These advancements led to the development of three main research areas of organolanthanide chemistry: catalysis in organic synthesis, small molecule activation using reduction chemistry and polymerization catalysis. After some general remarks on the unique properties of the lanthanides and an overview on the ligands that can be used with these metals, all three fields will be shortly introduced, with a special focus on the (possible) impact of organophosphorus ligands.

1 Physical and chemical properties of the lanthanide elements[3, 6] [7, 8]

The lanthanide series consists of the 14 elements following lanthanum in the periodic table - going from cerium ($_{58}$Ce) to lutetium ($_{71}$Lu) - which are characterized by a gradual filling of the 4f electron subshell. The group 3 elements scandium ($_{21}$Sc), yttrium ($_{39}$Y) and lanthanum ($_{57}$La) are often associated to the lanthanides due to their similar physical properties and chemical behavior. This 17-element group is often referred to as “Rare Earths”, however, in this text we will employ the term “lanthanide” for all these elements. This also avoids the misleading interpretation of the name “Rare Earths” which was not given to these elements because of their low terrestrial abundance but because of the late discovery of their metal oxides. In fact, some of these elements, cerium, lanthanum and neodymium, are as common as cobalt and lead and even the least common lanthanides, thulium and europium, are still as common as silver, mercury and the precious metals.[9] It should be noted that the elements having even atomic numbers are more abundant than the elements with uneven atomic

numbers. Finally it should be mentioned that all isotopes of promethium ($_{61}$Pr) are radioactive with short lifetimes, incompatible with the presence of this element on the earth surface.

The lanthanide metals are strong reducing agents and will react with water or acids with concomitant dihydrogen evolution to form aqueous Ln^{3+}-solutions. The preferred trivalent oxidation state of the lanthanide ions is formed by abstraction of the 6s and 5d valence electrons, leading to an extended xenon core electron-configuration [Xe] f^n $6s^0$ $5d^0$ (n = 1-14). The 4f-orbitals have limited radial extensions and are embedded in the interior of the ion. Hence, they are well shielded externally by the filled 5s and 5p orbitals and experience therefore only negligible interactions with ligand orbitals (Figure 2). For the same reasons they also lack the capacity of π-backbonding, e.g. no M-O double bonds or M-N triple bonds, which play an important role in transition metal chemistry, have been reported. The isolation of the f-electrons from the influence of the ligands results in very small crystal-field effects and thus spectroscopic and magnetic properties of the lanthanides are essentially unaffected by the environment. The Ln^{3+} ions are therefore often described as "triple-positively charged closed shell inert gas electron cloud".[10]

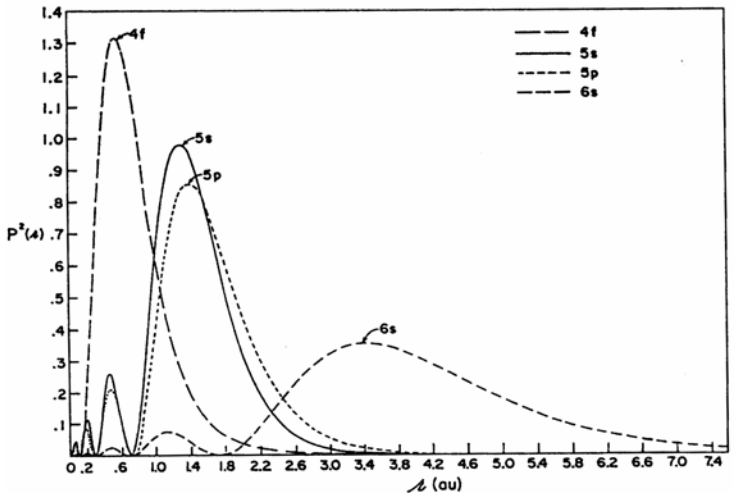

Figure 2. Plot of the radial charge densities for the 4f-, 5s-, 5p-, and 6s-electrons of Gd^+.[10]

The 4f-orbitals also experience internal shielding as can be deducted from the low probability of electron density close to the nucleus (Figure 2). As a consequence, the positive nuclear charge is only partially shielded by the f-electrons, leading to the well-known lanthanide contraction, i.e. the monotonically decreasing ionic radii with increasing atomic number. Although similar contractions can be observed in main block and transition metal chemistry, the unique feature of the lanthanide contraction is the stable oxidation state +3 throughout the series. Hence, one can induce important changes in reactivity when going from the larger early lanthanides to the smaller late lanthanides, and vice versa, allowing for the easy fine-tuning of catalytic systems.

Although the most common oxidation state of the lanthanides is +3, other oxidation states are also encountered. In the tetravalent state, only cerium has allowed for the isolation of some stable compounds.[11-13] The stability of Ce^{4+} can be explained by its f^0 electron configuration. In contrast, divalent lanthanide halide complexes have been prepared in the solid state for a large number of elements.[14, 15] These complexes can be divided into two groups: the "ionic" salt-like compounds of the $[Ln^{II}X_2]$ type for Ln = Eu, Yb, Sm, Tm, Dy, Nd and the "metallic", conducting compounds of the $[Ln^{III}(X)_2(e^-)]$-type for Ln = Ce, Pr, Gd, Ho. These complexes are very strong reducing agents and only a small number of them, the so-called "classical" divalent lanthanides Eu, Yb and Sm, are stable in water for a short time. This finding can be explained by their electron-configurations: half-filled (f^7, Eu^{2+}), nearly half-filled (f^6, Sm^{2+}) or filled (f^{14}, Yb^{2+}) f subshells stabilize the divalent oxidation state. In recent years, investigations on the so-called "new" divalent lanthanides Tm, Dy and Nd have increased. The following electronic considerations may be put forward to explain their accessibility: for Nd^{2+} (f^3) the f subshell is filled to one quarter, for Dy^{2+} (f^{10}) to three-quarters and for Tm^{2+} (f^{13}) it is nearly completely filled. These "new" lanthanides require special reaction conditions due to their very negative redox potentials and their low thermal stability.

Table 1. Intrinsic properties of the lanthanides.

Ln	Ln^{2+} [$E^0(M^{2+}/M^{3+})$, V]	Ln^{3+}	Ln^{4+} [$E^0(M^{4+}/M^{3+})$, V]	Ionic radii (Ln^{3+}, CN 6) [ppm]	Ln^{3+} electronic ground state	μ_{eff}^{calc} (μ_{eff}^{exp}) (Ln^{3+}, $(Ln\text{-}1)^{2+}$) [μ_B]
Sc		[Ar]		74.5	$^1S_0$	0.000
Y		[Kr]		90.0	$^1S_0$	0.000
La		[Xe]		103.2	$^1S_0$	0.000
Ce		[Xe] $4f^1$	1.74	101.0	$^2F_{5/2}$	2.535
Pr		[Xe] $4f^2$	3.2	99.0	$^3H_4$	3.578
Nd	-2.6	[Xe] $4f^3$		98.3	$^4I_{9/2}$	3.618
Pm		[Xe] $4f^4$		97.0	$^5I_4$	2.683
Sm	-1.55	[Xe] $4f^5$		95.8	$^6H_{5/2}$	0.845 (1.6)
Eu	-0.35	[Xe] $4f^6$		94.7	$^7F_0$	0.000 (3.5)
Gd		[Xe] $4f^7$		93.8	$^8S_{7/2}$	7.937
Tb		[Xe] $4f^8$	3.1	92.3	$^7F_6$	9.721
Dy	-2.5	[Xe] $4f^9$		91.2	$^6H_{15/2}$	10.646
Ho		[Xe] $4f^{10}$		90.1	$^5I_8$	10.607
Er		[Xe] $4f^{11}$		89.0	$^4H_{15/2}$	9.581
Tm	-2.3	[Xe] $4f^{12}$		88.0	$^3H_6$	7.561
Yb	-1.05	[Xe] $4f^{13}$		86.8	$^2F_{7/2}$	4.536
Lu		[Xe] $4f^{14}$		86.1	$^1S_0$	0.000

Most Ln^{n+} ions (n = 2,3,4) contain unpaired f-electrons and are thus paramagnetic. The exceptions are Sc^{3+} and Y^{3+} (no f subshell), La^{3+} and Ce^{4+} (f^0) and Yb^{2+} and Lu^{3+} (f^{14}), which are diamagnetic. Except for the f^5 (Sm^{3+}) and f^6 (Sm^{2+} and Eu^{3+}) configurations, the magnetic properties are determined by the electronic ground state only, and are conveniently described by the Russell-Saunders spin-orbit coupling scheme. The magnetic moment μ_{eff} is unaffected by the environment and given by the equation:

$$\mu_{eff} = g_J\sqrt{J(J+1)}$$

$$\text{with } g_J = \frac{3}{2} + \frac{S(S+1) - L(L+1)}{2J(J+1)} \text{ (Landé factor)}$$

In the case of Sm^{3+}, Sm^{2+} and Eu^{3+}, low-lying paramagnetic excited states are substantially populated at room temperature and contribute to the observed magnetic moments (1.6 instead of 0.85 for Sm^{3+}, and 3.5 instead of 0 for Eu^{3+} and Sm^{2+}).

Most trivalent lanthanide ions absorb electromagnetic radiation, particularly in the visible region, leading to characteristic colors for certain elements. The ion is excited from the ground state to a higher electronic state due to the partly filled 4f subshell. These f-f transitions are Laporte-forbidden and result in weak intensities, which are responsible for the pale color of the trivalent species. Due to the weakness of crystal field effects in the lanthanides, the thermal motion of the ligands has very little effect upon them, so the f-f absorption bands in the spectra are very narrow - in contrast to the broad d-d bands in transition metals. The reduced charge of Ln^{2+} ions causes the energy levels to be closer together and Laporte-allowed 4f-5d transitions become possible. These ions show therefore more intense and ligand dependent colors e.g. the Yb^{3+} ion is colorless whereas the isoelectronic Tm^{2+} ion shows intense violet or green colors.

In conclusion, lanthanides can be described as large, highly electropositive metals with gradually changing size and limited orbital extension. The next chapters will show how these special properties can be used in organometallic chemistry to develop unique chemistry with these elements.

2 Ligands and synthetic methods in organolanthanide chemistry[4, 7, 8]

Ligand design plays a very important role in organolanthanide chemistry. The poor overlap of f-orbitals with ligand orbitals in organolanthanide complexes contributes to the predominantly ionic character of these compounds. Hence, the number of ligands that can be coordinated around the metal does not depend on crystal field effects but on the size, the basicity and the functionalization of the ligand. It should also be noted that there is no 18-electron rule as in transition metal chemistry. Coordination numbers are usually between 7 and 9, but can go down to 2 or 3 and up to 10 or 12.

According to the HSAB terminology lanthanide cations are considered as hard acids and therefore prefer hard donor ligands, such as alkoxides or amides. Cyclopentadienyls are also widely used, although they are usually not classified as hard ligands. However, the size of the Cp ligand, which covers an important part of the coordination sphere of the lanthanide, and the negative charge contribute to the good stabilization of organolanthanide complexes. The lack of π-backbonding is responsible for the fact that a number of ligands that play an important role in transition metal chemistry, namely carbon monoxide and isonitriles, are very rarely used in lanthanide chemistry. For the same reason, carbene complexes of the lanthanides are still very scarce and no Ln-O double bond or Ln-N triple bond has been reported. Studies on the π-accepting properties of the lanthanides have shown that arenes - as well as alkenes and alkynes - are much less suitable ligands than Cp ligands. Hence it is not surprising, that organolanthanide chemistry has been dominated for a long-time by cyclopentadienyl-substituted complexes. During the last decade, the search for non-Cp ligands has made enormous progress and allowed for the development of many new types of compounds.[16] Phosphorus-containing ligands, a subclass of non-Cp ligands, have been investigated only marginally in organolanthanide chemistry.[16-19] However, in recent years, interest in this sub-class has grown and many new ligand systems have appeared.

2.1 Cp ligands

Three main classes of Cp ligands can be distinguished: unsubstituted, alkyl or aryl-substituted Cp ligands (class A), Cp ligands carrying additional neutral donor atoms (class B) and bridged (ansa) Cp ligands (class C) (Figure 3).

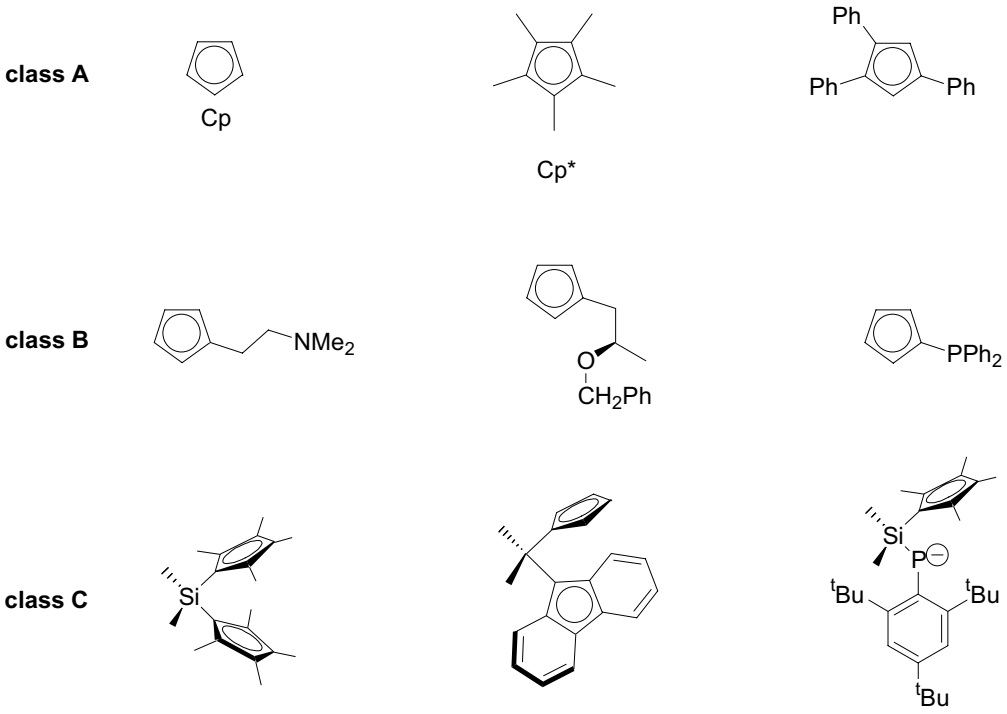

Figure 3. Different classes of Cp ligands used in organolanthanide chemistry.

Organolanthanide chemistry started with the unsubstituted Cp ligand. However, the resulting complexes exhibited very low solubility and were therefore not suitable for further investigations. A major improvement came with the introduction of the more bulky permethylated Cp* ligand into organolanthanide chemistry. This still very widely used ligand, has allowed for the synthesis of more soluble and more stable complexes as well as for their derivatization and use in catalysis. In order to further increase the steric bulk, Cp ligands with variable numbers of tBu, TMS or phenyl substituents have also been employed in organolanthanide chemistry.[2]

Another possibility of covering the coordination sphere of the lanthanide metal is the introduction of additional neutral donor atoms on the Cp ligand. These ligands can help for the fine-tuning of the activity of an organolanthanide complex in catalysis by differing the steric bulk and influencing the electronic environment around the metal center. Chiral side-arms on the Cp ligand can lead to non-racemic complexes.[20] The diphenylphosphine-substituted Cp ligand has allowed for the synthesis of heterobimetallic 4f-3d complexes.[21]

Introducing too much steric bulk reduces the reactivity of the organolanthanide complexes, especially in polymerization catalysis. Ansa-type ligands have been found to be a good compromise: the lanthanide is still stabilized by two Cp-ligands, however, because of the connection of the two ligands, the bite angle opens up and leads to higher reactivity. Instead of bridging two Cp ligands, the combination of one Cp ligand and one anionic donor ligand, for example amide or phosphide, has also led to very important improvements in the design of organolanthanide complexes for polymerization catalysis.[22, 23]

The main class of compounds obtained with these Cp ligands are metallocene complexes of the $[(Cp^{A,B})_2LnX(S)_n]$ or the $[(Cp^{C})LnX(S)_n]$ (X = H, halide, alkyl, amide, alkoxide, aryloxide, S = solvent) type for trivalent compounds and $[(Cp^{A,B})_2Ln(S)_n]$ or $[(Cp^{C})Ln(S)_n]$ for divalent complexes. Different synthetic strategies can be adopted to access these compounds. For trivalent complexes the most important ones are (i) salt metathesis, (ii) σ-bond metathesis and (iii) metal exchange reactions. For divalent complexes an additional pathway is often encountered: (iv) the reduction of trivalent precursors (Scheme 1). The coordination of solvent molecules can be prevented by using very bulky Cp ligands or additional donor groups on the Cp ring.

(i) Salt metathesis

$LnX_3(S)_n + 2\,[M\text{-}Cp] \xrightarrow[-\,2\,MX]{solvent} [Cp_2LnX(S)_n]$ X = halide, BH_4; M = Na, K; solvent: THF, Et_2O, DME

(ii) Sigma-bond metathesis

$LnX_3(S)_n + 2\,Cp\text{-}H \xrightarrow[-\,2\,HX]{solvent} [Cp_2LnX(S)_n]$ X = amide, alkyl; solvent: pentane

(iii) Metal exchange reaction

$Ln + 3\,[TlCp] \xrightarrow[-\,3\,Tl]{solvent} [Cp_3Ln(S)_n]$ solvent: THF

(iv) Reduction

$[Cp_2LnX(S)] + M \xrightarrow[-\,MX]{solvent} [Cp_2Ln(S)_n]$

$[Cp_3Ln] + M \xrightarrow[-\,MCp]{solvent} [Cp_2Ln(S)_n]$

X = halide; M = Na, K; Ln = Eu, Yb, Sm; solvent: THF, benzene

Scheme 1. Synthetic pathways to divalent and trivalent lanthanidocene complexes.

2.2 Non-Cp ligands[16]

This very large class of ligands can be divided roughly into two groups: σ-donor ligands and π-ligands (Figure 4). The first group includes anionic alkyl, aryl, benzyl, alkynyl and neutral N-heterocyclic carbene ligands, whereas the second group is constituted by anionic allyl, pentadienyl, cyclooctatetraenyl, aza-allyl, benzamidinato, β-diketiminato, pyrrolyl, pyrazolyl, carborane and neutral aryl ligands. It should be noted that the pyrrolyl and pyrazolyl ligands can also act as σ-donor ligands via the lone pair on nitrogen.

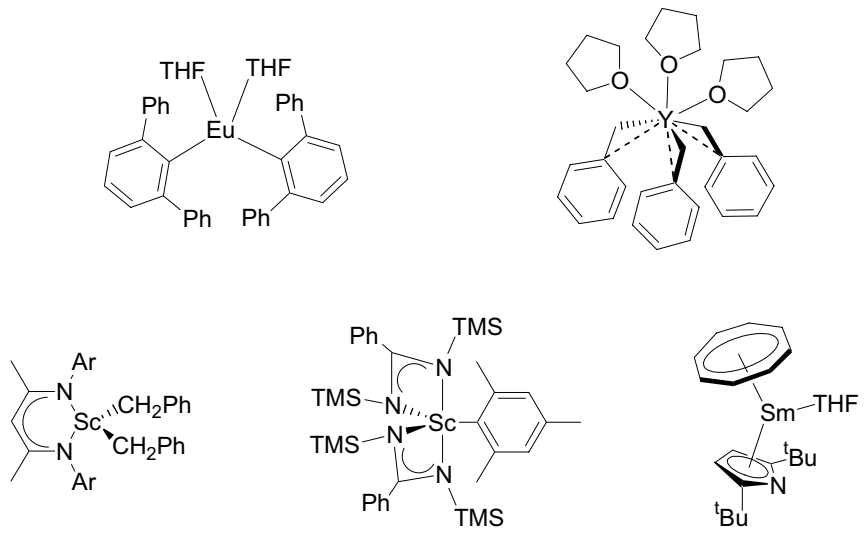

Figure 4. Examples of organolanthanide complexes carrying non-cyclopentadienyl ligands.[24-28]

With these ligands a vast array of divalent and trivalent organolanthanide complexes can be obtained using mainly salt-metathesis or metal-exchange reactions. Most importantly, as many of these ligands are sterically less hindered than Cp-ligands the formation of ate-complexes and the observation of agostic interactions to compensate the steric unsaturation are more frequent than with Cp ligands (Figure 5). In addition, solvent coordination is facilitated and special reaction pathways need to be developed to exclude solvent molecules, e.g. high-temperature salt metathesis in non-polar solvents, metal-vapor sublimation.

Figure 5. Examples of ate-complex formation and agostic interactions in non-Cp organolanthanide complexes.[29, 30]

2.3 Phosphorus-containing ligands

According to the HSAB classification, bonding interactions between soft phosphorus atoms and hard lanthanide ions are disfavored. This assumption may have contributed to the rare use of phosphorus containing ligands in organolanthanide chemistry. However, as early as 1983, Schlesener and coworkers showed, that triethylphosphine was approximately as good a ligand as pyrrolidine and better than THF in the adduct-formation with [Cp_3Yb] in benzene.[31]

Today, two important classes of organophosphorus ligands used in lanthanide chemistry can be distinguished: pincer-type ligands and π-ligands (Figure 6).

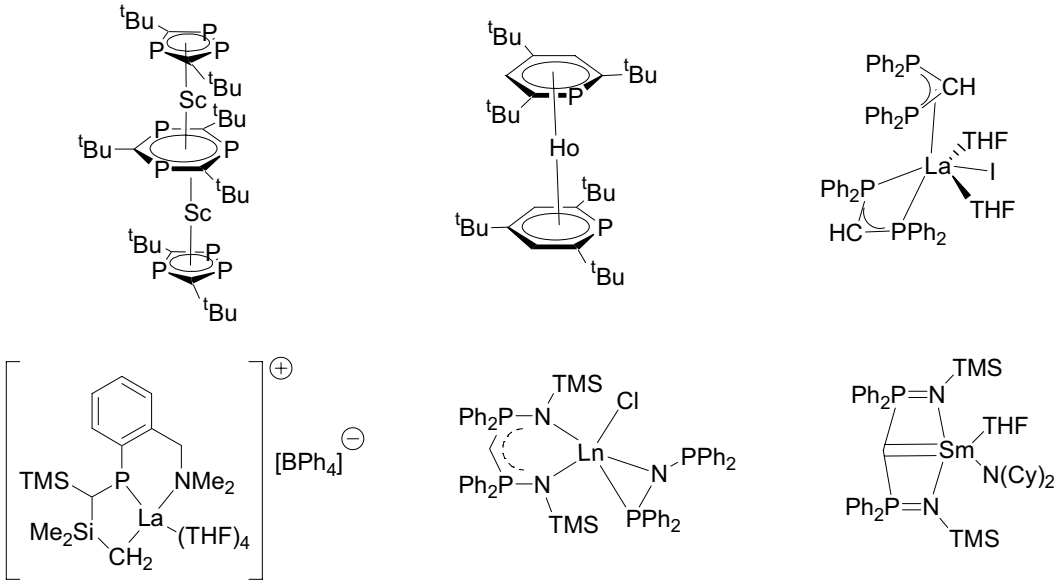

Figure 6. Examples of organolanthanide complexes carrying phosphorus-containing ligands.[32-37]

In the former class the pincer can contain (a) neutral phosphines or (b) anionic phosphides which give rise to Ln-P bonds, or (c) P=X groups (X= O, N, S) which lead to the formation of Ln-X bonds. Whereas in (a) the main driving force of the Ln-P bond formation is chelation, in (b) and (c) additional (partial) negative charges also contribute. In particular, iminophosphorane ligands (P=N) have recently attracted growing interest, due to the catalytic activity of the corresponding lanthanide complexes in organic transformations and polymerization. The bis(iminophosphorane)methane ligand has also allowed the synthesis of the first structurally characterized lanthanide alkylidene complex (Figure 6).[37, 38] Lanthanide carbene complexes are very rare, in contrast to their transition metal analogues, because of the lack of π-backbonding from the lanthanide to the ligand,[39] and virtually no chemistry has been developed with these complexes.

Among the π-ligands, anionic phospholyl ligands are the most studied ones, although several other ligand systems have also been employed, e.g. anionic di- and tri-phospholyl, annulated benzophospholyl and neutral mono- and triphosphabenzene ligands.

As in this work phospholyl ligands play an important role a short overview on their properties, synthesis and use in organolanthanide chemistry will be given.

The phospholyl ligand can be considered as cyclopentadienyl analog with one CH group being replaced by a P atom. Theoretical investigations have shown that the aromaticity of Cp and phospholyl ligands are nearly the same.[40] In contrast, electrochemical investigations with a number of transition metal and actinide complexes have revealed, that the phospholyl ligand is much less electron donating than the Cp ligand.[41-44]

The phospholyl anions are usually obtained by the cleavage of exocyclic P-R, P-X or P-P bonds of the corresponding phospholes using alkali metals (Scheme 2).[45-49]

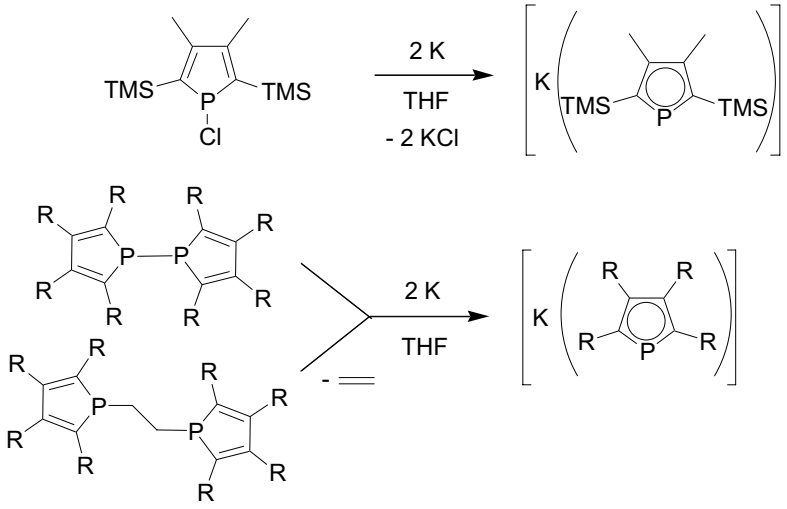

Scheme 2. Synthesis of phospholyl anions.

Several synthetic pathways to substituted phosphole ligands have been proposed. As lanthanide chemistry mainly requires bulky ligands the syntheses of the three phosphole ligands Dtp, Dsp and Htp are shown as representative examples in scheme 3.[45, 50, 51] The regioselectivity in the Zr intermediate is determined by the steric bulk of the R groups and by their ability to stabilize the negative charge on the carbon atom next to Zr.

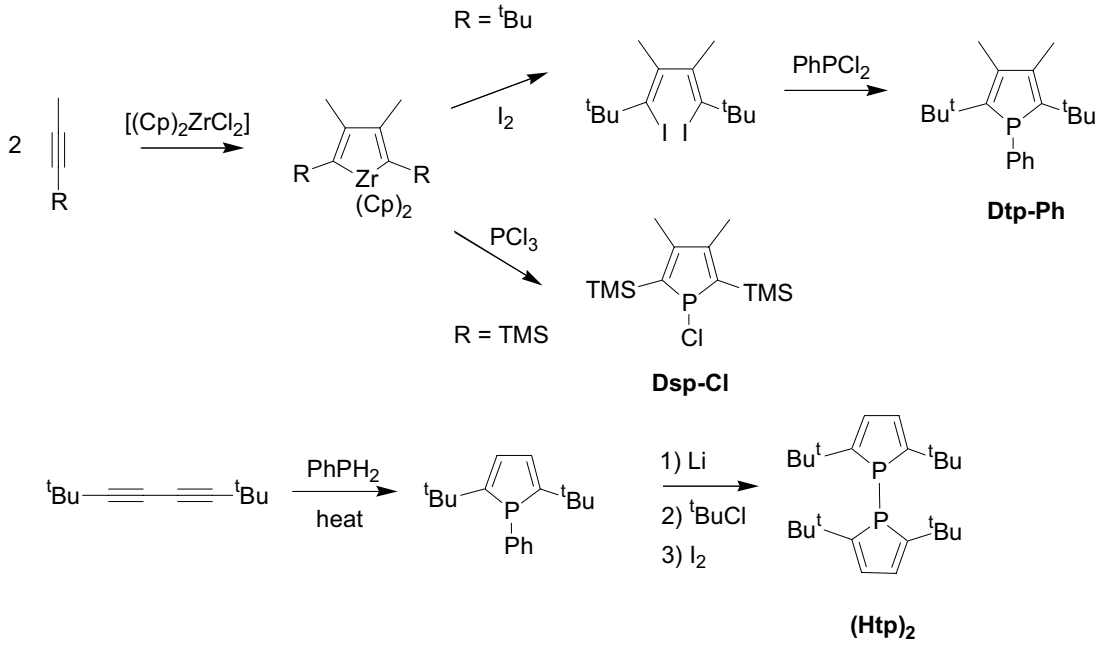

Scheme 3. Synthesis of different phospholes

The use of phospholyl ligands in lanthanide chemistry has been well established. Three main binding modes have been observed: η^5-coordination via the delocalized π-system, η^1-coordination via the lone pair on phosphorus and a combination of both.[17, 19] Divalent lanthanide complexes bearing phospholyl ligands are not only accessible via salt metathesis reactions but also via the insertion of the metal into the P-P bond of biphospholes or into the P-Cl bond of phospholes. The lone pair on P has also allowed for the synthesis of a bimetallic Yb-Ru complex.[52]

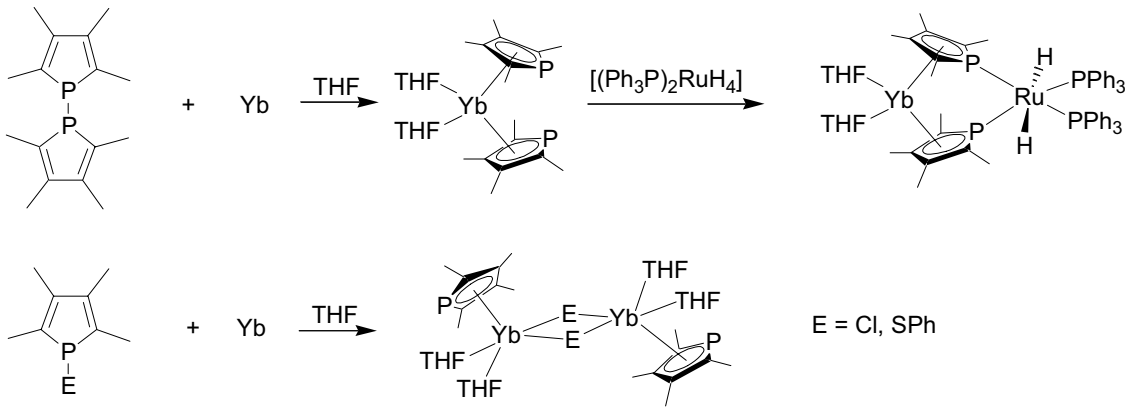

Scheme 4. Synthesis of divalent lanthanide complexes bearing phospholyl ligands.

3 Applications of organolanthanide complexes

3.1 Organic Synthesis

Lanthanides are usually found in the oxidation state +3 and for none of the elements the oxidation state +2 and +4 have been found on the same metal. Hence, two-electron redox processes which form the basis of many transition metal catalyzed reactions, e.g. oxidative addition and reductive elimination, cannot occur on a single lanthanide metal center. As will be shown below, the main transformations with organolanthanide complexes are insertion and σ-bond metathesis reactions.

The use of organolanthanide complexes in organic synthesis started in the mid-1980s with the works by Marks and coworkers who used some bis(cyclopentadienyl)Ln alkyl complexes in the catalytic hydrogenation of alkenes.[53] Since then, a large number of complexes carrying Cp and non-Cp ligands have been applied to catalytic hydrosilylation, hydroamination and combined cyclization- functionalization reactions (Figure 7).[54-56]

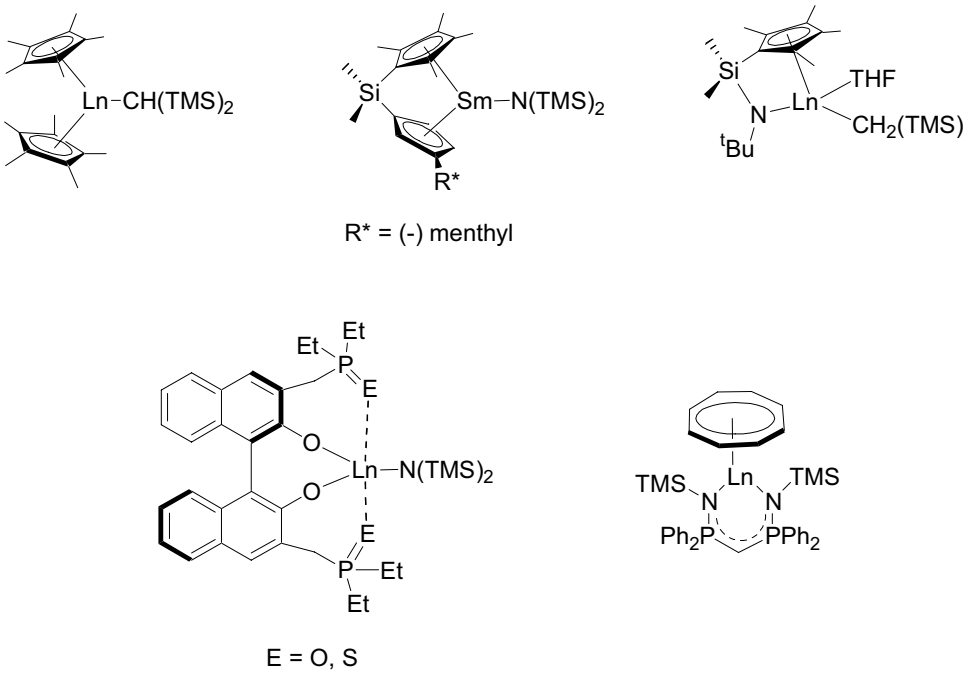

Figure 7. Catalysts for organolanthanide based functionalization reactions. [57-61]

Two different reaction mechanisms are proposed depending on the electronegativity of the heteroatom (Scheme 5).[54, 55] Each mechanism starts with the generation of the catalytically active species (**A**) via σ-bond metathesis: for electropositive elements (Si, B) a lanthanide hydride species forms, whereas in the case of the electronegative elements (N, P) a Ln-X bond results. This species **A** undergoes alkene insertion into the lanthanide hydride or Ln-X bond to form a new lanthanide carbon bond (**B**). The final step is the σ-bond metathesis between this organometallic and another substrate molecule with release of the final product and

regeneration of the catalyst (**A**). The use of enantiomerically pure organolanthanide complexes has allowed for the induction of stereoselectivity in some reactions.[54, 62] The successful use of [(COT)Ln{CH(PN(TMS)$_2$)$_2$}] in hydroamination reactions shows that other mechanistic pathways also need to be considered, as this complex does not have an obvious active ligand.[57]

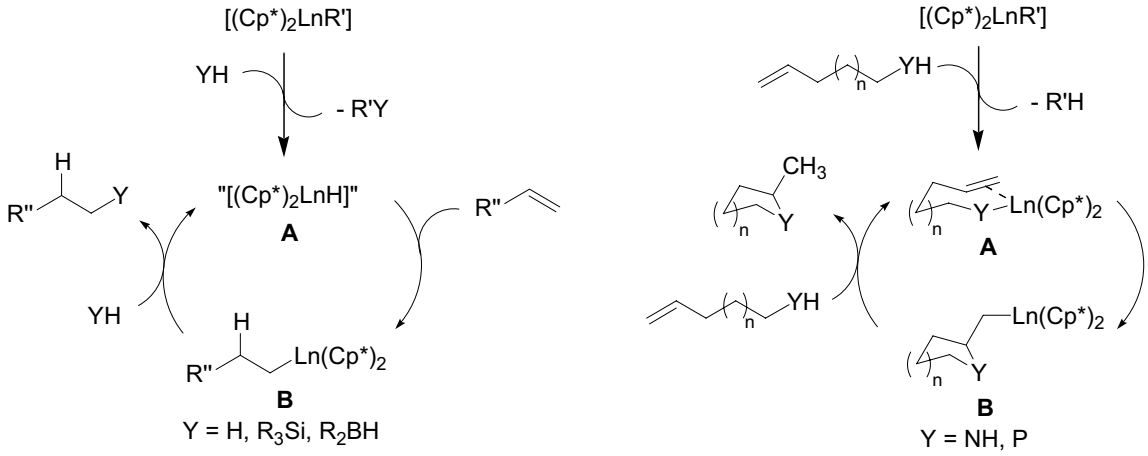

Scheme 5. Catalytic cycles of organolanthanide catalyzed transformations of alkenes.

3.2 Reduction chemistry

For a long time only the three elements Eu, Yb and Sm were considered to have an accessible divalent oxidation state in addition to the usual trivalent oxidation state.[4] The discovery of a convenient synthesis of SmI_2 by Kagan and its use in many organic reactions (Scheme 6) can be considered as the starting point for the development of reduction chemistry with divalent organolanthanide compounds.[63, 64]

SmI_2 is a one-electron reducing agent (-1.55 V vs. NHE) which can be prepared in-situ as dark green solution by stirring 1,2-diiodoethane with Sm powder in THF. It reduces chemoselectively a large number of functional groups, for example organic halides, carbonyl compounds, epoxides and azo-compounds.[65] The reactivity of SmI_2 can be increased by the use of solvents other than THF,[66] elevated temperature and also by addition of co-activators like HMPA or Ni-salts.[67, 68] One major drawback of this reagent is its use in stoichiometric amounts. However, in recent years a catalytic version making use of Mischmetal as co-reducing agent has been successfully developed.[69, 70]

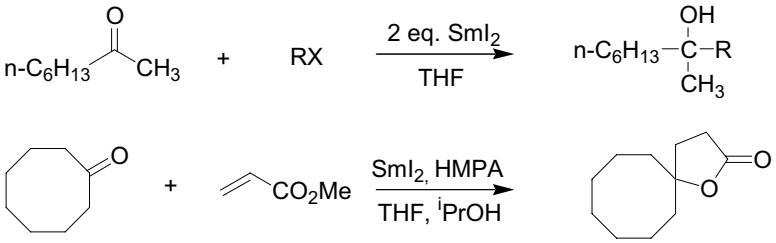

Scheme 6. Use of SmI_2 in organic synthesis.[71, 72]

Shortly after the discovery of the convenient synthesis of SmI_2, Evans reported on the synthesis of $[(Cp^*)_2Sm(THF)_2]$ and consequently of $[(Cp^*)_2Sm]$, which are among the most reactive organometallic reducing agents reported so far.[73, 74] These compounds react with a large variety of substrates of which only two examples are shown in Scheme 7.[75-77]

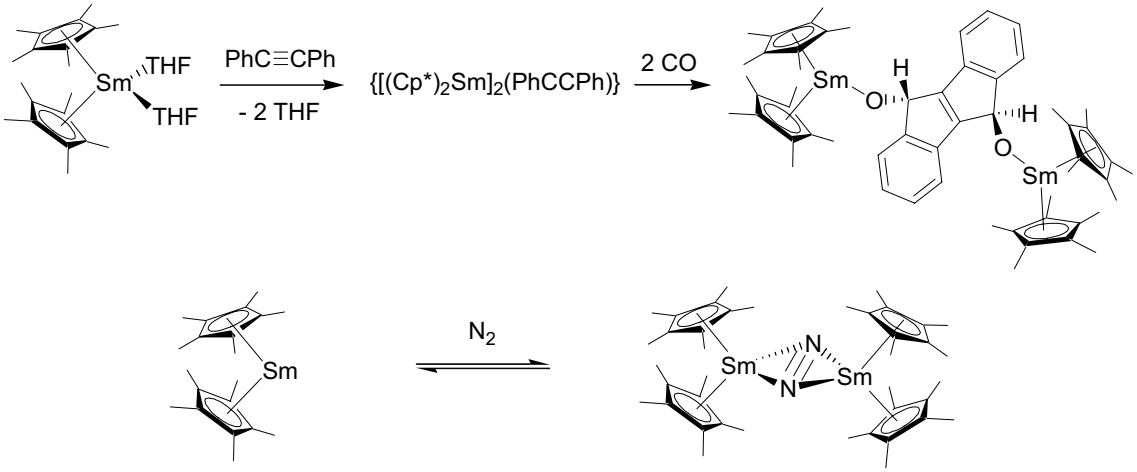

Scheme 7. Activation of diphenylacetylene/CO and N_2 with $[(Cp^*)_2Sm]$.

The dinitrogen adduct was the first example of coplanar coordination of two metals to dinitrogen. However, the short N-N bond length and the reversibility of this reaction show that no dinitrogen reduction has taken place.

In the quest for even more powerful reducing agents three new areas of lanthanide reduction chemistry opened up:

a) "New" divalent lanthanide chemistry

According to the redox potentials the next accessible divalent lanthanides after Sm should be Tm, Dy and Nd. Divalent halides were reported for all three elements in the 1960s, however, they were expected to be too reactive to be stable in organic solvents.[15] In 1998, Evans and Bochkarev managed to isolate the first molecular compound of divalent thulium, $TmI_2(DME)_3$, from the reaction of metallic Tm and TmI_3 in refluxing DME (Scheme 8).[78] This compound was shown to be more reactive than SmI_2/HMPA in the coupling of alkyl halides to ketones.[79]

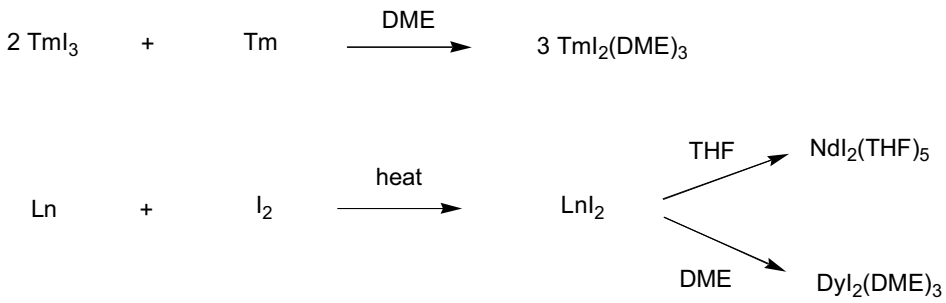

Scheme 8. Synthesis of "new" divalent LnI_2.

In the following years, the DME or THF solvated divalent $DyI_2(DME)_3$ and $NdI_2(THF)_5$ could also be prepared and characterized crystallographically.[80, 81] These new LnI_2 complexes react with a large number of organic and inorganic substrates, e.g. the reaction with metallocenes of d-transition metals has opened up a new synthetic route to bis(arene) complexes of the transition metals and they also show good activity in the polymerisation of isoprene.[82, 83]

The attempted preparation of organometallic compounds with these diiodides by salt metathesis reactions using anionic Cp ligands allowed for the isolation of new dinitrogen complexes (Scheme 9).[84, 85] These reactions are irreversible and true dinitrogen reduction takes place. In contrast, using the bulky Cp'' ligand and working under an argon atmosphere allowed for the isolation of the first divalent organothulium complex $[(Cp'')_2Tm(THF)]$, which was characterized by X-ray analysis.[85]

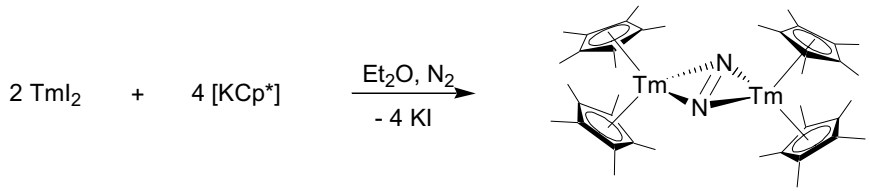

Scheme 9. Dinitrogen activation in the attempted synthesis of divalent Tm compounds.

Some more divalent organothulium complexes with high stability have been reported, making use of phospholyl and arsolyl ligands,[50, 86, 87] however, the synthetic methods and the investigation of their reactivity remain still very limited. Furthermore, no organodysprosium or organoneodymium complex has been isolated.

b) Sterically induced reduction chemistry

Tris(cyclopentadienyl) lanthanide compounds have been known since the beginning of organolanthanide chemistry. However, it was assumed that only two of the bulky Cp* star ligands could fit around the lanthanide center. Very surprisingly, the reduction of cyclooctatetraene by $[(Cp^*)_2Sm]$ allowed for the isolation of $[(Cp^*)_3Sm]$ (Scheme 10).[88] This compound exhibits significantly longer Sm-C distances than in other Sm^{3+} complexes of Cp*.

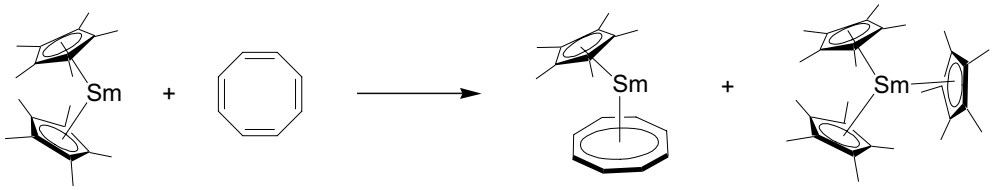

Scheme 10. First synthesis of $[(Cp^*)_3Sm]$.

The extreme steric crowding provided a good basis for high reactivity. This compound showed similar reaction behaviour as the divalent $[(Cp^*)_2Sm]$ with many substrates, e.g. reduction of $Ph_3P{=}S$ to Ph_3P and reduction of azobenzene.[89, 90] As one of the by-products which was always obtained was $(Cp^*)_2$ and no formation of Sm^{4+} was observed, the third Cp* ligand was held responsible for this reduction chemistry. $(Cp^*)_2$ can form if the anionic $(Cp^*)^-$ gives up one electron and forms a $(Cp^*)^\bullet$ radical which can easily dimerize.

In the meantime, $[(Cp^*)_3Ln]$ complexes have been synthesized for the whole lanthanide series.[91, 92] However, as most of these elements do not possess an accessible divalent state, another synthetic route has been developed making use of unsolvated cations of the general formula $[(Cp^*)_2Ln(BPh_4)]$ (Scheme 11).[93]

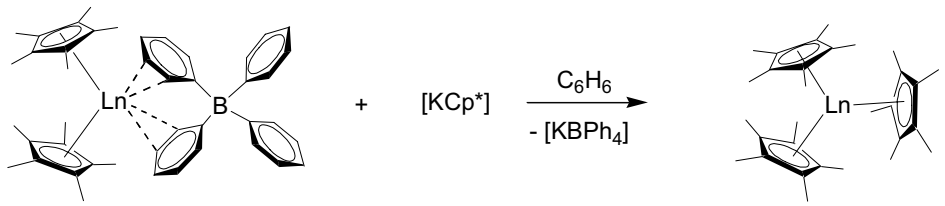

Scheme 11. General synthesis of $[(Cp^*)_3Ln]$ complexes.

As all these complexes exhibit reduction chemistry in analogy to Sm^{2+} it is possible to effect size optimization of the reduction chemistry.

c) LnZ_3/K reduction chemistry

Over the last years it has been shown, that dinitrogen activation cannot only occur with "true" divalent lanthanides but also by the in-situ reduction of trivalent precursors along the whole series of the lanthanides. For example, $[Ln\{N(TMS)_2\}_3]$ led to the dinitrogen containing products $[\{Ln[N(TMS)_2]_2\}_2(\mu\text{-}\eta^2\text{:}\eta^2\text{-}N_2)]$ upon reduction with potassium in THF (Scheme 12), even with Ln = Er, Tb, Gd, Y and Lu which all possess more negative reduction potentials Ln^{3+}/Ln^{2+} than -2.9 V vs. NHE, the reduction potential of the potassium reductant.[94-96] This approach is also possible for a $[LnZ_2Z']$ system like $[(Cp^*)_2Ln(BPh_4)]$ precursors.[97]

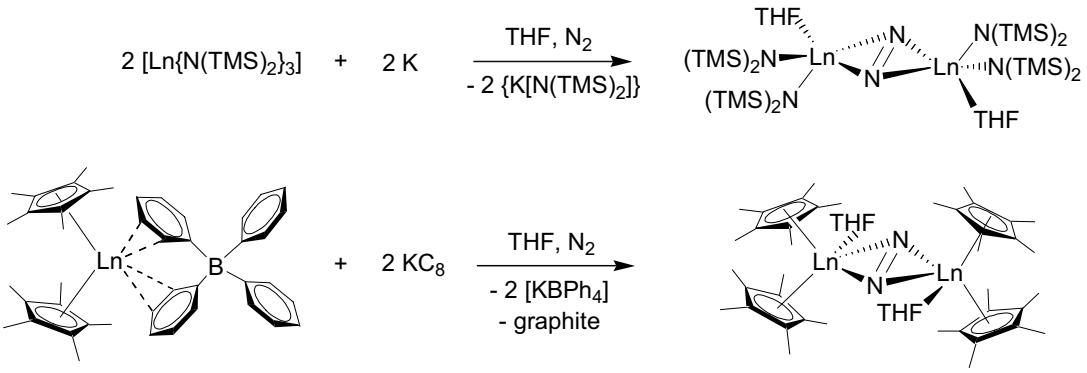

Scheme 12. Examples of the LnZ_3/K reduction chemistry.

This approach allows again the full range of size optimization. In addition, as even diamagnetic La^{3+}, Y^{3+} and Lu^{3+} dinitrogen complexes can be accessed, follow-up reactions can now be conveniently followed by NMR spectroscopy.[97]

3.3 Polymerization Catalysis

Trivalent organolanthanide complexes have been used as initiators in polymerization and copolymerization reactions of polar and non-polar monomers for 30 years. Since the pioneering work by Ballard, Watson and Marks which was mainly based on lanthanidocene complexes many new types of complexes have been developed to increase the activity and selectivity in these processes.[98-103] Especially the use of bridged Cp ligands, half-sandwich complexes and of divalent or cationic species has recently led to many new discoveries.[22, 23, 104, 105]

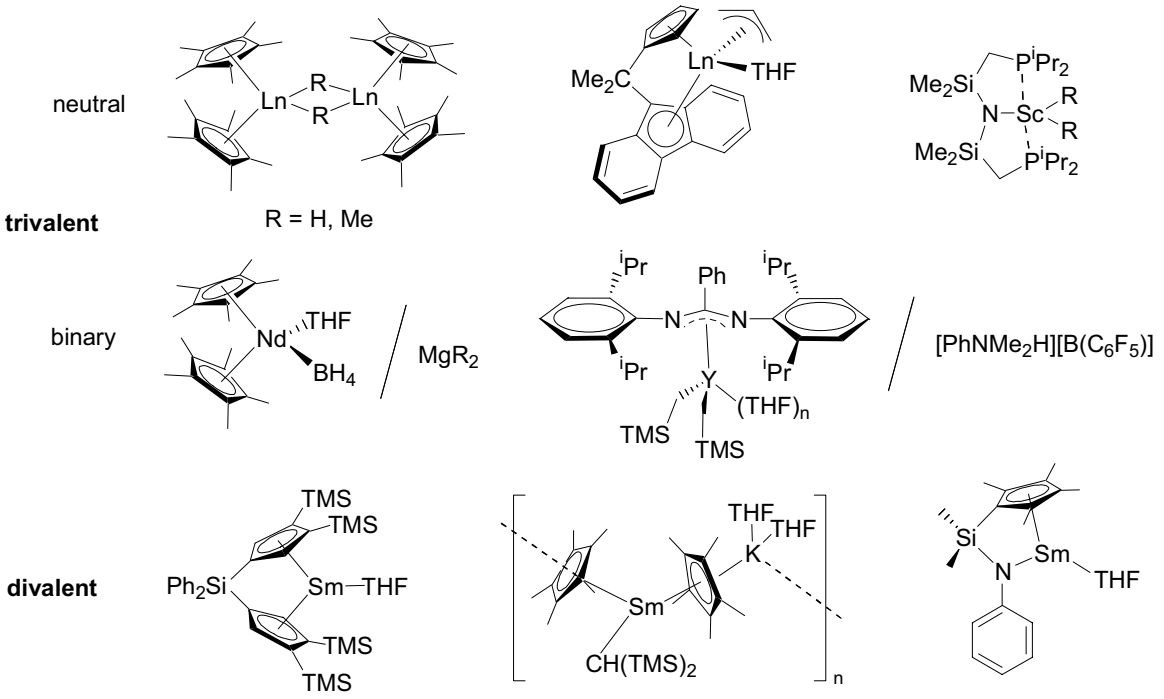

Figure 8. Examples of lanthanide-based polymerization initiators. [100, 106-113]

For non-polar monomers (ethylene, styrene) the essential reaction steps are similar to the above described transformations of alkenes. The catalytically active species (**A**) undergoes alkene insertion (**B**) followed by σ-bond metathesis with other monomers (**C**). The termination step often involves H-abstraction or chain transfer (Scheme 13).[114]

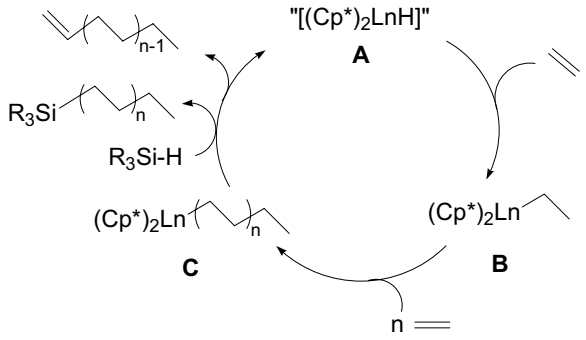

Scheme 13. Polymerization of ethylene.[114]

For polar monomers (acrylates, esters) the initiation step is the 1,2 or 1,4 nucleophilic attack of the lanthanide bound alkyl or hydride group onto the functional group of the monomer.[115, 116] The resulting alkoxide group can then attack the functional group of another monomer (Scheme 14). Many of these polymerization reactions have been reported to be of a "living fashion".

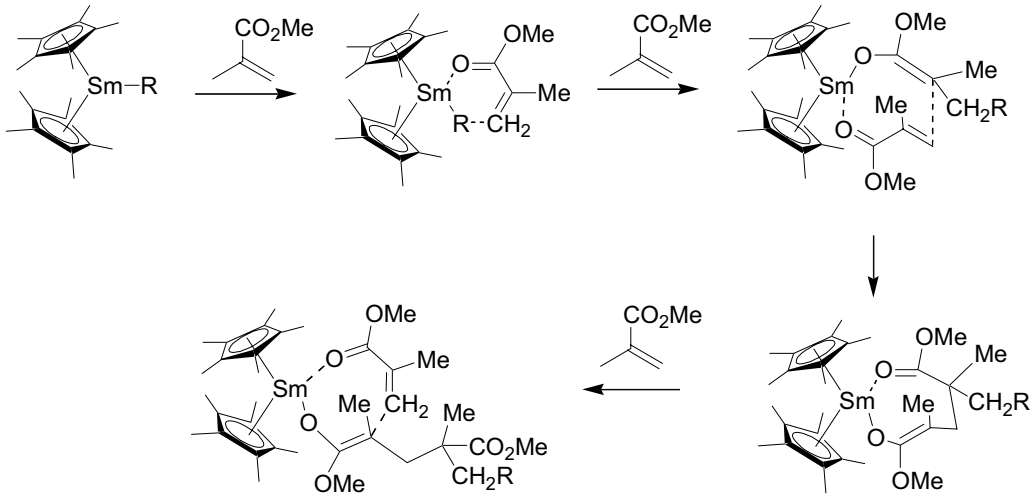

Scheme 14. Reaction mechanism for the syndiotactic polymerization of MMA.

Divalent organolanthanide complexes were introduced in polymerization catalysis some years after the trivalent complexes. In particular, $[(Cp^*)_2Sm]$ has been intensively investigated in the polymerization of both polar and non-polar monomers.[111, 117, 118] In both cases, $[(Cp^*)_2Sm]$ can act as bifunctional initiator: in a first step the divalent compound is oxidized via one electron transfer to the monomer which undergoes reductive coupling to form a bimetallic complex. Chain growth can then take place at both Sm centers (Scheme 15).

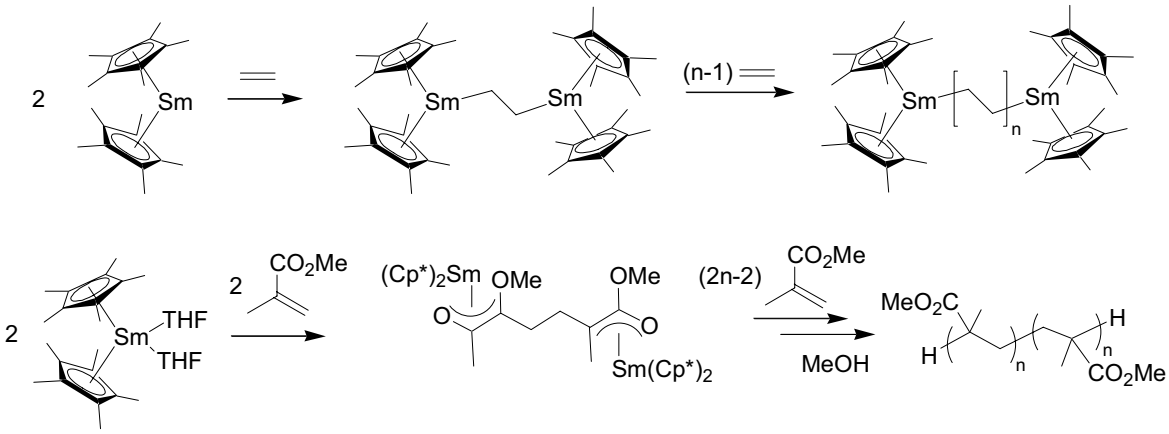

Scheme 15. Ethylene and MMA polymerization with [$(Cp^*)_2Sm$].

Organophosphorus-based complexes have recently been introduced to polymerization catalysis.[108, 119] However, so far no catalytically active phospholyl substituted lanthanide complex has been reported.

4 Project presentation

This bibliographical overview shows that a lot of progress has been made in both the synthesis and applications of organolanthanide complexes, which has led to some exciting new chemistry. However, some areas are still under-developed, including organophosphorus chemistry, carbene chemistry and "new" divalent organolanthanide chemistry.

In this work we will focus on the contribution of organophosphorus ligands to organolanthanide chemistry in three different areas.

First, we will present a new synthetic approach towards "new" divalent organolanthanide complexes using both cyclopentadienyl and phospholyl ligands. The difference between the two ligand systems will be shown in the coordination behavior of the ligands and the observed stability and reactivity of the new complexes.

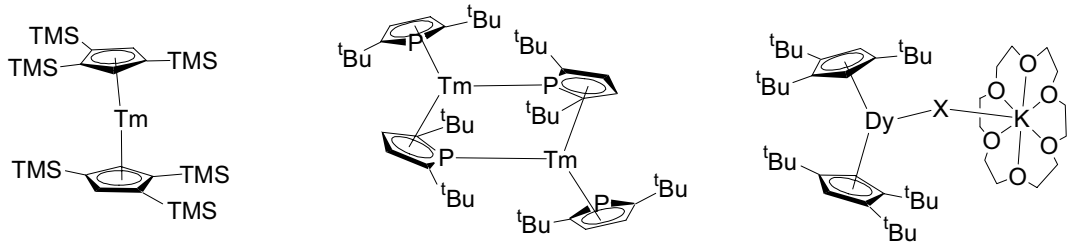

Figure 9. "New" divalent organolanthanide complexes.

In the second part, investigations concerning the synthesis of half-sandwich lanthanide complexes with phospholyl ligands will be described. New synthetic routes have been developed and the obtained complexes have been studied in polymerization reactions.

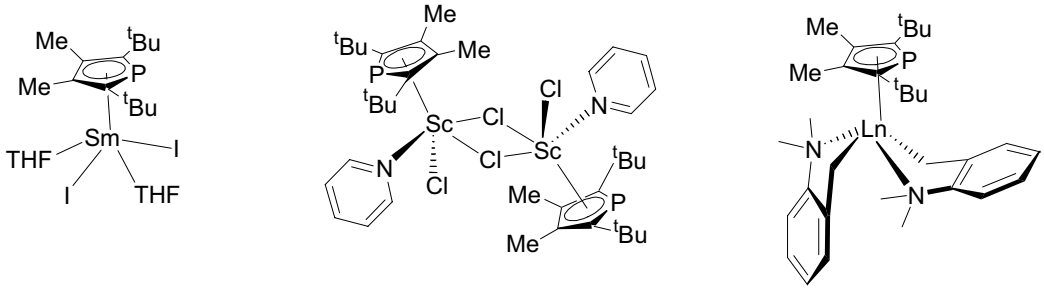

Figure 10. Half-sandwich lanthanide complexes with phospholyl ligands.

The third part will illustrate how a dianionic precursor can be used to access new lanthanide carbene complexes. The first reactivity studies of these complexes and structural evidence on the nature of the Ln-C multiple bond will be presented.

Figure 11. Lanthanide carbene complexes.

References

[1] H. B. Kagan, *Chem. Rev.* **2002**, *102*, 1805.
[2] H. Schumann, J. A. Meese-Marktscheffel, L. Esser, *Chem. Rev.* **1995**, *95*, 865.
[3] T. J. Marks, R. D. Ernst, in *Comp. Organomet. Chem., Vol. 3, Chap. 2* (Eds.: E. W. Abel, F. G. A. Stone, G. Wilkinson), Pergamon, Oxford, **1982**.
[4] F. T. Edelmann, in *Comp. Organomet. Chem. II, Vol. 4, Chap. 2* (Eds.: E. W. Abel, F. G. A. Stone, G. Wilkinson), Pergamon, Oxford, **1995**.
[5] G. Wilkinson, J. M. Birmingham, *J. Am. Chem. Soc.* **1954**, *76*, 6210.
[6] S. A. Cotton, *Lanthanide and Actinide Chemistry (Inorganic Chemistry: A textbook series)*, 2nd revised ed., John Wiley & Sons, West Sussex, **2006**.
[7] R. Anwander, in *Topics in Organometallic Chemistry, Vol. 2* (Ed.: S. Kobayashi), Springer-Verlag, Berlin Heidelberg, **1999**.
[8] C. Elschenbroich, *Organometallics*, 3rd ed., Wiley-VCH, Weinheim, **2006**.
[9] K. H. Wedepohl, *Geochim. Cosmochim. Acta* **1995**, *59*, 1217.
[10] A. J. Freeman, R. E. Watson, *Phys. Rev.* **1962**, *127*, 2058.
[11] A. Streitwieser, S. A. Kinsley, J. T. Rigsbee, I. L. Fragala, E. Ciliberto, N. Rosch, *J. Am. Chem. Soc.* **1985**, *107*, 7786.
[12] A. Streitwieser, S. A. Kinsley, C. H. Jenson, J. T. Rigsbee, *Organometallics* **2004**, *23*, 5169.
[13] U. Kilimann, R. Herbstirmer, D. Stalke, F. T. Edelmann, *Angew. Chem. Int. Ed.* **1994**, *33*, 1618.
[14] G. Meyer, N. Gerlitzki, S. Hammerich, *J. Alloy Compd.* **2004**, *380*, 71.
[15] G. Meyer, *Chem. Rev.* **1988**, *88*, 93.
[16] F. T. Edelmann, D. M. M. Freckmann, H. Schumann, *Chem. Rev.* **2002**, *102*, 1851.
[17] P. Le Floch, *Coord. Chem. Rev.* **2006**, *250*, 627.
[18] F. Nief, *Coord. Chem. Rev.* **1998**, *178-180*, 13.
[19] F. Nief, *Eur. J. Inorg. Chem.* **2001**, 891.
[20] H. Schumann, E. C. E. Rosenthal, J. Demtschuk, *Organometallics* **1998**, *17*, 5324.
[21] G. B. Deacon, A. Dietrich, C. M. Forsyth, H. Schumann, *Angew. Chem. Int. Ed.* **1989**, *28*, 1370.
[22] J. Gromada, J. F. Carpentier, A. Mortreux, *Coord. Chem. Rev.* **2004**, *248*, 397.
[23] Z. M. Hou, Y. Wakatsuki, *Coord. Chem. Rev.* **2002**, *231*, 1.
[24] S. Bambirra, A. Meetsma, B. Hessen, *Organometallics* **2006**, *25*, 3454.
[25] G. Heckmann, M. Niemayer, *J. Am. Chem. Soc.* **2000**, *122*, 4227.
[26] H. Schumann, E. C. E. Rosenthal, J. Winterfeld, R. Weimann, J. Demtschuk, *J. Organomet. Chem.* **1996**, *507*, 287.
[27] J. R. Hagadorn, J. Arnold, *Organometallics* **1996**, *15*, 984.
[28] L. W. M. Lee, W. E. Piers, M. R. J. Elsegood, W. Clegg, M. Parvez, *Organometallics* **1999**, *18*, 2947.
[29] C. Eaborn, P. B. Hitchcock, K. Izod, J. D. Smith, *J. Am. Chem. Soc.* **1994**, *116*, 12071.
[30] H. Schumann, W. Genthe, N. Bruncks, J. Pickardt, *Organometallics* **1982**, *1*, 1194.
[31] C. J. Schlesener, A. B. Ellis, *Organometallics* **1983**, *2*, 529.
[32] P. L. Arnold, F. G. N. Cloke, P. B. Hitchcock, J. F. Nixon, *J. Am. Chem. Soc.* **1996**, *118*, 7630.
[33] P. L. Arnold, F. G. N. Cloke, P. B. Hitchcock, *Chem. Commun.* **1997**, 481.
[34] S. T. Liddle, K. Izod, *J. Organomet. Chem.* **2006**, *691*, 2599.
[35] K. Izod, S. T. Liddle, W. Clegg, *Chem. Commun.* **2004**, 1748.
[36] M. T. Gamer, M. Rastatter, P. W. Roesky, A. Steffens, M. Glanz, *Chem.-Eur. J.* **2005**, *11*, 3165.
[37] K. Aparna, M. Ferguson, R. G. Cavell, *J. Am. Chem. Soc.* **2000**, *122*, 726.
[38] R. G. Cavell, R. P. K. Babu, K. Aparna, *J. Organomet. Chem.* **2001**, *617*, 158.
[39] G. R. Giesbrecht, J. C. Gordon, *Dalton Trans.* **2004**, 2387.
[40] L. Nyulaszi, *Chem. Rev.* **2001**, *101*, 1229.
[41] P. Lemoine, M. Gross, P. Braunstein, F. Mathey, B. Deschamps, J. M. Nelson, *Organometallics* **1984**, *3*, 1303.

[42] C. Burney, D. Carmichael, K. Forissier, J. C. Green, F. Mathey, L. Ricard, *Chem.-Eur. J.* **2003**, *9*, 2567.
[43] C. Burney, D. Carmichael, K. Forissier, J. C. Green, F. Mathey, L. Ricard, *Chem.-Eur. J.* **2005**, *11*, 5381.
[44] P. Gradoz, D. Baudry, M. Ephritikhine, M. Lance, M. Nierlich, J. Vigner, *J. Organomet. Chem.* **1994**, *466*, 107.
[45] M. Visseaux, F. Nief, L. Ricard, *J. Organomet. Chem.* **2002**, *647*, 139.
[46] F. Mathey, F. Mercier, F. Nief, J. Fischer, A. Mitschler, *J. Am. Chem. Soc.* **1982**, *104*, 2077.
[47] C. Charrier, H. Bonnard, F. Mathey, *J. Org. Chem.* **1982**, *47*, 2376.
[48] C. Charrier, N. Maigrot, F. Mathey, *Organometallics* **1987**, *6*, 586.
[49] C. Charrier, F. Mathey, *Tetrahedron Lett.* **1987**, *28*, 5025.
[50] D. Turcitu, F. Nief, L. Ricard, *Chem.-Eur. J.* **2003**, *9*, 4916.
[51] D. Carmichael, L. Ricard, F. Mathey, *J. Chem. Soc., Chem. Commun.* **1994**, 1167.
[52] P. Desmurs, M. Visseaux, D. Baudry, A. Dormond, F. Nief, L. Ricard, *Organometallics* **1996**, *15*, 4178.
[53] G. Jeske, H. Lauke, H. Mauermann, H. Schumann, T. J. Marks, *J. Am. Chem. Soc.* **1985**, *107*, 8111.
[54] G. A. Molander, J. A. C. Romero, *Chem. Rev.* **2002**, *102*, 2161.
[55] S. Hong, T. J. Marks, *Acc. Chem. Res.* **2004**, *37*, 673.
[56] T. J. Marks, M. R. Gagne, *US patent 5,043,453*, **1991**.
[57] T. K. Panda, A. Zulys, M. T. Gainer, P. W. Roesky, *Organometallics* **2005**, *24*, 2197.
[58] X. H. Yu, T. J. Marks, *Organometallics* **2007**, *26*, 365.
[59] M. R. Gagné, L. Brard, V. P. Conticello, C. L. Stern, T. J. Marks, *J. Am. Chem. Soc.* **1992**, *114*, 2003.
[60] D. Robert, A. A. Trifonov, P. Voth, J. Okuda, *J. Organomet. Chem.* **2006**, *691*, 4393.
[61] V. M. Arredondo, F. E. McDonald, T. J. Marks, *J. Am. Chem. Soc.* **1998**, *120*, 4871.
[62] H. C. Aspinall, *Chem. Rev.* **2002**, *102*, 1807.
[63] J. L. Namy, P. Girard, H. B. Kagan, *New J. Chem.* **1977**, *1*, 5.
[64] H. B. Kagan, *J. Alloy Compd.* **2006**, *408-412*, 421.
[65] A. Krief, A.-M. Laval, *Chem. Rev.* **1999**, *99*, 745.
[66] H. B. Kagan, J. L. Namy, in *Topics in Organometallic Chemistry, Vol. 2* (Ed.: S. Kobayashi), Springer-Verlag, Berlin Heidelberg, **1999**.
[67] F. Machrouhi, J. L. Namy, *Tetrahedron Lett.* **1999**, *40*, 1315.
[68] A. Cabrera, H. Alper, *Tetrahedron Lett.* **1992**, *33*, 5007.
[69] A. Di Scala, S. Garbacia, F. Hélion, M. I. Lannou, J. L. Namy, *Eur. J. Org. Chem.* **2002**, 2989.
[70] M. I. Lannou, F. Hélion, J. L. Namy, *Tetrahedron Lett.* **2002**, *43*, 8007.
[71] T. Tabuchi, J. Inanaga, M. Yamaguchi, *Tetrahedron Lett.* **1986**, *27*, 5763.
[72] P. Girard, J. L. Namy, H. B. Kagan, *J. Am. Chem. Soc.* **1980**, *102*, 2693.
[73] W. J. Evans, I. Bloom, W. E. Hunter, J. L. Atwood, *Organometallics* **1985**, *4*, 112.
[74] W. J. Evans, J. W. Grate, H. W. Choi, I. Bloom, W. E. Hunter, J. L. Atwood, *J. Am. Chem. Soc.* **1985**, *107*, 941.
[75] W. J. Evans, D. G. Giarikos, C. B. Robledo, V. S. Leong, J. W. Ziller, *Organometallics* **2001**, *20*, 5648.
[76] W. J. Evans, L. A. Hughes, D. K. Drummond, H. Zhang, J. L. Atwood, *J. Am. Chem. Soc.* **1986**, *108*, 1722.
[77] W. J. Evans, T. A. Ulibarri, J. W. Ziller, *J. Am. Chem. Soc.* **1988**, *110*, 6877.
[78] M. N. Bochkarev, I. L. Fedushkin, A. A. Fagin, T. V. Petrovskaya, J. W. Ziller, R. N. R. BroomhallDillard, W. J. Evans, *Angew. Chem. Int. Ed.* **1997**, *36*, 133.
[79] W. J. Evans, N. T. Allen, *J. Am. Chem. Soc.* **2000**, *122*, 2118.
[80] M. N. Bochkarev, I. L. Fedushkin, S. Dechert, A. A. Fagin, H. Schumann, *Angew. Chem. Int. Ed.* **2001**, *40*, 3176.
[81] W. J. Evans, N. T. Allen, J. W. Ziller, *J. Am. Chem. Soc.* **2000**, *122*, 11749.
[82] W. J. Evans, D. G. Giarikos, N. T. Allen, *Macromolecules* **2003**, *36*, 4256.
[83] M. E. Burin, M. V. Smirnova, G. K. Fukin, E. V. Baranov, M. N. Bochkarev, *Eur. J. Inorg. Chem.* **2006**, 351.

[84] W. J. Evans, N. T. Allen, J. W. Ziller, *J. Am. Chem. Soc.* **2001**, *123*, 7927.
[85] W. J. Evans, N. T. Allen, J. W. Ziller, *Angew. Chem. Int. Ed.* **2002**, *41*, 359.
[86] F. Nief, D. Turcitu, L. Ricard, *Chem. Commun.* **2002**, 1646.
[87] F. Nief, B. T. de Borms, L. Ricard, D. Carmichael, *Eur. J. Inorg. Chem.* **2005**, 637.
[88] W. J. Evans, S. L. Gonzales, J. W. Ziller, *J. Am. Chem. Soc.* **1991**, *113*, 7423.
[89] W. J. Evans, *J. Organomet. Chem.* **2002**, *652*, 61.
[90] W. J. Evans, *Coord. Chem. Rev.* **2000**, *206*, 263.
[91] W. J. Evans, B. L. Davis, *Chem. Rev.* **2002**, *102*, 2119.
[92] W. J. Evans, J. M. Perotti, S. A. Kozimor, T. M. Champagne, B. L. Davis, G. W. Nyce, C. H. Fujimoto, R. D. Clark, M. A. Johnston, J. W. Ziller, *Organometallics* **2005**, *24*, 3916.
[93] W. J. Evans, C. A. Seibel, J. W. Ziller, *J. Am. Chem. Soc.* **1998**, *120*, 6745.
[94] W. J. Evans, G. Zucchi, J. W. Ziller, *J. Am. Chem. Soc.* **2003**, *125*, 10.
[95] W. J. Evans, D. S. Lee, C. Lie, J. W. Ziller, *Angew. Chem. Int. Ed.* **2004**, *43*, 5517.
[96] W. J. Evans, D. S. Lee, D. B. Rego, J. M. Perotti, S. A. Kozimor, E. K. Moore, J. W. Ziller, *J. Am. Chem. Soc.* **2004**, *126*, 14574.
[97] W. J. Evans, D. S. Lee, J. W. Ziller, N. Kaltsoyannis, *J. Am. Chem. Soc.* **2006**, *128*, 14176.
[98] J. Holton, M. F. Lappert, D. G. H. Ballard, R. Pearce, J. L. Atwood, W. E. Hunter, *J. Chem. Soc., Chem. Commun.* **1976**, 480.
[99] D. G. H. Ballard, A. Courtis, J. Holton, J. McMeeking, R. Pearce, *J. Chem. Soc., Chem. Commun.* **1978**, 994.
[100] P. L. Watson, G. W. Parshall, *Acc. Chem. Res.* **1985**, *18*, 51.
[101] T. J. Marks, H. Mauermann, *US patent 4,668,773*, **1987**.
[102] F. Garbassi, P. Biagini, P. Andreussi, G. Lugli, *US patent 5,484,897*, **1996**.
[103] V. Monteil, R. Spitz, C. Boisson, *US patent 7,094,854*, **2006**.
[104] P. M. Zeimentz, S. Arndt, B. R. Elvidge, J. Okuda, *Chem. Rev.* **2006**, *106*, 2404.
[105] Y. Nakayama, H. Yasuda, *J. Organomet. Chem.* **2004**, *689*, 4489.
[106] G. Jeske, H. Lauke, H. Mauermann, P. N. Swepston, H. Schumann, T. J. Marks, *J. Am. Chem. Soc.* **1985**, *107*, 8091.
[107] E. Kirillov, C. W. Lehmann, A. Razavi, J. F. Carpentier, *J. Am. Chem. Soc.* **2004**, *126*, 12240.
[108] M. D. Fryzuk, G. Giesbrecht, S. J. Rettig, *Organometallics* **1996**, *15*, 3329.
[109] M. Visseaux, T. Chenal, P. Roussel, A. Mortreux, *J. Organomet. Chem.* **2006**, *691*, 86.
[110] S. Bambirra, M. J. R. Brandsma, E. A. C. Brussee, A. Meetsma, B. Hessen, J. H. Teuben, *Organometallics* **2000**, *19*, 3197.
[111] E. Ihara, M. Nodono, K. Katsura, Y. Adachi, H. Yasuda, M. Yamagashira, H. Hashimoto, N. Kanehisa, Y. Kai, *Organometallics* **1998**, *17*, 3945.
[112] Z. Hou, T. A. Koizumi, M. Nishiura, Y. Wakatsuki, *Organometallics* **2001**, *20*, 3323.
[113] Z. Hou, Y. Zhang, M. Nishiura, Y. Wakatsuki, *Organometallics* **2003**, *22*, 129.
[114] P. F. Fu, T. J. Marks, *J. Am. Chem. Soc.* **1995**, *117*, 10747.
[115] H. Yasuda, H. Yamamoto, K. Yokota, S. Miyake, A. Nakamura, *J. Am. Chem. Soc.* **1992**, *114*, 4908.
[116] H. Yasuda, in *Topics in Organometallic Chemistry, Vol.2* (Ed.: S. Kobayashi), Springer-Verlag, Berlin Heidelberg, **1999**.
[117] L. S. Boffa, B. M. Novak, *Polyhedron* **1997**, *53*, 15367.
[118] W. J. Evans, D. M. DeCoster, J. Greaves, *Macromolecules* **1995**, *28*, 7929.
[119] O. Tardif, Z. Hou, M. Nishiura, T. A. Koizumi, Y. Wakatsuki, *Organometallics* **2001**, *20*, 4565.

Part I

Synthesis and reactivity of “new” divalent organolanthanide complexes: Exploring the reductive approach

1 Introduction

The synthesis and isolation of the first divalent organothulium complex, $[(Cp'')_2Tm(THF)]$,[1] by the metathesis reaction between TmI_2 and two equivalents of [KCp''] under argon (Scheme 1) led to much excitement in the lanthanide community – even a new era in organolanthanide chemistry was predicted.[2] This compound was the first - and still remains the only – fully characterized divalent complex capable of reducing dinitrogen. During the following years, several more divalent organothulium compounds were synthesized by the same synthetic pathway, making use of bulky phospholyl and arsolyl ligands (Figure 1).[3-5] Interestingly, these complexes did not reduce dinitrogen, probably due to the higher stability induced by the hetero-cyclopentadienyl ligands.

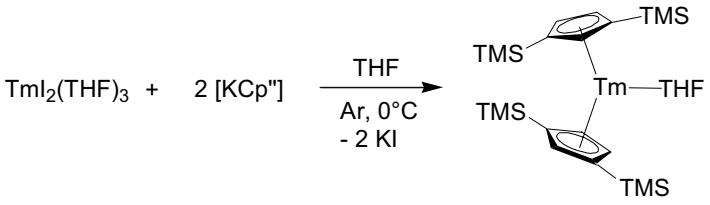

Scheme 1. Synthesis of the first divalent organothulium complex by metathesis reaction.

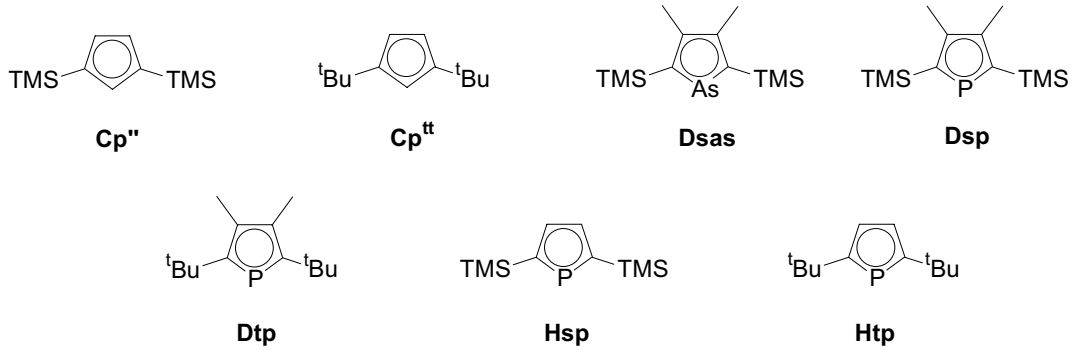

Figure 1. Ligands used for all known divalent thulium complexes of type $[(\eta^5\text{-L})_2Tm(THF)]$.

One major drawback of the metathesis reaction is the use of polar solvents, which often coordinate to the divalent metal; the resulting adducts are rather unstable because the highly reducing divalent species can react with the solvent molecule leading, for example, to diethyl ether cleavage in the attempted synthesis of "$[(Cp^*)_2Tm]$" (Scheme 2).[6]

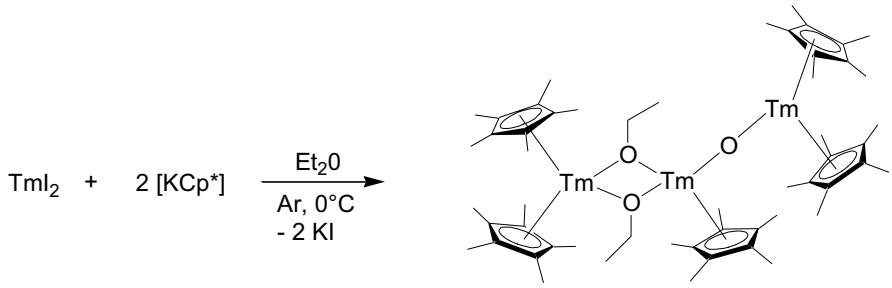

Scheme 2. Diethyl ether cleavage by "[(Cp*)$_2$Tm]".

Only in the case of the bulky Dtp ligand, the solvent-free product [(Dtp)$_2$Tm] which exhibited much higher stability, could be obtained under special conditions (Scheme 3).[4]

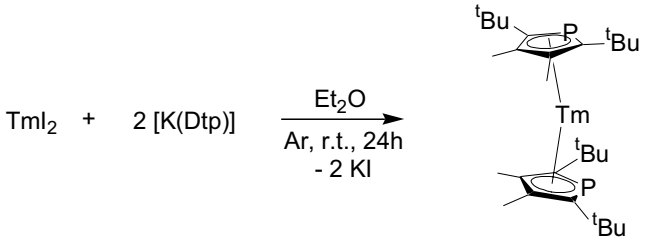

Scheme 3. Synthesis of solvent-free [(Dtp)$_2$Tm].

This reactivity towards polar solvents also prevented the extension of the metathesis approach to dysprosium or neodymium chemistry. In the few examples reported in the literature, the presumably formed divalent species reacted even at low temperature with the solvent or ligand molecules giving either intractable products or trivalent species.[7, 8] It should be noted that even the solvated divalent iodide precursors $DyI_2(S)_n$ and $NdI_2(S)_n$ (S = THF, DME) are not stable at room temperature.[9] Another synthetic pathway avoiding polar solvents was therefore desirable to access "new" divalent organolanthanide species.

Early attempts on the synthesis of "new" low-valent organolanthanide complexes – some even before the discovery of a suitable synthesis of TmI_2 - made use of the reduction of trivalent precursor molecules, mainly of the [(Cp)$_3$Ln] or [(Cp)$_2$LnX] type, by alkali metals in THF or DME (Scheme 4).[10-14] Although most of the reactions carried out with neodymium or thulium precursors did not afford isolable products – in some cases trivalent compounds resulting from the reaction with the solvent were identified - some important information could be obtained for the improvement of this approach. However, the reduction of the trivalent lanthanum precursor [(Cp^{tt})$_3$La] by K/crown ether in benzene allowed for the isolation of the first crystallographically characterized La(II) species, [{K([18]crown-6)(η^2-C_6H_6)$_2$}{[(Cp^{tt})$_2$La]$_2$(μ-η^6:η^6-C_6H_6)}•2C_6H_6].[15] More recently, a formally divalent, but more likely mixed-valent scandium compound, [($P_3C_2{}^tBu_2$)$_2$Sc], resulted from the reduction of the corresponding trivalent precursor, [($P_3C_2{}^tBu_2$)$_3$Sc], using potassium graphite (KC_8) in toluene (Scheme 4).[16]

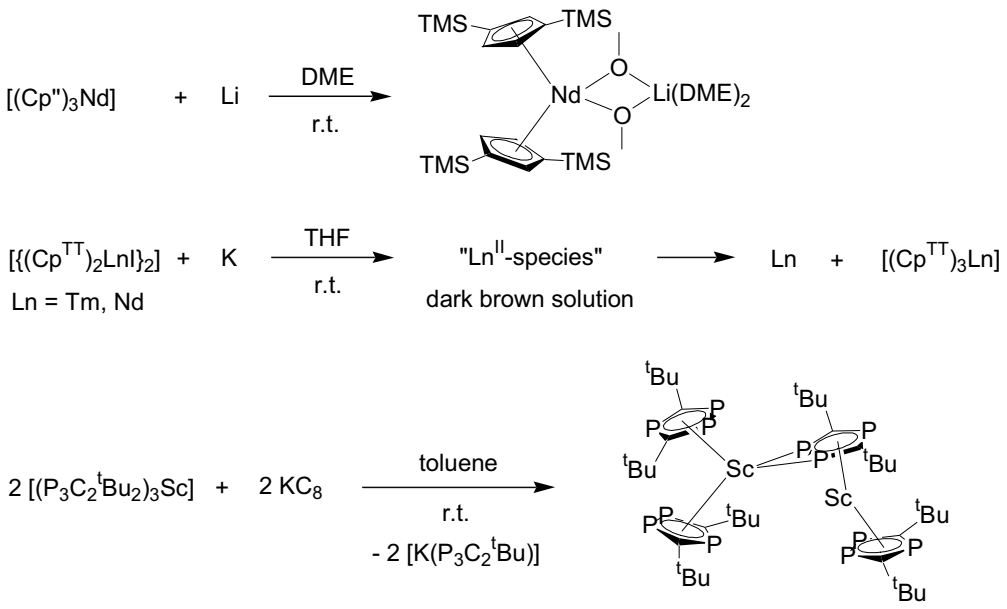

Scheme 4. Some examples of low-valent organolanthanide complexes accessed through chemical reduction of trivalent precursors; ($Cp^{TT} = C_5H_3TBS_2$).

Reaction conditions

From the above examples we deduced the following guidelines in order to successfully carry out the reductive approach, first with organosamarium complexes and then with organothulium, -dysprosium and -neodymium compounds:

a) The absence of polar solvent molecules in the starting materials and during the reaction should enhance the stability of the divalent product because the possibility of adduct formation and solvent cleavage would be reduced.

b) The trivalent precursors should be chosen so as to be soluble in non-polar solvents. in order to allow a rapid reduction process. This is a non-trivial task as can be seen from the above-mentioned examples.

c) The steric bulk of the ligands should be sufficient to stabilize the newly formed divalent species.

d) The use of activated alkali metals – K/crown-ether, KC_8 - which can be employed in non-polar solvents should be envisaged.

Ligand choice

It has been shown, that the divalent thulium complexes carrying Cp^{tt} and Cp'' ligands exhibit very low stability at room temperature[5, 8] and these ligands were therefore initially deemed not suitable in the development of the reductive approach. Instead, addition of one

more bulky group on the cyclopentadienyl-ring, either tBu (Cp^{ttt}) or TMS (Cp''') (Figure 2), was conceived to better stabilize the divalent complexes.

Cp^{ttt} **Cp'''**

Figure 2. Bulky **c**yclopentadienyl ligands for reductive approach.

The Cp^{ttt} ligand, which has recently been investigated in both divalent and trivalent lanthanide chemistry, allows i) the synthesis of solvent-free $[(Cp^{ttt})_2Ln]$ complexes (Ln = Eu, Yb, Sm) by metathesis reaction[17] and ii) the isolation of very soluble, monomeric $[(Cp^{ttt})_2CeX]$ complexes (X = H, F, C_6H_6).[18, 19] The latter examples particularly attracted our interest as most of the reported trivalent thulium precursors of the $[(Cp)_2TmX]$ type are solid-state dimers and thus lack solubility in non-polar solvents.[13, 14] In addition, the very high steric bulk of the Cp^{ttt} could allow for the synthesis of non-solvated thulium complexes even by metathesis and the comparison of the results obtained by reduction and metathesis should lead to rapid conclusions on the feasibility of the project. Less bulky ligands, e.g. Cp^{tt}, Cp'' and Cp*, would next be considered as potential candidates once the reaction conditions for the reductive approach were established.

Among the phospholyl ligands which had previously allowed the stabilisation of divalent thulium complexes,[3-5] the Dtp ligand seemed to be most promising for the development of the reductive approach due to its steric bulk. It offers the supplementary practical advantage that the data already obtained for the solvent-free divalent complex, $[(Dtp)_2Tm]$, could be compared with crude reaction data and therefore provide a rapid check upon the viability of the reduction attempts. The other ligands, Dsp, Htp and Hsp, would be considered at a later stage of the development.

In order to test the Cp^{ttt}, Cp''' and Dtp ligands in the reductive approach, and to get an idea on the possible problems that could be encountered, we started our investigations with the classical, more stable organosamarium compounds. For the Cp^{ttt} and Dtp ligand the existing data on the corresponding divalent samarium complexes, $[(Cp^{ttt})_2Sm]$[17] and $[\{(Dtp)_2Sm\}_2]$[4], provided a good basis for the rapid development of this synthetic route. After this "honing period" we then moved on to unknown territory introducing the reductive pathway to divalent thulium, dysprosium and neodymium chemistry.

2 Development of the reductive approach using samarium chemistry

Although some reports on the reduction of trivalent organosamarium precursors by alkali metals exist in the literature,[20-23] most divalent organosamarium complexes have been obtained by the salt metathesis reaction between SmI_2 and the alkali-metal ligands.[4, 17, 24-27] In both approaches, the reactions were carried out in THF or DME, which give rise to the corresponding adducts of the divalent compounds. Because our aim was to develop a new synthetic pathway avoiding polar solvents, new trivalent precursors based on the above mentioned ligands were necessary. The following compounds were considered for synthesis and testing in reduction:

a) For Cp^{ttt} and Cp''': These bulky Cp ligands were not expected to allow the synthesis of $[(Cp)_3Ln]$ type complexes, in contrast to the lesser substituted Cp^{tt}, Cp'' and Cp* ligands.[1, 28-33] The target molecules were therefore defined as $[(Cp^{ttt})_2SmI]$ and $[(Cp''')_2SmI]$, which should be accessible from simple salt metathesis reactions.

b) For Dtp: The lone pair on the phosphorus atom of the ligand should provide the possibility of η^1-coordination to samarium as reported in the literature[4, 34, 35] and therefore the synthesis of $[(Dtp)_3Sm]$ was envisaged. In addition, $[(Dtp)_2SmI]$ also appeared to be an alternative precursor.

2.1 Attempted preparation of a tris(phospholyl)samarium(III) precursor

In the cyclopentadienyl series a number of $[(Cp)_3Ln]$ complexes have been synthesized.[1] These even include sterically demanding Cp* ligand, with this special case leading to the discovery of the "sterically induced reduction chemistry".[36] In contrast, tris(phospholyl)lanthanide complexes remain very rare. To date only one crystallographically characterized compound of the type $[(phospholyl)_3Sm]$ carrying the small 3,4-dimethylphospholyl ligand (Dmp) has been reported in the literature.[34] $[(Dmp)_3Sm]$ was obtained by the reaction between anhydrous $SmCl_3$ and [K(Dmp)] in refluxing toluene. It forms a dimeric structure with one phospholyl being η^5,η^1 bound to the two Sm centers (Figure 3). For the larger 2,3,4,5-tetramethylphospholyl ligand (Tmp), the third chloride ion could not be replaced and a complex including coordinated KCl resulted.[34]

Further examples of the possibility of η^1-coordination of the phosphorus lone pair to the lanthanide center have been demonstrated in the oxidation of the divalent organosamarium complex $[(Cp^*)_2Sm]$ with biphosphole Tmp-Tmp or thallium phospholide (Figure 3).[35] In contrast, changing the substitution pattern of the biphosphole from Tmp to Htp led to the η^5-coordination of the phospholyl ligand. Additionally, a tris(triphospholyl)scandium complex showing η^2-coordination of two phosphorus atoms to Sc has been described by Cloke and coworkers (Figure 3).[16]

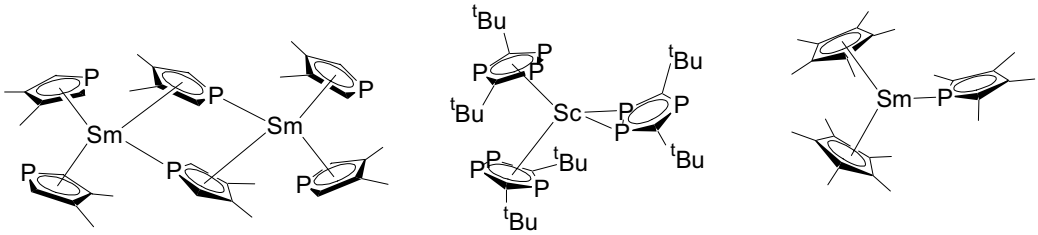

Figure 3. (Phospholyl)$_3$Ln complexes and η^1-coordination of the phosphorus lone pair to Sm.

As it therefore seemed problematical to access [(phospholyl)$_3$Ln] complexes having bulky ligands by salt metathesis another approach was investigated. Evans reported the oxidation of [(Cp*)$_2$Sm] with [(Cp*)$_2$Pb] to obtain the highly reactive [(Cp*)$_3$Sm].[37] Hence, we attempted the synthesis of [(Dtp)$_3$Sm] by oxidation of [(Dtp)$_2$Sm] with [(Dtp)$_2$Pb]. The new bis(phospholyl)plumbocene [(Dtp)$_2$Pb] (**1**) was synthesized from $PbCl_2$ and [K(Dtp)] in the presence of LiCl in THF (Scheme 5). Without LiCl, no reaction took place, even at higher temperatures. **1** was characterized by multinuclear NMR spectroscopy and X-ray studies (Figure 4).

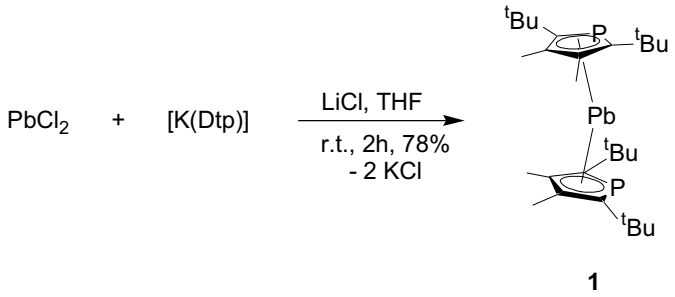

Scheme 5. Synthesis of [(Dtp)$_2$Pb] (**1**).

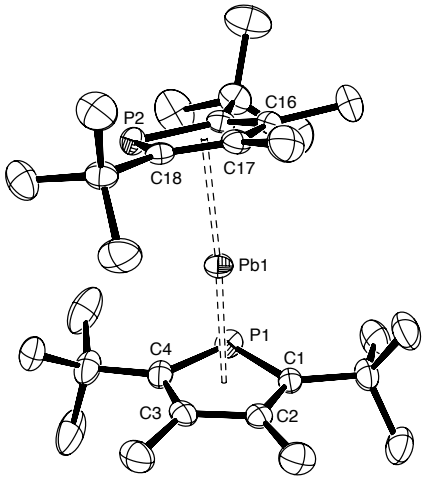

Figure 4. ORTEP-plot (50% probability ellipsoids) of one molecule of [(Dtp)$_2$Pb] (**1**). Hydrogen atoms were omitted for clarity. Selected bond distances (Å) and angles (°): Pb(1)-P(1) = 2.8422(6), Pb(1)-P(2) = 2.8413(6), P(2)-Pb(1)-P(1) = 122.70(2).

As in the similar [$(Htp)_2Pb$] complex[38] the phospholyl rings are staggered with the tBu groups adopting a least sterically demanding configuration. The interplane angle is slightly bigger for **1** than in [$(Htp)_2Pb$] (18.38° vs 17.24°) and the Pb-P bonds (2.84 Å vs 2.89 Å) are shorter.

Unfortunately, the reaction between [$(Dtp)_2Sm$] and **1** in ether or toluene at room temperature did not afford the new [$(Dtp)_3Sm$] complex but only the starting materials were recovered (Scheme 6). Elevated temperatures were then employed but again formation of the desired product was not observed. Instead, upon prolonged heating in toluene (90°C, 3h), formation of biphosphole (Dtp-Dtp) (^{31}P NMR: - 24 ppm) and precipitation of elemental lead was observed. Thus, **1** has similar stability to [$(Htp)_2Pb$], which decomposes at 80°C in benzene.[38]

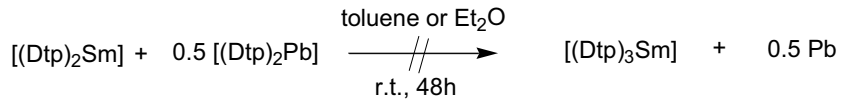

Scheme 6. Attempted synthesis of [$(Dtp)_3Sm$].

First, the inaccessibility of [$(Dtp)_3Sm$] by oxidation was thought to be a consequence of the steric bulk of the ligand which prevents the redox reaction between the two metal centers. However, further studies with the corresponding thulium complex, [$(Dtp)_2Tm$] (which we will discuss later), showed that the size was not responsible for this behaviour. It therefore seemed more likely to be a problem of reactivity. Phospholyl ligands are known to stabilize divalent compounds better than Cp ligands and therefore diminish their reactivity towards oxidizing agents.[4, 5] In addition, the low solubility of the [$(Dtp)_2Sm$] complex, which forms a dimer in the solid state and is only slightly soluble in toluene at room temperature,[4] may also contribute to the observed lack of reactivity.

2.2 Preparation of organosamarium(III) precursors carrying bulky cyclopentadienyl and phospholyl ligands

As the preparation of [tris(phospholyl)Ln] precursors had failed, we turned our interest towards the synthesis of trivalent precursors of the type [L_2SmI], which were accessible from the reaction of $SmI_3(THF)_{3.5}$ with 2 equivalents of an alkali metal salt of the ligand precursor [M-L] (M = Na, K and L = Cp^{ttt}, Cp''', Dtp) (Scheme 7).

In the case of Cp^{ttt} the unsolvated compound [$(Cp^{ttt})_2SmI$] (**2**), obtained after workup, was characterized by ^{1}H NMR. Very recently, Sitzmann reported the synthesis of **2** by oxidation of [$(Cp^{ttt})_2Sm$] with CuI and the same NMR shifts were observed.[39] Although no X-ray studies could be performed, the good solubility in non-polar solvents indicated that this compound was probably monomeric in solution, as were some similar cerium compounds.[18]

Three peaks with an integration of 1:1:1 were observed in the ^{1}H NMR spectrum and were attributed to the tBu groups of **2**. Similar observations had been made for [$(Cp^{ttt})_2$CeX] complexes with large substituents X, e.g. OTf and $CH_2C_6H_5$, which may imply that free rotation around the metal is restricted and the tBu groups become non-equivalent. In contrast for small X, e.g. H or F, or upon heating the complexes with large X, 2 peaks with integration 2:1 were reported.[18] No observable interaction between **2** and THF could be detected, as the peaks did not shift when the spectrum was recorded in THF-d_8. This indicates the steric shielding of the metal by the bulky tBu groups of the ligand.

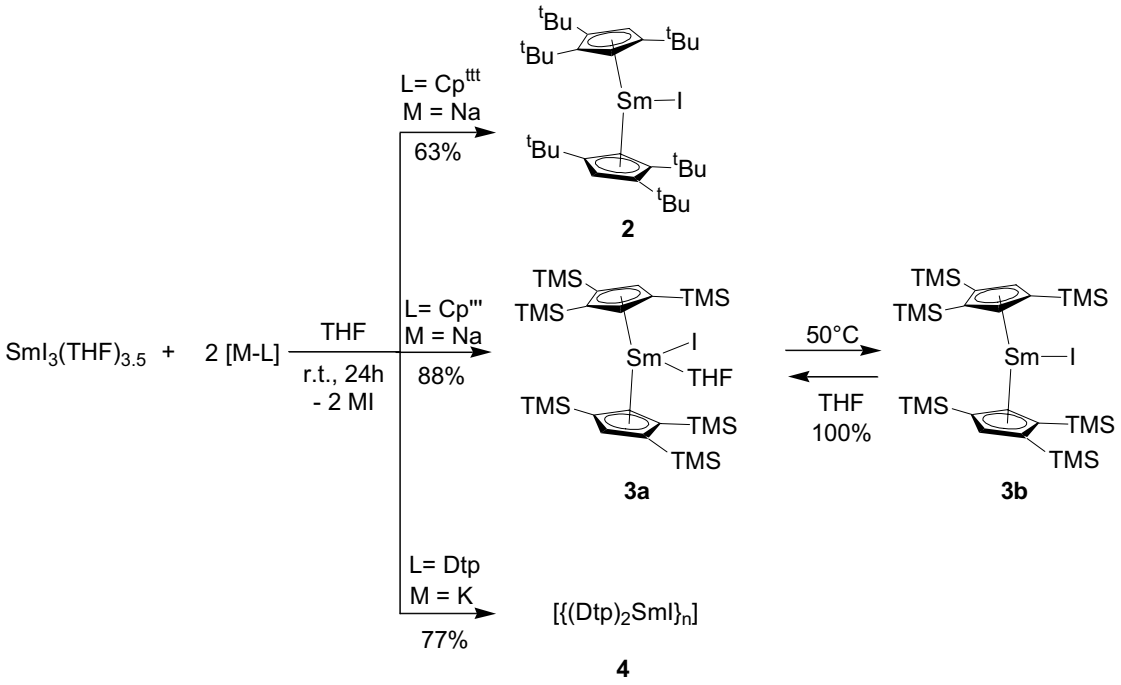

Scheme 7. Synthesis of trivalent organosamarium precursors.

With the Cp''' ligand, we did not obtain a solvent-free complex. Instead, the THF adduct [$(Cp'''')_2$SmI(THF)] (**3a**) was isolated and characterized by NMR and X-ray studies. Similarly, a solvated La compound was reported as a pyridine adduct [$(Cp'''')_2$LaI(py)] in the literature.[40] **3a** confirms that the Cp''' ligand is sterically less hindered than the Cp^{ttt} ligand due to the more flexible TMS groups which exhibit longer C-Si bonds. In addition, the three TMS groups render the Cp ligand less π-donating whereas the three tBu groups in Cp^{ttt} increase the electron density of the ligand. Hence, the samarium center is more Lewis acidic in the case of Cp''' than in the case of Cp^{ttt}. Surprisingly, despite the presence of the iodide and the THF ligand, free rotation around the Sm remains possible, as indicated by the ^{1}H NMR spectrum: 2 peaks with a 2:1 integration are observed for the TMS groups.

The X-ray structure of **3a** shows that the TMS groups are staggered in a 2:1 fashion, i.e. the neighbouring TMS groups on one Cp ligand are intercalated with the single TMS group on the other Cp ligand and vice versa (Figure 5). The Sm-centroid distances are 2.45 Å and

the angle between the ligand planes is 49.0°. The Sm-I bond length (3.034 Å) is in the typical range of monomeric Sm compounds and slightly longer than in [(Cp'')$_2$SmI(THF)] (3.007 Å).[41] The Sm-O bond lengths are in the same range (Cp''': 2.434 Å vs. Cp'': 2.411 Å), indicating that the THF molecule is not tightly bound to the metal. As in the latter complex, THF could be removed in **3a** upon heating at 50°C for 2 hours, affording quantitatively the solvent-free compound [(Cp''')$_2$SmI] (**3b**) as a yellow powder. In the ^{1}H NMR spectrum a shift of the peaks for the TMS groups occurred. Addition of THF to this compound regenerated **3a**.

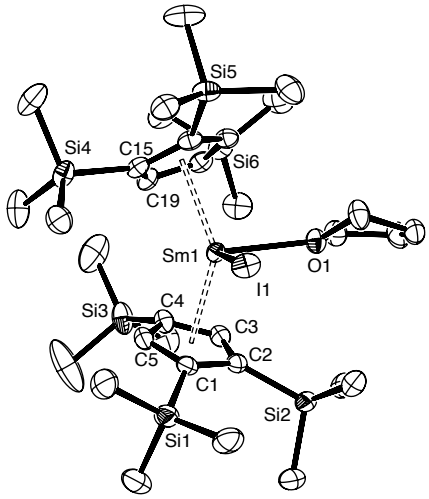

Figure 5. ORTEP-plot (50% probability ellipsoids) of one molecule of [(Cp''')$_2$SmI(THF)] (**3a**). Hydrogen atoms were omitted for clarity. Selected bond distances (Å) and angles (°): Sm(1)-O(1) = 2.434(1), Sm(1)-I(1) = 3.0343(2), O(1)-Sm(1)-I(1) = 88.83(4).

With the Dtp ligand, a non-solvated [{(Dtp)$_2$SmI}$_n$] (**4**) complex was isolated and characterized by NMR studies. The signal at 28 ppm in the ^{31}P NMR spectrum is close to the observed value for the [(Dtp)$_2$Sm(azobenzene)] complex (46 ppm).[4] Different ^{1}H NMR spectra in the presence and the absence of THF could be recorded, indicating that this ligand has properties between those of the Cp^{ttt} ligand (no visible interaction with THF) and the Cp''' (THF cannot be easily removed).

4 showed low solubility in toluene and was completely insoluble in aliphatic solvents which suggests that it may be dimeric in the solid state. Unfortunately no crystals suitable for X-ray studies could be isolated. However, we could show that **4** was not an ionic complex of the type [{K(THF)$_n$}{L$_2$SmI$_2$}] by using another synthetic pathway to access **4**: the oxidation of [(Dtp)$_2$Sm] with AgI in THF led to the immediate precipitation of metallic silver and the appearance of the signal at 28 ppm in the ^{31}P NMR spectra indicated the formation of **4**. No formation of biphosphole (Dtp-Dtp) from the oxidative coupling of two phospholyl ligands was observed.

2.3 Reduction of new organosamarium(III) precursors

Although classical divalent complexes are relatively stable to polar and aromatic solvents, the "new" divalent lanthanides were reported to react with both classes of solvents.[6, 42] The feasibility of the reduction in completely non-polar solvents was therefore explored. The commercially available perdeuterated cyclohexane seemed to be a suitable solvent as it allowed for the facile monitoring of the reduction process by ^{1}H NMR.

In contrast to the reported conditions by Cloke for the reduction of $[(P_3C_2{}^tBu_2)_3Sc]$ (toluene, 1eq. KC_8),[16] the reduction of **2** in C_6D_{12} required an excess of KC_8 (10 eq.) to go to completion at room temperature (Scheme 8). A colour change from orange-red to violet became visible after several hours. The complete formation of $[(Cp^{ttt})_2Sm]$ (**5**) was observed after 24h as indicated by ^{1}H NMR. The signals for the divalent complex were in agreement with the values in the literature.[43]

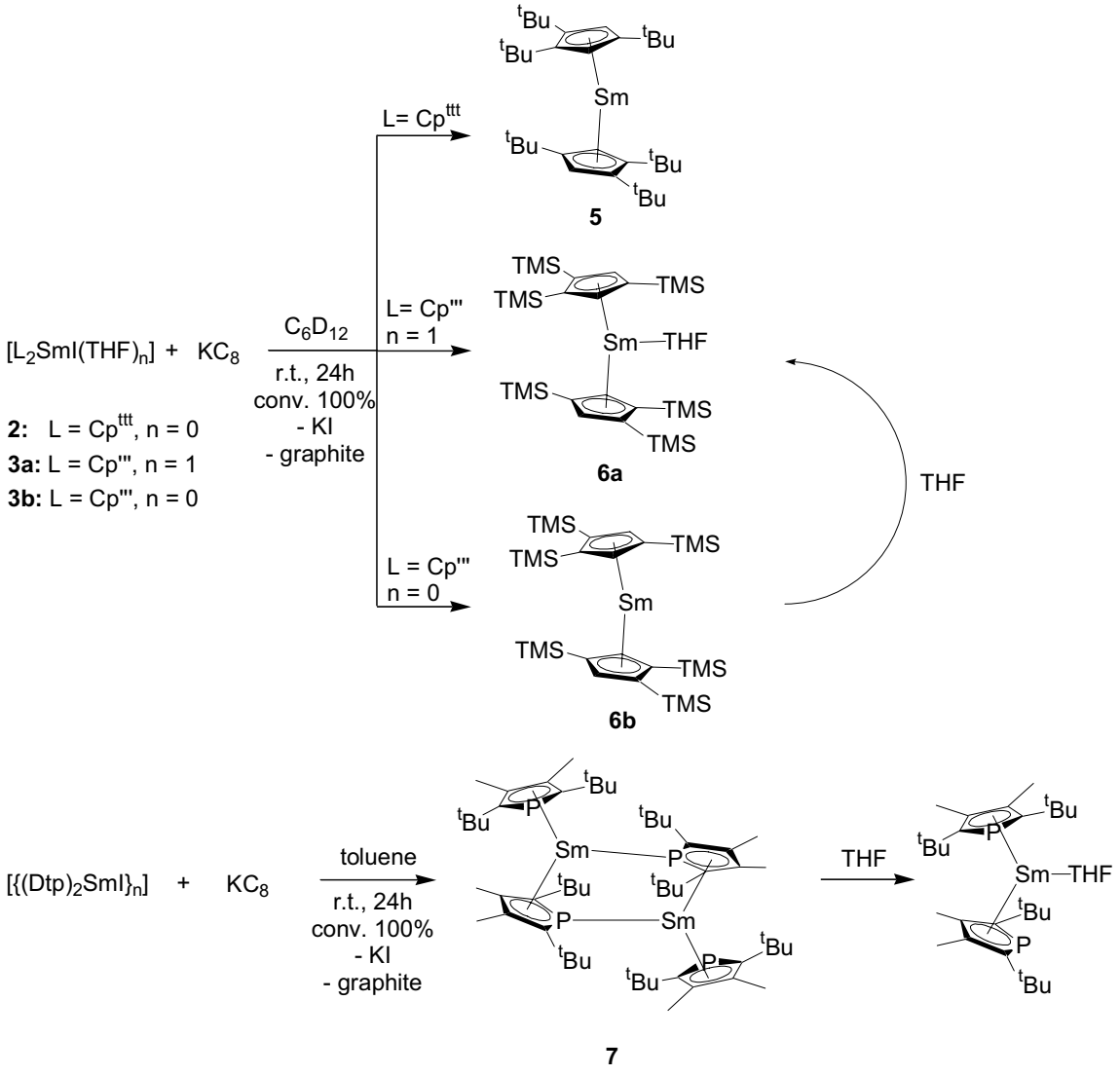

Scheme 8. Reduction of trivalent organosamarium precursors

Although **3a** did not fulfil our criterion of the absence of polar solvent molecules, we attempted its reduction in C_6D_{12} with KC_8 in order to check the suitability of the ligand in this approach and to obtain data on the new [(Cp''')$_2$Sm(THF)] (**6a**) compound. A colour change from orange to purple was observed after several minutes, indicating the divalent oxidation state of the product. Further confirmation was obtained from the ^{1}H NMR spectrum which showed similarities to the spectrum of [(Cp^{ttt})$_2$Sm(THF)], reported in the literature.[43] Evans reported on the attempted synthesis of compound **6a** by metathesis but obtained the mixed-ligand complex [(Cp''')(Cp'')Sm(THF)] instead, which exhibited a more complicated NMR spectrum.[25] The much faster reduction of **3a**, compared to **2**, may again be the result of the electronic properties of the Cp''' ligand. The less π-donating ability allows for a better stabilization of the additional electron density of the divalent compound.

In the same way the non-solvated **3b** was reduced to give the solvent-free violet [(Cp''')$_2$Sm] (**6b**) after several minutes. Addition of THF to this solution regenerated **6a**.

Despite the low solubility of **4** in toluene the reduction could be carried out in this solvent with the disappearance of the peak at 28 ppm. However, as the formed divalent compound [{(Dtp)$_2$Sm}$_2$] (**7**) is a dimer,[4] precipitation from the solution occurred rapidly. Addition of THF allowed re-dissolving the complex and a purple solution with a characteristic peak at -513 ppm in the ^{31}P NMR was observed.

2.4 Conclusion

These results show that it is possible to reduce trivalent organosamarium precursors in non-polar solvents to obtain neutral divalent complexes. This synthetic route has allowed the preparation of the new divalent complexes [(Cp''')$_2$Sm(THF)] (**6a**) and [(Cp''')$_2$Sm] (**6b**). However, these first tests already indicated that care had to be taken in the choice of the ligand and the preparation of the trivalent precursors in order to retain their solubility and to exclude solvent molecules.

3 Accessing divalent organothulium compounds by metathesis and reductive approach

The successful exploration of the reductive approach in divalent organosamarium chemistry encouraged us to extend this synthetic route to organothulium chemistry, in the hope of obtaining new unsolvated divalent complexes. As the size of the lanthanide ion plays a crucial role in its behaviour, some important adaptations had to be made when transferring the chemistry from samarium to the smaller thulium. The bulky ligands were again to be tested first: whereas the Dtp containing divalent complex [$(Dtp)_2Tm$] had already been characterized,[4] no data existed for divalent complexes carrying Cp^{ttt} and Cp''' ligands. In a first step, we tried to obtain some information on these compounds by using the metathesis approach before further investigating the chemical reduction pathway. These studies were then completed by testing the influence of other ligands and different counterions in this approach. Finally, reactivity studies were carried out with several divalent organothulium complexes.

3.1 Synthesis of [$(Cp^{ttt})_2Tm$] and [$(Cp''')_2Tm(THF)$] by the metathesis reaction

The use of bulky Cp-ligands, e.g. Cp^{ttt}, Cp^{4i}, in the salt metathesis reaction of classical divalent organolanthanide complexes in THF had allowed for the isolation of solvent-free compounds, [$(Cp^{ttt})_2Sm$] and [$(Cp^{4i})_2Sm$].[17, 26] We therefore tried to expand the use of very bulky ligands, Cp^{ttt} and Cp''', to divalent thulium chemistry. Reaction of two equivalents of [$NaCp^{ttt}$] with $TmI_2(THF)_3$ in THF and usual workup led to the formation of a violet solid (Scheme 9). In contrast to the synthesis of other organothulium(II) complexes,[3-5, 8] the reaction did not proceed in diethyl ether.

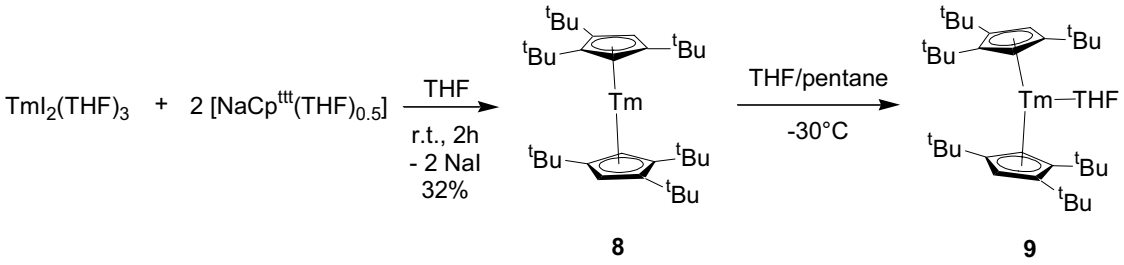

Scheme 9. Synthesis of [$(Cp^{ttt})_2Tm$] (**8**) and [$(Cp^{ttt})_2Tm(THF)$] (**9**) by metathesis reaction.

In the ^1H NMR spectrum two close and sharp signals for the tBu groups (32.5 and 22.2 ppm, 1:2 integration) and one broad signal for the Cp-H protons (-63.7 ppm) were observed. The absence of THF peaks was taken as evidence that the first solvent-free thulocene complex [$(Cp^{ttt})_2Tm$] (**8**) had formed. In order to verify this assumption many crystallisation attempts were carried out. However, due to the very high solubility of this compound in all solvents,

even pentane and hexane, and the quasi-spherical form of the molecule caused by the tBu groups of the ligand, no crystals suitable for X-ray studies could be obtained.

Another possibility to investigate the possible coordination of THF to Tm was to check the chemical shift variation of the tBu peaks in ^{1}H NMR upon addition of THF to a solution of the isolated compound **8** in C_6D_{12}. Sitzmann had shown that the addition of several equivalents of THF to [$(Cp^{ttt})_2$Sm] led to the formation of [$(Cp^{ttt})_2$Sm(THF)], which was demonstrated by the downfield shift of one peak of the tBu groups.[43] In contrast, [$(Cp^{ttt})_2$Yb] was reported not to show any interaction with THF.[43] Addition of one up to 120 equivalents of THF to **8** in C_6D_{12} led to a steady increase in the separation of the two tBu peaks, starting from 10 ppm (0-3 eq. THF) and increasing to 60 ppm (> 80 eq. THF). In addition, the appearance of THF signals in the typical diamagnetic area (1.7 and 3.7 ppm) was observed. This result showed that at room temperature THF interacted weakly with Tm.

This observation prompted us to try to crystallize the THF adduct and, in this case, dark violet crystals of [$(Cp^{ttt})_2$Tm(THF)] (**9**) could be obtained from a pentane/THF solution at -30°C (Figure 6). The long Tm-O bond (2.473(2) Å) clearly indicates the weak binding of the THF molecule (Table 1).

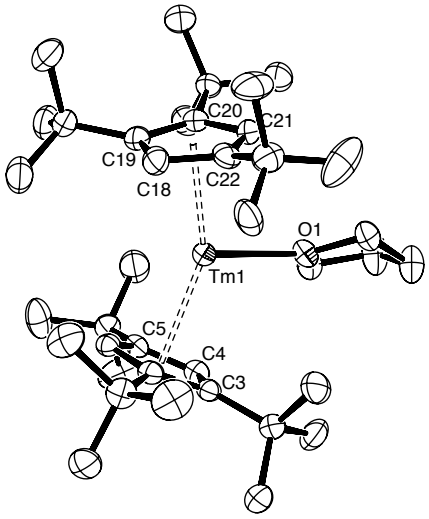

Figure 6. ORTEP-plot (50% probability ellipsoids) of one molecule of [$(Cp^{ttt})_2$Tm(THF)] (**9**). Hydrogen atoms were omitted for clarity. Selected bond distance (Å): Tm(1)-O(1) = 2.473(2).

Surprisingly, when the metathesis reaction was carried out in THF with KCp^{ttt} instead of $NaCp^{ttt}$, the formation of another product was observed as indicated by ^{1}H NMR, with peaks at 27.7 and 9.5 ppm, and an integration of 1:2. However, this product, which may be an anionic complex such as for instance [{K(THF)$_n$}{$(Cp^{ttt})_2$TmI}] because of its low solubility in aliphatic solvents, transformed cleanly into [$(Cp^{ttt})_2$Tm] after 48 h in C_6D_{12}.

As shown for the samarium complexes **2** and **3**, the Cp''' ligand is less bulky than the Cp^{ttt} ligand. It was therefore interesting to see if the solvent-free divalent complex $[(Cp''')_2Tm]$ could be obtained by a metathesis reaction between $TmI_2(THF)_3$ and [NaCp''']. Stirring this mixture in diethyl ether for 2 hours resulted in the formation of a violet product (Scheme 10). Again, no THF peaks could be detected in the ^1H NMR spectrum, but this time the peaks were broader and the chemical shift difference between the two signals attributed to the TMS groups were larger (53 ppm and 14 ppm) than in the case of **8** and resembled the NMR shifts observed for **9** (55 ppm and 20 ppm). This indication of the possible presence of THF was confirmed by X-ray studies of isolated crystals of $[(Cp''')_2Tm(THF)]$ (**10**) (Figure 7). The shorter Tm-O bond (2.457(2) Å) confirms the stronger interaction between the THF and Tm, which did not allow for the synthesis of the solvent-free complex by this route.

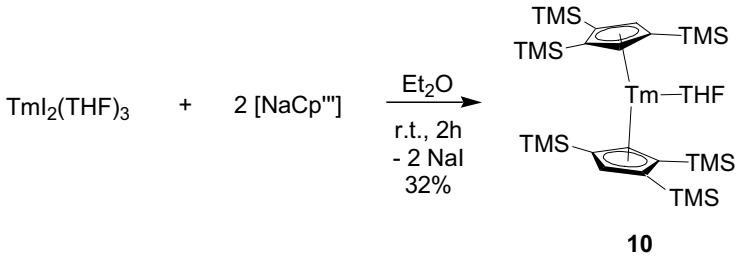

Scheme 10. Synthesis of $[(Cp''')_2Tm(THF)]$ (**10**) by metathesis reaction.

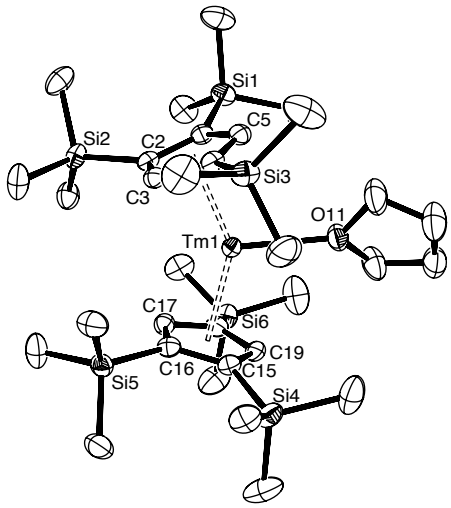

Figure 7. ORTEP-plot (50% probability ellipsoids) of one molecule of $[(Cp''')_2Tm(THF)]$ (**10**). Hydrogen atoms were omitted for clarity. Selected bond distance (Å): Tm(1)-O(1) = 2.457(2).

In both structures, **9** and **10**, the tBu or TMS groups are in a staggered 2:1 conformation. The interplane angle is smaller for **9** (32°) than for **10** (35°). The Tm-centroid distances are in the typical range of divalent organothulium compounds, slightly shorter for **10** (2.453 and 2.442 Å) than for **9** (2.464 and 2.479 Å). The steric difference between Cp^{ttt} and Cp''' may be

mainly due to the different mean bond lengths of the C(Cp)-C(tBu) and C(Cp)-Si(TMS) bonds (1.54 vs. 1.86 A), whereas the out-of-plane bending of the bulky groups is comparable in the two complexes, varying from 0° to 20°, with a mean value of 12° in both complexes. Table 1 gives an overview on selected bond distances and angles of all crystallographically characterized divalent organothulium complexes of the composition $[(\eta^5\text{-L})_2\text{Tm(THF)}]$.

Table 1. Comparison of structural parameters for divalent organothulium compounds

Complex	Tm-O (Å)	Tm-Ct (Å)	Ct-Tm-Ct (°)	Interplane angle (°)
$[(Cp'')_2Tm(THF)]$[8]	2.365(5)	2.39	135	47
$[(Cp^{tt})_2Tm(THF)]$[5]	2.388(7)	2.40	136	49
$[(Cp''')_2Tm(THF)]$ (10)	2.457(2)	2.45	144	35
$[(Cp^{ttt})_2Tm(THF)]$ (9)	2.473(2)	2.47	149	32
$[(Hsp)_2Tm(THF)]$[5]	2.398(3)	2.46	130	52
$[(Htp)_2Tm(THF)]$[5]	2.393(2)	2.45	135	49
$[(Dsas)_2Tm(THF)]$[3]	2.410(4)	2.48	146	34
$[(Dtp)_2Tm(THF)]$[3]	2.455(2)	2.53	145	34

3.2 Preparation of organothulium(III) precursors with bulky Cp ligands

The development of the reductive approach for divalent organothulium complexes required the synthesis of suitable trivalent precursors. As pointed out earlier, these complexes should be base-free, remain soluble in non-polar solvents and the steric bulk of the ligands should be sufficient to stabilize divalent species. We therefore chose the Cp^{ttt} ligand to start the investigation of this new approach as it had fulfilled the three criteria in the synthesis of $[(Cp^{ttt})_2SmI]$.

The synthesis of $[(Cp^{ttt})_2TmI]$ (**11**) turned out to be more complicated than expected. Using an approach analogous to the Sm case, from the reaction of $TmI_3(THF)_{3.5}$ and two equivalents of $[NaCp^{ttt}]$ or $[KCp^{ttt}]$ in THF only starting material was recovered. Elevated temperatures and the use of solvent mixtures, e.g. toluene/THF or toluene/pyridine, led to yellow polymeric products, which could not be identified. Finally, applying the reaction conditions that had led to $[(Dmp)_3Sm]$[34] and $[(P_3C_2{}^tBu_2)_3Sc]$[16], i.e. heating non-solvated TmI_3 and 2 equivalents of $[NaCp^{ttt}]$ or $[KCp^{ttt}]$ in refluxing toluene for several days, allowed the new complex **11** to be obtained in reasonable yields (Scheme 11). This compound was analyzed by X-ray studies which confirmed that this was the first monomeric, base-free, non-

chelating bis(cyclopentadienyl)thulium iodide complex (Figure 8). The tBu groups are staggered in a 2:1 fashion as already observed in the divalent compound **9**.

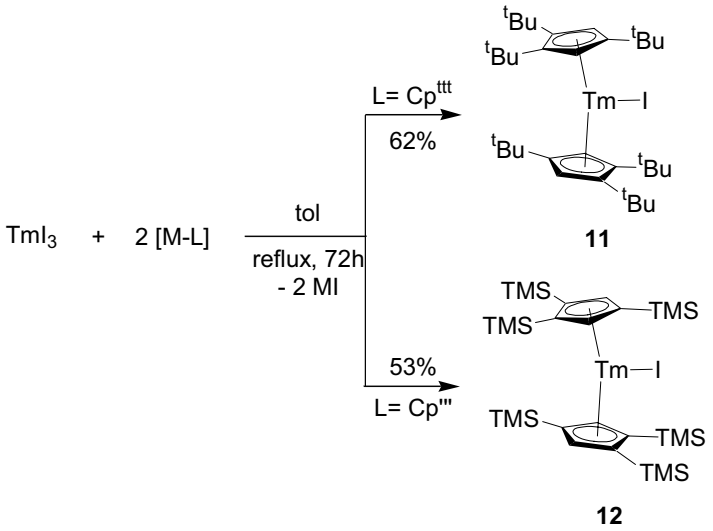

Scheme 11. Synthesis of $[(Cp^{ttt})_2TmI]$ (**11**) and $[(Cp''')_2TmI]$ (**12**).

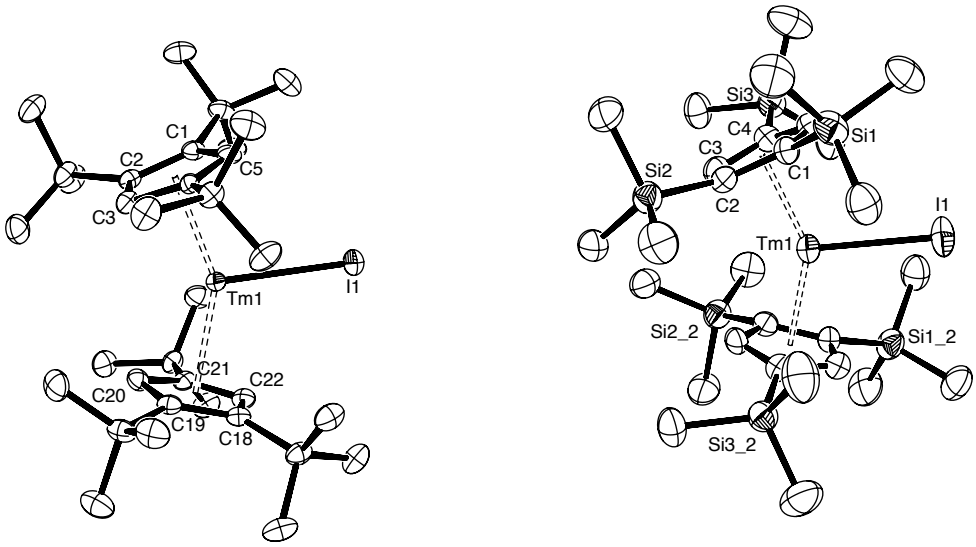

Figure 8. ORTEP-plot (50% probability ellipsoids) of one molecule of $[(Cp^{ttt})_2TmI]$ (**11**) (left) and one molecule of $[(Cp''')_2TmI]$ (**12**) (right). Hydrogen atoms were omitted for clarity. There are three independent molecules in the lattice of **12**; only one is represented here. Selected bond distances (Å): **11**: Tm(1)-I(1) = 2.8999(5); **12**: Tm(1)-I(1) = 2.8697(7).

The preparation of the trivalent precursor using the Cp''' ligand was carried out by analogy with the Cp^{ttt} ligand. In addition, this approach excluded possible THF coordination as had been observed in the case of **3a**. $[(Cp''')_2TmI]$ (**12**) could be obtained from the reaction of TmI_3 and [NaCp'''] or [KCp'''] in refluxing toluene (Scheme 11). X-ray analysis revealed again its monomeric structure (Figure 8). However, this time 3 molecules are in the unit cell,

one of which exhibits a similar staggering pattern (2:1) as **11**, whereas in the two other molecules the two neighbouring tBu groups of each Cp ring are intercalated (2:2 pattern). Table 2 gives an overview on the different bond distances and angles of the di- and trivalent complexes **9**, **10**, **11** and **12**. As expected the Tm-Ct distances are longer for the divalent complexes. The interplane angles are in the same range for the four complexes due to coordinated THF or iodide ligands, with a more open conformation for the Cp''' complexes. The Tm-iodide bond lengths are among the shortest reported so far, due to the monomeric form of the complexes. The recently reported [$(Cp^{4i})_2TmI$] has similar geometrical parameters.[39]

Table 2. Comparison of divalent and trivalent [$(Cp)_2TmX$] complexes (Cp = Cp^{ttt}, Cp''', Cp^{4i}; X = I, O(THF))

Complex	Tm-X (Å)	Tm-Ct (Å)	Ct-Tm-Ct (°)	Interplane angle (°)	Conformation
$(Cp^{ttt})_2TmI$ (11)	2.8999(5)	2.37	148	35	2:1
$(Cp''')_2TmI$ (12)	2.8697(7)	2.31	144	38	2:1
	2.8877(5)	2.30	139	41	2:2
	2.8977(6)	2.30	139	42	2:2
$(Cp^{4i})_2Tm^{III}I$[39]	2.8866(3)	2.33	144	39	--
$(Cp^{ttt})_2Tm(THF)$ (9)	2.473(2)	2.47	149	32	2:1
$(Cp''')_2Tm(THF)$ (10)	2.457(2)	2.45	144	35	2:1

3.3 NMR studies of organothulium(III) complexes with bulky Cp ligands

Whereas NMR data of paramagnetic divalent organothulium complexes (μ_{eff} = 4.5 μ_B) has been successfully utilized for the identification of these compounds, NMR data of highly paramagnetic organothulium(III) complexes (μ_{eff} = 7.0 μ_B) is often considered as inconclusive, due to the general assumption that with these complexes no interpretable NMR spectra can be obtained.

It was therefore surprising that the recorded ^1H NMR spectra of **11** and **12** showed the following signals: three large peaks of equal intensities at 350, 90 and -15 ppm were obtained in the spectrum of **11**, whereas two large peaks with integration 2:1 at 150 and 15 ppm were observed for **12**. The observed peaks were then related to the spectra obtained for the corresponding Sm compounds **2** and **3b**: a 1:1:1 pattern for the tBu groups in **2** and **11**, due to restricted rotation around the metal center, and a 2:1 pattern for the TMS groups in **3b** and **12**,

resulting from free rotation, were proposed. In order to explain these observations, we will give a short survey on the theory of paramagnetic NMR spectroscopy.[44, 45]

In general, NMR spectroscopy with lanthanide complexes (except those of Gd^{III} and Eu^{II}) is possible because of a usable combination of two magnetic properties: anisotropy of the magnetic susceptibility and electron spin relaxation. Whereas the first one causes the so-called paramagnetic chemical shift, the latter one is a determining factor for the peak width and hence the observation of a signal. Due to these properties, the development of lanthanide shift reagents in organic chemistry became possible.

The large chemical shifts observed in NMR spectra of paramagnetic lanthanide complexes arise from hyperfine coupling between the nuclei of the ligand and the electron spin of the metal. There are two major independent mechanisms for this hyperfine interaction: (i) the contact interaction which results from a finite probability of finding unpaired electronic spin density on an atomic s orbital and (ii) the dipolar interaction which takes place via space and causes shifts only if the magnetic susceptibility of the central ion is anisotropic, which is the case for all paramagnetic lanthanide ions except Gd^{3+} and Eu^{2+} (f^7) where no dipolar shift is observed as the magnetic susceptibility is averaged out. The net shift Δ_n in frequency units can be expressed as the sum of the two contributions, the contact shift Δ_c and the dipolar shift Δ_d.

$$\Delta_n = \Delta_c + \Delta_d \tag{1}$$

The contact shift can be expressed as

$$\Delta_c = A\langle S_z \rangle \tag{2}$$

with A is the hyperfine coupling constant (in frequency units) and $\langle S_z \rangle$ is the projection of the total electron spin magnetization of the lanthanide on the direction of the external magnetic field. In ^{1}H NMR, Δ_c is usually very small compared to Δ_d and can therefore be neglected.

The dipolar shift of an axially symmetric complex is conveniently expressed as

$$\Delta_d^i = DG_i = D[(3\cos^2\theta_i - 1)/r_i^3] \tag{3}$$

where G_i is the geometrical function specific for a given ligand nucleus, i, defined by r (distance between the central ion and the ligand nucleus) and θ (angle between the vector **r** and the principal axis of symmetry of the complex). D is a temperature dependent factor characteristic of each lanthanide ion. In ^{1}H NMR, the shifts are dominated by dipolar contributions. When plotting the observed shifts of several isostructural complexes versus the

calculated *D* values a straight line can often be obtained. Deviations from the linear correlation are often due to the influence of other shift mechanisms.

As the *D*-value for Tm^{3+} is +53, peaks are mainly expected to be found in the far low-field area of the spectrum. This is confirmed in the spectra of **11** and **12**, with peaks at 350, 150, 90 and 15 ppm.

The observation of a peak in the ^1H NMR spectrum depends on the nuclear relaxation rate which is given for a rapidly tumbling complex by the following expression

$$1/T_1 \approx 1/T_2 = (20/15)(\gamma_N)^2(g_N)^2\beta^2 J(J+1)r^{-6}T_e \quad (4)$$

where T_e is the electron spin relaxation time, T_1 and T_2 are the longitudinal and transverse relaxation times, respectively, γ_N is the nuclear magnetogyric ratio, β the Bohr magneton and g_N the mean value of the anisotropic nuclear g-tensor. The line-width at half-height $w_{1/2}$ can be calculated from

$$w_{1/2} = (1/T_2)\,\pi^{-1}. \quad (5)$$

A closer look at the factors that determine T_2 is warranted here. As already mentioned, lanthanide complexes are suitable for NMR spectroscopy due to their short electron spin relaxation times T_e, which is in the order of 10^{-13} sec. In contrast, the high magnetic and orbital moments of several ions, which are reflected in the $J(J+1)$ values, e.g. 42 for Tm^{3+}, are not favorable. Another important contribution comes from the inverse sixth power dependence on the metal-proton distance. The possibility of observing ^1H signals thus appears considerably higher for bulky ligands with protons far away from the metal center.

In the case of **11** and **12**, the bulky Cp^{ttt} and Cp''' ligands lead to relatively long metal-proton distances which dominate over the unfavorable impact of the high magnetic moment of Tm^{3+}. This allows for relatively short relaxation times T_2 and makes the observation of the protons of the bulky tBu or TMS groups with $w_{1/2}$ = 2-3 kHz possible. In contrast, the ring-protons, much closer to the metal, could not be observed in these spectra.

Eq. 4 also explains why the divalent organothulium complexes **8** and **13** have finer peaks and more easily interpretable ^1H NMR spectra. The lower magnetic and orbital moments ($J(J+1) = 16$), as well as the slightly longer metal-proton distances lead to shorter relaxation times T_2 and therefore diminish the peak width. In addition to the bulky tBu or TMS groups, the ring protons can also be observed. The peak broadening observed for the THF adducts **9** and **10** is probably due to exchange processes which are independent of eq. 4.

3.4 Reduction of organothulium(III) precursors

The observation of ^{1}H NMR spectra for the trivalent complexes **11** and **12** allowed us to follow the reduction reaction step by step. The choice of solvent played an important role with regards to experimental time and the stability of the divalent complexes. The best results and the purest compounds were obtained when the reaction was carried out in aliphatic solvents, such as cyclohexane or pentane. However, in these solvents 10 equivalents KC_8 and 48 hours were necessary to get the reaction to completion (Scheme 12). On the other hand, using benzene or toluene allowed for a faster reaction in the case of **11** with some minor decomposition, but gave none of the desired product with **12**.

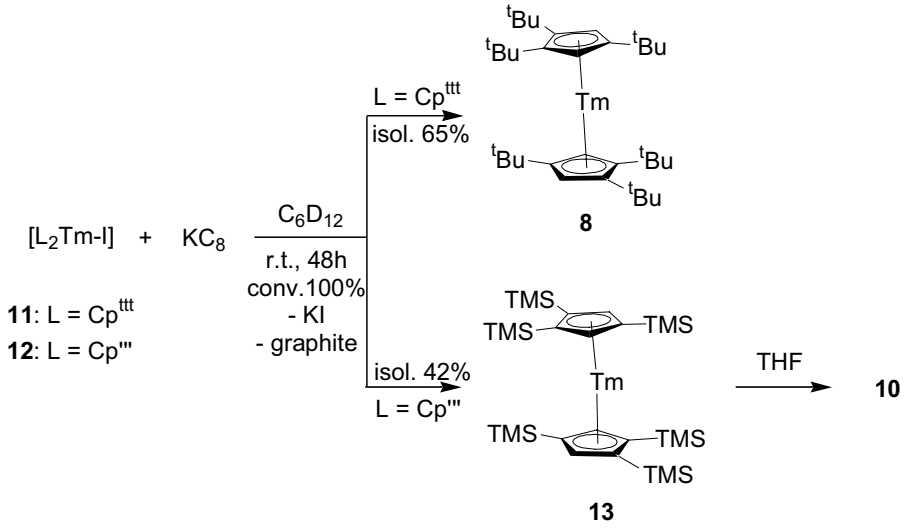

Scheme 12. Synthesis of solvent-free [$(Cp^{ttt})_2$Tm] (**8**) and [$(Cp''')_2$Tm] (**13**) by reduction

When the reduction of **11** was carried out in C_6D_{12} the slow disappearance of the three peaks belonging to the tBu groups was observed. The concomitant appearance of three new peaks and a colour change from yellow to purple indicated the successful reduction to **8**. The new signals showed the same NMR shifts as those observed for the product in the metathesis reaction and therefore confirmed that the solvent-free complex [$(Cp^{ttt})_2$Tm] could be obtained by both approaches.

The reduction of **12** under the same conditions led to a green solution and a different NMR spectrum compared to **10**, obtained from the metathesis reaction. As in the case of **8**, two sharp peaks for the TMS groups in a 2:1 integration and a broad peak attributed to the ring protons were observed. Unfortunately, this product also proved to be too soluble to form crystals suitable for X-ray studies. However, we could establish its identity by adding one equivalent THF to a solution of C_6D_{12}. A colour change to purple occurred immediately and an NMR spectrum identical to the one observed for **10** was recorded. We therefore concluded that the green product was the second base-free divalent thulocene complex [$(Cp''')_2$Tm] (**13**).

3.5 Use of other counterions

Although the successful reduction of trivalent precursors opened up the way to new divalent organothulium complexes, one major drawback was that it required the use of the expensive TmI_3 building block (5g/430 euros). We therefore envisaged the use of a cheaper precursor, $TmCl_3$ (5g/290 euros), which can even be obtained from the cheapest thulium source, Tm_2O_3 (5g/170 euros).

3.5.1 Precursor synthesis

The reaction between $TmCl_3$ and [$NaCp^{ttt}$] or [KCp^{ttt}] in refluxing toluene did not give any of the desired product, [$(Cp^{ttt})_2TmCl$] (Scheme 13). This observation was in agreement with reports on the attempted synthesis of the corresponding Yb and Lu complexes, which have similar ion size as thulium, and which only afforded mono-substituted products [$(Cp^{ttt})LnCl_2(THF)_2$], when the reaction was carried out in THF.[39]

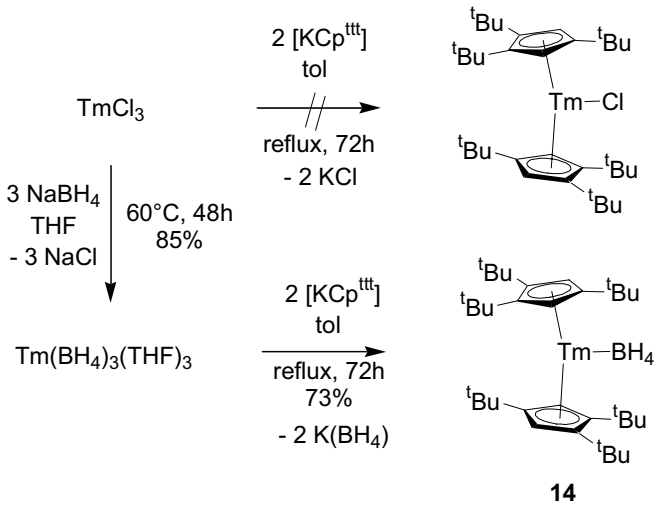

Scheme 13. Attempted synthesis of [$(Cp^{ttt})_2TmCl$] and the synthesis of [$(Cp^{ttt})_2Tm(BH)_4$] (**14**)

Another readily available precursor was the borohydride complex $Tm(BH_4)_3(THF)_3$ which resulted from the reaction of $TmCl_3$ with $NaBH_4$ in THF. In contrast to the chloride compound, the borohydride showed good solubility in toluene, which greatly favoured its reactivity. The reaction of two equivalents [KCp^{ttt}] with $Tm(BH_4)_3(THF)_3$ in refluxing toluene allowed for the isolation of [$(Cp^{ttt})_2Tm(BH_4)$] (**14**) in good yields (Scheme 13). Crystals of this first organothulium borohydride complex could be obtained from a pentane solution at -30°C. The X-ray structure shows that, despite the presence of small amounts of THF in the reaction mixture, **14** could be obtained as solvent-free monomeric complex (Figure 9). Its structural parameters are similar to those of the iodide **11**, with an interplane angle of 33° and Tm-centroid distances of 2.36 Å. The borohydride is only dihapto-bound to the Tm centre due

to steric hindrance. A similar binding mode was observed in the sterically crowded $[(Cp^{4i})_2Sm(BH_4)]$.[46]

14 remained soluble in non-polar solvents and its ^1H NMR spectrum showed three peaks for the tBu groups at 279, 107 and -26 ppm with $w_{1/2}$ = 2-3 kHz in analogy to **11**.

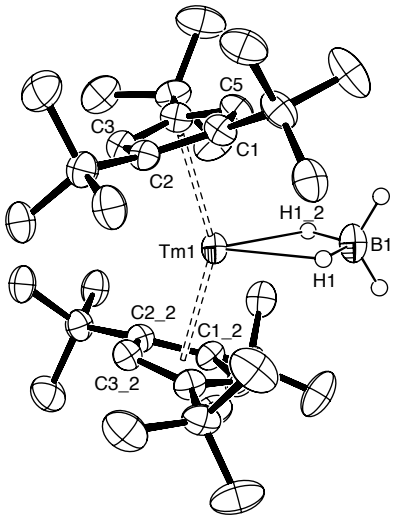

Figure 9. ORTEP-plot (50% probability ellipsoids) of one molecule of $[(Cp^{ttt})_2Tm(BH_4)]$ (**14**). Hydrogen atoms were omitted for clarity, except in the borohydride. Selected bond distances (Å): Tm(1)-B(1) = 2.631(5), Tm(1)-H(1) = 2.14(4).

3.5.2 Reduction of the borohydride precursor

The reduction of **14** under standard conditions, i.e. cyclohexane and KC_8, led to the quantitative conversion to the already described divalent complex **8** after 48h at room temperature as indicated by the colour change to purple and the ^1H NMR spectrum.

This possibility of accessing divalent organothulium complexes from a relatively cheap thulium precursor could make this chemistry more attractive for organic chemists and lead to a better exploitation of the unique reductive properties of thulium(II). Furthermore, the borohydride complexes will play an important role in the synthesis of mono-cyclopentadienyl and mixed ligand complexes which will be discussed later.

3.6 Use of less bulky ligands

Having established the reaction conditions for the reduction of trivalent precursors carrying bulky Cp ligands, the next challenge was the application of this method to precursors with

less bulky ligands, e.g. Cp^{tt}, Cp'' and Cp*. This research was guided by the idea that the known divalent complexes $[(Cp'')_2Tm(THF)]$ and $[(Cp^{tt})_2Tm(THF)]$ may be more stable in a solvent-free form and their chemistry could be better investigated. Furthermore, it may also allow to access $[(Cp^*)_2Tm]$, which is supposed to be an even more reactive reducing agent than $[(Cp^*)_2Sm]$. Despite several synthetic attempts, $[(Cp^*)_2Tm]$ species were only observed intrinsically during the metathesis reaction of TmI_2 and [KCp*] or the reduction of $[(Cp^*)_2TmI(THF)]$ in DME but could not be isolated.[6, 14] In contrast, for Yb the stable, base-free complexes $[(Cp'')_2Yb]$[47], $[(Cp^{tt})_2Yb]$[48] and $[(Cp^*)_2Yb]$[48] could be synthesized by desolvating their diethyl ether adducts either by sublimation or by the toluene reflux method. However, as neither of these methods was suitable for the divalent thulium compounds, we investigated their syntheses using the reductive approach.

However, with the less bulky ligands, there is a potential difficulty: as the steric bulk around the metal decreases, the coordination number increases and unsolvated complexes of type $[(L)_2TmX]$ may no longer be monomeric, even in solution, which may result in strongly reduced solubility in non-polar solvents. This is why we excluded the Cp'' ligand, as two trivalent dimeric thulium complexes were already known: $[\{(Cp'')_2TmCl\}_2]$[14] and the related $[\{(Cp^{TT})_2TmI\}_2]$[13], which were reported to be insoluble in non-polar solvents.

3.6.1 Synthesis of trivalent precursors with less bulky Cp ligands

With the Cp^{tt} ligand, the trivalent precursor $[\{(Cp^{tt})_2TmI\}_2]$ (**15**) was obtained from the reaction of TmI_3 and $[KCp^{tt}]$ in refluxing toluene (Scheme 14). The resulting product remained soluble in non-polar solvents, although X-ray studies revealed its dimeric form in the solid state (Figure 10). The structure resembles closely the one for $[\{(Cp^{TT})_2TmI\}_2]$[13], with similar Tm-I bond lengths (3.044 Å for **15** versus 3.048 Å), equal Tm-centroid distances (2.35 Å) and more open conformation (133.6° for **15** vs. 131.5°). **15** is reasonably soluble in cyclohexane and the ^1H NMR in this solvent shows one single peak at 220 ppm which was attributed to the tBu groups. This may be because **15** is now monomeric in solution.

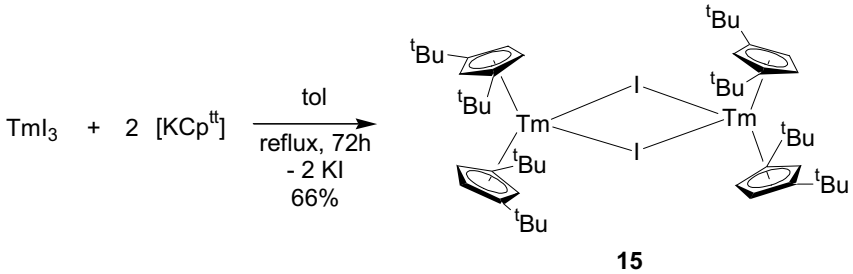

Scheme 14. Synthesis of $[\{(Cp^{tt})_2TmI\}_2]$ (**15**).

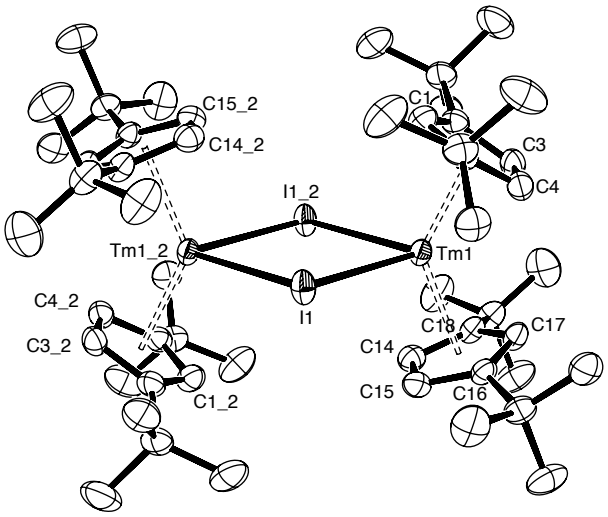

Figure 10. ORTEP-plot (50% probability ellipsoids) of one molecule of $[\{(Cp^{tt})_2TmI\}_2]$ (**15**). Hydrogen atoms were omitted for clarity. Selected bond distances (Å) and angles (°): Tm(1)-I(1) = 3.0424(4), Tm(1)-I(1_2) = 3.0459(4), I(1)-Tm(1)-I(1_2) = 81.46(1), Tm(1)-I(1)-Tm(1_2) = 98.54(1).

For Cp*, the precursor synthesis turned out to be less straight-forward. The reaction between TmI_3 and [KCp*] in refluxing toluene resulted in the formation of a mixture of $[\{(Cp^*)_2TmI\}_n]$ (**16**) and other non-identified products (Scheme 15). However, traces of THF in the glove box led to the immediate formation of $[(Cp^*)_2TmI(THF)]$ (**17**) as indicated by a shift in the ^1H NMR from +12 ppm to -10 ppm for the Cp* protons and the appearance of a peak at 90 ppm for the THF.

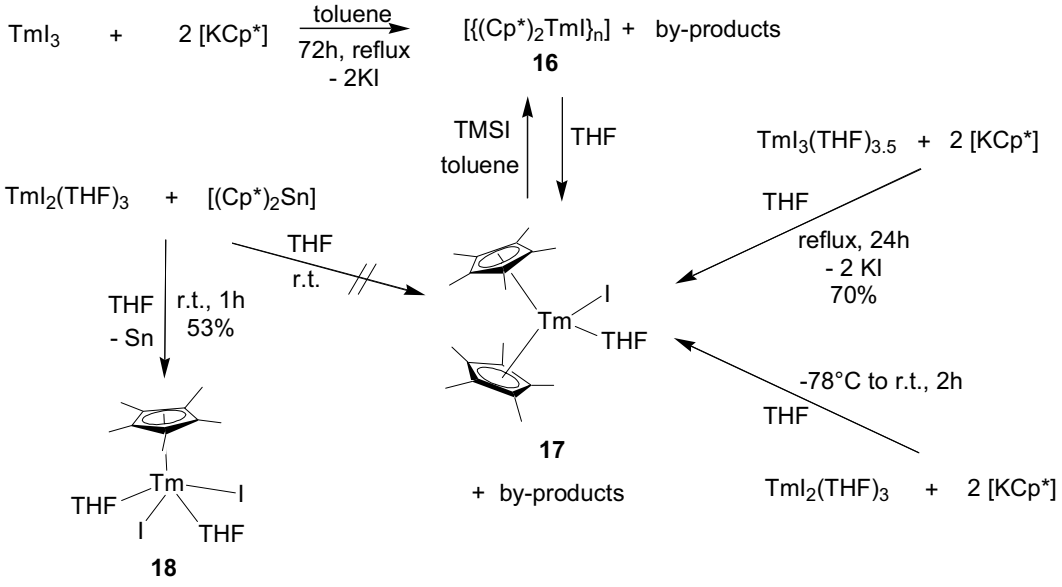

Scheme 15. Synthesis of $[(Cp^*)_2TmI(THF)]$ (**17**) and $[(Cp^*)TmI_2(THF)_2]$ (**18**).

17 could be analyzed by X-ray crystallography although the data were only good enough to show its composition (Figure 11). As it seemed difficult to obtain the pure solvent-free complex **16** directly from metathesis reaction, THF removal of **17** was envisaged as alternative route. Therefore several synthetic routes were explored, some according to literature reports,[14, 49] to access **17**, each time leading to different product mixtures (Scheme 15). The best result was obtained from the metathesis reaction of $TmI_3(THF)_{3.5}$ with [KCp*] in refluxing THF.

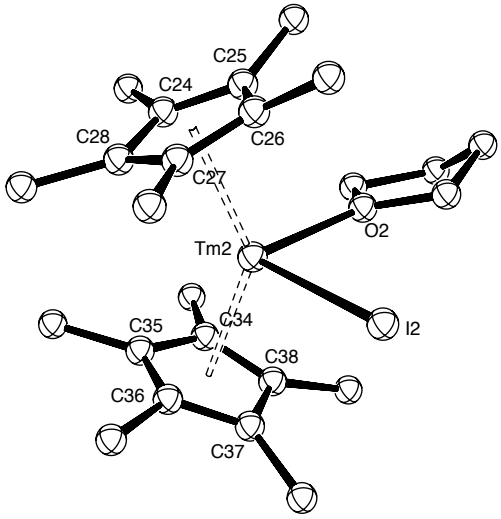

Figure 11. X-ray structure of $[(Cp^*)_2TmI(THF)]$ (**17**) as ball and stick model.

To our surprise, the reaction of $TmI_2(THF)_3$ with $[(Cp^*)_2Sn]$ gave only traces of the desired product **17** in contrast to the reported reaction of YbI_2 with $[(Cp^*)_2Sn]$, which afforded mainly $[(Cp^*)_2YbI]$.[50] Instead, the main product of this reaction was the monocyclopentadienyl product **18** which could be isolated and analyzed by X-ray studies (Figure 12). It crystallizes in a typical four-legged pianostool conformation with the two iodide and THF ligands trans to each other. In the ^1H NMR spectrum, **18** shows a peak at -5 ppm for the methyl protons and can therefore be nicely distinguished from **17.**

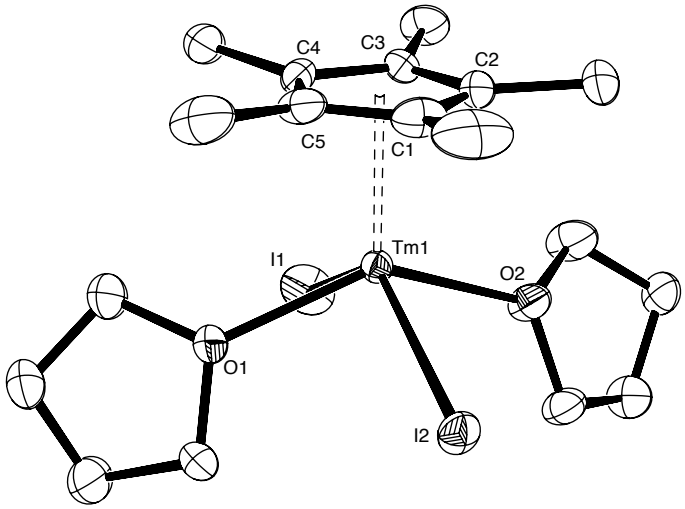

Figure 12. ORTEP-plot (50% probability ellipsoids) of one molecule of $[(Cp^*)TmI_2(THF)_2]$ (**18**). Hydrogen atoms were omitted for clarity. Selected bond distances (Å) and angles (°): Tm(1)-O(1) = 2.316(3), Tm(1)-O(2) = 2.317(3), Tm(1)-I(2) = 2.9576(4), Tm(1)-I(1) = 2.9884(4), O(2)-Tm(1)-I(1) = 80.11(8), O(1)-Tm(1)-I(1) = 79.53(7), I(2)-Tm(1)-I(1) = 132.45(1), O(1)-Tm(1)-O(2) = 139.7(1).

A possibility for the removal of THF from **17** under mild conditions was the use of iodotrimethylsilane (TMSI) according to a procedure described by Schaverien in the synthesis of $[(Cp^*)LaI_2]$ from $[(Cp^*)LaI_2(THF)_2]$.[51] Upon addition of TMSI to a solution of **17** in toluene-d8, a shift of the peak from -10 ppm to +12 ppm was observed, with the disappearance of the peak at 98 ppm. However, rapidly the formation of a yellow precipitate, presumably $[\{(Cp^*)_2TmI\}_n]$ (**16**), which could not be re-dissolved upon heating, was observed. Note that the Sm analogue forms a trimer $[\{(Cp^*)_2SmI\}_3]$ in the solid state.[31] Dissolving **16** in THF-d_8 gave very pure $[(Cp^*)_2TmI(THF\text{-}d_8)]$ (peak at -10ppm, no peak at 98 ppm). No solvent-free precursor suitable for the reductive approach could therefore be obtained for the Cp* ligand.

3.6.2. Attempted reduction of the trivalent precursor carrying the Cp^{tt} ligand

Addition of KC_8 to a cyclohexane solution of **15** led to the slow disappearance of the peak at 220 ppm, but instead of observing a change to an intense colour as expected for divalent species, the solution turned colourless. We therefore concluded that even in the absence of donor solvents, the divalent complex $[(Cp^{tt})_2Tm]$ was not stable at room temperature but underwent rapid evolution. In toluene the reduction occurred much faster but degradation was observed immediately.

3.7 Use of phospholyl ligands in the reductive approach

Phospholyl ligands have been shown to stabilize divalent organothulium complexes better than the corresponding Cp analogues.[3-5] This observation is attributed to the good π-accepting and poor π-donating properties of this type of ligand.[52] Having explored the reductive approach with a number of substituted Cp ligands we then wanted to know if this approach would also be suitable for the phospholyl ligands. The first target molecule was $[(Dtp)_2Tm]$ as it had already been synthesized as solvent-free compound by metathesis reaction.[4] We then envisaged the use of other ligands, such as Dsp and also the less bulky Htp, to generalize this synthetic route.

3.7.1 Preparation of trivalent precursors with phospholyl ligands

The synthesis of the trivalent precursors was carried out according to the well-established method for the Cp ligands. Reaction of TmI_3 with two equivalents potassium phospholide allowed the isolation of $[(Dtp)_2TmI]$ (**19**), $[\{(Dsp)_2TmI\}_n]$ (**20**) and $[\{(Htp)_2TmI\}_2]$ (**21**) in reasonable to good yields (Scheme 16).

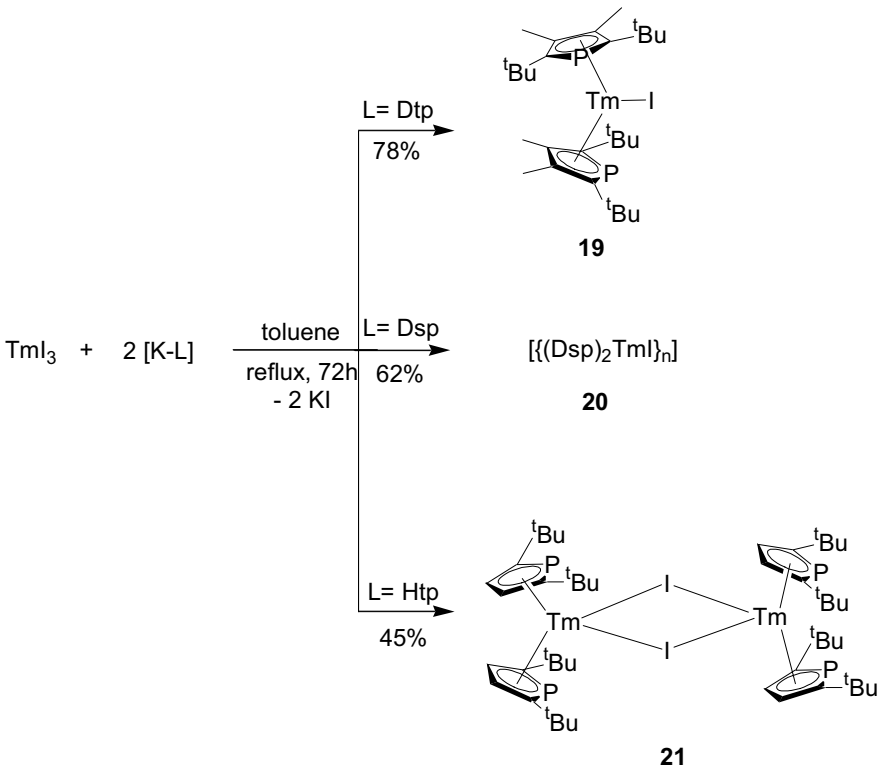

Scheme 16. Synthesis of $[(Dtp)_2TmI]$ (**19**), $[\{(Dsp)_2TmI\}_n]$ (**20**) and $[\{(Htp)_2TmI\}_2]$ (**21**).

For **19** and **21**, X-ray studies were carried out (Figure 13), but the crystals obtained for **20** were not suitable for X-ray analysis. The very bulky Dtp ligand gave the first monomeric bis(phospholyl)thulium iodide complex, with a very short Tm-I bond length of 2.8864(8) Å. The tBu groups are in a typical staggered conformation as already observed for **1**, with a P-

Tm-P angle of 94°. In contrast, the smaller Htp ligand led to the formation of a dimer in the solid state, in analogy to the Cp^{tt} ligand. However, the two compounds **15** and **21** did not crystallize in the same way. In **21**, the tBu groups are eclipsed with the phosphorus atoms pointing in the same direction. This leads to a large interplane angle on Tm2 (63°) whereas on Tm1 a small angle of 33° is measured. In contrast, in **15**, the carbon atom on the Cp ring between the tBu groups point in opposite directions which avoids direct overlap of the tBu groups, leading to an interplane angle of 51°. The mean Tm-I bond lengths in **15** and **21** are equal with 3.04 Å.

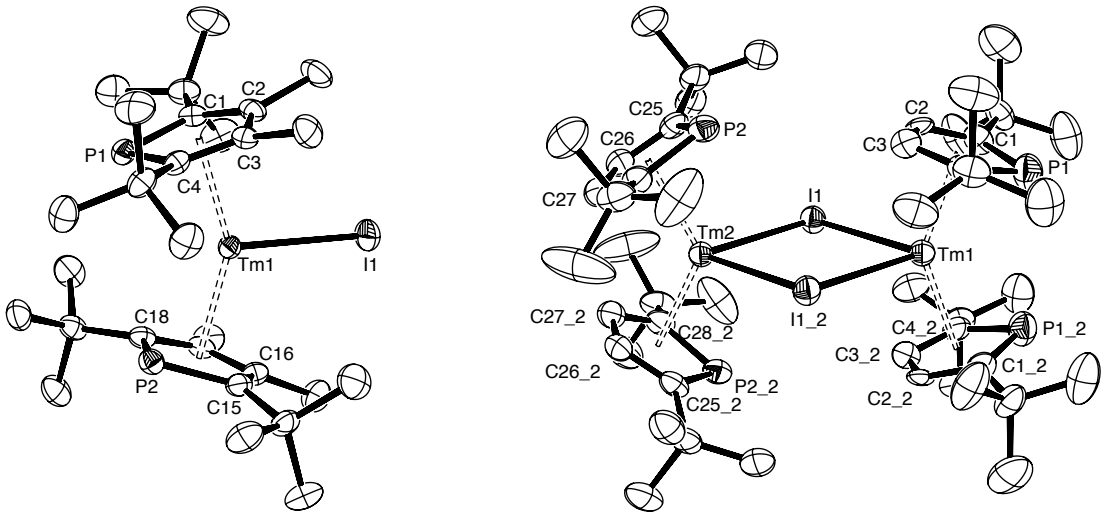

Figure 13. ORTEP-plot (50% probability ellipsoids) of one molecule of $[(Dtp)_2TmI]$ (**19**) and one molecule of $[\{(Htp)_2TmI\}_2]$ (**21**). Hydrogen atoms were omitted for clarity. Selected bond distances (Å) and angles (°): **19:** Tm(1)-P(1) = 2.812(1), Tm(1)-P(2) = 2.817(1), Tm(1)-I(1) = 2.8864(8), P(1)-Tm(1)-P(2) = 94.27(3); **21:** Tm(1)-P(1) = 2.906(2), Tm(1)-I(1) = 3.0612(4), Tm(2)-P(2) = 2.950(1), Tm(2)-I(1) = 3.0189(4), I(1_2)-Tm(1)-I(1) = 79.35(1), I(1)-Tm(2)-I(1_2) = 80.69(1), Tm(2)-I(1)-Tm(1) = 99.98(1).

In the ^{1}H NMR the three compounds were characterized by one broad single peak for the tBu or TMS groups, at 167 ppm for **19**, 135 ppm for **20** and 85 ppm for **21**, whereas the Me groups in **19** and **20** and the ring protons in **21** could not be observed. Again, although **21** is a solid-state dimer, it was reasonably soluble in aliphatic solvents.

3.7.2 Reduction of trivalent precursors with phospholyl ligands

The reduction of **19** and **21** under standard conditions led to the well known divalent $[(Dtp)_2Tm]$ (**22**), as indicated by ^{1}H and ^{31}P NMR measurements, and the new $[\{(Htp)_2Tm\}_2]$ (**23**), as shown by the colour change to green and a new ^{1}H NMR spectrum with peaks at 40

ppm for the tBu groups and at -26 ppm for the ring protons (Scheme 17). Addition of THF to a solution of **23** gave the already known ^{1}H and ^{31}P NMR spectra of $[(Htp)_2Tm(THF)]$.[5]

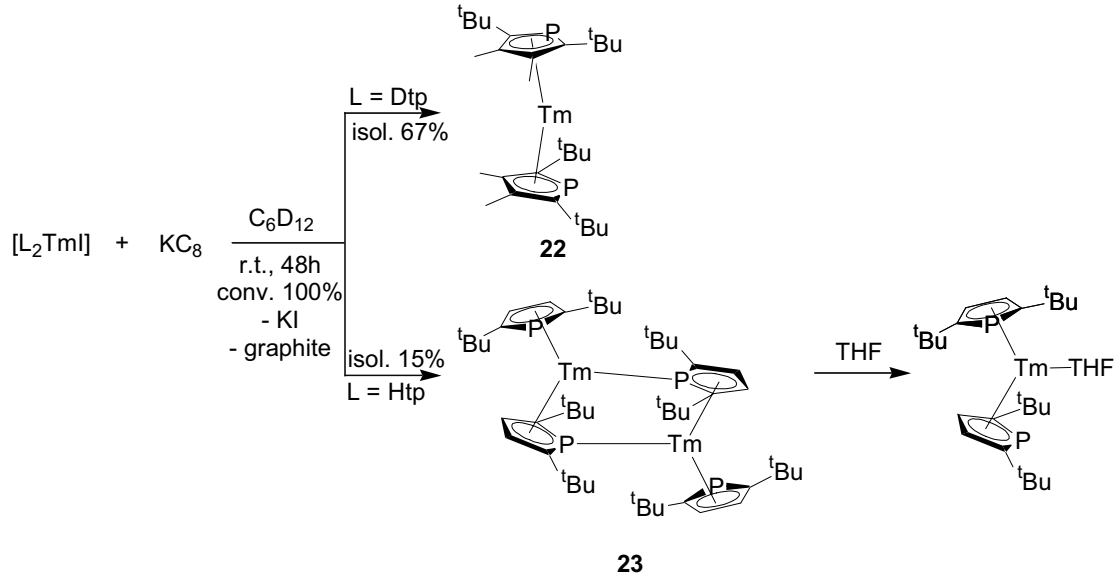

Scheme 17. Synthesis of $[(Dtp)_2Tm]$ (**22**) and $[\{(Htp)_2Tm\}_2]$ (**23**) by reduction.

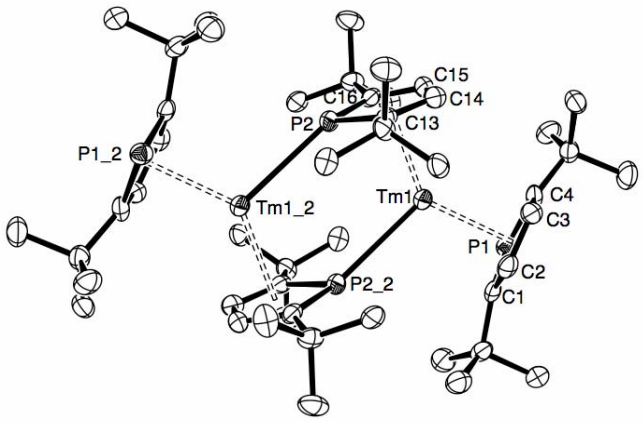

Figure 14. ORTEP-plot (50% probability ellipsoids) of one molecule of $[\{(Htp)_2Tm\}_2]$ (**23**). Hydrogen atoms were omitted for clarity. Selected bond distances (Å): Tm(1)-P(1) = 2.960(2), Tm(1)-P(2) = 3.014(2), Tm(1)-P(2_2) = 3.001(2).

X-ray studies allowed the identification of the new divalent compound **23**, which is only the second structurally characterized solvent-free complex (Figure 14). In the solid state, **23** forms a dimer via σ-π bonding of one phospholyl ligand to Tm. This structure resembles the previously described structure of $[(Dtp)_2Sm]_2$.[4] In both complexes, there is also an interaction between the metal and a methyl group belonging to one of the *t*-Bu groups α to phosphorus (Tm1-C18_2 = 3.20 Å in **23** *vs.* Sm1-C20_2 = 3.25 Å in $[(Dtp)_2Sm]_2$).

Reduction of **19** did not allow the isolation of the new solvent-free [$(Dsp)_2Tm$], but a large number of peaks in the 1H NMR spectrum indicated the degradation of the product. A plausible explanation was found in the rather labile C-Si bonds, which also caused problems in the synthesis of the alkali metal precursor [K(Dsp)].

3.8 Synthesis of mixed ligand complexes

So far only two divalent mixed Cp ligand complexes have been reported: the fortuitously synthesised compound [(Cp''')(Cp'')Sm(THF)][25] and the stepwise-prepared complex [$(C_{13}H_9)$(Cp*)Yb(DME)][53]. One major problem in the synthesis of these complexes is ligand redistribution which may occur in polar solvents. We therefore wanted to test if mixed-ligand complexes could be accessed by the reductive approach taking advantage of the non-polar reaction medium.

3.8.1 Preparation of trivalent mixed-ligand precursors

In order to access mixed ligand trivalent precursors, the first requirement was the synthesis of stable mono-Cp thulium complexes. With bulky ligands, the metathesis approach as demonstrated with $TmCl_3$ and [$NaCp^{4i}$][39] seemed to be favourable over the oxidation of TmI_2 as shown with Cp-H or [$(Cp^*)_2Sn$] (see section 3.6.1). As iodide precursors have been shown to be very suitable for the reduction process we started our investigations with the metathesis reaction between the bulky anionic Cp^{ttt} ligand and $TmI_3(THF)_{3.5}$. However, the high insolubility of the thulium precursor did not allow reaction to occur in THF at room temperature, even after stirring for several days, whereas heating the reaction led to a mixture of products.

As shown in section 3.5.2 the borohydride precursor **14** could be successfully reduced to a divalent compound. We therefore turned our interest towards the synthesis of mono-Cp thulium complexes starting from $Tm(BH_4)_3(THF)_3$. As already mentioned above, this precursor is soluble even in toluene. In Sm chemistry the use of borohydride precursors had allowed for the synthesis of mono-Cp complexes and several mixed ligand complexes.[46, 54] The reaction of $Tm(BH_4)_3(THF)_3$ with [KCp^{ttt}] in THF at room temperature led to the quantitative transformation to [$(Cp^{ttt})Tm(BH_4)_2(THF)_x$] (**24**) (Scheme 18).

In order to avoid ligand redistribution, as observed for [$(Cp^{ttt})YbCl_2(THF)_2$][39], **24** was then reacted with one equivalent of [K(Dtp)] or [KCp'''] in refluxing toluene, according to the usual preparation of trivalent bis(cyclopentadienyl)thulium complexes. Despite the presence of small amounts of THF, the solvent-free, monomeric products [(Cp^{ttt})(Dtp)$Tm(BH_4)$] (**25**) and [(Cp^{ttt})(Cp''')$Tm(BH_4)$] (**26**) were obtained in good yields and could be identified by ^{1}H NMR and X-ray analysis (Figure 15).

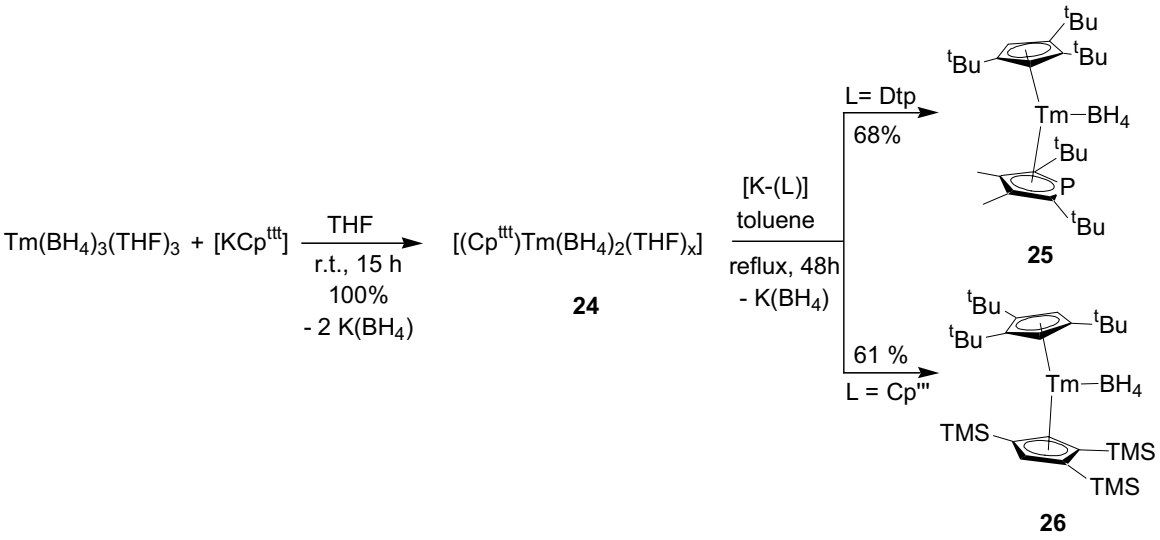

Scheme 18. Synthesis of mixed-ligand complexes [(Cp^{ttt})(Dtp)Tm(BH_4)] (**25**) and [(Cp^{ttt})(Cp''')Tm(BH_4)] (**26**).

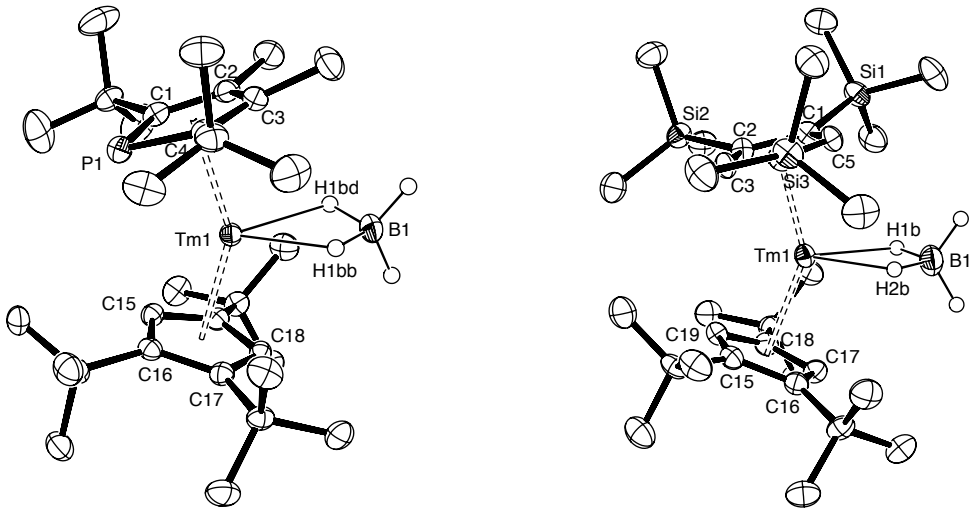

Figure 15. ORTEP-plot (50% probability ellipsoids) of one molecule of [(Cp^{ttt})(Dtp)Tm(BH_4)] (**25**) (left) and one molecule of [(Cp^{ttt})(Cp''')Tm(BH_4)] (**26**) (right). Hydrogen atoms were omitted for clarity, except in the borohydride. Selected bond distances (Å): **25:** Tm(1)-B(1) = 2.638(3), Tm(1)-P(1) = 2.8098(6), Tm(1)-H(1bb) = 2.12(2), Tm(1)-H(1bd) = 2.17(2); **26:** Tm(1)-B(1) = 2.653(4), Tm(1)-H(1b) = 2.12(3).

As in **14**, the borohydride is η^2-bound to Tm in **25** and **26** due to steric constraints. The tBu and TMS groups in **26** show a 2:1 staggering pattern as in **14**. Table 3 summarizes some structural parameters of **14**, **25** and **26**. The steric influence of the Cp''' ligand in **26** can be seen in the more open conformation.

Table 3. Comparison of structural parameters for $[(Cp^{ttt})_2Tm(BH_4)]$ (**14**), $[(Cp^{ttt})(Dtp)Tm(BH_4)]$ (**25**) and $[(Cp^{ttt})(Cp''')Tm(BH_4)]$ (**26**)

Complex	Tm-BH_4 (Å)	Tm-Ct (Å)	Ct-Tm-Ct (°)	Interplane angle (°)
$[(Cp^{ttt})_2Tm(BH_4)]$ (14)	2.631(5)	2.36	149	33
$[(Cp^{ttt})(Dtp)Tm(BH_4)]$ (25)	2.638(3)	2.40 (Dtp) 2.32 (Cp^{ttt})	148	33
$[(Cp^{ttt})(Cp''')Tm(BH_4)]$ (26)	2.653(4)	2.33 (Cp''') 2.33 (Cp^{ttt})	145	36

The ^{1}H NMR spectrum of **25** shows five peaks with equal intensities in the range from 285 ppm to -100 ppm which correspond to the tBu peaks of the Cp^{ttt} and Dtp ligand. In the ^{1}H NMR spectrum of **26** three peaks can be observed at 342, 93 and 24 ppm with an integration of 1:1:2. No definite attribution of these peaks to the tBu and TMS groups could be made.

3.8.2 Reduction of mixed ligand precursors

The attempted reduction of $[(Cp^{ttt})(Dtp)Tm(BH_4)]$ (**25**) in cyclohexane with KC_8 did not afford the new mixed ligand $[(Cp^{ttt})(Dtp)Tm]$. In the ^{1}H NMR spectrum the peaks disappeared very slowly over several days but no colour change occurred.

The reduction of **26** was slow compared to **12**, despite the presence of a Cp''' ligand. After 48h, the starting material had disappeared and the solution had changed to purple (Scheme 19). In the ^{1}H NMR four new peaks were obtained: two peaks at 28 ppm and 19 ppm with an integration of 2:1 for the freely rotating tBu and TMS groups, and two signals at -52 and -62 ppm for the ring protons. These peaks do not correspond to **8** or **13** and we therefore postulate that this newly formed compound can be formulated as the first divalent mixed-ligand organothulium complex $[(Cp^{ttt})(Cp''')Tm]$ (**27**). No crystals suitable for X-ray analysis have been obtained so far.

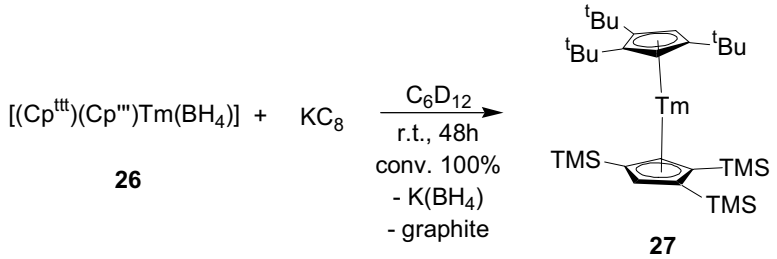

Scheme 19. Synthesis of the first divalent mixed-ligand complex $[(Cp^{ttt})(Cp''')Tm]$ (**27**).

3.9 Reactivity studies on divalent organothulium complexes

3.9.1 Dinitrogen activation

One of the most exciting discoveries in divalent organolanthanide chemistry was the activation of dinitrogen by the most reactive species.[55] We therefore investigated all new compounds towards their reactivity with dinitrogen.

The new divalent Cp complexes **8** and **13** did not show any obvious interaction with dinitrogen, i.e. no colour change, no change in the ^{1}H NMR spectra, in contrast to their analogues carrying the less bulky Cp^{tt} and Cp'' ligands.[5, 8] In the case of **8** this behaviour can be explained by the steric bulk of the ligand which reduces the space around the metal center and therefore the reactivity of the complex. Even THF, a very good donor ligand in lanthanide chemistry, shows only weak coordination towards the thulium centre, so it is not surprising that the much less donating dinitrogen does not interact with the metal. This observation even allowed for the synthesis of **8** under dinitrogen. In the case of **13**, steric considerations alone might permit interaction with dinitrogen. However, the three TMS groups also contribute to the stabilization of the divalent complex as they reduce the π-donating properties of the Cp ligand.

With divalent phospholyl complexes no activation of dinitrogen has been observed so far, and this may be viewed as proof of their higher stability compared to the corresponding Cp complexes. However, exposing a freshly prepared solution of the new solvent-free complex **23** in hexanes to dinitrogen at room temperature led to an immediate colour change, first to dark green and some seconds later to orange. Unfortunately, so far no crystals of the final product have been isolated. This surprising result – the THF analogue **23a** did not show any interaction with dinitrogen[5] – may be mainly explained by the absence of a strong donor ligand, and only partly by the structural parameters in the solid state , e.g. interplane angle (129° for **23** vs. 131° for **23a**) and metal-centroid distances (2.50 A for **23** vs. 2.45 A for **23a**).[5] In solution, **23** may even be monomeric with complete absence of a stabilizing σ-donor interaction.

3.9.2 Oxidation with I_2 and AgI

In order to establish a reduction/oxidation cycle for di- and trivalent thulium complexes, we explored the oxidation of the divalent complexes **8** and **13** with iodine and silver iodide.

Addition of iodine to **8** in THF led to an immediate colour change from violet to yellow. After workup **11** could be isolated in good yields. However, due to a slight excess of I_2, some [(Cp^{ttt})TmI_2(THF)] (**28**) was formed by oxidation of the ligand (Scheme 20).

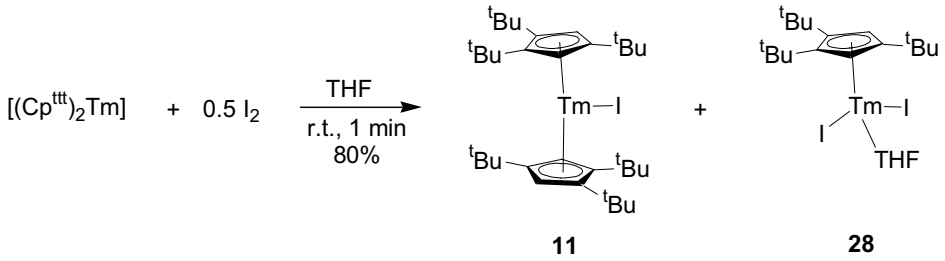

Scheme 20. Oxidation of $[(Cp^{ttt})_2Tm]$ (**8**) with I_2.

The new half-sandwich compound **28** was characterized by X-ray studies (Figure 16). It crystallized as monomeric, three-legged piano stool. The bulky Cp^{ttt} ligand allows only for the coordination of one THF molecule in contrast to the Cp*-analogue **18**. Recently, a similar complex $[(Cp^{ttt})YbCl_2(THF)_2]$[39] was reported which shows that with the less bulky chloride ligands two THF molecules can be bound to Tm.

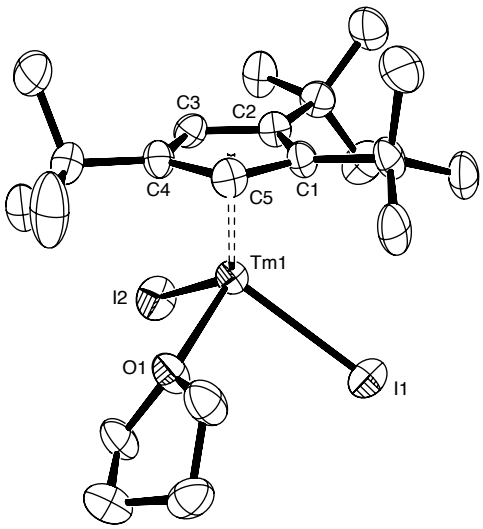

Figure 16. ORTEP-plot (50% probability ellipsoids) of one molecule of $[(Cp^{ttt})TmI_2(THF)]$ (**28**). Hydrogen atoms were omitted for clarity. Selected bond distances (Å) and angles (°): Tm(1)-I(1) = 2.8851(5), Tm(1)-I(2) = 2.8725(5), Tm(1)-O(1) = 2.258(4), I(2)-Tm(1)-I(1) = 102.69(1), O(1)-Tm(1)-I(2) = 101.7(1), O(1)-Tm(1)-I(1) = 89.7(1).

Table 4 gives an overview on the structural parameters of $[(\eta^5\text{-Cp})TmI_2]$ complexes. A clear trend in the Tm-I, Tm-O and Tm-centroid distance shortening can be observed when going from the unsubstituted Cp to the Cp^{ttt} ligand, which can be explained with the different coordination numbers on Tm resulting from the steric bulk of the ligands.

Table 4. Structural comparison of different [(η^5-Cp)TmI_2] complexes

Complex	Tm-I (Å)	Tm-Ct (Å)	Tm-O (Å)
[(Cp^{ttt})TmI_2(THF)] (28)	2.8725(5)	2.28	2.258(4)
	2.8851(5)		
[(Cp*)TmI_2($THF)_2$] (18)	2.9576(4)	2.31	2.316(3)
	2.9884(4)		2.317(3)
[{(Cp*)Tm($MeCN)_6$}I_2] [56]	--	2.31	--
[(Cp)TmI_2($THF)_3$] [57]	3.0655(11)	2.35	2.323(9)
	3.1072(11)		2.366(9)
			2.395(9)

In order to avoid over-oxidation, the more easily handled AgI was then used as the oxidizing agent. The reaction with **8** in THF led quantitatively to the non-solvated **11**, as shown by ^{1}H NMR. This was confirmed by reducing the obtained product with KC_8, which regenerated the divalent compound **8** (Scheme 21). In contrast, reaction of green **13** with AgI gave a compound formulated as the yellow THF-solvate [(Cp''')$_2$TmI(THF)] (**12a)**, the Tm analogue of **3a**, on the basis of its ^{1}H NMR spectrum. In contrast to the spectrum for the solvent-free **12**, only one large peak at 40 ppm remained, whereas the peak at 150 ppm was no longer observable due to the presence of THF. Consequently, the reduction of **12a** led to the purple THF-adduct **10**, as indicated by ^{1}H NMR, and not to the solvent-free complex **13** (Scheme 21).

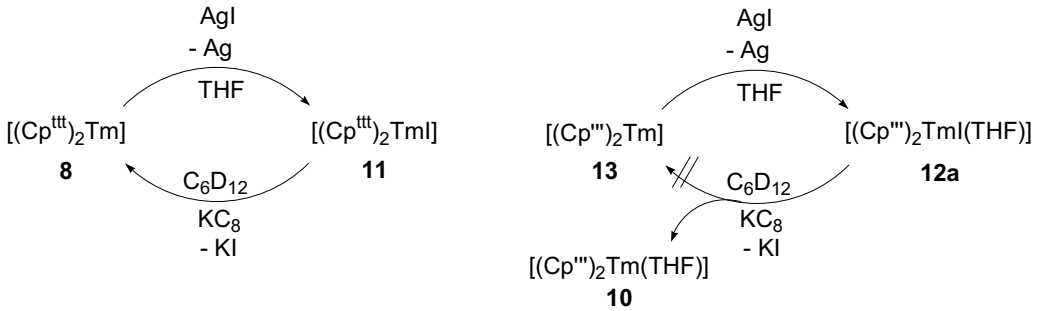

Scheme 21. Oxidation of [(Cp^{ttt})$_2$Tm] (**8**) and [(Cp''')$_2$Tm] (**13**) with AgI.

3.9.3 Oxidation with [(Dtp)$_2$Pb]

The oxidation of [(Dtp)$_2$Sm] with [(Dtp)$_2$Pb] (**1**) did not result in the formation of the trisphospholyl complex [(Dtp)$_3$Sm], as already described above. The corresponding Tm-complex **22**, seemed to be a good candidate for this reaction, despite its smaller cation size, as

it is monomeric in the solid state and therefore highly soluble, but also due its lower reduction potential.

Indeed, **22** reacted immediately with **1** as seen by the colour change from green to orange-red, the disappearance of the peak for the divalent compound with the concomitant appearance of a new, sharp peak at 63 ppm in the ^{31}P NMR spectrum and the precipitation of elemental lead from the solution (Scheme 22). In the ^{1}H NMR spectrum a new large peak at 114 ppm and two new peaks at 2.1 and 0.3 ppm in the diamagnetic area with integration 36:6:18 were observed. The resonances in the diamagnetic area and the observed ^{31}P signal at 63 ppm are similar to that found for the free Dtp anion. Treatment of this reaction mixture with KC_8 resulted in the shift of the peak at 63 ppm to 58 ppm in the ^{31}P spectrum, in accordance with the formation of [K(Dtp)], which disappeared slowly due to its precipitation from the benzene solution. In addition, the reappearance of the proton and ^{31}P resonances characteristic of **22** was observed.

A tentative explanation for these observations would be that **22** is oxidized by **1** into a tris(phospholyl)thulium complex which could be in the dissociated form [{(Dtp)$_2$Tm}{Dtp}], with one Dtp ligand acting as counterion, and thus giving rise to the observed diamagnetic peaks; this new compound, by reduction with KC8, would revert back to the divalent form with the concomitant precipitation of [KDtp]. However, further investigations, especially a crystal structure of the trivalent species, is necessary to confirm this hypothesis.

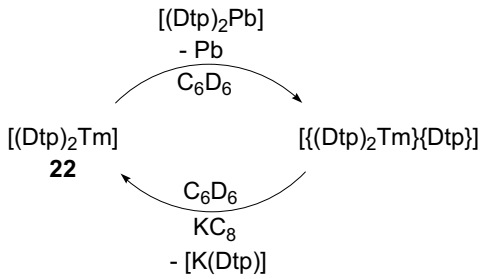

Scheme 22. A tentative scheme for the reaction of [(Dtp)$_2$Tm] (**22)** with [(Dtp)$_2$Pb] (**1**).

3.9.4 Reaction with Ph_3PS and Ph_3PO

In the case of **22** the reaction with Ph_3PS has been reported.[4] This reaction allowed the isolation of the dimeric, sulphide bridged compound [{(Dtp)$_2$Tm}$_2$(μ-S)]. We wished to see if the slightly more bulky Cp^{ttt} ligand would also allow for the formation of a dimeric species.

Addition of Ph_3PS to a solution of **8** led to the immediate formation of Ph_3P as shown by ^{31}P NMR, which was accompanied by a colour change to yellow. However, no crystals of the co-products could be obtained from the reaction mixture and the ^{1}H NMR spectrum was inconclusive.

In contrast, the reaction of Ph_3PO with **8** did not lead to the formation of Ph_3P, but a new signal in the ^{31}P NMR at -102 ppm appeared. So far, no X-ray studies have been performed on the resulting product, which may be a trivalent compound such as for instance $[(Cp^{ttt})_2Tm(OPPh_3)]$ resulting from one-electron reduction of the P=O bond. However, from these results it is clear that the reduction potential of **8** is not as high as that of $[(Cp^*)_3Sm]$, which was reported to reduce Ph_3PS and Ph_3PO readily to afford Ph_3P.[36]

3.9.5 Reaction with pyridine

Bochkarev and Schumann have recently reported the reductive dimerization of pyridine by thulium diiodide.[58] As already described above, phospholyl complexes of divalent Tm have shown higher stability in THF compared to their cyclopentadienyl analogues. The reaction with pyridine constituted therefore a useful test of the respective reducing powers of phospholyl and Cp complexes.

Reaction of **8** with pyridine resulted in an instantaneous color change from purple to orange and, as in Bochkarev's case, we were able to isolate crystals of a product containing the 1,1'-bis(1,4-dihydropyridylamide) ligand: $[\{(Cp^{ttt})_2Tm\}_2\{\mu\text{-}(NC_5H_5\text{-}C_5H_5N)\}]$ (**29**) (Scheme 23 and Figure 17).

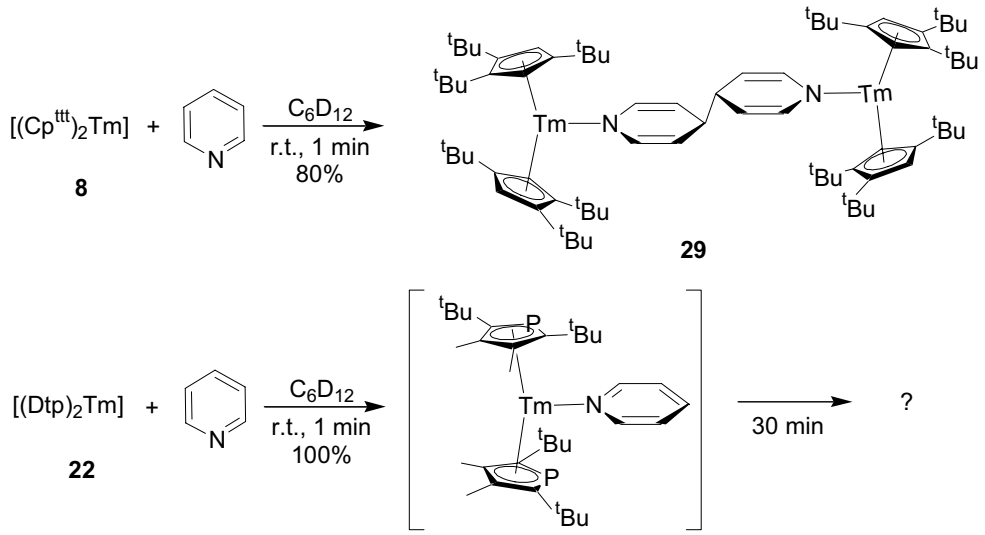

Scheme 23. Reaction of pyridine with **8** and **22**.

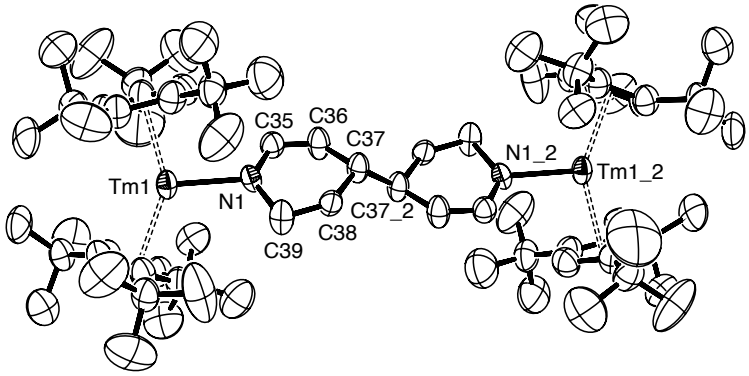

Figure 17. ORTEP Plot (50% ellipsoids) of one molecule of [{$(Cp^{ttt})_2Tm$}$_2${μ-(NC_5H_5-C_5H_5N)}] (**29**). Hydrogen atoms have been omitted for clarity; the bipyridine ligand is disordered over two positions; only one is presented in the figure. Selected bond distances (Å) and angles (°): Tm(1)-N(1) = 2.28(7), N(1)-C(35) = 1.43(8), N(1)-C(39) = 1.5(1), (35)-C(36) = 1.29(5), C(36)-C(37) = 1.49(3), C(37)-C(37_2) = 1.39(4), C(37)-C(38) = 1.50(3), C(38)-C(39) = 1.39(7).

However, when **22** was treated with pyridine, the reaction mixture turned deep red and we were unable to obtain any tractable material after workup (Scheme 23); we therefore decided to investigate the reaction between **22** and pyridine by NMR. Initially, the proton spectrum of an equimolecular mixture of **22** and pyridine displayed two peaks corresponding respectively to the tBu protons at 45 ppm and to the Me protons at -22 ppm; additionally, a broad signal at 3 ppm that was attributed to pyridine was observed. The chemical shift of the tBu and Me protons are similar to that found in $[(Dtp)_2Tm(THF)]$[3] (59 ppm and -23 ppm, respectively). The phosphorus spectrum of the **22**/pyridine mixture was found at -270 ppm, in the range of other solvated divalent Tm species such as $[(Dtp)_2Tm(THF)]$[3] (-338 ppm) or $[(Htp)_2Tm(THF)]$[5] (-290 ppm). However, after 5 min at room temperature, the proton spectrum began to degrade and after 30 min the tBu and Me protons could no longer be detected. On these bases, we postulate that the initial species present in the **22**/pyridine mixture was still a divalent Tm complex, most likely a simple adduct of **22** with pyridine such as $[(Dtp)_2Tm(pyridine)]$, that further decomposed at room temperature, presumably into unidentified Tm^{III} species.

The observed difference in reactivity towards pyridine between homoleptic divalent Tm complexes with cyclopentadienyl and phospholyl ligands confirms the higher stability and lower reactivity of the phospholylthulium(II) complexes than their Cp analogues. Since the Dtp and Cp^{ttt} ligands are sterically very similar, this difference is likely of electronic origin: in related uranium chemistry, it has been shown that phospholyl ligands are less electron-donating than cyclopentadienyl ligands of similar steric bulk.[52]

3.9.6 Reaction with nitrile

The reaction of LnI_2 (Ln = Tm, Dy) with acetonitrile was reported to afford a new bis(imino)amine ligand by reductive coupling of three acetonitrile molecules,[59] whereas in the reaction with benzonitrile a mixture of triazines, pyrazines and imidazoles was obtained after workup.[60] Evans very recently reported on the reaction of $[(Cp^*)_2Sm]$ with tBuCN leading to the formation of orange polymeric $[\{(Cp^*)_2Sm(CN)\}_n]$.[61] This latter reaction was interesting to study with our complexes, as the bulky ligands may prevent polymerization and allow for the isolation of new products.

However, addition of tBuCN to a solution of **8** led to a colour change to orange and the formation of a precipitate, possibly $[\{(Cp^{ttt})_2Tm(CN)\}_n]$, which has not been further characterized. The only compound which could be identified was the trivalent complex $[(Cp^{ttt})_2TmI(NCtBu)]$ (**30**), that resulted from some $[(Cp^{ttt})_2TmI]$ impurities in the starting material. The X-ray structure of **30** shows that, although no interaction between THF and **11** could be observed in ^{1}H NMR , a linear molecule could form an adduct with **11** (Figure 18).

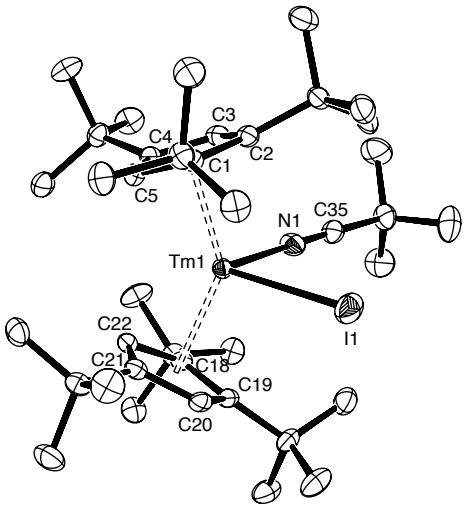

Figure 18. ORTEP Plot (50% ellipsoids) of one molecule of $[(Cp^{ttt})_2TmI(NCtBu)]$ (**30**). Hydrogen atoms have been omitted for clarity. Selected bond distances (Å) and angles (°): Tm(1)-N(1) = 2.394(3), Tm(1)-I(1) = 2.9754(6), N(1)-Tm(1)-I(1) = 88.91(8).

The binding of the nitrile leads to a much more open conformation compared to **11** (141° for **30** vs. 148° for **11**) with longer Tm-centroid distances (2.42 Å for **30** vs. 2.37 Å for **11**) and a longer Tm-I bond (2.9754(6) Å for **30** vs 2.8999(5) Å for **11**).

These geometric changes also influenced the ^{1}H NMR spectrum: the three peaks for the tBu groups in **11** disappeared and only two new broad peaks for the tBu groups in **30** with an integration of 2:1 formed at 55 and 24 ppm. In addition, a large peak in the diamagnetic area (3 ppm) which may be attributed to the protons of the nitrile, was observed, indicating a

dynamic behaviour as in the case of **8** with THF. By analogy to **12**, the possible free rotation of the ligands, may arise from the above-mentioned longer Tm-centroid distance (between divalent and trivalent complexes) and the more open conformation.

3.9.7 Further observations

The reactions of LnI_2 with azobenzene[4, 62-64] and ketones, mainly benzophenone and fluorenone,[58, 65, 66] have been widely studied. Although typical colour changes, indicative of the reduction process, were observed when reacting these substrates with complex **8** (green for azobenzene and violet for the ketones), no further characterization of the formed products was obtained. The high solubility of the complexes did not allow for the isolation of crystals suitable for X-ray studies.

3.10 Conclusion

The studies presented here show that there are now two distinct synthetic approaches to divalent organothulium complexes:

The metathesis approach, requiring the synthesis of TmI_2, can be used with several bulky Cp and phospholyl ligands but leads in most cases to THF-solvates which exhibit low to medium stability. The new divalent complexes $[(Cp^{ttt})_2Tm]$ (**8**), $[(Cp^{ttt})_2Tm(THF)]$ (**9**) and [(Cp''')Tm(THF)] (**10**) have been synthesized by this route. The isolation of **8** by metathesis reaction confirms that, with very bulky ligands, solvent-free complexes can be obtained, as already observed in the case of the Dtp ligand.

The reductive approach allows the synthesis of solvent-free divalent organothulium complexes which show very high stability. The divalent complexes $[(Cp^{ttt})_2Tm]$ (**8**), [(Cp''')Tm] (**13**), $[(Dtp)_2Tm]$ (**22**) and $[\{(Htp)_2Tm\}_2]$ (**23**) are obtained from the reduction of their iodide precursors $[(Cp^{ttt})_2TmI]$ (**11**), [(Cp''')TmI] (**12**), $[(Dtp)_2TmI]$ (**19**) and $[\{(Htp)_2TmI\}_2]$ (**21**) with KC_8 in cyclohexane. A general method for the synthesis of non-solvated precursors has been developed: reaction of TmI_3 with two equivalents alkali metal ligand in refluxing toluene for 72h leads to clean products after workup in moderate to good yields. Despite the high paramagnetism of Tm^{3+}, interpretable ^1H NMR spectra can be obtained for these complexes.

It has further been shown that the borohydride complex $Tm(BH_4)(THF)_3$ can be a cheap alternative to TmI_3: the solvent-free trivalent precursor $[(Cp^{ttt})_2Tm(BH_4)]$ (**14**) has been obtained in analogy to **11** and can be reduced to **8** under usual reaction conditions. The use of the borohydride precursor also gives access to the mixed-ligand trivalent complexes $[(Cp^{ttt})(Dtp)Tm(BH_4)]$ (**25**) and $[(Cp^{ttt})(Cp''')Tm(BH_4)]$ (**26**), of which only the latter one has

been successfully reduced to the first divalent mixed-ligand organothulium complex [(Cp^{ttt})(Cp''')Tm] (**27**).

For the less bulky Cp ligands, Cp^{tt}, Cp'' and Cp*, the reductive approach cannot be applied as either the precursors are not suitable due to insolubility in non-polar solvents (Cp'' and Cp*) or the reduction is too slow and follow-up reactions occur (Cp^{tt}). The TMS substituted phospholyl ligand, Dsp, is also not suitable for this approach as the ligand is destroyed during the reduction process.

Reactivity studies on the new divalent complexes have shown that THF coordination can influence the reactivity: the new solvent-free **23** reacts immediately with dinitrogen, whereas its THF-adduct is inert. Confirmation of the electronic influence of the phospholyl ligands on the stability of the divalent complexes has been obtained from the reaction of **8** and **22** with pyridine: whereas **8** is oxidized immediately, which has been confirmed by the isolation of the bis(pyridinyl) coupling product [{(Cp^{ttt})$_2$Tm}$_2${μ-(NC_5H_5-C_5H_5N)}] (**29**), **22** forms first a divalent pyridine adduct which slowly decomposes to give intractable products. Finally, oxidation of **22** with [(Dtp)$_2$Pb] has led to the first tris(phospholyl)thulium complex "[(Dtp)$_3$Tm]" in which one of the Dtp ligands may not be bound to the metal center.

4 Expanding the reductive approach to divalent organodysprosium chemistry

Although some examples on the use of DyI_2 in organic synthesis such as the coupling of alkyl halides to ketones[67] or the cyclotrimerization of terminal alkynes[68], have been reported, divalent organodysprosium chemistry has been mostly neglected, with chemists being more interested in divalent thulium (the least reactive) and neodymium (the most reactive and cheapest element of the triad): no attempt to reduce trivalent organodysprosium precursors has been reported and only Evans has briefly described the metathesis reaction between DyI_2 and [NaCp''].[8] When conducted under nitrogen atmosphere, this reaction led to a typical dinitrogen reduction product $[\{(Cp'')_2Dy\}_2(\mu\text{-}\eta^2\text{-}\eta^2\text{-}N_2)]$ and when conducted under argon, to a highly reactive species which could not be isolated. For the development of the reductive approach and for a better understanding of divalent organolanthanide chemistry, the exploration of divalent dysprosium complexes seemed indispensable to us. In comparison to thulium chemistry, it would allow for significant variation of one parameter, the lower redox potential (-2.56 V vs. -2.22 V) whilst retaining similar cation size (121 pm vs. 117 pm, CN = 6), whereas in the case of neodymium both influences, lower redox potential (-2.62 V) and much bigger cation size (143 pm, CN = 8), have to be considered.

4.1 Preparation of organodysprosium(III) precursors with bulky ligands

The successful use of the Cp^{ttt}, Cp''' and Dtp ligand in the reduction of organothulium precursors prompted us to investigate these three ligands in the synthesis of divalent organodysprosium complexes. The preparation of the trivalent organodysprosium precursors was carried out in an analogous fashion to the corresponding thulium compounds. As the Cp^{ttt} ligand was the most promising, due to the steric bulk of the tBu groups, trivalent precursors with different counterions were synthesized for this ligand. For purely structural investigations a trivalent Dsp-containing complex was also synthesized. Note that as seen in the previous chapter, the Dsp ligand cannot be used in the reductive approach due to the possible C-Si bond cleavage.

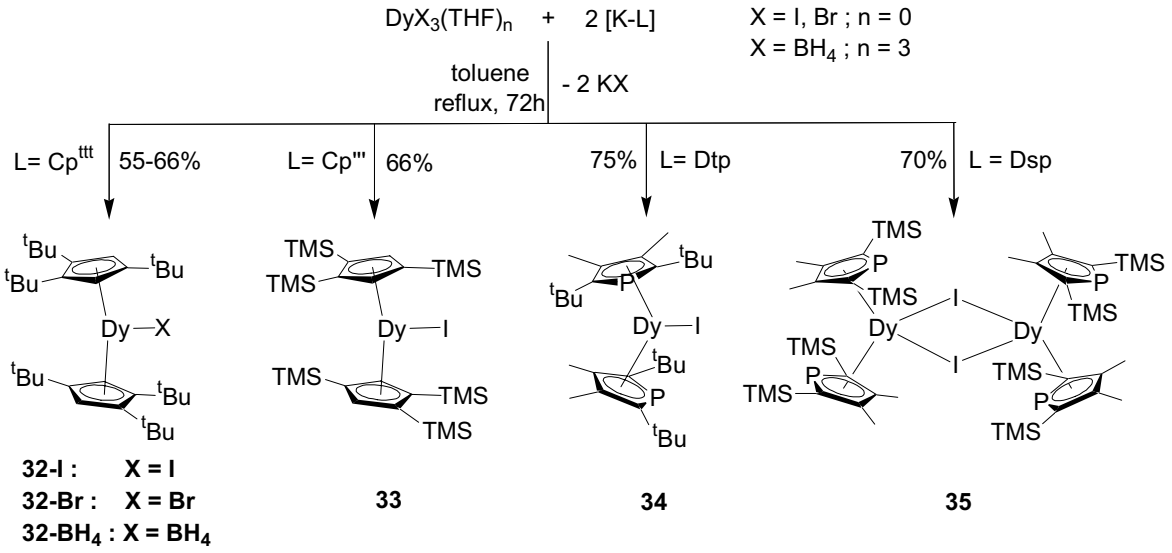

Scheme 24. Synthesis of $[(Cp^{ttt})_2DyX]$ (X = I, Br, BH_4) (**32**), $[(Cp''')_2DyI]$ (**33**), $[(Dtp)_2DyI]$ (**34**) and $[\{(Dsp)_2DyI\}_2]$ (**35**).

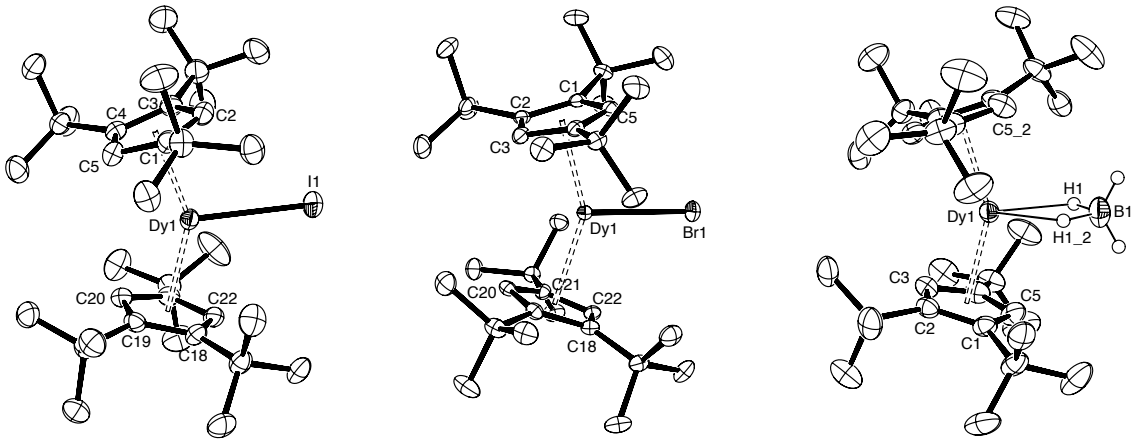

Figure 19. ORTEP-plot (50% probability ellipsoids) of one molecule of $[(Cp^{ttt})_2DyI]$ (**32-I**) (left), one molecule of $[(Cp^{ttt})_2DyBr]$ (**32-Br**) (middle) and one molecule of $[(Cp^{ttt})_2Dy(BH_4)]$ (**32-BH$_4$**) (right). Hydrogen atoms were omitted for clarity, except in the borohydride. Selected bond distances (Å): Dy(1)-I(1) = 2.9619(5), Dy(1)-Br(1) = 2.7138(4), Dy(1)-B(1) = 2.660(4), Dy(1)-H(1) = 2.12(3).

The solvent-free monomeric complexes $[(Cp^{ttt})_2DyI]$ (**32-I**), $[(Cp^{ttt})_2DyBr]$ (**32-Br**) and $[(Cp^{ttt})_2Dy(BH_4)]$ (**32-BH$_4$**) were obtained in moderate to good yields and could be characterized by X-ray studies (Figure 19). They exhibit the typical 2:1 staggering pattern for the tBu groups, also found in the Tm-analogues. The borohydride counterion in **32-BH$_4$** is η^2-bound to Dy in analogy to the Tm complexes. Most interestingly, one can see the influence of the size of the counterion on its distance to the metal (Dy-I > Dy-Br > Dy-(BH_4)). In

comparison to the thulium compounds, the distances are longer in agreement with the lanthanide contraction (Table 5).

Table 5. Comparison of structural parameters of $[(\eta^5\text{-L})_2\text{LnX}]$ complexes (Ln = Tm, Dy; L = Cpttt, Cp''', Dtp; X = I, Br, B).

Complex	Ln-X (Å)	Ln-Ct (Å)	Ct-Ln-Ct (°)	Interplane angle (°)
$[(Cp^{ttt})_2TmI]$ (11)	2.8999(5)	2.37	148	35
$[(Cp^{ttt})_2Tm(BH_4)]$ (14)	2.631(5)	2.36	149	33
$[(Cp^{ttt})_2DyI]$ (32-I)	2.9619(5)	2.39	147	33
$[(Cp^{ttt})_2DyBr]$ (32-Br)	2.7138(4)	2.41	147	34
$[(Cp^{ttt})_2Dy(BH_4)]$ (32-BH_4)	2.660(4)	2.39	149	33
$[(Cp''')_2TmI]$[a] (12)	2.8697(7)	2.31	144	38
$[(Cp''')_2DyI]$ [a] (33)	2.9012(4)	2.35	145	38
$[(Dtp)_2TmI]$ (19)	2.8864(8)	2.38	148	35
$[(Dtp)_2DyI]$ (34)	2.9235(2)	2.42	147	35

[a] only the 2:1 staggering is considered

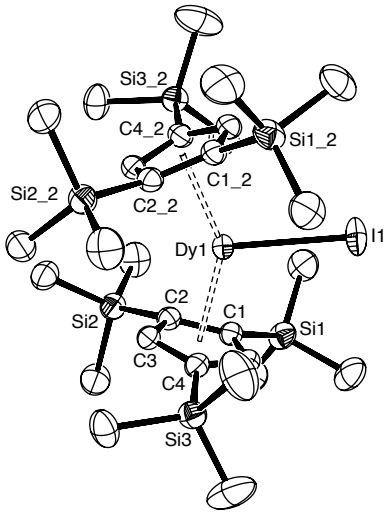

Figure 20. ORTEP-plot (50% probability ellipsoids) of one molecule of $[(Cp''')_2DyI]$ (**33**). Hydrogen atoms were omitted for clarity. There are three independent molecules in the lattice of **33**; only one is represented here. Selected bond distance (Å): Dy(1)-I(1) = 2.9012(4).

For the Cp''' ligand, the obtained complex $[(Cp''')_2DyI]$ (**33**) (Figure 20) exhibited the same structural conformation as the corresponding Tm-complex **12**, with slightly longer bond distances (Table 5). Whereas in one molecule the TMS groups are staggered in a 2:1 conformation, the other two molecules of the unit cell show a 2:2 pattern.

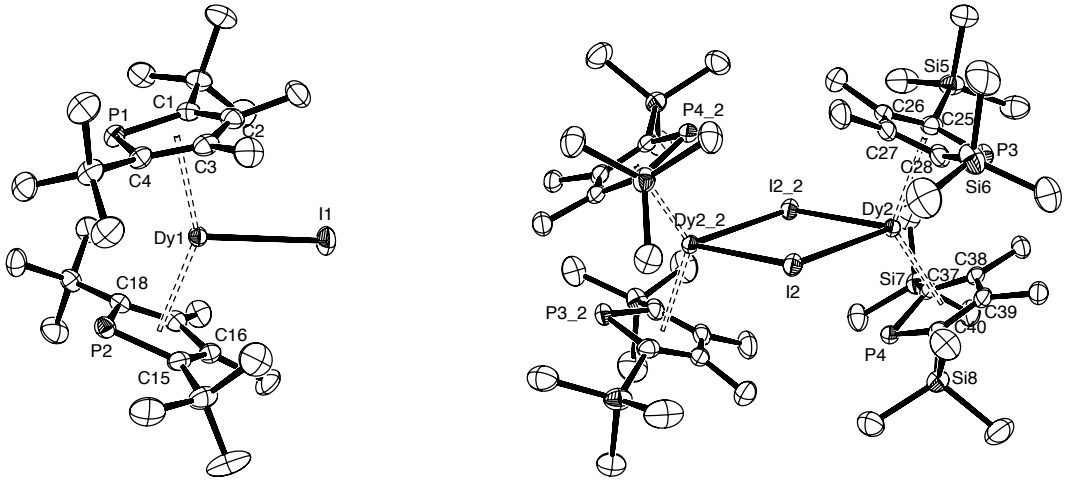

Figure 21. ORTEP-plot (50% probability ellipsoids) of one molecule of $[(Dtp)_2DyI]$ (**34**) and one molecule of $[\{(Dsp)_2DyI\}_2]$ (**35**). Hydrogen atoms were omitted for clarity. Selected bond distances (Å) and angles (°): **34**: Dy(1)-P(2) = 2.8440(6), Dy(1)-P(1) = 2.8528(6), Dy(1)-I(1) = 2.9235(2); **35**: Dy(2)-P(4) = 2.8500(7), Dy(2)-P(3) = 2.8595(7), Dy(2)-I(2) = 3.1473(2), Dy(2)-I(2_2) = 3.1585(3), I(2)-Dy(2)-I(2_2) = 77.299(7), Dy(2)-I(2)-Dy(2_2) = 102.701(8).

In the case of the phospholyl ligands, a small change in the steric bulk due to an exchange of the bulky groups from tBu (Dtp) to TMS (Dsp) allowed for the isolation of two different products. For the less flexible Dtp-ligand the first monomeric bis(phospholyl)dysprosium iodide complex $[(Dtp)_2DyI]$ (**34**) (Figure 21) was obtained in good yields, which compared well with the thulium complex **19** (Table 5). In contrast, the complex containing the Dsp ligand, $[\{(Dsp)_2DyI\}_2]$(**35**) formed a μ-iodo bridged dimer in the solid state (Figure 21). In contrast to the dimeric structure of the Tm-complex **21**, the phospholyl rings have no symmetrical arrangement towards the metal in **35** with the two phosphorus atoms pointing in opposite directions. The structure of **35** resembles therefore more the structure of the Tm-complex **15**. The interplane angle is 49.5°, compared to 51.1° in **15,** with a Dy-centroid distance of 2.45 Å. The mean Dy-I distance of 3.15 Å is expectedly much longer than in the monomeric compound **34** (2.92 Å). The observation that **35** formed a dimer in the solid state furnished a possible explanation why the crystals of the corresponding thulium compound **20** showed low stability. With the smaller thulium, the ligand may lead to a product which depending on the conditions forms either a monomeric or a dimeric form in the solid state, which is not stable at room temperature.

4.2 Characterization of trivalent organodysprosium complexes by ^{1}H NMR

The observation of interpretable ^{1}H NMR spectra for many trivalent organothulium complexes encouraged us to investigate the even more paramagnetic trivalent organodysprosium complexes (μ_{eff} = 10.8μ_B). According to theoretical considerations, NMR spectroscopy should be possible - depending especially on the metal-proton distances - and

data on coordination complexes of Dy^{3+} have already been reported. As the *D*-value of Dy^{3+} was fixed at -100, peaks were supposed to be shifted far upfield.[44, 45]

Indeed, all the synthesized trivalent complexes **32**-**35** showed interpretable and reproducible ^1H NMR spectra. The observed shifts, integrations and half-width values are summarized in table 6.

Table 6. ^1H NMR data on trivalent organodysprosium complexes.

	32-I	**32-Br**	**32-BH_4**	**33**	**34**	**35**
δ (ppm)	12, -191, -390	-31, -168, -362	-6, -173, -275	-70, -230	-242	-218
integration	1:1:1	1:1:1	1:1:1	2:1	1	1
$w_{1/2}$ (kHz)	3, 3, 4	4, 4, 3	2, 2, 1	3, 2	3	2
attribution	tBu	tBu	tBu	TMS	tBu	TMS

For the Cp^{ttt} containing complexes **32**, the usual three-peak scheme (1:1:1 integration) was observed, independently of the counterion. However, the shift interval, i.e. the difference between the most upfield and most downfield peak, seems to be influenced by the nature of the counterion: I (402 ppm) > Br (331 ppm) > BH_4 (269 ppm). For the Cp''' ligand in **33**, a two peak spectrum with integration 2:1 was recorded, in analogy to the Sm and Tm complexes. In the case of the phospholyl complexes **34** and **35**, only the bulky tBu and TMS groups were visible and no peak in the ^{31}P spectrum was observed.

4.3 Reduction of organodysprosium(III) precursors carrying the Cp^{ttt} ligand

Having in hand several trivalent precursors and being able to characterize them by ^1H NMR, it seemed likely that the reduction of these compounds under the well-established conditions in thulium chemistry should straightforwardly give the first divalent organodysprosium complexes.

As already discussed, the Cp^{ttt} carrying complexes **32** were the most promising ones due to the stabilization of the low-coordinate dysprosium centre by the bulky tBu groups, and we therefore started our investigations with these complexes. In an attempt to reduce **32-I** with KC_8 in cyclohexane at room temperature, the initial peaks in the ^1H NMR spectrum disappeared very slowly over several days, but the colour change which typically accompanies the reduction to divalent species, was not observed. From the resulting orange solution, no product could be isolated. Similar observations were made in the case of the other precursors **32-Br** and **32-BH_4**. The use of other solvents, toluene or benzene, led to slightly faster reactions, but again no divalent species could be obtained. In these cases, reaction with the solvent molecules also can be considered as possible degradation pathway. Apparently,

the reduction potential of KC_8 in these solvents was not sufficient to reduce the trivalent precursors.

In order to further activate KC_8, we next attempted to use a crown ether to assist the reduction of the dysprosium precursors. Addition of one equivalent of [18]crown-6, best suited for the complexation of K^+, to a solution of **32-I** in cyclohexane, followed by addition of KC_8 (2 equivalents) led to the immediate formation of a dark red solution, from which most of the product crystallised after 24 hours (Scheme 25). The red crystalline product was suitable for X-ray studies, which revealed the first divalent organodysprosium species in the form of an ate-complex, $[(Cp^{ttt})_2Dy(\mu\text{-}I)K([18]crown\text{-}6)]$ (**36-I**) (Figure 22). Unfortunately, due to disorder problems in the crown-ether, the structure could not be resolved completely. We therefore attempted the reduction of the other precursors under the same conditions (Scheme 25). With **32-Br** and **32-BH$_4$**, the new divalent complexes $[(Cp^{ttt})_2Dy(\mu\text{-}X)K([18]crown\text{-}6)]$ (X = Br (**36-Br**), BH_4 (**36-BH$_4$**)) were isolated and fully characterized by X-ray analysis (Figure 23).

The most striking structural feature of the divalent complexes concerns the degree of elongation of the Dy-counterion distance compared to their trivalent precursors. The well-precedented increase in the metal-centroid distance when going from the trivalent to the divalent compound is much less pronounced in these complexes (Table 7).

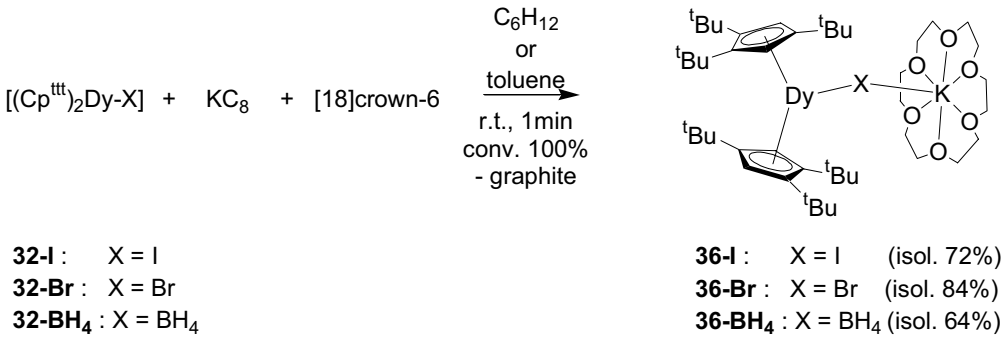

32-I : X = I
32-Br : X = Br
32-BH$_4$: X = BH_4

36-I : X = I (isol. 72%)
36-Br : X = Br (isol. 84%)
36-BH$_4$: X = BH_4 (isol. 64%)

Scheme 25. Synthesis of the first divalent organodysprosium complexes **36**.

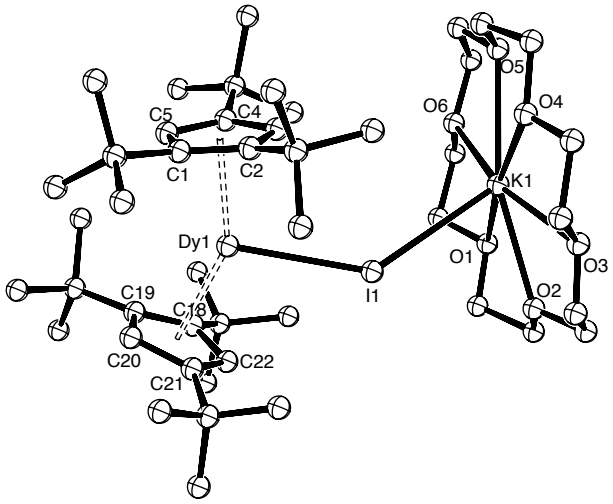

Figure 22. X-ray structure of $[(Cp^{ttt})_2Dy(\mu\text{-}I)K([18]crown\text{-}6)]$ (**36-I**) as ball-and-stick model. A disorder was observed in the crown-ether of the second molecule of the unit cell.

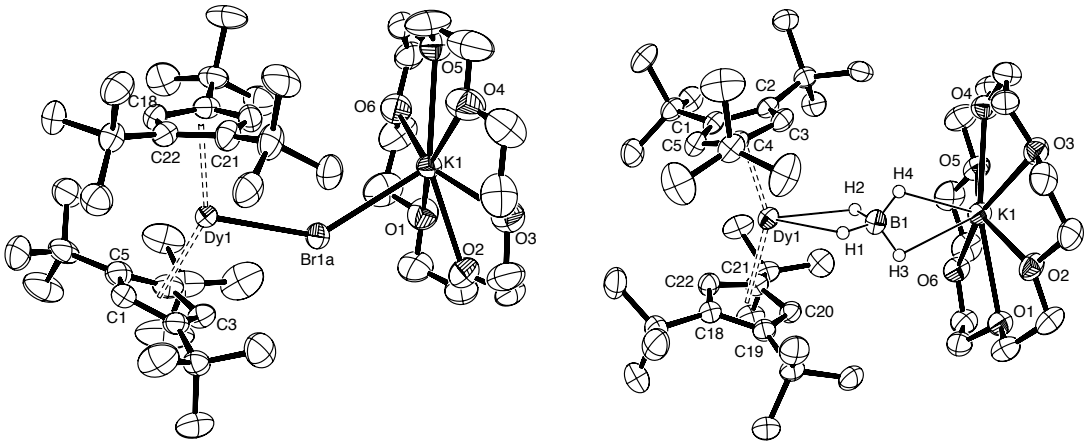

Figure 23. ORTEP-plot (50% probability ellipsoids) of one molecule of $[(Cp^{ttt})_2Dy(\mu\text{-}Br)K([18]crown\text{-}6)]$ (**36-Br**) (left) and one molecule of $[(Cp^{ttt})_2Dy(\mu\text{-}BH_4)K([18]crown\text{-}6)]$ (**36-BH$_4$**) (right). Hydrogen atoms were omitted for clarity, except in the borohydride. In **36-Br**, two tBu groups and the Br are disordered. Selected bond distances (Å) and angles (°): **36-Br**: Dy(1)-Br(1a) = 2.810(5), Br(1a)-K(1) = 3.234(7), Dy(1)-Br(1a)-K(1) = 137.5(2); **36-BH$_4$**: Dy(1)-B(1) = 2.735(4), Dy(1)-H(1) = 2.25(5), Dy(1)-H(2) = 2.28(5), K(1)-B(1) = 3.092(5), Dy(1)-B(1)-K(1) = 144.9(2).

Table 7. Comparison of structural parameters of divalent and trivalent organodysprosium complexes.

Complex	Dy-X (Å)	Dy-Ct (Å)	Ct-Dy-Ct (°)	Interplane angle (°)	Dy-X-K (°)
32-I	2.9619(5)	2.39	147	33	--
32-Br	2.7138(4)	2.41	147	34	--
32-BH_4	2.660(4)	2.39	149	33	--
36-I	3.06	2.44	149	27	136
36-Br	2.85 (av.)	2.42	148	26	137
36-BH_4	2.735(4)	2.42	148	31	145

The new divalent complexes could be dissolved in toluene. The ^{1}H NMR spectra revealed four new peaks: three peaks with the integration 1:1:1, around 200 ppm downfield compared to the starting materials, which were attributed to the tBu groups, and one peak between -40 and -60 ppm for the crown-ether (Table 8). It should be noted that Dy^{2+} complexes are as paramagnetic as their trivalent analogues (μ_{eff} = 10.61 μ_B) and therefore only the bulky tBu groups and the crown-ether could be observed in the spectra. The surprising stability of the divalent complexes observed in toluene - complete degradation only after 48-72h – allowed their synthesis directly in this solvent.

Table 8: ^{1}H NMR data on divalent organodysprosium complexes

	36-I	**36-Br**	**36-BH_4**
δ (ppm)	236, 109, -32, -233	209, 99, -63, -232	343, 133, -49, -178
integration	1:1:1.4:1	1:1:1.4:1	1:1:1.4:1
$w_{1/2}$ (kHz)	4, 4, 2, 4	3, 3, 2, 3	3, 3, 2, 3
attribution	tBu, crown-ether	tBu, crown-ether	tBu, crown-ether

Four possibilities were envisaged in order to go from these ate-complexes to neutral complexes:

a) Reducing the size of the counterion

The use of different counterions, iodide, bromide and borohydride, in order to bring the coordinated KI-(crown-ether) adduct closer to the Cp^{ttt} ligands and therefore force its precipitation, have failed so far. As the trivalent chloride precursor, having the smallest counterion, was not accessible under the usual metathesis conditions, we attempted its synthesis by oxidation of the divalent complex **36-BH_4** with chlorobenzene or $CHCl_3$ according to literature reports.[69] However, the ^{1}H NMR spectrum of the crude reaction

mixture a large number of products formed from which no clean material could be isolated. In contrast, reaction with 0.5 equivalents of C_2Cl_6 resulted in a much clearer spectrum. The new trivalent ate complex $[(Cp^{ttt})_2Dy(\mu\text{-}Cl)_2K([18]crown\text{-}6)]$ (**37**) was obtained as the main product and this was characterized by X-ray studies (Figure 24). One of the by-products of this reaction was identified as the mono-Cp product $[(Cp^{ttt})_2DyCl(BH_4)(\mu\text{-}Cl)K([18]crown\text{-}6)]$ (**38**) (Figure 24), which was accessible in high yield and in pure form from the reaction between **36-BH$_4$** and one equivalent C_2Cl_6 (Scheme 26).

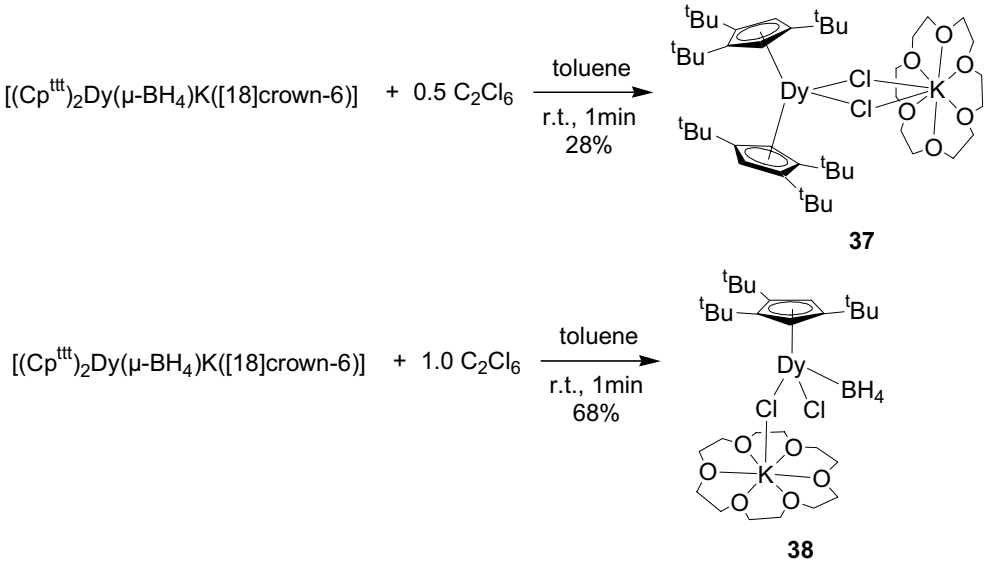

Scheme 26. Oxidation of $[(Cp^{ttt})_2Dy(\mu\text{-}BH_4)K([18]crown\text{-}6)]$ with C_2Cl_6.

The X-ray structure of **37** shows a bigger interplane angle of 41.6° than is observed in the other trivalent precursors **32** (33-34°) with longer mean Dy-centroid distances (2.48 Å for **37** vs. 2.40 Å for **32**), which probably result from the coordination of the two chlorides. A similar observation was made in the Tm complexes **11** and **30**. Most interestingly, the Dy-K distance in **37** (4.60 Å) is much shorter than in the shortest divalent complex **36-BH$_4$** (5.56 Å). However, despite this reduced distance, the crown-ether remains coordinated to the complex. This result shows that neutral complexes are not accessible by this approach.

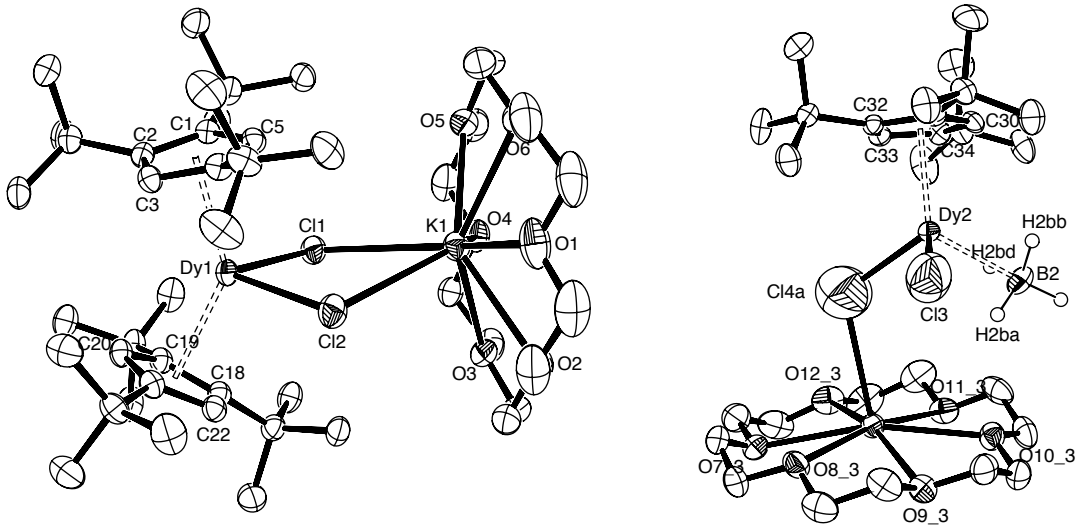

Figure 24. ORTEP-plot (50% probability ellipsoids) of one molecule of $[(Cp^{ttt})_2Dy(\mu\text{-}Cl)_2K([18]crown\text{-}6)]$ (**37**) (left) and one molecule of $[(Cp^{ttt})_2DyCl(BH_4)(\mu\text{-}Cl)K([18]crown\text{-}6)]$ (**38**) (right). Hydrogen atoms were omitted for clarity, except in the borohydride. In **38**, the Cl and BH_4 are disordered. Selected bond distances (Å) and angles (°): **37**: Dy(1)-Cl(1) = 2.6043(7), Dy(1)-Cl(2) = 2.6327(8), K(1)-Cl(2) = 3.202(1), K(1)-Cl(1) = 3.348(1), Cl(1)-Dy(1)-Cl(2) = 85.82(3), Dy(1)-Cl(1)-K(1) = 100.39(3), Dy(1)-Cl(2)-K(1) = 103.54(3); **38**: Dy(2)-B(2) = 2.51(1), Dy(2)-Cl(3) = 2.523(5), Dy(2)-Cl(4A) = 2.58(1), Dy(2)-H(2ba) = 2.42(4), Dy(2)-H(2bb) = 2.33(5), Dy(2)-H(2bd) = 2.42(5), Dy(2)-Cl(4a)-K(2_3) = 116.5(3).

b) Using other sequestrating agents

The aim of this approach was again the precipitation of KI, this time due to steric hindrance between the bulky tBu groups on the complex and a large cryptand. Carrying out the reduction of **32-I** with one equivalent of [2.2.2]cryptand, best-suited for K^+, instead of [18]crown-6, led again to the formation of a red solution. Unfortunately, the crystals that precipitated from this solution were not suitable for X-ray studies. However, the ^1H NMR spectrum was comparable to the one recorded for the crown-ether adduct **36-I**, showing three peaks for the tBu groups and a doublet for the cryptand instead of the single peak for the crown-ether. The new divalent product may probably have the composition $[\{K([2.2.2]cryptand)\}\{(Cp^{ttt})_2DyI\}]$, indicating that this method was not suitable for the synthesis of a neutral compound either.

$$[(Cp^{ttt})_2Dy\text{-}I] + KC_8 + [2.2.2]cryptand \xrightarrow[\text{r.t., 1min}\\ \text{conv. 100\%}\\ \text{isol. 72\%}\\ \text{- graphite}]{\text{toluene}} [\{K([2.2.2]cryptand)\}\{(Cp^{ttt})_2Dy\text{-}I\}]$$

Scheme 27. Reduction of $[(Cp^{ttt})_2DyI]$ (**32-I**) in the presence of [2.2.2]cryptand.

c) Adding Lewis-bases

The replacement of the KI-(crown-ether) adduct in **36-I** by Lewis bases, such as TMEDA, DME or THF was investigated by ^{1}H NMR experiments. Surprisingly, addition of TMEDA or DME to toluene solutions of the divalent compounds **36** did not influence the stability of the complexes at all and no change was observed in the NMR spectra after 48h. In contrast, addition of THF led to the degradation of the divalent complexes within 15min, a colour change to brown and the disappearance of all peaks in the spectra occurred. During that 15-min period, no new peaks indicating the formation of a neutral species became visible. These results showed, that once a crown-ether was used for the activation of KC_8 it was very difficult to remove it.

d) Carrying out the reduction without crown-ether in THF

In order to avoid the use of crown-ethers, the reduction of the trivalent complexes in THF at low temperatures was attempted. For the divalent complexes $[(Cp^{ttt})_2Sm(THF)]$[43] and $[(Cp^{ttt})_2Tm(THF)]$ (**9**), THF-coordination was shown to be very weak, allowing for the easy removal of THF after the metathesis reaction. Similar behaviour was expected for $[(Cp^{ttt})_2Dy(THF)]$, as Dy has an intermediate size between Sm and Tm. The experiments carried out under c) had shown, that at room temperature the THF adduct was not stable. Preliminary low-temperature NMR experiments in THF-d_8 were therefore performed to investigate the stability of this complex at different temperatures.

Condensation of THF-d_8 onto a mixture of **32-I** and KC_8 at -78°C afforded immediately a red solution, hence indicating that presumably reduction had taken place. The ^{1}H NMR spectrum recorded at -50°C confirmed this observation as a peak shift in the area of the divalent complexes had occurred: two peaks at 384 and 150 ppm were observed. Slow warming of this solution to -30°C revealed three new peaks at 120, -319 and -341 in addition to the first ones, which moved to 334 and 149 ppm. Further warming to -20°C and then to -10°C showed that the peak at 150 ppm split into two peaks at 145 and 131 ppm and the remaining four peaks further approached each other, going from 293 to -308 ppm. At 0°C the rise of many new peaks indicated the onset of degradation and we therefore decided to re-cool the solution to -50°C at which temperature the initial spectrum was obtained. These results showed that the presumed divalent compound was stable up to -10°C.

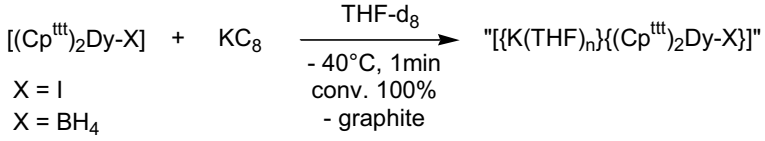

Scheme 28. Reduction of trivalent precursors in THF at low temperatures.

Further information on the possible divalent species was obtained, when the reduction of **32-BH$_4$** was carried out in THF-d$_8$ at low temperatures. From -50°C on (450, 250, -350 ppm) and up to room temperature (343, 138, -180 ppm), at which this compound was stable for a few minutes, only 3 peaks were observed. The final spectrum shows the same chemical shifts for the tBu groups as the spectrum for **36-BH$_4$**, indicating that even in THF the formation of a divalent ate complex, presumably [{K(THF)$_n$}{(Cp^{ttt})$_2$Dy(BH$_4$)}], occurred and no neutral species could be obtained. We therefore conclude that in the above described reduction of the iodide precursor **32-I** a similar complex formed, e.g. [{K(THF)$_n$}{(Cp^{ttt})$_2$DyI}], which is more reactive due to the longer and more labile Dy-I bond and hence not stable at temperatures above 0°C. The observation of up to 6 peaks in the case of the iodide against only 3 peaks in the case of the borohydride may be explained by the larger anion size which has a stronger influence on the rotation of the ligand around the metal centre.

4.4 Attempted reduction of other precursors

For the samarium and thulium precursors **3** and **12** carrying the Cp''' ligand, the reduction with KC$_8$ is much faster than for the corresponding Cp^{ttt}-containing complexes **2** and **11**. This is attributed to the higher Lewis acidity of the metal in these complexes upon changing Cp^{ttt} for the less-electron donating Cp''' ligand. It was therefore interesting to see if similar behaviour could also be observed for dysprosium.

Indeed, reduction of **33** with KC$_8$ in C$_6$D$_{12}$ at room temperature led to a rapid colour change to red. ^{1}H NMR indicated the slow disappearance of the initial signals and the formation of new products (Scheme 29). After 24 hours, the intense red colour had changed to orange, the typical colour of trivalent complexes and in the ^{1}H NMR spectrum only one new set of signals was observed. This product has not been characterized further.

The addition of one equivalent crown-ether to the reduction reaction led to the immediate decomposition of the products, as indicated by a large number of peaks in the ^{1}H NMR, probably due to C-Si bond cleavage.

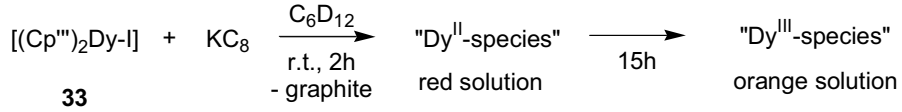

Scheme 29. Reduction of [(Cp''')$_2$DyI] (**33**)

The Dtp ligand gave access to a highly stable divalent organothulium complex and expectations were high that it could also allow for the isolation of stable divalent organodysprosium complexes.

However, the reduction of **34** with KC_8 in the presence or absence of crown-ether in either cyclohexane or toluene did not lead to any observable products, i.e. no colour change and no change in the shift of the tBu peak in the ^1H NMR spectrum were seen. So far, no explanation has been found for this unexpected behaviour.

4.5 Reactivity tests

4.5.1 Dinitrogen activation

Due to the highly negative redox potential of divalent Dy, it seemed that dinitrogen activation might be possible with the new complexes, despite the steric hindrance of the ligand and the coordination of KX-(crown-ether). Indeed, exposing a toluene solution of the isolated **36-I** under nitrogen atmosphere at room temperature led to a rapid colour change from dark red to intense purple. This product was stable for 30 min at room temperature and 24 hours at -30°C before a colour change to yellow was observed. Despite numerous crystallisation attempts, the reaction product with dinitrogen could not be identified by X-ray studies, nor could any product be isolated from the yellow solution.

Surprisingly, the two other characterized divalent complexes **36-Br** and **36-BH$_4$** did not show any visible interaction with dinitrogen; the starting materials were recovered after 30 min. The longer and weaker Dy-I bond may be held responsible for the higher reactivity of **36-I** compared to its bromide and borohydride analogues.

4.5.2 Reaction with diphenylacetylene

Evans recently reported the reaction of DyI_2 with diphenylacetylene to afford cis-stilbene exclusively after aqueous workup.[67] In order to compare this result with our isolated divalent organodysprosium complexes, an equimolar reaction was carried out between diphenylacetylene and **36-BH$_4$**. The immediate formation of a green product, which could not be obtained crystalline, was observed. After aqueous workup one major product could be obtained and identified by NMR, mass spectroscopy and X-ray studies: the reductive coupling product (*E*,*E*)-1,2,3,4-tetraphenylbuta-1,3-diene (Scheme 30).

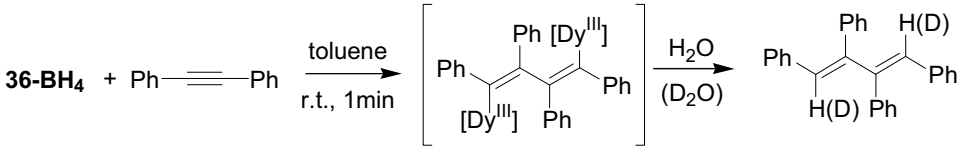

Scheme 30. Reaction between **36-BH$_4$** and diphenylacetylene

This reaction probably goes via the formation of a butadiene-bridged bimetallic complex, the green intermediate, by analogy with the 1,1'-bis(1,4-dihydropyridylamide)thulium-complex **29**. Some support for this hypothesis comes from the observation that workup with D_2O led only to the 1,4-deuterated butadiene product. The butadiene product can also be obtained after aqueous quenching of the reaction of lithium with diphenylacetylene,[70] indicating that the reactivity of the divalent organodysprosium complexes comes closer to alkali metal type chemistry than SmI_2 type chemistry.

4.5.3 Reaction with Ph_3PS and Ph_3PO

Divalent Sm and Tm complexes were reported to reduce Ph_3PS but not Ph_3PO to afford Ph_3P.[4, 71] When reacting the more reducing divalent organodysprosium complex **36-I** with Ph_3PS or Ph_3PO, the immediate quantitative formation of Ph_3P could be observed in ^{31}P NMR. However, no metal-containing co-product could be isolated or characterized.

4.5.4 Reaction with fluorenone

In the case of the divalent thulium compounds **8** and **13** we could only observe a colour change upon reaction with ketones but no product could be isolated (see 3.9.7). In the literature, fluorenone complexes are reported to be easier to isolate than benzophenone complexes due to the more rigid ring system.[66] Hence, we attempted the reduction of this ketone with the new divalent organodysprosium complexes.

The addition of fluorenone to a toluene solution of **36-Br** led to an immediate colour change to orange-brown and after several minutes most of the product had crystallized from the solution. The crystals obtained were suitable for X-ray studies, which revealed a new zwitterionic ate complex **39** having the bromide and the reduced fluorenone attached to dysprosium. The K(crown-ether) counterion is out of the binding distance of the bromide. The C-O bond in the fluorenyl unit shows a typical bond length for a ketone radical anion (1.32(1) Å).[66] As with the dichloride complex **37**, the Dy-centroid distances are long (2.50 Å for **39** vs. 2.48 Å for **37**) and the interplane angle is very large (44.4° for **39** vs. 41.6° for **37**).

In contrast, when the reaction was carried out with **36-I**, the solution immediately lightened from dark red to red and a white precipitate formed. The separated and weighed precipitate corresponded to the amount of KI-(crown-ether) employed in the reaction. Unfortunately, from the red solution no product could be characterized, but due to the colour, we postulate the formation of the $[(Cp^{ttt})_2Dy(OC_{13}H_8)]$ complex. Therefore, as in the case of the reduction of dinitrogen, it seemed that the different counterions had again influenced the reactivity of the divalent compounds.

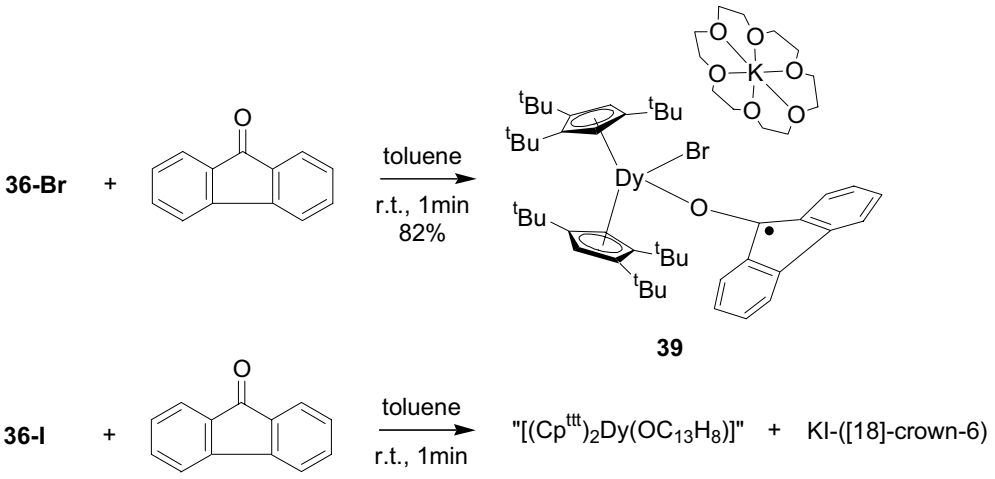

Scheme 31. Reaction between the divalent complexes **36-Br** and **36-I** and fluorenone

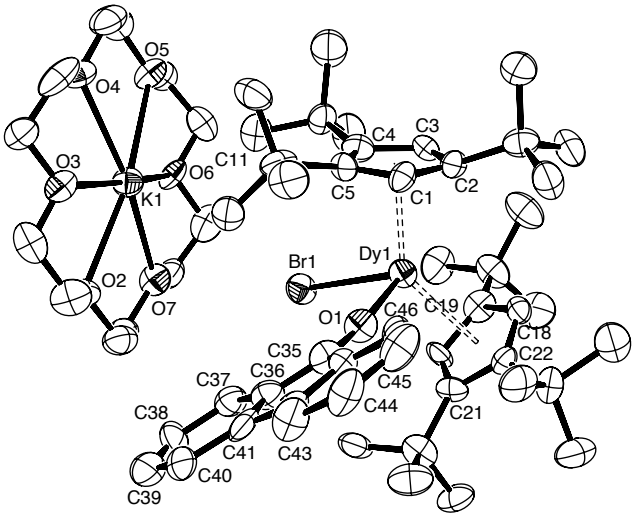

Figure 25. ORTEP-plot (50% probability ellipsoids) of one molecule of [{K([18]-crown-6)}{(Cp^{ttt})$_2$DyBr($OC_{13}H_8$)}] (**39**). Hydrogen atoms were omitted for clarity. Selected bond distances (Å) and angles (°): Dy(1)-O(1) = 2.133(7), Dy(1)-Br(1) = 2.806(1), O(1)-C(35) = 1.32(1), O(1)-Dy(1)-Br(1) = 93.1(2).

4.5.5 Reaction with biphospholes and thalliumphospholide

[(Cp*)$_2$Sm] has been reported to react with biphospholes and thallium phospholide, (PC_4H_4)Tl, to yield η^1- or η^5- bound phospholyl complexes.[35] Similar reactions with the divalent dysprosium complexes might be expected to lead to the precipitation of the KX-(crown-ether) adduct and formation of bis(cyclopentadienyl)-phospholyl complexes.

However, although reduction of (Dpp)$_2$ or (Tmp)$_2$ occurred in the reaction with **36-BH$_4$**, as observed from the ^{31}P spectra, the phospholides were not nucleophilic enough to replace the

borohydride at the metal center and **32-BH_4** was recovered nearly quantitatively. Similar results were obtained for Tl-phospholide, where metallic Tl precipitated immediately, but only the trivalent **32-BH_4** resulted.

In order to investigate the difference of reactivity of the counterion, the reaction of Tl-phospholide with the **36-I** was carried out, but again only the formation of **32-I** was observed.

4.6 Conclusion

The first stable divalent organodysprosium complexes $[(Cp^{ttt})_2Dy(\mu\text{-}X)K([18]crown\text{-}6)]$ (X = I, Br, BH_4**) (36)** have been synthesized by chemical reduction of the corresponding trivalent precursors $[(Cp^{ttt})_2DyX]$ (X = I, Br, BH_4**) (32)** and characterized by X-ray crystallography. As the reduction potential of KC_8 in non-polar solvents is not sufficient to reduce the trivalent complexes, addition of crown-ether is necessary and this leads to the formation of divalent ate-complexes. ^1H NMR spectroscopy has been shown to be a very useful tool for the characterization of both trivalent and divalent complexes, despite the high magnetic moment of Dy^{2+} and Dy^{3+}. Neutral complexes could not be obtained by varying the size of the counterion in the trivalent precursor, by using bigger crown-ethers or by adding Lewis bases to the ate-complexes. The reduction of the trivalent precursors in THF at low temperatures, avoiding the use of crown-ether, also led to the formation of divalent ate complexes. From the reduction of other trivalent precursors **33** and **34**, containing Cp''' and phospholyl ligands, no divalent products could be isolated.

The reactivity of the divalent complexes has been shown to depend on the counterion. Whereas the more weakly bound iodide ligand allows for the reaction with dinitrogen, the more strongly bound bromide and borohydride ligands did not show any visible reaction. With fluorenone, two different products are obtained, an ate-complex in the case of the bromide and (presumably) a neutral species in the case of the iodide. The high reducing power of these complexes has been demonstrated in the reactions with diphenylacetylene, Ph_3PS, Ph_3PO and bi(phospholes).

5 Further development of the reductive approach towards divalent organoneodymium compounds

Neodymium is certainly one of the most studied lanthanides due to its high abundance and the relatively low price of the metal itself and of the commercially available compounds. For the synthesis of divalent species two important facts need to be considered: the extremely high reactivity due to the redox potential (-2.62 V) and the cation size which requires very bulky ligands for stabilization. In the early days of "new" divalent lanthanide chemistry these properties were certainly known but also under-estimated. Several synthetic attempts to access divalent organoneodymium compounds have been reported, however, no structural evidence of an isolated divalent complex has been given so far.[10, 12, 13, 72] In most reactions, coloured intermediates – presumably divalent species - were observed which rapidly decomposed.

On the basis of the results obtained in organothulium and organodysprosium chemistry using the reductive approach, it was obvious that the most suitable of our ligands for stabilizing a divalent neodymium species would be the Cp^{ttt} ligand. The Cp''' ligand could not be used with crown ethers and had failed to stabilize a possible neutral divalent organodysprosium species. With the Dtp ligand no reduction of the corresponding trivalent Dy complex was observed at all. In addition, an eventual reduction product of $[(Dtp)_2NdI]$ like the hypothetical $[(Dtp)_2Nd]$ may be difficult to deal with since it would likely dimerize into an insoluble compound like $[\{(Dtp)_2Sm\}_2]$ does,[4] the size of Nd and Sm being similar.

The synthesis of several trivalent precursors carrying the Cp^{ttt} ligand and different counterions was envisaged in order to examine their suitability in the reductive approach.

5.1 Preparation of organoneodymium(III) precursors bearing the Cp^{ttt} ligand

A recent report on the synthesis of Cp^{ttt} substituted lanthanide complexes showed, that the salt metathesis between $NdCl_3$ and $[NaCp^{ttt}]$ in a THF/toluene mixture led to $[(Cp^{ttt})_2NdCl]$ (**40-Cl**) – a perfect precursor, as cheap and easily available.[39] Unfortunately, when trying to reproduce this reaction, some impurities, which could not be removed by washing or re-crystallisation, remained in the final product as indicated by ^1H NMR (Scheme 32). Hence, this complex was not considered as suitable for testing in the reductive approach. It should also be noted, that when using the potassium instead of the sodium salt of the ligand none of the desired product was obtained.

Investigations on the borohydride precursor $Nd(BH_4)_3(THF)_3$ led to similar observations. With $[NaCp^{ttt}]$, a mixture of products was obtained which could not be separated. However, one of the products, the monomeric, salt-free $[(Cp^{ttt})_2Nd(BH_4)]$ (**40-BH_4**) was obtained

crystalline and identified by X-ray studies (Figure 26). When using the potassium salt in analogy to the preparation of the thulium and dysprosium precursors **14** and **32-BH$_4$**, i.e. heating in toluene for several days, resulted in the formation of a completely different compound (Scheme 31). According to its ^{1}H NMR spectrum and its low solubility in THF, one possible formulation might be that of an ate-complex, [{K(THF)$_n$}{(Cp^{ttt})$_2$Nd(BH$_4$)$_2$}] (**41**). Similar observations have been made by Sitzmann in the synthesis of [(Cp^{4i})$_2$LnCl] complexes (Ln = La, Nd).[73, 74] The unexpected complexes [{(Cp^{4i})$_2$Ln(μ-Cl)(μ$_3$-Cl)Na(OEt$_2$)}$_2$] formed, which could be transformed into the salt-free complexes by stirring in toluene. In the case of **41**, no salt precipitation was observed during stirring in toluene.

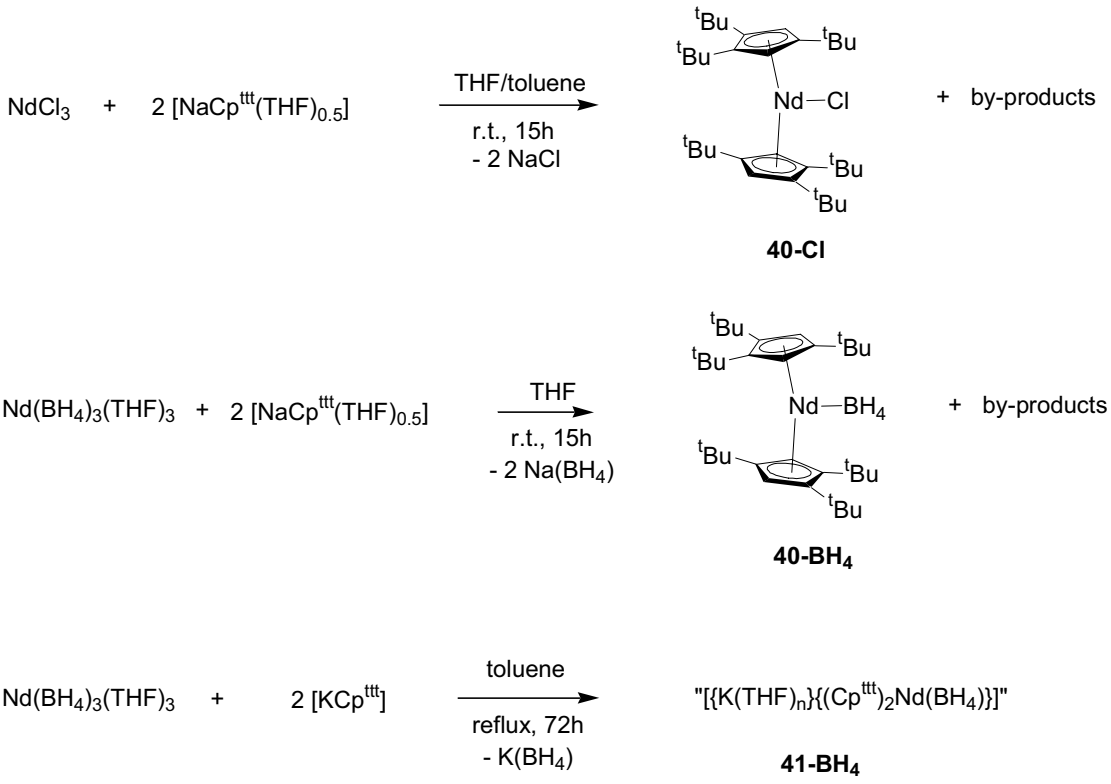

Scheme 32. Attempted synthesis of [(Cp^{ttt})$_2$NdX] (X = Cl, BH$_4$) precursors.

The ^{1}H NMR spectra of **40-Cl** and **40-BH$_4$** showed only two peaks with a 2:1 integration for the tBu groups, similarly to some related Ce complexes (X = H, F, C$_6$H$_5$, C$_6$F$_5$).[18] In all the other recorded spectra for [(Cp^{ttt})$_2$LnX] type complexes (Ln = Sm, Dy, Tm; X = I, Br, BH$_4$) a 1:1:1 pattern was obtained. This shows that free rotation around the metal depends on both, the metal size and the size of the counterion.

This difference in size can also be seen from the X-ray structure of **40-BH$_4$** (Figure 26). In contrast to the smaller Tm and Dy complexes, the borohydride is bound in a pseudo-trihapto fashion: one Nd-H bond is surprisingly long 2.76(3) Å, however the angle between the metal and the free hydride, Nd-B-H1b1, of 175° indicates the trihapto binding mode. The larger Nd-centroid distances and the larger interplane angles (Table 9) are held responsible for this

different BH_4 coordination. Consequently, the Nd-B bond distance becomes as short as in the Tm analogue and can be compared to similar neodymium borohydride complexes, e.g. $[(Cp^*)_2Nd(BH_4)(THF)]$ (2.63(5) Å).[75]

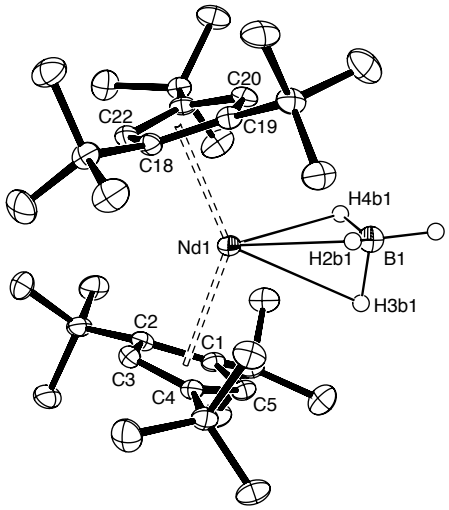

Figure 26. ORTEP-plot (50% probability ellipsoids) of one molecule of $[(Cp^{ttt})_2Nd(BH_4)]$ (**40-BH_4**). Hydrogen atoms were omitted for clarity, except in the borohydride. Selected bond distances (Å): Nd(1)-B(1) = 2.634(4), Nd(1)-H(2b1) = 2.33(3), Nd(1)-H(4b1) = 2.45(3), Nd(1)-H(3b1) = 2.76(3), Nd(1)-B(1)-H(1b1) = 175(2).

Table 9. Comparison of structural parameters for $[(Cp^{ttt})_2Ln(BH_4)]$ complexes (Ln = Nd, Dy, Tm)

Complex	Ln-B (Å)	Ln-H (Å)	Ln-Ct (Å)	Ct-Ln-Ct (°)	Interplane angle (°)
$[(Cp^{ttt})_2Tm(BH_4)]$ (14)	2.631(5)	2.14(4)	2.36	149	33
$[(Cp^{ttt})_2Dy(BH_4)]$ (32-BH_4)	2.660(4)	2.12(3)	2.39	149	33
$[(Cp^{ttt})_2Nd(BH_4)]$ (40-BH_4)	2.634(4)	2.33(3), 2.45(3), 2.76(3)	2.51	143	37

As the "cheap" precursors did not give reliable results, the iodide precursor was then investigated. Using the conditions that had allowed for the synthesis of $[(Cp^{ttt})_2SmI]$, i.e. reacting $NdI_3(THF)_{3.5}$ with 2 equivalents of $[NaCp^{ttt}]$ in THF, did not lead to the expected $[(Cp^{ttt})_2NdI]$. ^1H NMR studies revealed similarities to the compound obtained from the reaction of $[KCp^{ttt}]$ with $Nd(BH_4)_3$. In addition, only small amounts of NaI precipitated from the solution, hence, further strengthening the hypothesis of the formation of an ate-complex

41-I. Carrying out the reaction with the potassium salt in THF at room temperature afforded the mono(cyclopentadienyl) product $[(Cp^{ttt})NdI_2(THF)_n]$, as seen from the remaining $[KCp^{ttt}]$ in the ^1H NMR sprectrum. Addition of toluene and refluxing the reaction for 48 hours resulted in a mixture of products, from which some $[(Cp^{ttt})_2NdI]$ (**40-I**) could be isolated in poor yield (Scheme 33).

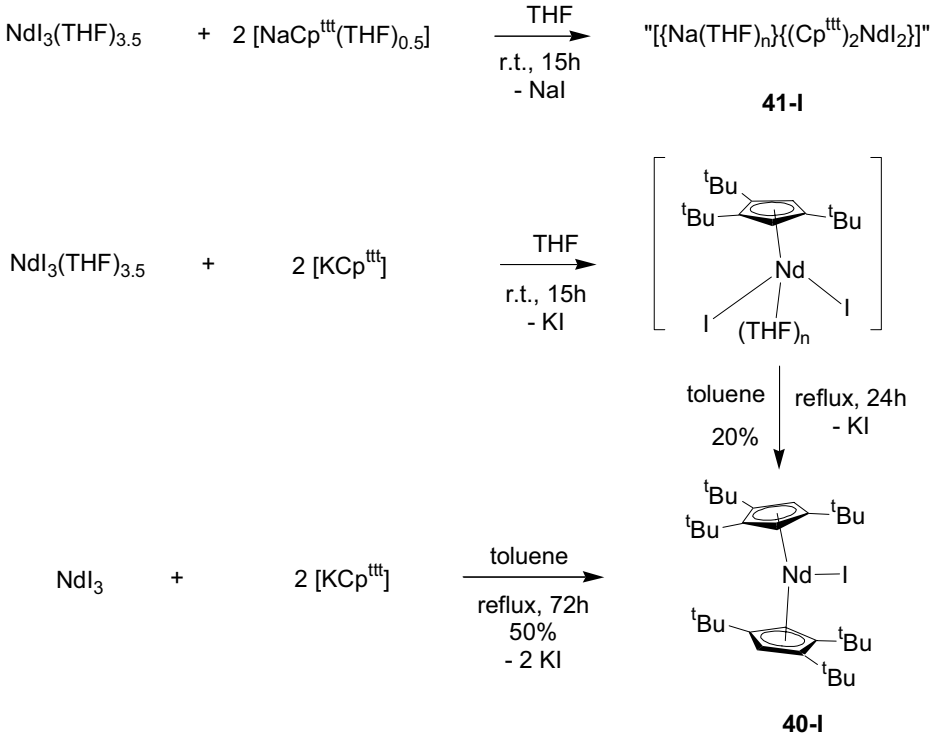

Scheme 33. Synthesis of $[(Cp^{ttt})_2NdI]$ (**40-I**).

Finally, the reaction of non-solvated NdI_3 and $[KCp^{ttt}]$ in refluxing toluene was tested. Pure $[(Cp^{ttt})_2NdI]$ could be obtained in moderate yield after recrystallisation from pentane (Scheme 33). The crystals were not suitable for X-ray studies, however, their solubility and their ^1H NMR spectrum indicated their composition. As in the case of Sm, Dy and Tm this compound exhibited three independent peaks in the ^1H NMR spectrum for the tBu groups, with a 1:1:1 integration pattern. Hence, this is another example where the size of the counterion influences the free rotation of the cyclopentadienyl rings around the metal center.

5.2 Reduction of organoneodymium(III) precursors

The reduction of pure **40-I** in cyclohexane with KC_8 and one equivalent of crown-ether, [18]crown-6, led to an immediate colour change from green to dark red and after one night crystals suitable for X-ray studies had grown from the solution (Scheme 34). The complex has the composition $[(Cp^{ttt})_2Nd(\mu\text{-}I)K([18]crown\text{-}6)]$ (**42-I**), in analogy to the dysprosium complexes **36**, and is the first example of a divalent organoneodymium compound.

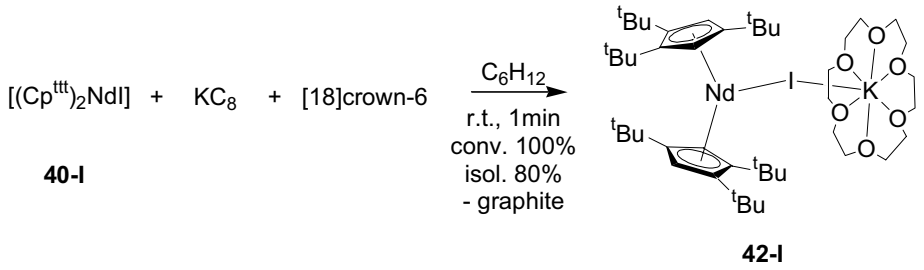

Scheme 34. Synthesis of the first divalent organoneodymium complex $[(Cp^{ttt})_2Nd(\mu\text{-}I)K([18]crown\text{-}6)]$ (**42-I**).

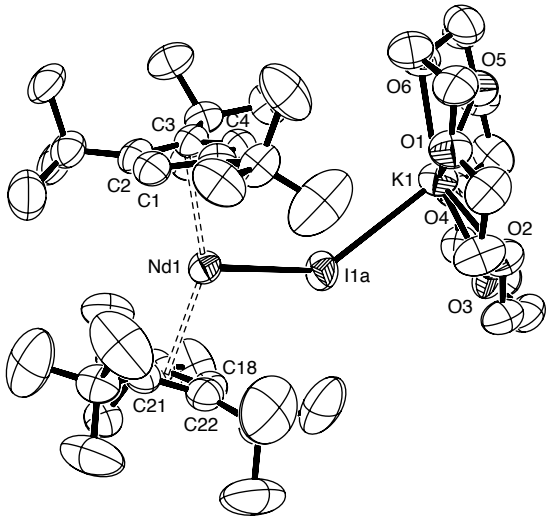

Figure 27. ORTEP-plot (50% probability ellipsoids) of one molecule of $[(Cp^{ttt})_2Nd(\mu\text{-}I)K([18]crown\text{-}6)]$ (**42-I**). Hydrogen atoms were omitted for clarity. Selected bond distances (Å) and angles (°): Nd(1)-I(1A) = 3.1565(6), Nd(1)-I(1A)-K(1) = 132.89(3).

The X-ray structure of **42-I** (Figure 27) shows many similarities to the Dy complex **36-I**. The distance elongations Ln-I (3.16 Å vs. 3.06 Å) and Ln-centroid (2.53 Å vs. 2.44 Å) are in good agreement with the lanthanide contraction. The Nd compound has a slightly more open conformation as indicted by the interplane angles (29.2° vs 27.0°). Unfortunately, no comparisons could be made with the trivalent precursor, for which no crystals suitable for X-ray studies could be obtained. However, compared to other trivalent compounds, the Nd-I bond length is significantly longer, e.g. 3.065 Å in [(Cp*)(Cp')NdI(py)].[76]

In the ^1H NMR spectrum the approach of two tBu groups (-12.3 and -0.3 ppm) of the trivalent precursor to form one peak with a shoulder at -4.9 ppm gave rise to a pseudo 2:1 integration. This observation may result from the elongation of the Nd-I bond and allow for nearly free rotation of the Cp ligands around the metal center.

5.3 Reactivity studies

5.3.1 Aromatic solvents

The instability of highly reactive divalent lanthanide species in aromatic solvents has been demonstrated.[42] However, it seems that for **42-I** the reactivity is such, that the crystallised compound could not be re-dissolved in benzene or toluene without degradation, nor could the reduction be carried out in these solvents. This contrasts the observation made for **36-I** which showed reasonable stability in toluene for 48h. One reason for this behaviour may be the more available space around the metal center which may allow easier interaction with the solvent molecules.

5.3.2 Dinitrogen activation

Organoneodymium compounds containing the typical (μ-η^2:η^2-N_2)-moiety have not been isolated so far, probably because of their high reactivity which may arise from steric reasons. In contrast, using the harder amide or aryloxide ligands, N_2-containing Nd-complexes could be characterized.[77] Having observed an interaction between the divalent dysprosium complex **36-I** and dinitrogen we then wished to know if **42-I** would react in the same way. Exposing a cyclohexane solution of this compound to dinitrogen at room temperature led to a rapid colour change to orange. However, so far no product has been isolated or characterized from this reaction.

5.3.3 Reaction with fluorenone

The difference in reactivity between the divalent dysprosium complexes **36-I** and **36-Br** towards fluorenone prompted us to investigate this reaction with **42-I** in cyclohexane. As in the case of **36-Br**, a strongly coloured precipitate formed upon addition of fluorenone, which has not been characterized further. A compound of the composition [{K([18]crown-6)}{$(Cp^{ttt})_2$NdI(fluorenyl)}] may have formed, which may be even favoured in the case of Nd due to more space around the metal center.

5.4 Conclusion

The first divalent organoneodymium compound [$(Cp^{ttt})_2$Nd(μ-I)K([18]crown-6)] has been synthesized by reduction of the trivalent precursor [$(Cp^{ttt})_2$NdI]. Other Nd complexes with the Cp^{ttt} ligand, including the crystallographically characterized [$(Cp^{ttt})_2$Nd(BH_4)], have been prepared. However, it has not been possible to obtain these compounds sufficiently pure or in a high enough yield to undertake further reduction experiments. Preliminary reactivity tests with the divalent compound have shown its high potential for the activation of small molecules.

6 Conclusion and Outlook

In the first part of this work we have explored a new synthetic approach to "new" divalent organolanthanide complexes. We have thus obtained new divalent organosamarium and organothulium complexes and the first stable divalent organodysprosium and organoneodymium complexes.

Trivalent precursors

A general procedure for the clean and efficient synthesis of trivalent iodide precursors $[\{(L)_2LnI\}_n]$ (Ln = Nd, Dy, Tm; L = Cp^{ttt}, Cp''', Cp^{tt}, Dtp, Dsp, Htp; n = 1 or 2), using a salt-metathesis reaction in a non-polar solvent such as toluene, has been developed (Scheme 34). For the borohydride precursors $[(Cp^{ttt})_2Ln(BH_4)]$ this approach is only valid for the smaller Dy and Tm.

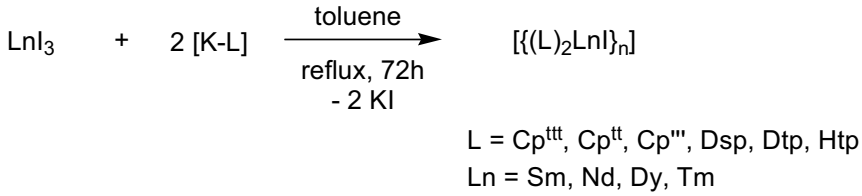

Scheme 35. General procedure for the synthesis of trivalent precursors $[\{(L)_2LnI\}_n]$.

Depending on the ligand and the metal size, monomeric or dimeric solvent-free precursors are obtained: with the bulky Cp^{ttt} and Cp''' ligands, very soluble, monomeric complexes have been isolated with the four elements Sm, Nd, Dy and Tm, whereas in the case of the phospholyl ligands the metal size plays an important role. The bulky Dtp ligand leads to monomeric complexes for Tm and Dy, whereas with Sm it is likely to give a dimeric species. For the more flexible Dsp ligand dimer formation is already observed with Dy. The sterically less demanding Cp^{tt} and Htp ligands form dimers even with the smallest Tm.

All these complexes can be characterized by ^1H NMR spectroscopy. Despite the high paramagnetism of some of them, namely Tm^{3+} and Dy^{3+}, reproducible and interpretable NMR spectra can be obtained.

The precursors carrying the bulky Cp^{ttt}, Cp''' and Dtp show different behaviour towards THF coordination. Whereas no obvious interaction is observed for the Cp^{ttt} ligand complexes, the Cp''' ligand complexes bind THF tightly, so that it can only be removed under vacuum upon heating. The Dtp ligand complexes take an intermediate position. In contrast, the coordination of a linear molecule, such as tBuCN is possible even in the case of the Cp^{ttt} ligand.

Divalent complexes

Two different protocols for the reduction of the trivalent precursors have been established depending on the reduction potential of the metal involved.

Divalent organosamarium and organothulium complexes are obtained from the slow reduction of their trivalent iodide or borohydride precursors in aliphatic solvents using KC_8 as reducing agent. With the bulky Cp^{ttt} and Cp''' ligands new samarocenes and the first base-free thulocenes have been obtained. The reduction can also be carried out with phospholyl complexes: with the Htp ligand the first dimeric divalent thulium complex has been isolated.

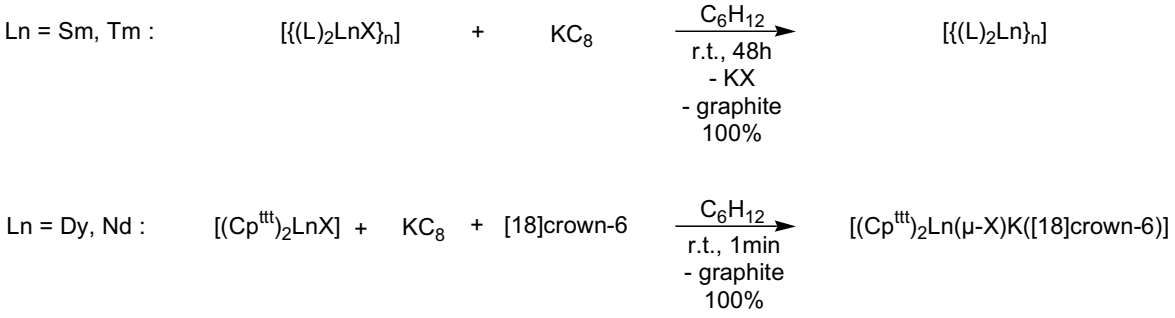

Scheme 36. Two different reduction protocols depending on the lanthanide involved.

The reduction potential of KC_8 in non-polar solvents has been shown to be insufficient to reduce trivalent dysprosium or neodymium complexes. Upon further activation of KC_8 by addition of one equivalent of crown-ether, the first divalent organodysprosium and organoneodymium species carrying the Cp^{ttt} ligand have been obtained as ate-complexes.

All the divalent complexes, even the paramagnetic Dy^{2+} complexes, can be characterized by ^1H NMR spectroscopy.

Reactivity studies

The reactivity of the divalent compounds depends strongly on the metal and the ligands used.

Among the divalent thulium complexes isolated during these studies, dinitrogen activation is only observed in the case of the solvent-free Htp substituted complex, whereas the complexes with the more bulky Cp^{ttt} and Cp''' ligands are inert towards dinitrogen. With the new divalent dysprosium complexes only the iodide compound shows interaction with dinitrogen, the bromide and borohydride remain unchanged during exposure to dinitrogen. Both cases confirm that the steric environment around the metal as well as electronic influences from the ligands play an important role in the reaction with dinitrogen. It is therefore not surprising, that the divalent neodymium complex with the most reducing metal

and the most open coordination sphere in the "$[(Cp^{ttt})_2Ln]$" series reacts readily with dinitrogen.

Similar observations to the dinitrogen case are observed in other reduction attempts, for example the reduction of Ph_3PS and Ph_3PO or the reaction with $[(Dtp)_2Pb]$. Whereas Ph_3PS is readily reduced to Ph_3P by the obtained divalent samarium and thulium complexes, only the divalent dysprosium complexes reduce PhPO to Ph_3P, hence indicating the differences in reduction potential. In a similar fashion, only the divalent Dtp carrying thulium complex is oxidised by $[(Dtp)_2Pb]$ to form probably a zwitterionic species; the corresponding samarium complex shows no reaction even at elevated temperatures.

The difference in reactivity between bulky Cp and phospholyl ligands has been observed in the reaction of divalent thulium complexes with pyridine. The Cp^{ttt} substituted complex reduces pyridine immediately to form a bimetallic bipyridinyl bridged complex, whereas in the case of the Dtp substituted complex a stable divalent adduct is obtained which slowly decomposes.

The divalent Dy complexes have demonstrated their important reduction potential in the reaction with 1,2-diphenylactetylene. This reaction affords the reductive coupling product tetraphenylbutadiene by analogy with metallic lithium, hence indicating the closeness of the Dy complexes to Birch-type reducing agents.

Outlook

These studies have opened up a new field of organolanthanide chemistry. Divalent lanthanide chemistry is no longer restricted to the four elements Eu, Yb, Sm and Tm but divalent Dy and Nd species can also be accessed. However, divalent compounds of the latter elements are still restricted to the Cp^{ttt} ligand and no neutral complexes have been obtained. In order to isolate new Dy and Nd complexes with other ligands, variations of the reductive approach need to be developed. One possibility for the synthesis of neutral complexes may be the reduction of cationic complexes of the $[(L)_2Ln(BPh_4)]$ type, which should be accessible from the iodide or borohydride precursors by reaction with $[Ag(BPh_4)]$ or $[Tl(BPh_4)]$. As alternative precursors zwitterionic tris(phospholyl) complexes can also be envisaged.

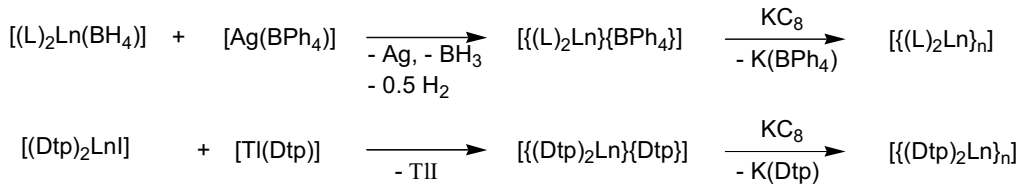

Scheme 37. Proposed synthesis for neutral divalent organolanthanide complexes.

For a better understanding of the influence of the ligand on the stability of the divalent complexes, electrochemical and theoretical investigations should also be carried out. This would allow the quantification of the observed differences in reactivity between Cp and phospholyl substituted complexes. The influence of steric bulk and electronic environment could also be better differentiated. These studies would also encourage a further development of the divalent mixed-ligand complexes: the fine-tuning of the reduction potential could be investigated making use of a whole array of Cp, phospholyl, and other related ligands such as for instance pyrrolyl.

The reactivity tests carried out so far have shown the high potential of the divalent complexes. More in-depth studies are necessary, especially with small molecules like dinitrogen, carbon monoxide and dihydrogen, to evaluate the usefulness of these new complexes.

References

[1] W. J. Evans, B. L. Davis, *Chem. Rev.* **2002**, *102*, 2119.
[2] K. Izod, *Angew. Chem. Int. Ed.* **2002**, *41*, 743.
[3] F. Nief, D. Turcitu, L. Ricard, *Chem. Commun.* **2002**, 1646.
[4] D. Turcitu, F. Nief, L. Ricard, *Chem.-Eur. J.* **2003**, *9*, 4916.
[5] F. Nief, B. T. de Borms, L. Ricard, D. Carmichael, *Eur. J. Inorg. Chem.* **2005**, 637.
[6] W. J. Evans, N. T. Allen, J. W. Ziller, *J. Am. Chem. Soc.* **2001**, *123*, 7927.
[7] L. J. Bowman, K. Izod, W. Clegg, R. W. Harrington, *J. Organomet. Chem.* **2007**, *692*, 806.
[8] W. J. Evans, N. T. Allen, J. W. Ziller, *Angew. Chem. Int. Ed.* **2002**, *41*, 359.
[9] M. N. Bochkarev, A. A. Fagin, *Chem.-Eur. J.* **1999**, *5*, 2990.
[10] Y. K. Gunko, P. B. Hitchcock, M. F. Lappert, *J. Organomet. Chem.* **1995**, *499*, 213.
[11] W. J. Evans, C. A. Seibel, J. W. Ziller, *J. Am. Chem. Soc.* **1998**, *120*, 6745.
[12] S. Al-Juaid, Y. K. Gun'ko, P. B. Hitchcock, M. F. Lappert, S. Tian, *J. Organomet. Chem.* **1999**, *582*, 143.
[13] P. B. Hitchcock, M. F. Lappert, S. Tian, *Organometallics* **2000**, *19*, 3420.
[14] I. L. Fedushkin, F. Girgsdies, H. Schumann, M. N. Bochkarev, *Eur. J. Inorg. Chem.* **2001**, 2405.
[15] M. C. Cassani, D. J. Duncalf, M. F. Lappert, *J. Am. Chem. Soc.* **1998**, *120*, 12958.
[16] G. K. B. Clentsmith, F. G. N. Cloke, J. C. Green, J. Hanks, P. B. Hitchcock, J. F. Nixon, *Angew. Chem. Int. Ed.* **2003**, *42*, 1038.
[17] H. Sitzmann, T. Dezember, O. Schmitt, F. Weber, G. Wolmershauser, M. Ruck, *Z. Anorg. Allg. Chem.* **2000**, *626*, 2241.
[18] L. Maron, E. L. Werkema, L. Perrin, O. Eisenstein, R. A. Andersen, *J. Am. Chem. Soc.* **2005**, *127*, 279.
[19] E. L. Werkema, E. Messines, L. Perrin, L. Maron, O. Eisenstein, R. A. Andersen, *J. Am. Chem. Soc.* **2005**, *127*, 7781.
[20] C. T. Qian, C. J. Zhu, Y. H. Lin, Y. Xing, *J. Organomet. Chem.* **1996**, *507*, 41.
[21] C. T. Qian, G. Zou, W. H. Jiang, Y. F. Chen, J. Sun, N. Li, *Organometallics* **2004**, *23*, 4980.
[22] M. Ganesan, C. D. Berube, S. Gambarotta, G. P. A. Yap, *Organometallics* **2002**, *21*, 1707.
[23] G. B. Deacon, G. N. Pain, T. D. Tuong, *Polyhedron* **1985**, *4*, 1149.
[24] W. J. Evans, J. W. Grate, H. W. Choi, I. Bloom, W. E. Hunter, J. L. Atwood, *J. Am. Chem. Soc.* **1985**, *107*, 941.
[25] W. J. Evans, G. Kociokkohn, S. E. Foster, J. W. Ziller, R. J. Doedens, *J. Organomet. Chem.* **1993**, *444*, 61.
[26] M. Visseaux, D. Barbier-Baudry, O. Blacque, A. Hafid, P. Richard, F. Weber, *New J. Chem.* **2000**, *24*, 939.
[27] J. L. Namy, P. Girard, H. B. Kagan, P. E. Caro, *New J. Chem.* **1981**, *5*, 479.
[28] Z. W. Xie, K. L. Chui, Z. X. Liu, F. Xue, Z. Y. Zhang, T. C. W. Mak, J. Sun, *J. Organomet. Chem.* **1997**, *549*, 239.
[29] S. D. Stults, R. A. Andersen, A. Zalkin, *Organometallics* **1990**, *9*, 115.
[30] C. D. Sofield, R. A. Andersen, *J. Organomet. Chem.* **1995**, *501*, 271.
[31] W. J. Evans, J. M. Perotti, S. A. Kozimor, T. M. Champagne, B. L. Davis, G. W. Nyce, C. H. Fujimoto, R. D. Clark, M. A. Johnston, J. W. Ziller, *Organometallics* **2005**, *24*, 3916.
[32] W. J. Evans, R. A. Keyer, J. W. Ziller, *J. Organomet. Chem.* **1990**, *394*, 87.
[33] W. J. Evans, S. L. Gonzales, J. W. Ziller, *J. Am. Chem. Soc.* **1991**, *113*, 7423.
[34] H. J. Gosink, F. Nief, L. Ricard, F. Mathey, *Inorg. Chem.* **1995**, *34*, 1306.
[35] F. Nief, L. Ricard, *Organometallics* **2001**, *20*, 3884.
[36] W. J. Evans, K. J. Forrestal, J. W. Ziller, *J. Am. Chem. Soc.* **1998**, *120*, 9273.
[37] W. J. Evans, K. J. Forrestal, J. T. Leman, J. W. Ziller, *Organometallics* **1996**, *15*, 527.
[38] D. Carmichael, L. Ricard, F. Mathey, *J. Chem. Soc., Chem. Commun.* **1994**, 1167.
[39] M. D. Walter, D. Bentz, F. Weber, O. Schmitt, G. Wolmershauser, H. Sitzmann, *New J. Chem.* **2007**, *31*, 305.

[40] G. R. Giesbrecht, G. E. Collis, J. C. Gordon, D. L. Clark, B. L. Scott, N. J. Hardman, *J. Organomet. Chem.* **2004**, *689*, 2177.
[41] Z. W. Xie, Z. X. Liu, F. Xue, Z. Y. Zhang, T. C. W. Mak, *J. Organomet. Chem.* **1997**, *542*, 285.
[42] M. N. Bochkarev, A. A. Fagin, G. V. Khoroshenkov, *Russ. Chem. Bull., Int. Ed.* **2002**, *51*, 1909.
[43] F. Weber, H. Sitzmann, M. Schultz, C. D. Sofield, R. A. Andersen, *Organometallics* **2002**, *21*, 3139.
[44] J. Reuben, G. A. Elgavish, in *Handbook on the physics and chemistry of Rare Earths, chap 38* (Eds.: K. A. Gschneidner Jr., L. Eyring), North-Holland Publishing Company, Amsterdam, **1979**.
[45] I. Bertini, C. Luchinat, S. Aime, *Coord. Chem. Rev.* **1996**, *150*, R7.
[46] D. Barbier-Baudry, O. Blacque, A. Hafid, A. Nyassi, H. Sitzmann, M. Visseaux, *Eur. J. Inorg. Chem.* **2000**, 2333.
[47] P. B. Hitchcock, J. A. K. Howard, M. F. Lappert, S. Prashar, *J. Organomet. Chem.* **1992**, *437*, 177.
[48] M. Schultz, C. J. Burns, D. J. Schwartz, R. A. Andersen, *Organometallics* **2000**, *19*, 781.
[49] W. J. Evans, R. N. R. Broomhall-Dillard, S. E. Foster, J. W. Ziller, *J. Coord. Chem.* **1998**, *43*, 199.
[50] G. Lima, PhD thesis, University of Sussex, UK **1997**.
[51] J. van der Heijden, C. J. Schaverien, A. G. Orpen, *Organometallics* **1989**, *8*, 255.
[52] P. Gradoz, D. Baudry, M. Ephritikhine, M. Lance, M. Nierlich, J. Vigner, *J. Organomet. Chem.* **1994**, *466*, 107.
[53] A. A. Trifonov, E. N. Kirillov, S. Dechert, H. Schumann, M. N. Bochkarev, *Eur. J. Inorg. Chem.* **2001**, 3055.
[54] D. Barbier-Baudry, F. Bouyer, A. S. M. Bruno, M. Visseaux, *Appl. Organomet. Chem.* **2006**, *20*, 24.
[55] W. J. Evans, D. S. Lee, *Can. J. Chem.* **2005**, *83*, 375.
[56] W. J. Evans, T. M. Champagne, B. L. Davis, N. T. Allen, G. W. Nyce, M. A. Johnston, Y. C. Lin, A. Khvostov, J. W. Ziller, *J. Coord. Chem.* **2006**, *59*, 1069.
[57] G. V. Khoroshen'kov, A. A. Fagin, M. N. Bochkarev, S. Dechert, S. H., *Russ. Chem. Bull., Int. Ed.* **2003**, *52*, 1715.
[58] I. L. Fedushkin, V. I. Nevodchikov, M. N. Bochkarev, S. Dechert, H. Schumann, *Russ. Chem. Bull., Int. Ed.* **2003**, *52*, 154.
[59] M. N. Bochkarev, G. V. Khoroshenkov, H. Schumann, S. Dechert, *J. Am. Chem. Soc.* **2003**, *125*, 2894.
[60] T. V. Balashova, G. V. Khoroshen'kov, D. M. Kusyaev, I. L. Eremenko, G. G. Aleksandrov, G. K. Fukin, M. N. Bochkarev, *Russ. Chem. Bull., Int. Ed.* **2004**, *53*, 825.
[61] W. J. Evans, E. Montalvo, S. E. Foster, K. A. Harada, J. W. Ziller, *Organometallics* **2007**, *26*, 2904.
[62] M. A. Katkova, G. K. Fukin, A. A. Fagin, M. N. Bochkarev, *J. Organomet. Chem.* **2003**, *682*, 218.
[63] W. J. Evans, D. K. Drummond, *J. Am. Chem. Soc.* **1986**, *108*, 7440.
[64] W. J. Evans, D. K. Drummond, S. G. Bott, J. L. Atwood, *Organometallics* **1986**, *5*, 2389.
[65] Z. Hou, Y. Wakatsuki, in *Topics in Organometallic Chemistry, Vol. 2* (Ed.: S. Kobayashi), Springer, Heidelberg, **1999**.
[66] Z. M. Hou, A. Fujita, Y. G. Zhang, T. Miyano, H. Yamazaki, Y. Wakatsuki, *J. Am. Chem. Soc.* **1998**, *120*, 754.
[67] W. J. Evans, N. T. Allen, J. W. Ziller, *J. Am. Chem. Soc.* **2000**, *122*, 11749.
[68] Z. Zhu, C. Wang, X. Xiang, C. Pi, X. Zhou, *Chem. Commun.* **2006**, 2066.
[69] R. G. Finke, S. R. Keenan, D. A. Schiraldi, P. L. Watson, *Organometallics* **1987**, *6*, 1356.
[70] E. H. Braye, W. Hubel, I. Caplier, *J. Am. Chem. Soc.* **1961**, *83*, 4406.
[71] W. J. Evans, G. W. Rabe, J. W. Ziller, R. J. Doedens, *Inorg. Chem.* **1994**, *33*, 2719.
[72] M. Wedler, A. Recknagel, F. T. Edelmann, *J. Organomet. Chem.* **1990**, *395*, C26.
[73] H. Sitzmann, O. Schmitt, F. Weber, G. Wolmershauser, *Z. Anorg. Allg. Chem.* **2001**, *627*, 12.

[74] O. Schmitt, G. Wolmershauser, H. Sitzmann, *Eur. J. Inorg. Chem.* **2003**, 3105.
[75] M. Visseaux, T. Chenal, P. Roussel, A. Mortreux, *J. Organomet. Chem.* **2006**, *691*, 86.
[76] D. L. Clark, J. C. Gordon, B. L. Scott, J. G. Watkin, *Polyhedron* **1999**, *18*, 1389.
[77] W. J. Evans, G. Zucchi, J. W. Ziller, *J. Am. Chem. Soc.* **2003**, *125*, 10.

Part II

Synthesis and characterization of mono(phospholyl)lanthanide complexes and their use in polymerization catalysis

1 Introduction

Lanthanide complexes bearing two cyclopentadienyl ancillary ligands (e.g. type **A** and **B**, Figure 1) have a special place in organolanthanide chemistry due to their high activity in numerous catalytic processes.[1-5] Especially their ability to act as well-defined single-site catalysts in polymerization reactions has accelerated their development.[6-8]

Mono-cyclopentadienyl or half-sandwich complexes (e.g. type **D**, Figure 1) are electronically more unsaturated and sterically more open than lanthanocenes and may therefore exhibit increased activity in catalytic processes by analogy with d-block transition metal half-sandwich complexes.[9] However, these properties of the half-sandwich complexes make their synthesis in general more difficult than the synthesis of the corresponding bis(cyclopentadienyl) lanthanide complexes.[10] Ligand redistribution has often been observed in these systems to yield the thermodynamically more stable metallocene derivatives. In addition, the half-sandwich compounds are more difficult to handle with respect to Lewis base complexation (solvents and alkali-metal halides), air and moisture sensitivity and thermal stability. For these reasons, special care has to be taken in the choice of the ligands and the synthetic approach: the classical salt metathesis reactions are often not adequate to access these complexes, but more suitable synthetic methods need to be developed.

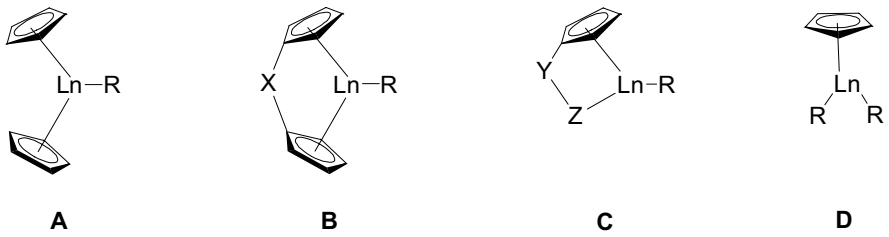

Figure 1. Schematic presentation of metallocene (**A**), ansa-metallocene (**B**), geometrically constrained (**C**) and mono-cyclopentadienyl (**D**) complexes.

An intermediate form of complexes, the so-called geometrically constrained complexes (e.g. type **C**, Figure 1), has been investigated since the early 1990s.[11] In these complexes, the ancillary cyclopentadienyl ligands are tethered with non-Cp ligands which offer additional binding sites and induce some steric strain into the molecules, in analogy to ansa-metallocenes, to increase their activity. Complexes bearing amido or phosphido groups (X = NR_2 or PR) linked by silyl or alkylsilyl groups (Y = $SiMe_2$ or CH_2SiMe_2) have been synthesized and have proven their utility as reactive single-site catalysts in a number of polymerization reactions as well as in organic synthesis.[12, 13]

In order to develop monophospholyl lanthanide chemistry - only very recently, the synthesis of the first monophospholyl scandium complexes[14] was published without further investigations on their reactivity - the following observations concerning ligand choice (ancillary and active) and synthetic pathways were considered.

Choice of ancillary ligand

Bulky ligands, such as for instance Cp*, were shown to reduce ligand redistribution in half-sandwich complexes and gave access to the first solvent-free mono(cyclopentadienyl)-bis(alkyl) complexes by metathesis reaction in 1989 (Scheme 1).[15] Although these complexes showed some activity in the polymerization of alkenes, they were not suitable for stereochemically selective processes as intermolecular ligand scrambling could occur during polymerization.

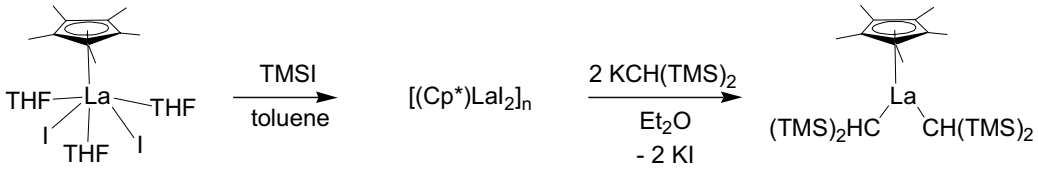

Scheme 1. Synthesis of the first monomeric solvent-free mono(cyclopentadienyl) lanthanide complex.

In order to gain control on the stereoselectivity, more rigid ligand systems were needed. This requirement was fulfilled with the geometrically constrained complexes. However, despite their good activity in many polymerization processes, until recently, one of the main aims could still not be achieved with these complexes: the syndiospecific polymerization of styrene, which had already been reported with titanium based complexes in 1986.[16]

Finally, in 2004, it was shown that activation of bulky mono(cyclopentadienyl) bis(alkyl)scandium complexes with borates led to highly active, cationic catalysts for the syndiospecific polymerization of styrene (Scheme 2).[17] Since then, a number of cationic complexes, incorporating bulky cyclopentadienyl ligands with and without additional donor groups, have been reported to exhibit very high activity and selectivity in numerous homo-and copolymerization reactions of α-olefins.[18, 19]

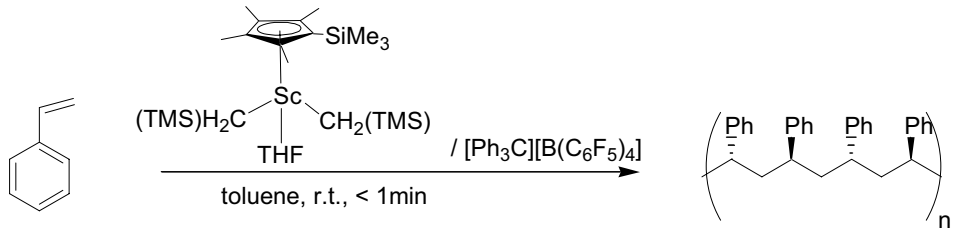

Scheme 2. Syndiospecific polymerization of styrene with a cationic mono-cyclopentadienyl complex.[17]

The development of bulky phospholyl ligands in our laboratory and their successful use in divalent lanthanide chemistry[20-22] encouraged us to investigate their utility in half-sandwich complexes for polymerization reactions. In particular, the different electronic properties of phospholyl ligands compared to cyclopentadienyl ligands, as observed in divalent lanthanide

complexes (see Part I), were supposed to have a positive influence on the catalytic properties of the monophospholyl species. The already well-investigated sterically hindered Dtp ligand seemed very suitable for the development of this chemistry as it shows good similarities to the Cp*' ligand [Cp*' = $C_5Me_4SiMe_3$], one of the most successful ligands in mono-Cp chemistry.[17, 23, 24]

Synthetic approaches

As already pointed out earlier, salt metathesis does not always afford the desired mono(cyclopentadienyl) complexes. Especially in the presence of alkyl or hydride ligands, ate-complex formation with concomitant incorporation of alkali-metal salt has been observed.[25, 26] The most successful and most widely used alternative is the synthesis by σ-bond metathesis[10], i.e. reaction of a tris(alkyl) or tris(amide)lanthanide precursor with a sterically hindered cyclopentadiene (Scheme 3). The same synthetic pathway can also be used for multidentate cyclopentadienyl-ligands, as shown in the double deprotonation of an amino-functionalized cyclopentadiene (Scheme 3).

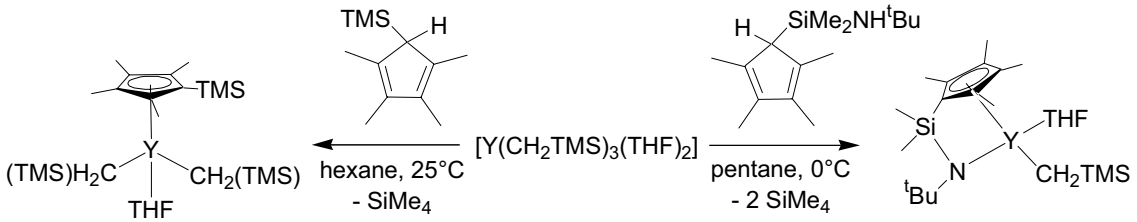

Scheme 3. Synthesis of a mono-cyclopentadienyl bis(alkyl) yttrium complex (left) and an alkyl yttrium complex containing a linked amido-cyclopentadienyl ligand (right) by σ-bond metathesis.

In the case of the phospholyl ligands, no example has been reported using σ-bond metathesis to form metal complexes. This is mainly due to the instability of most 1*H*-phospholes which can be detected at low temperatures but readily undergo [1,5]-*H* shift at room temperature. The resulting 2*H*-phospholes form immediately Diels-Alder or other coupling products (Scheme 4).[27]

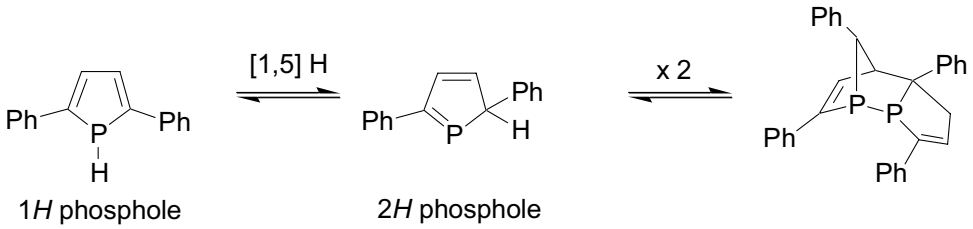

Scheme 4. Example of a typical rearrangement of 1*H*-phospholes.

Bulky substituents on the phosphole ring should inhibit follow-up reactions and allow for the stabilization of 2*H*-phospholes and hence, due to the reversibility of [1,5]-*H* shifts, give

access to 1*H* phospholes. The bulky Dtp ligand, in which not only the α-positions are blocked by tBu groups but the additional steric bulk induced by the two methyl groups in the β-positions should disfavor following Diels-Alder reactions, seemed to be a good candidate to investigate this new synthetic approach. It should be noted that previously, the only 1*H* phospholes known to be stable at room temperature were those with annelated benzo rings that prevented the [1,5] *H*-shift: a 1*H*-dibenzophosphole has already been successfully used for the synthesis of a new ligand[28] and recently the first crystallographically characterized 1*H*-phosphindole has been reported (Figure 2).[29]

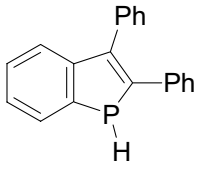

2,3-diphenyl-1*H*-phosphindole

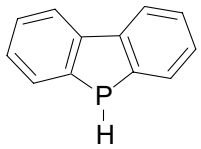

dibenzophosphole

Figure 2. A phosphindole and a dibenzophosphole.

Choice of alkyl ligand

Different alkyl, allyl and amide ligands have been studied in half-sandwich complexes, among which, the most popular are the CH_2TMS, $CH(TMS)_2$ and $N(TMS)_2$ ligands.[10] Benzyl ligands have also been introduced into organolanthanide complexes, however, they are still much less often used.[30-38] The chelating o-dimethylaminobenzyl ligand has recently been re-investigated in lanthanide chemistry as a readily available alternative to alkyl and allyl ligands.[39, 40] The homoleptic complexes $[Ln(CH_2C_6H_4NMe_2\text{-}o)_3]$ (Ln = Y, La) are stabilized by σ-bonding and intramolecular NMe_2 coordination. The unstabilized benzylic CH_2 functionality has revealed its high basicity in the double deprotonation of 9-t-BuN(H)$SiMe_2$-fluorene.[40] For these reasons, this ligand seemed to be suitable for our purpose: the stabilization of mono-phospholyl lanthanide complexes could be achieved via σ-bonding and intramolecular NMe_2 coordination of the ligand, whereas the high reactivity of the benzyl group should allow for the formation of cationic species in the polymerization process.

As this area of organolanthanide chemistry was still unexplored with the phospholyl ligands, the synthesis of monophospholyl lanthanide complexes was first investigated using the salt metathesis approach. Different lanthanide ions (Sm, Y, Sc) were used in combination with the Dtp ligand and the chelating o-dimethylaminobenzyl ligand in order to detect possible size dependent effects. In the case of Sc, the synthetic studies were extended to the σ-bond metathesis approach. The obtained complexes were then subject to polymerization tests.

2 Synthesis of monophospholyl lanthanide complexes

2.1 Synthesis of Sm and Y complexes

The reaction between equimolar amounts of $SmI_3(THF)_{3.5}$ and [K(Dtp)] in THF at room temperature yielded the corresponding monophospholyl samarium diiodide complex $[(Dtp)SmI_2(THF)_2]$ (**1**) which was isolated in good yield and fully characterized by multinuclear NMR studies, X-ray diffraction and elemental analysis. (Scheme 5). The reaction between YCl_3 and [K(Dtp)] in the same conditions had a different outcome. The ^{31}P NMR spectrum showed complete disappearance of [K(Dtp)] and the appearance of two signals at 92 and 99 ppm, in the typical region of an η^5-bound phospholyl ligand,[41, 42] with relative intensities depending on the concentration. These signals thus clearly belong to species in which the Dtp ligand is η^5-bonded to yttrium. A tentative explanation to this could be that both a neutral and an anionic species, such as respectively $[(Dtp)YCl_2(THF)_x]$ (**2a**) and $[(Dtp)YCl_3K(THF)_x]$ (**2b**), are present in solution. This hypothesis is supported by the fact that by switching to a less polar reaction medium like THF/toluene the reaction led mostly to the product at 92 ppm, which could then correspond to the neutral, less polar compound **2a**. Surprisingly, no Y-P coupling was observed, in contrast to the previously reported $[(PC_4Me_4)_2YCl_2Li(DME)_2]$.[43] In the case of the samarium complex **1**, some minor amounts of bisphospholyl complex formed, as indicated by ^{31}P NMR (28 ppm), in addition to the monosubstituted product (80 ppm).

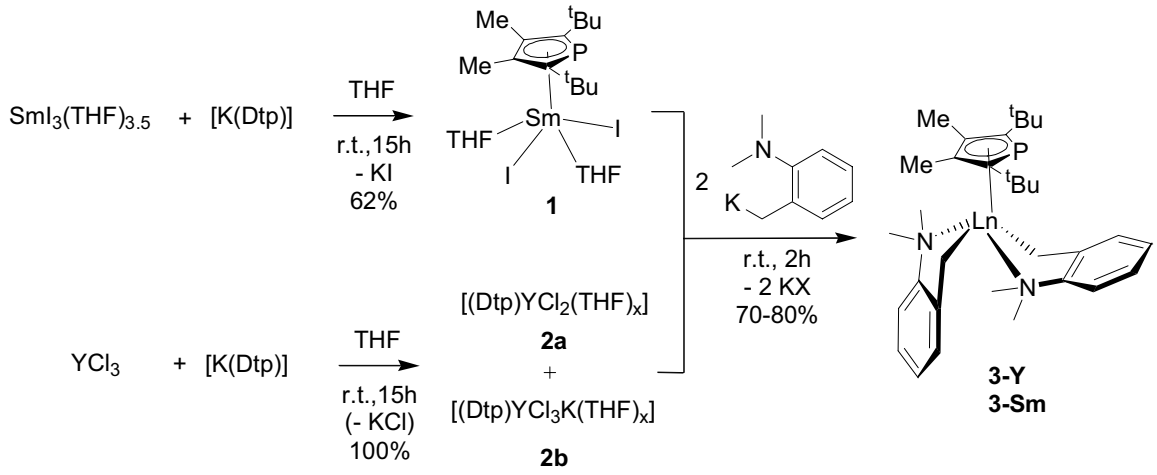

Scheme 5. Synthesis of mono(phospholyl) complexes of samarium and yttrium.

Further addition of two equivalents of *o*-dimethylaminobenzyl potassium $[K(CH_2C_6H_4NMe_2\text{-}o)]$ to the in-situ generated compounds **1** and **2** resulted in an immediate color change and ^{31}P NMR indicated quantitative transformation of the starting materials. After workup the monophospholylbis(benzyl) complexes $[(Dtp)Ln(CH_2C_6H_4NMe_2\text{-}o)_2]$ (Ln = Y (**3-Y**), Sm (**3-Sm**)) were isolated in good yields and fully characterized by multinuclear

NMR, X-ray studies and elemental analysis (Scheme 5). In the ^{31}P NMR spectra single peaks were observed at 92 ppm and 63 ppm for **3-Y** and **3-Sm**, respectively. Again, no Y-P coupling was observed for **3-Y**.

2.2 Synthesis of Sc complexes

2.2.1 Salt metathesis approach

In the case of Sc, the reaction between $ScCl_3$ and one equivalent of [K(Dtp)] in THF at room temperature probably resulted initially in the formation of the corresponding monophospholyl dichloride complex **4**, which was detected by a resonance at 100 ppm in the ^{31}P NMR spectrum; however, **4** was not stable in the reaction conditions because this resonance disappeared completely within 72h with the concomitant appearance of a signal at 6 ppm, in the typical region of P-substituted phospholes.[27] Compound **5**, a product resulting from a ring-opening reaction with THF could be isolated in nearly quantitative yield and characterized by NMR and X-ray studies (Scheme 6).

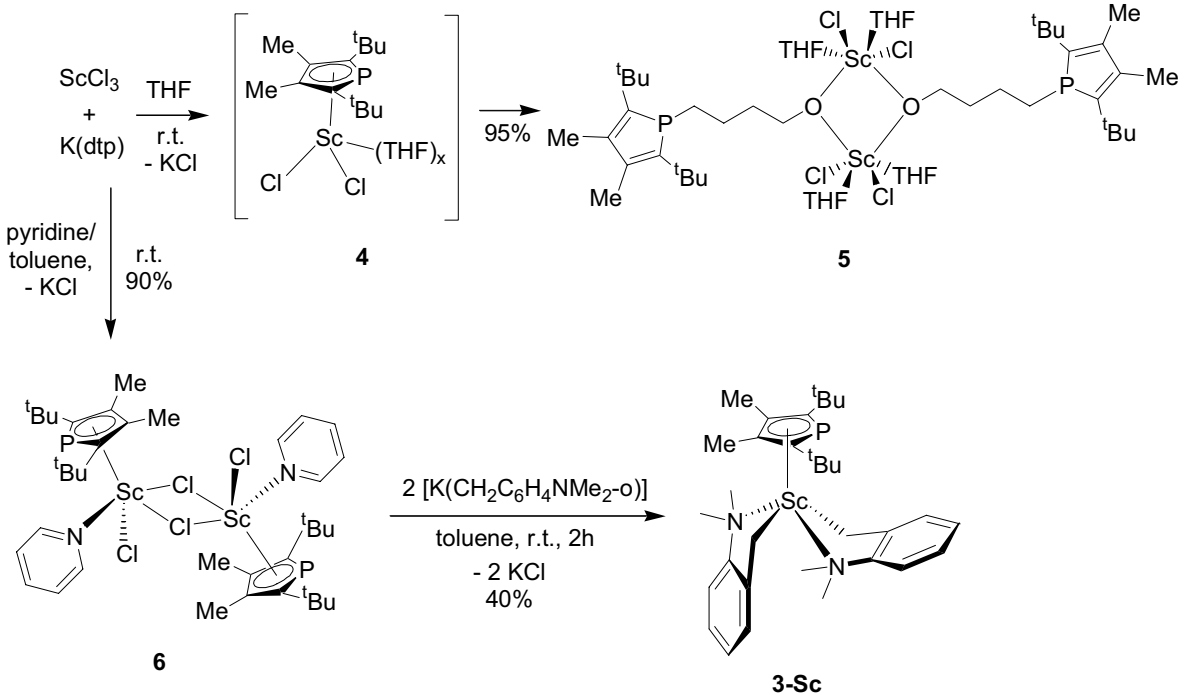

Scheme 6. Synthesis of monophospholylscandium complexes by salt metathesis reaction.

In order to prevent this unwanted ring-opening reaction, the reaction between $ScCl_3$ and [K(Dtp)] was performed in a 5:1 toluene:pyridine mixture instead of THF. This time the monophospholyldichloride complex **6** (^{31}P NMR : 120 ppm) was obtained in very good yield (scheme 6). X-ray studies confirmed the η^5 coordination of the phospholyl ligand to scandium. Addition of 2 equivalents of [K($CH_2C_6H_4NMe_2$-*o*)] to the in-situ formed complex

6 resulted in a mixture of products. In contrast, the reaction of the isolated compound **6** with two equivalents of [K($CH_2C_6H_4NMe_2$-*o*)] in toluene afforded the monophospholyl bis(benzyl) scandium complex **3-Sc** as major product as shown by NMR studies.

2.2.2 σ-bond metathesis approach

Since the synthesis of **3-Sc** using the salt metathesis approach had proven to be less efficient than the one-pot syntheses of **3-Y** and **3-Sm**, the σ-bond metathesis approach was investigated to access **3-Sc**.

Protonation of [K(Dtp)] with one equivalent of *p*-toluenesulfonic acid (PTH) in toluene resulted in the formation of 1*H*-phosphole **7** as the major compound, as indicated by the shift in the ^{31}P NMR from 58 to -53 ppm, a doublet with a typical P-H coupling of 211 Hz.[27] A small peak at 220 ppm, in the typical range of di-coordinated phosphorus compounds,[44] was attributed to 2*H*-phosphole **8**. The ratio between these two peaks remain constant over time, suggesting that an equilibrium between **7** and **8** is present, strongly shifted to the side of the 1*H*-phosphole **7**. No trace of a phosphole dimer could be detected in the reaction mixture. It thus seems that the substitution pattern on the Dtp ring kinetically stabilizes the Dtp-H phosphole both in the 1*H* and the 2*H* forms; however, all attempts to isolate **7** were unsuccessful.

Nonetheless, addition of one equivalent of [Sc($CH_2C_6H_4NMe_2$-*o*)$_3$] to the in-situ generated **7** and heating the reaction mixture at 60°C for one night led to the quantitative formation of complex **3-Sc**, as indicated by ^{31}P NMR (Scheme 7). **3-Sc** was characterized by multinuclear NMR and X-ray studies. To the best of our knowledge this is the first example of the successful synthesis of a phospholyl-metal complex using the deprotonation of a 1*H* phosphole.

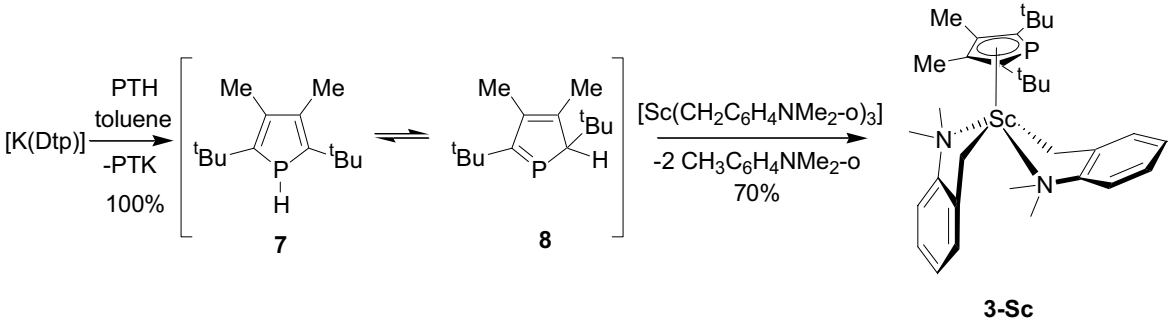

Scheme 7. Synthesis of monophospholylscandium complex **3-Sc** by σ-bond metathesis reaction.

3 X-ray structure analyses

3.1 Monophospholyl dihalide complexes

An X-ray study was carried out for [(Dtp)$SmI_2(THF)_2$] (**2**), which crystallized in the conformation of a four-legged pianostool with the two iodide ligands and the two THF molecules trans to each other (Figure 3). Whereas all the reported monocyclopentadienyl samariumdiiodo complexes crystallized with three solvent molecules,[45-49] the bulky Dtp ligand allowed only for the coordination of two solvent molecules.

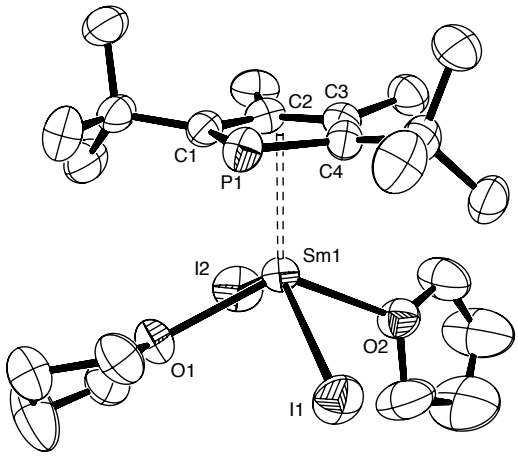

Figure 3. ORTEP plot (50% ellipsoids) of one molecule of [(Dtp)$SmI_2(THF)_2$] (2). Hydrogen atoms have been omitted for clarity. Selected bond distances (Å) and angles (°): Sm(1)-O(2) = 2.443(4), Sm(1)-O(1) = 2.442(4), Sm(1)- P(1) = 2.9112(14), Sm(1)-I(2) = 3.0575(5), Sm(1)-I(1) = 3.0663(6), O(2)-Sm(1)-O(1) = 131.37(13), O(2)-Sm(1)-I(2) = 77.97(9), O(1)-Sm(1)-I(2) = 83.41(9), O(2)-Sm(1)-I(1) = 79.92(1), O(1)-Sm(1)-I(1) = 81.27(9), I(2)-Sm(1)-I(1) = 133.363(16).

In contrast to the monomeric structure of the samarium diiodide **1**, the scandium dichloride complex [(Dtp)Sc(μ-Cl)Cl(NC_5H_5)]$_2$ (**6**) (Figure 4) formed a dimer in the solid state with two bridging chlorides and one pyridine coordinated to the metal center. The Sc-$(Dtp)_{centroid}$ distance (2.252 Å) lies between the ones observed for [$(Me_4C_4P)_2ScCl_2Li$(tmeda)] (2.29(1) Å) and for [$(Me_4C_4P)Sc[CH(SiMe_3)_2]Cl_2Li$(tmeda)] (2.220(3) Å).[14] This is in agreement with the different coordination numbers observed in these complexes. The bridging chlorides in **6** show Sc-Cl bond distances of 2.623 Å and 2.502 Å which are significantly longer than in [$(Me_4C_4P)Sc[CH(SiMe_3)_2]Cl_2Li$(tmeda)] (2.445 Å and 2.444 Å), due to the presence of the strong donating pyridine and the free chloride ligand. In contrast the Sc-Cl nonbridging bond distances in **6** are comparable to those observed in **5** or in other mono(cyclopentadienyl)scandium complexes.[50, 51]

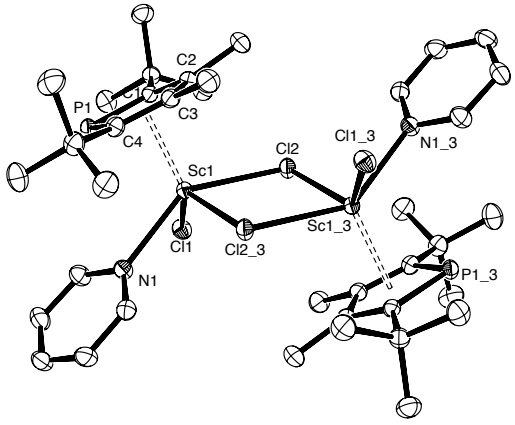

Figure 4. ORTEP plot (50% ellipsoids) of one molecule of $[(Dtp)Sc(\mu\text{-}Cl)Cl(NC_5H_5)]_2$ (6). Hydrogen atoms and one molecule of co-crystallized toluene have been omitted for clarity. Selected bond distances (Å) and angles (°): Sc(1)-N(1) = 2.383(1), Sc(1)-Cl(1) = 2.4090(5), Sc(1)-Cl(2) = 2.6231(5), Sc(1)-Cl(2_3) = 2.5022(5), Sc(1)-P(1) = 2.6960(5), N(1)-Sc(1)-Cl(1) = 82.42(3), N(1)-Sc(1)-Cl(2_3) = 83.38(3), Cl(1)-Sc(1)-Cl(2_3) = 124.71(2), N(1)-Sc(1)-Cl(2) = 140.83(4), Sc(1_3)-Cl(2)-Sc(1) = 103.84(2), Cl(1)-Sc(1)-Cl(2) = 82.40(2), Cl(2_3)-Sc(1)-Cl(2) = 76.16(2).

3.2 Monophospholylbis(benzyl)complexes

3-Sm and **3-Y** were obtained as monoclinic crystals in the space group $P2_1$ with two molecules of a single enantiomer in the unit cell, whereas **3-Sc** crystallized as monoclinic crystals in the space group $P2_1/n$ with one molecule of each enantiomer in the unit cell (Figure 5). Some selected bond distances and angles are summarized in table 1.

The average Ln-$(Dtp)_{centroid}$ distances increase in consistency with the metal size going from **3-Sc** (2.36 Å) over **3-Y** (2.52 Å) to **3-Sm** (2.59 Å). These values also show the elongation of the metal-$(Dtp)_{centroid}$ distance when the two halide ligands in **2** and **6**, with Ln-$(Dtp)_{centroid}$ distances of 2.51 Å and 2.25 Å, respectively, are replaced by the dimethylaminobenzyl ligand. These observations were attributed to the higher steric demand of the benzyl ligand. The average Y-CH_2 (2.44 Å) and Y-NMe_2 (2.58 Å) distances of **3-Y**, are similar to the distances observed in $[Y(CH_2C_6H_4NMe_2\text{-}o)_3]$, 2.47 Å and 2.56 Å, respectively. [40] Å multihapto binding mode was reported for the benzyl ligand in $[Ln(CH_2C_6H_4NMe_2\text{-}o)_3]$ (Ln = Y, La).[40] This observation was confirmed by **3-Y** and **3-Sm**, although less pronounced, in which some interactions between Y and C_{ipso} and between Sm and C_{ipso} and C_{ortho} could be considered. In contrast, **3-Sc** did not show any interaction between the metal and the C_{ipso} or C_{ortho} atoms of the benzyl ligand.

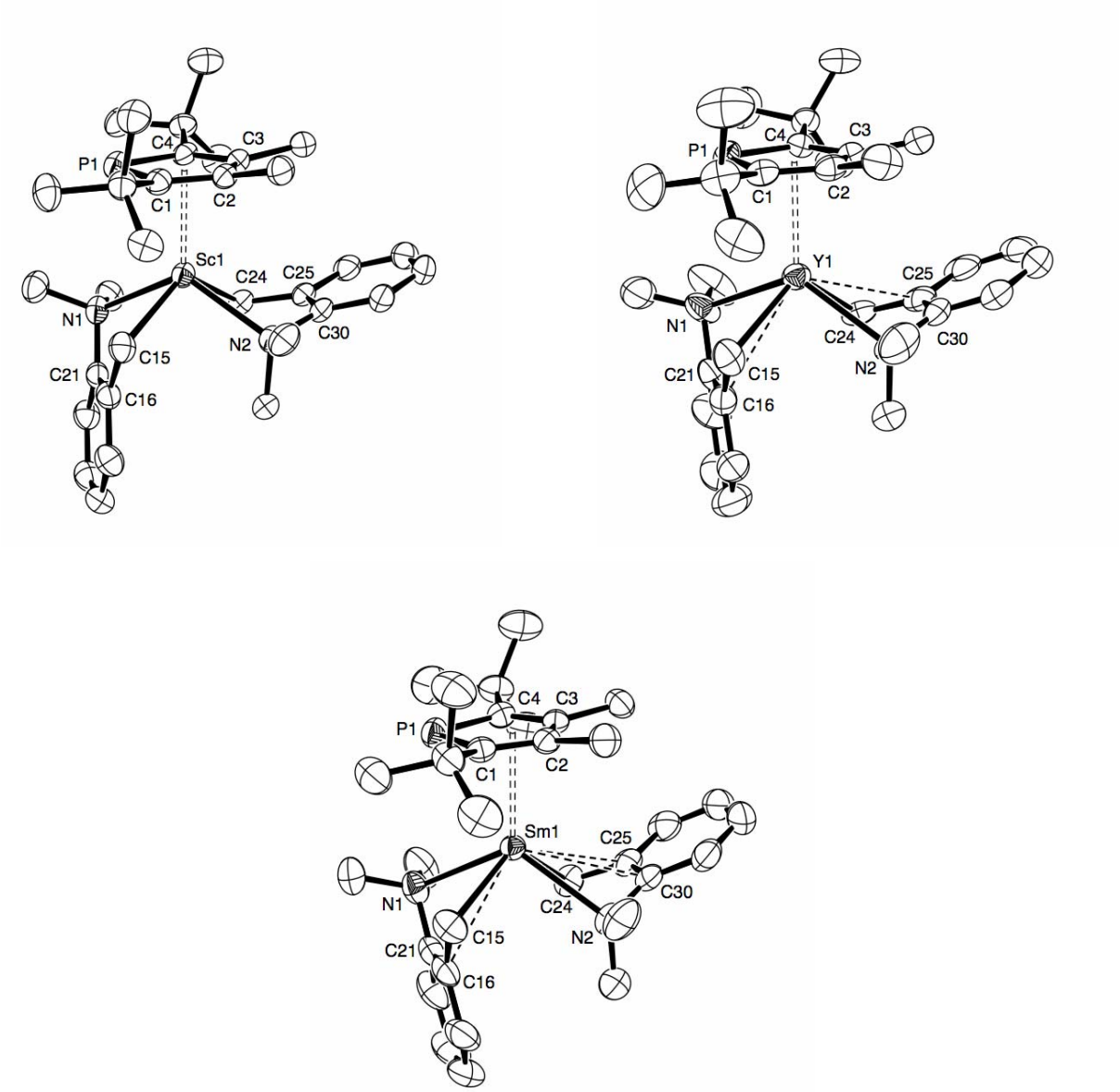

Figure 5. ORTEP plot (50% ellipsoids) of one molecule of [(Dtp)(o-Me_2N-benzyl)$_2$Sc] (**3-Sc**), [(Dtp)(o-Me_2N-benzyl)$_2$Y] (**3-Y**) and [(Dtp)(o-Me_2N-benzyl)$_2$Sm] (**3-Sm**). Hydrogen atoms have been omitted for clarity. In each case, only one molecule of the two independent molecules in the unit cell is shown. The additional bonding interactions (Sm1-C16, Sm1-C25 and Sm1-C30; Y1-C16 and Y1-C25) are shown with dashed lines.

Table 1. Selected bond distances (Å) and angles (°) for complexes **3-Ln**

	3-Sc	**3-Y**	**3-Sm**		**3-Sc**	**3-Y**	**3-Sm**
Ln1-P1	2.769(1)	2.928(1)	3.009(1)	**Ln1-C16**	3.043(4)	3.025(5)	3.022(4)
Ln1-C1	2.631(3)	2.793(4)	2.862(3)	**Ln1-C25**	2.995(4)	3.013(5)	2.981(4)
Ln1-C2	2.673(3)	2.814(4)	2.834(3)	**Ln1-C30**	3.071(4)	3.084(5)	3.029(3)
Ln1-C3	2.717(3)	2.820(4)	2.866(3)	**N1-Ln-C15**	69.9(1)	67.4(1)	66.4(1)
Ln1-C4	2.724(3)	2.862(4)	2.926(4)	**N2-Ln-C24**	71.1(1)	68.6(1)	67.6(1)
Ln1-C15	2.289(3)	2.443(3)	2.505(3)	**N1-Ln-C24**	84.6(1)	87.8(2)	86.8(1)
Ln1-C24	2.283(3)	2.447(4)	2.519(4)	**N2-Ln-C15**	83.8(1)	84.2(1)	84.5(1)
Ln1-N1	2.529(2)	2.595(4)	2.630(3)	**C15-Ln-C24**	121.9(1)	116.9(2)	120.6(1)
Ln1-N2	2.453(2)	2.576(3)	2.620(3)	**N1-Ln-N2**	126.93(8)	129.6(1)	123.8(1)

3.3 THF-ring opening with Sc

THF ring opening with phosphide complexes was observed by Evans[52] in $[(Cp^*)_2SmPPh_2(THF)]$ and Schumann[53] in $[(Cp)_2LuPPh_2(THF)]$, leading to $[(Cp^*)_2Sm[O(CH_2)_4PPh_2](THF)]$ and $[\{(Cp)_2Lu[\mu\text{-}O(CH_2)_4PPh_2]\}_2]$, respectively. In both cases, nucleophilic attack of the phosphide on the activated metal-bound THF can be presumed. With the η^5-bound phospholyl ligand, a similar transformation seems less likely. However, from group 4 chemistry it is known that an equilibrium between the η^5- and η^1-coordination of the phospholyl ligand to the metal center can occur.[54]

On this basis the following mechanism for the formation of **5** is proposed: the reaction of $ScCl_3$ and [K(Dtp)] leads first to the formation of $[(\eta^5\text{-Dtp})ScCl_2(THF)_x]$ which can be observed for a short time in ^{31}P NMR. This compound is in equilibrium with $[(\eta^1\text{-Dtp})ScCl_2(THF)_x]$ (not detectable in ^{31}P) which can undergo THF ring-opening by nucleophilic attack of the phosphide on the ether group of THF which is highly activated by the Lewis acidic Sc center. The resulting low-coordinated Sc-complex further dimerizes immediately to **5**.

The X-ray structure of **5** (Figure 6) reveals many similarities to the above-mentioned Lu-compound. The Sc_2O_2 center is quasi planar (dihedral angle 3.5°) with a Sc-Sc distance (3.285 Å) that is shorter than the corresponding Lu-Lu distance (3.475 Å) due to the differences in metal size and coordination numbers. The chloride ligands and the THF molecules are trans to each other as already observed for **2**. In the phosphole ring the double bonds (1.355-1.360 Å) can be clearly distinguished from the single bond (1.475 Å) and the P-CH_2 bond (1.862 Å) is close to that observed in the Lu-compound (1.847 Å).[53]

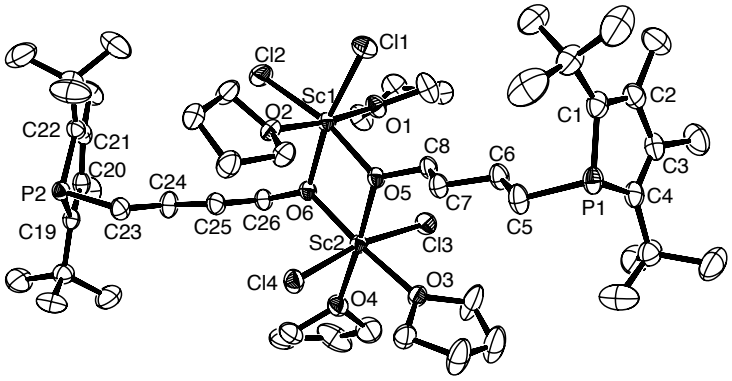

Figure 6. ORTEP plot (50% ellipsoids) of one molecule of [{Sc[μ-O$(CH_2)_4$(Dtp)]$Cl_2(THF)_2\}_2$] (**5**). Hydrogen atoms have been omitted for clarity. Selected bond distances (Å) and angles (°): P(1)-C(5) = 1.862(2), Sc(1)-O(5) = 2.092(1), Sc(1)-Sc(2) = 3.2848(5), O(5)-Sc(1)-O(6) = 74.73(4), Sc(2)-O(5)-Sc(1) = 104.16(4), Cl(2)-Sc(1)-Cl(1) = 97.87(2), Cl(4)-Sc(2)-Cl(3) = 169.94(2), O(1)-Sc(1)-O(2) = 174.26(4), O(4)-Sc(2)-O(3) = 91.20(4).

4 Polymerization tests with monophospholylbis(benzyl) complexes

Neutral mono-Cp bis(alkyl) lanthanide complexes have been reported to show no or very low activity in the polymerization of α-olefins,[55-57] in contrast to the isoelectronic cationic group 4 metal mono-Cp analogues. However, the use of cationic lanthanide alkyl complexes bearing Cp ligands for the syndiospecific polymerization of styrene has recently been reported.[18, 19] Complexes **3-Ln** were therefore tested in this reaction to see the influence of the phospholyl ligand on the reaction outcome (Table 2).

Table 2. Syndiospecific polymerisation of styrene by **3-Ln** complexes[a]

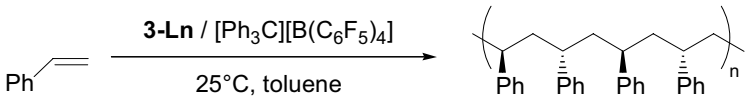

run	Ln	[M]/[Ln]	T (min)	Yield[b](%)	Activity[c]	M_n[d] (10^3)	M_w/M_n[d]	Efficiency[e](%)
1	Sc	500	<1	100	>3125	300.0	2.07	17
2	Y	500	30	84	87	77.7	1.55	67
3	Y	100	1	50	308	8.8	1.67	118
4	Sm	100	30	0	0	-	-	-

[a] Conditions: Ln, 21μmol; [Ln]/[B] = 1/1 (mol/mol); solvent/monomer = 5/1 (v/v). [b] Weight of polymer obtained/ weight of monomer used. [c] Given in (kg of sPS) x (mol Ln)$^{-1}$ x h^{-1}. [d] Determined by GPC in trichlorobenzene at 145 °C against polystyrene standard. [e] Catalyst efficiency = M_n(calculated)/M_n(measured)

Addition of styrene to a 1:1 reaction mixture of **3-Sc** or **3-Y** and $[Ph_3C][(C_6F_5)_4B]$ in toluene at room temperature led to the immediate formation of syndiotactic polystyrene. **3-Sc** gave excellent results which could be well compared with those reported for the Cp*'-ligated Sc bis(alkyl) complex $[(Cp^{*'})Sc(CH_2SiMe_3)_2(THF)]$.[17] The phospholyl ligand did not negatively influence the polymerisation as it was observed for some group 4 catalysts.[58] Surprisingly, the activity observed for **3-Y** was much higher than that for $[(Cp^{*'})Y(CH_2SiMe_3)_2(THF)]$.[17] However, the activated **3-Sm** complex did not show any activity under the same conditions in accordance with a previous observation on the reactivity of monocyclopentadienyl complexes of the larger lanthanides in styrene polymerisation.[17] It should also be noted that none of the neutral complexes afforded polystyrene.

5 Conclusion and Outlook

In this part we have shown that solvent-free mono(phospholyl)lanthanide bis(aminobenzyl) complexes [(Dtp)Ln($CH_2C_6H_4NMe_2$-*o*)$_2$] (**3-Ln**) (Ln = Sm, Y, Sc) can be obtained by two distinct reaction pathways:

The one-pot reactions of lanthanide trihalides $LnCl_3$ with one equivalent of [K(Dtp)] and two equivalents of [K($CH_2C_6H_4NMe_2$-*o*)] in THF afford the samarium and yttrium complexes **3-Sm** and **3-Y**. The analogous Sc complex cannot be prepared in a one-pot fashion as THF-ring opening occurs at the Lewis acidic Sc center. By changing the solvent from THF to toluene/pyridine a scandium monophospholyldichloride compound can be isolated from the reaction of $ScCl_3$ with one equivalent of [K(Dtp)]. This complex reacts further with two equivalents of [K($CH_2C_6H_4NMe_2$-*o*)] in toluene to yield **3-Sc**.

An alternative approach is the σ-metathesis reaction between the protonated Dtp-H ligand and [Sc($CH_2C_6H_4NMe_2$-*o*)$_3$]. This pathway is accessible, probably, because of the steric bulk of the Dtp ligand which hinders Diels-Alder reactions of the 1*H*-phosphole. Hence, the 1*H*-phosphole is even stable at room temperature and deprotonation using the basic benzyl ligands can occur.

The obtained **3-Sc** and **3-Y** complexes show high activity for the syndiospecific polymerization of styrene when treated with one equivalent of [Ph_3C][$(C_6F_5)_4B$]. In contrast, the neutral complexes and activated **3-Sm** do not give any polystyrene product.

Outlook

In order to evaluate the full potential of mono-phospholyl lanthanide complexes as polymerization catalysts, the synthesized “prototype” complexes need to be investigated in other homo-and copolymerization reactions using ethylene, α-olefins and cyclic olefins.

Structural variations of the catalytic complexes may include the use of differently substituted phospholyl rings and the exchange of the bis(benzyl) ligands against more reactive alkyl or allyl ligands.

The variations on the phospholyl ring may concern the steric bulk, for example, the exchange of the Dtp ligand against the Htp ligand, or may have electronic influence as in the case of the Dsp ligand, i.e. exchange of electron-donating tBu groups against electron-stabilizing TMS groups, or both, the steric and electronic factors, as in the case of the Hsp ligand (Scheme 8). These ligands would therefore allow the investigation of the factors that govern the stability of half-sandwich complexes.

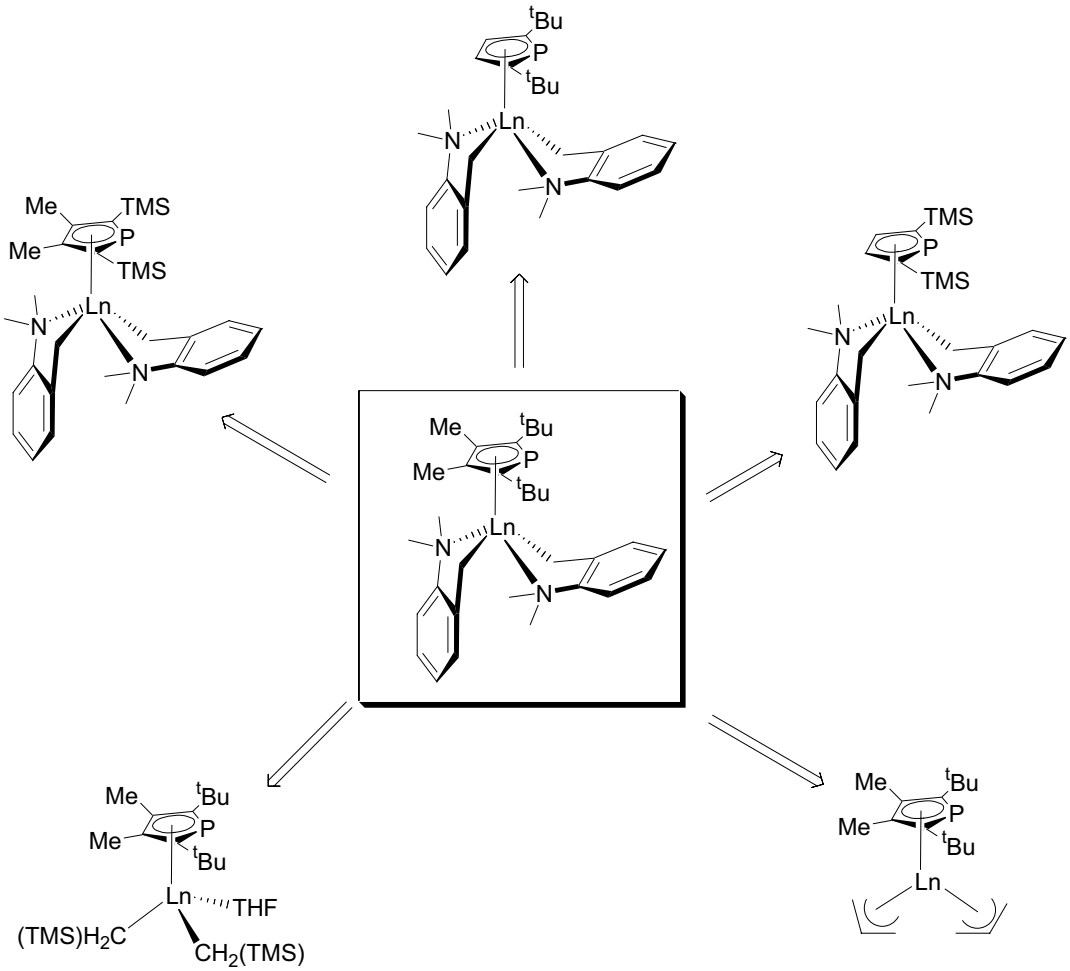

Scheme 8. Possible variations on the monophospholylbis(aminobenzyl) complexes.

The exchange of the aminobenzyl ligand against alkyl or allyl ligands may increase the reactivity of the resulting complexes as no additional, stabilizing σ-donation (dimethylamino groups) is possible with these ligands (Scheme 8). For these complexes the newly developed σ-metathesis approach will be more favorable than the salt-metathesis reactions as it avoids ate-complex formation.

In addition, the use of alkyl ligands may also facilitate the synthesis of monophospholyl hydride complexes. The analogous mono-Cp hydride complexes have attracted much interest, due to their new reactivities, e.g. in the copolymerization of cyclohexene oxide with carbon monoxide or the hydrogenation of carbon monoxide.[13, 59, 60] If the phospholyl ligands also lead to the formation of hydride clusters as in the case of the Cp ligands, one can imagine the synthesis of heterobimetallic complexes via σ-bonding of the lone-pairs on the phosphorus (Scheme 9).

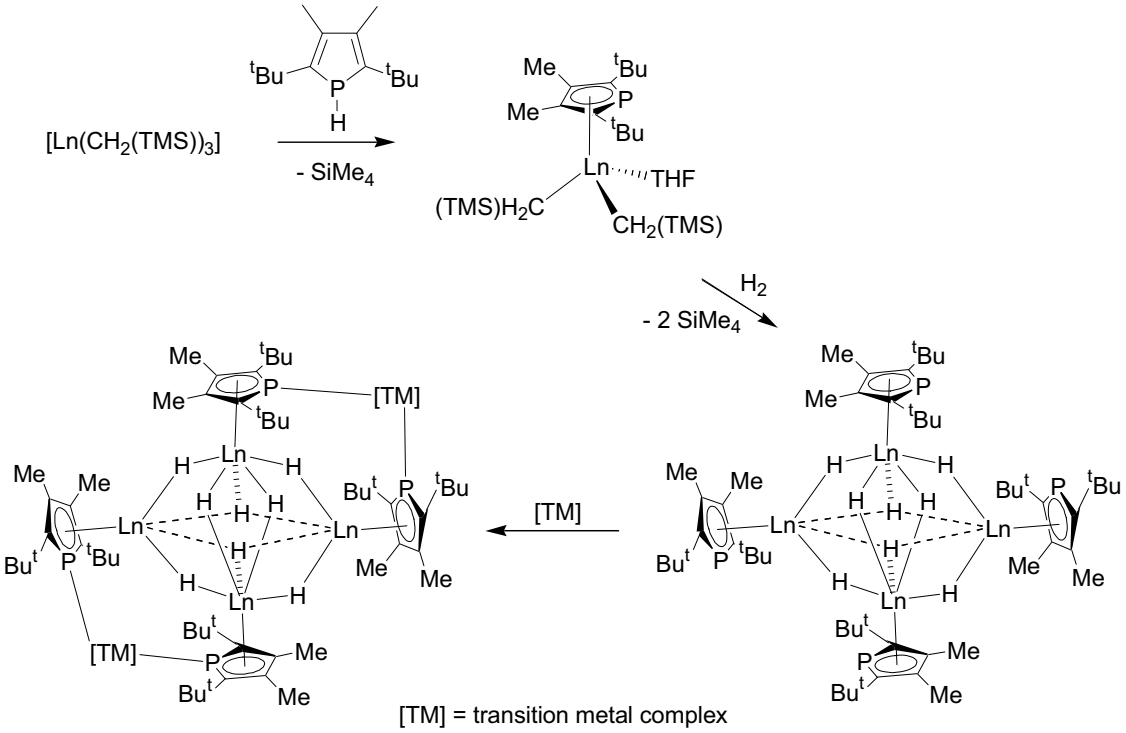

Scheme 9. Proposed synthesis of a monophospholyl polyhydride heterobimetallic cluster.

6 References

[1] S. Hong, T. J. Marks, *Acc. Chem. Res.* **2004**, *37*, 673.
[2] G. A. Molander, J. A. C. Romero, *Chem. Rev.* **2002**, *102*, 2161.
[3] H. Schumann, J. A. Meese-Marktscheffel, L. Esser, *Chem. Rev.* **1995**, *95*, 865.
[4] V. Monteil, R. Spitz, C. Boisson, *US patent 7,094,854*, **2006**.
[5] T. J. Marks, H. Mauermann, *US patent 4,668,773*, **1987**.
[6] J. Gromada, J. F. Carpentier, A. Mortreux, *Coord. Chem. Rev.* **2004**, *248*, 397.
[7] Z. M. Hou, Y. Wakatsuki, *Coord. Chem. Rev.* **2002**, *231*, 1.
[8] Y. Nakayama, H. Yasuda, *J. Organomet. Chem.* **2004**, *689*, 4489.
[9] R. Poli, *Chem. Rev.* **1991**, *91*, 509.
[10] S. Arndt, J. Okuda, *Chem. Rev.* **2002**, *102*, 1953.
[11] P. J. Shapiro, E. E. Bunel, W. P. Schaefer, J. E. Bercaw, *Organometallics* **1990**, *9*, 867.
[12] J. Okuda, *Dalton Trans.* **2003**, 2367.
[13] O. Tardif, M. Nishiura, Z. M. Hou, *Organometallics* **2003**, *22*, 1171.
[14] F.-G. Fontaine, K. A. Tupper, T. D. Tilley, *J. Organomet. Chem.* **2006**, *691*, 4595.
[15] J. van der Heijden, C. J. Schaverien, A. G. Orpen, *Organometallics* **1989**, *8*, 255.
[16] N. Ishihara, T. Seimiya, M. Kuramoto, M. Uoi, *Macromolecules* **1986**, *19*, 2464.
[17] Y. Luo, J. Baldamus, Z. Hou, *J. Am. Chem. Soc.* **2004**, *126*, 13910.
[18] P. M. Zeimentz, S. Arndt, B. R. Elvidge, J. Okuda, *Chem. Rev.* **2006**, *106*, 2404.
[19] Z. M. Hou, Y. J. Luo, X. F. Li, *J. Organomet. Chem.* **2006**, *691*, 3114.
[20] F. Nief, B. T. de Borms, L. Ricard, D. Carmichael, *Eur. J. Inorg. Chem.* **2005**, 637.
[21] D. Turcitu, F. Nief, L. Ricard, *Chem.-Eur. J.* **2003**, *9*, 4916.
[22] F. Nief, D. Turcitu, L. Ricard, *Chem. Commun.* **2002**, 1646.
[23] K. C. Hultzsch, T. P. Spaniol, J. Okuda, *Angew. Chem. Int. Ed.* **1999**, *38*, 227.
[24] X. F. Li, J. Baldamus, Z. Hou, *Angew. Chem. Int. Ed.* **2005**, *44*, 962.
[25] I. Albrecht, H. Schumann, *J. Organomet. Chem.* **1986**, *310*, C29.
[26] H. Schumann, I. Albrecht, J. Pickardt, E. Hahn, *J. Organomet. Chem.* **1984**, *276*, C5.
[27] F. Mathey, *Chem. Rev.* **1988**, *88*, 429.
[28] C. Thoumazet, L. Ricard, H. Grützmacher, P. Le Floch, *Chem. Commun.* **2005**, 1592.
[29] J. G. Cordaro, D. Stein, H. Grützmacher, *J. Am. Chem. Soc.* **2006**, *128*, 14962.
[30] A. G. Avert, F. G. N. Cloke, B. R. Elvidge, P. B. Hitchcock, *Dalton Trans.* **2004**, 1083.
[31] S. Bambirra, M. J. R. Brandsma, E. A. C. Brussee, A. Metsma, B. Hessen, J. H. Teuben, *Organometallics* **2000**, *19*, 3197.
[32] S. Bambirra, A. Meetsma, B. Hessen, *Organometallics* **2006**, *25*, 3454.
[33] W. J. Evans, T. A. Ulibarri, J. W. Ziller, *Organometallics* **1991**, *10*, 134.
[34] S. Harder, *Angew. Chem. Int. Ed.* **2004**, *43*, 2714.
[35] P. G. Hayes, W. E. Piers, L. W. M. Lee, L. K. Knight, M. Parvez, M. R. J. Elsegood, W. Clegg, *Organometallics* **2001**, *20*, 2533.
[36] L. W. M. Lee, W. E. Piers, M. R. J. Elsegood, W. Clegg, M. Parvez, *Organometallics* **1999**, *18*, 2947.
[37] A. Mandell, J. Magull, *Z. Anorg. Allg. Chem.* **1996**, *622*, 1913.
[38] A. A. Trifonov, T. P. Spaniol, J. Okuda, *Organometallics* **2001**, *20*, 4869.
[39] L. E. Manzer, *J. Am. Chem. Soc.* **1978**, *100*, 8068.
[40] S. Harder, *Organometallics* **2005**, *24*, 373.
[41] F. Nief, *Eur. J. Inorg. Chem.* **2001**, 891.
[42] P. Le Floch, *Coord. Chem. Rev.* **2006**, *250*, 627.
[43] F. Nief, F. Mathey, *Chem. Commun.* **1989**, 800.

[44] F. Zurmühlen, M. Regitz, *J. Organomet. Chem.* **1987**, *332*, C1.
[45] A. A. Trifonov, P. Van der Weghe, J. Collin, A. Domingos, I. Santos, *J. Organomet. Chem.* **1997**, *527*, 225.
[46] D. Stellfeldt, G. Meyer, G. B. Deacon, *Z. Anorg. Allg. Chem.* **1999**, *625*, 1252.
[47] W.-P. Leung, F.-Q. Song, F. Xue, Z.-Y. Zhang, T. C. W. Mak, *J. Organomet. Chem.* **1999**, *582*, 292.
[48] W. J. Evans, T. S. Gummersheimer, J. W. Ziller, *Appl. Organomet. Chem.* **1995**, *9*, 437.
[49] V. K. Belskii, Y. K. Gunko, E. B. Lobkovskii, B. M. Bulychev, G. L. Soloveichik, *Metalloorg. Khim. (Russ.)* **1991**, *4*, 420.
[50] L. D. Henderson, G. D. MacInnis, W. E. Piers, M. Parvez, *Can. J. Chem.* **2004**, *82*, 182.
[51] M. D. Fryzuk, G. R. Giesbrecht, S. G. Rettig, *Can. J. Chem.* **2000**, *78*, 2003.
[52] W. J. Evans, J. T. Leman, J. W. Ziller, S. I. Khan, *Inorg. Chem.* **1996**, *35*, 4283.
[53] H. Schumann, E. Palamidis, J. Loebel, *J. Organomet. Chem.* **1990**, *384*, C49.
[54] Y. J. Ahn, R. J. Rubio, T. K. Hollis, F. S. Tham, B. Donnadieu, *Organometallics* **2006**, *25*, 1079.
[55] K. C. Hultzsch, T. P. Spaniol, J. Okuda, *Angew. Chem. Int. Ed.* **1999**, *38*, 227.
[56] K. C. Hultzsch, P. Voth, K. Beckerle, T. P. Spaniol, J. Okuda, *Organometallics* **2002**, *19*, 228.
[57] P. J. Shapiro, W. D. Cotter, W. P. Schaefer, J. A. Labinger, J. E. Bercaw, *J. Am. Chem. Soc.* **1994**, *116*, 4623.
[58] C. Janiak, *Coord. Chem. Rev.* **2006**, *250*, 66.
[59] D. M. Cui, M. Nishiura, Z. Hou, *Macromolecules* **2005**, *38*, 4089.
[60] D. M. Cui, O. Tardif, Z. M. Hou, *J. Am. Chem. Soc.* **2004**, *126*, 1312.

Part III

Synthesis and characterization of new lanthanide mono- and bis-carbene complexes: Investigations on the nature of the Ln-C multiple bond

1 Introduction

Over the past decades, the chemistry of transition metal carbene complexes has been thoroughly explored and recent works have clearly demonstrated the relevance of carbenes as ancillary or active ligands in many catalytic processes of important synthetic value, as for example in olefin metathesis reactions and Fischer-Tropsch processes.[1-11] In contrast, examples of well-defined lanthanide species incorporating these ligandsremain scarce.[12]

Transition metal carbene complexes can be divided into two main groups.[3] In Fischer carbenes metals in a low formal oxidation state interact with carbene ligands which are further stabilized by -OR or -NR_2 ligands. The orbital interactions can be described as σ-donation from a filled σ-type ligand orbital into a an empty σ-type metal orbital and subsequent π-back-donation from a metal d-orbital to an empty p(π) orbital on the carbon atom. Fischer carbenes are therefore in general electrophilic (Figure 1).

In contrast, Schrock-type carbene or alkylidene complexes contain transition metals in a high formal oxidation state and alkyl substituted carbene ligands. The bonding is best described as a covalent double bond between a triplet carbene and a triplet metal fragment, which leads to a nucleophilic carbene and shorter metal carbon bond distances compared to Fischer carbenes (Figure 1).

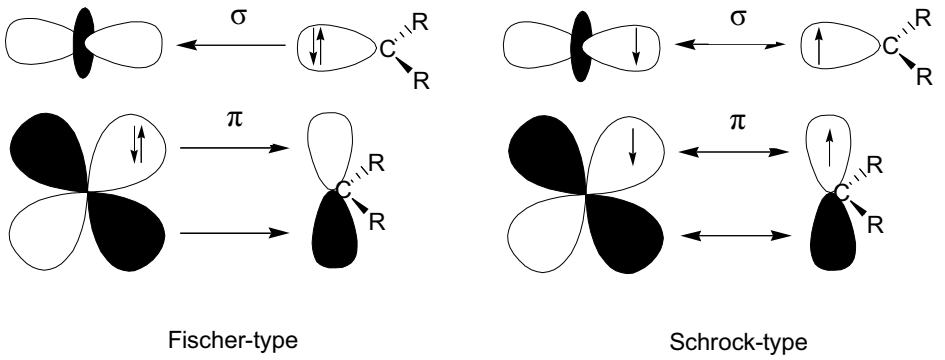

Figure 1. Orbital interactions in Fischer-type carbene complexes (left) and Schrock-type carbene complexes (right).

The development of analogous lanthanide carbene chemistry is hampered by the fact, that the 4f-orbitals are very contracted and cannot participate directly in bonding interactions.[13-15] As a consequence, bonding is mainly electrostatic in nature in lanthanide complexes[16] and no contribution from the lanthanide ion (d^0-configuration) to the carbene stabilization via π-backbonding is possible. In addition, the empty $5d_\pi$-orbitals – which partially control the charge on the carbene carbon in transition metal complexes - are more energetic in the more electropositive lanthanides than in d-block metals such as Ta and W, thus resulting in a greater energy mismatch of relevant metal and ligand orbitals.[12]

For these reasons, mainly N-heterocyclic carbene (NHC) complexes (Fischer-type) of both divalent and trivalent lanthanides have been synthesized and investigated as in these complexes the carbene fragment is stable without back-donation from the metal center (Figure 2).[17-28] The NHC ligand acts as neutral two-electron σ-donor, in analogy to phosphines and THF, and forms metal-carbene carbon single bonds as recently confirmed by theoretical studies.[29]

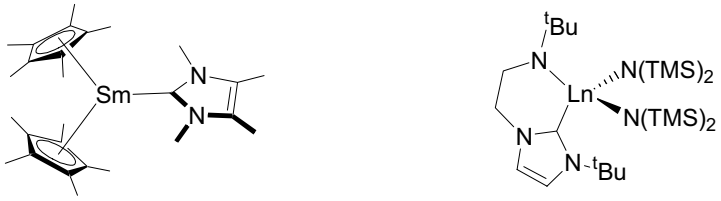

Figure 2. Examples of a divalent (left) and a trivalent (right) NHC lanthanide complexes.

Only two examples of structurally characterized lanthanide alkylidene complexes have been reported so far. The first example was obtained by Cavell by the in-situ deprotonation of a bis(iminophosphorane)methylene ligand using a tris(alkylamide) samarium precursor (Scheme 1).[30, 31] The second examples are yttrium and lanthanum clusters in which a dianionic methylidene ligand (H_2C^{2-}) is stabilized by Y(III) or La(III).[32] However, neither the reactivity nor the electronic nature of the lanthanide carbon multiple bond in these complexes have been studied in detail.

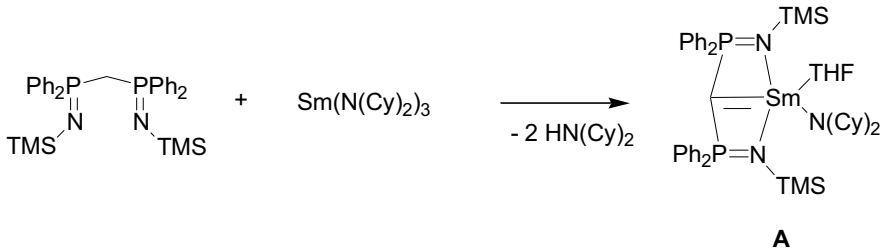

Scheme 1. Synthesis of the first lanthanide alkylidene complex **A**.

In order to explore a more general synthesis for lanthanide alkylidene complexes and to obtain a better insight into the nature of the lanthanide carbon multiple bond we based our choice of the ligand and the synthetic approach on the following considerations.

Ligand choice

For the formation of a formal lanthanide carbon double four electrons are necessary. As none of these electrons can derive from the trivalent metal ion, the ligand has to provide the entire four electrons. In our group, the synthesis and coordination behavior of the stable dianionic ligand 1,1-dilithio-bis(diphenylthiophosphinoyl)methane [Li_2(SPCPS)] (**1**) towards different metals has been explored (Scheme 2).[33, 34] These investigations have allowed the

synthesis of a number of new carbene complexes of both electron-rich and electron-deficient metal fragments by a formal two electron reduction of the metal. In addition, the thiophosphinoyl groups can contribute to the stabilization of the carbene complexes by coordination to the metal center. Theoretical studies have revealed that the negative charges on the dianionic ligand are stabilized by negative hyperconjugation with the P-S and P-C(phenyl) antibonding orbitals.[35]

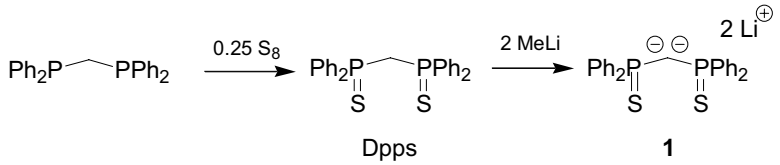

Scheme 2. Synthesis of Dpps and the dianionic ligand [Li_2(SPCPS)] (**1**).

This dianionic ligand **1** therefore seemed to be a suitable precursor for exploring the synthesis of new lanthanide alkylidene complexes.

Reaction conditions

The σ-bond metathesis reaction employed for the synthesis of Cavell's alkylidene complex **A** was shown to be only suitable for highly reactive tris(alkylamide) precursors - for example, the less basic [Ln(N(SiHMe$_2$)$_2$)$_3$] precursors did not form the corresponding alkylidene complexes.[36, 37] We therefore envisaged the use of the dianionic ligand **1** in salt metathesis reactions with lanthanide trihalides. This would not only allow for the possible nucleophilic substitution of the remaining halide ligand, but also the synthesis of bis(carbene) complexes could be attempted, which was not possible by a σ-bond metathesis reaction. As the cation size plays an important role in the reactivity of lanthanide complexes, an example of both, early (Sm) and late (Tm) lanthanide metal, needed to be investigated.

2 Synthesis of mono(carbene) complexes of samarium and thulium

Addition of one equivalent of dianion **1** to $LnI_3(THF)_{3.5}$ (Ln = Sm, Tm) under an argon atmosphere yielded the quantitative formation of complexes [{(SPCPS)Ln(μ-I)(THF)$_2$}$_2$] (Ln = Sm (**2**), Tm (**3**)) (Scheme 3). After workup yellow **2** and white **3** were isolated and **2** was fully characterized by multi-nuclear NMR techniques. In contrast, for **3** no interpretable NMR spectrum could be obtained due to the high paramagnetism of Tm, the rather short Tm-proton and Tm-phosphorus distances and possible THF exchange in solution (see Part I, 3.3).

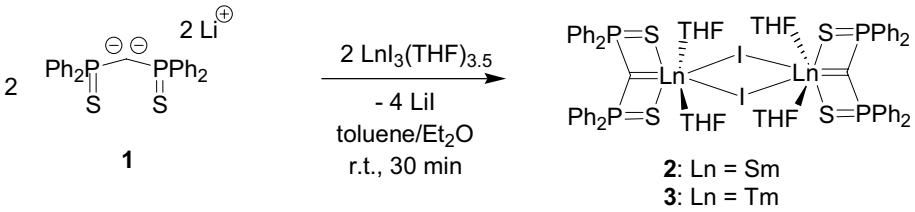

Scheme 3. Synthesis of mono(carbene) complexes of samarium and thulium.

In ^{31}P NMR spectroscopy, complex **2** is characterized by a broad singlet markedly low-shifted relative to the dianionic precursor (**2**, 51.8 ppm; **1**, 20.6 ppm). Though no ^{13}C NMR signal could be recorded for the carbenic carbon atom which is directly bound to the paramagnetic Sm(III) center, the absence of methylenic protons was confirmed by ^{1}H NMR. Crystals of **2** suitable for X-ray analysis were grown by cooling a solution of the complex in a diethyl ether/toluene/hexanes mixture, whereas crystals of **3** were obtained by diffusion of hexanes into a toluene solution of the complex (Figure 3).

2 and **3** crystallize as iodine bridged dimers with two molecules of THF bound to the lanthanide center. The coordination sphere of the lanthanide adopts a distorted C2-symmetrical edge-capped octahedral geometry with the metal in the PCP plane. Considering the coordination number in these complexes, the most striking feature is the short Ln-C bond (2.36 Å (av.) for **2**; 2.32 Å for **3)** which possesses multiple bond character, since it is considerably shorter - by over 0.1 Å - than the average Ln-C distance (2.48 Å for Sm; 2.44 Å for Tm).[38] Compared to the Sm-C bond length in the carbene complex **A** (2.467(4) Å), a shortening is observed in **2** which may be due to the planarity of the carbene fragment: in **2** the samarium atom lies in the SPCPS plane and the sum of the angles around the carbene atom equals 360°, whereas compound **A** forms an open-book structure and the angles at the carbene sum up to 321°.[30, 31] The short P-C bond distances measured in **2** and **3** (1.66 Å av.) result very likely from negative hyperconjugation from carbon to phosphorus σ* orbitals as in the case of free **1**.[35] The bond shortenings observed for the Tm-C, Tm-S and Tm-I bonds are in agreement with the well-known lanthanide contraction. In contrast, no change in bond lengths or angles is observed for the alkylidene fragment. The electronic nature of the metal carbon bond seems therefore to be similar for early and late lanthanide centers.

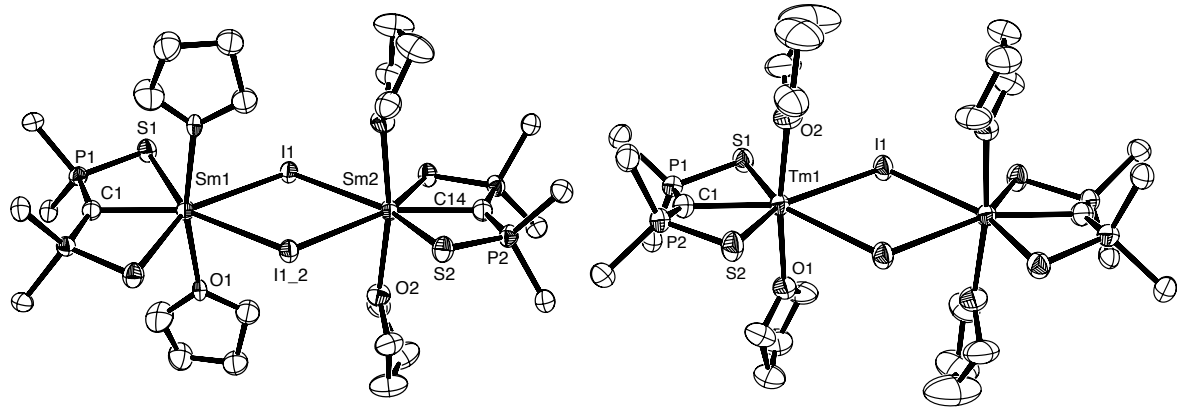

Figure 3. ORTEP-plot (50% probability ellipsoids) of one molecule of **2** (left) and **3 (**right). Hydrogen atoms, phenyl rings (only ipso-carbon atoms are shown) and co-crystallized toluene molecules were omitted for clarity. Selected bond distances (Å) and angles (°): **2** : Sm(1)-C(1) = 2.371(6), Sm(2)-C(14) = 2.352(6), Sm(1)-S(1) = 2.891(1), Sm(1)-S(2) = 2.922(1), Sm(1)-I(1) = 3.3021(4), Sm(2)-I(1) = 3.2413(4), Sm(1)-O(1) = 2.476(3), Sm(1)-O(2) = 2.435(3), P(1)-C(1) = 1.675(2), P(2)-C(1) = 1.667(2), P(1)-C(1)-P(1_2) = 146.2(4), P(2)-C(14)-P(2_2) = 145.4(4), P(1)-C(1)-Sm(1) = 106.9(2), P(2)-C(14)-Sm(2) = 107.3(2) ; **3** : Tm(1)-C(1) = 2.325(5), Tm(1)-S(1) = 2.822(1), Tm(1)-S(2) = 2.777(1), Tm(1)-I(1) = 3.1575(4), Tm(1)-O(1) = 2.307(3), Tm(1)-O(2) = 2.323(3), P(1)-C(1) = 1.661(5), P(2)-C(1) = 1.653(5), P(1)-S(1) = 2.024(2), P(2)-S(2) = 2.030(2), P(1)-C(1)-P(2) = 150.8(3), P(1)-C(1)-Tm(1) = 104.6(2), Tm(1)-C(1)-P(2) =104.0(2).

However, the observed short Ln-C bond lengths are not sufficient to fully determine the nature of the Ln-C multiple bond as they could be the result of purely electrostatic interactions without any orbital overlap. Further information was obtained from the synthesis of bis(carbene) complexes and reactivity tests.

3 Synthesis of homoleptic bis(carbene) complexes of samarium and thulium

In order to assert the strong Lewis basicity of dianion **1**, substitution of the three iodide ligands in $LnI_3(THF)_{3.5}$ by two equivalents of the dianionic ligand **1** was attempted. This reaction led to the new complexes $[\{Li(THF)_4\}\{(SPCPS)_2Ln\}]$ (Ln = Sm (**4**), Tm(**5**)) (Scheme 4) which are the first examples of homoleptic bis(carbene) complexes in the lanthanide series.

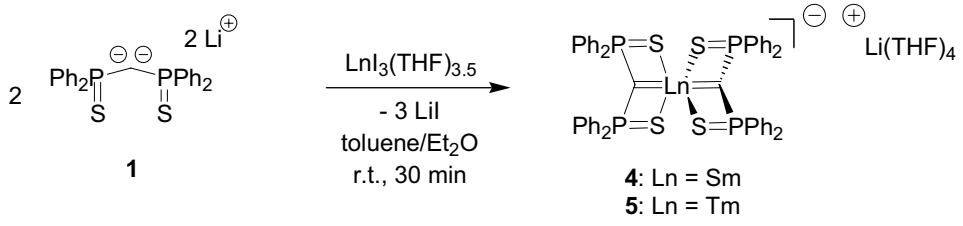

Scheme 4. Synthesis of homoleptic bis(carbene) complexes of samarium and thulium.

4 was fully characterized by multinuclear NMR spectroscopy. Its ^{31}P NMR spectrum shows a large peak at 46.2 ppm and, as in the case of **2**, no resonance could be observed in the ^{13}C NMR spectrum for the two carbenic centers. Crystals of **4** and **5** suitable for X-ray analysis were grown from slow diffusions of hexanes into toluene solutions of the compounds. The crystals of both complexes exhibited a phase transition at low temperature (near 177 K for **5**, not exactly determinable for **4**), which allowed us to obtain two significantly different structures at 150 K (**4a** and **5a**, two molecules in unit cell, Figure 4) and at 230 K (**4b** and **5b**, one molecule in unit cell, Figure 5).[39]

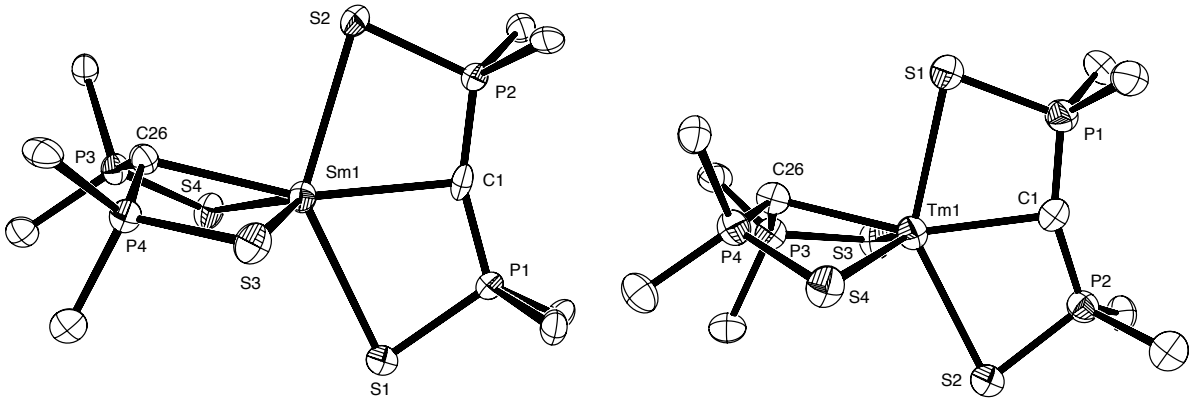

Figure 4. ORTEP plot (50% probability ellipsoids) of the anionic part of **4a** (left) and **5a** (right) (the solvated $Li(THF)_4^+$ cation was omitted for clarity). H atoms were also omitted and only the ipso carbon atoms of the phenyl rings are shown. Selected bond distances (Å) and angles (°): **4a** : Sm(1)-C(1) = 2.491(5), Sm(1)-C(26) = 2.507(5), Sm(1)-S(1) = 2.858(2), Sm(1)-S(2) = 2.816(2), Sm(1)-S(3) = 2.851(2), Sm(1)-S(4) = 2.824(2), P(1)-C(1)-P(2) = 156.4(4), P(3)-C(2)-P(4) = 136.5(4), P(1)-C(1)-Sm(1) = 99.1(3), P(2)-C(1)-Sm(1) = 100.8(3), P(4)-C(26)-Sm(1) = 97.8(2), P(3)-C(26)-Sm(1) = 98.0(2), C(1)-Sm(1)-C(26) = 160.4(2) ; **5a** : Tm(1)-C(26) = 2.423(9), Tm(1)-(C1) = 2.378(9), Tm(1)-S(1) = 2.751(2), Tm(1)-S(2)= 2.788(2), Tm(1)-S(3) = 2.754(2), Tm(1)-S(4) = 2.747(2), P(1)-C(1) = 1.657(9), P(2)-C(1) = 1.647(9), P(3)-C(26) = 1.673(9), P(4)-C(26) = 1.655(9), P(1)-C(1)-P(2) = 158.0(6), P(1)-C(1)-Tm(1) = 101.3(4), P(2)-C(1)-Tm(1) = 100.6(4), P(3)-C(26)-P(4) = 134.6(6), P(3)-C(26)-Tm(1) = 96.1(4), P(4)-C(26)-Tm(1) =97.7(4).

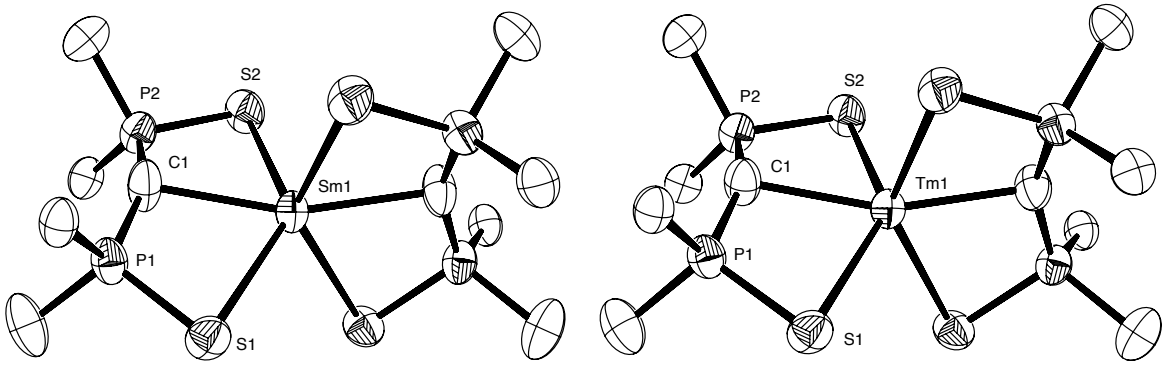

Figure 5. ORTEP plot (50% probability ellipsoids) of the anionic part of **4b** (left) and **5b** (right) (the solvated $Li(THF)_4^+$ cation was omitted for clarity). H atoms were also omitted and only the ipso carbon atoms of the phenyl rings are shown. Selected bond distances (Å) and angles (°): **4b** : Sm(1)-C(1) = 2.448(8), Sm(1)-S(1) = 2.833(2), Sm(1)-S(2) = 2.835(2), P(1)-C(1) = 1.645(8), P(2)-C(1) = 1.632(8), P(1)-C(1)-P(2) = 151.2(6), P(1)-C(1)-Sm(1) = 100.5(4), P(2)-C(1)-Sm(1) = 101.4(4) ; **5b** : Tm(1)-C(1) = 2.368(3), Tm(1)-S(1) = 2.7655(7), Tm(1)-S(2) = 2.7618(7), P(1)-C(1) = 1.652(3), P(2)-C(1) = 1.647(3), P(1)-C(1)-P(2) = 151.1(2), P(1)-C(1)-Tm(1) = 100.1(1), P(2)-C(1)-Tm(1) = 100.7(1).

The crystals of the samarium and the thulium complexes have similar geometries and only the typical distance variations due to the lanthanide contraction were observed. We will therefore focus our discussion on the thulium complexes **5a** and **5b**, however, the same conclusions can be drawn for the samarium compounds.

In the low temperature form **5a**, the two carbenic moieties are geometrically different. In one fragment, the carbon C26 is tetrahedral with Σangles = 332° (av.). The corresponding Tm1-C26 bond distance of 2.42 Å (av.) falls in the range of Tm-C single bonds. In the second fragment, the geometry at the carbon atom is strictly planar (Σangles = 360° (av.)) and a shorter Tm1-C1 bond distance of 2.38 Å is measured (however longer than in **3**). These geometrical parameters are in favor of a double bond character for the C1-Tm1 bond. Therefore, as shown in scheme 5, in this structure a strongly localized electron distribution is observed. The overall charge is mainly located on the tetrahedral C26 atom, which clearly exhibits a significant sp^3 character. While the C26 carbon center behaves as a two electron X-type ligand, the C1 center donates four electrons to stabilize the thulium(III) center.

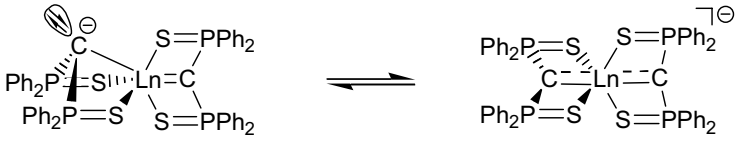

4a: Ln=Sm
5a: Ln=Tm
low temperature

4b: Ln=Sm
5b: Ln=Tm
high temperature

Scheme 5. Schematic drawing of the bonding situation in the bis(carbene) complexes **4** and **5** at low-temperature (left) and at high temperature (right).

At 230 K, another structure was observed for complex **5**. In this form (**5b**), the two carbenic moieties are identical (related by a C_2 axis). The P-C and P=S bonds as well as the Tm-S bonds are not perturbed by this modification of geometry (**5a** to **5b**). Moreover, the Tm1-C1 bond distance of 2.368(3) Å is the average between double (2.32 Å in **3**) and single (Tm1-C26: 2.42 in form **5a**) bonds and is similar to the Tm1-C1 bond length in **5a** (2.38 Å). Most interestingly, the geometry at both carbon atoms is here nearly planar (Σangles = 351.9°) and suggests the coordination of formally two four electron donor ligands. Taken together, these data can be attributed to a delocalization of the anionic charge over the two carbon and the thulium atoms, as shown in scheme 5, thereby indicating that a π-overlap develops between these three atoms. Indeed, Gordon and coworkers recently showed, that empty lanthanide d-orbitals are involved in the stabilization of lanthanide imido complexes via π-donation from the imido ligand to the metal fragment.[12] In the same way, we propose that the two alkylidene fragments interact via both σ and π donation with the thulium center in form **5b**.

The solid state dimorphism of **4** and **5** emphasizes the different electronic effects involved in the stabilization of this class of alkylidene complexes. First the additional charge involved in these complexes can be centered at the carbon atom (low-temperature form). This geometry is in complete agreement with the ability of the bis(thiophosphinoyl)methylene ligand to accommodate a dianionic center. More surprisingly, the high temperature form of these complexes reveals that to a certain extent the metal center is also able to participate in stabilizing this extra charge via its delocalization on the Ln-C backbone using the empty d-orbitals on the lanthanide center.

4 Reactivity tests

4.1 Reactivity towards electrophiles

As no data on the reactivity of lanthanide carbene complexes was reported, we investigated the reactivity of the carbene complexes **2**-**5**. Since all these complexes were derived from coordination of dianion **1** to an electron-deficient lanthanide center, one could expect that these species exhibit a reactivity similar to that of Schrock-type carbene complexes. In order to assess the nucleophilicity of **2** and **3**, reaction with benzophenone was attempted. As expected, the Wittig-like reaction resulted in the formation of the tetra-substituted olefin **6** which was fully characterized by NMR techniques and X-ray crystallography (Scheme 6, Figure 6).[40-42] This product could not be obtained by reacting the dianion **1** itself with benzophenone. This result establishes the carbenic nature of the Ln-C bonds in **2** and **3** and their nucleophilic character.

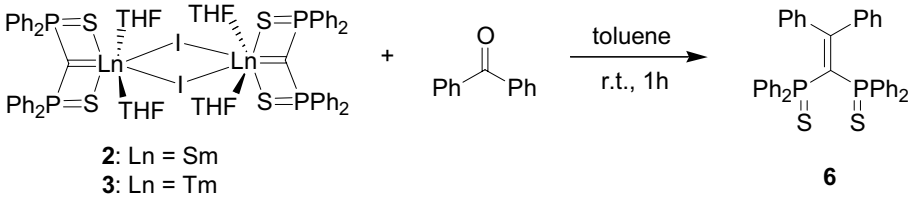

Scheme 6. Reaction of mono(carbene) complexes **2** and **3** with benzophenone.

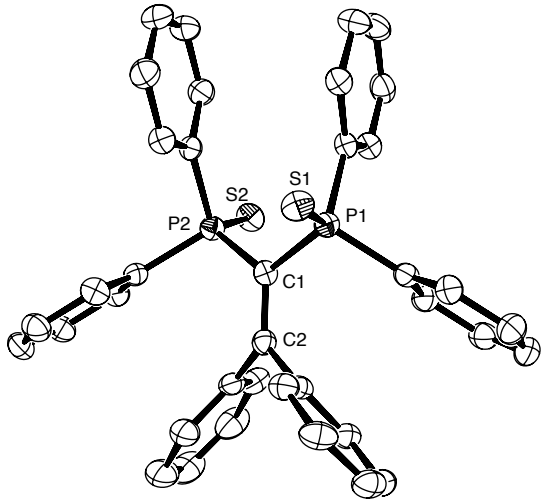

Figure 6. ORTEP-plot (50% probability ellipsoids) of one molecule of **6**. Hydrogen atoms were omitted for clarity. Selected bond distances (Å) and angles (°): C(1)-C(2) = 1.368(3), P(1)-C(1) = 1.845(2), P(2)-C(1) = 1.836(2), P(1)-S(1) = 1.9532(7), P(2)-S(2) = 1.9593(7), P(1)-C(1)-P(2) = 119.9(1).

Since the reaction between benzophenone and **2** or **3** was fast, no intermediate could be observed in ^{31}P NMR. In order to shed some light on the synthetic pathway, we also attempted to react benzophenone with the anionic complexes **4** and **5**. This time the reaction was less rapid and led to the final product **6** only after several hours. Indeed, the driving force of this reaction being the formation of ionic samarium oxide, we expected that the overall negative charge in **4** or **5** would kinetically stabilize a monomeric intermediate which would not easily rearrange into the highly energetic samarium oxide.

Addition of one equivalent of benzophenone to **4** in toluene led to the immediate disappearance of the signal of **4** in the ^{31}P NMR spectrum with the concomitant appearance of a new complex **7** characterized by two broad singlets at 43.9 and 49.4 ppm (Scheme 7). Multinuclear NMR spectra recorded for this compound support the structure assigned for complex **7** which involves the addition of one benzophenone molecule onto one carbene moiety of complex **4** while the other carbene fragment remains intact. However, rearrangement of this kinetic isomer **7** to the more stable final products (**6**, samarium oxide and other intractable products) occurs in solution over a period of about ten hours at room temperature. Our efforts have thus concentrated on trapping this intermediate by crystallization. Slow diffusion of a saturated solution of benzophenone in hexanes onto a

solution of **4** (or **5**) in toluene, resulted in the growth of pale yellow crystals on the interface of the two solutions within one hour. X-ray structure analysis of these crystals revealed the unexpected formation of the new complexes **8** (Sm) and **9** (Tm) (Figure 7). These two complexes result from the addition of one molecule of benzophenone on each carbene moiety. Dissolution of the crystals in toluene or THF (^{31}P NMR: 50.2 ppm for **8**) led to the rapid formation of olefin **6**, hence confirming that **8** and **9** are reaction intermediates in this transformation.

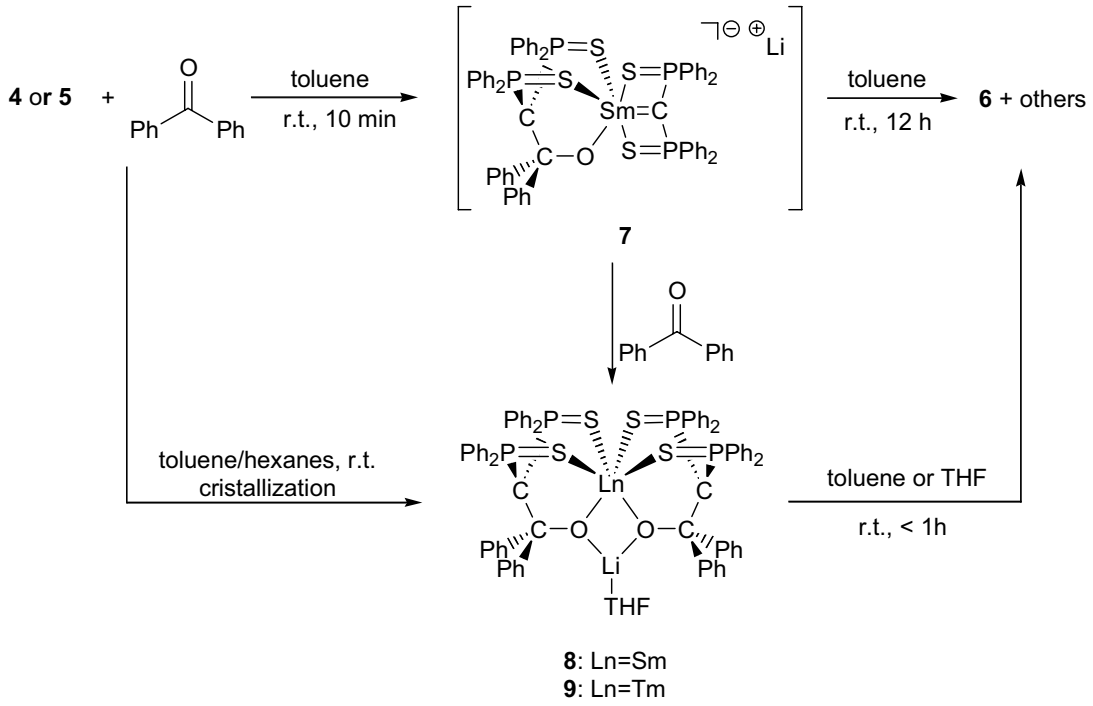

Scheme 7. Reaction of bis(carbene) complexes **4** and **5** with benzophenone.

Complexes **8** and **9** are isostructural and we will therefore concentrate our discussion only on the samarium complex **8**. The recorded structure confirms **8** as an intermediate in the transformation of carbene complex **4** into olefin **6**. Indeed, a new C-C sigma bond has formed (1.56 Å vs. 1.37 Å in the final product **6**) whilst the Sm-C multiple bond has been cleaved (3.57 Å vs. 2.46 Å in reactant **4**). Simultaneously, the benzophenone C=O bond is significantly elongated (1.42 Å in 6 vs. 1.22 Å in free benzophenone) and a new energetic Sm-O bond interaction arises (2.24 Å). Metalla-oxetanes have often been proposed as intermediates in the reaction of early transition metal carbene complexes with carbonyl compounds.[40-44] Due to their instability, only few related intermediates have been isolated so far. In our case, the structures of **8** and **9** support the idea that this transformation very likely proceeds through the formation of an open metalla-oxetane in which the lanthanide carbene bond is cleaved because of geometric constraints. The sp^3 character found for the C1 atom (Σangles = 345°) in **8** is consistent with a significant remaining negative charge induced by such cleavage.

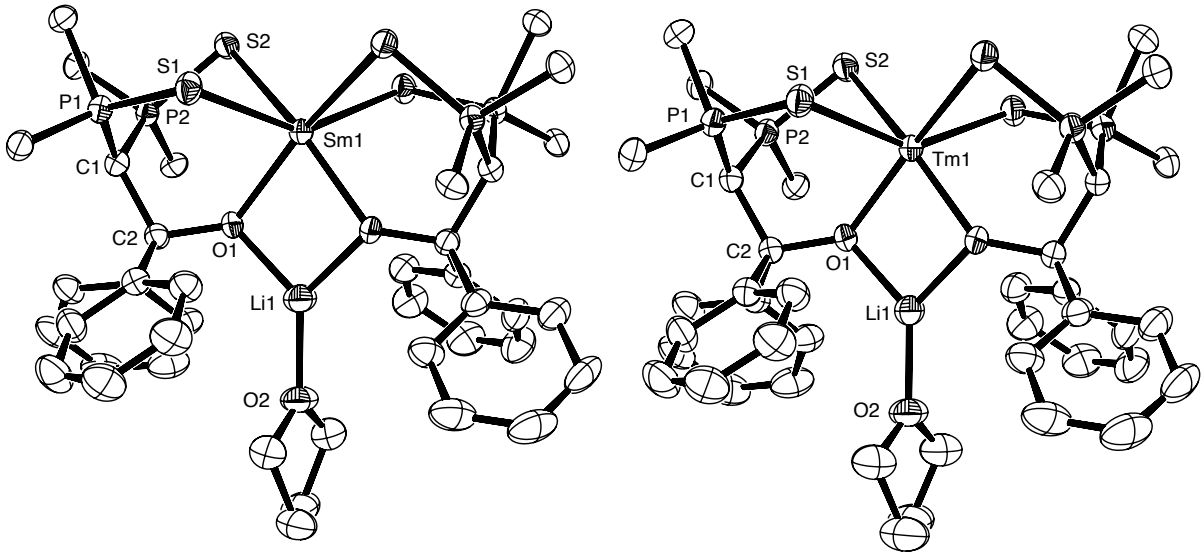

Figure 7. ORTEP-plot (50% probability ellipsoids) of one molecule of **8** (left) and **9 (**right). Hydrogen atoms and phenyl rings (only ipso-carbon atoms are shown, except on benzophenone) were omitted for clarity. Selected bond distances (Å) and angles (°): **8**: Sm(1)-O(1) = 2.237(2), Sm(1)-S(1) = 2.843(1), Sm(1)-S(2) = 2.856(1), P(2)-C(1) = 1.768(4), P(1)-C(1) = 1.755(4), O(1)-C(2) = 1.418(4), C(1)-C(2) = 1.558(5), S(1)-P(1) = 2.031(1), S(2)-P(2) = 2.022(1), P(1)-C(1)-P(2) = 112.5(2) ; **9** : Tm(1)-O(1) = 2.154(2), Tm(1)-S(1) = 2.7566(8), Tm(1)-S(2) = 2.772(1), S(1)-P(1) = 2.033(1), S(2)-P(2) = 2.022(1), P(1)-C(1) = 1.751(3), P(2)-C(1) = 1.767(3), O(1)-C(2) = 1.427(4), C(1)-C(2) = 1.559(5), P(1)-C(1)-P(2) = 111.8(2).

4.2 Nucleophilic substitution

One advantage of using the dianionic ligand **1** as carbene precursor in the synthesis of **2** and **3** is, as already pointed out earlier, the possibility of nucleophilic substitution at the lanthanide center to replace the remaining iodide ligand by alkali metal alkyls, amides or cyclopentadienyls, hence giving access to a large variety of new carbene complexes. We will concentrate on reactions of the samarium complex **2** with nucleophiles as it was possible to follow the reactions by NMR spectroscopy.

Addition of one equivalent of [Li(CH(TMS)$_2$)] or [K(N(TMS)$_2$)] to a solution of **2** in toluene or THF resulted in the formation of new products as indicated by the shifts in the ^{31}P NMR spectra. However, no product could be isolated from these reactions and the ^{1}H NMR spectra were not conclusive. In contrast, addition of one equivalent of [NaCp*] to a solution of **2** in THF or toluene led to the immediate formation of two new signals in the ^{31}P NMR spectrum while the signal for some remaining carbene complex **2** was strongly reduced. The new peaks could be attributed to one major product, presumably the neutral mono-Cp* product **10,** characterized by a large peak at 57.8 ppm and one minor product, the anionic bis-Cp* product [{Na(THF)$_3$}{(SPCPS)Sm(Cp*)$_2$}] (**11**)**,** showing a peak at 46.5 ppm (Scheme 8). The separation of **10** and **11** on a large scale could not be achieved, however, crystals of **11**, suitable for X-ray analysis were grown from slow diffusion of hexanes into a solution of

the mixture of **10** and **11** in toluene (Figure 8). Compound **11** could also be obtained quantitatively from the reaction of two equivalents of [NaCp*] with **2** in THF.

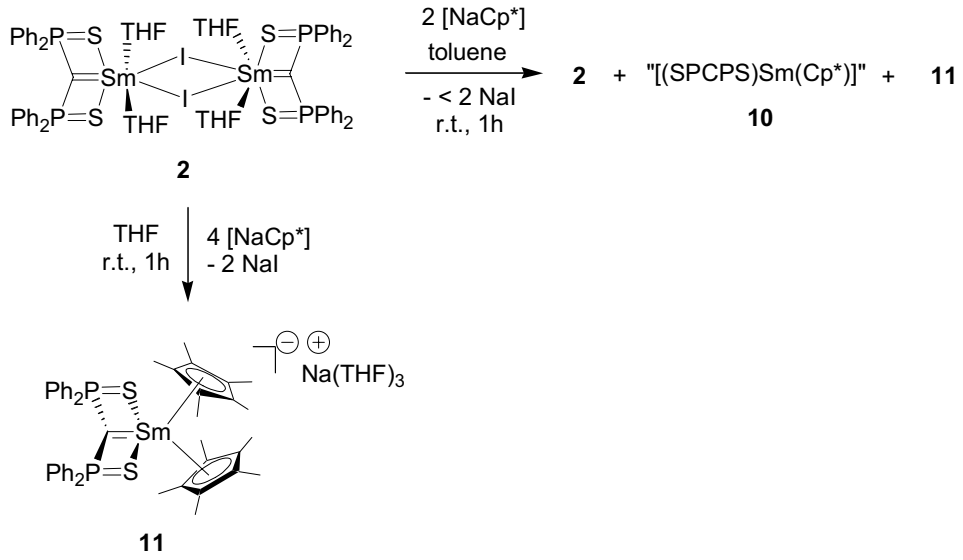

Scheme 8. Nucleophilic substitution at the samarium center in mono(carbene) complex **2**.

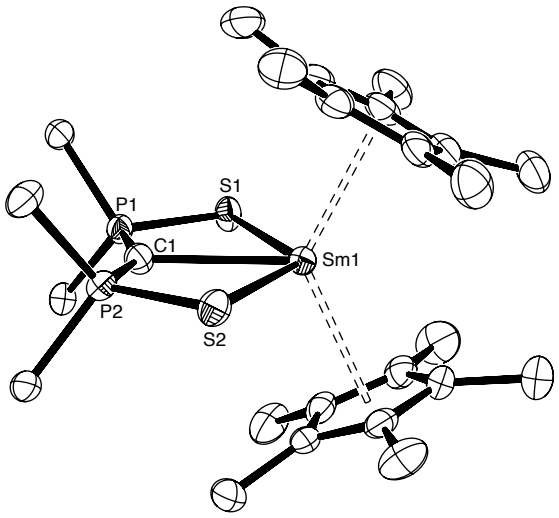

Figure 8. ORTEP plot (50% probability ellipsoids) of the anionic part of **11** (the solvated $Na(THF)_3^+$ cation was omitted for clarity). H atoms were also omitted and only the ipso carbon atoms of the phenyl rings are shown. Selected bond distances (Å) and angles (°): Sm(1)-C(1) = 2.527(2), Sm(1)-S(2) = 2.9561(6), S(2)-P(2) = 2.0250(7), S(1)-P(1) = 2.0398(7), P(1)-C(1) = 1.646(2), P(2)-C(1) = 1.664(2), P(1)-C(1)-P(2) = 149.9(1).

The structure of **11** reveals a planar carbene center with a much longer lanthanide carbene bond distance compared to **4a** (2.53 Å vs. 2.49 Å for planar carbene moiety in **4a**). The P-C and P=S bond lengths are in the same range as in **4a**. One interpretation of these geometrical parameters may be that the electronic saturation of the Sm-center by the electron-donating

Cp* ligands does not allow for the accommodation of further electron density from the carbene fragment and therefore a long Sm-C bond is observed. The reactivity of this new carbene complex still needs to be investigated.

5 Conclusions on the nature of the Ln-C multiple bond

In lanthanide carbene complexes, the stability of the carbenic center cannot be provided by the metal center through π-backdonation and has thus to be ensured by the substituents at the carbon atom. Due to the lanthanide carbon bond polarity ($\chi_C = 2.5$; $\chi_{Ln} < 1.2$) the electrons of the Ln-C multiple bond are strongly polarized towards the carbon center. Two cases are therefore to be discussed, depending on the ability of the substituents to stabilize the metal-free carbene fragment in its neutral or dianionic form (Figure 9).

First, the carbene ligand could behave as a two electron donor ligand and should therefore be stabilized in its free form as a neutral singlet carbene (case A, Figure 9). This formally corresponds to the well-known transition metal Fischer carbene complexes, in which the stability of the carbene center is partly provided by π-donor substituents so that little back donation is required from the metal. Thus, little or no double bond character is found between the metal and the carbene fragment. This case has clearly been illustrated by the isolation of some lanthanide complexes bearing NHC ligands.[17-29]

In a second case, the metal-free carbene ligand is a dianionic ligand which behaves as a four electron X_2-type ligand (case B, Figure 9). Complexes **2-5**, which result from the coordination of a dianionic ligand stabilized by electron-withdrawing substituents illustrate this second class of lanthanide carbene complexes, namely alkylidene complexes. Their reactivity towards benzophenone together with short lanthanide carbon bond distances support the analogy to transition metal Schrock-type carbene complexes.

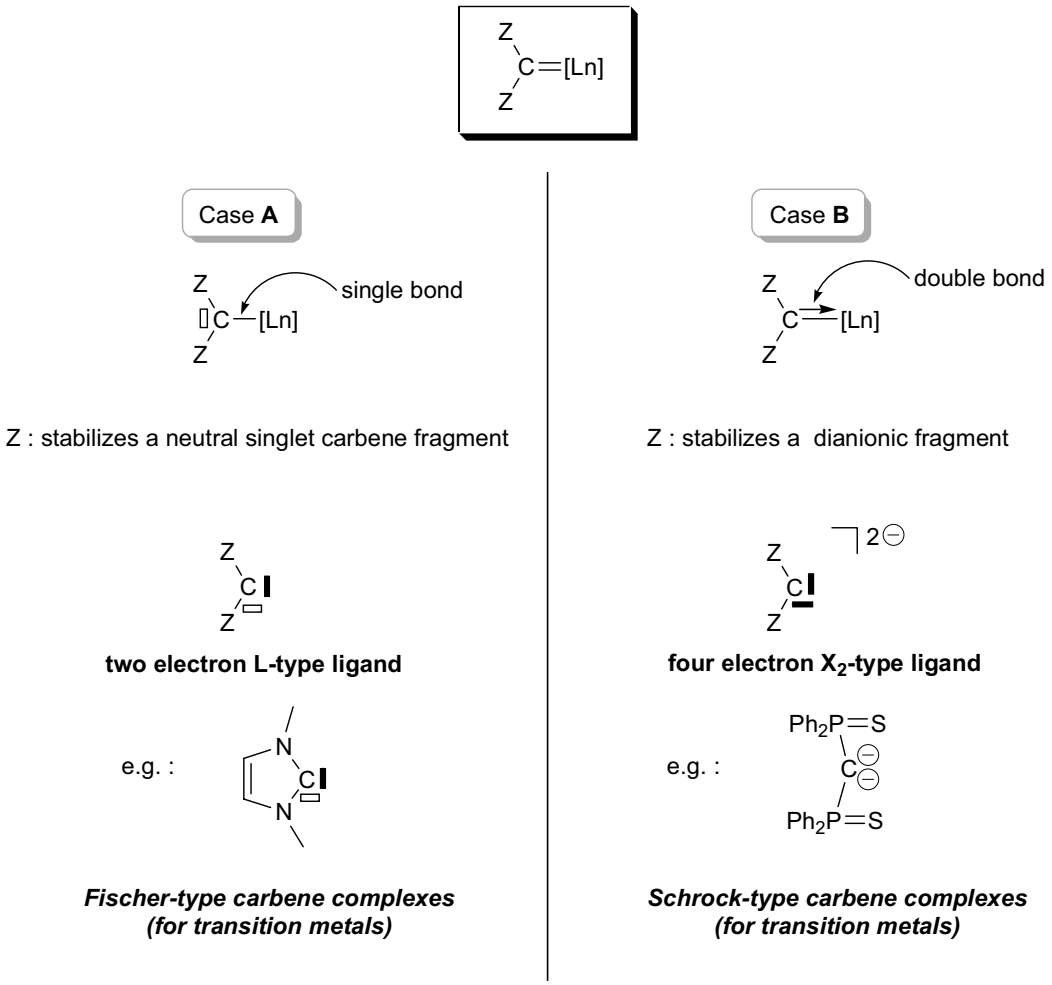

Figure 9. Lanthanide carbene complexes in analogy to transition metal carbenes.

6 Conclusion and Outlook

The work presented in this part has focused on the synthesis and reactivity of new lanthanide carbene complexes. The use of a stable dianionic ligand as precursor has proven successful to access early and late lanthanide alkylidene complexes. The structures of these complexes show a strong interaction between the carbenic center and the metal. Although this interaction is predominantly electrostatic in nature, there is also a contribution from orbital overlap: the observed dimorphism of the biscarbene complexes reveals that σ- and π-donation from the dianionic ligand to the empty d-orbital on the metal may develop. This π-bonding is also held responsible for the very short Ln-C bond distances and the planarity of the carbenic center.

The reactivity of the new complexes towards benzophenone confirms the carbenic nature of the Ln-C multiple bond and reveals the nucleophilic character of these complexes. This transformation proceeds via the formation of an open-metallaoxetane intermediate. On the bases of these results the new carbene complexes can be considered as the lanthanide analogues of Schrock-type transition metal carbenes.

Outlook

The substitution of the remaining iodide ligand in the samarium mono(carbene) complex by Cp* ligands has initiated the search for new carbene complexes. However, as the replacement is not as straightforward as expected, especially with amide and alkyl ligands, the variation may also occur on the dianionic ligand. Recently, the formation of a bisphosphonate dianion has been reported.[35] This ligand system is interesting as it may be possible to introduce chirality into the molecule via the OR groups (Figure 10). The stability of the resulting carbene complexes with these ligands may be enhanced because of the strong Ln-O interaction. However, solubility problems of the dianionic precursor still have to be overcome.[35]

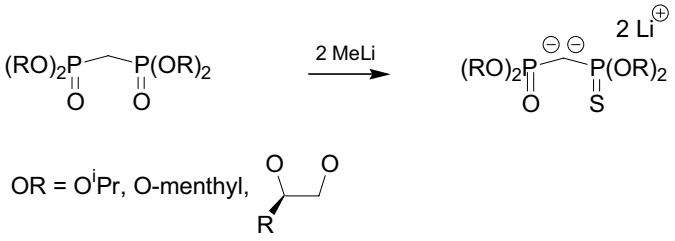

Figure 10. Proposed dianionic precursors for new carbene complexes.

The investigations on the nature of the Ln-C multiple bond have been restricted to structural analysis and reactivity tests so far. In order to quantify the contribution of orbital overlap in the carbene bonds of these complexes, theoretical studies should also be envisaged. They may result in a better understanding of how the different ligands on the metal influence

the multiple bond character, e.g. the different bond lengths observed in mono- and biscarbene complexes.

Although the reaction with benzophenone has allowed to learn more about the nature and reactivity of the new carbene complexes further tests are necessary to determine the full potential of these complexes. In particular, their use as polymerization catalysts of polar monomers may be envisaged.

References and Notes

[1] K. H. Dotz, *Angew. Chem. Int. Ed.* **1984**, *23*, 587.
[2] W. Kirmse, *Angew. Chem. Int. Ed.* **1997**, *36*, 1164.
[3] S. F. Vyboishchikov, G. Frenking, *Chem.-Eur. J.* **1998**, *4*, 1428.
[4] J. Barluenga, J. Santamaria, M. Tomas, *Chem. Rev.* **2004**, *104*, 2259.
[5] A. Furstner, *Angew. Chem. Int. Ed.* **2000**, *39*, 3013.
[6] W. A. Herrmann, *Angew. Chem. Int. Ed.* **2002**, *41*, 1291.
[7] R. R. Schrock, A. H. Hoveyda, *Angew. Chem. Int. Ed.* **2003**, *42*, 4592.
[8] T. M. Trnka, R. H. Grubbs, *Acc. Chem. Res.* **2001**, *34*, 18.
[9] T. R. Cundari, *Chem. Rev.* **2000**, *100*, 807.
[10] G. Frenking, N. Frohlich, *Chem. Rev.* **2000**, *100*, 717.
[11] E. Peris, R. H. Crabtree, *Coord. Chem. Rev.* **2004**, *248*, 2239.
[12] G. R. Giesbrecht, J. C. Gordon, *Dalton Trans.* **2004**, 2387.
[13] L. Maron, O. Eisenstein, *J. Phys. Chem. A* **2000**, *104*, 7140.
[14] L. Maron, L. Perrin, O. Eisenstein, *Dalton Trans.* **2003**, 4313.
[15] L. Maron, L. Perrin, O. Eisenstein, R. A. Andersen, *J. Am. Chem. Soc.* **2002**, *124*, 5614.
[16] K. N. Raymond, C. W. Eigenbrot, *Acc. Chem. Res.* **1980**, *13*, 276.
[17] P. L. Arnold, S. A. Mungur, A. J. Blake, C. Wilson, *Angew. Chem. Int. Ed.* **2003**, *42*, 5981.
[18] H. Schumann, M. Glanz, J. Winterfeld, H. Hemling, N. Kuhn, T. Kratz, *Angew. Chem. Int. Ed.* **1994**, *33*, 1733.
[19] P. L. Arnold, S. T. Liddle, *Chem. Commun.* **2005**, 5638.
[20] P. L. Arnold, S. T. Liddle, *Chem. Commun.* **2006**, 3959.
[21] T. Mehdoui, J. C. Berthet, P. Thuery, M. Ephritikhine, *Chem. Commun.* **2005**, 2860.
[22] D. Baudry-Barbier, N. Andre, A. Dormond, C. Pardes, P. Richard, M. Visseaux, C. J. Zhu, *Eur. J. Inorg. Chem.* **1998**, 1721.
[23] G. M. Ferrence, A. J. Arduengo, A. Jockisch, H. J. Kim, R. McDonald, J. Takats, *J. Alloy Comp.* **2006**, *418*, 184.
[24] A. J. Arduengo, M. Tamm, S. J. McLain, J. C. Calabrese, F. Davidson, W. J. Marshall, *J. Am. Chem. Soc.* **1994**, *116*, 7927.
[25] P. L. Arnold, S. T. Liddle, *Organometallics* **2006**, *25*, 1485.
[26] M. Glanz, S. Dechert, H. Schumann, D. Wolff, J. Springer, *Z. Anorg. All. Chem.* **2000**, *626*, 2467.
[27] W. A. Herrmann, F. C. Munck, G. R. J. Artus, O. Runte, R. Anwander, *Organometallics* **1997**, *16*, 682.
[28] S. T. Liddle, P. L. Arnold, *Organometallics* **2005**, *24*, 2597.
[29] L. Maron, D. Bourissou, *Organometallics* **2007**, *26*, 1100.
[30] K. Aparna, M. Ferguson, R. G. Cavell, *J. Am. Chem. Soc.* **2000**, *122*, 726.
[31] R. G. Cavell, R. P. K. Babu, K. Aparna, *J. Organomet. Chem.* **2001**, *617*, 158.
[32] H. M. Dietrich, K. W. Tornroos, R. Anwander, *J. Am. Chem. Soc.* **2006**, *128*, 9298.
[33] T. Cantat, M. Demange, N. Mézailles, L. Ricard, Y. Jean, P. Le Floch, *Organometallics* **2005**, *24*, 4838.
[34] T. Cantat, N. Mézailles, L. Ricard, Y. Jean, P. Le Floch, *Angew. Chem. Int. Ed.* **2004**, *43*, 6382.
[35] T. Cantat, L. Ricard, P. Le Floch, N. Mézailles, *Organometallics* **2006**, *25*, 4965.
[36] M. Rastatter, A. Zulys, P. W. Roesky, *Chem.-Eur. J.* **2007**, *13*, 3606.
[37] M. Rastatter, A. Zulys, P. W. Roesky, *Chem. Commun.* **2006**, 874.
[38] These values result from a search on the Cambridge Structural Database on complexes containing an eta-1 Ln-C bond
[39] This irreversible transition cracks the crystals. A usable sample was obtained by slowly ramping through the transition temperature
[40] L. L. Whinnery, L. M. Henling, J. E. Bercaw, *J. Am. Chem. Soc.* **1991**, *113*, 7575.
[41] G. C. Bazan, R. R. Schrock, M. B. Oregan, *Organometallics* **1991**, *10*, 1062.
[42] K. A. Jorgensen, B. Schiott, *Chem. Rev.* **1990**, *90*, 1483.

[43] F. N. Tebbe, G. W. Parshall, G. S. Reddy, *J. Am. Chem. Soc.* **1978**, *100*, 3611.
[44] S. H. Pine, G. S. Shen, H. Hoang, *Synthesis* **1991**, 165.

Conclusion and Perspectives

Conclusion and Perspectives

In this work we have shown that, despite the « hard-soft » mismatch between lanthanide ions and phosphorus, exciting new organolanthanide chemistry can be developed making use of phosphorus-containing ligands.

In the field of divalent lanthanide chemistry, the poor electron-donating nature of the phospholyl ligands and the possibility of η1-coordination via the phosphorus lone-pair have allowed the synthesis of divalent thulium complexes with higher stability compared to their Cp analogues. However, some refinements are still necessary in order to access divalent organodysprosium and neodymium complexes with these ligands.

In polymerization catalysis, the electronic properties of the phospholyl ligand have been exploited in the synthesis and application of mono-phospholyl lanthanide complexes in cationic styrene polymerization. The good results should encourage further development of these ligands in polymerization reactions.

A dianionic P=S pincer ligand, the 1,1 dilithio-bis(diphenylthiophosphoryl)methane, has given access to new lanthanide carbene complexes and their reactivity has been studied. Data from X-ray analysis has also allowed to obtain new insights into the nature of the Ln-C multiple bond.

The interesting properties of the phospholyl ligand, make this ligand a candidate for further investigations in the field of organolanthanide catalysis. As already mentioned earlier, geometrically constrained organolanthanide complexes play an important role in organic and polymerization catalysis. So far, only Cp-based ligands with amido or phosphido groups have been successfully employed. We have demonstrated that the introduction of phospholyl ligands in polymerization catalysis has a beneficial effect on the activity of the catalyst system. On this basis the combination of phospholyl ligands and phosphide or amide side-arms may further enhance the reactivity of the catalysts. One direction of future development could therefore be the synthesis and application of new phospholyl-phosphido and phospholyl-amido ligands. (Figure 1).

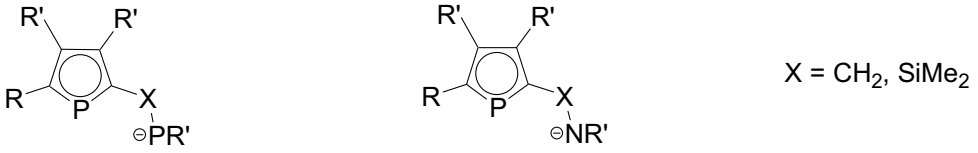

Figure 1. New phosphorus-based ligands for organolanthanide based catalysts.

Some few examples of phospholyl ligands carrying additional neutral donor atoms in a side-chain have already been reported (Figure 2).[1, 2] However, they have all been obtained by transformation of the phospholyl ligand in a phosphaferrocene complex. Only one example of a bridged phospholyl amido titanium complex has been described (Figure 2). This compound has been successfully used as catalyst for ethylene polymerization.[3] In the

following we will propose two new reaction pathways to access phospholyl phosphido or amido lanthanide complexes.

Figure 2. Phospholyl ligands with linked neutral or anionic donor substituents

The synthesis of a free phosphine or amine carrying phospholyl ligand can be envisaged by reacting the recently reported thio-phosphole **1** with primary phosphides or amides (Scheme 1).[4] After de-sulfurization the potential precursor ligands **2** and **3** should be accessible. Cleavage of the P-Ph bond and deprotonation of the phosphine or amine followed by the complexation with lanthanide halide or borohydride precursors may allow the synthesis of phospholyl based geometrically constrained complexes. In the case of phosphine groups, the advantage of this ligand over the reported silyl linked ligand used in the titanium complex should be the higher stability in the reaction with alkali metals: there is the risk of P-Si cleavage as already observed in phospholyl chemistry. In contrast, the low steric bulk of the proposed ligand may lead to some ligand redistribution. An additional substituent in the 4-position is therefore desirable.

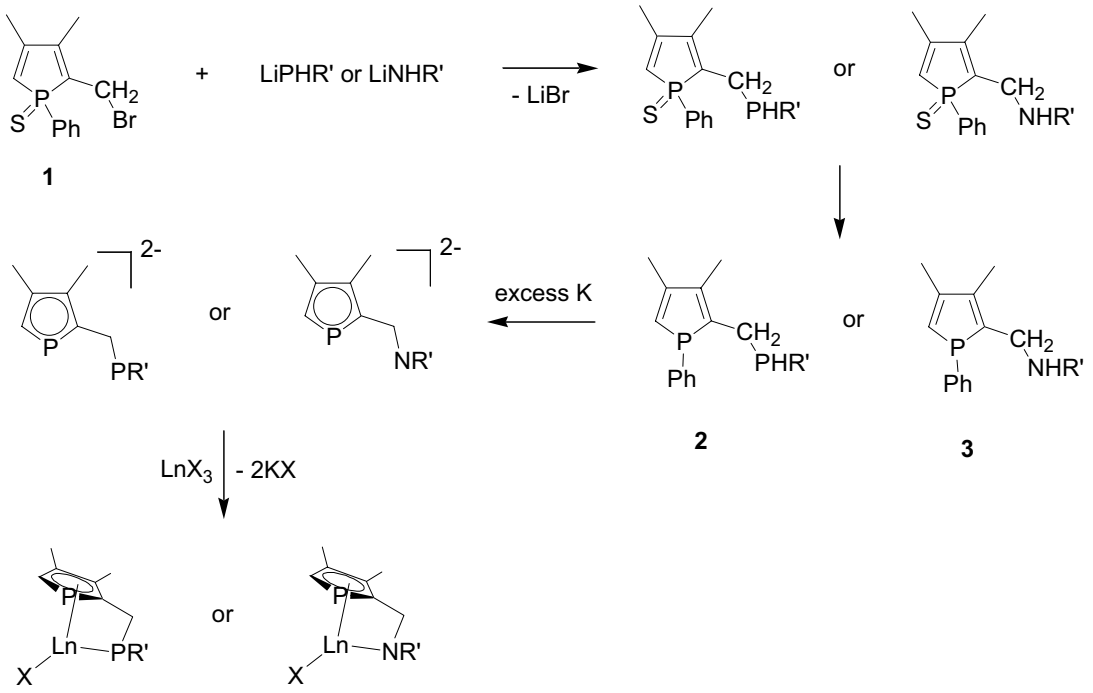

Scheme 1: Possible pathway to geometrically constrained phospholyl lanthanide complexes.

An alternative ligand may be synthesized from the recently reported ester-substituted phosphole **4**.[5] Reaction with a primary amine followed by the reduction of the amide may lead to the amino-phosphole **5**, which can serve as ligand precursor.

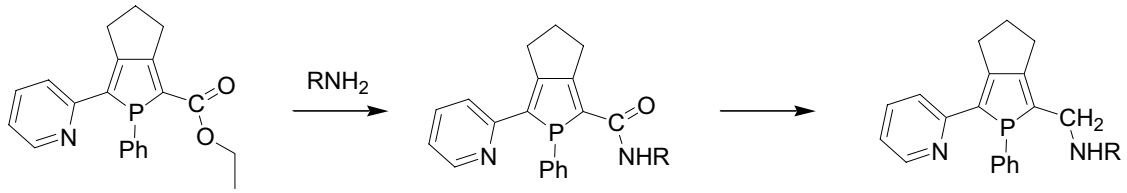

4 **5**

Scheme 2: Alternative ligand for geometrically constrained phospholyl lanthanide complexes.

In relation to the monophospholyl complexes another ligand system, the anionic phosphinines, may also lead to further advances in the field of polymerization catalysis. As lanthanides prefer hard donor ligands, arene-ligands are not very often encountered in lanthanide chemistry. Whereas several examples with substituted benzene ligands have been reported, there is only one example of a zero-valent complex carrying two neutral phosphinine ligands. Anionic phosphinine ligands exhibit three different binding modes: η^5, η^2 and η^1 coordination, depending on the metal fragment and the presence or absence of an SPS pincer.[6] A recent study has shown that anionic SPS phosphinines coordinate lanthanide and actinide metals in an η^1 fashion.[7] In contrast, a rhodium(I) complex showed η^5 coordination with the bulky 2,3,5,6 tetraphenylphosphinine and the 2,6-bis(trimethylsilyl)-4,5-diphenylphosphinine.[8] These latter ligands seem therefore suitable alternatives to Cp ligands. They should allow the synthesis of mono-substituted phosphinine complexes which could then be tested in polymerization reactions or organic transformations.

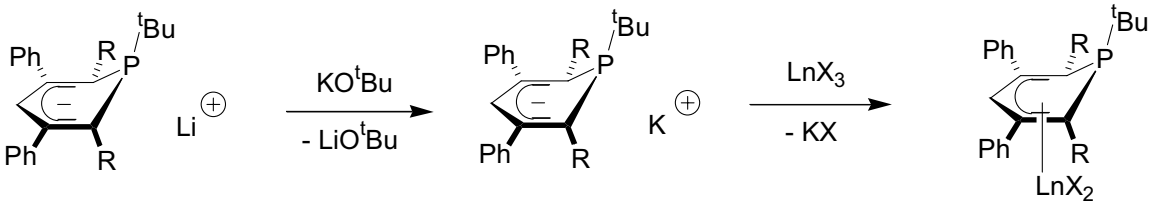

R = Ph, TMS

X = halide, borohydride

References

[1] C. Ganter, L. Brassat, B. Ganter, *Chem. Ber.* **1997**, *130*, 1771-1776.
[2] C. Ganter, L. Brassat, C. Glinsbockel, B. Ganter, *Organometallics* **1997**, *16*, 2862.
[3] S. J. Brown, X. L. Gao, D. G. Harrison, L. Koch, R. E. V. Spence, G. P. A. Yap, *Organometallics* **1998**, *17*, 5445.
[4] E. Deschamps, L. Ricard, F. Mathey, *Organometallics* **2001**, *20*, 1499.
[5] Y. Matano, T. Miyajima, T. Nakabuchi, Y. Matsutani, H. Imahori, *J. Org. Chem.* **2006**, *71*, 5792.
[6] P. Le Floch, *Coord. Chem. Rev.* **2006**, *250*, 627.
[7] T. Arliguie, M. Doux, N. Mezailles, P. Thuery, P. Le Floch, M. Ephritikhine, *Inorganic Chemistry* **2006**, *45*, 9907.
[8] A. Moores, N. Mezailles, L. Ricard, P. Le Floch, *Organometallics* **2005**, *24*, 508.

Experimental Part

General

All manipulations were performed under strict exclusion of air or moisture on a vacuum line using Schlenk techniques or in dry boxes under purified argon. THF, diethyl ether, pentane, hexanes and cyclohexane were distilled from sodium benzophenone ketyl. Toluene was distilled from sodium and pyridine from calcium hydride. All solvents were degassed by three freeze-pump-thaw cycles prior to use. Deuterated solvents (C_6D_6, C_6D_{12}, tol-d_8 and THF-d_8) purchased from Sigma-Aldrich were stored over activated 4 Å molecular sieves.

NMR measurements were obtained using a Bruker 300 Avance spectrometer operating at 300 MHz for ^1H, 75.5 MHz for ^{13}C and 121.5 for ^{31}P. The spectra were recorded at room temperature unless mentioned otherwise. Chemical shifts δ are reported in parts per million (ppm) relative to TMS (internal reference) for ^1H and ^{13}C and relative to 85% H_3PO_4 (external reference) for ^{31}P. The following abbreviations are used for the description of the NMR spectra: s (singlet), d (doublet), t (triplet), m (multiplet), br (broad). For paramagnetic compounds the line-width at half height $w_{1/2}$ is given in kHz. The room temperature Evans magnetic susceptibility determination were made following the procedure described by the literature for supraconducting equipment.[1]

Elemental analyses were performed at the "Service de microanalyse de l'université de Dijon", Dijon (Bourgogne), France and at the "Organometallic Chemistry Laboratory" at RIKEN, Wako, Japan. The polymer reactions and the polymer analyses were also carried out at RIKEN.

Metal precursors

The anhydrous $LnCl_3$ (Ln = Sc, Y, Nd, Dy, Tm), $DyBr_3$, LnI_3 (Ln = Nd, Dy, Tm), $PbCl_2$, $SnCl_2$ and the metal powders of Nd, Sm, Dy and Tm were used as purchased from Strem Chemicals or Sigma-Aldrich.

The following metal precursors were prepared according to literature methods:

$LnI_3(THF)_{3.5}$ (Ln = Nd, Sm, Dy and Tm) was prepared by reaction of the respective metal powders with iodine in THF.[2]
$Ln(BH_4)_3(THF)_3$ (Ln = Nd, Dy, Tm) was synthesized by reaction of the respective trichloride with $NaBH_4$ in refluxing THF.[3]
Solvent-free TmI_2 was prepared by the high-temperature reaction of metallic Tm with iodine.[4]
Potassium graphite KC_8 was prepared according to a literature procedure by heating potassium metal with graphite.[5]

Synthesis of $TmI_2(THF)_3$

A new synthesis of $TmI_2(THF)_3$ was developed: In the glove box a mixture of $TmI_3(THF)_{3.5}$ (0.50 g, 0.74 mmol) and KC_8 (0.20 g, 1.48 mmol) was prepared in a centrifuge tube. THF (20 mL) was added onto this mixture and the reaction was shaken, leading to an immediate color change to malachite-green. After centrifugation, the solution was transferred to a 250 mL round-bottom flask. The remaining residue in the centrifuge tube was extracted several times with THF and after each centrifugation the solution was transferred to the glass flask. The extraction was stopped when no colour change to green occurred upon addition of THF. The round-bottom flask was then connected to a filtration apparatus and the solution was evaporated at the vacuum line. Washing the residue with diethyl ether and drying for several hours led to pure $TmI_2(THF)_3$ as a brown powder in 95% yield (0.45g, 0.70 mmol).

Other reagents

KH, NaH, n-Butyllithium (2.6 M in hexane), Methyllithium (1.6 M in Et_2O), KOtBu, $NaBH_4$, iodine, AgI, C_2Cl_6, Ph_3PS, Ph_3PO, 1,2-diphenylacetylene, fluorenone, benzophenone, TMSI, *o*-(dimethylamino)toluene, [18]crown-6, [2.2.2]cryptand are commercial and were used as purchased.
Styrene was distilled from CaH_2, tBuCN was dried over P_2O_5 and both were degassed prior to use.
[(Cp^*_2)Sn] was prepared according to a literature procedure from $SnCl_2$ and [KCp*] in THF.[6]

Ligands

a) Cp-ligands

The syntheses of [NaCp*][7], [KCp*][8], [$NaCp^{ttt}(THF)_{0.5}$][9], [KCp^{ttt}][9], [NaCp'''][10] and [KCp'''][11] were carried out according to literature procedures.

Synthesis of [KCp^{tt}] from Cp^{tt}-H[12] and KH (in analogy to [KCp^{ttt}])

In a Schlenk tube, Cp^{tt}-H (1.0 g, 5.6 mmol) and KH (0.17 g, 4.2 mmol) were reacted in refluxing THF for 24 h, generating gaseous dihydrogen. After this time [KCp^{tt}] precipitated from the solution. The cold solution was filtered and the precipitate was rinsed twice with hexanes to remove remaining Cp^{tt}-H. After drying overnight under vacuum at 60°C, white [KCp^{tt}] was obtained in 80% yield (0.73 g, 3.3 mmol).
^{1}H NMR (THF-d_8): δ 5.41(br s, 1H, C*H*), 5.33 (br d, 2H, C*H*), 1.18 (s, 18H, C(CH_3)$_3$).

b) Phospholyl ligands

[K(Dtp)][13], [K(Dsp)][14] and [K(Htp)][15] were prepared according to literature procedures.

c) Other ligands

Synthesis of *o*-dimethylaminobenzyl potassium [K($CH_2C_6H_4NMe_2$-*o*)]

The synthesis of [K($CH_2C_6H_4NMe_2$-o)] was carried out by a modification of a literature procedure:[16] In a Schlenk tube, *n*-Butyllithium (2.6 M, 100 mL, 260 mmol) was added to a solution of *o*-(dimethylamino)toluene (35.15 g; 260 mmol) in hexane (100 mL) and ether (50 mL) at room temperature. Potassium t-butoxide (29.18 g, 260 mmol) was added in small portions. Then, ether (150 ml) was added and the solution was stirred for 24h during which time a yellow powder slowly precipitated. Subsequently, the solvents were concentrated to half of the amount under vacuum. Hexanes (150 mL) was added to this suspension, the yellow precipitate was filtrated and washed four times with 100 mL portions of hexane. Drying the product under vacuum resulted in the quantitative isolation of o-dimethylaminobenzyl potassium as a yellow powder.
^{1}H NMR (THF-d_8): δ 1.85 (d, 2.8 Hz, 1H, CH_2), 2.39 (d, 2.8 Hz, 1H, CH_2), 2.48 (s, 6H, N, N(CH_3)$_2$), 4.94 (t, 6.9 Hz, 1H, aromatic), 5.85 (d, 8.0 Hz, 1H, aromatic), 5.99 (t, 7.5 Hz, 1H, aromatic), 6.09 (d, 6.8 Hz, 1H, aromatic).

Synthesis of bis(diphenylphosphino)methane disulfide (Dpps)

The synthesis of Dpps was carried out by a modification of a literature procedure:[17] To a suspension of bis(diphenylphosphino)methane (6.00 g, 15.6 mmol) in THF (20 mL) was added elemental sulphur (0.25 equivalents of S_8: 1.00, 3.9 mmol) at room temperature. The resulting solution was stirred for 3 h at 60°C. Pure Dpps was obtained as a white solid after evaporation of the solvents in 100% yield (7.00 g, 15.6 mmol).
^{31}P NMR ($CDCl_3$): δ 35.1 (s).

Part I

Chapter 2

Synthesis of [$(Dtp)_2$Pb] (1)

A mixture of anhydrous $PbCl_2$ (0.30 g, 1.08 mmol), [K(Dtp)] (0.57 g, 2.16 mmol) and LiCl (0.09 g, 2.16 mmol) in THF (10 mL) was stirred for 2 hours at room temperature resulting in an orange solution and a white precipitate. After centrifugation, the solution was evaporated and the residue was taken up in pentane. The insoluble salts were separated by centrifugation and the solution was evaporated leading to orange **1** in 78% yield (0.55 g, 0.84 mmol).

^{1}H NMR (C_6D_6): δ 2.18 (s, 6H, CCH_3), 1.44 (d, 18H, J = 1.5 Hz, C(CH_3)$_3$).
^{13}C NMR (C_6D_6): δ 150.4 (d, $^{1}J_{P\text{-}C}$ = 45.8 Hz, PC), 131.7 (d, $^{2}J_{P\text{-}C}$ = 3.4 Hz, PCC), 27.9 (d, $^{2}J_{P\text{-}C}$ = 16.2 Hz, C(CH$_3$)$_3$), 26.6 (d, $^{3}J_{P\text{-}C}$ = 10.3 Hz, C(CH$_3$)$_3$), 9.8 (s, CCH$_3$).
^{31}P NMR (C_6D_6): δ 58.8 (s).
Crystals suitable for X-ray studies were grown from a pentane solution at -78°C.

Synthesis of [(Cp^{ttt})$_2$SmI] (2)

SmI$_3$(THF)$_{3.5}$ (0.20 g, 0.26 mmol) and [NaCp^{ttt}(THF)$_{0.5}$] (0.15 g, 0.51 mmol) were stirred in THF (10 mL) for 24 hours. After evaporation of the solvent, toluene was added onto the red residue and the solution was centrifuged to remove all remaining salts. Evaporation and recrystallisation from pentane at –30°C afforded dark red **2** in 63% yield (0.12 g, 0.16 mmol).
^{1}H NMR in agreement with literature reports.[18]

Synthesis of [(Cp’’’)$_2$SmI(THF)] (3a)

SmI$_3$(THF)$_{3.5}$ (0.20 g, 0.26 mmol) and [NaCp’’’] (0.16 g, 0.51 mmol) were stirred in THF (10 mL) for 24 hours. After evaporation of the solvent, toluene was added onto the red residue and the solution was centrifuged to remove all remaining salts. Evaporation and recrystallisation from pentane at –30°C afforded orange **3a** in 88% yield (0.21 g, 0.23 mmol).
^{1}H NMR (C_6D_6): δ 14.6 (br s, $w_{1/2}$ = 0.2 kHz, 4H, CH), 1.56 (br s, $w_{1/2}$ = 0.1 kHz, 4H, THF), 0.41 (s, 4H, THF), -0.42 (s, 36H, Si(CH_3)$_3$), -1.68 (s, 18H, Si(CH_3)$_3$).
Crystals suitable for X-ray studies were grown from a pentane solution at -30°C.

Synthesis of [(Cp’’’)$_2$SmI] (3b)

A solution of [(Cp’’’)$_2$SmI(THF)] (0.05 g, 0.06 mmol) in toluene was heated to 50°C and the solvent was evaporated at this temperature for 2 hours. The solvent-free **3b** was obtained as a yellow powder in quantitative yield (0.05 g, 0.06 mmol). Addition of THF to this product gave back the ^{1}H NMR spectrum of **3a**.
^{1}H NMR (C_6D_{12}): δ 17.3 (br s, $w_{1/2}$ = 0.1 kHz, 4H, CH), -0.79 (s, 36H, Si(CH_3)$_3$), -3.3 (s, 18H, Si(CH_3)$_3$).

Synthesis of [{(Dtp)$_2$SmI}$_n$] (4)

SmI$_3$(THF)$_{3.5}$ (0.30 g, 0.38 mmol) and [K(Dtp)] (0.20 g, 0.76 mmol) were stirred in THF (15 mL) for 24 hours. ^{31}P NMR indicated the complete disappearance of the starting materials. After centrifugation, the solvent was evaporated and the crude product was washed with pentane to afford red **4** in 77% yield (0.21 g, 0.29 mmol).
^{1}H NMR (tol-d_8): δ 2.8 (br s, $w_{1/2}$ = 0.1 kHz, 12H, CH_3), -2.2 (s, $w_{1/2}$ = 0.1 kHz, 36H, C(CH_3)$_3$).
^{31}P NMR (C_6D_6): δ 28.8 (s).

Synthesis of [(Cp^{ttt})$_2$Sm] (5) by reduction of 2 (NMR experiment)

To a solution of [(Cp^{ttt})$_2$SmI] (10 mg, 13 µmol) in C_6D_{12} was added KC_8 (18 mg, 130 µmol) leading to a colour change from red to dark purple after 5 h. The reduction was completed after 24 h as indicated by ^{1}H NMR.
^{1}H NMR in agreement with literature reports.[9]

Synthesis of [(Cp’’’)$_2$Sm(THF)] (6a) by reduction of 3a (NMR experiment)

To a solution of [(Cp’’’)$_2$SmI(THF)] (10 mg, 11 µmol) in C_6D_{12} was added KC_8 (15 mg, 110 µmol) leading immediately to a colour change from orange to purple. After 1 h the reduction was completed as indicated by ^{1}H NMR.
^{1}H NMR (C_6D_{12}): δ 11.6 (s, 18H, Si(CH_3)$_3$), 9.8 (s, 4H, THF), 7.4 (s, 4H, THF), 4.0 (s, 36H, Si(CH_3)$_3$), -1.9 (s, 4H, C*H*).

Synthesis of [(Cp’’’)$_2$Sm] (6b) by reduction of 3b (NMR experiment)

To a solution of [($Cp^{'''}$)$_2$SmI] (10 mg,12 µmol) in in C_6D_{12} was added KC_8 (16 mg, 120 µmol) leading immediately to a colour change from yellow to purple. After 1 h the reduction was completed as indicated by ^{1}H NMR. Addition of THF to the final product led to the ^{1}H NMR spectrum of **6a**.
^{1}H NMR (C_6D_{12}): δ 8.1 (br s, $w_{1/2}$ = 0.5 kHz, 18H, Si(CH_3)$_3$), 3.5 (br s, $w_{1/2}$ = 0.3 kHz, 36H, Si(CH_3)$_3$).

Synthesis of [(Dtp)$_2$Sm] (7) by reduction of 4 (NMR experiment)

To a solution of [{(Dtp)$_2$SmI}$_n$] (10 mg, 14 µmol) in toluene-d_8 was added potassium graphite (11 mg, 83 µmol) leading to the disappearance of the signal for the starting material in the ^{31}P NMR spectrum and the precipitation of a green solid. Addition of THF to the reaction mixture allowed for the dissolving of the green precipitate and the observation of a signal at -512 ppm in the ^{31}P NMR for [(Dtp)$_2$Sm(THF)].
^{1}H NMR in agreement with literature reports.[13]

Chapter 3

General Procedure 1 (GP-1) for the preparation of [L_2TmX] precursors (L = Cp^{ttt}, Cp’’’, Cp^{tt}, Dtp, Dsp, Htp; X = I, BH_4)

In the glovebox a mixture of $TmX_3(THF)_y$ (for X = I: y = 0, for X = BH_4: y = 3) (1.0 eq) and [K(L)] (2.2 eq) was prepared in a Schlenk tube fitted with a J. Young valve. Toluene (20mL) was condensed onto this mixture at -78°C and the suspension was allowed to warm to room temperature. Under stirring the reaction was heated to reflux for 48h. After that time the

yellow solution was cooled to room temperature and centrifuged. The solvent was evaporated and the crude product was recrystallised from pentane at -30°C.

Synthesis of [(Cp^{ttt})$_2$Tm] (8) and [(Cp^{ttt})$_2$Tm(THF)] (9) by metathesis

A mixture of $TmI_2(THF)_3$ (0.50 g, 0.78 mmol) and [$NaCp^{ttt}(THF)_{0.5}$] (0.46 g, 1.57 mmol) was stirred at 0°C in THF (15 mL) for 2 h, evaporated to dryness and pentane was added to the residue. After filtration and evaporation of the solvent, the crude product was washed with cold pentane to yield pure **8** as a purple crystalline solid in 32% yield (0.16 g, 0.25 mmol).
^{1}H NMR (C_6D_{12}): δ 32.4 (br s, 18H, $w_{1/2} \approx 0.3$ kHz, C(C*H*$_3$)$_3$), 22.2 (br s, 36H, $w_{1/2} \approx 0.3$ kHz, C(C*H*$_3$)$_3$), -63.7 (br s, 4H, $w_{1/2} \approx 0.8$ kHz, C*H*).
$\mu_{eff} = 5.0\ \mu_B$ (Evans' NMR method).
Crystals of **9** suitable for X-Ray analysis were grown from a solution of **8** in THF/pentane at -30°C.

Synthesis of [(Cp’’’)$_2$Tm(THF)] (10) by metathesis

Onto a mixture of $TmI_2(THF)_3$ (0.10 g, 0.16 mmol) and [NaCp'''] (0.09 g, 0.31 mmol) diethyl ether (10mL) was condensed at -78°C and the reaction was allowed to warm to room temperature under stirring. After 2h the resulting violet solution was filtered and evaporated. Recrystallization from pentane at -30°C led to the isolation of pure **10** as a purple crystalline solid in 32% yield (0.04 g, 0.05mmol).
^{1}H NMR (C_6D_6): δ 53.1 (br s, 18H, $w_{1/2} \approx 1$ kHz, Si(C*H*$_3$)$_3$), 14.0 (br s, 36H $w_{1/2} \approx 1$ kHz, Si(C*H*$_3$)$_3$), -23.2 (br s, 4H, $w_{1/2} \approx 1$ kHz, C*H*).
$\mu_{eff} = 5.0\ \mu_B$ (Evans' NMR method)
Crystals suitable for X-Ray analysis were grown from pentane at -30°C.

Synthesis of [(Cp^{ttt})$_2$TmI] (11)

From the reaction of TmI_3 (0.40 g, 0.73 mmol) and [KCp^{ttt}] (0.40 g, 1.61 mmol) according to the GP-1, **11** was obtained as a yellow powder in 62% yield (0.25 g, 0.29 mmol).
^{1}H NMR (C_6D_{12}): δ 450 (br s, 18H, $w_{1/2} \approx 3$ kHz, C(C*H*$_3$)$_3$), 92 (br s, 18H, $w_{1/2} \approx 3$ kHz, C(C*H*$_3$)$_3$), -15 (br s, 18H, $w_{1/2} \approx 2$ kHz, C(C*H*$_3$)$_3$).
Anal. Calcd for $C_{34}H_{58}ITm$ (762.66): C, 53.55; H, 7.67. Found : C, 53.94 H, 7.57.
Crystals suitable for X-Ray analysis were grown from toluene at -30°C.

Synthesis of [(Cp’’’)$_2$TmI] (12)

From the reaction of TmI_3 (0.30 g, 0.55 mmol) and [KCp'''] (0.38 g, 1.2 mmol) according to the GP-1, **12** was obtained as a yellow powder in 53% yield (0.25 g, 0.29 mmol).
^{1}H NMR (C_6D_{12}) : δ 157 (br s, 18H, $w_{1/2} \approx 2$ kHz, Si(C*H*$_3$)$_3$), 48 (br s, 36H, $w_{1/2} \approx 4$ kHz, Si(C*H*$_3$)$_3$).

Anal. Calcd for $C_{28}H_{58}ISi_6Tm$ (859.11): C, 39.15; H, 6.80. Found : C, 39.52 H, 6.54.
Crystals suitable for X-Ray analysis were obtained from sublimation at 220°C and 10^{-3} mbar.

Synthesis of [$(Cp^{ttt})_2Tm$] (8) by reduction of 11

A mixture of [$(Cp^{ttt})_2TmI$] (90 mg, 0.12 mmol) and KC_8 (193 mg, 1.43 mmol) was stirred in cyclohexane (3 mL) for 48 h. After centrifugation, the solvent was evaporated and the resulting purple residue was washed with cold pentane to yield pure **8** in 65% (46 mg, 0.08 mmol).
^{1}H NMR spectrum in agreement with that of **8** obtained by metathesis.

Synthesis of [$(Cp''')_2Tm$] (13) by reduction of 12

To a solution of [$(Cp''')_2TmI$] (0.10 g, 0.11 mmol) in cyclohexane (6 mL) was added KC_8 (0.16 g, 1.2 mmol) in small portions. After 48 h the dark green solution was centrifuged and evaporated. Addition of some drops of cyclohexane to the oily residue led to the precipitation of pure **13** as a dark green solid in 42% yield (0.03 g, 0.05 mmol).
^{1}H NMR (C_6D_{12}): δ 24 (br s, 18H, $w_{1/2} \approx 60$ Hz, $Si(CH_3)_3$), 21 (br s, 36H $w_{1/2} \approx 90$ Hz, $Si(CH_3)_3$), -54 (br s, 4H, $w_{1/2} \approx 600$ Hz, C*H*).

Synthesis of [$(Cp^{ttt})_2Tm(BH_4)$] (14)

From the reaction of $Tm(BH_4)_3(THF)_3$ (0.30 g, 0.70 mmol) and [KCp^{ttt}] (0.42 g, 1.54 mmol) according to the GP-1, **14** was obtained as a yellow powder in 73% yield (0.33 g, 0.51 mmol).
^{1}H NMR (C_6D_{12}): δ 279 (br s, 18H, $w_{1/2} \approx 3$ kHz, $C(CH_3)_3$), 107 (br s, 18H, $w_{1/2} \approx 3$ kHz, $C(CH_3)_3$), -26 (br s, 18H, $w_{1/2} \approx 2$ kHz, $C(CH_3)_3$).
Anal. Calcd for $C_{34}H_{62}BTm$ (650.60): C, 62.77; H, 9.61. Found : C, 62.79 H, 9.69.
Crystals suitable for X-Ray analysis were obtained from pentane at -30°C.

Synthesis of [$(Cp^{ttt})_2Tm$] (8) by reduction of 14

To a solution of [$(Cp^{ttt})_2Tm(BH_4)$] (50 mg, 0.08 mmol) in pentane (4 mL) was added KC_8 (104 mg, 0.77 mmol) and the reaction was left for 48 h. The resulting violet solution was centrifuged and evaporated. After washing with cold pentane, pure **8** was obtained in 48% yield (23 mg, 0.04 mmol).
^{1}H NMR spectrum in agreement with that of **8** obtained by metathesis.

Synthesis of [$\{(Cp^{tt})_2TmI\}_2$] (15)

From the reaction of TmI_3 (0.30 g, 0.55 mmol) and [KCp^{tt}] (0.26 g, 1.2 mmol) according to the GP-1, **15** was obtained as a yellow powder in 66% yield (0.23 g, 0.18 mmol).
^{1}H NMR (C_6D_{12}): δ 214 (br s, $w_{1/2} \approx 3$ kHz, $C(CH_3)_3$).

Anal. Calcd for $C_{52}H_{84}I_2Tm_2$ (1300.90): C, 48.01; H, 6.51. Found : C, 47.99; H, 6.69.
Crystals suitable for X-Ray analysis were obtained from pentane at -30°C.

Synthesis of [(Cp*)$_2$TmI(THF)] (17)

A mixture of $TmI_3(THF)_{3.5}$ (0.30 g, 0.38 mmol) and [KCp*] (0.14 g, 0.82 mmol) were reacted in refluxing THF for 48 h. After evaporation of the solvent, toluene was added onto the residue and the reaction mixture was centrifuged. The yellow solution was evaporated and washed with cold pentane to yield pure **17** in 70% yield (0.17 g, 0.26 mmol).
^{1}H NMR (C_6D_{12}): δ 90.8 (br s, 4H, $w_{1/2} \approx 0.6$ kHz, THF), -10.3 (br s, $w_{1/2} \approx 0.3$ kHz, CH_3).
Crystals suitable for X-Ray analysis were obtained from toluene/pentane at -30°C.

Synthesis of [{(Cp*)$_2$TmI}$_n$] (16) (NMR experiment)

Addition of an excess TMSI (420 µL, 120 µmol) to a solution of (Cp*)$_2$TmI(THF) (10 mg, 16 µmol) in toluene-d_8 led to the quantitative formation of a light yellow precipitate of **16** after 2 h. Removing the supernatant and dissolving the solid in THF-d8 gave back the peak at -10 ppm in the ^{1}H NMR spectrum of **17**.
^{1}H NMR (tol-d_8): δ 16.6 (br s, $w_{1/2} \approx 1.2$ kHz, CH_3).

Synthesis of [(Cp*)TmI$_2$(THF)$_2$] (18)

To a solution of [(Cp*)$_2$Sn] (15 mg, 39 µmol) in THF was added solid $TmI_2(THF)_3$ (25 mg, 39 µmol) leading to the immediate formation of a black precipitate which was removed by centrifugation. Concentrating the solution and addition of hexanes led to the precipitation of pure **18** as white crystals after 24 h in 53% yield (15 mg, 21 µmol).
^{1}H NMR (THF-d_8): δ -4.8 (br s, $w_{1/2} \approx 0.3$ kHz, CH_3).
Crystals suitable for X-Ray analysis were grown from slow diffusion of pentane in a toluene solution of **18** at room temperature.

Synthesis of [(Dtp)$_2$TmI] (19)

From the reaction of TmI_3 (0.40 g, 0.72 mmol) and [K(Dtp)] (0.42 g, 1.58 mmol) according to the GP-1, **19** was obtained as a yellow powder in 78% yield (0.42 g, 0.56 mmol).
^{1}H NMR (C_6D_6): δ 167 (br s, $w_{1/2} \approx 9$ kHz, C(CH_3)$_3$).
No correct elemental analysis could be obtained.
Crystals suitable for X-Ray analysis were obtained from sublimation at 190°C and 10^{-3}mbar.

Synthesis of [{(Dsp)$_2$TmI}$_n$] (20)

From the reaction of TmI_3 (0.20 g, 0.36 mmol) and [K(Dsp)] (0.24 g, 0.80 mmol) according to the GP-1, **20** was obtained as a yellow powder in 62% yield (0.18 g, 0.22 mmol).

^{1}H NMR (C_6D_{12}): δ 135 (br s, $w_{1/2} \approx 3$ kHz, Si(CH_3)$_3$).

Synthesis of [{(Htp)$_2$TmI}$_2$] (21)

From the reaction of TmI_3 (0.20 g, 0.36 mmol) and [K(Htp)] (0.18 g, 0.79 mmol) according to the GP-1, **21** was obtained as a yellow powder in 45% yield (0.11 g, 0.16 mmol).
^{1}H NMR (C_6D_{12}): δ 85 (br s, $w_{1/2} \approx 3$ kHz, C(CH_3)$_3$).
Anal. Calcd for $C_{48}H_{80}I_2P_4Tm_2$ (1372.72): C, 42.00; H, 5.87. Found : C, 42.11 H, 5.89. Crystals suitable for X-Ray analysis were obtained from pentane at -30°C.

Synthesis of [(Dtp)$_2$Tm] (22) by reduction of 19

To a solution of [(Dtp)$_2$TmI] (37 mg, 0.05 mmol) in pentane (4 mL) was added KC_8 (67 mg, 0.50 mmol) and the reaction was left for 48h. The resulting dark green solution was centrifuged and the volume was reduced to 2 mL under vacuum. From the solution pure **19** crystallized as a dark green solid in 67% yield (20 mg, 0.03 mmol).
^{1}H and ^{31}P NMR in agreement with literature reports.[13]

Synthesis of [{(Htp)$_2$Tm}$_2$] (23) by reduction of 21

To a solution of [{(Htp)$_2$TmI}$_2$] (25 mg, 0.018 mmol) in hexanes (2 mL) was added KC_8 (50 mg, 0.36 mmol) and the reaction was shaken for 1h. The resulting green solution was centrifuged and transferred to a crystallization tube. From this solution pure **23** crystallized at –30°C as a green solid in 15% yield (3 mg, 0.003 mmol).
^{1}H NMR (C_6D_{12}): δ 40 (br s, 36H, $w_{1/2} \approx 1$ kHz, C(CH_3)$_3$), -26 (br s, 4H, $w_{1/2} \approx 1$ kHz, CH).

Synthesis of [(Cp^{ttt})(Dtp)Tm(BH$_4$)] (25)

To a mixture of $Tm(BH_4)_3(THF)_3$ (0.20 g, 0.47 mmol) and [KCp^{ttt}] (0.16 g, 0.59 mmol) was added THF (10 mL) and the reaction was stirred for 15 h. The precipitated KBH_4 was removed by centrifugation and the solvent evaporated. Toluene (15 mL) was added onto the white residue and the insoluble solids were separated by centrifugation. The toluene solution was transferred into a Schlenk tube fitted with a J. Young valve and [K(Dtp)] (0.16 g, 0.59 mmol) was added. Heating this mixture to reflux with stirring for 15 h afforded a yellow solution, which was centrifuged and the solvent evaporated. Pure **25** was obtained from recrystallisation in pentane in 68% yield (0.20 g, 0.31 mmol).
^{1}H NMR (C_6D_{12}): δ 282 (br s, 9H, $w_{1/2} \approx 4$ kHz, C(CH_3)$_3$), 242 (br s, 9H, $w_{1/2} \approx 3$ kHz, C(CH_3)$_3$), 174 (br s, 9H, $w_{1/2} \approx 4$ kHz, C(CH_3)$_3$), 120 (br s, 9H, $w_{1/2} \approx 4$ kHz, C(CH_3)$_3$), -94 (br s, 9H, $w_{1/2} \approx 4$ kHz, C(CH_3)$_3$).
Crystals suitable for X-Ray analysis were obtained from pentane at -30°C.

Synthesis of [(Cp^{ttt})(Cp’’’)Tm(BH$_4$)] (26)

To a mixture of Tm(BH$_4$)$_3$(THF)$_3$ (0.20 g, 0.47 mmol) and [KCp^{ttt}] (0.16 g, 0.59 mmol) was added THF (10 mL) and the reaction was stirred for 15 h. The precipitated KBH$_4$ was removed by centrifugation and the solvent evaporated. Toluene (15 mL) was added onto the white residue and the insoluble solids were separated by centrifugation. The toluene solution was transferred into a Schlenk tube fitted with a J. Young valve and KCp’’’ (0.19 g, 0.59 mmol) was added. Heating this mixture to reflux with stirring for 15 h afforded a yellow solution, which was centrifuged and the solvent evaporated. Pure **26** was obtained from recrystallisation in pentane in 61% yield (0.20 g, 0.29 mmol).
^{1}H NMR (C$_6$D$_{12}$): δ 344 (br s, 9H, w$_{1/2}$ ≈ 2 kHz), 93 (br s, 9H, w$_{1/2}$ ≈ 1 kHz), 25 (br s, 18H, w$_{1/2}$ ≈ 3 kHz)
Crystals suitable for X-Ray analysis were obtained from pentane at -30°C.

Synthesis of [(Cp^{ttt})(Cp’’’)Tm] (27) by reduction of 25 (NMR experiment)

To a solution of [(Cp^{ttt})(Cp’’’)Tm(BH$_4$)] (10 mg, 14 μmol) in C$_6$D$_{12}$ was added KC$_8$ (19 mg, 143 μmol) leading slowly to a colour change from yellow to purple. After 24 h the reduction was completed as indicated by ^{1}H NMR.
^{1}H NMR (C$_6$D$_{12}$): δ 28.0 + 26.4 (br s, 36H, w$_{1/2}$ = 0.5 kHz), 18.2 (br s, 18H, w$_{1/2}$ = 0.2 kHz), -52 (br s, w$_{1/2}$ = 0.6 kHz, 2H, C*H*), -62 (br s, w$_{1/2}$ = 0.6 kHz, 2H, C*H*),

Reaction of [(Cp^{ttt})$_2$Tm] (8) with I$_2$

To a solution of [(Cp^{ttt})$_2$Tm] (50 mg, 78 μmol) in THF (3 mL) was added a solution of iodine (10 mg, 39 μmol) in THF (3 mL) at room temperature. The reaction turned immediately yellow and, after evaporation of the solvent, a ^{1}H NMR spectrum indicated the formation of **8**. Recrystallization of the crude product in toluene at 0°C allowed for the isolation of some crystals of [(Cp^{ttt})TmI$_2$(THF)] (**28**) suitable for X-ray analysis.

Reaction of [(Cp^{ttt})$_2$Tm] (8) with AgI

A solution of [(Cp^{ttt})$_2$Tm] (0.150 g, 0.24 mmol) in THF (5 mL) and AgI (0.06 g, 0.24 mmol) was stirred for 30 min at 0°C. After centrifugation, evaporation of the solvent resulted in the formation of yellow crystals which were washed with cold hexane. Pure **11** was isolated in 38% yield (0.07 g, 0.09 mmol).
^{1}H NMR spectrum in agreement with that of **11** obtained by metathesis.

Reaction of [(Cp’’’)$_2$Tm(THF)] (10) with AgI

A solution of [(Cp’’’)$_2$Tm(THF)] (0.100 g, 0.13 mmol) in THF (5 mL) and AgI (0.03 g, 0.13 mmol) was stirred for 30 min at 0°C. After centrifugation, evaporation of the solvent afforded

a yellow powder which was washed with cold hexane. Pure [(Cp’’’)$_2$TmI(THF)] was isolated in 30% yield (0.04 g, 0.04 mmol). The ^{1}H NMR spectrum corresponded to the spectrum of **12** in THF-d_8.
^{1}H NMR (C_6D_{12}): δ 43 (br s, $w_{1/2}$ = 1.5 kHz, Si(CH_3)$_3$).

Synthesis of [(Cp’’’)$_2$Tm(THF)] (10) by reduction of [(Cp’’’)$_2$TmI(THF)] (NMR experiment)

To a solution of [(Cp’’’)$_2$TmI(THF)] (10 mg, 11 μmol) in C_6D_{12} was KC_8 (15 mg, 110 μmol) leading to a colour change from yellow to purple. After 1 h the reduction was completed as indicated by ^{1}H NMR.
^{1}H NMR spectrum in agreement with that of **9** obtained by metathesis.

Reaction of [(Dtp)$_2$Tm] (22) with [(Dtp)$_2$Pb] (NMR experiment)

Addition of [(Dtp)$_2$Pb] (10 mg, 16 μmol) to a solution of [(Dtp)$_2$Tm] (20 mg, 32 μmol) in C_6D_6 (0.5 mL) led to the formation of an orange solution from which elemental lead precipitated.
^{1}H NMR (C_6D_6): δ 119 (br s, 36H, $w_{1/2}$ ≈ 3 kHz, tBu), 2.2 (s, 6H, CH_3), 0.2 (s, 18H, C(CH_3)$_3$).
^{31}P NMR (C_6D_6): δ 63.0 (s).

Synthesis of [(Dtp)$_2$Tm] (22) by reduction of [(Dtp)$_3$Tm] (NMR experiment)

To a solution of [(Dtp)$_3$Tm] (27 mg, 32 μmol) in C_6D_{12} (0.5 mL) was added KC_8 (43 mg, 320 μmol) leading to an immediate color change to green and the disappearance of the starting material as indicated by ^{31}P NMR.
^{1}H and ^{31}P NMR in agreement with literature reports.[13]

Reaction of [(Cp^{ttt})$_2$Tm] (8) with Ph$_3$PS

Addition of Ph_3PS (5 mg, 16 μmol) to a solution of [(Cp^{ttt})$_2$Tm] (20 mg, 31 μmol) in cyclohexane (2 mL) at room temperature led to an immediate colour change to yellow. The formation of Ph_3P was indicated in the ^{31}P NMR spectrum by a signal at -0.5 ppm and the disappearance of the starting material.

Reaction of [(Cp^{ttt})$_2$Tm] (8) with Ph$_3$PO

Addition of Ph_3PO (9 mg, 31 μmol) to a solution of [(Cp^{ttt})$_2$Tm] (20 mg, 31 μmol) in cyclohexane (2 mL) at room temperature led to an immediate colour change to green and the disappearance of the starting material as indicated by ^{31}P NMR.
^{31}P NMR (cyclohexane): δ -102 (br s).

Reaction of [(Cp^{ttt})$_2$Tm] (8) with pyridine

Addition of pyridine (2.5 µL, 0.03 mmol) to a solution of [(Cp^{ttt})$_2$Tm] (20 mg, 0.03 mmol) in toluene (2 mL) at room temperature led to an immediate colour change to orange. After evaporation of the solvent, the residue was dissolved in THF and crystals suitable for X-Ray analysis were grown from this solution at -30°C, yielding red [{(Cp^{ttt})$_2$Tm}$_2${µ-(NC$_5$H$_5$-C$_5$H$_5$N)}] (**29**) in 10% yield (4 mg, 0.003 mmol).

Reaction of [(Dtp)$_2$Tm] (22) with pyridine (NMR experiment)

Addition of pyridine (2.5 µL, 0.03 mmol) to a solution of [(Dtp)$_2$Tm] (19 mg, 0.03 mmol) in C_6D_6 (0.5 mL) led to the formation of a dark red solution which was stable for 30 min at room temperature.
^{1}H NMR (C_6D_6): δ 45 (br s, 36H, $w_{1/2} \approx 0.3$ kHz, tBu), 3 (br s, py), -22 (br s, 12H, $w_{1/2} \approx 0.6$ kHz, CH_3).
^{31}P NMR (C_6D_6): δ -260 (br s).

Reaction of [(Cp^{ttt})$_2$Tm] (8) with tBuCN

Addition of tBuCN (4.4 µL, 47 µmol) to a solution of (Cp^{ttt})$_2$Tm (20 mg, 31 µmol) in hexane (2 mL) at room temperature led to an immediate colour change to orange from which an orange solid precipitated after 24 h. Crystals suitable for X-Ray analysis of the yellow nitrile adduct [(Cp^{ttt})$_2$TmI(NCtBu)] (**30**) were grown from this solution at room temperature.
^{1}H NMR for **30** (C_6D_{12}): δ 55 (br s, 36H, $w_{1/2} \approx 1.5$ kHz, C(CH_3)$_3$), 23 (br s, 18H, $w_{1/2} \approx 1.5$ kHz, C(CH_3)$_3$), 3 (br s, C(CH_3)$_3$CN).

Chapter 4

General Procedure 2 (GP-2) for the preparation of [L$_2$DyX] precursors (L = Cp^{ttt}, Cp’’’, Dtp, Dsp; X = I, Br, BH$_4$)

In the glovebox a mixture of $DyX_3(THF)_y$ (for X = I or Br: y = 0, for X = BH_4: y = 3) (1.0 eq) and [K(L)] (2.2 eq) was prepared in a Schlenk tube fitted with a J. Young valve. Toluene (20mL) was condensed onto this mixture at -78°C and the suspension was allowed to warm to room temperature. Under stirring the reaction was heated to reflux for 48h. After that time the yellow solution was cooled to room temperature and centrifuged. The solvent was evaporated and the crude product was recrystallised from pentane at -30°C.

General Procedure (GP-3) for the reduction of [(Cp^{ttt})$_2$DyX] precursors (X = I, Br, BH$_4$)

In the glovebox a mixture of [(Cp^{ttt})$_2$DyX] (1.0 eq) and crown-ether (1.0 eq) was placed in a centrifugation tube and dissolved in cyclohexane (8 mL). After addition of KC_8 (2.0 eq) the

reaction mixture was shaken immediately to give a dark red solution from which the product precipitated over 24h. The supernatant was removed and the precipitate was taken up in toluene (15mL). After centrifugation the solution was evaporated yielding the pure product.

Synthesis of [(Cp^{ttt})$_2$DyI] (32-I)

From the reaction of DyI_3 (0.27 g, 0.50 mmol) and [KCp^{ttt}](0.30 g, 1.10 mmol) according to GP-2, **32-I** was obtained as a yellow powder in 66% yield (0.25 g, 0.33 mmol).
^{1}H NMR (C_6D_{12}): δ 12 (br s, 18H, $w_{1/2} \approx 3$ kHz, C(CH_3)$_3$), -191 (br s, 18H, $w_{1/2} \approx 3$ kHz, C(CH_3)$_3$), -390 (br s, 18H, $w_{1/2} \approx 4$ kHz, C(CH_3)$_3$).
Anal. Calcd for $C_{34}H_{58}DyI$ (756.23): C, 54.00; H, 7.73. Found : C, 54.28 H, 7.75.
Crystals suitable for X-Ray analysis were obtained from sublimation at 220°C and 10^{-3}mbar.

Synthesis of [(Cp^{ttt})$_2$DyBr] (32-Br)

From the reaction of $DyBr_3$ (0.30 g, 0.75 mmol) and [KCp^{ttt}](0.45 g, 1.65 mmol) according to the GP-2, **32-Br** was obtained as a white powder in 56% yield (0.30 g, 0.42 mmol).
^{1}H NMR (C_6D_{12}): δ -31 (br s, 18H, $w_{1/2} \approx 4$ kHz, C(CH_3)$_3$), -168 (br s, 18H, $w_{1/2} \approx 4$ kHz, C(CH_3)$_3$), -362 (br s, 18H, $w_{1/2} \approx 3$ kHz, C(CH_3)$_3$).
Anal. Calcd for $C_{34}H_{58}DyBr$ (709.23): C, 57.58; H, 8.24. Found : C, 57.87; H, 8.38.
Crystals suitable for X-Ray analysis were obtained from sublimation at 210°C and 10^{-3}mbar.

Synthesis of [(Cp^{ttt})$_2$Dy(BH_4)] (32-BH_4)

From the reaction of $Dy(BH_4)_3(THF)_3$ (0.30 g, 0.71 mmol) and [KCp^{ttt}](0.42 g, 1.56 mmol) according to the GP-2, **32-BH_4** was obtained as a pale yellow powder in 57% yield (0.26 g, 0.40 mmol).
^{1}H NMR (C_6D_{12}): δ -6 (br s, 18H, $w_{1/2} \approx 2$ kHz, C(CH_3)$_3$), -173 (br s, 18H, $w_{1/2} \approx 2$ kHz, C(CH_3)$_3$), -275 (br s, 18H, $w_{1/2} \approx 1$ kHz, C(CH_3)$_3$).
Anal. Calcd for $C_{34}H_{62}DyB$ (644.17): C, 63.39; H, 9.70. Found : C, 63.38 H, 9.91.
Crystals suitable for X-Ray analysis were grown in pentane at -30°C.

Synthesis of [(Cp’’’)$_2$DyI] (33)

From the reaction of DyI_3 (0.20 g, 0.37 mmol) and [NaCp’’’] (0.26 g, 0.85 mmol) according to the GP-2, **33** was obtained as a yellow powder in 66% yield (0.21 g, 0.24 mmol).
^{1}H NMR (C_6D_{12}): δ -70.1 (br s, 36H, $w_{1/2} \approx 1.5$ kHz, Si(CH_3)$_3$), -224 (br s, 18H, $w_{1/2} \approx 0.6$ kHz, Si(CH_3)$_3$).
Crystals suitable for X-Ray analysis were obtained from sublimation at 210°C and 10^{-3}mbar.

Synthesis of [(Dtp)$_2$DyI] (34)

From the reaction of DyI_3 (0.20 g, 0.37 mmol) and [K(Dtp)] (0.20 g, 0.77 mmol) according to the GP-2, **34** was obtained as a yellow powder in 75% yield (0.21 g, 0.28 mmol).
^{1}H NMR (C_6D_{12}): δ -241 (br s, $w_{1/2} \approx 2.5$ kHz, C(C*H*$_3$)$_3$).
Crystals suitable for X-Ray analysis were grown in pentane at -30°C.

Synthesis of [{(Dsp)$_2$DyI}$_2$] (35)

From the reaction of DyI_3 (0.20 g, 0.37 mmol) and [K(Dsp)] (0.23 g, 0.77 mmol) according to the GP-2, **35** was obtained as a yellow powder in 70% yield (0.21 g, 0.26 mmol).
^{1}H NMR (C_6D_{12}): δ -214 (br s, $w_{1/2} \approx 1.5$ kHz, Si(C*H*$_3$)$_3$).
Crystals suitable for X-Ray analysis were obtained from sublimation at 220°C and 10^{-3} mbar.

Synthesis of [(Cp^{ttt})$_2$Dy(μ-I)K([18]crown-6)] (36-I)

According to the GP-3, the reaction between [(Cp^{ttt})$_2$DyI] (70 mg, 92 μmmol), [18]crown-6 (24 mg, 92μmol) and KC_8 (24 mg, 184 μmol) led to pure **36-I** as a dark red powder in 72% yield (70 mg, 66 μmol).
^{1}H NMR (tol-d^8): δ 236 (br s, 18H, $w_{1/2}$ = 4 kHz, C(C*H*$_3$)$_3$), 109 (br s, 18H, $w_{1/2}$ = 4 kHz, C(C*H*$_3$)$_3$), -32 (br s, 24H, $w_{1/2}$ = 2 kHz, [18]crown-6), -233 (br s, 18H, $w_{1/2}$ = 4 kHz, C(C*H*$_3$)$_3$).
Crystals suitable for X-Ray analysis were grown in cyclohexane at room temperature.

Synthesis of [(Cp^{ttt})$_2$Dy(μ-Br)K([18]crown-6)] (36-Br)

According to the GP-3, the reaction between [(Cp^{ttt})$_2$DyBr] (50 mg, 71 μmol), [18]crown-6 (19 mg, 71 μmol) and KC_8 (19 mg, 140 μmol) led to pure **36-Br** as a dark red powder in 84% yield (60 mg, 59 μmol).
^{1}H NMR (tol-d^8): δ 209 (br s, 18H, $w_{1/2}$ = 3 kHz, C(C*H*$_3$)$_3$), 99 (br s, 18H, $w_{1/2}$ = 3 kHz, C(C*H*$_3$)$_3$), -63 (br s, 24H, $w_{1/2}$ = 2 kHz, [18]crown-6), -232 (br s, 18H, $w_{1/2}$ = 3 kHz, C(C*H*$_3$)$_3$).
Crystals suitable for X-Ray analysis were grown in cyclohexane at room temperature.

Synthesis of [(Cp^{ttt})$_2$Dy(μ-BH$_4$)K([18]crown-6)] (36-BH$_4$)

According to the GP-3, the reaction between [(Cp^{ttt})$_2$Dy(BH$_4$)] (100 mg, 156 μmol), [18]crown-6 (42 mg, 156 μmol) and KC_8 (42 mg, 312 μmol) led to pure **36-BH$_4$** as a dark red powder in 64% yield (95 mg, 100 μmol).
^{1}H NMR (tol-d^8): δ 343 (br s, 18H, $w_{1/2}$ = 3 kHz, C(C*H*$_3$)$_3$), 133 (br s, 18H, $w_{1/2}$ = 3 kHz, C(C*H*$_3$)$_3$), -49 (br s, 24H, $w_{1/2}$ = 2 kHz, [18]crown-6), -178 (br s, 18H, $w_{1/2}$ = 3 kHz, C(C*H*$_3$)$_3$).

Crystals suitable for X-Ray analysis were grown in toluene at -30°C.

Reaction of [(Cp^{ttt})$_2$DyI] with [2.2.2]cryptand

According to the GP-3, the reaction between [(Cp^{ttt})$_2$DyI] (20 mg, 26 μmmol), [2.2.2]cryptand (9 mg, 26 μmol) and KC_8 (5 mg, 40 μmol) led to "[{K([2.2.2]cryptand)}{(Cp^{ttt})$_2$DyI}]" as a dark red powder in 72% yield (22 mg, 19 μmol).
^{1}H NMR (tol-d^8): δ 249 (br s, $w_{1/2}$ = 1.5 kHz, C(CH_3)$_3$), 110 (br s, $w_{1/2}$ = 1.5 kHz, C(CH_3)$_3$), -8.4 (s, 12H, [2.2.2]cryptand), -9.7 (s, 24H, [2.2.2]cryptand), -231 (br s, w1/2 = 1 kHz, C(CH_3)$_3$).

Reactions of [(Cp^{ttt})$_2$Dy(μ-BH$_4$)K([18]crown-6)] (36-BH$_4$) with C_2Cl_6

a) Addition of hexachloroethane (9 mg, 39 μmol) to a solution of **36-BH$_4$** (75 mg, 78 μmol) in toluene (4 mL) led to an immediate colour change from dark red to yellow. The solvent was reduced and pentane was slowly added onto the solution. After 24 h white crystals suitable for X-Ray analysis of [(Cp^{ttt})$_2$Dy(μ-Cl)$_2$K([18]crown-6)] (**37**) were obtained in 28 % yield (22 mg, 22 μmol).
^{1}H NMR (tol-d^8): δ -10 (br s, 24H, $w_{1/2}$ = 0.3 kHz, [18]crown-6), -67 (br s, 18H, $w_{1/2}$ = 0.6 kHz, C(CH_3)$_3$).

b) Addition of hexachloroethane (18 mg, 78 μmol) to a solution of **36-BH$_4$** (75 mg, 78 μmol) in toluene (4 mL) led to an immediate colour change from dark red to yellow. The solvent was reduced and pentane was slowly added onto the solution. After 24 h white crystals suitable for X-Ray analysis of [(Cp^{ttt})DyCl(BH$_4$)(μ-Cl)K([18]crown-6)] (**38**) were obtained in 68 % yield (40 mg, 53 μmol).
^{1}H NMR (C_6D_6): δ 37 (br s, 24H, $w_{1/2}$ = 0.6 kHz, [18]crown-6), -24 (br s, 9H, $w_{1/2}$ = 0.3 kHz, C(CH_3)$_3$), -54 (br s, 9H, $w_{1/2}$ = 0.3 kHz, C(CH_3)$_3$), -85 (br s, 9H, $w_{1/2}$ = 0.3 kHz, C(CH_3)$_3$).

Synthesis of (*E*,*E*)-1,2,3,4-tetraphenyl-1,3-butadiene by reaction of [(Cp^{ttt})$_2$Dy(μ-BH$_4$)K([18]crown-6)] (36-BH$_4$) with diphenylacetylene

Addition of 1,2 diphenylacetylene (14 mg, 79 μmol) to a solution of **36-BH$_4$** (75 mg, 79 μmol) in toluene (8 mL) led to an immediate colour change from dark red to green. After hydrolysis, the yellow solution was dried over $MgSO_4$, filtered through silicon gel and evaporated. The obtained white residue was washed with hexane to give (*E*,*E*)-1,2,3,4-tetraphenyl-1,3-butadiene in 35% yield (5 mg, 14 μmol)
^{1}H NMR (THF-d^8): δ 7.25-7.45 (m, 10H), 6.90-7.01 (m, 6H), 6.66-6.75 (m, 4H), 6.34 (s, 2H)
EI-MS: 358 (100%)
Hydrolysis with D_2O gave the following data:
^{1}H NMR (THF-d^8): δ 7.25-7.45 (m, 10H), 6.90-7.01 (m, 6H), 6.66-6.75 (m, 4H)
EI-MS: 360 (100%)

Reaction of [(Cp^{ttt})$_2$Dy(μ-I)K([18]crown-6)] (36-I) with Ph$_3$PX (X = O, S)

a) Addition of Ph$_3$PS (4 mg, 14 μmol) to a solution of **36-I** (30 mg, 28 μmol) in toluene (3 mL) at room temperature led to an immediate colour change to yellow. The formation of Ph$_3$P was indicated in the ^{31}P NMR spectrum by a signal at -0.5 ppm and the disappearance of the starting material.

b) Addition of Ph$_3$PO (4 mg, 14 μmol) to a solution of **36-I** (30 mg, 28 μmol) in toluene (3 mL) at room temperature led to an immediate colour change to yellow. The formation of Ph$_3$P was indicated in the ^{31}P NMR spectrum by a signal at -0.5 ppm and the disappearance of the starting material.

Reaction of [(Cp^{ttt})$_2$Dy(μ-Br)K([18]crown-6)] (36-Br) with fluorenone

Addition of fluorenone (10 mg, 59 μmol) to a solution of **36-Br** (60 mg, 59 μmol) in toluene (4 mL) led to an immediate colour change from dark red to brown. After 24 h pure [{K([18]crown-6)}{(Cp^{ttt})$_2$DyBr(OC$_{13}$H$_8$)}] (**39**) precipitated from the solution in 82% (58 mg, 48 μmol).
Crystals suitable for X-ray analysis were grown from toluene at room temperature.

Chapter 5

Attempted synthesis of [(Cp^{ttt})$_2$NdCl] (40-Cl)

The synthesis of **40-Cl** was carried out according to literature reports. No pure product could be obtained.[18]

Synthesis of [(Cp^{ttt})$_2$Nd(BH$_4$)] (40-BH$_4$)

In the glovebox a mixture of Nd(BH$_4$)$_3$(THF)$_{3.5}$ (0.40 g, 0.98 mmol) and [NaCp^{ttt}(THF)$_{0.5}$] (0.63 g, 2.15 mmol) was prepared in a Schlenk tube fitted with a J. Young valve. THF (20mL) was condensed onto this mixture at -78°C and the suspension was allowed to warm to room temperature. After stirring for 24 h at room temperature THF was evaporated and toluene was condensed onto the residue. The reaction mixture was centrifuged, the solvent evaporated and the crude product was recrystallised from pentane at -30°C. **40-BH$_4$** was obtained with some impurities as a blue solid in 30% yield (0.18 g, 0.29 mmol).
^{1}H NMR (tol-d$_8$): δ 113 (br s, 4H, w$_{1/2}$ = 1 kHz, C*H*), 48 (br s, 4H, w$_{1/2}$ = 1 kHz, BH$_4$), -2.0 (s, 18H, C(C*H*$_3$)$_3$), -4.6 (s, 36H, C(C*H*$_3$)$_3$).
Crystals suitable for X-ray analysis were grown from pentane at -30°C.

Synthesis of [$(Cp^{ttt})_2NdI$] (40-I)

a) In the glovebox a mixture of $NdI_3(THF)_{3.5}$ (1.0 g, 1.29 mmol) and [KCp^{ttt}] (0.77 g, 2.86 mmol) was prepared in a Schlenk tube fitted with a J. Young valve. THF (20mL) was condensed onto this mixture at -78°C and the suspension was allowed to warm to room temperature. After stirring for 24 h at room temperature THF was evaporated. Toluene was condensed onto the residue and the reaction was left with stirring for 15h in refluxing toluene. After that time the green-blue solution was cooled to room temperature and centrifuged. The solvent was evaporated and the crude product was recrystallised from pentane at -30°C. **40-I** was obtained as a blue solid in 10% yield (0.10 g, 0.13 mmol).

b) In the glovebox a mixture of NdI_3 (0.30 g, 0.572 mmol) and [KCp^{ttt}] (0.39 g, 1.43 mmol) was prepared in a Schlenk tube fitted with a J. Young valve. Toluene (20mL) was condensed onto this mixture at -78°C and the suspension was allowed to warm to room temperature. Under stirring the reaction was heated to reflux for 48h. After that time the green-blue solution was cooled to room temperature and centrifuged. The solvent was evaporated and the crude product was recrystallised from pentane at -30°C. Pure **40-I** was obtained as a blue solid in 50% yield (0.21 g, 0.29 mmol).
^{1}H NMR (C_6D_{12}): δ 106 (br s, 4H, $w_{1/2}$ = 1 kHz, C*H*), -0.9 (br s, 18H, $w_{1/2}$ = 0.6 kHz, C(CH_3)$_3$), -11.6 (s, 18H, C(CH_3)$_3$), -18.1 (s, 18H, C(CH_3)$_3$).

Synthesis of [$(Cp^{ttt})_2Nd(\mu\text{-}I)K([18]crown\text{-}6)$] (42-I)

In the glovebox a mixture of $(Cp^{ttt})_2NdI$ (20 mg, 27 μmol) and crown-ether (7.2 mg, 27 μmol) was placed in a centrifugation tube and dissolved in cyclohexane (4 mL). After addition of KC_8 (10 mg, 74 μmol) the reaction mixture was shaken immediately to give a dark red solution. After centrifugation the solution was placed in another tube and pure dark red **42-I** precipitated during 24 h at room temperature in 80% yield (22 mg, 22 μmol).
^{1}H NMR (C_6D_{12}): 1.0 (s, 24H, [18]crown-6), -4.8 and -6.7 (br s, 36H, $w_{1/2}$ = 1 kHz, C(CH_3)$_3$), -19.4 (s, 18H, C(CH_3)$_3$).
Crystals suitable for X-Ray analysis were grown in cyclohexane at room temperature.

Part II

Synthesis of [(Dtp)$SmI_2(THF)_2$] (1)

$SmI_3(THF)_{3.5}$ (0.400 g, 0.510 mmol) and [K(Dtp)] (0.134 g, 0.510 mmol) were stirred in THF (10mL) for 15 hours. The reaction was checked by ^{31}P NMR which indicated that no starting material was left. The red solution was filtered and the solvent evaporated. The residue was taken up in toluene and filtered again. After evaporation the product was washed with diethyl ether to give a red powder of **2** in 62% yield (0.244 g, 0.316 mmol).

^{1}H NMR (THF-d_8): δ 3.73 (m, 8H, THF), 2.57 (s, 6H, CCH_3), 1.88 (m, 8H, THF), 0.58 (s, 18H, C(CH_3)$_3$).
^{13}C NMR (THF-d_8): δ 18.4 (s, C*C*H$_3$), 27.7 (d, $^{3}J_{P\text{-}C}$ = 7.1 Hz, C(*C*H$_3$)$_3$), 33.9 (d, $^{2}J_{P\text{-}C}$ = 8.3 Hz, *C*(CH$_3$)$_3$), 135.5 (s, PC*C*), 157.7 (d, $^{1}J_{P\text{-}C}$ = 10.3 Hz, P*C*).
^{31}P NMR (THF-d_8): δ 77.5 (s).
Anal. Calcd for $C_{22}H_{38}I_2O_2PSm$ (769.68): C, 34,33, H, 4,98. Found: C, 35.06, H, 4.99. Crystals suitable for X-ray analysis were grown from a diethyl ether solution at -30ºC.

Synthesis of [(Dtp)Y(CH$_2$C$_6$H$_4$NMe$_2$-*o*)$_2$] (3-Y)

Anhydrous YCl_3 (0.125 g, 0.641 mmol) and [K(Dtp)] (0.168 g, 0.641 mmol) were stirred in THF (10mL) for 15 hours. The reaction was checked by ^{31}P NMR which indicated that no starting material was left. To the reaction mixture a solution of [K(CH$_2$C$_6$H$_4$NMe$_2$-***o***)] (0.222 g, 1.282mmol) in THF (4mL) was added and a color change to yellow-green occurred immediately. After 2 hours a ^{31}P NMR spectrum showed that the reaction was finished. The solvent was evaporated and diethyl ether was added onto the residue. After filtration and evaporation a yellow foam was obtained which was washed with hexane to give **3-Y** in 68% yield (0.253 g, 0.436 mmol).
^{1}H NMR(C_6D_6, 50ºC): δ 6.85 (s, 4H, CH_{arom}) 6.66 (s, 4H, CH_{arom}), 2.41 (br s, 12H, N(CH_3)$_2$), 1.74 (br s, 6H, CCH_3), 1.51 (s, 18H, C(CH_3)$_3$), 1.43 (br s, 4H, YCH_2).
^{13}C NMR (C_6D_{12}): δ 17.8 (C*C*H$_3$), 32.5 (d, $^{3}J_{P\text{-}C}$ = 10.5Hz, C(*C*H$_3$)$_3$,), 36.1 (d, $^{2}J_{P\text{-}C}$ = 16.6 Hz, *C*(CH$_3$)$_3$), 44.0 (s, N(*C*H$_3$)$_2$), 45.7 (d, $^{1}J_{C\text{-}Y}$ = 31.7 Hz, Y*C*H$_2$), 117.3, 120.0, 127.3, 130.6 (aromatics), 135.2 (s, PC*C*), 142.2, 143.4 (aromatics), 152.9 (s, P*C*).
^{31}P NMR (C_6D_{12}): δ 88.9 (s).
Anal. Calcd for $C_{32}H_{46}N_2PY$ (578.60): C, 66,43, H, 8.01, N, 4.84. Found: C, 66.54, H, 8.40, N, 5.19.
Crystals suitable for X-ray analysis were grown from a diethyl ether solution at -30ºC.

Synthesis of [(Dtp)Sm(CH$_2$C$_6$H$_4$NMe$_2$-*o*)$_2$] (3-Sm)

a) To a solution of **2** (0.150 g, 0.239 mmol) in THF (6mL) was added a solution of [K(CH$_2$C$_6$H$_4$NMe$_2$-***o***)] (0.082 g, 0.478 mmol) in THF (4mL) and a color change to red-violet occurred immediately. After stirring the reaction mixture for 2 hours ^{31}P NMR indicated that no starting material was left. The solvent was evaporated and the residue was taken up in diethyl ether. After filtration and evaporation **3-Sm** was obtained as a dark red powder in 80% yield (0.123 g, 0.191 mmol).

b) $SmI_3(THF)_{3.5}$ (0.400 g, 0.510 mmol) and [K(Dtp)] (0.134 g, 0.510 mmol) were stirred in THF (10mL) for 15 hours. The reaction was checked by ^{31}P NMR which indicated that no starting material was left. To the reaction mixture a solution of [K(CH$_2$C$_6$H$_4$NMe$_2$-***o***)] (0.176 g, 1.020 mmol) in THF (4mL) was added and a color change to red-violet occurred immediately. After 2h a ^{31}P NMR spectrum showed that the reaction was finished. The

solvent was evaporated and diethyl ether was added onto the residue. After filtration and evaporation the product was washed with some cold diethyl ether to give pure **3-Sm** in 64% yield (0.209 g, 0.326 mmol).
^{1}H NMR (tol-d_8, 80ºC): δ 14.44 (v br s, 4H, SmCH_2), 9.79 (s. 2H, aromatics), 7.56-7.70 (m, 4H, aromatics), 4.68 (s, 2H, aromatics), 2.03 (s, 18H, C(CH_3)$_3$), 0.59 (br s, 6H, CCH_3), -2.29 (br s, 12H, N(CH_3)$_2$).
^{31}P NMR (tol-d_8): δ 62.2 (s).
Anal. Calcd for $C_{32}H_{46}N_2PSm$ (640.05): C, 60.05, H, 7.24, N, 4.38. Found: C, 59.79, H, 7.36, N, 4.63.
Crystals suitable for X-ray analysis were grown from a diethyl ether solution at -30ºC.

Synthesis of [{Sc[μ-O(CH$_2$)$_4$(Dtp)]Cl$_2$(THF)$_2$}$_2$] (5)

Anhydrous $ScCl_3$ (0.097 g, 0.641mmol) and [K(Dtp)] (0.168 g, 0.641 mmol) were stirred in THF (10mL) for 72 hours. The reaction was checked by ^{31}P NMR which indicated that no starting material was left. After centrifugation the solvent was evaporated and **5** was obtained as a white powder in 95% yield (0.338 g, 0.304 mmol).
^{1}H NMR (THF-d_8): δ 0.98 (br s, 4H, CH_2CH$_2$P), 1.33 (s, 36H, C(CH_3)$_3$), 1.80 (br s, 20H, THF + OCH$_2$CH_2), 2.06 (s, 16H, CH_3 + PCH_2), 3.65 (br s, 16H, THF), 4.09 (m, 4H, OCH_2).
^{13}C NMR (THF-d_8): δ 14.6 (d, $^{1}J_{P\text{-}C}$ = 3.8 Hz, C*C*H$_3$), 19.1 (d, $^{3}J_{P\text{-}C}$ = 10.9 Hz, P(CH$_2$)$_2$*C*H$_2$), 23.5 (d, $^{2}J_{P\text{-}C}$ = 32.9 Hz, PCH$_2$*C*H$_2$), 23.8 (s, THF), 29.1 (d, $^{3}J_{P\text{-}C}$ =10.4 Hz, C(*C*H$_3$)$_3$), 32.3 (d, $^{2}J_{P\text{-}C}$ = 25.7 Hz, *C*(CH$_3$)$_3$), 32.5 (d, $^{1}J_{P\text{-}C}$ = 6.0 Hz, P*C*H$_2$), 65.6 (s, THF), 67.6 (s, P(CH$_2$)$_3$*C*H$_2$), 141.1 (d, $^{2}J_{P\text{-}C}$ = 10.0 Hz, PC*C*), 143.9 (d, $^{1}J_{P\text{-}C}$ = 6.5 Hz, P*C*).
^{31}P NMR (THF-d_8): δ 6.0 (s).
No correct elemental analysis could be obtained for this compound.
Crystals suitable for X-ray analysis were obtained from slow diffusion of hexanes into a THF solution of **5**.

Synthesis of [{(Dtp)Sc(μ-Cl)Cl(NC$_5$H$_5$)}$_2$] (6)

Anhydrous $ScCl_3$ (0.097 g, 0.641mmol) and [K(Dtp)] (0.168 g, 0.641 mmol) were stirred in a toluene/pyridine mixture (5/1) (6 mL) for 15 hours. The reaction was checked by ^{31}P NMR which indicated that no starting material was left. After centrifugation the solvent was evaporated and a white powder of **6** was obtained in 90% yield (0.242 g, 0.288 mmol).
^{1}H NMR (C_6D_6): δ 1.52 (s, 18H, C(CH_3)$_3$), 2.56 (s, 6H, CCH_3), 6.31 (m, 2H, pyridine), 6.65 (m, 1H, pyridine), 8.78 (d, 2H, ^{3}J = 4.8Hz, pyridine)
^{13}C NMR (C_6D_6): δ 18.2 (C*C*H$_3$), 32.8 (d, $^{3}J_{P\text{-}C}$ = 9.8 Hz, C(*C*H$_3$)$_3$), 37.3 (d, *C*(CH$_3$)$_3$), $^{2}J_{P\text{-}C}$ = 15.8 Hz), 124.8, 140.2 (pyridine), 142.5 (d, $^{2}J_{P\text{-}C}$ = 3.8 Hz, PC*C*), 150.6 (pyridine), 168.1 (d, $^{1}J_{P\text{-}C}$ = 55.5Hz, P*C*).
^{31}P NMR (C_6D_6): δ 123.0 (s).

Anal. Calcd for $C_{38}H_{54}Cl_3N_2P_2Sc_2$ (797.07) : C, 57.26, H, 6.83, N, 3.51; found: C, 55.95, H, 7.11, N, 2.97.
Crystals suitable for X-ray analysis were obtained from slow diffusion of hexanes into a THF solution of **6**.

Synthesis of [(Dtp)Sc($CH_2C_6H_4NMe_2$-*o*)$_2$] (3-Sc)

a) To a solution of **6** (0.100 g, 0.240 mmol) in toluene (5 mL) was slowly added under vigorous stirring a suspension of [K($CH_2C_6H_4NMe_2$-***o***)] (0.083 g, 0.480 mmol) in toluene (5mL) resulting in an orange solution. The reaction was left with stirring for 2 hours, after which ^{31}P NMR indicated that all the starting material had been consumed. After centrifugation the solvent was evaporated at 40°C for 5 hours and the residue was recrystallised from hexanes to afford pure **3-Sc** as a yellow solid in 40 % yield (0.052 g, 0.096 mmol).

b) Addition of *p*-toluene sulfonic acid (0.047 g, 0.250 mmol) to a solution of [K(Dtp)] (0.066 g, 0.252 mmol) in toluene (4mL) resulted in the protonation of Dtp as indicated by ^{31}P NMR. After addition of [Sc(*o*-Me_2N-benzyl)$_3$] (0.112 g, 0.251 mmol) the reaction was heated to 50°C and left with stirring for 15h. After this period ^{31}P NMR indicated that no starting material was left. Evaporation of the solvent at 40°C for 5 hours and recrystallisation from hexanes gave **3-Sc** as a yellow powder in 70% yield (0.094 g, 0.175 mmol).
^{1}H NMR (C_6D_{12}): δ 1.38 (s, 18H, C(C*H*$_3$)$_3$), 1.44 (s, 4H, ScC*H*$_2$), 1.60 (s, 6H, CC*H*$_3$), 2.63 (s, 12H, N(C*H*$_3$)$_2$), 6.55-6.73 (m, 8H, aromatics).
^{13}C NMR (C_6D_{12}): δ 16.8 (C*C*H$_3$), 32.4 (d, $^3J_{P\text{-}C}$ = 10.5Hz, C(*C*H$_3$)$_3$), 36.7 (d, $^2J_{P\text{-}C}$ = 17.3 Hz, *C*(CH$_3$)$_3$), 48.5 (N(*C*H$_3$)$_2$), 50.3 (Sc*C*H$_2$), 115.8, 121.1, 126.3, 130.5 (aromatics), 135.4 (d, $^2J_{P\text{-}C}$ = 3.8 Hz, PC*C*), 144.3, 147.4 (aromatics), 163.7 (d, $^1J_{P\text{-}C}$ = 54Hz, P*C*).
^{31}P NMR (C_6D_{12}): δ 99.0 (s).
Anal. Calcd for $C_{32}H_{46}N_2PSc$ (534.65): C, 71.89, H, 8.67, N, 5.24. Found C, 69.55, H, 8.99, N, 4.70.
Crystals suitable for X-ray analysis were obtained from a saturated benzene solution.

Synthesis of Dtp-H (7) (NMR experiment)

To a mixture of [K(Dtp)] (0.010 g, 0.038 mmol) and *p*-toluene sulfonic acid (0.007 g, 0.038 mmol) in an NMR tube, THF-d_8 was added, leading to the immediate protonation of Dtp.
^{1}H NMR (THF-d_8): δ 1.32 (s, 18H, C(C*H*$_3$)$_3$), 2.08 (s, 6H, CC*H*$_3$), 4.91 (d, 1H, $^1J_{P\text{-}H}$ = 219Hz, P*H*).
^{13}C NMR (THF-d_8): δ 16.3 (d, $^3J_{P\text{-}C}$ = 3Hz, C*C*H$_3$), 30.8 (d, $^3J_{P\text{-}C}$ = 7.3 Hz, C(*C*H$_3$)$_3$), 34.1 (d, $^2J_{P\text{-}C}$ = 14.9 Hz, *C*(CH$_3$)$_3$), 143.7 (d, $^1J_{P\text{-}C}$ = 18.7 Hz, P*C*), 145.4 (d, $^2J_{P\text{-}C}$ = 2.5 Hz, PC*C*).
^{31}P NMR (THF-d_8): -53.3 (d, 211.2 Hz).

Typical polymerisation procedure for styrene:

In the glove box, a toluene solution (7 mL) of $[Ph_3C][B(C_6F_5)_4]$ (0.019 g, 0.021 mmol) was added to a toluene solution (5 mL) of $[(Dtp)Sc(CH_2C_6H_4NMe_2\text{-}o)_2]$ (0.011 g, 0.021 mmol) in a 100-mL flask. The mixture was stirred at room temperature for a few minutes, and styrene (1.074 g, 10.5 mmol) was added under vigorous stirring. After a few seconds the stirring ceased due to the viscosity. The flask was then taken outside the glovebox and after ca. 1 min, methanol (2 mL) was added to stop the polymerization. The mixture was poured into methanol (200 mL) to precipitate the polymer product. The white polymer was collected by filtration and dried under vacuum at 60°C to a constant weight (1.074 g, 10.5 mmol).

Part III

Synthesis of $[Li_2(SPCPS)]$ (1)

Methyllithium (4.0 mL, 1.6 M in diethyl ether, 6.4 mmol) was added to a solution of bis(diphenylthiophosphinoyl)methane (1.43 g, 3.2 mmol) in a toluene/diethyl ether solution (5/1, 20 mL) at -78°C. The resulting mixture was warmed to room temperature and stirred for 15 h, leading quantitatively to a yellow solution of **1** as indicated by ^{31}P NMR.
^{31}P NMR (toluene): δ 24.3 (br s).

Synthesis of $[\{(SPCPS)Sm(\mu\text{-}I)(THF)_2\}_2]$ (2)

A solution of **1** in toluene (3.0 mL, 0.40 mmol) was added onto $SmI_3(THF)_{3.5}$ (0.31 g, 0.40 mmol) and the reaction was stirred for 15 min. After centrifugation LiI salt was removed and diethyl ether (5 mL) was condensed onto the solution. After 24 hours, **2** was isolated as a yellow precipitate in 81% yield (0.28 g, 0.32 mmol).
^{1}H NMR (tol-d_8): δ 8.4 (m, 4 H, ortho-aryl), 7.15-7.03 (m, 16 H, meta+para-aryl), 3.2 (br s, 8 H, THF), 1.04 (br s, 8 H, THF).
^{13}C NMR (tol-d_8): δ 141.2 (d, $^{2}J_{P\text{-}C}$ =75.5 Hz, ipso), 131.7 (s, ortho), 129.7 (s, para), 128.1 (s, meta), C-Sm not observed.
^{31}P NMR (tol-d_8): δ 51.8 (br s).
Crystals suitable for X-ray analysis were obtained from a toluene/diethyl ether/hexanes solution at -30°C.

Synthesis of $[\{(SPCPS)Tm(\mu\text{-}I)(THF)_2\}_2]$ (3)

To $TmI_3(THF)_{3.5}$ (325 mg, 0.40 mmol) was added a solution of **1** in toluene (3.0 mL, 0.40 mmol) and stirred for 30 minutes at room temperature. LiI salt was removed by centrifugation and diethyl ether (5 mL) was condensed onto the solution. A white precipitate of **3** was collected after 24 hours in 78% yield (276 mg, 0.31 mmol).
Anal. Calcd. for $C_{66}H_{72}I_2O_4P_4S_4Tm_2$: C, 44.71; H, 4.09. Found C, 44.83; H, 4.16.

Crystals suitable for X-ray analysis were obtained from slow diffusion of hexanes into a toluene solution.

Synthesis of [{Li(THF)$_4$}{(SPCPS)$_2$Sm}] (4)

In a centrifugation tube two equivalents of **1** in toluene (6.0 mL, 0.80 mmol) were added onto $SmI_3(THF)_{3.5}$ (0.31 g, 0.40 mmol) and the reaction was stirred for 5 min, at room temperature. LiI salt was eliminated via centrifugation. Evaporation of the solvent affords a yellow solid which was washed with a THF (0.5 mL) diethyl ether (10 mL) mixture. Pure complex **4** was isolated in 87% yield (0.47 g, 0.35 mmol).
^{1}H NMR (tol-d$_8$): δ 8.42 (br s, 16H, ortho), 7.11-7.05 (m, 24H, meta+para), 2.96 (br s, 16H, THF), 1.11 (br s, 16H, THF).
^{13}C NMR (tol-d$_8$): δ 144.1 (d, $^1J_{C\text{-}P}$ = 81.6 Hz, ipso), 131.6 (s, ortho), 129.0 (s, para), 127.8 (s, meta); 68.1 (s, THF), 25.1 (s, THF).
^{31}P NMR (tol-d$_8$): δ 46.2 (br s).
Crystals suitable for X-ray analysis were obtained from slow diffusion of hexanes into a toluene solution.

Synthesis of [{Li(THF)$_4$}{(SPCPS)$_2$Tm}] (5)

Two equivalents of **1** in toluene (3.0 mL, 0.40 mmol) were added onto $TmI_3(THF)_{3.5}$ (163 mg, 0.20 mmol) at room temperature. Elimination of the LiI salt by centrifugation and evaporation of the solvent yielded a yellow solid which was purified by washing with a THF (0.5 mL) diethyl ether (10 mL) mixture. Pure product **5** was obtained in 81% yield (218 mg, 0.16 mmol).
Anal. Calcd. for $C_{66}H_{72}LiO_4P_4S_4Tm$: C, 58.40; H, 5.35. Found C, 58.63; H, 5.29.
Crystals suitable for X-ray analysis were obtained from slow diffusion of hexanes into a toluene solution.

Reaction of 2 with benzophenone

Benzophenone (10 mg, 0.06 mmol) and samarium carbene **2** (50 mg, 0.06 mmol) were reacted in toluene (5 mL) for 1 hour upon which a white precipitate formed. After centrifugation the precipitate was removed and the solution evaporated affording $Ph_2C{=}C(P(S)Ph_2)_2$ (**6**) as a pale yellow solid in 94% yield (0.034 g, 0.056 mmol).
^{1}H NMR (tol-d$_8$): δ 8.2 (br s, 4 H, ortho-aryl), 7.1-6.7 (m, 16 H, meta+para-aryl).
^{13}C NMR (tol-d$_8$): δ 177.5 (d, $^2J_{P\text{-}C}$ = 2.3 Hz, C=CPh$_2$), 142.7 (d, $^1J_{P\text{-}C}$ = 11.5 Hz C=CPh$_2$), 132.2-125.6 (phenyl).
^{31}P NMR (tol-d$_8$): δ 40.1 (s).
Crystals suitable for X-ray analysis were obtained from slow diffusion of hexanes into a toluene solution.

Reaction of 3 with benzophenone

Benzophenone (10 mg, 0.06 mmol) and thulium carbene **3** (50 mg, 0.06 mmol) were reacted in toluene (5 mL) for 1 hour upon which a white precipitate formed. After centrifugation the precipitate was removed and the solution evaporated giving $Ph_2C=C(P(S)Ph_2)_2$ (**6**) as a pale yellow solid in 94% yield (0.034 g, 0.056 mmol).

Reaction of 4 with benzophenone

a) Addition of one equivalent of benzophenone (5.5 mg, 0.03 mmol) to a solution of **4** (40 mg, 0.03 mmol) in C_6D_6 (1 mL) yielded the quantitative formation of the intermediate complex **7** within 10 minutes, which was was quantitatively transformed into $Ph_2C=C(P(S)Ph_2)_2$ (**6**) after 12 h at room temperature.
^{1}H NMR for **7** (C_6D_6): δ 8.67-6.42 (m, H of phenyl).
^{13}C NMR for **7** (C_6D_6): δ 148.8 (t, $^2J_{P-C}$ = 8.1 Hz, CO), 138.1 (d, $^1J_{P-C}$ = 101.8 Hz, SPCipso), 137.5 (d, $^1J_{P-C}$ = 88.9 Hz, SPCipso), 134.6 (s, OCCipso), 135.6-126.3 (m, ortho+meta+para aryl), 55.3 (t, $^1J_{P-C}$ = 49.4 Hz, PCCO).
^{31}P NMR for **7** (C_6D_6): δ 49.4 (br s, PCCP), 43.9 (br s, PCSmP).

b) Crystals of complex $[Sm\{\mu\text{-}OCPh_2C(P(S)Ph_2)_2\}_2Li(THF)]$ (**8**) were grown by diffusing a saturated solution of benzophenone in hexanes in a solution of complex **4** in toluene (0.07 mmol, 1 mL).
^{31}P NMR (tol-d_8): δ 50.2 (s).

Reaction of 5 with benzophenone

a) Addition of one equivalent of benzophenone (5.5 mg, 0.03 mmol) to a solution of **5** (41 mg, 0.03 mmol) in C_6D_6 (1 mL) yielded the quantitative formation of $Ph_2C=C(P(S)Ph_2)_2$ (**6**) after 12 h at room temperature.
b) Crystals of complex $[Tm\{\mu\text{-}OCPh_2C(P(S)Ph_2)_2\}_2Li(THF)]$ (**9**) were grown by diffusing a saturated solution of benzophenone in hexanes in a solution of complex **5** in toluene (0.07 mmol, 1 mL).

Synthesis of $[\{Na(THF)_3\}\{(SPCPS)Sm(Cp^*)_2\}]$ (11)

A solution of **2** (50 mg, 0.06 mmol) and NaCp* (18 mg, 0.12 mmol) in THF (5 mL) was stirred for 30 min at room temperature. ^{31}P NMR indicated the disappearance of the starting material. The solvent was evaporated and toluene (5 mL) was added onto the residue. After centrifugation, the solvent was evaporated and the residue washed with pentane. Pure **11** was obtained in 54% (36 mg, 0.03 mmol).
^{1}H NMR (THF-d_8): δ 8.4-6.4 (m, H of phenyl), -0.2 (s, CH_3).
^{31}P NMR (THF-d_8): δ 44.5 (s).

Crystals suitable for X-ray analysis were obtained from slow diffusion of hexanes into a toluene solution.

References

[1] D. H. Grant, *J. Chem. Educ.* **1995**, *72*, 39.
[2] K. Izod, S. T. Liddle, W. Clegg, *Inorg. Chem.* **2004**, *43*, 214.
[3] S. M. Cendrowski-Guillaume, G. Le Gland, M. Nierlich, M. Ephritikhine, *Organometallics* **2000**, *19*, 5654.
[4] M. N. Bochkarev, A. A. Fagin, *Chem.-Eur. J.* **1999**, *5*, 2990.
[5] I. S. Weitz, M. J. Rabinovitz, *J. Chem. Soc., Perkin Trans. I* **1993**, 117.
[6] P. Jutzi, F. Kohl, P. Hofmann, C. Kruger, Y.-H. Tsay, *Chem. Ber.* **1980**, *113*, 757.
[7] H. Schumann, I. Albrecht, J. Loebel, E. Hahn, M. B. Hossain, D. Van der Helm, *Organometallics* **1986**, *5*, 1296.
[8] P. L. Watson, J. F. Whitney, R. L. Harlow, *Inorg. Chem.* **1981**, *20*, 3271.
[9] F. Weber, H. Sitzmann, M. Schultz, C. D. Sofield, R. A. Andersen, *Organometallics* **2002**, *21*, 3139.
[10] M. A. Edelmann, P. B. Hitchcock, J. Hu, M. F. Lappert, *New J. Chem.* **1995**, *19*, 481.
[11] M. J. Harvey, T. P. Hanusa, *Organometallics* **2000**, *19*, 1556.
[12] R. Riemschneider, *Z. Naturforsch. Teil B* **1963**, *18*, 641.
[13] D. Turcitu, F. Nief, L. Ricard, *Chem.-Eur. J.* **2003**, *9*, 4916.
[14] M. Visseaux, F. Nief, L. Ricard, *J. Organomet. Chem.* **2002**, *647*, 139.
[15] D. Carmichael, L. Ricard, F. Mathey, *J. Chem. Soc., Chem. Commun.* **1994**, 1167.
[16] S. Harder, *Organometallics* **2005**, *24*, 373.
[17] S. O. Grim, J. D. Mitchell, *Inorg. Chem.* **1977**, *16*, 1762.
[18] M. D. Walter, D. Bentz, F. Weber, O. Schmitt, G. Wolmershauser, H. Sitzmann, *New J. Chem.* **2007**, *31*, 305.

Supplementary Material

Paramagnetic ^{1}H NMR spectra

X-ray crystallographic data

Annex I: NMR spectra of paramagnetic Tm^{3+}, Tm^{2+}, Dy^{3+} and Dy^{2+} complexes

a) Examples of Tm^{3+} complexes

$[(Cp^{ttt})_2TmI]$ (11)

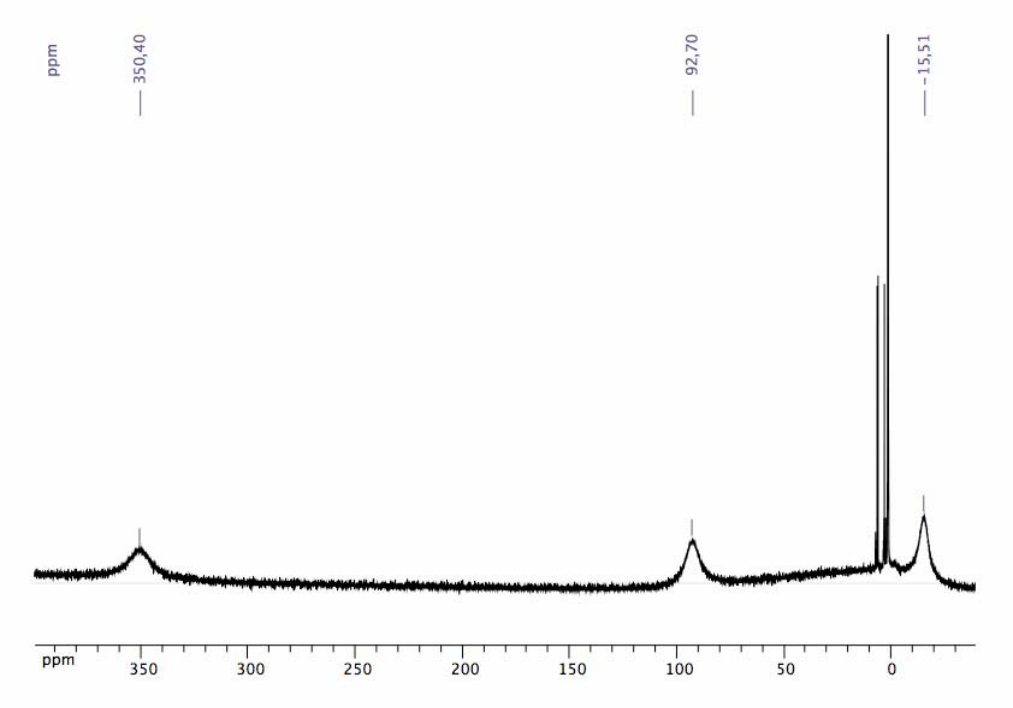

$[(Cp^{ttt})_2Tm(BH_4)]$ (14)

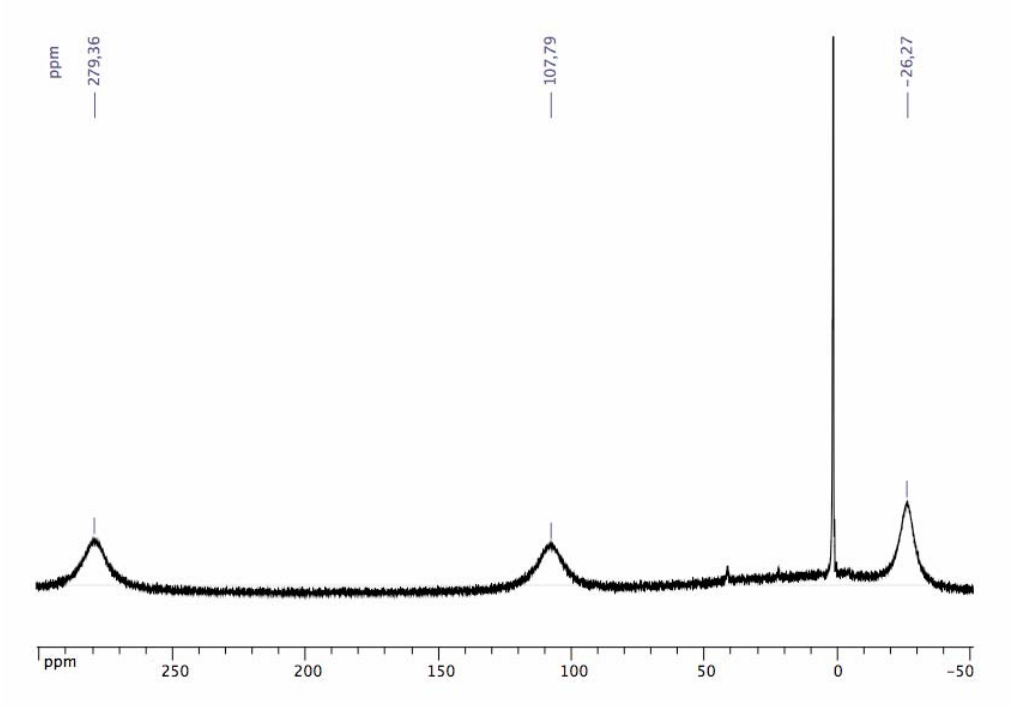

[(Cp$^{'''}$)$_2$TmI] (12)

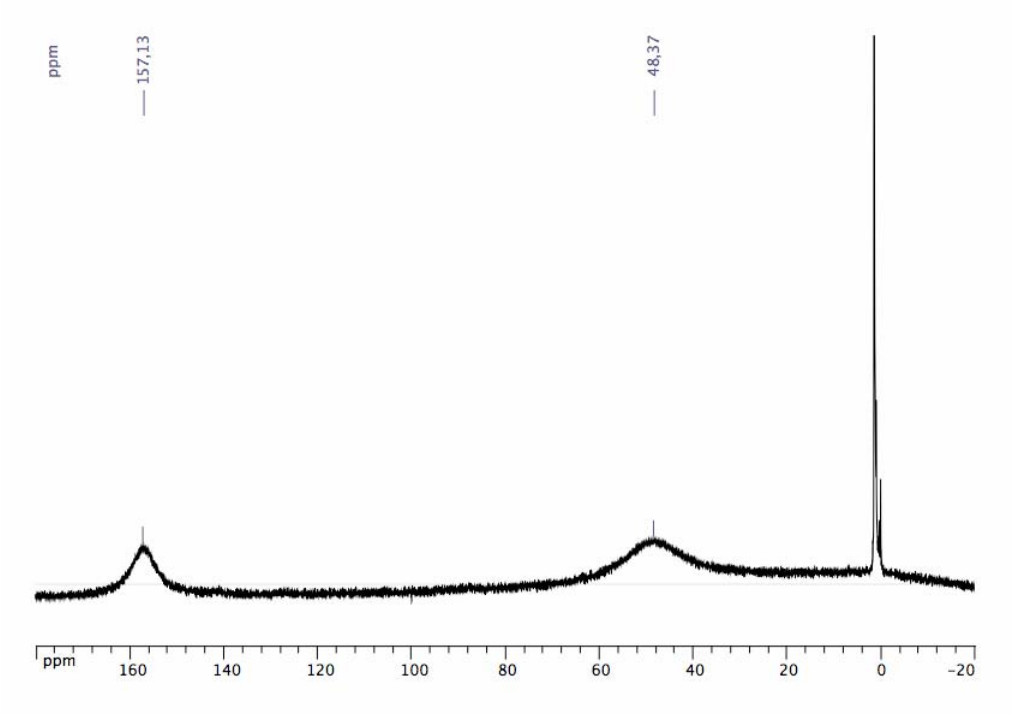

b) Examples of Tm^{2+} complexes

[(Cp^{ttt})$_2$Tm] (8)

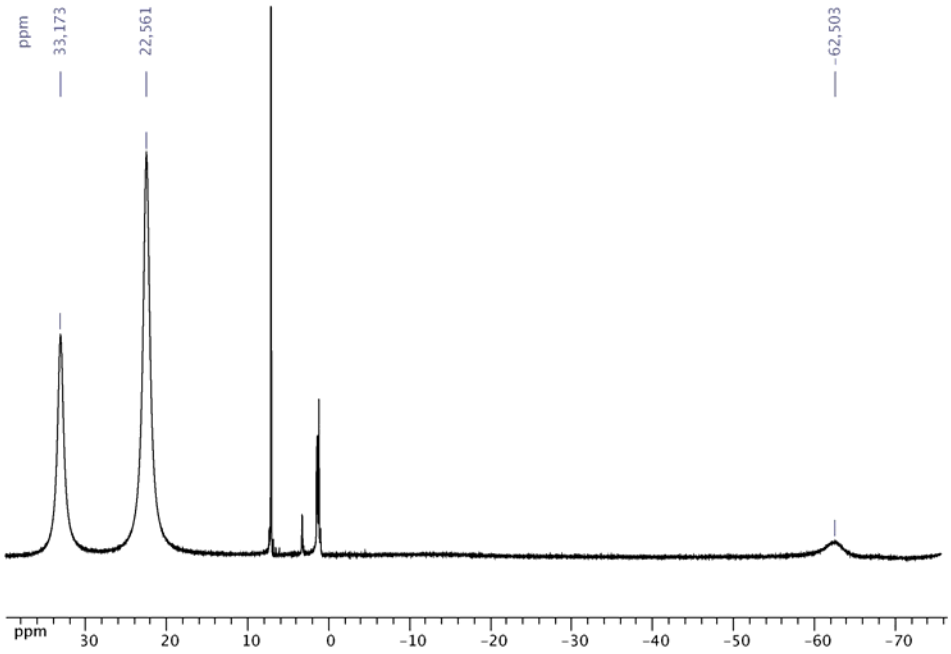

[(Cp‴)$_2$Tm] (13)

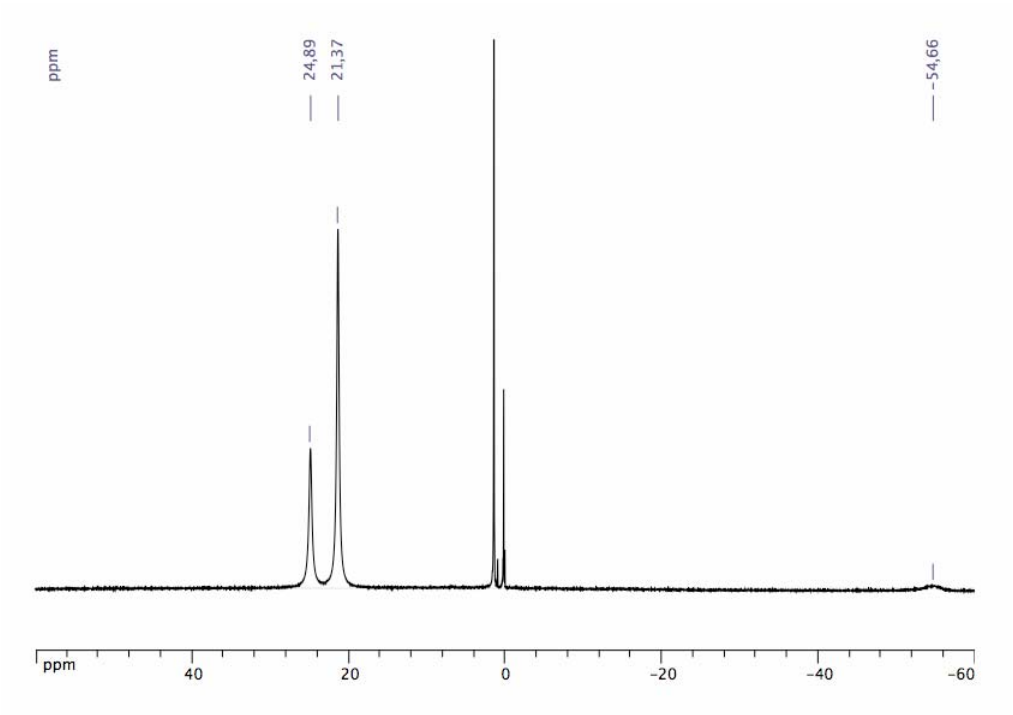

[(Cp‴)$_2$Tm(THF)] (10)

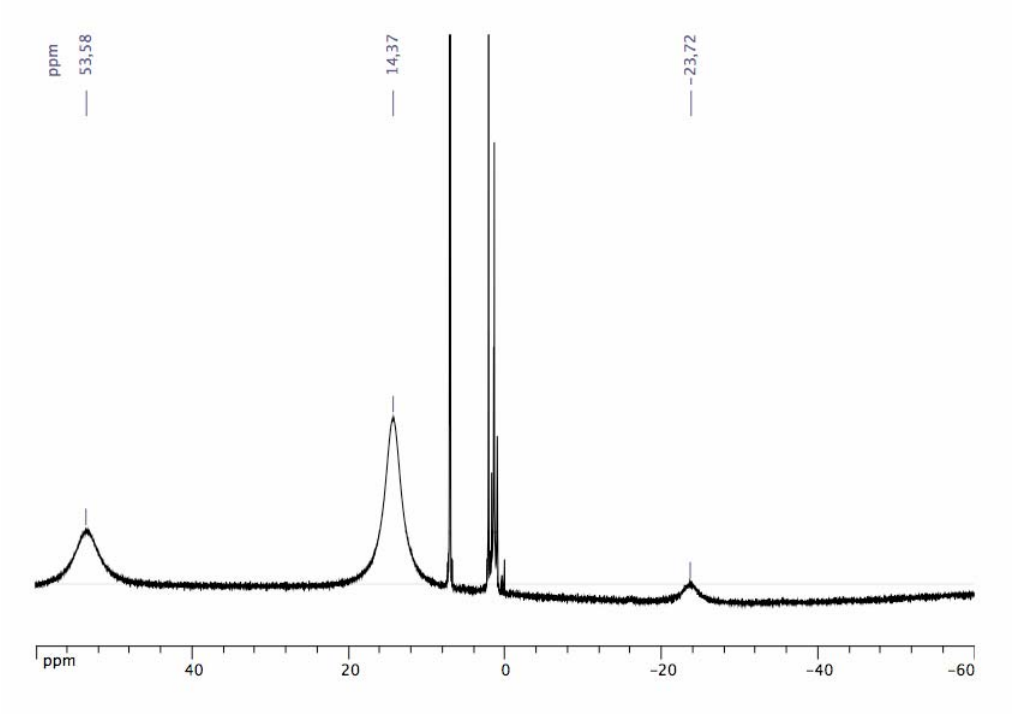

[(Cp^{ttt})(Cp’’’)Tm] (27)

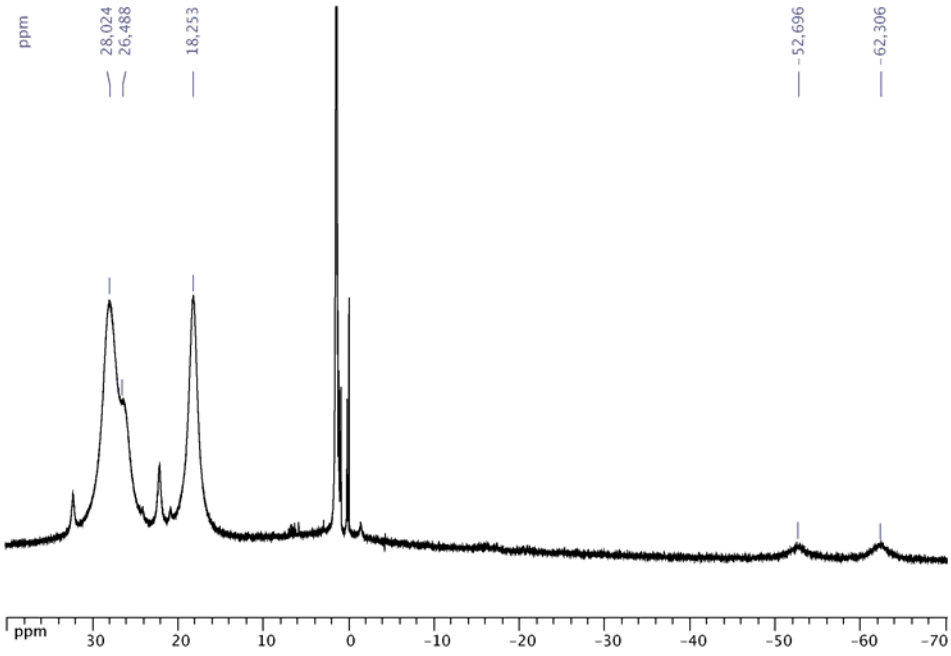

[{(Htp)$_2$Tm}$_2$] (23)

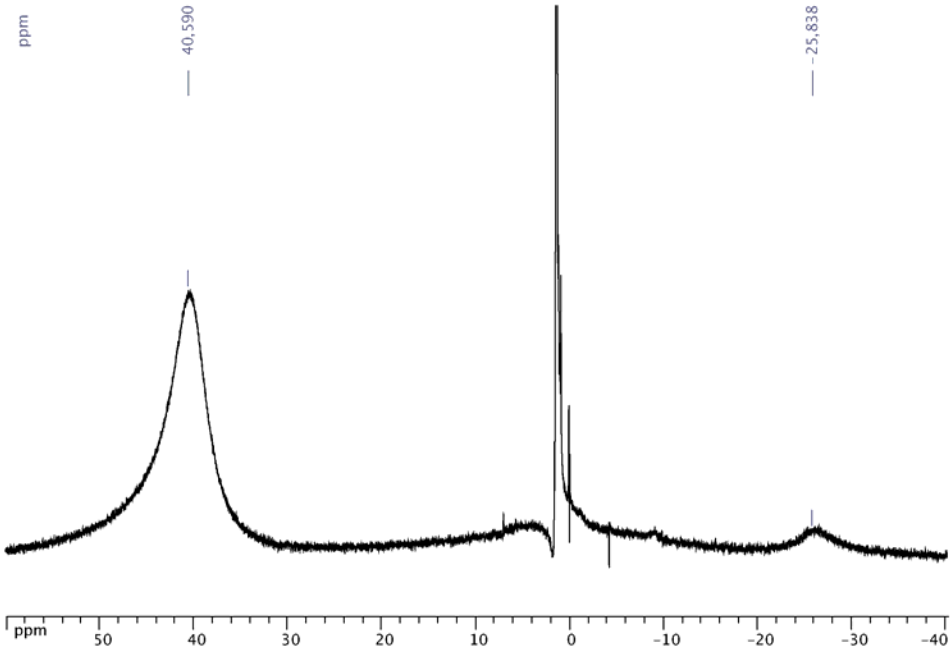

b) Examples of Dy^{3+} complexes

[$(Cp^{ttt})_2DyI$] (32-I)

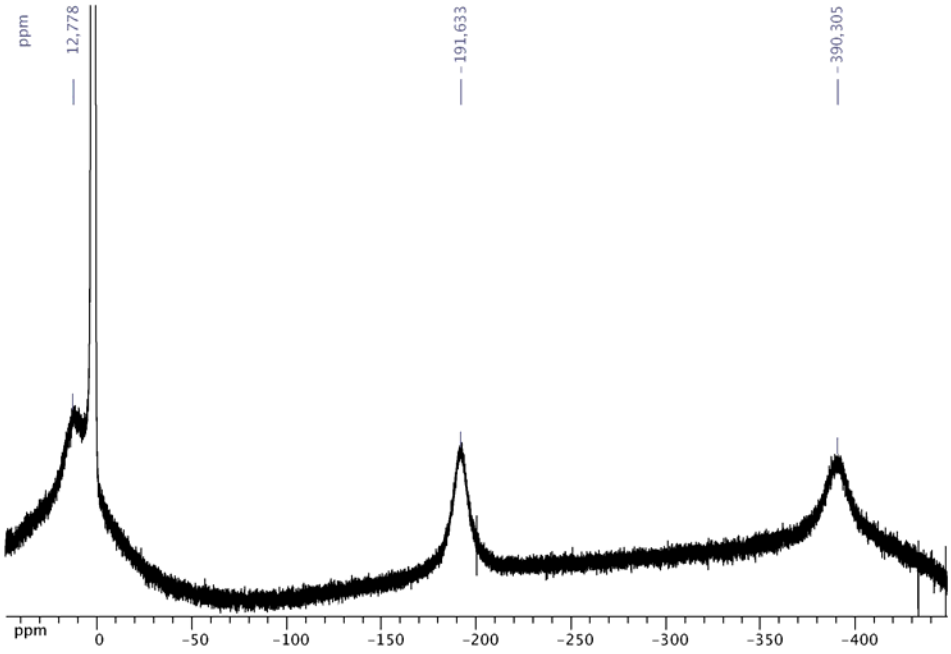

[$(Cp^{ttt})_2DyBr$] (32-Br)

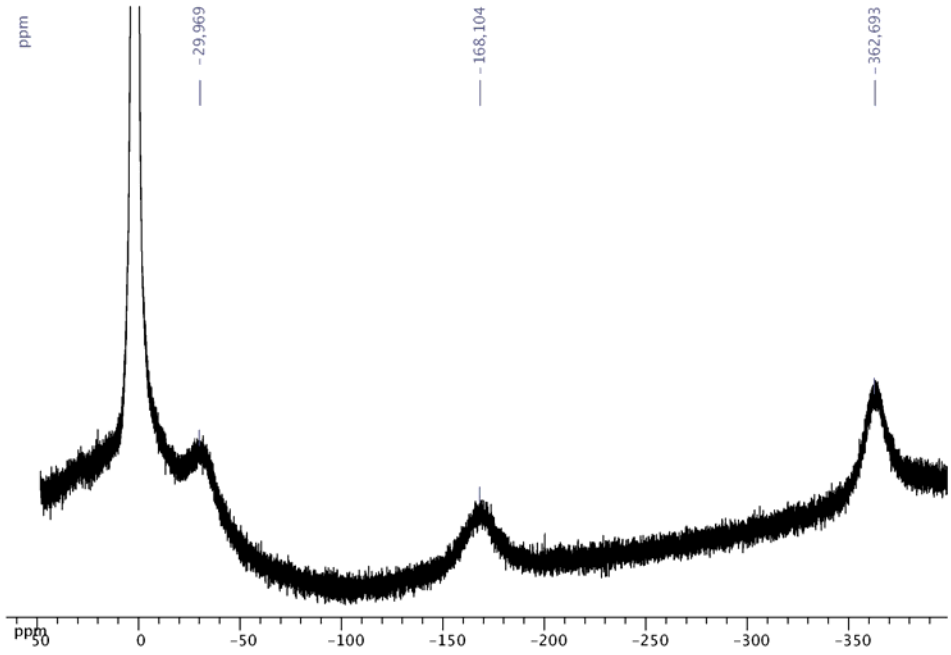

[(Cp^{ttt})$_2$Dy(BH$_4$)] (32-BH$_4$)

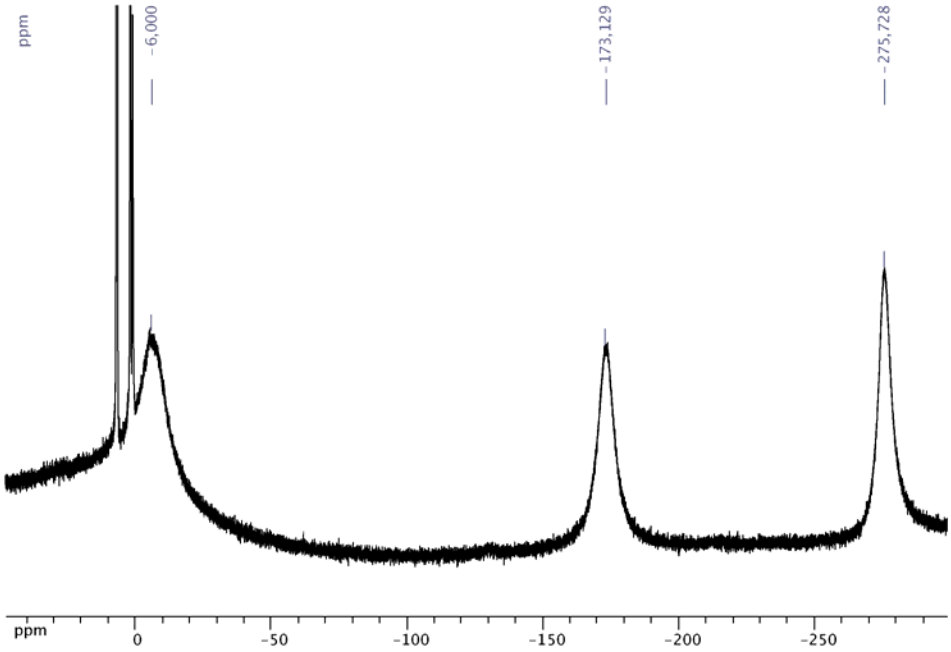

[(Cp$^{'''}$)$_2$DyI] (33)

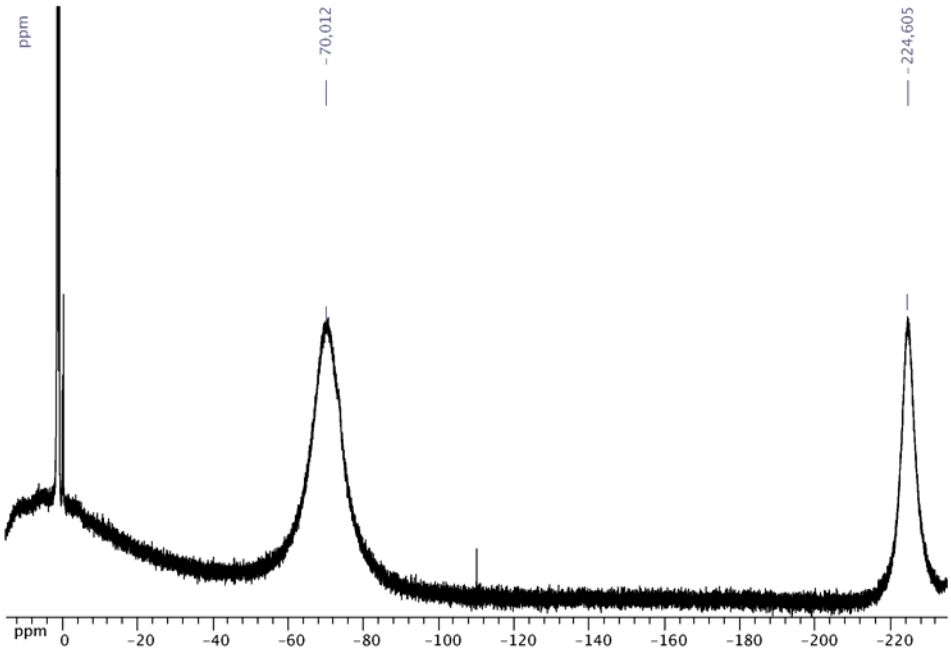

c) Examples of Dy^{2+} complexes

$[(Cp^{ttt})_2Dy(\mu\text{-}I)K([18]crown\text{-}6)]$ (36-I)

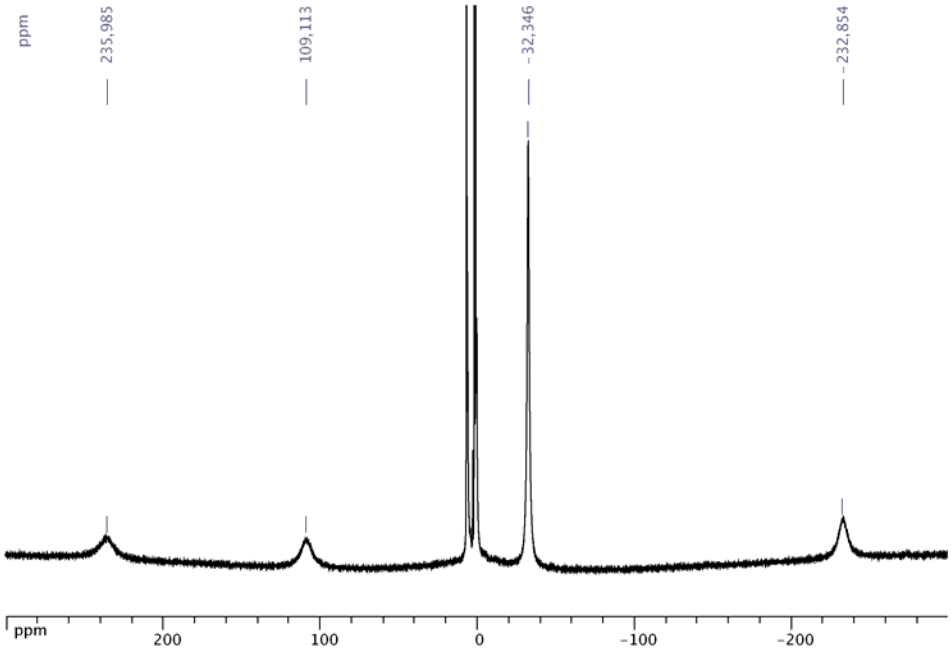

$[(Cp^{ttt})_2Dy(\mu\text{-}Br)K([18]crown\text{-}6)]$ (36-Br)

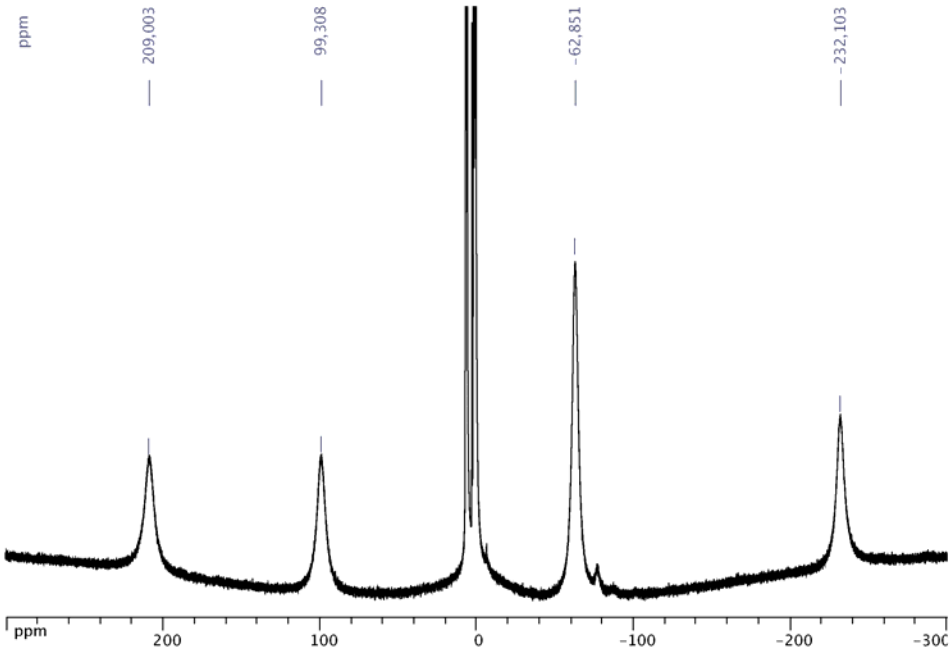

[(Cp^{ttt})$_2$Dy(μ-BH$_4$)K([18]crown-6)] (36-BH$_4$)

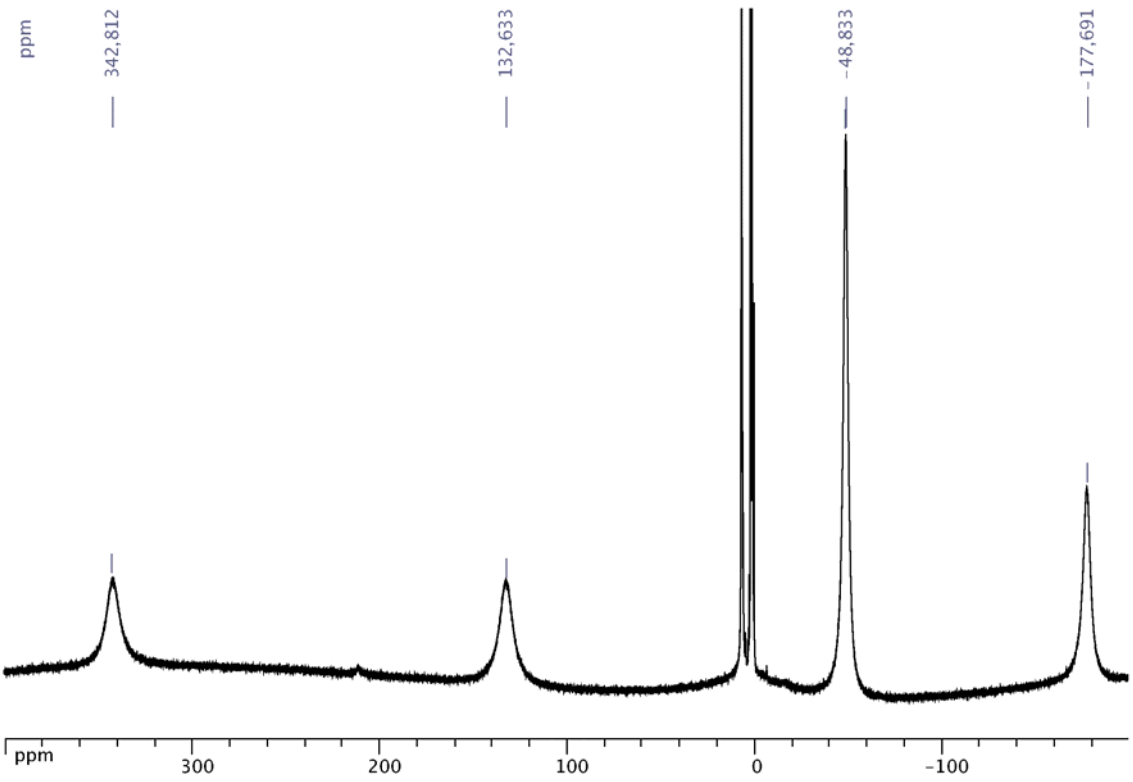

Annex II: X-ray crystallographic data

For all measurements at the Ecole Polytechnique, crystals suitable for X-ray analysis were covered with Parathon oil in the glovebox and mounted on a fiberglass needle outside the glovebox. Data collection was carried out using a Nonius Kappa CCD diffractometer with a graphite-monochromated Mo Kα source (λ = 0.71069 Å) at 150 K.

For the measurements at RIKEN, Japan, the crystals were sealed in thin-walled glass capillaries in the glovebox. Data collection were performed at 150-160 K on a Bruker SMART APEX diffractrometer with a CCD area detector, using graphite monochromated Mo-Ka radiation (λ = 0.71069 Å).

The determination of crystal class and unit cell parameters was carried out by the SMART program package.[1] The raw frame data were processed using SAINT[2] and SADABS[3] to yield the reflection data file. The structures were solved by using SHELXTL program.[4] Refinement for all compounds was performed on F^2 anisotropically for all the non-hydrogen atoms by the full-matrix least-squares methods. The analytical scattering factors for neutral atoms were used throughout the analysis. Hydrogen atoms were placed at the calculated positions and were included in the structure calculation without further refinement of the parameters. The residual electron densities were of no chemical significance.

X-ray crystallographic data for published complexes can be accessed on the internet by the following links:

Part I

[(Cp^{ttt})$_2$Tm(THF)] (9)
[(Cp^{ttt})$_2$TmI] (11)
http://www.rsc.org/suppdata/CC/b5/b514818a/b514818a.txt

[(Cp$^{'''}$)$_2$Tm(THF)] (10)
[(Cp$^{'''}$)$_2$TmI] (12)
[(Cp^{ttt})$_2$Tm(BH$_4$)] (14)
[{(Cp^{tt})$_2$TmI}$_2$] (15)
[(Dtp)$_2$TmI] (19)
[{(Htp)$_2$TmI}$_2$] (21)
[{(Htp)$_2$Tm}$_2$] (23)
[{(Cp^{ttt})$_2$Tm}$_2${μ-(NC$_5$H$_5$-C$_5$H$_5$N)}] (29)
http://pubs.acs.org/subscribe/journals/orgnd7/suppinfo/om700316a/om700316a-File002.cif

[1] SMART Software Users Guide, version 4.21; Bruker AXS, Inc.: Madison, WI, 1997.
[2] SAINT PLUS, version 6.02; Bruker AXS, Inc.: Madison, WI, 1999.
[3] Sheldrick, G. M. SADABS; Bruker AXS, Inc.: Madison, WI, 1998.
[4] Sheldrick, G. M. SHELXTL, version 5.1; Bruker AXS, Inc.: Madison, WI, 1998.

[(Cp^{ttt})$_2$DyI] (32-I)
[(Cp^{ttt})$_2$DyBr] (32-Br)
[(Cp^{ttt})$_2$Dy(BH$_4$)] (32-BH$_4$)
[(Cp^{ttt})$_2$Dy(μ-Br)K([18]crown-6)] (36-Br)
[(Cp^{ttt})$_2$Dy(μ-BH$_4$)K([18]crown-6)] (36-BH$_4$)
[(Cp^{ttt})$_2$Dy(μ-Cl)$_2$K([18]crown-6)] (37)
http://pubs.acs.org/subscribe/journals/orgnd7/suppinfo/om0700213/om0700213si20070109_034632.cif

Part II

[(Dtp)SmI$_2$(THF)$_2$] (1)
[(Dtp)Y(CH$_2$C$_6$H$_4$NMe$_2$-*o*)$_2$] (3-Y)
[(Dtp)Sm(CH$_2$C$_6$H$_4$NMe$_2$-*o*)$_2$] (3-Sm)
[(Dtp)Sc(CH$_2$C$_6$H$_4$NMe$_2$-*o*)$_2$] (3-Sc)
[{Sc[*μ*-O(CH$_2$)$_4$(Dtp)]Cl$_2$(THF)$_2$}$_2$] (5)
[{(Dtp)Sc(*μ*-Cl)Cl(NC$_5$H$_5$)}$_2$] (6)
http://pubs.acs.org/subscribe/journals/orgnd7/suppinfo/om7005936/om7005936-File003.cif

Part III

[{(SPCPS)Sm(μ-I)(THF)$_2$}$_2$] (2)
[{Li(THF)$_4$}{(SPCPS)$_2$Sm}] (4a)
Ph$_2$CC(P(S)Ph$_2$)$_2$ (6)
[Sm{μ-OCPh$_2$C(P(S)Ph$_2$)$_2$}$_2$Li(THF)] (8)
http://www.rsc.org/suppdata/CC/b5/b510327d/b510327d.txt

[{(SPCPS)Tm(μ-I)(THF)$_2$}$_2$] (3)
[{Li(THF)$_4$}{(SPCPS)$_2$Tm}] (5a) and (5b)
[Tm{μ-OCPh$_2$C(P(S)Ph$_2$)$_2$}$_2$Li(THF)] (9)
http://pubs.acs.org/subscribe/journals/orgnd7/suppinfo/om050877c/om050877csi20051011_010650.cif

Unpublished complexes

Part I

[(Dtp)$_2$Pb] (1)

Compound	pbp2tbu
Molecular formula	$C_{28}H_{48}P_2Pb$

Molecular weight	653.79
Crystal habit	orange block
Crystal dimensions(mm)	0.22x0.20x0.16
Crystal system	monoclinic
Space group	$P2_1/n$
a(Å)	11.8450(10)
b(Å)	15.6650(10)
c(Å)	15.9570(10)
α(°)	90.00
β(°)	91.5400(10)
γ(°)	90.00
V(Å^3)	2959.8(4)
Z	4
d(g-cm^{-3})	1.467
F(000)	1312
μ(cm^{-1})	5.821
Absorption corrections	multi-scan ; 0.3608 min, 0.4561 max
Diffractometer	KappaCCD
X-ray source	MoKα
λ(Å)	0.71069
Monochromator	graphite
T (K)	150.0(1)
Scan mode	phi and omega scans
Maximum θ	30.00
HKL ranges	-16 16 ; -21 19 ; -22 22
Reflections measured	15019
Unique data	8590
Rint	0.0218
Reflections used	6682
Criterion	I > 2σI)
Refinement type	Fsqd
Hydrogen atoms	mixed
Parameters refined	297
Reflections / parameter	22
wR2	0.0511
R1	0.0247
Weights a, b	0.0156 ; 0.0000
GoF	1.009
difference peak / hole (e Å^{-3})	0.982(0.093) / -0.901(0.093)

Table. Bond lengths (A) and angles (deg) for pbp2tbu

Pb(1)-C(4)	2.762(2)	Pb(1)-C(15)	2.770(2)
Pb(1)-P(2)	2.8413(6	Pb(1)-P(1)	2.8422(6)
P(1)-C(4)	1.782(2)	P(1)-C(1)	1.786(2)
P(2)-C(18)	1.775(2)	P(2)-C(15)	1.783(2)
C(1)-C(2)	1.383(3)	C(1)-C(5)	1.532(3)
C(2)-C(3)	1.436(3)	C(2)-C(9)	1.512(3)
C(3)-C(4)	1.397(4)	C(3)-C(10)	1.513(3)
C(4)-C(11)	1.538(3)	C(5)-C(6)	1.537(4)
C(5)-C(7)	1.540(4)	C(5)-C(8)	1.543(4)
C(11)-C(13)	1.526(4)	C(11)-C(12)	1.529(4)

C(11)-C(14)	1.536(3)	C(15)-C(16)	1.411(3)
C(15)-C(19)	1.526(3)	C(16)-C(17)	1.437(3)
C(16)-C(23)	1.518(3)	C(17)-C(18)	1.386(3)
C(17)-C(24)	1.520(3)	C(18)-C(25)	1.540(3)
C(19)-C(20)	1.535(4)	C(19)-C(22)	1.538(4)
C(19)-C(21)	1.546(4)	C(25)-C(28)	1.526(3)
C(25)-C(27)	1.528(3)	C(25)-C(26)	1.534(3)

C(4)-Pb(1)-C(15)	134.94(7)	C(4)-Pb(1)-P(2)	115.20(5)
C(15)-Pb(1)-P(2)	37.02(5)	C(4)-Pb(1)-P(1)	37.04(5)
C(15)-Pb(1)-P(1)	115.84(5)	P(2)-Pb(1)-P(1)	122.70(2)
C(4)-P(1)-C(1)	90.9(1)	C(4)-P(1)-Pb(1)	69.04(8)
C(1)-P(1)-Pb(1)	73.73(7)	C(18)-P(2)-C(15)	91.3(1)
C(18)-P(2)-Pb(1)	73.58(7)	C(15)-P(2)-Pb(1)	69.31(7)
C(2)-C(1)-C(5)	126.8(2)	C(2)-C(1)-P(1)	111.1(2)
C(5)-C(1)-P(1)	122.1(2)	C(1)-C(2)-C(3)	113.8(2)
C(1)-C(2)-C(9)	126.3(2)	C(3)-C(2)-C(9)	119.8(2)
C(4)-C(3)-C(2)	113.1(2)	C(4)-C(3)-C(10)	126.9(2)
C(2)-C(3)-C(10)	119.9(2)	C(3)-C(4)-C(11)	127.2(2)
C(3)-C(4)-P(1)	111.1(2)	C(11)-C(4)-P(1)	121.1(2)
C(3)-C(4)-Pb(1)	80.8(1)	C(11)-C(4)-Pb(1)	119.4(2)
P(1)-C(4)-Pb(1)	73.91(8)	C(1)-C(5)-C(6)	110.8(2)
C(1)-C(5)-C(7)	110.4(2)	C(6)-C(5)-C(7)	107.4(2)
C(1)-C(5)-C(8)	111.1(2)	C(6)-C(5)-C(8)	110.2(2)
C(7)-C(5)-C(8)	106.9(2)	C(13)-C(11)-C(12)	108.8(3)
C(13)-C(11)-C(14)	109.9(3)	C(12)-C(11)-C(14)	106.8(2)
C(13)-C(11)-C(4)	108.0(2)	C(12)-C(11)-C(4)	109.9(2)
C(14)-C(11)-C(4)	113.3(2)	C(16)-C(15)-C(19)	127.6(2)
C(16)-C(15)-P(2)	110.5(2)	C(19)-C(15)-P(2)	121.3(2)
C(16)-C(15)-Pb(1)	80.4(1)	C(19)-C(15)-Pb(1)	119.3(2)
P(2)-C(15)-Pb(1)	73.67(7)	C(15)-C(16)-C(17)	113.0(2)
C(15)-C(16)-C(23)	126.3(2)	C(17)-C(16)-C(23)	120.6(2)
C(18)-C(17)-C(16)	113.7(2)	C(18)-C(17)-C(24)	127.0(2)
C(16)-C(17)-C(24)	119.2(2)	C(17)-C(18)-C(25)	127.1(2)
C(17)-C(18)-P(2)	111.4(2)	C(25)-C(18)-P(2)	121.5(2)
C(15)-C(19)-C(20)	111.0(2)	C(15)-C(19)-C(22)	108.6(2)
C(20)-C(19)-C(22)	107.1(2)	C(15)-C(19)-C(21)	113.0(2)
C(20)-C(19)-C(21)	106.7(2)	C(22)-C(19)-C(21)	110.3(2)
C(28)-C(25)-C(27)	106.5(2)	C(28)-C(25)-C(26)	109.9(2)
C(27)-C(25)-C(26)	107.3(2)	C(28)-C(25)-C(18)	110.3(2)
C(27)-C(25)-C(18)	110.8(2)	C(26)-C(25)-C(18)	111.8(2)

[(Cp’’’)$_2$SmI(THF)] (3a)

Compound	smcpttmsi
Molecular formula	$C_{32}H_{66}IOSi_6Sm$
Molecular weight	912.64
Crystal habit	plate yellow
Crystal dimensions(mm)	0.22x0.18x0.10
Crystal system	monoclinic
Space group	$P2_1/c$
a(Å)	16.9270(10)
b(Å)	12.9810(10)
c(Å)	20.5490(10)
α(°)	90.00
β(°)	92.7610(10)
γ(°)	90.00
V(Å^3)	4510.0(5)
Z	4
d(g-cm^{-3})	1.344

F(000)	1860
μ(cm^{-1})	2.167
Absorption corrections	multi-scan ; 0.6471 min, 0.8125 max
Diffractometer	KappaCCD
X-ray source	MoKα
λ(Å)	0.71069
Monochromator	graphite
T (K)	150.0(1)
Scan mode	phi and omega scans
Maximum θ	30.03
HKL ranges	-23 23 ; -18 16 ; -28 28
Reflections measured	22737
Unique data	13160
Rint	0.0171
Reflections used	11132
Criterion	I > 2σI)
Refinement type	Fsqd
Hydrogen atoms	mixed
Parameters refined	388
Reflections / parameter	28
wR2	0.0769
R1	0.0277
Weights a, b	0.0440 ; 0.2893
GoF	1.032
difference peak / hole (e $Å^{-3}$)	0.954(0.089) / -1.240(0.089)

Table. Bond lengths (A) and angles (deg) for smcpttmsi

Sm(1)-O(1)	2.434(1)	Sm(1)-C(19)	2.687(2)
Sm(1)-C(5)	2.714(2)	Sm(1)-C(15)	2.716(2)
Sm(1)-C(3)	2.728(2)	Sm(1)-C(18)	2.749(2)
Sm(1)-C(2)	2.751(2)	Sm(1)-C(1)	2.753(2)
Sm(1)-C(17)	2.757(2)	Sm(1)-C(4)	2.761(2)
Sm(1)-C(16)	2.764(2)	Sm(1)-I(1)	3.0343(2)
Si(1)-C(6)	1.865(2)	Si(1)-C(8)	1.869(3)
Si(1)-C(7)	1.873(3)	Si(1)-C(1)	1.878(2)
Si(2)-C(9)	1.869(2)	Si(2)-C(11)	1.872(3)
Si(2)-C(10)	1.874(3)	Si(2)-C(2)	1.879(2)
Si(3)-C(14)	1.847(4)	Si(3)-C(12)	1.855(3)
Si(3)-C(4)	1.877(2)	Si(3)-C(13)	1.880(3)
Si(4)-C(22)	1.856(2)	Si(4)-C(20)	1.871(3)
Si(4)-C(15)	1.872(2)	Si(4)-C(21)	1.879(3)
Si(5)-C(23)	1.861(2)	Si(5)-C(25)	1.868(3)
Si(5)-C(16)	1.872(2)	Si(5)-C(24)	1.878(3)
Si(6)-C(27)	1.867(3)	Si(6)-C(18)	1.869(2)
Si(6)-C(26)	1.870(3)	Si(6)-C(28)	1.873(3)
O(1)-C(32)	1.447(3)	O(1)-C(29)	1.453(3)
C(1)-C(5)	1.415(3)	C(1)-C(2)	1.447(3)
C(2)-C(3)	1.420(3)	C(3)-C(4)	1.419(3)
C(3)-H(3)	0.9500	C(4)-C(5)	1.429(3)
C(5)-H(5)	0.9500	C(6)-H(6A)	0.9800
C(6)-H(6B)	0.9800	C(6)-H(6C)	0.9800
C(7)-H(7A)	0.9800	C(7)-H(7B)	0.9800
C(7)-H(7C)	0.9800	C(8)-H(8A)	0.9800
C(8)-H(8B)	0.9800	C(8)-H(8C)	0.9800
C(9)-H(9A)	0.9800	C(9)-H(9B)	0.9800
C(9)-H(9C)	0.9800	C(10)-H(10A)	0.9800
C(10)-H(10B)	0.9800	C(10)-H(10C)	0.9800

C(11)-H(11A)	0.9800	C(11)-H(11B)	0.9800
C(11)-H(11C)	0.9800	C(12)-H(12A)	0.9800
C(12)-H(12B)	0.9800	C(12)-H(12C)	0.9800
C(13)-H(13A)	0.9800	C(13)-H(13B)	0.9800
C(13)-H(13C)	0.9800	C(14)-H(14A)	0.9800
C(14)-H(14B)	0.9800	C(14)-H(14C)	0.9800
C(15)-C(19)	1.418(3)	C(15)-C(16)	1.452(3)
C(16)-C(17)	1.416(3)	C(17)-C(18)	1.422(3)
C(17)-H(17)	0.9500	C(18)-C(19)	1.420(3)
C(19)-H(19)	0.9500	C(20)-H(20A)	0.9800
C(20)-H(20B)	0.9800	C(20)-H(20C)	0.9800
C(21)-H(21A)	0.9800	C(21)-H(21B)	0.9800
C(21)-H(21C)	0.9800	C(22)-H(22A)	0.9800
C(22)-H(22B)	0.9800	C(22)-H(22C)	0.9800
C(23)-H(23A)	0.9800	C(23)-H(23B)	0.9800
C(23)-H(23C)	0.9800	C(24)-H(24A)	0.9800
C(24)-H(24B)	0.9800	C(24)-H(24C)	0.9800
C(25)-H(25A)	0.9800	C(25)-H(25B)	0.9800
C(25)-H(25C)	0.9800	C(26)-H(26A)	0.9800
C(26)-H(26B)	0.9800	C(26)-H(26C)	0.9800
C(27)-H(27A)	0.9800	C(27)-H(27B)	0.9800
C(27)-H(27C)	0.9800	C(28)-H(28A)	0.9800
C(28)-H(28B)	0.9800	C(28)-H(28C)	0.9800
C(29)-C(30)	1.508(3)	C(29)-H(29A)	0.9900
C(29)-H(29B)	0.9900	C(30)-C(31)	1.531(3)
C(30)-H(30A)	0.9900	C(30)-H(30B)	0.9900
C(31)-C(32)	1.516(3)	C(31)-H(31A)	0.9900
C(31)-H(31B)	0.9900	C(32)-H(32A)	0.9900
C(32)-H(32B)	0.9900		

O(1)-Sm(1)-C(19)	116.33(6)	O(1)-Sm(1)-C(5)	131.85(6)
C(19)-Sm(1)-C(5)	92.24(6)	O(1)-Sm(1)-C(15)	126.17(6)
C(19)-Sm(1)-C(15)	30.43(6)	C(5)-Sm(1)-C(15)	98.44(6)
O(1)-Sm(1)-C(3)	85.61(5)	C(19)-Sm(1)-C(3)	103.58(6)
C(5)-Sm(1)-C(3)	48.80(6)	C(15)-Sm(1)-C(3)	129.26(6)
O(1)-Sm(1)-C(18)	86.07(6)	C(19)-Sm(1)-C(18)	30.27(6)
C(5)-Sm(1)-C(18)	115.09(6)	C(15)-Sm(1)-C(18)	50.83(6)
C(3)-Sm(1)-C(18)	103.09(6)	O(1)-Sm(1)-C(2)	83.80(5)
C(19)-Sm(1)-C(2)	131.06(6)	C(5)-Sm(1)-C(2)	49.50(6)
C(15)-Sm(1)-C(2)	147.76(6)	C(3)-Sm(1)-C(2)	30.04(6)
C(18)-Sm(1)-C(2)	132.57(6)	O(1)-Sm(1)-C(1)	111.41(5)
C(19)-Sm(1)-C(1)	122.14(6)	C(5)-Sm(1)-C(1)	30.00(6)
C(15)-Sm(1)-C(1)	122.42(6)	C(3)-Sm(1)-C(1)	49.62(7)
C(18)-Sm(1)-C(1)	143.30(6)	C(2)-Sm(1)-C(1)	30.48(6)
O(1)-Sm(1)-C(17)	76.77(5)	C(19)-Sm(1)-C(17)	48.74(6)
C(5)-Sm(1)-C(17)	140.97(6)	C(15)-Sm(1)-C(17)	49.59(6)
C(3)-Sm(1)-C(17)	129.45(6)	C(18)-Sm(1)-C(17)	29.93(6)
C(2)-Sm(1)-C(17)	153.86(6)	C(1)-Sm(1)-C(17)	170.79(6)
O(1)-Sm(1)-C(4)	113.33(5)	C(19)-Sm(1)-C(4)	81.01(6)
C(5)-Sm(1)-C(4)	30.25(6)	C(15)-Sm(1)-C(4)	101.19(6)
C(3)-Sm(1)-C(4)	29.96(6)	C(18)-Sm(1)-C(4)	93.24(7)
C(2)-Sm(1)-C(4)	50.35(6)	C(1)-Sm(1)-C(4)	50.51(7)
C(17)-Sm(1)-C(4)	123.11(7)	O(1)-Sm(1)-C(16)	98.85(6)
C(19)-Sm(1)-C(16)	49.80(6)	C(5)-Sm(1)-C(16)	128.38(6)
C(15)-Sm(1)-C(16)	30.71(6)	C(3)-Sm(1)-C(16)	152.15(6)
C(18)-Sm(1)-C(16)	50.35(6)	C(2)-Sm(1)-C(16)	176.42(6)
C(1)-Sm(1)-C(16)	146.09(6)	C(17)-Sm(1)-C(16)	29.72(6)
C(4)-Sm(1)-C(16)	129.86(6)	O(1)-Sm(1)-I(1)	88.83(4)
C(19)-Sm(1)-I(1)	128.19(4)	C(5)-Sm(1)-I(1)	103.41(4)
C(15)-Sm(1)-I(1)	97.90(4)	C(3)-Sm(1)-I(1)	123.94(5)
C(18)-Sm(1)-I(1)	132.12(4)	C(2)-Sm(1)-I(1)	93.89(5)
C(1)-Sm(1)-I(1)	81.96(5)	C(17)-Sm(1)-I(1)	102.91(4)
C(4)-Sm(1)-I(1)	131.78(5)	C(16)-Sm(1)-I(1)	83.78(4)
C(6)-Si(1)-C(8)	107.7(1)	C(6)-Si(1)-C(7)	106.9(1)
C(8)-Si(1)-C(7)	109.0(1)	C(6)-Si(1)-C(1)	110.9(1)
C(8)-Si(1)-C(1)	117.0(1)	C(7)-Si(1)-C(1)	104.9(1)
C(9)-Si(2)-C(11)	106.1(1)	C(9)-Si(2)-C(10)	110.2(1)
C(11)-Si(2)-C(10)	108.4(1)	C(9)-Si(2)-C(2)	108.9(1)
C(11)-Si(2)-C(2)	108.5(1)	C(10)-Si(2)-C(2)	114.5(1)

C(14)-Si(3)-C(12)	110.0(2)	C(14)-Si(3)-C(4)	106.4(2)
C(12)-Si(3)-C(4)	108.0(1)	C(14)-Si(3)-C(13)	107.8(2)
C(12)-Si(3)-C(13)	106.4(2)	C(4)-Si(3)-C(13)	118.2(1)
C(22)-Si(4)-C(20)	110.3(1)	C(22)-Si(4)-C(15)	113.5(1)
C(20)-Si(4)-C(15)	109.3(1)	C(22)-Si(4)-C(21)	107.8(1)
C(20)-Si(4)-C(21)	107.2(1)	C(15)-Si(4)-C(21)	108.4(1)
C(23)-Si(5)-C(25)	107.4(1)	C(23)-Si(5)-C(16)	116.5(1)
C(25)-Si(5)-C(16)	105.5(1)	C(23)-Si(5)-C(24)	109.5(1)
C(25)-Si(5)-C(24)	107.4(1)	C(16)-Si(5)-C(24)	110.1(1)
C(27)-Si(6)-C(18)	106.1(1)	C(27)-Si(6)-C(26)	107.1(2)
C(18)-Si(6)-C(26)	109.5(1)	C(27)-Si(6)-C(28)	110.1(1)
C(18)-Si(6)-C(28)	115.0(1)	C(26)-Si(6)-C(28)	108.8(1)
C(32)-O(1)-C(29)	105.0(2)	C(32)-O(1)-Sm(1)	123.9(1)
C(29)-O(1)-Sm(1)	125.2(1)	C(5)-C(1)-C(2)	106.2(2)
C(5)-C(1)-Si(1)	119.0(2)	C(2)-C(1)-Si(1)	131.2(2)
C(5)-C(1)-Sm(1)	73.5(1)	C(2)-C(1)-Sm(1)	74.7(1)
Si(1)-C(1)-Sm(1)	133.4(1)	C(3)-C(2)-C(1)	106.7(2)
C(3)-C(2)-Si(2)	121.3(2)	C(1)-C(2)-Si(2)	130.5(2)
C(3)-C(2)-Sm(1)	74.1(1)	C(1)-C(2)-Sm(1)	74.8(1)
Si(2)-C(2)-Sm(1)	127.1(1)	C(4)-C(3)-C(2)	111.3(2)
C(4)-C(3)-Sm(1)	76.3(1)	C(2)-C(3)-Sm(1)	75.9(1)
C(4)-C(3)-H(3)	124.3	C(2)-C(3)-H(3)	124.3
Sm(1)-C(3)-H(3)	115.2	C(3)-C(4)-C(5)	104.2(2)
C(3)-C(4)-Si(3)	123.5(2)	C(5)-C(4)-Si(3)	124.9(2)
C(3)-C(4)-Sm(1)	73.7(1)	C(5)-C(4)-Sm(1)	73.1(1)
Si(3)-C(4)-Sm(1)	141.4(1)	C(1)-C(5)-C(4)	111.6(2)
C(1)-C(5)-Sm(1)	76.5(1)	C(4)-C(5)-Sm(1)	76.7(1)
C(1)-C(5)-H(5)	124.2	C(4)-C(5)-H(5)	124.2
Sm(1)-C(5)-H(5)	114.3	Si(1)-C(6)-H(6A)	109.5
Si(1)-C(6)-H(6B)	109.5	H(6A)-C(6)-H(6B)	109.5
Si(1)-C(6)-H(6C)	109.5	H(6A)-C(6)-H(6C)	109.5
H(6B)-C(6)-H(6C)	109.5	Si(1)-C(7)-H(7A)	109.5
Si(1)-C(7)-H(7B)	109.5	H(7A)-C(7)-H(7B)	109.5
Si(1)-C(7)-H(7C)	109.5	H(7A)-C(7)-H(7C)	109.5
H(7B)-C(7)-H(7C)	109.5	Si(1)-C(8)-H(8A)	109.5
Si(1)-C(8)-H(8B)	109.5	H(8A)-C(8)-H(8B)	109.5
Si(1)-C(8)-H(8C)	109.5	H(8A)-C(8)-H(8C)	109.5
H(8B)-C(8)-H(8C)	109.5	Si(2)-C(9)-H(9A)	109.5
Si(2)-C(9)-H(9B)	109.5	H(9A)-C(9)-H(9B)	109.5
Si(2)-C(9)-H(9C)	109.5	H(9A)-C(9)-H(9C)	109.5
H(9B)-C(9)-H(9C)	109.5	Si(2)-C(10)-H(10A)	109.5
Si(2)-C(10)-H(10B)	109.5	H(10A)-C(10)-H(10B)	109.5
Si(2)-C(10)-H(10C)	109.5	H(10A)-C(10)-H(10C)	109.5
H(10B)-C(10)-H(10C)	109.5	Si(2)-C(11)-H(11A)	109.5
Si(2)-C(11)-H(11B)	109.5	H(11A)-C(11)-H(11B)	109.5
Si(2)-C(11)-H(11C)	109.5	H(11A)-C(11)-H(11C)	109.5
H(11B)-C(11)-H(11C)	109.5	Si(3)-C(12)-H(12A)	109.5
Si(3)-C(12)-H(12B)	109.5	H(12A)-C(12)-H(12B)	109.5
Si(3)-C(12)-H(12C)	109.5	H(12A)-C(12)-H(12C)	109.5
H(12B)-C(12)-H(12C)	109.5	Si(3)-C(13)-H(13A)	109.5
Si(3)-C(13)-H(13B)	109.5	H(13A)-C(13)-H(13B)	109.5
Si(3)-C(13)-H(13C)	109.5	H(13A)-C(13)-H(13C)	109.5
H(13B)-C(13)-H(13C)	109.5	Si(3)-C(14)-H(14A)	109.5
Si(3)-C(14)-H(14B)	109.5	H(14A)-C(14)-H(14B)	109.5
Si(3)-C(14)-H(14C)	109.5	H(14A)-C(14)-H(14C)	109.5
H(14B)-C(14)-H(14C)	109.5	C(19)-C(15)-C(16)	106.2(2)
C(19)-C(15)-Si(4)	121.2(2)	C(16)-C(15)-Si(4)	131.4(2)
C(19)-C(15)-Sm(1)	73.6(1)	C(16)-C(15)-Sm(1)	76.5(1)
Si(4)-C(15)-Sm(1)	124.5(1)	C(17)-C(16)-C(15)	106.3(2)
C(17)-C(16)-Si(5)	118.6(2)	C(15)-C(16)-Si(5)	132.2(2)
C(17)-C(16)-Sm(1)	74.9(1)	C(15)-C(16)-Sm(1)	72.8(1)
Si(5)-C(16)-Sm(1)	132.4(1)	C(16)-C(17)-C(18)	111.4(2)
C(16)-C(17)-Sm(1)	75.4(1)	C(18)-C(17)-Sm(1)	74.7(1)
C(16)-C(17)-H(17)	124.3	C(18)-C(17)-H(17)	124.3
Sm(1)-C(17)-H(17)	117.2	C(19)-C(18)-C(17)	104.5(2)
C(19)-C(18)-Si(6)	126.3(2)	C(17)-C(18)-Si(6)	125.0(2)
C(19)-C(18)-Sm(1)	72.4(1)	C(17)-C(18)-Sm(1)	75.4(1)
Si(6)-C(18)-Sm(1)	134.7(1)	C(15)-C(19)-C(18)	111.4(2)

C(15)-C(19)-Sm(1)	75.9(1)	C(18)-C(19)-Sm(1)	77.3(1)
C(15)-C(19)-H(19)	124.3	C(18)-C(19)-H(19)	124.3
Sm(1)-C(19)-H(19)	114.3	Si(4)-C(20)-H(20A)	109.5
Si(4)-C(20)-H(20B)	109.5	H(20A)-C(20)-H(20B)	109.5
Si(4)-C(20)-H(20C)	109.5	H(20A)-C(20)-H(20C)	109.5
H(20B)-C(20)-H(20C)	109.5	Si(4)-C(21)-H(21A)	109.5
Si(4)-C(21)-H(21B)	109.5	H(21A)-C(21)-H(21B)	109.5
Si(4)-C(21)-H(21C)	109.5	H(21A)-C(21)-H(21C)	109.5
H(21B)-C(21)-H(21C)	109.5	Si(4)-C(22)-H(22A)	109.5
Si(4)-C(22)-H(22B)	109.5	H(22A)-C(22)-H(22B)	109.5
Si(4)-C(22)-H(22C)	109.5	H(22A)-C(22)-H(22C)	109.5
H(22B)-C(22)-H(22C)	109.5	Si(5)-C(23)-H(23A)	109.5
Si(5)-C(23)-H(23B)	109.5	H(23A)-C(23)-H(23B)	109.5
Si(5)-C(23)-H(23C)	109.5	H(23A)-C(23)-H(23C)	109.5
H(23B)-C(23)-H(23C)	109.5	Si(5)-C(24)-H(24A)	109.5
Si(5)-C(24)-H(24B)	109.5	H(24A)-C(24)-H(24B)	109.5
Si(5)-C(24)-H(24C)	109.5	H(24A)-C(24)-H(24C)	109.5
H(24B)-C(24)-H(24C)	109.5	Si(5)-C(25)-H(25A)	109.5
Si(5)-C(25)-H(25B)	109.5	H(25A)-C(25)-H(25B)	109.5
Si(5)-C(25)-H(25C)	109.5	H(25A)-C(25)-H(25C)	109.5
H(25B)-C(25)-H(25C)	109.5	Si(6)-C(26)-H(26A)	109.5
Si(6)-C(26)-H(26B)	109.5	H(26A)-C(26)-H(26B)	109.5
Si(6)-C(26)-H(26C)	109.5	H(26A)-C(26)-H(26C)	109.5
H(26B)-C(26)-H(26C)	109.5	Si(6)-C(27)-H(27A)	109.5
Si(6)-C(27)-H(27B)	109.5	H(27A)-C(27)-H(27B)	109.5
Si(6)-C(27)-H(27C)	109.5	H(27A)-C(27)-H(27C)	109.5
H(27B)-C(27)-H(27C)	109.5	Si(6)-C(28)-H(28A)	109.5
Si(6)-C(28)-H(28B)	109.5	H(28A)-C(28)-H(28B)	109.5
Si(6)-C(28)-H(28C)	109.5	H(28A)-C(28)-H(28C)	109.5
H(28B)-C(28)-H(28C)	109.5	O(1)-C(29)-C(30)	104.3(2)
O(1)-C(29)-H(29A)	110.9	C(30)-C(29)-H(29A)	110.9
O(1)-C(29)-H(29B)	110.9	C(30)-C(29)-H(29B)	110.9
H(29A)-C(29)-H(29B)	108.9	C(29)-C(30)-C(31)	103.6(2)
C(29)-C(30)-H(30A)	111.1	C(31)-C(30)-H(30A)	111.1
C(29)-C(30)-H(30B)	111.1	C(31)-C(30)-H(30B)	111.1
H(30A)-C(30)-H(30B)	109.0	C(32)-C(31)-C(30)	105.0(2)
C(32)-C(31)-H(31A)	110.7	C(30)-C(31)-H(31A)	110.7
C(32)-C(31)-H(31B)	110.7	C(30)-C(31)-H(31B)	110.7
H(31A)-C(31)-H(31B)	108.8	O(1)-C(32)-C(31)	106.3(2)
O(1)-C(32)-H(32A)	110.5	C(31)-C(32)-H(32A)	110.5
O(1)-C(32)-H(32B)	110.5	C(31)-C(32)-H(32B)	110.5
H(32A)-C(32)-H(32B)	108.7		

[(Cp*)TmI$_2$(THF)$_2$] (18)

Compound	tmcpstari2
Molecular formula	$C_{18}H_{31}I_2O_2Tm$
Molecular weight	702.16
Crystal habit	pale yellow plate
Crystal dimensions(mm)	0.20x0.16x0.10
Crystal system	monoclinic
Space group	$P2_1/n$
a(Å)	7.9920(10)
b(Å)	21.5800(10)
c(Å)	12.9860(10)
α(°)	90.00
β(°)	105.9600(10)
γ(°)	90.00
V(Å^3)	2153.3(3)
Z	4
d(g-cm^{-3})	2.166

F(000)	1320
μ(cm^{-1})	6.994
Absorption corrections	multi-scan ; 0.3352 min, 0.5414 max
Diffractometer	KappaCCD
X-ray source	MoKα
λ(Å)	0.71069
Monochromator	graphite
T (K)	150.0(1)
Scan mode	phi and omega scans
Maximum θ	30.03
HKL ranges	-11 11 ; -27 30 ; -18 18
Reflections measured	10645
Unique data	6234
Rint	0.0281
Reflections used	5205
Criterion	I > 2σI)
Refinement type	Fsqd
Hydrogen atoms	mixed
Parameters refined	214
Reflections / parameter	24
wR2	0.1064
R1	0.0368
Weights a, b	0.0631 ; 0.1714
GoF	1.064
difference peak / hole (e Å^{-3})	2.738(0.202) / -2.066(0.202)

Table. Bond lengths (A) and angles (deg) for tmcpstari2

Tm(1)-O(1)	2.316(3)	Tm(1)-O(2)	2.317(3)
Tm(1)-C(1)	2.594(5)	Tm(1)-C(4)	2.597(4)
Tm(1)-C(2)	2.605(4)	Tm(1)-C(3)	2.606(4)
Tm(1)-C(5)	2.608(4)	Tm(1)-I(2)	2.9576(4)
Tm(1)-I(1)	2.9884(4	C(1)-C(2)	1.414(6)
C(1)-C(5)	1.426(6)	C(1)-C(6)	1.501(7)
C(2)-C(3)	1.423(5)	C(2)-C(7)	1.518(6)
C(3)-C(4)	1.409(6)	C(3)-C(8)	1.498(5)
C(4)-C(5)	1.425(6)	C(4)-C(9)	1.503(5)
C(5)-C(10)	1.505(6)	O(1)-C(14)	1.465(5)
O(1)-C(11)	1.474(5)	C(11)-C(12)	1.491(7)
C(12)-C(13)	1.494(7)	C(13)-C(14)	1.487(6)
O(2)-C(18)	1.468(5)	O(2)-C(15)	1.471(5)
C(15)-C(16)	1.513(6)	C(16)-C(17)	1.499(7)
C(17)-C(18)	1.490(7)		

O(1)-Tm(1)-O(2)	139.7(1)	O(1)-Tm(1)-C(1)	109.7(1)
O(2)-Tm(1)-C(1)	107.4(1)	O(1)-Tm(1)-C(4)	91.9(1)
O(2)-Tm(1)-C(4)	123.5(1)	C(1)-Tm(1)-C(4)	52.7(1)
O(1)-Tm(1)-C(2)	136.7(1)	O(2)-Tm(1)-C(2)	83.6(1)
C(1)-Tm(1)-C(2)	31.6(1)	C(4)-Tm(1)-C(2)	52.2(1)
O(1)-Tm(1)-C(3)	122.7(1)	O(2)-Tm(1)-C(3)	92.4(1)
C(1)-Tm(1)-C(3)	52.6(1)	C(4)-Tm(1)-C(3)	31.4(1)
C(2)-Tm(1)-C(3)	31.7(1)	O(1)-Tm(1)-C(5)	84.6(1)
O(2)-Tm(1)-C(5)	135.6(1)	C(1)-Tm(1)-C(5)	31.8(1)
C(4)-Tm(1)-C(5)	31.8(1)	C(2)-Tm(1)-C(5)	52.1(2)
C(3)-Tm(1)-C(5)	52.2(1)	O(1)-Tm(1)-I(2)	84.34(7)
O(2)-Tm(1)-I(2)	84.30(7)	C(1)-Tm(1)-I(2)	84.0(1)
C(4)-Tm(1)-I(2)	132.4(1)	C(2)-Tm(1)-I(2)	102.0(1)

C(3)-Tm(1)-I(2)	133.27(8)	C(5)-Tm(1)-I(2)	100.8(1)
O(1)-Tm(1)-I(1)	79.53(7)	O(2)-Tm(1)-I(1)	80.11(8)
C(1)-Tm(1)-I(1)	143.5(1)	C(4)-Tm(1)-I(1)	92.8(1)
C(2)-Tm(1)-I(1)	120.3(1)	C(3)-Tm(1)-I(1)	92.2(1)
C(5)-Tm(1)-I(1)	121.5(1)	I(2)-Tm(1)-I(1)	132.45(1)
C(2)-C(1)-C(5)	107.5(4)	C(2)-C(1)-C(6)	125.8(4)
C(5)-C(1)-C(6)	125.6(4)	C(2)-C(1)-Tm(1)	74.7(3)
C(5)-C(1)-Tm(1)	74.6(3)	C(6)-C(1)-Tm(1)	126.0(4)
C(1)-C(2)-C(3)	108.5(4)	C(1)-C(2)-C(7)	122.9(4)
C(3)-C(2)-C(7)	128.5(4)	C(1)-C(2)-Tm(1)	73.8(3)
C(3)-C(2)-Tm(1)	74.2(2)	C(7)-C(2)-Tm(1)	121.2(3)
C(4)-C(3)-C(2)	107.9(3)	C(4)-C(3)-C(8)	124.3(3)
C(2)-C(3)-C(8)	127.2(4)	C(4)-C(3)-Tm(1)	73.9(2)
C(2)-C(3)-Tm(1)	74.1(2)	C(8)-C(3)-Tm(1)	124.9(3)
C(3)-C(4)-C(5)	108.1(3)	C(3)-C(4)-C(9)	123.8(4)
C(5)-C(4)-C(9)	127.2(4)	C(3)-C(4)-Tm(1)	74.6(2)
C(5)-C(4)-Tm(1)	74.5(2)	C(9)-C(4)-Tm(1)	124.9(3)
C(4)-C(5)-C(1)	107.9(4)	C(4)-C(5)-C(10)	129.0(4)
C(1)-C(5)-C(10)	123.0(4)	C(4)-C(5)-Tm(1)	73.7(2)
C(1)-C(5)-Tm(1)	73.5(3)	C(10)-C(5)-Tm(1)	121.6(3)
C(14)-O(1)-C(11)	108.0(3)	C(14)-O(1)-Tm(1)	120.2(2)
C(11)-O(1)-Tm(1)	126.8(3)	O(1)-C(11)-C(12)	105.2(4)
C(11)-C(12)-C(13)	103.2(4)	C(14)-C(13)-C(12)	104.6(4)
O(1)-C(14)-C(13)	106.3(4)	C(18)-O(2)-C(15)	107.4(3)
C(18)-O(2)-Tm(1)	126.2(3)	C(15)-O(2)-Tm(1)	121.7(3)
O(2)-C(15)-C(16)	105.9(4)	C(17)-C(16)-C(15)	103.9(4)
C(18)-C(17)-C(16)	102.1(4)	O(2)-C(18)-C(17)	104.7(4)

[(Cp^{ttt})(Dtp)Tm(BH$_4$)] (25)

Compound	fj209
Molecular formula	$C_{31}H_{57}BPTm$
Molecular weight	640.48
Crystal habit	Yellow Block
Crystal dimensions(mm)	0.26x0.22x0.22
Crystal system	monoclinic
Space group	C2/c
a(≈)	34.436(1)
b(≈)	9.870(1)
c(≈)	18.443(1)
α(∞)	90.00
β(∞)	94.175(1)
γ(∞)	90.00
V(≈^{3})	6251.8(7)
Z	8
d(g-cm^{-3})	1.361
F(000)	2656
μ(cm^{-1})	2.906
Absorption corrections	multi-scan ; 0.5187 min, 0.5673 max
Diffractometer	KappaCCD
X-ray source	MoKα
λ(≈)	0.71069
Monochromator	graphite
T (K)	150.0(1)
Scan mode	phi and omega scans
Maximum θ	30.03

HKL ranges	-47 48 ; -13 12 ; -25 25
Reflections measured	15432
Unique data	9116
Rint	0.0180
Reflections used	7514
Criterion	I > 2σ(I)
Refinement type	Fsqd
Hydrogen atoms	mixed
Parameters refined	340
Reflections / parameter	22
wR2	0.0592
R1	0.0259
Weights a, b	0.0258 ; 0.0000
GoF	1.029
difference peak / hole (e ≈$^{-3}$)	1.906(0.092) / -0.821(0.092)

Table. Bond lengths (A) and angles (deg) for fj209

Tm(1)-C(18)	2.583(2)	Tm(1)-C(15)	2.611(2)
Tm(1)-C(17)	2.617(2)	Tm(1)-B(1)	2.638(3)
Tm(1)-C(19)	2.641(2)	Tm(1)-C(16)	2.643(2)
Tm(1)-C(1)	2.695(2)	Tm(1)-C(2)	2.710(2)
Tm(1)-C(4)	2.752(2)	Tm(1)-C(3)	2.762(2)
Tm(1)-P(1)	2.8098(6	Tm(1)-H(1BB)	2.12(2)
Tm(1)-H(1BD)	2.17(2)	P(1)-C(1)	1.779(2)
P(1)-C(4)	1.781(2)	C(1)-C(2)	1.411(3)
C(1)-C(11)	1.546(3)	C(2)-C(3)	1.441(3)
C(2)-C(10)	1.509(3)	C(3)-C(4)	1.397(3)
C(3)-C(9)	1.512(3)	C(4)-C(5)	1.541(3)
C(5)-C(6)	1.527(3)	C(5)-C(7)	1.538(3)
C(5)-C(8)	1.545(3)	C(6)-H(6A)	0.9800
C(6)-H(6B)	0.9800	C(6)-H(6C)	0.9800
C(7)-H(7A)	0.9800	C(7)-H(7B)	0.9800
C(7)-H(7C)	0.9800	C(8)-H(8A)	0.9800
C(8)-H(8B)	0.9800	C(8)-H(8C)	0.9800
C(9)-H(9A)	0.9800	C(9)-H(9B)	0.9800
C(9)-H(9C)	0.9800	C(10)-H(10A)	0.9800
C(10)-H(10B)	0.9800	C(10)-H(10C)	0.9800
C(11)-C(14)	1.511(3)	C(11)-C(12)	1.516(3)
C(11)-C(13)	1.529(3)	C(12)-H(12A)	0.9800
C(12)-H(12B)	0.9800	C(12)-H(12C)	0.9800
C(13)-H(13A)	0.9800	C(13)-H(13B)	0.9800
C(13)-H(13C)	0.9800	C(14)-H(14A)	0.9800
C(14)-H(14B)	0.9800	C(14)-H(14C)	0.9800
C(15)-C(19)	1.404(3)	C(15)-C(16)	1.437(3)
C(15)-H(15)	0.9500	C(16)-C(17)	1.441(3)
C(16)-C(28)	1.541(3)	C(17)-C(18)	1.422(3)
C(17)-C(24)	1.556(3)	C(18)-C(19)	1.413(3)
C(18)-H(18)	0.9498	C(19)-C(20)	1.528(3)
C(20)-C(22)	1.535(3)	C(20)-C(21)	1.538(3)
C(20)-C(23)	1.536(3)	C(21)-H(21A)	0.9800
C(21)-H(21B)	0.9800	C(21)-H(21C)	0.9800
C(22)-H(22A)	0.9800	C(22)-H(22B)	0.9800
C(22)-H(22C)	0.9800	C(23)-H(23A)	0.9800
C(23)-H(23B)	0.9800	C(23)-H(23C)	0.9800
C(24)-C(26)	1.524(3)	C(24)-C(27)	1.529(3)
C(24)-C(25)	1.538(3)	C(25)-H(25A)	0.9800
C(25)-H(25B)	0.9800	C(25)-H(25C)	0.9800
C(26)-H(26A)	0.9800	C(26)-H(26B)	0.9800
C(26)-H(26C)	0.9800	C(27)-H(27A)	0.9800
C(27)-H(27B)	0.9800	C(27)-H(27C)	0.9800

C(28)-C(31)	1.529(3)	C(28)-C(29)	1.543(3)
C(28)-C(30)	1.544(3)	C(29)-H(29A)	0.9800
C(29)-H(29B)	0.9800	C(29)-H(29C)	0.9800
C(30)-H(30A)	0.9800	C(30)-H(30B)	0.9800
C(30)-H(30C)	0.9800	C(31)-H(31A)	0.9800
C(31)-H(31B)	0.9800	C(31)-H(31C)	0.9800
B(1)-H(1BA)	1.09(2)	B(1)-H(1BB)	1.21(2)
B(1)-H(1BC)	1.08(3)	B(1)-H(1BD)	1.19(2)

C(18)-Tm(1)-C(15)	51.21(6)	C(18)-Tm(1)-C(17)	31.73(6)
C(15)-Tm(1)-C(17)	52.13(6)	C(18)-Tm(1)-B(1)	78.89(8)
C(15)-Tm(1)-B(1)	126.69(8)	C(17)-Tm(1)-B(1)	96.10(8)
C(18)-Tm(1)-C(19)	31.35(6)	C(15)-Tm(1)-C(19)	31.01(6)
C(17)-Tm(1)-C(19)	52.67(6)	B(1)-Tm(1)-C(19)	96.28(8)
C(18)-Tm(1)-C(16)	52.17(6)	C(15)-Tm(1)-C(16)	31.74(6)
C(17)-Tm(1)-C(16)	31.80(6)	B(1)-Tm(1)-C(16)	127.39(8)
C(19)-Tm(1)-C(16)	52.56(6)	C(18)-Tm(1)-C(1)	144.58(6)
C(15)-Tm(1)-C(1)	97.97(6)	C(17)-Tm(1)-C(1)	144.40(7)
B(1)-Tm(1)-C(1)	119.02(8)	C(19)-Tm(1)-C(1)	113.25(6)
C(16)-Tm(1)-C(1)	112.60(6)	C(18)-Tm(1)-C(2)	149.54(6)
C(15)-Tm(1)-C(2)	123.29(6)	C(17)-Tm(1)-C(2)	174.63(6)
B(1)-Tm(1)-C(2)	89.09(8)	C(19)-Tm(1)-C(2)	125.50(6)
C(16)-Tm(1)-C(2)	142.85(6)	C(1)-Tm(1)-C(2)	30.26(6)
C(18)-Tm(1)-C(4)	157.55(6)	C(15)-Tm(1)-C(4)	134.34(7)
C(17)-Tm(1)-C(4)	128.46(6)	B(1)-Tm(1)-C(4)	98.88(8)
C(19)-Tm(1)-C(4)	164.44(6)	C(16)-Tm(1)-C(4)	118.60(6)
C(1)-Tm(1)-C(4)	55.61(6)	C(2)-Tm(1)-C(4)	51.59(6)
C(18)-Tm(1)-C(3)	157.96(6)	C(15)-Tm(1)-C(3)	149.21(6)
C(17)-Tm(1)-C(3)	152.24(6)	B(1)-Tm(1)-C(3)	79.09(8)
C(19)-Tm(1)-C(3)	154.54(6)	C(16)-Tm(1)-C(3)	147.30(6)
C(1)-Tm(1)-C(3)	51.47(6)	C(2)-Tm(1)-C(3)	30.53(6)
C(4)-Tm(1)-C(3)	29.37(6)	C(18)-Tm(1)-P(1)	145.10(5)
C(15)-Tm(1)-P(1)	98.16(5)	C(17)-Tm(1)-P(1)	119.02(5)
B(1)-Tm(1)-P(1)	134.76(7)	C(19)-Tm(1)-P(1)	127.10(5)
C(16)-Tm(1)-P(1)	93.14(5)	C(1)-Tm(1)-P(1)	37.63(5)
C(2)-Tm(1)-P(1)	57.23(5)	C(4)-Tm(1)-P(1)	37.35(4)
C(3)-Tm(1)-P(1)	56.39(5)	C(18)-Tm(1)-H(1BB)	81.9(6)
C(15)-Tm(1)-H(1BB)	132.7(6)	C(17)-Tm(1)-H(1BB)	85.6(6)
B(1)-Tm(1)-H(1BB)	26.7(6)	C(19)-Tm(1)-H(1BB)	108.8(6)
C(16)-Tm(1)-H(1BB)	116.2(6)	C(1)-Tm(1)-H(1BB)	128.5(6)
C(2)-Tm(1)-H(1BB)	99.7(6)	C(4)-Tm(1)-H(1BB)	86.5(6)
C(3)-Tm(1)-H(1BB)	78.1(6)	P(1)-Tm(1)-H(1BB)	123.2(6)
C(18)-Tm(1)-H(1BD)	83.1(6)	C(15)-Tm(1)-H(1BD)	117.2(6)
C(17)-Tm(1)-H(1BD)	109.8(6)	B(1)-Tm(1)-H(1BD)	26.4(6)
C(19)-Tm(1)-H(1BD)	87.2(6)	C(16)-Tm(1)-H(1BD)	134.9(6)
C(1)-Tm(1)-H(1BD)	100.8(6)	C(2)-Tm(1)-H(1BD)	74.4(6)
C(4)-Tm(1)-H(1BD)	105.0(6)	C(3)-Tm(1)-H(1BD)	77.6(6)
P(1)-Tm(1)-H(1BD)	130.7(6)	H(1BB)-Tm(1)-H(1BD)	52.8(8)
C(1)-P(1)-C(4)	91.1(1)	C(1)-P(1)-Tm(1)	67.67(7)
C(4)-P(1)-Tm(1)	69.55(7)	C(2)-C(1)-C(11)	126.0(2)
C(2)-C(1)-P(1)	111.5(2)	C(11)-C(1)-P(1)	121.1(2)
C(2)-C(1)-Tm(1)	75.5(1)	C(11)-C(1)-Tm(1)	127.9(1)
P(1)-C(1)-Tm(1)	74.70(7)	C(1)-C(2)-C(3)	112.4(2)
C(1)-C(2)-C(10)	126.8(2)	C(3)-C(2)-C(10)	120.4(2)
C(1)-C(2)-Tm(1)	74.3(1)	C(3)-C(2)-Tm(1)	76.7(1)
C(10)-C(2)-Tm(1)	122.3(2)	C(4)-C(3)-C(2)	113.7(2)
C(4)-C(3)-C(9)	126.3(2)	C(2)-C(3)-C(9)	119.5(2)
C(4)-C(3)-Tm(1)	74.9(1)	C(2)-C(3)-Tm(1)	72.8(1)
C(9)-C(3)-Tm(1)	127.2(2)	C(3)-C(4)-C(5)	127.0(2)
C(3)-C(4)-P(1)	111.2(2)	C(5)-C(4)-P(1)	120.4(2)
C(3)-C(4)-Tm(1)	75.7(1)	C(5)-C(4)-Tm(1)	128.9(1)
P(1)-C(4)-Tm(1)	73.10(7)	C(6)-C(5)-C(7)	107.4(2)
C(6)-C(5)-C(4)	111.0(2)	C(7)-C(5)-C(4)	114.5(2)
C(6)-C(5)-C(8)	107.4(2)	C(7)-C(5)-C(8)	109.5(2)
C(4)-C(5)-C(8)	106.9(2)	C(5)-C(6)-H(6A)	109.5
C(5)-C(6)-H(6B)	109.5	H(6A)-C(6)-H(6B)	109.5
C(5)-C(6)-H(6C)	109.5	H(6A)-C(6)-H(6C)	109.5
H(6B)-C(6)-H(6C)	109.5	C(5)-C(7)-H(7A)	109.5
C(5)-C(7)-H(7B)	109.5	H(7A)-C(7)-H(7B)	109.5

C(5)-C(7)-H(7C)	109.5	H(7A)-C(7)-H(7C)	109.5
H(7B)-C(7)-H(7C)	109.5	C(5)-C(8)-H(8A)	109.5
C(5)-C(8)-H(8B)	109.5	H(8A)-C(8)-H(8B)	109.5
C(5)-C(8)-H(8C)	109.5	H(8A)-C(8)-H(8C)	109.5
H(8B)-C(8)-H(8C)	109.5	C(3)-C(9)-H(9A)	109.5
C(3)-C(9)-H(9B)	109.5	H(9A)-C(9)-H(9B)	109.5
C(3)-C(9)-H(9C)	109.5	H(9A)-C(9)-H(9C)	109.5
H(9B)-C(9)-H(9C)	109.5	C(2)-C(10)-H(10A)	109.5
C(2)-C(10)-H(10B)	109.5	H(10A)-C(10)-H(10B)	109.5
C(2)-C(10)-H(10C)	109.5	H(10A)-C(10)-H(10C)	109.5
H(10B)-C(10)-H(10C)	109.5	C(14)-C(11)-C(12)	107.2(2)
C(14)-C(11)-C(13)	109.2(2)	C(12)-C(11)-C(13)	107.6(2)
C(14)-C(11)-C(1)	113.7(2)	C(12)-C(11)-C(1)	111.1(2)
C(13)-C(11)-C(1)	107.7(2)	C(11)-C(12)-H(12A)	109.5
C(11)-C(12)-H(12B)	109.5	H(12A)-C(12)-H(12B)	109.5
C(11)-C(12)-H(12C)	109.5	H(12A)-C(12)-H(12C)	109.5
H(12B)-C(12)-H(12C)	109.5	C(11)-C(13)-H(13A)	109.5
C(11)-C(13)-H(13B)	109.5	H(13A)-C(13)-H(13B)	109.5
C(11)-C(13)-H(13C)	109.5	H(13A)-C(13)-H(13C)	109.5
H(13B)-C(13)-H(13C)	109.5	C(11)-C(14)-H(14A)	109.5
C(11)-C(14)-H(14B)	109.5	H(14A)-C(14)-H(14B)	109.5
C(11)-C(14)-H(14C)	109.5	H(14A)-C(14)-H(14C)	109.5
H(14B)-C(14)-H(14C)	109.5	C(19)-C(15)-C(16)	110.9(2)
C(19)-C(15)-Tm(1)	75.7(1)	C(16)-C(15)-Tm(1)	75.4(1)
C(19)-C(15)-H(15)	124.6	C(16)-C(15)-H(15)	124.6
Tm(1)-C(15)-H(15)	116.2	C(15)-C(16)-C(17)	105.9(2)
C(15)-C(16)-C(28)	119.7(2)	C(17)-C(16)-C(28)	132.1(2)
C(15)-C(16)-Tm(1)	72.9(1)	C(17)-C(16)-Tm(1)	73.1(1)
C(28)-C(16)-Tm(1)	132.0(1)	C(18)-C(17)-C(16)	106.8(2)
C(18)-C(17)-C(24)	120.0(2)	C(16)-C(17)-C(24)	133.2(2)
C(18)-C(17)-Tm(1)	72.8(1)	C(16)-C(17)-Tm(1)	75.1(1)
C(24)-C(17)-Tm(1)	117.7(1)	C(19)-C(18)-C(17)	110.8(2)
C(19)-C(18)-Tm(1)	76.6(1)	C(17)-C(18)-Tm(1)	75.4(1)
C(19)-C(18)-H(18)	124.5	C(17)-C(18)-H(18)	124.7
Tm(1)-C(18)-H(18)	115.7	C(15)-C(19)-C(18)	105.7(2)
C(15)-C(19)-C(20)	128.6(2)	C(18)-C(19)-C(20)	124.9(2)
C(15)-C(19)-Tm(1)	73.3(1)	C(18)-C(19)-Tm(1)	72.1(1)
C(20)-C(19)-Tm(1)	127.2(1)	C(19)-C(20)-C(22)	112.3(2)
C(19)-C(20)-C(21)	110.9(2)	C(22)-C(20)-C(21)	110.0(2)
C(19)-C(20)-C(23)	108.0(2)	C(22)-C(20)-C(23)	108.2(2)
C(21)-C(20)-C(23)	107.2(2)	C(20)-C(21)-H(21A)	109.5
C(20)-C(21)-H(21B)	109.5	H(21A)-C(21)-H(21B)	109.5
C(20)-C(21)-H(21C)	109.5	H(21A)-C(21)-H(21C)	109.5
H(21B)-C(21)-H(21C)	109.5	C(20)-C(22)-H(22A)	109.5
C(20)-C(22)-H(22B)	109.5	H(22A)-C(22)-H(22B)	109.5
C(20)-C(22)-H(22C)	109.5	H(22A)-C(22)-H(22C)	109.5
H(22B)-C(22)-H(22C)	109.5	C(20)-C(23)-H(23A)	109.5
C(20)-C(23)-H(23B)	109.5	H(23A)-C(23)-H(23B)	109.5
C(20)-C(23)-H(23C)	109.5	H(23A)-C(23)-H(23C)	109.5
H(23B)-C(23)-H(23C)	109.5	C(26)-C(24)-C(27)	109.7(2)
C(26)-C(24)-C(25)	106.6(2)	C(27)-C(24)-C(25)	107.0(2)
C(26)-C(24)-C(17)	112.4(2)	C(27)-C(24)-C(17)	111.0(2)
C(25)-C(24)-C(17)	110.1(2)	C(24)-C(25)-H(25A)	109.5
C(24)-C(25)-H(25B)	109.5	H(25A)-C(25)-H(25B)	109.5
C(24)-C(25)-H(25C)	109.5	H(25A)-C(25)-H(25C)	109.5
H(25B)-C(25)-H(25C)	109.5	C(24)-C(26)-H(26A)	109.5
C(24)-C(26)-H(26B)	109.5	H(26A)-C(26)-H(26B)	109.5
C(24)-C(26)-H(26C)	109.5	H(26A)-C(26)-H(26C)	109.5
H(26B)-C(26)-H(26C)	109.5	C(24)-C(27)-H(27A)	109.5
C(24)-C(27)-H(27B)	109.5	H(27A)-C(27)-H(27B)	109.5
C(24)-C(27)-H(27C)	109.5	H(27A)-C(27)-H(27C)	109.5
H(27B)-C(27)-H(27C)	109.5	C(31)-C(28)-C(16)	116.4(2)
C(31)-C(28)-C(29)	109.8(2)	C(16)-C(28)-C(29)	107.4(2)
C(31)-C(28)-C(30)	105.2(2)	C(16)-C(28)-C(30)	110.8(2)
C(29)-C(28)-C(30)	107.0(2)	C(28)-C(29)-H(29A)	109.5
C(28)-C(29)-H(29B)	109.5	H(29A)-C(29)-H(29B)	109.5
C(28)-C(29)-H(29C)	109.5	H(29A)-C(29)-H(29C)	109.5
H(29B)-C(29)-H(29C)	109.5	C(28)-C(30)-H(30A)	109.5

C(28)-C(30)-H(30B)	109.5	H(30A)-C(30)-H(30B)	109.5
C(28)-C(30)-H(30C)	109.5	H(30A)-C(30)-H(30C)	109.5
H(30B)-C(30)-H(30C)	109.5	C(28)-C(31)-H(31A)	109.5
C(28)-C(31)-H(31B)	109.5	H(31A)-C(31)-H(31B)	109.5
C(28)-C(31)-H(31C)	109.5	H(31A)-C(31)-H(31C)	109.5
H(31B)-C(31)-H(31C)	109.5	Tm(1)-B(1)-H(1BA)	129(1)
Tm(1)-B(1)-H(1BB)	52(1)	H(1BA)-B(1)-H(1BB)	109(2)
Tm(1)-B(1)-H(1BC)	111(1)	H(1BA)-B(1)-H(1BC)	119(2)
H(1BB)-B(1)-H(1BC)	107(2)	Tm(1)-B(1)-H(1BD)	54(1)
H(1BA)-B(1)-H(1BD)	109(2)	H(1BB)-B(1)-H(1BD)	105(2)
H(1BC)-B(1)-H(1BD)	106(2)		

[(Cp^{ttt})(Cp''')Tm(BH_4)] (26)

Compound	fj221
Molecular formula	$C_{31}H_{62}BSi_3Tm$
Molecular weight	698.82
Crystal habit	colorless needle
Crystal dimensions(mm)	0.18x0.10x0.08
Crystal system	monoclinic
Space group	$P2_1/n$
a(Å)	10.9850(10)
b(Å)	19.4660(10)
c(Å)	17.2080(10)
α(°)	90.00
β(°)	107.7760(10)
γ(°)	90.00
V(Å^3)	3504.0(4)
Z	4
d(g-cm^{-3})	1.325
F(000)	1456
μ(cm^{-1})	2.652
Absorption corrections	multi-scan ; 0.6468 min, 0.8158 max
Diffractometer	KappaCCD
X-ray source	MoKα
λ(Å)	0.71069
Monochromator	graphite
T (K)	150.0(1)
Scan mode	phi and omega scans
Maximum θ	30.05
HKL ranges	-15 12 ; -24 27 ; -15 24
Reflections measured	28952
Unique data	10261
Rint	0.0260
Reflections used	8121
Criterion	I > 2σI)
Refinement type	Fsqd
Hydrogen atoms	mixed
Parameters refined	355
Reflections / parameter	22
wR2	0.0814
R1	0.0314

Weights a, b	0.0411 ; 0.7377
GoF	1.019
difference peak / hole (e Å^{-3})	1.644(0.104) / -1.604(0.104)

Table. Bond lengths (A) and angles (deg) for fj221

Tm(1)-C(19)	2.576(3)	Tm(1)-C(18)	2.584(3)
Tm(1)-C(17)	2.592(3)	Tm(1)-C(5)	2.604(3)
Tm(1)-C(3)	2.615(3)	Tm(1)-C(4)	2.623(3)
Tm(1)-B(1)	2.653(4)	Tm(1)-C(2)	2.654(3)
Tm(1)-C(1)	2.655(3)	Tm(1)-C(15)	2.687(3)
Tm(1)-C(16)	2.714(3)	Tm(1)-H(1B)	2.12(3)
Tm(1)-H(2B)	2.12(3)	Si(1)-C(7)	1.858(4)
Si(1)-C(8)	1.859(3)	Si(1)-C(6)	1.860(3)
Si(1)-C(1)	1.877(3)	Si(2)-C(10)	1.854(3)
Si(2)-C(11)	1.855(3)	Si(2)-C(9)	1.861(3)
Si(2)-C(2)	1.867(3)	Si(3)-C(13)	1.846(3)
Si(3)-C(12)	1.858(3)	Si(3)-C(14)	1.861(3)
Si(3)-C(4)	1.871(2)	C(1)-C(5)	1.429(3)
C(1)-C(2)	1.447(4)	C(2)-C(3)	1.433(3)
C(3)-C(4)	1.421(4)	C(3)-H(999)	0.9500
C(4)-C(5)	1.418(4)	C(5)-H(5)	0.9500
C(6)-H(6A)	0.9800	C(6)-H(6B)	0.9800
C(6)-H(6C)	0.9800	C(7)-H(7A)	0.9800
C(7)-H(7B)	0.9800	C(7)-H(7C)	0.9800
C(8)-H(8A)	0.9800	C(8)-H(8B)	0.9800
C(8)-H(8C)	0.9800	C(9)-H(9A)	0.9800
C(9)-H(9B)	0.9800	C(9)-H(9C)	0.9800
C(10)-H(10A)	0.9800	C(10)-H(10B)	0.9800
C(10)-H(10C)	0.9800	C(11)-H(11A)	0.9800
C(11)-H(11B)	0.9800	C(11)-H(11C)	0.9800
C(12)-H(12A)	0.9800	C(12)-H(12B)	0.9800
C(12)-H(12C)	0.9800	C(13)-H(13A)	0.9800
C(13)-H(13B)	0.9800	C(13)-H(13C)	0.9800
C(14)-H(14A)	0.9800	C(14)-H(14B)	0.9800
C(14)-H(14C)	0.9800	C(15)-C(19)	1.437(3)
C(15)-C(16)	1.444(4)	C(15)-C(20)	1.563(4)
C(16)-C(17)	1.428(3)	C(16)-C(24)	1.576(3)
C(17)-C(18)	1.410(4)	C(17)-H(17)	0.9500
C(18)-C(19)	1.404(4)	C(18)-C(28)	1.551(4)
C(19)-H(19)	0.9500	C(20)-C(22)	1.516(4)
C(20)-C(21)	1.534(4)	C(20)-C(23)	1.548(4)
C(21)-H(21A)	0.9800	C(21)-H(21B)	0.9800
C(21)-H(21C)	0.9800	C(22)-H(22A)	0.9800
C(22)-H(22B)	0.9800	C(22)-H(22C)	0.9800
C(23)-H(23A)	0.9800	C(23)-H(23B)	0.9800
C(23)-H(23C)	0.9800	C(24)-C(25)	1.526(4)
C(24)-C(26)	1.535(4)	C(24)-C(27)	1.555(4)
C(25)-H(25A)	0.9800	C(25)-H(25B)	0.9800
C(25)-H(25C)	0.9800	C(26)-H(26A)	0.9800
C(26)-H(26B)	0.9800	C(26)-H(26C)	0.9800
C(27)-H(27A)	0.9800	C(27)-H(27B)	0.9800
C(27)-H(27C)	0.9800	C(28)-C(29)	1.512(4)
C(28)-C(30)	1.534(4)	C(28)-C(31)	1.537(4)
C(29)-H(29A)	0.9800	C(29)-H(29B)	0.9800
C(29)-H(29C)	0.9800	C(30)-H(30A)	0.9800
C(30)-H(30B)	0.9800	C(30)-H(30C)	0.9800
C(31)-H(31A)	0.9800	C(31)-H(31B)	0.9800
C(31)-H(31C)	0.9800	B(1)-H(1B)	1.20(3)
B(1)-H(2B)	1.18(3)	B(1)-H(3B)	1.09(4)
B(1)-H(4B)	1.09(3)		

C(19)-Tm(1)-C(18)	31.57(8)	C(19)-Tm(1)-C(17)	51.7(1)
C(18)-Tm(1)-C(17)	31.63(8)	C(19)-Tm(1)-C(5)	145.56(8)
C(18)-Tm(1)-C(5)	160.12(8)	C(17)-Tm(1)-C(5)	162.7(1)
C(19)-Tm(1)-C(3)	94.5(1)	C(18)-Tm(1)-C(3)	121.0(1)

C(17)-Tm(1)-C(3)	145.5(1)	C(5)-Tm(1)-C(3)	51.26(8)
C(19)-Tm(1)-C(4)	119.8(1)	C(18)-Tm(1)-C(4)	150.4(1)
C(17)-Tm(1)-C(4)	156.08(8)	C(5)-Tm(1)-C(4)	31.48(8)
C(3)-Tm(1)-C(4)	31.48(8)	C(19)-Tm(1)-B(1)	135.9(1)
C(18)-Tm(1)-B(1)	109.7(1)	C(17)-Tm(1)-B(1)	84.3(1)
C(5)-Tm(1)-B(1)	78.4(1)	C(3)-Tm(1)-B(1)	128.8(1)
C(4)-Tm(1)-B(1)	99.5(1)	C(19)-Tm(1)-C(2)	97.75(8)
C(18)-Tm(1)-C(2)	110.85(8)	C(17)-Tm(1)-C(2)	142.43(8)
C(5)-Tm(1)-C(2)	51.98(8)	C(3)-Tm(1)-C(2)	31.55(7)
C(4)-Tm(1)-C(2)	52.85(8)	B(1)-Tm(1)-C(2)	123.0(1)
C(19)-Tm(1)-C(1)	127.25(8)	C(18)-Tm(1)-C(1)	128.63(8)
C(17)-Tm(1)-C(1)	151.11(7)	C(5)-Tm(1)-C(1)	31.52(7)
C(3)-Tm(1)-C(1)	51.91(8)	C(4)-Tm(1)-C(1)	52.79(8)
B(1)-Tm(1)-C(1)	91.4(1)	C(2)-Tm(1)-C(1)	31.64(8)
C(19)-Tm(1)-C(15)	31.61(8)	C(18)-Tm(1)-C(15)	52.47(8)
C(17)-Tm(1)-C(15)	51.62(8)	C(5)-Tm(1)-C(15)	139.59(8)
C(3)-Tm(1)-C(15)	96.80(8)	C(4)-Tm(1)-C(15)	108.24(8)
B(1)-Tm(1)-C(15)	120.9(1)	C(2)-Tm(1)-C(15)	115.40(8)
C(1)-Tm(1)-C(15)	146.54(8)	C(19)-Tm(1)-C(16)	51.62(8)
C(18)-Tm(1)-C(16)	52.16(8)	C(17)-Tm(1)-C(16)	31.13(7)
C(5)-Tm(1)-C(16)	147.55(7)	C(3)-Tm(1)-C(16)	125.30(8)
C(4)-Tm(1)-C(16)	124.95(8)	B(1)-Tm(1)-C(16)	90.7(1)
C(2)-Tm(1)-C(16)	146.20(8)	C(1)-Tm(1)-C(16)	177.21(8)
C(15)-Tm(1)-C(16)	31.01(8)	C(19)-Tm(1)-H(1B)	130(1)
C(18)-Tm(1)-H(1B)	99(1)	C(17)-Tm(1)-H(1B)	84(1)
C(5)-Tm(1)-H(1B)	81(1)	C(3)-Tm(1)-H(1B)	130(1)
C(4)-Tm(1)-H(1B)	110(1)	B(1)-Tm(1)-H(1B)	26.1(8)
C(2)-Tm(1)-H(1B)	109.3(8)	C(1)-Tm(1)-H(1B)	80(1)
C(15)-Tm(1)-H(1B)	133(1)	C(16)-Tm(1)-H(1B)	102.6(8)
C(19)-Tm(1)-H(2B)	131(1)	C(18)-Tm(1)-H(2B)	117.8(8)
C(17)-Tm(1)-H(2B)	87(1)	C(5)-Tm(1)-H(2B)	78(1)
C(3)-Tm(1)-H(2B)	118.4(8)	C(4)-Tm(1)-H(2B)	87.0(8)
B(1)-Tm(1)-H(2B)	26(1)	C(2)-Tm(1)-H(2B)	130(1)
C(1)-Tm(1)-H(2B)	102(1)	C(15)-Tm(1)-H(2B)	105(1)
C(16)-Tm(1)-H(2B)	80(1)	H(1B)-Tm(1)-H(2B)	52(1)
C(7)-Si(1)-C(8)	107.4(2)	C(7)-Si(1)-C(6)	107.1(2)
C(8)-Si(1)-C(6)	108.5(1)	C(7)-Si(1)-C(1)	107.1(1)
C(8)-Si(1)-C(1)	116.9(1)	C(6)-Si(1)-C(1)	109.5(1)
C(10)-Si(2)-C(11)	107.4(2)	C(10)-Si(2)-C(9)	109.7(2)
C(11)-Si(2)-C(9)	108.2(1)	C(10)-Si(2)-C(2)	109.3(1)
C(11)-Si(2)-C(2)	107.3(1)	C(9)-Si(2)-C(2)	114.6(1)
C(13)-Si(3)-C(12)	107.6(2)	C(13)-Si(3)-C(14)	107.3(2)
C(12)-Si(3)-C(14)	113.3(2)	C(13)-Si(3)-C(4)	107.9(1)
C(12)-Si(3)-C(4)	110.6(1)	C(14)-Si(3)-C(4)	110.0(1)
C(5)-C(1)-C(2)	106.5(2)	C(5)-C(1)-Si(1)	118.9(2)
C(2)-C(1)-Si(1)	133.2(2)	C(5)-C(1)-Tm(1)	72.3(1)
C(2)-C(1)-Tm(1)	74.1(2)	Si(1)-C(1)-Tm(1)	128.8(1)
C(3)-C(2)-C(1)	106.4(2)	C(3)-C(2)-Si(2)	118.1(2)
C(1)-C(2)-Si(2)	132.8(2)	C(3)-C(2)-Tm(1)	72.8(2)
C(1)-C(2)-Tm(1)	74.2(1)	Si(2)-C(2)-Tm(1)	132.1(1)
C(4)-C(3)-C(2)	110.8(2)	C(4)-C(3)-Tm(1)	74.6(2)
C(2)-C(3)-Tm(1)	75.7(2)	C(4)-C(3)-H(999)	124.6
C(2)-C(3)-H(999)	124.6	Tm(1)-C(3)-H(999)	116.8
C(5)-C(4)-C(3)	105.4(2)	C(5)-C(4)-Si(3)	122.6(2)
C(3)-C(4)-Si(3)	130.4(2)	C(5)-C(4)-Tm(1)	73.5(1)
C(3)-C(4)-Tm(1)	73.9(1)	Si(3)-C(4)-Tm(1)	128.5(1)
C(4)-C(5)-C(1)	111.0(2)	C(4)-C(5)-Tm(1)	75.0(2)
C(1)-C(5)-Tm(1)	76.2(2)	C(4)-C(5)-H(5)	124.5
C(1)-C(5)-H(5)	124.5	Tm(1)-C(5)-H(5)	116.1
Si(1)-C(6)-H(6A)	109.5	Si(1)-C(6)-H(6B)	109.5
H(6A)-C(6)-H(6B)	109.5	Si(1)-C(6)-H(6C)	109.5
H(6A)-C(6)-H(6C)	109.5	H(6B)-C(6)-H(6C)	109.5
Si(1)-C(7)-H(7A)	109.5	Si(1)-C(7)-H(7B)	109.5
H(7A)-C(7)-H(7B)	109.5	Si(1)-C(7)-H(7C)	109.5
H(7A)-C(7)-H(7C)	109.5	H(7B)-C(7)-H(7C)	109.5
Si(1)-C(8)-H(8A)	109.5	Si(1)-C(8)-H(8B)	109.5
H(8A)-C(8)-H(8B)	109.5	Si(1)-C(8)-H(8C)	109.5
H(8A)-C(8)-H(8C)	109.5	H(8B)-C(8)-H(8C)	109.5
Si(2)-C(9)-H(9A)	109.5	Si(2)-C(9)-H(9B)	109.5
H(9A)-C(9)-H(9B)	109.5	Si(2)-C(9)-H(9C)	109.5

H(9A)-C(9)-H(9C)	109.5	H(9B)-C(9)-H(9C)	109.5
Si(2)-C(10)-H(10A)	109.5	Si(2)-C(10)-H(10B)	109.5
H(10A)-C(10)-H(10B)	109.5	Si(2)-C(10)-H(10C)	109.5
H(10A)-C(10)-H(10C)	109.5	H(10B)-C(10)-H(10C)	109.5
Si(2)-C(11)-H(11A)	109.5	Si(2)-C(11)-H(11B)	109.5
H(11A)-C(11)-H(11B)	109.5	Si(2)-C(11)-H(11C)	109.5
H(11A)-C(11)-H(11C)	109.5	H(11B)-C(11)-H(11C)	109.5
Si(3)-C(12)-H(12A)	109.5	Si(3)-C(12)-H(12B)	109.5
H(12A)-C(12)-H(12B)	109.5	Si(3)-C(12)-H(12C)	109.5
H(12A)-C(12)-H(12C)	109.5	H(12B)-C(12)-H(12C)	109.5
Si(3)-C(13)-H(13A)	109.5	Si(3)-C(13)-H(13B)	109.5
H(13A)-C(13)-H(13B)	109.5	Si(3)-C(13)-H(13C)	109.5
H(13A)-C(13)-H(13C)	109.5	H(13B)-C(13)-H(13C)	109.5
Si(3)-C(14)-H(14A)	109.5	Si(3)-C(14)-H(14B)	109.5
H(14A)-C(14)-H(14B)	109.5	Si(3)-C(14)-H(14C)	109.5
H(14A)-C(14)-H(14C)	109.5	H(14B)-C(14)-H(14C)	109.5
C(19)-C(15)-C(16)	106.4(2)	C(19)-C(15)-C(20)	118.3(2)
C(16)-C(15)-C(20)	133.5(2)	C(19)-C(15)-Tm(1)	69.9(2)
C(16)-C(15)-Tm(1)	75.5(2)	C(20)-C(15)-Tm(1)	130.5(2)
C(17)-C(16)-C(15)	106.4(2)	C(17)-C(16)-C(24)	120.0(2)
C(15)-C(16)-C(24)	132.9(2)	C(17)-C(16)-Tm(1)	69.7(1)
C(15)-C(16)-Tm(1)	73.5(1)	C(24)-C(16)-Tm(1)	128.1(2)
C(18)-C(17)-C(16)	110.5(2)	C(18)-C(17)-Tm(1)	73.8(2)
C(16)-C(17)-Tm(1)	79.1(2)	C(18)-C(17)-H(17)	124.8
C(16)-C(17)-H(17)	124.8	Tm(1)-C(17)-H(17)	114.1
C(19)-C(18)-C(17)	106.3(2)	C(19)-C(18)-C(28)	128.1(2)
C(17)-C(18)-C(28)	125.4(2)	C(19)-C(18)-Tm(1)	73.9(2)
C(17)-C(18)-Tm(1)	74.5(2)	C(28)-C(18)-Tm(1)	113.8(2)
C(18)-C(19)-C(15)	110.3(2)	C(18)-C(19)-Tm(1)	74.5(2)
C(15)-C(19)-Tm(1)	78.4(2)	C(18)-C(19)-H(19)	124.8
C(15)-C(19)-H(19)	124.8	Tm(1)-C(19)-H(19)	114.1
C(22)-C(20)-C(21)	107.0(3)	C(22)-C(20)-C(23)	106.4(2)
C(21)-C(20)-C(23)	109.8(2)	C(22)-C(20)-C(15)	111.9(2)
C(21)-C(20)-C(15)	107.8(2)	C(23)-C(20)-C(15)	113.8(2)
C(20)-C(21)-H(21A)	109.5	C(20)-C(21)-H(21B)	109.5
H(21A)-C(21)-H(21B)	109.5	C(20)-C(21)-H(21C)	109.5
H(21A)-C(21)-H(21C)	109.5	H(21B)-C(21)-H(21C)	109.5
C(20)-C(22)-H(22A)	109.5	C(20)-C(22)-H(22B)	109.5
H(22A)-C(22)-H(22B)	109.5	C(20)-C(22)-H(22C)	109.5
H(22A)-C(22)-H(22C)	109.5	H(22B)-C(22)-H(22C)	109.5
C(20)-C(23)-H(23A)	109.5	C(20)-C(23)-H(23B)	109.5
H(23A)-C(23)-H(23B)	109.5	C(20)-C(23)-H(23C)	109.5
H(23A)-C(23)-H(23C)	109.5	H(23B)-C(23)-H(23C)	109.5
C(25)-C(24)-C(26)	107.3(3)	C(25)-C(24)-C(27)	109.8(2)
C(26)-C(24)-C(27)	105.7(2)	C(25)-C(24)-C(16)	114.6(2)
C(26)-C(24)-C(16)	109.6(2)	C(27)-C(24)-C(16)	109.4(2)
C(24)-C(25)-H(25A)	109.5	C(24)-C(25)-H(25B)	109.5
H(25A)-C(25)-H(25B)	109.5	C(24)-C(25)-H(25C)	109.5
H(25A)-C(25)-H(25C)	109.5	H(25B)-C(25)-H(25C)	109.5
C(24)-C(26)-H(26A)	109.5	C(24)-C(26)-H(26B)	109.5
H(26A)-C(26)-H(26B)	109.5	C(24)-C(26)-H(26C)	109.5
H(26A)-C(26)-H(26C)	109.5	H(26B)-C(26)-H(26C)	109.5
C(24)-C(27)-H(27A)	109.5	C(24)-C(27)-H(27B)	109.5
H(27A)-C(27)-H(27B)	109.5	C(24)-C(27)-H(27C)	109.5
H(27A)-C(27)-H(27C)	109.5	H(27B)-C(27)-H(27C)	109.5
C(29)-C(28)-C(30)	110.2(3)	C(29)-C(28)-C(31)	110.6(2)
C(30)-C(28)-C(31)	108.6(2)	C(29)-C(28)-C(18)	108.0(2)
C(30)-C(28)-C(18)	110.1(2)	C(31)-C(28)-C(18)	109.5(2)
C(28)-C(29)-H(29A)	109.5	C(28)-C(29)-H(29B)	109.5
H(29A)-C(29)-H(29B)	109.5	C(28)-C(29)-H(29C)	109.5
H(29A)-C(29)-H(29C)	109.5	H(29B)-C(29)-H(29C)	109.5
C(28)-C(30)-H(30A)	109.5	C(28)-C(30)-H(30B)	109.5
H(30A)-C(30)-H(30B)	109.5	C(28)-C(30)-H(30C)	109.5
H(30A)-C(30)-H(30C)	109.5	H(30B)-C(30)-H(30C)	109.5
C(28)-C(31)-H(31A)	109.5	C(28)-C(31)-H(31B)	109.5
H(31A)-C(31)-H(31B)	109.5	C(28)-C(31)-H(31C)	109.5
H(31A)-C(31)-H(31C)	109.5	H(31B)-C(31)-H(31C)	109.5
Tm(1)-B(1)-H(1B)	51(2)	Tm(1)-B(1)-H(2B)	51(2)

H(1B)-B(1)-H(2B)	102(2)	Tm(1)-B(1)-H(3B)	122(2)
H(1B)-B(1)-H(3B)	109(2)	H(2B)-B(1)-H(3B)	109(2)
Tm(1)-B(1)-H(4B)	121(2)	H(1B)-B(1)-H(4B)	109(2)
H(2B)-B(1)-H(4B)	110(2)	H(3B)-B(1)-H(4B)	117(3)

[(Cp^{ttt})TmI_2(THF)] (28)

Compound	tmtcpi2
Molecular formula	$C_{21}H_{37}I_2OTm$
Molecular weight	2912.94
Crystal habit	yellow plate
Crystal dimensions(mm)	0.22x0.19x0.03
Crystal system	monoclinic
Space group	$P2_1/c$
a(Å)	18.0220(10)
b(Å)	9.1030(10)
c(Å)	16.8040(10)
α(°)	90.00
β(°)	114.8190(10)
γ(°)	90.00
V(Å^3)	2502.1(3)
Z	1
d(g-cm^{-3})	1.933
F(000)	1384
μ(cm^{-1})	6.020
Absorption corrections	multi-scan ; 0.3510 min, 0.8400 max
Diffractometer	KappaCCD
X-ray source	MoKα
λ(Å)	0.71069
Monochromator	graphite
T (K)	150.0(1)
Scan mode	phi and omega scans
Maximum θ	27.46
HKL ranges	-23 23 ; -10 11 ; -21 21
Reflections measured	9774
Unique data	5687
Rint	0.0422
Reflections used	4400
Criterion	I > 2σI)
Refinement type	Fsqd
Hydrogen atoms	mixed
Parameters refined	235
Reflections / parameter	18
wR2	0.1124
R1	0.0396
Weights a, b	0.0666 ; 0.0000
GoF	1.008
difference peak / hole (e Å^{-3})	1.782(0.181) / -1.613(0.181)

Table. Bond lengths (A) and angles (deg) for tmtcpi2

Tm(1)-O(1)	2.258(4)	Tm(1)-C(5)	2.553(5)
Tm(1)-C(3)	2.568(5)	Tm(1)-C(4)	2.586(5)
Tm(1)-C(1)	2.587(5)	Tm(1)-C(2)	2.601(5)
Tm(1)-I(2)	2.8725(5	Tm(1)-I(1)	2.8851(5)
O(1)-C(21)	1.457(7)	O(1)-C(18)	1.481(6)
C(1)-C(5)	1.410(8)	C(1)-C(2)	1.456(7)
C(1)-C(6)	1.555(7)	C(2)-C(3)	1.422(8)
C(2)-C(10)	1.535(8)	C(3)-C(4)	1.419(8)
C(3)-H(3)	0.9507	C(4)-C(5)	1.411(8)
C(4)-C(14)	1.517(8)	C(5)-H(5)	0.9501
C(6)-C(8)	1.538(8)	C(6)-C(7)	1.548(8)
C(6)-C(9)	1.552(9)	C(7)-H(7A)	0.9800
C(7)-H(7B)	0.9800	C(7)-H(7C)	0.9800
C(8)-H(8A)	0.9800	C(8)-H(8B)	0.9800
C(8)-H(8C)	0.9800	C(9)-H(9A)	0.9800
C(9)-H(9B)	0.9800	C(9)-H(9C)	0.9800
C(10)-C(13)	1.526(8)	C(10)-C(11)	1.543(8)
C(10)-C(12)	1.544(8)	C(11)-H(11A)	0.9800
C(11)-H(11B)	0.9800	C(11)-H(11C)	0.9800
C(12)-H(12A)	0.9800	C(12)-H(12B)	0.9800
C(12)-H(12C)	0.9800	C(13)-H(13A)	0.9800
C(13)-H(13B)	0.9800	C(13)-H(13C)	0.9800
C(14)-C(15)	1.523(9)	C(14)-C(17)	1.527(9)
C(14)-C(16)	1.546(9)	C(15)-H(15A)	0.9800
C(15)-H(15B)	0.9800	C(15)-H(15C)	0.9800
C(16)-H(16A)	0.9800	C(16)-H(16B)	0.9800
C(16)-H(16C)	0.9800	C(17)-H(17A)	0.9800
C(17)-H(17B)	0.9800	C(17)-H(17C)	0.9800
C(18)-C(19)	1.495(9)	C(18)-H(18A)	0.9900
C(18)-H(18B)	0.9900	C(19)-C(20)	1.50(1)
C(19)-H(19A)	0.9900	C(19)-H(19B)	0.9900
C(20)-C(21)	1.492(8)	C(20)-H(20A)	0.9900
C(20)-H(20B)	0.9900	C(21)-H(21A)	0.9900
C(21)-H(21B)	0.9900		

O(1)-Tm(1)-C(5)	88.0(2)	O(1)-Tm(1)-C(3)	122.2(2)
C(5)-Tm(1)-C(3)	52.1(2)	O(1)-Tm(1)-C(4)	91.6(2)
C(5)-Tm(1)-C(4)	31.9(2)	C(3)-Tm(1)-C(4)	32.0(2)
O(1)-Tm(1)-C(1)	114.2(2)	C(5)-Tm(1)-C(1)	31.8(2)
C(3)-Tm(1)-C(1)	53.0(2)	C(4)-Tm(1)-C(1)	53.6(2)
O(1)-Tm(1)-C(2)	140.7(2)	C(5)-Tm(1)-C(2)	52.9(2)
C(3)-Tm(1)-C(2)	31.9(2)	C(4)-Tm(1)-C(2)	53.7(2)
C(1)-Tm(1)-C(2)	32.6(2)	O(1)-Tm(1)-I(2)	101.7(1)
C(5)-Tm(1)-I(2)	139.2(1)	C(3)-Tm(1)-I(2)	90.8(1)
C(4)-Tm(1)-I(2)	107.6(1)	C(1)-Tm(1)-I(2)	138.5(1)
C(2)-Tm(1)-I(2)	105.9(1)	O(1)-Tm(1)-I(1)	89.7(1)
C(5)-Tm(1)-I(1)	117.1(1)	C(3)-Tm(1)-I(1)	142.3(1)
C(4)-Tm(1)-I(1)	148.8(1)	C(1)-Tm(1)-I(1)	97.8(1)
C(2)-Tm(1)-I(1)	110.5(1)	I(2)-Tm(1)-I(1)	102.69(1)
C(21)-O(1)-C(18)	108.8(4)	C(21)-O(1)-Tm(1)	121.2(3)
C(18)-O(1)-Tm(1)	124.9(4)	C(5)-C(1)-C(2)	106.4(5)
C(5)-C(1)-C(6)	119.6(5)	C(2)-C(1)-C(6)	132.6(5)
C(5)-C(1)-Tm(1)	72.8(3)	C(2)-C(1)-Tm(1)	74.2(3)
C(6)-C(1)-Tm(1)	128.3(3)	C(3)-C(2)-C(1)	106.1(5)
C(3)-C(2)-C(10)	120.9(5)	C(1)-C(2)-C(10)	133.0(5)
C(3)-C(2)-Tm(1)	72.8(3)	C(1)-C(2)-Tm(1)	73.2(3)
C(10)-C(2)-Tm(1)	120.6(3)	C(4)-C(3)-C(2)	110.9(5)
C(4)-C(3)-Tm(1)	74.7(3)	C(2)-C(3)-Tm(1)	75.3(3)
C(4)-C(3)-H(3)	124.3	C(2)-C(3)-H(3)	124.8
Tm(1)-C(3)-H(3)	117.1	C(5)-C(4)-C(3)	105.1(5)
C(5)-C(4)-C(14)	128.6(5)	C(3)-C(4)-C(14)	126.1(5)
C(5)-C(4)-Tm(1)	72.8(3)	C(3)-C(4)-Tm(1)	73.3(3)
C(14)-C(4)-Tm(1)	122.1(3)	C(1)-C(5)-C(4)	111.5(5)
C(1)-C(5)-Tm(1)	75.4(3)	C(4)-C(5)-Tm(1)	75.3(3)
C(1)-C(5)-H(5)	123.8	C(4)-C(5)-H(5)	124.7
Tm(1)-C(5)-H(5)	116.7	C(8)-C(6)-C(7)	108.0(5)
C(8)-C(6)-C(9)	105.0(5)	C(7)-C(6)-C(9)	109.8(5)

C(8)-C(6)-C(1)	109.1(4)	C(7)-C(6)-C(1)	107.6(5)
C(9)-C(6)-C(1)	117.0(5)	C(6)-C(7)-H(7A)	109.5
C(6)-C(7)-H(7B)	109.5	H(7A)-C(7)-H(7B)	109.5
C(6)-C(7)-H(7C)	109.5	H(7A)-C(7)-H(7C)	109.5
H(7B)-C(7)-H(7C)	109.5	C(6)-C(8)-H(8A)	109.5
C(6)-C(8)-H(8B)	109.5	H(8A)-C(8)-H(8B)	109.5
C(6)-C(8)-H(8C)	109.5	H(8A)-C(8)-H(8C)	109.5
H(8B)-C(8)-H(8C)	109.5	C(6)-C(9)-H(9A)	109.5
C(6)-C(9)-H(9B)	109.5	H(9A)-C(9)-H(9B)	109.5
C(6)-C(9)-H(9C)	109.5	H(9A)-C(9)-H(9C)	109.5
H(9B)-C(9)-H(9C)	109.5	C(13)-C(10)-C(2)	112.4(5)
C(13)-C(10)-C(11)	111.0(6)	C(2)-C(10)-C(11)	111.4(4)
C(13)-C(10)-C(12)	106.2(5)	C(2)-C(10)-C(12)	109.8(5)
C(11)-C(10)-C(12)	105.6(5)	C(10)-C(11)-H(11A)	109.5
C(10)-C(11)-H(11B)	109.5	H(11A)-C(11)-H(11B)	109.5
C(10)-C(11)-H(11C)	109.5	H(11A)-C(11)-H(11C)	109.5
H(11B)-C(11)-H(11C)	109.5	C(10)-C(12)-H(12A)	109.5
C(10)-C(12)-H(12B)	109.5	H(12A)-C(12)-H(12B)	109.5
C(10)-C(12)-H(12C)	109.5	H(12A)-C(12)-H(12C)	109.5
H(12B)-C(12)-H(12C)	109.5	C(10)-C(13)-H(13A)	109.5
C(10)-C(13)-H(13B)	109.5	H(13A)-C(13)-H(13B)	109.5
C(10)-C(13)-H(13C)	109.5	H(13A)-C(13)-H(13C)	109.5
H(13B)-C(13)-H(13C)	109.5	C(4)-C(14)-C(15)	110.4(5)
C(4)-C(14)-C(17)	111.6(5)	C(15)-C(14)-C(17)	108.7(6)
C(4)-C(14)-C(16)	108.1(5)	C(15)-C(14)-C(16)	107.5(5)
C(17)-C(14)-C(16)	110.5(6)	C(14)-C(15)-H(15A)	109.5
C(14)-C(15)-H(15B)	109.5	H(15A)-C(15)-H(15B)	109.5
C(14)-C(15)-H(15C)	109.5	H(15A)-C(15)-H(15C)	109.5
H(15B)-C(15)-H(15C)	109.5	C(14)-C(16)-H(16A)	109.5
C(14)-C(16)-H(16B)	109.5	H(16A)-C(16)-H(16B)	109.5
C(14)-C(16)-H(16C)	109.5	H(16A)-C(16)-H(16C)	109.5
H(16B)-C(16)-H(16C)	109.5	C(14)-C(17)-H(17A)	109.5
C(14)-C(17)-H(17B)	109.5	H(17A)-C(17)-H(17B)	109.5
C(14)-C(17)-H(17C)	109.5	H(17A)-C(17)-H(17C)	109.5
H(17B)-C(17)-H(17C)	109.5	O(1)-C(18)-C(19)	104.2(5)
O(1)-C(18)-H(18A)	110.9	C(19)-C(18)-H(18A)	110.9
O(1)-C(18)-H(18B)	110.9	C(19)-C(18)-H(18B)	110.9
H(18A)-C(18)-H(18B)	108.9	C(18)-C(19)-C(20)	103.3(5)
C(18)-C(19)-H(19A)	111.1	C(20)-C(19)-H(19A)	111.1
C(18)-C(19)-H(19B)	111.1	C(20)-C(19)-H(19B)	111.1
H(19A)-C(19)-H(19B)	109.1	C(21)-C(20)-C(19)	102.4(5)
C(21)-C(20)-H(20A)	111.3	C(19)-C(20)-H(20A)	111.3
C(21)-C(20)-H(20B)	111.3	C(19)-C(20)-H(20B)	111.3
H(20A)-C(20)-H(20B)	109.2	O(1)-C(21)-C(20)	105.2(5)
O(1)-C(21)-H(21A)	110.7	C(20)-C(21)-H(21A)	110.7
O(1)-C(21)-H(21B)	110.7	C(20)-C(21)-H(21B)	110.7
H(21A)-C(21)-H(21B)	108.8		

[(Cp^{ttt})$_2$TmI(NCtBu)] (30)

Compound	tmitbucn
Molecular formula	$C_{39}H_{67}INTm$
Molecular weight	845.77
Crystal habit	lemon yellow plate
Crystal dimensions(mm)	0.22x0.18x0.12
Crystal system	monoclinic
Space group	$P2_1/n$
a(Å)	10.435(5)
b(Å)	35.368(5)
c(Å)	11.290(5)
α(°)	90.000(5)
β(°)	107.460(5)

γ(°)	90.000(5)
V(Å^3)	3975(3)
Z	4
d(g-cm^{-3})	1.413
F(000)	1720
μ(cm^{-1})	3.033
Absorption corrections	multi-scan ; 0.5550 min, 0.7123 max
Diffractometer	KappaCCD
X-ray source	MoKα
λ(Å)	0.71069
Monochromator	graphite
T (K)	150.0(1)
Scan mode	phi and omega scans
Maximum θ	30.02
HKL ranges	-14 14 ; -49 44 ; -15 15
Reflections measured	16026
Unique data	10436
Rint	0.0196
Reflections used	8978
Criterion	I > 2σI)
Refinement type	Fsqd
Hydrogen atoms	mixed
Parameters refined	401
Reflections / parameter	22
wR2	0.0954
R1	0.0334
Weights a, b	0.0534 ; 4.1062
GoF	1.022
difference peak / hole (e Å^{-3})	1.789(0.117) / -2.192(0.117)

Table. Bond lengths (A) and angles (deg) for tmitbucn

Tm(1)-N(1)	2.394(3)	Tm(1)-C(22)	2.615(3)
Tm(1)-C(21)	2.617(3)	Tm(1)-C(5)	2.660(3)
Tm(1)-C(3)	2.663(3)	Tm(1)-C(4)	2.667(3)
Tm(1)-C(20)	2.668(3)	Tm(1)-C(2)	2.762(3)
Tm(1)-C(18)	2.768(3)	Tm(1)-C(1)	2.787(3)
Tm(1)-C(19)	2.806(3)	Tm(1)-I(1)	2.9754(6)
N(1)-C(35)	1.133(4)	C(1)-C(5)	1.424(4)
C(1)-C(2)	1.446(4)	C(1)-C(6)	1.547(4)
C(2)-C(3)	1.429(4)	C(2)-C(10)	1.550(5)
C(3)-C(4)	1.399(4)	C(4)-C(5)	1.420(4)
C(4)-C(14)	1.528(4)	C(6)-C(8)	1.532(5)
C(6)-C(7)	1.536(5)	C(6)-C(9)	1.544(5)
C(10)-C(11)	1.535(5)	C(10)-C(13)	1.544(5)
C(10)-C(12)	1.551(5)	C(14)-C(16)	1.527(5)
C(14)-C(17)	1.529(5)	C(14)-C(15)	1.548(5)
C(18)-C(22)	1.431(4)	C(18)-C(19)	1.445(4)
C(18)-C(23)	1.542(4)	C(19)-C(20)	1.426(4)
C(19)-C(27)	1.550(5)	C(20)-C(21)	1.410(4)
C(21)-C(22)	1.419(4)	C(21)-C(31)	1.527(4)
C(23)-C(25)	1.535(5)	C(23)-C(24)	1.537(5)
C(23)-C(26)	1.542(5)	C(27)-C(28)	1.531(5)
C(27)-C(30)	1.540(5)	C(27)-C(29)	1.543(5)
C(31)-C(34)	1.525(5)	C(31)-C(33)	1.529(5)
C(31)-C(32)	1.543(5)	C(35)-C(36)	1.482(5)

C(36)-C(38)	1.528(6)	C(36)-C(39)	1.534(5)
C(36)-C(37)	1.543(6)		

N(1)-Tm(1)-C(22)	106.1(1)	N(1)-Tm(1)-C(21)	130.6(1)
C(22)-Tm(1)-C(21)	31.5(1)	N(1)-Tm(1)-C(5)	122.1(1)
C(22)-Tm(1)-C(5)	93.8(1)	C(21)-Tm(1)-C(5)	92.9(1)
N(1)-Tm(1)-C(3)	73.7(1)	C(22)-Tm(1)-C(3)	120.1(1)
C(21)-Tm(1)-C(3)	138.0(1)	C(5)-Tm(1)-C(3)	49.9(1)
N(1)-Tm(1)-C(4)	93.2(1)	C(22)-Tm(1)-C(4)	92.7(1)
C(21)-Tm(1)-C(4)	107.7(1)	C(5)-Tm(1)-C(4)	30.9(1)
C(3)-Tm(1)-C(4)	30.4(1)	N(1)-Tm(1)-C(20)	113.2(1)
C(22)-Tm(1)-C(20)	50.5(1)	C(21)-Tm(1)-C(20)	30.9(1)
C(5)-Tm(1)-C(20)	121.0(1)	C(3)-Tm(1)-C(20)	168.9(1)
C(4)-Tm(1)-C(20)	138.5(1)	N(1)-Tm(1)-C(2)	88.5(1)
C(22)-Tm(1)-C(2)	142.1(1)	C(21)-Tm(1)-C(2)	139.3(1)
C(5)-Tm(1)-C(2)	50.1(1)	C(3)-Tm(1)-C(2)	30.5(1)
C(4)-Tm(1)-C(2)	50.9(1)	C(20)-Tm(1)-C(2)	152.3(1)
N(1)-Tm(1)-C(18)	79.6(1)	C(22)-Tm(1)-C(18)	30.7(1)
C(21)-Tm(1)-C(18)	51.4(1)	C(5)-Tm(1)-C(18)	121.5(1)
C(3)-Tm(1)-C(18)	126.3(1)	C(4)-Tm(1)-C(18)	109.5(1)
C(20)-Tm(1)-C(18)	50.0(1)	C(2)-Tm(1)-C(18)	156.8(1)
N(1)-Tm(1)-C(1)	118.4(1)	C(22)-Tm(1)-C(1)	121.1(1)
C(21)-Tm(1)-C(1)	109.3(1)	C(5)-Tm(1)-C(1)	30.2(1)
C(3)-Tm(1)-C(1)	49.8(1)	C(4)-Tm(1)-C(1)	50.7(1)
C(20)-Tm(1)-C(1)	126.8(1)	C(2)-Tm(1)-C(1)	30.2(1)
C(18)-Tm(1)-C(1)	150.9(1)	N(1)-Tm(1)-C(19)	84.1(1)
C(22)-Tm(1)-C(19)	50.2(1)	C(21)-Tm(1)-C(19)	50.9(1)
C(5)-Tm(1)-C(19)	142.1(1)	C(3)-Tm(1)-C(19)	152.1(1)
C(4)-Tm(1)-C(19)	139.3(1)	C(20)-Tm(1)-C(19)	30.1(1)
C(2)-Tm(1)-C(19)	167.6(1)	C(18)-Tm(1)-C(19)	30.0(1)
C(1)-Tm(1)-C(19)	156.9(1)	N(1)-Tm(1)-I(1)	88.91(8)
C(22)-Tm(1)-I(1)	129.49(7)	C(21)-Tm(1)-I(1)	104.44(7)
C(5)-Tm(1)-I(1)	118.72(7)	C(3)-Tm(1)-I(1)	110.35(7)
C(4)-Tm(1)-I(1)	135.22(7)	C(20)-Tm(1)-I(1)	79.11(6)
C(2)-Tm(1)-I(1)	84.51(7)	C(18)-Tm(1)-I(1)	114.82(7)
C(1)-Tm(1)-I(1)	89.57(7)	C(19)-Tm(1)-I(1)	85.39(7)
C(35)-N(1)-Tm(1)	166.2(3)	C(5)-C(1)-C(2)	106.3(3)
C(5)-C(1)-C(6)	119.4(3)	C(2)-C(1)-C(6)	132.3(3)
C(5)-C(1)-Tm(1)	69.9(2)	C(2)-C(1)-Tm(1)	73.9(2)
C(6)-C(1)-Tm(1)	132.5(2)	C(3)-C(2)-C(1)	106.1(3)
C(3)-C(2)-C(10)	117.7(3)	C(1)-C(2)-C(10)	134.3(3)
C(3)-C(2)-Tm(1)	70.9(2)	C(1)-C(2)-Tm(1)	75.9(2)
C(10)-C(2)-Tm(1)	129.5(2)	C(4)-C(3)-C(2)	111.3(3)
C(4)-C(3)-Tm(1)	74.9(2)	C(2)-C(3)-Tm(1)	78.6(2)
C(3)-C(4)-C(5)	105.5(3)	C(3)-C(4)-C(14)	125.8(3)
C(5)-C(4)-C(14)	123.4(3)	C(3)-C(4)-Tm(1)	74.6(2)
C(5)-C(4)-Tm(1)	74.2(2)	C(14)-C(4)-Tm(1)	136.6(2)
C(4)-C(5)-C(1)	110.7(3)	C(4)-C(5)-Tm(1)	74.8(2)
C(1)-C(5)-Tm(1)	79.9(2)	C(8)-C(6)-C(7)	106.5(3)
C(8)-C(6)-C(9)	105.4(3)	C(7)-C(6)-C(9)	110.6(3)
C(8)-C(6)-C(1)	111.0(3)	C(7)-C(6)-C(1)	114.4(3)
C(9)-C(6)-C(1)	108.6(3)	C(11)-C(10)-C(13)	105.9(3)
C(11)-C(10)-C(2)	117.6(3)	C(13)-C(10)-C(2)	110.2(3)
C(11)-C(10)-C(12)	108.7(3)	C(13)-C(10)-C(12)	107.1(3)
C(2)-C(10)-C(12)	106.8(3)	C(16)-C(14)-C(4)	111.8(3)
C(16)-C(14)-C(17)	110.3(3)	C(4)-C(14)-C(17)	113.1(3)
C(16)-C(14)-C(15)	107.9(3)	C(4)-C(14)-C(15)	106.0(3)
C(17)-C(14)-C(15)	107.4(3)	C(22)-C(18)-C(19)	106.5(3)
C(22)-C(18)-C(23)	118.8(3)	C(19)-C(18)-C(23)	132.7(3)
C(22)-C(18)-Tm(1)	68.8(2)	C(19)-C(18)-Tm(1)	76.5(2)
C(23)-C(18)-Tm(1)	131.1(2)	C(20)-C(19)-C(18)	106.4(3)
C(20)-C(19)-C(27)	120.4(3)	C(18)-C(19)-C(27)	132.2(3)
C(20)-C(19)-Tm(1)	69.6(2)	C(18)-C(19)-Tm(1)	73.5(2)
C(27)-C(19)-Tm(1)	130.0(2)	C(21)-C(20)-C(19)	110.9(3)
C(21)-C(20)-Tm(1)	72.5(2)	C(19)-C(20)-Tm(1)	80.3(2)
C(20)-C(21)-C(22)	105.7(3)	C(20)-C(21)-C(31)	124.0(3)
C(22)-C(21)-C(31)	127.0(3)	C(20)-C(21)-Tm(1)	76.5(2)
C(22)-C(21)-Tm(1)	74.2(2)	C(31)-C(21)-Tm(1)	130.8(2)
C(21)-C(22)-C(18)	110.4(3)	C(21)-C(22)-Tm(1)	74.3(2)

C(18)-C(22)-Tm(1)	80.6(2)	C(25)-C(23)-C(24)	105.7(3)
C(25)-C(23)-C(18)	117.6(3)	C(24)-C(23)-C(18)	110.2(3)
C(25)-C(23)-C(26)	109.4(3)	C(24)-C(23)-C(26)	106.9(3)
C(18)-C(23)-C(26)	106.6(3)	C(28)-C(27)-C(30)	106.5(3)
C(28)-C(27)-C(29)	110.4(3)	C(30)-C(27)-C(29)	104.2(3)
C(28)-C(27)-C(19)	114.7(3)	C(30)-C(27)-C(19)	110.3(3)
C(29)-C(27)-C(19)	110.1(3)	C(34)-C(31)-C(21)	112.6(3)
C(34)-C(31)-C(33)	110.5(3)	C(21)-C(31)-C(33)	110.8(3)
C(34)-C(31)-C(32)	107.9(3)	C(21)-C(31)-C(32)	106.5(3)
C(33)-C(31)-C(32)	108.3(3)	N(1)-C(35)-C(36)	178.5(4)
C(35)-C(36)-C(38)	109.3(3)	C(35)-C(36)-C(39)	107.8(3)
C(38)-C(36)-C(39)	109.8(3)	C(35)-C(36)-C(37)	107.7(3)
C(38)-C(36)-C(37)	110.9(3)	C(39)-C(36)-C(37)	111.2(3)

[(Cp’’’)$_2$DyI] (33)

Compound	dysii
Molecular formula	$C_{28}H_{58}DyISi_6$
Molecular weight	852.68
Crystal habit	Colorless Block
Crystal dimensions(mm)	0.24x0.20x0.18
Crystal system	monoclinic
Space group	C2/c
a(Å)	41.095(2)
b(Å)	18.3960(10)
c(Å)	32.965(2)
α(°)	90.00
β(°)	125.6950(10)
γ(°)	90.00
V(Å^3)	20239.2(19)
Z	20
d(g-cm^{-3})	1.399
F(000)	8580
μ(cm^{-1})	2.801
Absorption corrections	multi-scan ; 0.5529 min, 0.6325 max
Diffractometer	KappaCCD
X-ray source	MoKα
λ(Å)	0.71069
Monochromator	graphite
T (K)	150.0(1)
Scan mode	phi and omega scans
Maximum θ	27.48
HKL ranges	-53 53 ; -23 22 ; -42 42
Reflections measured	42689
Unique data	23151
Rint	0.0312
Reflections used	17056
Criterion	I > 2σI)
Refinement type	Fsqd
Hydrogen atoms	mixed
Parameters refined	857
Reflections / parameter	19

wR2	0.1030
R1	0.0377
Weights a, b	0.0582 ; 0.0000
GoF	1.035
difference peak / hole (e Å^{-3})	1.642(0.116) / -2.007(0.116)

Table. Bond lengths (A) and angles (deg) for dysii

Dy(1)-C(3)	2.607(3)	Dy(1)-C(3)#2	2.607(3)
Dy(1)-C(4)	2.642(3)	Dy(1)-C(4)#2	2.642(3)
Dy(1)-C(5)	2.643(3)	Dy(1)-C(5)#2	2.643(3)
Dy(1)-C(2)#2	2.650(3)	Dy(1)-C(2)	2.650(3)
Dy(1)-C(1)#2	2.677(3)	Dy(1)-C(1)	2.677(3)
Dy(1)-I(1)	2.9012(4	Si(1)-C(8)	1.859(4)
Si(1)-C(6)	1.862(4)	Si(1)-C(7)	1.876(4)
Si(1)-C(1)	1.891(4)	Si(2)-C(10)	1.862(4)
Si(2)-C(11)	1.874(4)	Si(2)-C(2)	1.875(4)
Si(2)-C(9)	1.891(4)	Si(3)-C(12)	1.857(4)
Si(3)-C(14)	1.865(4)	Si(3)-C(4)	1.868(4)
Si(3)-C(13)	1.872(5)	C(1)-C(5)	1.412(5)
C(1)-C(2)	1.451(5)	C(2)-C(3)	1.421(5)
C(3)-C(4)	1.415(5)	C(3)-H(3)	0.9500
C(4)-C(5)	1.421(5)	C(5)-H(5)	0.9500
C(6)-H(6A)	0.9800	C(6)-H(6B)	0.9800
C(6)-H(6C)	0.9800	C(7)-H(7A)	0.9800
C(7)-H(7B)	0.9800	C(7)-H(7C)	0.9800
C(8)-H(8A)	0.9800	C(8)-H(8B)	0.9800
C(8)-H(8C)	0.9800	C(9)-H(9A)	0.9800
C(9)-H(9B)	0.9800	C(9)-H(9C)	0.9800
C(10)-H(10A)	0.9800	C(10)-H(10B)	0.9800
C(10)-H(10C)	0.9800	C(11)-H(11A)	0.9800
C(11)-H(11B)	0.9800	C(11)-H(11C)	0.9800
C(12)-H(12A)	0.9800	C(12)-H(12B)	0.9800
C(12)-H(12C)	0.9800	C(13)-H(13A)	0.9800
C(13)-H(13B)	0.9800	C(13)-H(13C)	0.9800
C(14)-H(14A)	0.9800	C(14)-H(14B)	0.9800
C(14)-H(14C)	0.9800	Dy(2)-C(31)	2.588(3)
Dy(2)-C(32)	2.618(3)	Dy(2)-C(17)	2.622(3)
Dy(2)-C(16)	2.636(3)	Dy(2)-C(33)	2.640(3)
Dy(2)-C(15)	2.641(3)	Dy(2)-C(30)	2.643(3)
Dy(2)-C(19)	2.645(3)	Dy(2)-C(29)	2.663(3)
Dy(2)-C(18)	2.681(4)	Dy(2)-I(2)	2.9233(3)
Si(4)-C(21)	1.861(5)	Si(4)-C(22)	1.870(4)
Si(4)-C(15)	1.884(4)	Si(4)-C(20)	1.884(5)
Si(5)-C(24)	1.835(5)	Si(5)-C(23)	1.859(4)
Si(5)-C(25)	1.878(5)	Si(5)-C(16)	1.884(4)
Si(6)-C(27)	1.869(3)	Si(6)-C(28)	1.876(4)
Si(6)-C(18)	1.881(4)	Si(6)-C(26)	1.881(4)
Si(7)-C(35)	1.860(4)	Si(7)-C(34)	1.861(4)
Si(7)-C(36)	1.865(4)	Si(7)-C(29)	1.888(4)
Si(8)-C(39)	1.854(4)	Si(8)-C(37)	1.855(4)
Si(8)-C(38)	1.869(4)	Si(8)-C(30)	1.879(4)
Si(9)-C(42)	1.855(4)	Si(9)-C(40)	1.858(4)
Si(9)-C(32)	1.869(4)	Si(9)-C(41)	1.869(4)
C(15)-C(16)	1.430(5)	C(15)-C(19)	1.430(5)
C(16)-C(17)	1.419(5)	C(17)-C(18)	1.429(5)
C(17)-H(17)	0.9500	C(18)-C(19)	1.420(5)
C(19)-H(19)	0.9500	C(20)-H(20A)	0.9800
C(20)-H(20B)	0.9800	C(20)-H(20C)	0.9800
C(21)-H(21A)	0.9800	C(21)-H(21B)	0.9800
C(21)-H(21C)	0.9800	C(22)-H(22A)	0.9800
C(22)-H(22B)	0.9800	C(22)-H(22C)	0.9800
C(23)-H(23A)	0.9800	C(23)-H(23B)	0.9800
C(23)-H(23C)	0.9800	C(24)-H(24A)	0.9800
C(24)-H(24B)	0.9800	C(24)-H(24C)	0.9800
C(25)-H(25A)	0.9800	C(25)-H(25B)	0.9800
C(25)-H(25C)	0.9800	C(26)-H(26A)	0.9800
C(26)-H(26B)	0.9800	C(26)-H(26C)	0.9800

C(27)-H(27A)	0.9800	C(27)-H(27B)	0.9800
C(27)-H(27C)	0.9800	C(28)-H(28A)	0.9800
C(28)-H(28B)	0.9800	C(28)-H(28C)	0.9800
C(29)-C(33)	1.416(5)	C(29)-C(30)	1.443(5)
C(30)-C(31)	1.418(5)	C(31)-C(32)	1.424(5)
C(31)-H(31)	0.9500	C(32)-C(33)	1.424(5)
C(33)-H(33)	0.9500	C(34)-H(34A)	0.9800
C(34)-H(34B)	0.9800	C(34)-H(34C)	0.9800
C(35)-H(35A)	0.9800	C(35)-H(35B)	0.9800
C(35)-H(35C)	0.9800	C(36)-H(36A)	0.9800
C(36)-H(36B)	0.9800	C(36)-H(36C)	0.9800
C(37)-H(37A)	0.9800	C(37)-H(37B)	0.9800
C(37)-H(37C)	0.9800	C(38)-H(38A)	0.9800
C(38)-H(38B)	0.9800	C(38)-H(38C)	0.9800
C(39)-H(39A)	0.9800	C(39)-H(39B)	0.9800
C(39)-H(39C)	0.9800	C(40)-H(40A)	0.9800
C(40)-H(40B)	0.9800	C(40)-H(40C)	0.9800
C(41)-H(41A)	0.9800	C(41)-H(41B)	0.9800
C(41)-H(41C)	0.9800	C(42)-H(42A)	0.9800
C(42)-H(42B)	0.9800	C(42)-H(42C)	0.9800
Dy(3)-C(59)	2.594(3)	Dy(3)-C(60)	2.596(3)
Dy(3)-C(45)	2.618(3)	Dy(3)-C(61)	2.627(3)
Dy(3)-C(44)	2.630(3)	Dy(3)-C(47)	2.643(4)
Dy(3)-C(58)	2.645(4)	Dy(3)-C(43)	2.647(3)
Dy(3)-C(46)	2.656(4)	Dy(3)-C(57)	2.674(3)
Dy(3)-I(3)	2.9321(4	Si(10)-C(50)	1.872(5)
Si(10)-C(48)	1.872(5)	Si(10)-C(49)	1.879(5)
Si(10)-C(43)	1.882(4)	Si(11)-C(53)	1.845(5)
Si(11)-C(51)	1.867(4)	Si(11)-C(52)	1.878(5)
Si(11)-C(44)	1.886(4)	Si(12)-C(54)	1.840(4)
Si(12)-C(55)	1.843(4)	Si(12)-C(56)	1.846(5)
Si(12)-C(46)	1.886(4)	Si(13)-C(57)	1.861(4)
Si(13)-C(62)	1.870(4)	Si(13)-C(63)	1.874(5)
Si(13)-C(64)	1.889(5)	Si(14)-C(67)	1.871(5)
Si(14)-C(65)	1.872(4)	Si(14)-C(66)	1.882(4)
Si(14)-C(58)	1.894(4)	Si(15)-C(68)	1.853(4)
Si(15)-C(70)	1.866(5)	Si(15)-C(69)	1.869(4)
Si(15)-C(60)	1.869(4)	C(43)-C(47)	1.423(5)
C(43)-C(44)	1.442(5)	C(44)-C(45)	1.420(5)
C(45)-C(46)	1.418(5)	C(45)-H(45)	0.9500
C(46)-C(47)	1.409(5)	C(47)-H(47)	0.9500
C(48)-H(48A)	0.9800	C(48)-H(48B)	0.9800
C(48)-H(48C)	0.9800	C(49)-H(49A)	0.9800
C(49)-H(49B)	0.9800	C(49)-H(49C)	0.9800
C(50)-H(50A)	0.9800	C(50)-H(50B)	0.9800
C(50)-H(50C)	0.9800	C(51)-H(51A)	0.9800
C(51)-H(51B)	0.9800	C(51)-H(51C)	0.9800
C(52)-H(52A)	0.9800	C(52)-H(52B)	0.9800
C(52)-H(52C)	0.9800	C(53)-H(53A)	0.9800
C(53)-H(53B)	0.9800	C(53)-H(53C)	0.9800
C(54)-H(54A)	0.9800	C(54)-H(54B)	0.9800
C(54)-H(54C)	0.9800	C(55)-H(55A)	0.9800
C(55)-H(55B)	0.9800	C(55)-H(55C)	0.9800
C(56)-H(56A)	0.9800	C(56)-H(56B)	0.9800
C(56)-H(56C)	0.9800	C(57)-C(61)	1.421(5)
C(57)-C(58)	1.443(6)	C(58)-C(59)	1.436(5)
C(59)-C(60)	1.421(5)	C(59)-H(59)	0.9500
C(60)-C(61)	1.408(5)	C(61)-H(61)	0.9500
C(62)-H(62A)	0.9800	C(62)-H(62B)	0.9800
C(62)-H(62C)	0.9800	C(63)-H(63A)	0.9800
C(63)-H(63B)	0.9800	C(63)-H(63C)	0.9800
C(64)-H(64A)	0.9800	C(64)-H(64B)	0.9800
C(64)-H(64C)	0.9800	C(65)-H(65A)	0.9800
C(65)-H(65B)	0.9800	C(65)-H(65C)	0.9800
C(66)-H(66A)	0.9800	C(66)-H(66B)	0.9800
C(66)-H(66C)	0.9800	C(67)-H(67A)	0.9800
C(67)-H(67B)	0.9800	C(67)-H(67C)	0.9800
C(68)-H(68A)	0.9800	C(68)-H(68B)	0.9800

C(68)-H(68C)	0.9800	C(69)-H(69A)	0.9800
C(69)-H(69B)	0.9800	C(69)-H(69C)	0.9800
C(70)-H(70A)	0.9800	C(70)-H(70B)	0.9800
C(70)-H(70C)	0.9800		

C(3)-Dy(1)-C(3)#2	93.5(2)	C(3)-Dy(1)-C(4)	31.3(1)
C(3)#2-Dy(1)-C(4)	117.8(1)	C(3)-Dy(1)-C(4)#2	117.8(1)
C(3)#2-Dy(1)-C(4)#2	31.3(1)	C(4)-Dy(1)-C(4)#2	147.1(2)
C(3)-Dy(1)-C(5)	50.6(1)	C(3)#2-Dy(1)-C(5)	144.1(1)
C(4)-Dy(1)-C(5)	31.2(1)	C(4)#2-Dy(1)-C(5)	158.1(1)
C(3)-Dy(1)-C(5)#2	144.1(1)	C(3)#2-Dy(1)-C(5)#2	50.6(1)
C(4)-Dy(1)-C(5)#2	158.1(1)	C(4)#2-Dy(1)-C(5)#2	31.2(1)
C(5)-Dy(1)-C(5)#2	165.3(2)	C(3)-Dy(1)-C(2)#2	98.2(1)
C(3)#2-Dy(1)-C(2)#2	31.4(1)	C(4)-Dy(1)-C(2)#2	108.3(1)
C(4)#2-Dy(1)-C(2)#2	52.5(1)	C(5)-Dy(1)-C(2)#2	139.3(1)
C(5)#2-Dy(1)-C(2)#2	51.3(1)	C(3)-Dy(1)-C(2)	31.4(1)
C(3)#2-Dy(1)-C(2)	98.2(1)	C(4)-Dy(1)-C(2)	52.5(1)
C(4)#2-Dy(1)-C(2)	108.3(1)	C(5)-Dy(1)-C(2)	51.3(1)
C(5)#2-Dy(1)-C(2)	139.3(1)	C(2)#2-Dy(1)-C(2)	117.4(2)
C(3)-Dy(1)-C(1)#2	128.3(1)	C(3)#2-Dy(1)-C(1)#2	51.5(1)
C(4)-Dy(1)-C(1)#2	127.7(1)	C(4)#2-Dy(1)-C(1)#2	52.2(1)
C(5)-Dy(1)-C(1)#2	149.3(1)	C(5)#2-Dy(1)-C(1)#2	30.8(1)
C(2)#2-Dy(1)-C(1)#2	31.6(1)	C(2)-Dy(1)-C(1)#2	148.2(1)
C(3)-Dy(1)-C(1)	51.5(1)	C(3)#2-Dy(1)-C(1)	128.3(1)
C(4)-Dy(1)-C(1)	52.2(1)	C(4)#2-Dy(1)-C(1)	127.7(1)
C(5)-Dy(1)-C(1)	30.8(1)	C(5)#2-Dy(1)-C(1)	149.3(1)
C(2)#2-Dy(1)-C(1)	148.2(1)	C(2)-Dy(1)-C(1)	31.6(1)
C(1)#2-Dy(1)-C(1)	179.8(2)	C(3)-Dy(1)-I(1)	133.25(7)
C(3)#2-Dy(1)-I(1)	133.25(7)	C(4)-Dy(1)-I(1)	106.44(8)
C(4)#2-Dy(1)-I(1)	106.44(8)	C(5)-Dy(1)-I(1)	82.64(8)
C(5)#2-Dy(1)-I(1)	82.64(8)	C(2)#2-Dy(1)-I(1)	121.29(8)
C(2)-Dy(1)-I(1)	121.29(8)	C(1)#2-Dy(1)-I(1)	90.10(8)
C(1)-Dy(1)-I(1)	90.10(8)	C(8)-Si(1)-C(6)	107.5(2)
C(8)-Si(1)-C(7)	107.9(2)	C(6)-Si(1)-C(7)	107.5(2)
C(8)-Si(1)-C(1)	108.1(2)	C(6)-Si(1)-C(1)	115.1(2)
C(7)-Si(1)-C(1)	110.5(2)	C(10)-Si(2)-C(11)	108.1(2)
C(10)-Si(2)-C(2)	116.2(2)	C(11)-Si(2)-C(2)	108.5(2)
C(10)-Si(2)-C(9)	110.0(2)	C(11)-Si(2)-C(9)	108.0(2)
C(2)-Si(2)-C(9)	105.8(2)	C(12)-Si(3)-C(14)	109.5(2)
C(12)-Si(3)-C(4)	108.3(2)	C(14)-Si(3)-C(4)	107.0(2)
C(12)-Si(3)-C(13)	107.2(3)	C(14)-Si(3)-C(13)	114.1(2)
C(4)-Si(3)-C(13)	110.7(2)	C(5)-C(1)-C(2)	106.4(3)
C(5)-C(1)-Si(1)	119.4(3)	C(2)-C(1)-Si(1)	133.3(3)
C(5)-C(1)-Dy(1)	73.3(2)	C(2)-C(1)-Dy(1)	73.2(2)
Si(1)-C(1)-Dy(1)	127.2(2)	C(3)-C(2)-C(1)	106.1(3)
C(3)-C(2)-Si(2)	117.7(3)	C(1)-C(2)-Si(2)	132.2(3)
C(3)-C(2)-Dy(1)	72.7(2)	C(1)-C(2)-Dy(1)	75.2(2)
Si(2)-C(2)-Dy(1)	134.2(2)	C(4)-C(3)-C(2)	111.4(3)
C(4)-C(3)-Dy(1)	75.7(2)	C(2)-C(3)-Dy(1)	76.0(2)
C(4)-C(3)-H(3)	124.3	C(2)-C(3)-H(3)	124.3
Dy(1)-C(3)-H(3)	115.7	C(3)-C(4)-C(5)	104.7(3)
C(3)-C(4)-Si(3)	127.9(3)	C(5)-C(4)-Si(3)	126.2(3)
C(3)-C(4)-Dy(1)	73.0(2)	C(5)-C(4)-Dy(1)	74.4(2)
Si(3)-C(4)-Dy(1)	127.0(2)	C(1)-C(5)-C(4)	111.4(3)
C(1)-C(5)-Dy(1)	75.9(2)	C(4)-C(5)-Dy(1)	74.4(2)
C(1)-C(5)-H(5)	124.3	C(4)-C(5)-H(5)	124.3
Dy(1)-C(5)-H(5)	117.1	Si(1)-C(6)-H(6A)	109.5
Si(1)-C(6)-H(6B)	109.5	H(6A)-C(6)-H(6B)	109.5
Si(1)-C(6)-H(6C)	109.5	H(6A)-C(6)-H(6C)	109.5
H(6B)-C(6)-H(6C)	109.5	Si(1)-C(7)-H(7A)	109.5
Si(1)-C(7)-H(7B)	109.5	H(7A)-C(7)-H(7B)	109.5
Si(1)-C(7)-H(7C)	109.5	H(7A)-C(7)-H(7C)	109.5
H(7B)-C(7)-H(7C)	109.5	Si(1)-C(8)-H(8A)	109.5
Si(1)-C(8)-H(8B)	109.5	H(8A)-C(8)-H(8B)	109.5
Si(1)-C(8)-H(8C)	109.5	H(8A)-C(8)-H(8C)	109.5
H(8B)-C(8)-H(8C)	109.5	Si(2)-C(9)-H(9A)	109.5
Si(2)-C(9)-H(9B)	109.5	H(9A)-C(9)-H(9B)	109.5
Si(2)-C(9)-H(9C)	109.5	H(9A)-C(9)-H(9C)	109.5
H(9B)-C(9)-H(9C)	109.5	Si(2)-C(10)-H(10A)	109.5

Si(2)-C(10)-H(10B)	109.5	H(10A)-C(10)-H(10B)	109.5
Si(2)-C(10)-H(10C)	109.5	H(10A)-C(10)-H(10C)	109.5
H(10B)-C(10)-H(10C)	109.5	Si(2)-C(11)-H(11A)	109.5
Si(2)-C(11)-H(11B)	109.5	H(11A)-C(11)-H(11B)	109.5
Si(2)-C(11)-H(11C)	109.5	H(11A)-C(11)-H(11C)	109.5
H(11B)-C(11)-H(11C)	109.5	Si(3)-C(12)-H(12A)	109.5
Si(3)-C(12)-H(12B)	109.5	H(12A)-C(12)-H(12B)	109.5
Si(3)-C(12)-H(12C)	109.5	H(12A)-C(12)-H(12C)	109.5
H(12B)-C(12)-H(12C)	109.5	Si(3)-C(13)-H(13A)	109.5
Si(3)-C(13)-H(13B)	109.5	H(13A)-C(13)-H(13B)	109.5
Si(3)-C(13)-H(13C)	109.5	H(13A)-C(13)-H(13C)	109.5
H(13B)-C(13)-H(13C)	109.5	Si(3)-C(14)-H(14A)	109.5
Si(3)-C(14)-H(14B)	109.5	H(14A)-C(14)-H(14B)	109.5
Si(3)-C(14)-H(14C)	109.5	H(14A)-C(14)-H(14C)	109.5
H(14B)-C(14)-H(14C)	109.5	C(31)-Dy(2)-C(32)	31.7(1)
C(31)-Dy(2)-C(17)	96.4(1)	C(32)-Dy(2)-C(17)	123.6(1)
C(31)-Dy(2)-C(16)	127.3(1)	C(32)-Dy(2)-C(16)	154.2(1)
C(17)-Dy(2)-C(16)	31.3(1)	C(31)-Dy(2)-C(33)	51.0(1)
C(32)-Dy(2)-C(33)	31.4(1)	C(17)-Dy(2)-C(33)	146.2(1)
C(16)-Dy(2)-C(33)	167.6(1)	C(31)-Dy(2)-C(15)	138.4(1)
C(32)-Dy(2)-C(15)	142.1(1)	C(17)-Dy(2)-C(15)	51.5(1)
C(16)-Dy(2)-C(15)	31.5(1)	C(33)-Dy(2)-C(15)	159.7(1)
C(31)-Dy(2)-C(30)	31.4(1)	C(32)-Dy(2)-C(30)	52.9(1)
C(17)-Dy(2)-C(30)	96.7(1)	C(16)-Dy(2)-C(30)	119.6(1)
C(33)-Dy(2)-C(30)	51.4(1)	C(15)-Dy(2)-C(30)	148.1(1)
C(31)-Dy(2)-C(19)	109.5(1)	C(32)-Dy(2)-C(19)	112.2(1)
C(17)-Dy(2)-C(19)	50.4(1)	C(16)-Dy(2)-C(19)	51.5(1)
C(33)-Dy(2)-C(19)	140.3(1)	C(15)-Dy(2)-C(19)	31.4(1)
C(30)-Dy(2)-C(19)	132.5(1)	C(31)-Dy(2)-C(29)	51.8(1)
C(32)-Dy(2)-C(29)	52.7(1)	C(17)-Dy(2)-C(29)	124.9(1)
C(16)-Dy(2)-C(29)	136.7(1)	C(33)-Dy(2)-C(29)	31.0(1)
C(15)-Dy(2)-C(29)	165.2(1)	C(30)-Dy(2)-C(29)	31.6(1)
C(19)-Dy(2)-C(29)	161.3(1)	C(31)-Dy(2)-C(18)	86.2(1)
C(32)-Dy(2)-C(18)	102.6(1)	C(17)-Dy(2)-C(18)	31.2(1)
C(16)-Dy(2)-C(18)	52.6(1)	C(33)-Dy(2)-C(18)	133.6(1)
C(15)-Dy(2)-C(18)	52.5(1)	C(30)-Dy(2)-C(18)	102.6(1)
C(19)-Dy(2)-C(18)	30.9(1)	C(29)-Dy(2)-C(18)	133.9(1)
C(31)-Dy(2)-I(2)	130.85(8)	C(32)-Dy(2)-I(2)	102.52(8)
C(17)-Dy(2)-I(2)	132.66(7)	C(16)-Dy(2)-I(2)	101.47(8)
C(33)-Dy(2)-I(2)	80.10(8)	C(15)-Dy(2)-I(2)	86.21(8)
C(30)-Dy(2)-I(2)	121.60(8)	C(19)-Dy(2)-I(2)	105.22(8)
C(29)-Dy(2)-I(2)	90.12(8)	C(18)-Dy(2)-I(2)	135.74(7)
C(21)-Si(4)-C(22)	108.9(2)	C(21)-Si(4)-C(15)	109.4(2)
C(22)-Si(4)-C(15)	116.4(2)	C(21)-Si(4)-C(20)	107.8(3)
C(22)-Si(4)-C(20)	109.7(2)	C(15)-Si(4)-C(20)	104.3(2)
C(24)-Si(5)-C(23)	109.6(3)	C(24)-Si(5)-C(25)	111.1(3)
C(23)-Si(5)-C(25)	106.9(2)	C(24)-Si(5)-C(16)	110.7(2)
C(23)-Si(5)-C(16)	110.5(2)	C(25)-Si(5)-C(16)	108.0(2)
C(27)-Si(6)-C(28)	107.6(2)	C(27)-Si(6)-C(18)	117.6(2)
C(28)-Si(6)-C(18)	107.6(2)	C(27)-Si(6)-C(26)	108.2(2)
C(28)-Si(6)-C(26)	110.7(2)	C(18)-Si(6)-C(26)	105.1(2)
C(35)-Si(7)-C(34)	107.8(2)	C(35)-Si(7)-C(36)	106.8(2)
C(34)-Si(7)-C(36)	108.9(2)	C(35)-Si(7)-C(29)	108.0(2)
C(34)-Si(7)-C(29)	114.6(2)	C(36)-Si(7)-C(29)	110.5(2)
C(39)-Si(8)-C(37)	109.2(2)	C(39)-Si(8)-C(38)	107.9(2)
C(37)-Si(8)-C(38)	110.4(2)	C(39)-Si(8)-C(30)	109.2(2)
C(37)-Si(8)-C(30)	112.5(2)	C(38)-Si(8)-C(30)	107.6(2)
C(42)-Si(9)-C(40)	109.7(2)	C(42)-Si(9)-C(32)	108.1(2)
C(40)-Si(9)-C(32)	111.1(2)	C(42)-Si(9)-C(41)	108.5(2)
C(40)-Si(9)-C(41)	108.9(2)	C(32)-Si(9)-C(41)	110.3(2)
C(16)-C(15)-C(19)	106.6(3)	C(16)-C(15)-Si(4)	133.4(3)
C(19)-C(15)-Si(4)	117.2(3)	C(16)-C(15)-Dy(2)	74.1(2)
C(19)-C(15)-Dy(2)	74.5(2)	Si(4)-C(15)-Dy(2)	131.0(2)
C(17)-C(16)-C(15)	106.6(3)	C(17)-C(16)-Si(5)	121.2(3)
C(15)-C(16)-Si(5)	131.6(3)	C(17)-C(16)-Dy(2)	73.8(2)
C(15)-C(16)-Dy(2)	74.5(2)	Si(5)-C(16)-Dy(2)	124.1(2)
C(16)-C(17)-C(18)	111.5(3)	C(16)-C(17)-Dy(2)	74.9(2)
C(18)-C(17)-Dy(2)	76.7(2)	C(16)-C(17)-H(17)	124.2

C(18)-C(17)-H(17)	124.2	Dy(2)-C(17)-H(17)	115.9
C(19)-C(18)-C(17)	104.0(3)	C(19)-C(18)-Si(6)	123.2(3)
C(17)-C(18)-Si(6)	128.0(3)	C(19)-C(18)-Dy(2)	73.2(2)
C(17)-C(18)-Dy(2)	72.1(2)	Si(6)-C(18)-Dy(2)	138.0(2)
C(18)-C(19)-C(15)	111.3(3)	C(18)-C(19)-Dy(2)	75.9(2)
C(15)-C(19)-Dy(2)	74.1(2)	C(18)-C(19)-H(19)	124.4
C(15)-C(19)-H(19)	124.4	Dy(2)-C(19)-H(19)	117.2
Si(4)-C(20)-H(20A)	109.5	Si(4)-C(20)-H(20B)	109.5
H(20A)-C(20)-H(20B)	109.5	Si(4)-C(20)-H(20C)	109.5
H(20A)-C(20)-H(20C)	109.5	H(20B)-C(20)-H(20C)	109.5
Si(4)-C(21)-H(21A)	109.5	Si(4)-C(21)-H(21B)	109.5
H(21A)-C(21)-H(21B)	109.5	Si(4)-C(21)-H(21C)	109.5
H(21A)-C(21)-H(21C)	109.5	H(21B)-C(21)-H(21C)	109.5
Si(4)-C(22)-H(22A)	109.5	Si(4)-C(22)-H(22B)	109.5
H(22A)-C(22)-H(22B)	109.5	Si(4)-C(22)-H(22C)	109.5
H(22A)-C(22)-H(22C)	109.5	H(22B)-C(22)-H(22C)	109.5
Si(5)-C(23)-H(23A)	109.5	Si(5)-C(23)-H(23B)	109.5
H(23A)-C(23)-H(23B)	109.5	Si(5)-C(23)-H(23C)	109.5
H(23A)-C(23)-H(23C)	109.5	H(23B)-C(23)-H(23C)	109.5
Si(5)-C(24)-H(24A)	109.5	Si(5)-C(24)-H(24B)	109.5
H(24A)-C(24)-H(24B)	109.5	Si(5)-C(24)-H(24C)	109.5
H(24A)-C(24)-H(24C)	109.5	H(24B)-C(24)-H(24C)	109.5
Si(5)-C(25)-H(25A)	109.5	Si(5)-C(25)-H(25B)	109.5
H(25A)-C(25)-H(25B)	109.5	Si(5)-C(25)-H(25C)	109.5
H(25A)-C(25)-H(25C)	109.5	H(25B)-C(25)-H(25C)	109.5
Si(6)-C(26)-H(26A)	109.5	Si(6)-C(26)-H(26B)	109.5
H(26A)-C(26)-H(26B)	109.5	Si(6)-C(26)-H(26C)	109.5
H(26A)-C(26)-H(26C)	109.5	H(26B)-C(26)-H(26C)	109.5
Si(6)-C(27)-H(27A)	109.5	Si(6)-C(27)-H(27B)	109.5
H(27A)-C(27)-H(27B)	109.5	Si(6)-C(27)-H(27C)	109.5
H(27A)-C(27)-H(27C)	109.5	H(27B)-C(27)-H(27C)	109.5
Si(6)-C(28)-H(28A)	109.5	Si(6)-C(28)-H(28B)	109.5
H(28A)-C(28)-H(28B)	109.5	Si(6)-C(28)-H(28C)	109.5
H(28A)-C(28)-H(28C)	109.5	H(28B)-C(28)-H(28C)	109.5
C(33)-C(29)-C(30)	106.6(3)	C(33)-C(29)-Si(7)	119.8(3)
C(30)-C(29)-Si(7)	132.8(3)	C(33)-C(29)-Dy(2)	73.6(2)
C(30)-C(29)-Dy(2)	73.5(2)	Si(7)-C(29)-Dy(2)	125.9(2)
C(31)-C(30)-C(29)	106.6(3)	C(31)-C(30)-Si(8)	121.5(3)
C(29)-C(30)-Si(8)	130.8(3)	C(31)-C(30)-Dy(2)	72.1(2)
C(29)-C(30)-Dy(2)	75.0(2)	Si(8)-C(30)-Dy(2)	127.2(2)
C(30)-C(31)-C(32)	111.1(3)	C(30)-C(31)-Dy(2)	76.4(2)
C(32)-C(31)-Dy(2)	75.3(2)	C(30)-C(31)-H(31)	124.5
C(32)-C(31)-H(31)	124.5	Dy(2)-C(31)-H(31)	115.6
C(31)-C(32)-C(33)	104.6(3)	C(31)-C(32)-Si(9)	130.8(3)
C(33)-C(32)-Si(9)	124.5(3)	C(31)-C(32)-Dy(2)	73.0(2)
C(33)-C(32)-Dy(2)	75.1(2)	Si(9)-C(32)-Dy(2)	119.4(2)
C(29)-C(33)-C(32)	111.1(3)	C(29)-C(33)-Dy(2)	75.4(2)
C(32)-C(33)-Dy(2)	73.5(2)	C(29)-C(33)-H(33)	124.4
C(32)-C(33)-H(33)	124.4	Dy(2)-C(33)-H(33)	118.3
Si(7)-C(34)-H(34A)	109.5	Si(7)-C(34)-H(34B)	109.5
H(34A)-C(34)-H(34B)	109.5	Si(7)-C(34)-H(34C)	109.5
H(34A)-C(34)-H(34C)	109.5	H(34B)-C(34)-H(34C)	109.5
Si(7)-C(35)-H(35A)	109.5	Si(7)-C(35)-H(35B)	109.5
H(35A)-C(35)-H(35B)	109.5	Si(7)-C(35)-H(35C)	109.5
H(35A)-C(35)-H(35C)	109.5	H(35B)-C(35)-H(35C)	109.5
Si(7)-C(36)-H(36A)	109.5	Si(7)-C(36)-H(36B)	109.5
H(36A)-C(36)-H(36B)	109.5	Si(7)-C(36)-H(36C)	109.5
H(36A)-C(36)-H(36C)	109.5	H(36B)-C(36)-H(36C)	109.5
Si(8)-C(37)-H(37A)	109.5	Si(8)-C(37)-H(37B)	109.5
H(37A)-C(37)-H(37B)	109.5	Si(8)-C(37)-H(37C)	109.5
H(37A)-C(37)-H(37C)	109.5	H(37B)-C(37)-H(37C)	109.5
Si(8)-C(38)-H(38A)	109.5	Si(8)-C(38)-H(38B)	109.5
H(38A)-C(38)-H(38B)	109.5	Si(8)-C(38)-H(38C)	109.5
H(38A)-C(38)-H(38C)	109.5	H(38B)-C(38)-H(38C)	109.5
Si(8)-C(39)-H(39A)	109.5	Si(8)-C(39)-H(39B)	109.5
H(39A)-C(39)-H(39B)	109.5	Si(8)-C(39)-H(39C)	109.5
H(39A)-C(39)-H(39C)	109.5	H(39B)-C(39)-H(39C)	109.5
Si(9)-C(40)-H(40A)	109.5	Si(9)-C(40)-H(40B)	109.5
H(40A)-C(40)-H(40B)	109.5	Si(9)-C(40)-H(40C)	109.5
H(40A)-C(40)-H(40C)	109.5	H(40B)-C(40)-H(40C)	109.5

Si(9)-C(41)-H(41A)	109.5	Si(9)-C(41)-H(41B)	109.5
H(41A)-C(41)-H(41B)	109.5	Si(9)-C(41)-H(41C)	109.5
H(41A)-C(41)-H(41C)	109.5	H(41B)-C(41)-H(41C)	109.5
Si(9)-C(42)-H(42A)	109.5	Si(9)-C(42)-H(42B)	109.5
H(42A)-C(42)-H(42B)	109.5	Si(9)-C(42)-H(42C)	109.5
H(42A)-C(42)-H(42C)	109.5	H(42B)-C(42)-H(42C)	109.5
C(59)-Dy(3)-C(60)	31.8(1)	C(59)-Dy(3)-C(45)	97.5(1)
C(60)-Dy(3)-C(45)	126.3(1)	C(59)-Dy(3)-C(61)	51.3(1)
C(60)-Dy(3)-C(61)	31.3(1)	C(45)-Dy(3)-C(61)	145.8(1)
C(59)-Dy(3)-C(44)	128.7(1)	C(60)-Dy(3)-C(44)	157.1(1)
C(45)-Dy(3)-C(44)	31.4(1)	C(61)-Dy(3)-C(44)	164.7(1)
C(59)-Dy(3)-C(47)	108.4(1)	C(60)-Dy(3)-C(47)	114.3(1)
C(45)-Dy(3)-C(47)	50.5(1)	C(61)-Dy(3)-C(47)	143.3(1)
C(44)-Dy(3)-C(47)	51.4(1)	C(59)-Dy(3)-C(58)	31.8(1)
C(60)-Dy(3)-C(58)	52.9(1)	C(45)-Dy(3)-C(58)	94.9(1)
C(61)-Dy(3)-C(58)	51.5(1)	C(44)-Dy(3)-C(58)	118.8(1)
C(47)-Dy(3)-C(58)	129.7(1)	C(59)-Dy(3)-C(43)	137.9(1)
C(60)-Dy(3)-C(43)	143.4(1)	C(45)-Dy(3)-C(43)	51.8(1)
C(61)-Dy(3)-C(43)	161.2(1)	C(44)-Dy(3)-C(43)	31.7(1)
C(47)-Dy(3)-C(43)	31.2(1)	C(58)-Dy(3)-C(43)	146.6(1)
C(59)-Dy(3)-C(46)	86.1(1)	C(60)-Dy(3)-C(46)	105.6(1)
C(45)-Dy(3)-C(46)	31.2(1)	C(61)-Dy(3)-C(46)	135.6(1)
C(44)-Dy(3)-C(46)	52.4(1)	C(47)-Dy(3)-C(46)	30.9(1)
C(58)-Dy(3)-C(46)	100.1(1)	C(43)-Dy(3)-C(46)	52.4(1)
C(59)-Dy(3)-C(57)	52.1(1)	C(60)-Dy(3)-C(57)	52.5(1)
C(45)-Dy(3)-C(57)	121.5(1)	C(61)-Dy(3)-C(57)	31.1(1)
C(44)-Dy(3)-C(57)	134.1(1)	C(47)-Dy(3)-C(57)	160.0(1)
C(58)-Dy(3)-C(57)	31.5(1)	C(43)-Dy(3)-C(57)	164.0(1)
C(46)-Dy(3)-C(57)	131.6(1)	C(59)-Dy(3)-I(3)	130.8(1)
C(60)-Dy(3)-I(3)	101.2(1)	C(45)-Dy(3)-I(3)	131.65(7)
C(61)-Dy(3)-I(3)	80.4(1)	C(44)-Dy(3)-I(3)	100.29(8)
C(47)-Dy(3)-I(3)	105.85(8)	C(58)-Dy(3)-I(3)	123.8(1)
C(43)-Dy(3)-I(3)	85.88(8)	C(46)-Dy(3)-I(3)	136.07(7)
C(57)-Dy(3)-I(3)	92.4(1)	C(50)-Si(10)-C(48)	108.9(3)
C(50)-Si(10)-C(49)	108.1(3)	C(48)-Si(10)-C(49)	107.0(3)
C(50)-Si(10)-C(43)	117.3(2)	C(48)-Si(10)-C(43)	105.4(2)
C(49)-Si(10)-C(43)	109.7(2)	C(53)-Si(11)-C(51)	107.8(2)
C(53)-Si(11)-C(52)	108.5(3)	C(51)-Si(11)-C(52)	110.3(2)
C(53)-Si(11)-C(44)	107.9(2)	C(51)-Si(11)-C(44)	108.7(2)
C(52)-Si(11)-C(44)	113.4(2)	C(54)-Si(12)-C(55)	105.9(2)
C(54)-Si(12)-C(56)	109.2(3)	C(55)-Si(12)-C(56)	109.2(2)
C(54)-Si(12)-C(46)	105.5(2)	C(55)-Si(12)-C(46)	118.5(2)
C(56)-Si(12)-C(46)	108.1(2)	C(57)-Si(13)-C(62)	110.5(2)
C(57)-Si(13)-C(63)	107.8(2)	C(62)-Si(13)-C(63)	108.2(2)
C(57)-Si(13)-C(64)	110.2(2)	C(62)-Si(13)-C(64)	111.5(2)
C(63)-Si(13)-C(64)	108.6(2)	C(67)-Si(14)-C(65)	108.2(2)
C(67)-Si(14)-C(66)	108.8(2)	C(65)-Si(14)-C(66)	108.5(2)
C(67)-Si(14)-C(58)	109.6(2)	C(65)-Si(14)-C(58)	113.8(2)
C(66)-Si(14)-C(58)	107.9(2)	C(68)-Si(15)-C(70)	110.1(2)
C(68)-Si(15)-C(69)	110.3(2)	C(70)-Si(15)-C(69)	108.8(2)
C(68)-Si(15)-C(60)	111.8(2)	C(70)-Si(15)-C(60)	106.7(2)
C(69)-Si(15)-C(60)	109.1(2)	C(47)-C(43)-C(44)	106.0(3)
C(47)-C(43)-Si(10)	116.5(3)	C(44)-C(43)-Si(10)	134.7(3)
C(47)-C(43)-Dy(3)	74.2(2)	C(44)-C(43)-Dy(3)	73.5(2)
Si(10)-C(43)-Dy(3)	131.4(2)	C(45)-C(44)-C(43)	106.8(3)
C(45)-C(44)-Si(11)	122.5(3)	C(43)-C(44)-Si(11)	129.5(3)
C(45)-C(44)-Dy(3)	73.8(2)	C(43)-C(44)-Dy(3)	74.8(2)
Si(11)-C(44)-Dy(3)	126.3(2)	C(46)-C(45)-C(44)	110.7(3)
C(46)-C(45)-Dy(3)	75.9(2)	C(44)-C(45)-Dy(3)	74.8(2)
C(46)-C(45)-H(45)	124.6	C(44)-C(45)-H(45)	124.6
Dy(3)-C(45)-H(45)	116.5	C(47)-C(46)-C(45)	105.1(3)
C(47)-C(46)-Si(12)	121.0(3)	C(45)-C(46)-Si(12)	128.6(3)
C(47)-C(46)-Dy(3)	74.1(2)	C(45)-C(46)-Dy(3)	72.9(2)
Si(12)-C(46)-Dy(3)	137.8(2)	C(46)-C(47)-C(43)	111.4(3)
C(46)-C(47)-Dy(3)	75.1(2)	C(43)-C(47)-Dy(3)	74.6(2)
C(46)-C(47)-H(47)	124.3	C(43)-C(47)-H(47)	124.3
Dy(3)-C(47)-H(47)	117.7	Si(10)-C(48)-H(48A)	109.5
Si(10)-C(48)-H(48B)	109.5	H(48A)-C(48)-H(48B)	109.5

Si(10)-C(48)-H(48C)	109.5	H(48A)-C(48)-H(48C)	109.5
H(48B)-C(48)-H(48C)	109.5	Si(10)-C(49)-H(49A)	109.5
Si(10)-C(49)-H(49B)	109.5	H(49A)-C(49)-H(49B)	109.5
Si(10)-C(49)-H(49C)	109.5	H(49A)-C(49)-H(49C)	109.5
H(49B)-C(49)-H(49C)	109.5	Si(10)-C(50)-H(50A)	109.5
Si(10)-C(50)-H(50B)	109.5	H(50A)-C(50)-H(50B)	109.5
Si(10)-C(50)-H(50C)	109.5	H(50A)-C(50)-H(50C)	109.5
H(50B)-C(50)-H(50C)	109.5	Si(11)-C(51)-H(51A)	109.5
Si(11)-C(51)-H(51B)	109.5	H(51A)-C(51)-H(51B)	109.5
Si(11)-C(51)-H(51C)	109.5	H(51A)-C(51)-H(51C)	109.5
H(51B)-C(51)-H(51C)	109.5	Si(11)-C(52)-H(52A)	109.5
Si(11)-C(52)-H(52B)	109.5	H(52A)-C(52)-H(52B)	109.5
Si(11)-C(52)-H(52C)	109.5	H(52A)-C(52)-H(52C)	109.5
H(52B)-C(52)-H(52C)	109.5	Si(11)-C(53)-H(53A)	109.5
Si(11)-C(53)-H(53B)	109.5	H(53A)-C(53)-H(53B)	109.5
Si(11)-C(53)-H(53C)	109.5	H(53A)-C(53)-H(53C)	109.5
H(53B)-C(53)-H(53C)	109.5	Si(12)-C(54)-H(54A)	109.5
Si(12)-C(54)-H(54B)	109.5	H(54A)-C(54)-H(54B)	109.5
Si(12)-C(54)-H(54C)	109.5	H(54A)-C(54)-H(54C)	109.5
H(54B)-C(54)-H(54C)	109.5	Si(12)-C(55)-H(55A)	109.5
Si(12)-C(55)-H(55B)	109.5	H(55A)-C(55)-H(55B)	109.5
Si(12)-C(55)-H(55C)	109.5	H(55A)-C(55)-H(55C)	109.5
H(55B)-C(55)-H(55C)	109.5	Si(12)-C(56)-H(56A)	109.5
Si(12)-C(56)-H(56B)	109.5	H(56A)-C(56)-H(56B)	109.5
Si(12)-C(56)-H(56C)	109.5	H(56A)-C(56)-H(56C)	109.5
H(56B)-C(56)-H(56C)	109.5	C(61)-C(57)-C(58)	106.3(3)
C(61)-C(57)-Si(13)	121.6(3)	C(58)-C(57)-Si(13)	132.0(3)
C(61)-C(57)-Dy(3)	72.6(2)	C(58)-C(57)-Dy(3)	73.1(2)
Si(13)-C(57)-Dy(3)	122.6(2)	C(59)-C(58)-C(57)	107.0(3)
C(59)-C(58)-Si(14)	120.2(3)	C(57)-C(58)-Si(14)	130.7(3)
C(59)-C(58)-Dy(3)	72.2(2)	C(57)-C(58)-Dy(3)	75.4(2)
Si(14)-C(58)-Dy(3)	130.4(2)	C(60)-C(59)-C(58)	109.6(3)
C(60)-C(59)-Dy(3)	74.2(2)	C(58)-C(59)-Dy(3)	76.0(2)
C(60)-C(59)-H(59)	125.2	C(58)-C(59)-H(59)	125.2
Dy(3)-C(59)-H(59)	116.5	C(61)-C(60)-C(59)	106.0(3)
C(61)-C(60)-Si(15)	124.2(3)	C(59)-C(60)-Si(15)	129.8(3)
C(61)-C(60)-Dy(3)	75.6(2)	C(59)-C(60)-Dy(3)	74.0(2)
Si(15)-C(60)-Dy(3)	115.0(2)	C(60)-C(61)-C(57)	111.1(4)
C(60)-C(61)-Dy(3)	73.2(2)	C(57)-C(61)-Dy(3)	76.3(2)
C(60)-C(61)-H(61)	124.4	C(57)-C(61)-H(61)	124.4
Dy(3)-C(61)-H(61)	117.7	Si(13)-C(62)-H(62A)	109.5
Si(13)-C(62)-H(62B)	109.5	H(62A)-C(62)-H(62B)	109.5
Si(13)-C(62)-H(62C)	109.5	H(62A)-C(62)-H(62C)	109.5
H(62B)-C(62)-H(62C)	109.5	Si(13)-C(63)-H(63A)	109.5
Si(13)-C(63)-H(63B)	109.5	H(63A)-C(63)-H(63B)	109.5
Si(13)-C(63)-H(63C)	109.5	H(63A)-C(63)-H(63C)	109.5
H(63B)-C(63)-H(63C)	109.5	Si(13)-C(64)-H(64A)	109.5
Si(13)-C(64)-H(64B)	109.5	H(64A)-C(64)-H(64B)	109.5
Si(13)-C(64)-H(64C)	109.5	H(64A)-C(64)-H(64C)	109.5
H(64B)-C(64)-H(64C)	109.5	Si(14)-C(65)-H(65A)	109.5
Si(14)-C(65)-H(65B)	109.5	H(65A)-C(65)-H(65B)	109.5
Si(14)-C(65)-H(65C)	109.5	H(65A)-C(65)-H(65C)	109.5
H(65B)-C(65)-H(65C)	109.5	Si(14)-C(66)-H(66A)	109.5
Si(14)-C(66)-H(66B)	109.5	H(66A)-C(66)-H(66B)	109.5
Si(14)-C(66)-H(66C)	109.5	H(66A)-C(66)-H(66C)	109.5
H(66B)-C(66)-H(66C)	109.5	Si(14)-C(67)-H(67A)	109.5
Si(14)-C(67)-H(67B)	109.5	H(67A)-C(67)-H(67B)	109.5
Si(14)-C(67)-H(67C)	109.5	H(67A)-C(67)-H(67C)	109.5
H(67B)-C(67)-H(67C)	109.5	Si(15)-C(68)-H(68A)	109.5
Si(15)-C(68)-H(68B)	109.5	H(68A)-C(68)-H(68B)	109.5
Si(15)-C(68)-H(68C)	109.5	H(68A)-C(68)-H(68C)	109.5
H(68B)-C(68)-H(68C)	109.5	Si(15)-C(69)-H(69A)	109.5
Si(15)-C(69)-H(69B)	109.5	H(69A)-C(69)-H(69B)	109.5
Si(15)-C(69)-H(69C)	109.5	H(69A)-C(69)-H(69C)	109.5
H(69B)-C(69)-H(69C)	109.5	Si(15)-C(70)-H(70A)	109.5
Si(15)-C(70)-H(70B)	109.5	H(70A)-C(70)-H(70B)	109.5
Si(15)-C(70)-H(70C)	109.5	H(70A)-C(70)-H(70C)	109.5
H(70B)-C(70)-H(70C)	109.5		

```
Estimated standard deviations are given in the parenthesis.
Symmetry operators ::
   1: x, y, z              2: -x, y, -z+1/2        3: x+1/2, y+1/2, z
   4: -x+1/2, y+1/2, -z+1/ 5: -x, -y, -z           6: x, -y, z-1/2
   7: -x+1/2, -y+1/2, -z   8: x+1/2, -y+1/2, z-1/2
```

[(Dtp)$_2$DyI] (34)

Compound	dydiphosi
Molecular formula	$C_{28}H_{48}DyIP_2$
Molecular weight	736.00
Crystal habit	pale yellow block
Crystal dimensions(mm)	0.22x0.20x0.20
Crystal system	monoclinic
Space group	$P2_1/c$
a(Å)	10.8260(10)
b(Å)	17.0250(10)
c(Å)	16.4470(10)
α(°)	90.00
β(°)	91.8290(10)
γ(°)	90.00
V(Å^3)	3029.8(4)
Z	4
d(g-cm^{-3})	1.614
F(000)	1460
μ(cm^{-1})	3.604
Absorption corrections	multi-scan ; 0.5044 min, 0.5326 max
Diffractometer	KappaCCD
X-ray source	MoKα
λ(Å)	0.71069
Monochromator	graphite
T (K)	150.0(1)
Scan mode	phi and omega scans
Maximum θ	30.03
HKL ranges	-15 15 ; -23 20 ; -23 23
Reflections measured	13982
Unique data	8824
Rint	0.0182
Reflections used	7458
Criterion	I > 2σI)
Refinement type	Fsqd
Hydrogen atoms	mixed
Parameters refined	306
Reflections / parameter	24
wR2	0.0747
R1	0.0278
Weights a, b	0.0401 ; 0.0000
GoF	1.060
difference peak / hole (e Å^{-3})	1.619(0.110) / -1.135(0.110)

Table. Bond lengths (A) and angles (deg) for dydiphosi

Dy(1)-C(18)	2.702(2)	Dy(1)-C(3)	2.703(2)
Dy(1)-C(4)	2.706(2)	Dy(1)-C(17)	2.715(2)
Dy(1)-C(2)	2.747(2)	Dy(1)-C(16)	2.748(2)
Dy(1)-C(15)	2.766(2)	Dy(1)-C(1)	2.778(2)
Dy(1)-P(2)	2.8440(6	Dy(1)-P(1)	2.8528(6)
Dy(1)-I(1)	2.9235(2	P(1)-C(1)	1.773(2)
P(1)-C(4)	1.780(2)	P(2)-C(15)	1.773(2)
P(2)-C(18)	1.786(2)	C(1)-C(2)	1.415(3)
C(1)-C(5)	1.541(3)	C(2)-C(3)	1.438(3)
C(2)-C(9)	1.505(3)	C(3)-C(4)	1.405(3)
C(3)-C(10)	1.518(3)	C(4)-C(11)	1.542(3)
C(5)-C(7)	1.533(4)	C(5)-C(8)	1.535(3)
C(5)-C(6)	1.538(4)	C(11)-C(12)	1.531(4)
C(11)-C(13)	1.532(4)	C(11)-C(14)	1.545(3)
C(15)-C(16)	1.404(3)	C(15)-C(19)	1.535(3)
C(16)-C(17)	1.442(3)	C(16)-C(23)	1.515(3)
C(17)-C(18)	1.402(3)	C(17)-C(24)	1.513(3)
C(18)-C(25)	1.535(3)	C(19)-C(21)	1.533(4)
C(19)-C(20)	1.533(4)	C(19)-C(22)	1.548(4)
C(25)-C(28)	1.520(3)	C(25)-C(27)	1.534(3)
C(25)-C(26)	1.543(3)		

C(18)-Dy(1)-C(3)	142.81(7)	C(18)-Dy(1)-C(4)	112.70(7)
C(3)-Dy(1)-C(4)	30.11(7)	C(18)-Dy(1)-C(17)	29.99(7)
C(3)-Dy(1)-C(17)	172.72(7)	C(4)-Dy(1)-C(17)	142.65(7)
C(18)-Dy(1)-C(2)	146.31(7)	C(3)-Dy(1)-C(2)	30.58(7)
C(4)-Dy(1)-C(2)	51.64(7)	C(17)-Dy(1)-C(2)	153.14(7)
C(18)-Dy(1)-C(16)	51.70(7)	C(3)-Dy(1)-C(16)	151.14(7)
C(4)-Dy(1)-C(16)	145.02(7)	C(17)-Dy(1)-C(16)	30.61(7)
C(2)-Dy(1)-C(16)	158.59(7)	C(18)-Dy(1)-C(15)	55.41(7)
C(3)-Dy(1)-C(15)	126.73(7)	C(4)-Dy(1)-C(15)	115.88(7)
C(17)-Dy(1)-C(15)	51.26(7)	C(2)-Dy(1)-C(15)	154.64(7)
C(16)-Dy(1)-C(15)	29.50(7)	C(18)-Dy(1)-C(1)	117.09(7)
C(3)-Dy(1)-C(1)	51.36(7)	C(4)-Dy(1)-C(1)	55.24(7)
C(17)-Dy(1)-C(1)	128.62(7)	C(2)-Dy(1)-C(1)	29.67(7)
C(16)-Dy(1)-C(1)	156.59(7)	C(15)-Dy(1)-C(1)	167.23(7)
C(18)-Dy(1)-P(2)	37.46(5)	C(3)-Dy(1)-P(2)	117.14(5)
C(4)-Dy(1)-P(2)	91.95(5)	C(17)-Dy(1)-P(2)	56.56(5)
C(2)-Dy(1)-P(2)	143.50(5)	C(16)-Dy(1)-P(2)	56.22(5)
C(15)-Dy(1)-P(2)	36.82(5)	C(1)-Dy(1)-P(2)	130.59(5)
C(18)-Dy(1)-P(1)	92.85(5)	C(3)-Dy(1)-P(1)	56.57(5)
C(4)-Dy(1)-P(1)	37.24(5)	C(17)-Dy(1)-P(1)	118.35(5)
C(2)-Dy(1)-P(1)	56.20(5)	C(16)-Dy(1)-P(1)	144.34(5)
C(15)-Dy(1)-P(1)	130.56(5)	C(1)-Dy(1)-P(1)	36.68(5)
P(2)-Dy(1)-P(1)	94.39(2)	C(18)-Dy(1)-I(1)	120.31(5)
C(3)-Dy(1)-I(1)	96.76(5)	C(4)-Dy(1)-I(1)	126.79(5)
C(17)-Dy(1)-I(1)	90.51(5)	C(2)-Dy(1)-I(1)	80.02(5)
C(16)-Dy(1)-I(1)	78.80(5)	C(15)-Dy(1)-I(1)	98.10(5)
C(1)-Dy(1)-I(1)	94.66(5)	P(2)-Dy(1)-I(1)	133.87(1)
P(1)-Dy(1)-I(1)	131.33(1)	C(1)-P(1)-C(4)	91.4(1)
C(1)-P(1)-Dy(1)	69.37(7)	C(4)-P(1)-Dy(1)	66.90(7)
C(15)-P(2)-C(18)	91.2(1)	C(15)-P(2)-Dy(1)	69.19(8)
C(18)-P(2)-Dy(1)	66.95(7)	C(2)-C(1)-C(5)	126.7(2)
C(2)-C(1)-P(1)	111.3(2)	C(5)-C(1)-P(1)	121.5(2)
C(2)-C(1)-Dy(1)	73.9(1)	C(5)-C(1)-Dy(1)	126.0(1)
P(1)-C(1)-Dy(1)	73.95(8)	C(1)-C(2)-C(3)	112.8(2)
C(1)-C(2)-C(9)	126.2(2)	C(3)-C(2)-C(9)	120.4(2)
C(1)-C(2)-Dy(1)	76.4(1)	C(3)-C(2)-Dy(1)	73.0(1)
C(9)-C(2)-Dy(1)	125.5(2)	C(4)-C(3)-C(2)	113.3(2)
C(4)-C(3)-C(10)	127.2(2)	C(2)-C(3)-C(10)	119.2(2)
C(4)-C(3)-Dy(1)	75.1(1)	C(2)-C(3)-Dy(1)	76.4(1)
C(10)-C(3)-Dy(1)	120.6(2)	C(3)-C(4)-C(11)	126.6(2)
C(3)-C(4)-P(1)	111.2(2)	C(11)-C(4)-P(1)	120.3(2)
C(3)-C(4)-Dy(1)	74.8(1)	C(11)-C(4)-Dy(1)	129.2(2)
P(1)-C(4)-Dy(1)	75.86(7)	C(7)-C(5)-C(8)	105.9(2)

C(7)-C(5)-C(6)	107.6(2)	C(8)-C(5)-C(6)	110.5(2)
C(7)-C(5)-C(1)	111.0(2)	C(8)-C(5)-C(1)	109.5(2)
C(6)-C(5)-C(1)	112.2(2)	C(12)-C(11)-C(13)	106.5(2)
C(12)-C(11)-C(4)	114.5(2)	C(13)-C(11)-C(4)	110.6(2)
C(12)-C(11)-C(14)	110.0(2)	C(13)-C(11)-C(14)	108.4(2)
C(4)-C(11)-C(14)	106.8(2)	C(16)-C(15)-C(19)	126.6(2)
C(16)-C(15)-P(2)	111.6(2)	C(19)-C(15)-P(2)	121.7(2)
C(16)-C(15)-Dy(1)	74.6(1)	C(19)-C(15)-Dy(1)	120.8(2)
P(2)-C(15)-Dy(1)	74.00(8)	C(15)-C(16)-C(17)	112.8(2)
C(15)-C(16)-C(23)	125.9(2)	C(17)-C(16)-C(23)	120.8(2)
C(15)-C(16)-Dy(1)	75.9(1)	C(17)-C(16)-Dy(1)	73.4(1)
C(23)-C(16)-Dy(1)	125.3(2)	C(18)-C(17)-C(16)	113.4(2)
C(18)-C(17)-C(24)	126.4(2)	C(16)-C(17)-C(24)	120.0(2)
C(18)-C(17)-Dy(1)	74.5(1)	C(16)-C(17)-Dy(1)	76.0(1)
C(24)-C(17)-Dy(1)	121.1(2)	C(17)-C(18)-C(25)	126.9(2)
C(17)-C(18)-P(2)	111.0(2)	C(25)-C(18)-P(2)	120.7(2)
C(17)-C(18)-Dy(1)	75.5(1)	C(25)-C(18)-Dy(1)	127.1(2)
P(2)-C(18)-Dy(1)	75.59(8)	C(21)-C(19)-C(20)	108.5(2)
C(21)-C(19)-C(15)	110.7(2)	C(20)-C(19)-C(15)	110.2(2)
C(21)-C(19)-C(22)	105.8(2)	C(20)-C(19)-C(22)	110.3(3)
C(15)-C(19)-C(22)	111.3(2)	C(28)-C(25)-C(27)	107.5(2)
C(28)-C(25)-C(18)	111.6(2)	C(27)-C(25)-C(18)	113.7(2)
C(28)-C(25)-C(26)	108.1(2)	C(27)-C(25)-C(26)	109.3(2)
C(18)-C(25)-C(26)	106.5(2)		

[{(Dsp)$_2$DyI}$_2$] (35)

Compound	dy2i2dsp4
Molecular formula	$C_{48}H_{96}Dy_2I_2P_4Si_8$
Molecular weight	1600.65
Crystal habit	Yellow Block
Crystal dimensions(mm)	0.12x0.10x0.10
Crystal system	triclinic
Space group	Pbar1
a(Å)	11.7130(10)
b(Å)	11.7720(10)
c(Å)	26.9880(10)
α(°)	78.9660(10)
β(°)	79.8550(10)
γ(°)	70.6780(10)
V(Å^3)	3421.1(4)
Z	2
d(g-cm^{-3})	1.554
F(000)	1588
μ(cm^{-1})	3.332
Absorption corrections	multi-scan ; 0.6906 min, 0.7317 max
Diffractometer	KappaCCD
X-ray source	MoKα
λ(Å)	0.71069
Monochromator	graphite
T (K)	150.0(1)
Scan mode	phi and omega scans
Maximum θ	30.03
HKL ranges	-16 16 ; -16 15 ; -36 38
Reflections measured	32162

Unique data	19986
Rint	0.0241
Reflections used	15182
Criterion	I > 2σI)
Refinement type	Fsqd
Hydrogen atoms	mixed
Parameters refined	609
Reflections / parameter	24
wR2	0.0637
R1	0.0315
Weights a, b	0.0210 ; 0.0000
GoF	1.005
difference peak / hole (e Å^{-3})	1.515(0.121) / -1.024(0.121)

Table. Bond lengths (A) and angles (deg) for dy2i2dsp4

Dy(1)-C(4)	2.742(3)	Dy(1)-C(1)	2.745(3)
Dy(1)-C(13)	2.746(3)	Dy(1)-C(3)	2.766(3)
Dy(1)-C(16)	2.773(3)	Dy(1)-C(2)	2.789(3)
Dy(1)-C(14)	2.792(3)	Dy(1)-C(15)	2.795(3)
Dy(1)-P(1)	2.8576(8	Dy(1)-P(2)	2.8690(7)
Dy(1)-I(1)	3.1490(2	Dy(1)-I(1)#2	3.1534(3)
I(1)-Dy(1)#2	3.1535(3	P(1)-C(4)	1.774(3)
P(1)-C(1)	1.775(3)	P(2)-C(16)	1.771(3)
P(2)-C(13)	1.783(3)	Si(1)-C(12)	1.856(3)
Si(1)-C(11)	1.860(3)	Si(1)-C(10)	1.870(3)
Si(1)-C(1)	1.882(3)	Si(2)-C(6)	1.849(3)
Si(2)-C(5)	1.853(3)	Si(2)-C(7)	1.866(4)
Si(2)-C(4)	1.881(3)	Si(3)-C(24)	1.858(3)
Si(3)-C(22)	1.863(3)	Si(3)-C(23)	1.873(3)
Si(3)-C(13)	1.881(3)	Si(4)-C(17)	1.860(3)
Si(4)-C(19)	1.865(3)	Si(4)-C(18)	1.871(3)
Si(4)-C(16)	1.879(3)	C(1)-C(2)	1.413(4)
C(2)-C(3)	1.428(4)	C(2)-C(9)	1.509(4)
C(3)-C(4)	1.413(4)	C(3)-C(8)	1.507(4)
C(5)-H(5A)	0.9800	C(5)-H(5B)	0.9800
C(5)-H(5C)	0.9800	C(6)-H(6A)	0.9800
C(6)-H(6B)	0.9800	C(6)-H(6C)	0.9800
C(7)-H(7A)	0.9800	C(7)-H(7B)	0.9800
C(7)-H(7C)	0.9800	C(8)-H(8A)	0.9800
C(8)-H(8B)	0.9800	C(8)-H(8C)	0.9800
C(9)-H(9A)	0.9800	C(9)-H(9B)	0.9800
C(9)-H(9C)	0.9800	C(10)-H(10A)	0.9800
C(10)-H(10B)	0.9800	C(10)-H(10C)	0.9800
C(11)-H(11A)	0.9800	C(11)-H(11B)	0.9800
C(11)-H(11C)	0.9800	C(12)-H(12A)	0.9800
C(12)-H(12B)	0.9800	C(12)-H(12C)	0.9800
C(13)-C(14)	1.407(4)	C(14)-C(15)	1.402(4)
C(14)-C(21)	1.503(4)	C(15)-C(16)	1.415(4)
C(15)-C(20)	1.514(4)	C(17)-H(17A)	0.9800
C(17)-H(17B)	0.9800	C(17)-H(17C)	0.9800
C(18)-H(18A)	0.9800	C(18)-H(18B)	0.9800
C(18)-H(18C)	0.9800	C(19)-H(19A)	0.9800
C(19)-H(19B)	0.9800	C(19)-H(19C)	0.9800
C(20)-H(20A)	0.9800	C(20)-H(20B)	0.9800
C(20)-H(20C)	0.9800	C(21)-H(21A)	0.9800
C(21)-H(21B)	0.9800	C(21)-H(21C)	0.9800
C(22)-H(22A)	0.9800	C(22)-H(22B)	0.9800
C(22)-H(22C)	0.9800	C(23)-H(23A)	0.9800
C(23)-H(23B)	0.9800	C(23)-H(23C)	0.9800
C(24)-H(24A)	0.9800	C(24)-H(24B)	0.9800
C(24)-H(24C)	0.9800	Dy(2)-C(25)	2.734(3)
Dy(2)-C(40)	2.739(3)	Dy(2)-C(37)	2.756(2)
Dy(2)-C(38)	2.784(2)	Dy(2)-C(39)	2.785(3)

Dy(2)-C(26)	2.787(3)	Dy(2)-C(28)	2.789(3)
Dy(2)-C(27)	2.812(3)	Dy(2)-P(4)	2.8500(7)
Dy(2)-P(3)	2.8595(7	Dy(2)-I(2)	3.1473(2)
Dy(2)-I(2)#2	3.1585(3	I(2)-Dy(2)#2	3.1585(3)
P(3)-C(28)	1.772(3)	P(3)-C(25)	1.775(3)
P(4)-C(40)	1.772(3)	P(4)-C(37)	1.776(3)
Si(5)-C(36)	1.863(4)	Si(5)-C(34)	1.867(3)
Si(5)-C(35)	1.870(3)	Si(5)-C(25)	1.874(3)
Si(6)-C(29)	1.862(3)	Si(6)-C(30)	1.872(4)
Si(6)-C(31)	1.873(3)	Si(6)-C(28)	1.878(3)
Si(7)-C(47)	1.855(3)	Si(7)-C(48)	1.864(3)
Si(7)-C(46)	1.871(3)	Si(7)-C(37)	1.878(3)
Si(8)-C(42)	1.857(3)	Si(8)-C(43)	1.861(3)
Si(8)-C(41)	1.867(3)	Si(8)-C(40)	1.881(3)
C(25)-C(26)	1.419(4)	C(26)-C(27)	1.399(4)
C(26)-C(33)	1.509(4)	C(27)-C(28)	1.409(4)
C(27)-C(32)	1.512(4)	C(29)-H(29A)	0.9800
C(29)-H(29B)	0.9800	C(29)-H(29C)	0.9800
C(30)-H(30A)	0.9800	C(30)-H(30B)	0.9800
C(30)-H(30C)	0.9800	C(31)-H(31A)	0.9800
C(31)-H(31B)	0.9800	C(31)-H(31C)	0.9800
C(32)-H(32A)	0.9800	C(32)-H(32B)	0.9800
C(32)-H(32C)	0.9800	C(33)-H(33A)	0.9800
C(33)-H(33B)	0.9800	C(33)-H(33C)	0.9800
C(34)-H(34A)	0.9800	C(34)-H(34B)	0.9800
C(34)-H(34C)	0.9800	C(35)-H(35A)	0.9800
C(35)-H(35B)	0.9800	C(35)-H(35C)	0.9800
C(36)-H(36A)	0.9800	C(36)-H(36B)	0.9800
C(36)-H(36C)	0.9800	C(37)-C(38)	1.411(4)
C(38)-C(39)	1.418(4)	C(38)-C(45)	1.517(4)
C(39)-C(40)	1.413(4)	C(39)-C(44)	1.513(4)
C(41)-H(41A)	0.9800	C(41)-H(41B)	0.9800
C(41)-H(41C)	0.9800	C(42)-H(42A)	0.9800
C(42)-H(42B)	0.9800	C(42)-H(42C)	0.9800
C(43)-H(43A)	0.9800	C(43)-H(43B)	0.9800
C(43)-H(43C)	0.9800	C(44)-H(44A)	0.9800
C(44)-H(44B)	0.9800	C(44)-H(44C)	0.9800
C(45)-H(45A)	0.9800	C(45)-H(45B)	0.9800
C(45)-H(45C)	0.9800	C(46)-H(46A)	0.9800
C(46)-H(46B)	0.9800	C(46)-H(46C)	0.9800
C(47)-H(47A)	0.9800	C(47)-H(47B)	0.9800
C(47)-H(47C)	0.9800	C(48)-H(48A)	0.9800
C(48)-H(48B)	0.9800	C(48)-H(48C)	0.9800

C(4)-Dy(1)-C(1)	55.27(8)	C(4)-Dy(1)-C(13)	137.43(8)
C(1)-Dy(1)-C(13)	106.59(8)	C(4)-Dy(1)-C(3)	29.73(8)
C(1)-Dy(1)-C(3)	51.03(8)	C(13)-Dy(1)-C(3)	107.79(8)
C(4)-Dy(1)-C(16)	108.27(8)	C(1)-Dy(1)-C(16)	135.99(8)
C(13)-Dy(1)-C(16)	55.02(8)	C(3)-Dy(1)-C(16)	93.4(1)
C(4)-Dy(1)-C(2)	50.80(8)	C(1)-Dy(1)-C(2)	29.59(8)
C(13)-Dy(1)-C(2)	93.4(1)	C(3)-Dy(1)-C(2)	29.80(8)
C(16)-Dy(1)-C(2)	106.71(8)	C(4)-Dy(1)-C(14)	157.60(8)
C(1)-Dy(1)-C(14)	132.56(8)	C(13)-Dy(1)-C(14)	29.43(8)
C(3)-Dy(1)-C(14)	132.52(8)	C(16)-Dy(1)-C(14)	50.29(8)
C(2)-Dy(1)-C(14)	122.79(8)	C(4)-Dy(1)-C(15)	134.01(8)
C(1)-Dy(1)-C(15)	155.79(8)	C(13)-Dy(1)-C(15)	50.27(8)
C(3)-Dy(1)-C(15)	122.82(8)	C(16)-Dy(1)-C(15)	29.44(8)
C(2)-Dy(1)-C(15)	131.74(8)	C(14)-Dy(1)-C(15)	29.07(8)
C(4)-Dy(1)-P(1)	36.87(6)	C(1)-Dy(1)-P(1)	36.86(6)
C(13)-Dy(1)-P(1)	143.40(6)	C(3)-Dy(1)-P(1)	55.80(6)
C(16)-Dy(1)-P(1)	145.14(6)	C(2)-Dy(1)-P(1)	55.55(6)
C(14)-Dy(1)-P(1)	163.68(6)	C(15)-Dy(1)-P(1)	165.80(6)
C(4)-Dy(1)-P(2)	104.39(6)	C(1)-Dy(1)-P(2)	102.93(6)
C(13)-Dy(1)-P(2)	36.94(6)	C(3)-Dy(1)-P(2)	77.36(6)
C(16)-Dy(1)-P(2)	36.53(6)	C(2)-Dy(1)-P(2)	76.77(6)
C(14)-Dy(1)-P(2)	55.21(6)	C(15)-Dy(1)-P(2)	55.04(6)
P(1)-Dy(1)-P(2)	130.89(2)	C(4)-Dy(1)-I(1)	87.23(6)

C(1)-Dy(1)-I(1)	123.06(5)	C(13)-Dy(1)-I(1)	128.23(6)
C(3)-Dy(1)-I(1)	114.00(5)	C(16)-Dy(1)-I(1)	92.65(5)
C(2)-Dy(1)-I(1)	137.24(6)	C(14)-Dy(1)-I(1)	99.04(6)
C(15)-Dy(1)-I(1)	81.15(6)	P(1)-Dy(1)-I(1)	86.92(1)
P(2)-Dy(1)-I(1)	129.15(2)	C(4)-Dy(1)-I(1)#2	121.94(6)
C(1)-Dy(1)-I(1)#2	87.65(6)	C(13)-Dy(1)-I(1)#2	91.59(6)
C(3)-Dy(1)-I(1)#2	137.52(6)	C(16)-Dy(1)-I(1)#2	127.91(6)
C(2)-Dy(1)-I(1)#2	114.82(6)	C(14)-Dy(1)-I(1)#2	80.46(6)
C(15)-Dy(1)-I(1)#2	98.80(6)	P(1)-Dy(1)-I(1)#2	86.05(2)
P(2)-Dy(1)-I(1)#2	128.49(2)	I(1)-Dy(1)-I(1)#2	77.728(7)
Dy(1)-I(1)-Dy(1)#2	102.272(7	C(4)-P(1)-C(1)	91.6(1)
C(4)-P(1)-Dy(1)	68.0(1)	C(1)-P(1)-Dy(1)	68.1(1)
C(16)-P(2)-C(13)	91.7(1)	C(16)-P(2)-Dy(1)	68.8(1)
C(13)-P(2)-Dy(1)	67.8(1)	C(12)-Si(1)-C(11)	106.8(2)
C(12)-Si(1)-C(10)	109.1(2)	C(11)-Si(1)-C(10)	110.1(2)
C(12)-Si(1)-C(1)	110.7(1)	C(11)-Si(1)-C(1)	113.8(1)
C(10)-Si(1)-C(1)	106.4(1)	C(6)-Si(2)-C(5)	107.0(2)
C(6)-Si(2)-C(7)	110.2(2)	C(5)-Si(2)-C(7)	107.8(2)
C(6)-Si(2)-C(4)	114.5(2)	C(5)-Si(2)-C(4)	110.8(1)
C(7)-Si(2)-C(4)	106.3(2)	C(24)-Si(3)-C(22)	107.6(2)
C(24)-Si(3)-C(23)	110.3(2)	C(22)-Si(3)-C(23)	107.3(2)
C(24)-Si(3)-C(13)	110.8(1)	C(22)-Si(3)-C(13)	105.2(1)
C(23)-Si(3)-C(13)	115.1(1)	C(17)-Si(4)-C(19)	106.6(2)
C(17)-Si(4)-C(18)	108.9(2)	C(19)-Si(4)-C(18)	108.9(2)
C(17)-Si(4)-C(16)	111.9(1)	C(19)-Si(4)-C(16)	105.7(1)
C(18)-Si(4)-C(16)	114.5(1)	C(2)-C(1)-P(1)	110.8(2)
C(2)-C(1)-Si(1)	124.6(2)	P(1)-C(1)-Si(1)	121.1(2)
C(2)-C(1)-Dy(1)	76.9(2)	P(1)-C(1)-Dy(1)	75.0(1)
Si(1)-C(1)-Dy(1)	132.5(1)	C(1)-C(2)-C(3)	113.3(2)
C(1)-C(2)-C(9)	125.1(2)	C(3)-C(2)-C(9)	121.1(2)
C(1)-C(2)-Dy(1)	73.5(2)	C(3)-C(2)-Dy(1)	74.2(2)
C(9)-C(2)-Dy(1)	127.2(2)	C(4)-C(3)-C(2)	113.2(2)
C(4)-C(3)-C(8)	124.9(2)	C(2)-C(3)-C(8)	121.1(2)
C(4)-C(3)-Dy(1)	74.2(2)	C(2)-C(3)-Dy(1)	76.0(2)
C(8)-C(3)-Dy(1)	126.1(2)	C(3)-C(4)-P(1)	110.9(2)
C(3)-C(4)-Si(2)	124.3(2)	P(1)-C(4)-Si(2)	121.4(2)
C(3)-C(4)-Dy(1)	76.1(2)	P(1)-C(4)-Dy(1)	75.1(1)
Si(2)-C(4)-Dy(1)	132.9(1)	Si(2)-C(5)-H(5A)	109.5
Si(2)-C(5)-H(5B)	109.5	H(5A)-C(5)-H(5B)	109.5
Si(2)-C(5)-H(5C)	109.5	H(5A)-C(5)-H(5C)	109.5
H(5B)-C(5)-H(5C)	109.5	Si(2)-C(6)-H(6A)	109.5
Si(2)-C(6)-H(6B)	109.5	H(6A)-C(6)-H(6B)	109.5
Si(2)-C(6)-H(6C)	109.5	H(6A)-C(6)-H(6C)	109.5
H(6B)-C(6)-H(6C)	109.5	Si(2)-C(7)-H(7A)	109.5
Si(2)-C(7)-H(7B)	109.5	H(7A)-C(7)-H(7B)	109.5
Si(2)-C(7)-H(7C)	109.5	H(7A)-C(7)-H(7C)	109.5
H(7B)-C(7)-H(7C)	109.5	C(3)-C(8)-H(8A)	109.5
C(3)-C(8)-H(8B)	109.5	H(8A)-C(8)-H(8B)	109.5
C(3)-C(8)-H(8C)	109.5	H(8A)-C(8)-H(8C)	109.5
H(8B)-C(8)-H(8C)	109.5	C(2)-C(9)-H(9A)	109.5
C(2)-C(9)-H(9B)	109.5	H(9A)-C(9)-H(9B)	109.5
C(2)-C(9)-H(9C)	109.5	H(9A)-C(9)-H(9C)	109.5
H(9B)-C(9)-H(9C)	109.5	Si(1)-C(10)-H(10A)	109.5
Si(1)-C(10)-H(10B)	109.5	H(10A)-C(10)-H(10B)	109.5
Si(1)-C(10)-H(10C)	109.5	H(10A)-C(10)-H(10C)	109.5
H(10B)-C(10)-H(10C)	109.5	Si(1)-C(11)-H(11A)	109.5
Si(1)-C(11)-H(11B)	109.5	H(11A)-C(11)-H(11B)	109.5
Si(1)-C(11)-H(11C)	109.5	H(11A)-C(11)-H(11C)	109.5
H(11B)-C(11)-H(11C)	109.5	Si(1)-C(12)-H(12A)	109.5
Si(1)-C(12)-H(12B)	109.5	H(12A)-C(12)-H(12B)	109.5
Si(1)-C(12)-H(12C)	109.5	H(12A)-C(12)-H(12C)	109.5
H(12B)-C(12)-H(12C)	109.5	C(14)-C(13)-P(2)	110.1(2)
C(14)-C(13)-Si(3)	122.8(2)	P(2)-C(13)-Si(3)	121.8(2)
C(14)-C(13)-Dy(1)	77.1(2)	P(2)-C(13)-Dy(1)	75.3(1)
Si(3)-C(13)-Dy(1)	135.6(1)	C(15)-C(14)-C(13)	113.8(3)
C(15)-C(14)-C(21)	120.7(3)	C(13)-C(14)-C(21)	125.0(3)
C(15)-C(14)-Dy(1)	75.6(2)	C(13)-C(14)-Dy(1)	73.5(2)
C(21)-C(14)-Dy(1)	125.7(2)	C(14)-C(15)-C(16)	114.1(3)
C(14)-C(15)-C(20)	121.2(3)	C(16)-C(15)-C(20)	124.1(3)
C(14)-C(15)-Dy(1)	75.3(2)	C(16)-C(15)-Dy(1)	74.4(2)

C(20)-C(15)-Dy(1)	125.6(2)	C(15)-C(16)-P(2)	110.0(2)
C(15)-C(16)-Si(4)	123.3(2)	P(2)-C(16)-Si(4)	122.3(2)
C(15)-C(16)-Dy(1)	76.1(2)	P(2)-C(16)-Dy(1)	74.7(1)
Si(4)-C(16)-Dy(1)	135.2(1)	Si(4)-C(17)-H(17A)	109.5
Si(4)-C(17)-H(17B)	109.5	H(17A)-C(17)-H(17B)	109.5
Si(4)-C(17)-H(17C)	109.5	H(17A)-C(17)-H(17C)	109.5
H(17B)-C(17)-H(17C)	109.5	Si(4)-C(18)-H(18A)	109.5
Si(4)-C(18)-H(18B)	109.5	H(18A)-C(18)-H(18B)	109.5
Si(4)-C(18)-H(18C)	109.5	H(18A)-C(18)-H(18C)	109.5
H(18B)-C(18)-H(18C)	109.5	Si(4)-C(19)-H(19A)	109.5
Si(4)-C(19)-H(19B)	109.5	H(19A)-C(19)-H(19B)	109.5
Si(4)-C(19)-H(19C)	109.5	H(19A)-C(19)-H(19C)	109.5
H(19B)-C(19)-H(19C)	109.5	C(15)-C(20)-H(20A)	109.5
C(15)-C(20)-H(20B)	109.5	H(20A)-C(20)-H(20B)	109.5
C(15)-C(20)-H(20C)	109.5	H(20A)-C(20)-H(20C)	109.5
H(20B)-C(20)-H(20C)	109.5	C(14)-C(21)-H(21A)	109.5
C(14)-C(21)-H(21B)	109.5	H(21A)-C(21)-H(21B)	109.5
C(14)-C(21)-H(21C)	109.5	H(21A)-C(21)-H(21C)	109.5
H(21B)-C(21)-H(21C)	109.5	Si(3)-C(22)-H(22A)	109.5
Si(3)-C(22)-H(22B)	109.5	H(22A)-C(22)-H(22B)	109.5
Si(3)-C(22)-H(22C)	109.5	H(22A)-C(22)-H(22C)	109.5
H(22B)-C(22)-H(22C)	109.5	Si(3)-C(23)-H(23A)	109.5
Si(3)-C(23)-H(23B)	109.5	H(23A)-C(23)-H(23B)	109.5
Si(3)-C(23)-H(23C)	109.5	H(23A)-C(23)-H(23C)	109.5
H(23B)-C(23)-H(23C)	109.5	Si(3)-C(24)-H(24A)	109.5
Si(3)-C(24)-H(24B)	109.5	H(24A)-C(24)-H(24B)	109.5
Si(3)-C(24)-H(24C)	109.5	H(24A)-C(24)-H(24C)	109.5
H(24B)-C(24)-H(24C)	109.5	C(25)-Dy(2)-C(40)	135.66(8)
C(25)-Dy(2)-C(37)	107.00(8)	C(40)-Dy(2)-C(37)	55.34(8)
C(25)-Dy(2)-C(38)	92.76(8)	C(40)-Dy(2)-C(38)	50.82(8)
C(37)-Dy(2)-C(38)	29.50(8)	C(25)-Dy(2)-C(39)	106.27(8)
C(40)-Dy(2)-C(39)	29.63(8)	C(37)-Dy(2)-C(39)	50.60(8)
C(38)-Dy(2)-C(39)	29.51(8)	C(25)-Dy(2)-C(26)	29.77(8)
C(40)-Dy(2)-C(26)	156.4(1)	C(37)-Dy(2)-C(26)	132.9(1)
C(38)-Dy(2)-C(26)	122.52(8)	C(39)-Dy(2)-C(26)	131.88(8)
C(25)-Dy(2)-C(28)	54.9(1)	C(40)-Dy(2)-C(28)	107.7(1)
C(37)-Dy(2)-C(28)	137.46(8)	C(38)-Dy(2)-C(28)	108.15(8)
C(39)-Dy(2)-C(28)	94.25(8)	C(26)-Dy(2)-C(28)	50.0(1)
C(25)-Dy(2)-C(27)	50.36(8)	C(40)-Dy(2)-C(27)	133.6(1)
C(37)-Dy(2)-C(27)	156.57(8)	C(38)-Dy(2)-C(27)	132.38(8)
C(39)-Dy(2)-C(27)	123.3(1)	C(26)-Dy(2)-C(27)	28.9(1)
C(28)-Dy(2)-C(27)	29.13(8)	C(25)-Dy(2)-P(4)	143.89(6)
C(40)-Dy(2)-P(4)	36.91(6)	C(37)-Dy(2)-P(4)	36.89(6)
C(38)-Dy(2)-P(4)	55.48(6)	C(39)-Dy(2)-P(4)	55.44(6)
C(26)-Dy(2)-P(4)	164.71(7)	C(28)-Dy(2)-P(4)	144.55(7)
C(27)-Dy(2)-P(4)	165.00(7)	C(25)-Dy(2)-P(3)	36.91(7)
C(40)-Dy(2)-P(3)	102.84(6)	C(37)-Dy(2)-P(3)	104.12(6)
C(38)-Dy(2)-P(3)	77.42(6)	C(39)-Dy(2)-P(3)	76.71(6)
C(26)-Dy(2)-P(3)	55.34(6)	C(28)-Dy(2)-P(3)	36.55(6)
C(27)-Dy(2)-P(3)	54.97(6)	P(4)-Dy(2)-P(3)	130.70(2)
C(25)-Dy(2)-I(2)	128.30(6)	C(40)-Dy(2)-I(2)	88.15(6)
C(37)-Dy(2)-I(2)	122.70(5)	C(38)-Dy(2)-I(2)	137.85(6)
C(39)-Dy(2)-I(2)	115.35(6)	C(26)-Dy(2)-I(2)	98.87(6)
C(28)-Dy(2)-I(2)	91.66(6)	C(27)-Dy(2)-I(2)	80.72(6)
P(4)-Dy(2)-I(2)	86.79(1)	P(3)-Dy(2)-I(2)	128.12(1)
C(25)-Dy(2)-I(2)#2	93.42(6)	C(40)-Dy(2)-I(2)#2	121.90(6)
C(37)-Dy(2)-I(2)#2	86.62(6)	C(38)-Dy(2)-I(2)#2	113.55(6)
C(39)-Dy(2)-I(2)#2	136.26(6)	C(26)-Dy(2)-I(2)#2	81.67(6)
C(28)-Dy(2)-I(2)#2	128.36(6)	C(27)-Dy(2)-I(2)#2	99.43(7)
P(4)-Dy(2)-I(2)#2	85.79(2)	P(3)-Dy(2)-I(2)#2	130.31(2)
I(2)-Dy(2)-I(2)#2	77.299(7)	Dy(2)-I(2)-Dy(2)#2	102.701(8)
C(28)-P(3)-C(25)	91.8(1)	C(28)-P(3)-Dy(2)	69.6(1)
C(25)-P(3)-Dy(2)	67.7(1)	C(40)-P(4)-C(37)	92.0(1)
C(40)-P(4)-Dy(2)	68.15(8)	C(37)-P(4)-Dy(2)	68.67(8)
C(36)-Si(5)-C(34)	109.9(2)	C(36)-Si(5)-C(35)	108.9(2)
C(34)-Si(5)-C(35)	107.3(2)	C(36)-Si(5)-C(25)	115.8(2)
C(34)-Si(5)-C(25)	102.4(1)	C(35)-Si(5)-C(25)	112.1(2)
C(29)-Si(6)-C(30)	107.9(2)	C(29)-Si(6)-C(31)	110.0(2)

C(30)-Si(6)-C(31)	108.2(2)	C(29)-Si(6)-C(28)	109.6(1)
C(30)-Si(6)-C(28)	104.6(2)	C(31)-Si(6)-C(28)	116.0(2)
C(47)-Si(7)-C(48)	107.7(2)	C(47)-Si(7)-C(46)	107.7(1)
C(48)-Si(7)-C(46)	109.5(2)	C(47)-Si(7)-C(37)	110.7(1)
C(48)-Si(7)-C(37)	113.8(1)	C(46)-Si(7)-C(37)	107.2(1)
C(42)-Si(8)-C(43)	107.7(2)	C(42)-Si(8)-C(41)	108.0(2)
C(43)-Si(8)-C(41)	109.2(2)	C(42)-Si(8)-C(40)	110.8(2)
C(43)-Si(8)-C(40)	107.8(1)	C(41)-Si(8)-C(40)	113.2(1)
C(26)-C(25)-P(3)	109.9(2)	C(26)-C(25)-Si(5)	122.7(2)
P(3)-C(25)-Si(5)	119.3(2)	C(26)-C(25)-Dy(2)	77.2(2)
P(3)-C(25)-Dy(2)	75.4(1)	Si(5)-C(25)-Dy(2)	140.5(1)
C(27)-C(26)-C(25)	113.8(3)	C(27)-C(26)-C(33)	121.5(3)
C(25)-C(26)-C(33)	124.1(3)	C(27)-C(26)-Dy(2)	76.5(2)
C(25)-C(26)-Dy(2)	73.1(2)	C(33)-C(26)-Dy(2)	125.8(2)
C(26)-C(27)-C(28)	114.1(3)	C(26)-C(27)-C(32)	121.7(3)
C(28)-C(27)-C(32)	123.7(3)	C(26)-C(27)-Dy(2)	74.5(2)
C(28)-C(27)-Dy(2)	74.5(2)	C(32)-C(27)-Dy(2)	126.2(2)
C(27)-C(28)-P(3)	110.2(2)	C(27)-C(28)-Si(6)	123.8(2)
P(3)-C(28)-Si(6)	120.5(2)	C(27)-C(28)-Dy(2)	76.4(2)
P(3)-C(28)-Dy(2)	73.9(1)	Si(6)-C(28)-Dy(2)	137.9(1)
Si(6)-C(29)-H(29A)	109.5	Si(6)-C(29)-H(29B)	109.5
H(29A)-C(29)-H(29B)	109.5	Si(6)-C(29)-H(29C)	109.5
H(29A)-C(29)-H(29C)	109.5	H(29B)-C(29)-H(29C)	109.5
Si(6)-C(30)-H(30A)	109.5	Si(6)-C(30)-H(30B)	109.5
H(30A)-C(30)-H(30B)	109.5	Si(6)-C(30)-H(30C)	109.5
H(30A)-C(30)-H(30C)	109.5	H(30B)-C(30)-H(30C)	109.5
Si(6)-C(31)-H(31A)	109.5	Si(6)-C(31)-H(31B)	109.5
H(31A)-C(31)-H(31B)	109.5	Si(6)-C(31)-H(31C)	109.5
H(31A)-C(31)-H(31C)	109.5	H(31B)-C(31)-H(31C)	109.5
C(27)-C(32)-H(32A)	109.5	C(27)-C(32)-H(32B)	109.5
H(32A)-C(32)-H(32B)	109.5	C(27)-C(32)-H(32C)	109.5
H(32A)-C(32)-H(32C)	109.5	H(32B)-C(32)-H(32C)	109.5
C(26)-C(33)-H(33A)	109.5	C(26)-C(33)-H(33B)	109.5
H(33A)-C(33)-H(33B)	109.5	C(26)-C(33)-H(33C)	109.5
H(33A)-C(33)-H(33C)	109.5	H(33B)-C(33)-H(33C)	109.5
Si(5)-C(34)-H(34A)	109.5	Si(5)-C(34)-H(34B)	109.5
H(34A)-C(34)-H(34B)	109.5	Si(5)-C(34)-H(34C)	109.5
H(34A)-C(34)-H(34C)	109.5	H(34B)-C(34)-H(34C)	109.5
Si(5)-C(35)-H(35A)	109.5	Si(5)-C(35)-H(35B)	109.5
H(35A)-C(35)-H(35B)	109.5	Si(5)-C(35)-H(35C)	109.5
H(35A)-C(35)-H(35C)	109.5	H(35B)-C(35)-H(35C)	109.5
Si(5)-C(36)-H(36A)	109.5	Si(5)-C(36)-H(36B)	109.5
H(36A)-C(36)-H(36B)	109.5	Si(5)-C(36)-H(36C)	109.5
H(36A)-C(36)-H(36C)	109.5	H(36B)-C(36)-H(36C)	109.5
C(38)-C(37)-P(4)	110.3(2)	C(38)-C(37)-Si(7)	124.5(2)
P(4)-C(37)-Si(7)	122.8(2)	C(38)-C(37)-Dy(2)	76.4(1)
P(4)-C(37)-Dy(2)	74.4(1)	Si(7)-C(37)-Dy(2)	130.2(1)
C(37)-C(38)-C(39)	113.7(2)	C(37)-C(38)-C(45)	124.8(3)
C(39)-C(38)-C(45)	120.9(3)	C(37)-C(38)-Dy(2)	74.1(1)
C(39)-C(38)-Dy(2)	75.3(1)	C(45)-C(38)-Dy(2)	126.4(2)
C(40)-C(39)-C(38)	113.7(3)	C(40)-C(39)-C(44)	124.5(3)
C(38)-C(39)-C(44)	121.3(2)	C(40)-C(39)-Dy(2)	73.4(2)
C(38)-C(39)-Dy(2)	75.2(2)	C(44)-C(39)-Dy(2)	126.7(2)
C(39)-C(40)-P(4)	110.3(2)	C(39)-C(40)-Si(8)	124.7(2)
P(4)-C(40)-Si(8)	122.8(2)	C(39)-C(40)-Dy(2)	77.0(2)
P(4)-C(40)-Dy(2)	74.9(1)	Si(8)-C(40)-Dy(2)	128.6(1)
Si(8)-C(41)-H(41A)	109.5	Si(8)-C(41)-H(41B)	109.5
H(41A)-C(41)-H(41B)	109.5	Si(8)-C(41)-H(41C)	109.5
H(41A)-C(41)-H(41C)	109.5	H(41B)-C(41)-H(41C)	109.5
Si(8)-C(42)-H(42A)	109.5	Si(8)-C(42)-H(42B)	109.5
H(42A)-C(42)-H(42B)	109.5	Si(8)-C(42)-H(42C)	109.5
H(42A)-C(42)-H(42C)	109.5	H(42B)-C(42)-H(42C)	109.5
Si(8)-C(43)-H(43A)	109.5	Si(8)-C(43)-H(43B)	109.5
H(43A)-C(43)-H(43B)	109.5	Si(8)-C(43)-H(43C)	109.5
H(43A)-C(43)-H(43C)	109.5	H(43B)-C(43)-H(43C)	109.5
C(39)-C(44)-H(44A)	109.5	C(39)-C(44)-H(44B)	109.5
H(44A)-C(44)-H(44B)	109.5	C(39)-C(44)-H(44C)	109.5
H(44A)-C(44)-H(44C)	109.5	H(44B)-C(44)-H(44C)	109.5
C(38)-C(45)-H(45A)	109.5	C(38)-C(45)-H(45B)	109.5
H(45A)-C(45)-H(45B)	109.5	C(38)-C(45)-H(45C)	109.5

H(45A)-C(45)-H(45C)	109.5	H(45B)-C(45)-H(45C)	109.5
Si(7)-C(46)-H(46A)	109.5	Si(7)-C(46)-H(46B)	109.5
H(46A)-C(46)-H(46B)	109.5	Si(7)-C(46)-H(46C)	109.5
H(46A)-C(46)-H(46C)	109.5	H(46B)-C(46)-H(46C)	109.5
Si(7)-C(47)-H(47A)	109.5	Si(7)-C(47)-H(47B)	109.5
H(47A)-C(47)-H(47B)	109.5	Si(7)-C(47)-H(47C)	109.5
H(47A)-C(47)-H(47C)	109.5	H(47B)-C(47)-H(47C)	109.5
Si(7)-C(48)-H(48A)	109.5	Si(7)-C(48)-H(48B)	109.5
H(48A)-C(48)-H(48B)	109.5	Si(7)-C(48)-H(48C)	109.5
H(48A)-C(48)-H(48C)	109.5	H(48B)-C(48)-H(48C)	109.5

Estimated standard deviations are given in the parenthesis.
Symmetry operators ::
1: x, y, z 2: -x, -y, -z

[(Cp^{ttt})DyCl(BH_4)(μ-Cl)K([18]crown-6)] (38)

Compound	fj186_2
Molecular formula	$C_{17}H_{33}BCl_2Dy$,$C_{12}H_{24}KO_6$
Molecular weight	1570.11
Crystal habit	Colorless Block
Crystal dimensions(mm)	0.24x0.14x0.14
Crystal system	monoclinic
Space group	$P2_1/a$
a(Å)	17.5970(10)
b(Å)	16.7150(10)
c(Å)	25.7750(10)
α(°)	90.00
β(°)	90.6430(10)
γ(°)	90.00
V(Å^3)	7580.8(7)
Z	4
d(g-cm^{-3})	1.376
F(000)	3224
μ(cm^{-1})	2.256
Absorption corrections	multi-scan ; 0.6135 min, 0.7430 max
Diffractometer	KappaCCD
X-ray source	MoKα
λ(Å)	0.71069
Monochromator	graphite
T (K)	150.0(1)
Scan mode	phi and omega scans
Maximum θ	26.37
HKL ranges	-21 21 ; -20 18 ; -32 32
Reflections measured	26009
Unique data	15318
Rint	0.0190
Reflections used	11736
Criterion	I > 2σI)
Refinement type	Fsqd
Hydrogen atoms	mixed

Parameters refined	784
Reflections / parameter	14
wR2	0.1520
R1	0.0503
Weights a, b	0.0775 ; 30.615
GoF	1.059
difference peak / hole (e Å^{-3})	3.738(0.143) / -2.217(0.143)

Table. Bond lengths (A) and angles (deg) for fj186_2

Dy(1)-B(1)	2.52(1)	Dy(1)-Cl(1)	2.55(1)
Dy(1)-Cl(2)	2.570(4)	Dy(1)-C(1)	2.636(7)
Dy(1)-C(4)	2.637(7)	Dy(1)-C(5)	2.650(7)
Dy(1)-C(2)	2.673(7)	Dy(1)-C(3)	2.689(7)
Dy(1)-H(1BA)	2.38(4)	Dy(1)-H(1BB)	2.34(4)
Dy(1)-H(1BD)	2.46(5)	Dy(2)-B(2)	2.51(1)
Dy(2)-Cl(3)	2.523(5)	Dy(2)-Cl(4A)	2.58(1)
Dy(2)-Cl(4B)	2.59(3)	Dy(2)-C(30)	2.638(7)
Dy(2)-C(33)	2.639(7)	Dy(2)-C(34)	2.662(7)
Dy(2)-C(32)	2.672(7)	Dy(2)-C(31)	2.674(7)
Dy(2)-H(2BA)	2.42(4)	Dy(2)-H(2BB)	2.33(5)
Dy(2)-H(2BD)	2.42(5)	B(1)-H(1BA)	1.112(1)
B(1)-H(1BB)	1.112(1)	B(1)-H(1BC)	1.112(1)
B(1)-H(1BD)	1.112(1)	B(2)-H(2BA)	1.112(1)
B(2)-H(2BB)	1.112(1)	B(2)-H(2BC)	1.112(1)
B(2)-H(2BD)	1.112(1)	K(1)-O(5)	2.836(6)
K(1)-O(6)	2.837(7)	K(1)-O(1)	2.844(6)
K(1)-O(2)	2.846(6)	K(1)-O(3)	2.907(6)
K(1)-O(4)	2.912(7)	K(1)-Cl(2)#2	3.324(4)
K(1)-C(41)#4	3.33(1)	K(2)-O(10)	2.747(6)
K(2)-O(8)	2.771(6)	K(2)-O(12)	2.800(7)
K(2)-O(7)	2.810(6)	K(2)-O(11)	2.815(7)
K(2)-O(9)	2.864(6)	K(2)-Cl(4A)#3	3.21(1)
K(2)-C(12)	3.418(8)	K(2)-Cl(4B)#3	3.58(3)
K(2)-H(12B)	2.85(3)	K(2)-H(12C)	3.08(5)
O(1)-C(18)	1.42(1)	O(1)-C(29)	1.43(1)
O(2)-C(20)	1.41(1)	O(2)-C(19)	1.42(1)
O(3)-C(21)	1.42(1)	O(3)-C(22)	1.43(1)
O(4)-C(24)	1.41(1)	O(4)-C(23)	1.44(1)
O(5)-C(25)	1.42(1)	O(5)-C(26)	1.43(1)
O(6)-C(28)	1.42(1)	O(6)-C(27)	1.42(1)
O(7)-C(58)	1.42(1)	O(7)-C(47)	1.43(1)
O(8)-C(49)	1.43(1)	O(8)-C(48)	1.43(1)
O(9)-C(50)	1.41(1)	O(9)-C(51)	1.42(1)
O(10)-C(52)	1.41(1)	O(10)-C(53)	1.41(1)
O(11)-C(54)	1.42(1)	O(11)-C(55)	1.43(1)
O(12)-C(56)	1.40(1)	O(12)-C(57)	1.44(1)
Cl(2)-K(1)#2	3.324(4)	Cl(4A)-K(2)#3	3.21(1)
Cl(4B)-K(2)#3	3.58(3)	C(1)-C(5)	1.41(1)
C(1)-C(2)	1.42(1)	C(1)-H(1)	0.9500
C(2)-C(3)	1.43(1)	C(2)-C(14)	1.56(1)
C(3)-C(4)	1.43(1)	C(3)-C(10)	1.55(1)
C(4)-C(5)	1.40(1)	C(4)-H(4)	0.9500
C(5)-C(6)	1.54(1)	C(6)-C(7)	1.53(1)
C(6)-C(8)	1.53(1)	C(6)-C(9)	1.54(1)
C(7)-H(7A)	0.9800	C(7)-H(7B)	0.9800
C(7)-H(7C)	0.9800	C(8)-H(8A)	0.9800
C(8)-H(8B)	0.9800	C(8)-H(8C)	0.9800
C(9)-H(9A)	0.9800	C(9)-H(9B)	0.9800
C(9)-H(9C)	0.9800	C(10)-C(12)	1.53(1)
C(10)-C(11)	1.54(1)	C(10)-C(13)	1.54(1)
C(11)-H(11A)	0.9800	C(11)-H(11B)	0.9800
C(11)-H(11C)	0.9800	C(12)-H(12A)	0.9800(2)
C(12)-H(12B)	0.9800(1	C(12)-H(12C)	0.98(4)
C(13)-H(13A)	0.9800	C(13)-H(13B)	0.9800
C(13)-H(13C)	0.9800	C(14)-C(16)	1.53(1)
C(14)-C(15)	1.53(1)	C(14)-C(17)	1.56(1)

C(15)-H(15A)	0.9800	C(15)-H(15B)	0.9800
C(15)-H(15C)	0.9800	C(16)-H(16A)	0.9800
C(16)-H(16B)	0.9800	C(16)-H(16C)	0.9800
C(17)-H(17A)	0.9800	C(17)-H(17B)	0.9800
C(17)-H(17C)	0.9800	C(18)-C(19)	1.50(1)
C(18)-H(18A)	0.9900	C(18)-H(18B)	0.9900
C(19)-H(19A)	0.9900	C(19)-H(19B)	0.9900
C(20)-C(21)	1.49(1)	C(20)-H(20A)	0.9900
C(20)-H(20B)	0.9900	C(21)-H(21A)	0.9900
C(21)-H(21B)	0.9900	C(22)-C(23)	1.49(1)
C(22)-H(22A)	0.9900	C(22)-H(22B)	0.9900
C(23)-H(23A)	0.9900	C(23)-H(23B)	0.9900
C(24)-C(25)	1.48(1)	C(24)-H(24A)	0.9900
C(24)-H(24B)	0.9900	C(25)-H(25A)	0.9900
C(25)-H(25B)	0.9900	C(26)-C(27)	1.49(1)
C(26)-H(26A)	0.9900	C(26)-H(26B)	0.9900
C(27)-H(27A)	0.9900	C(27)-H(27B)	0.9900
C(28)-C(29)	1.50(1)	C(28)-H(28A)	0.9900
C(28)-H(28B)	0.9900	C(29)-H(29A)	0.9900
C(29)-H(29B)	0.9900	C(30)-C(34)	1.41(1)
C(30)-C(31)	1.43(1)	C(30)-H(30)	0.9500
C(31)-C(32)	1.44(1)	C(31)-C(39)	1.54(1)
C(32)-C(33)	1.43(1)	C(32)-C(43)	1.55(1)
C(33)-C(34)	1.41(1)	C(33)-H(33)	0.9500
C(34)-C(35)	1.52(1)	C(35)-C(37)	1.53(1)
C(35)-C(36)	1.54(1)	C(35)-C(38)	1.55(1)
C(36)-H(36A)	0.9800	C(36)-H(36B)	0.9800
C(36)-H(36C)	0.9800	C(37)-H(37A)	0.9800
C(37)-H(37B)	0.9800	C(37)-H(37C)	0.9800
C(38)-H(38A)	0.9800	C(38)-H(38B)	0.9800
C(38)-H(38C)	0.9800	C(39)-C(42)	1.52(1)
C(39)-C(40)	1.53(1)	C(39)-C(41)	1.55(1)
C(40)-H(40A)	0.9800	C(40)-H(40B)	0.9800
C(40)-H(40C)	0.9800	C(41)-K(1)#4	3.33(1)
C(41)-H(41A)	0.9800(2	C(41)-H(41B)	0.9800(1)
C(41)-H(41C)	1.02(4)	C(42)-H(42A)	0.9800
C(42)-H(42B)	0.9800	C(42)-H(42C)	0.9800
C(43)-C(46)	1.53(1)	C(43)-C(45)	1.54(1)
C(43)-C(44)	1.54(1)	C(44)-H(44A)	0.9800
C(44)-H(44B)	0.9800	C(44)-H(44C)	0.9800
C(45)-H(45A)	0.9800	C(45)-H(45B)	0.9800
C(45)-H(45C)	0.9800	C(46)-H(46A)	0.9800
C(46)-H(46B)	0.9800	C(46)-H(46C)	0.9800
C(47)-C(48)	1.48(1)	C(47)-H(47A)	0.9900
C(47)-H(47B)	0.9900	C(48)-H(48A)	0.9900
C(48)-H(48B)	0.9900	C(49)-C(50)	1.50(1)
C(49)-H(49A)	0.9900	C(49)-H(49B)	0.9900
C(50)-H(50A)	0.9900	C(50)-H(50B)	0.9900
C(51)-C(52)	1.50(1)	C(51)-H(51A)	0.9900
C(51)-H(51B)	0.9900	C(52)-H(52A)	0.9900
C(52)-H(52B)	0.9900	C(53)-C(54)	1.49(1)
C(53)-H(53A)	0.9900	C(53)-H(53B)	0.9900
C(54)-H(54A)	0.9900	C(54)-H(54B)	0.9900
C(55)-C(56)	1.50(2)	C(55)-H(55A)	0.9900
C(55)-H(55B)	0.9900	C(56)-H(56A)	0.9900
C(56)-H(56B)	0.9900	C(57)-C(58)	1.45(2)
C(57)-H(57A)	0.9900	C(57)-H(57B)	0.9900
C(58)-H(58A)	0.9900	C(58)-H(58B)	0.9900

B(1)-Dy(1)-Cl(1)	103.4(4)	B(1)-Dy(1)-Cl(2)	103.4(2)
Cl(1)-Dy(1)-Cl(2)	97.4(4)	B(1)-Dy(1)-C(1)	136.7(3)
Cl(1)-Dy(1)-C(1)	115.9(3)	Cl(2)-Dy(1)-C(1)	89.5(2)
B(1)-Dy(1)-C(4)	89.1(3)	Cl(1)-Dy(1)-C(4)	134.8(4)
Cl(2)-Dy(1)-C(4)	122.0(2)	C(1)-Dy(1)-C(4)	50.4(2)
B(1)-Dy(1)-C(5)	106.3(3)	Cl(1)-Dy(1)-C(5)	145.4(3)
Cl(2)-Dy(1)-C(5)	92.7(2)	C(1)-Dy(1)-C(5)	30.9(2)
C(4)-Dy(1)-C(5)	30.8(2)	B(1)-Dy(1)-C(2)	134.5(3)

Cl(1)-Dy(1)-C(2)	94.4(3)	Cl(2)-Dy(1)-C(2)	115.4(2)
C(1)-Dy(1)-C(2)	31.0(2)	C(4)-Dy(1)-C(2)	51.0(2)
C(5)-Dy(1)-C(2)	51.7(2)	B(1)-Dy(1)-C(3)	103.6(3)
Cl(1)-Dy(1)-C(3)	104.1(4)	Cl(2)-Dy(1)-C(3)	140.2(2)
C(1)-Dy(1)-C(3)	51.1(2)	C(4)-Dy(1)-C(3)	31.1(2)
C(5)-Dy(1)-C(3)	51.7(2)	C(2)-Dy(1)-C(3)	31.0(2)
B(1)-Dy(1)-H(1BA)	26.0(1)	Cl(1)-Dy(1)-H(1BA)	92(1)
Cl(2)-Dy(1)-H(1BA)	128.6(4)	C(1)-Dy(1)-H(1BA)	131(1)
C(4)-Dy(1)-H(1BA)	81(1)	C(5)-Dy(1)-H(1BA)	108(1)
C(2)-Dy(1)-H(1BA)	114.1(6)	C(3)-Dy(1)-H(1BA)	84.2(7)
B(1)-Dy(1)-H(1BB)	26.1(1)	Cl(1)-Dy(1)-H(1BB)	129.2(4)
Cl(2)-Dy(1)-H(1BB)	94(1)	C(1)-Dy(1)-H(1BB)	113.5(5)
C(4)-Dy(1)-H(1BB)	73(1)	C(5)-Dy(1)-H(1BB)	82.6(5)
C(2)-Dy(1)-H(1BB)	124(1)	C(3)-Dy(1)-H(1BB)	98(1)
H(1BA)-Dy(1)-H(1BB)	45.3(5)	B(1)-Dy(1)-H(1BD)	25.8(2)
Cl(1)-Dy(1)-H(1BD)	87.3(8)	Cl(2)-Dy(1)-H(1BD)	85.9(8)
C(1)-Dy(1)-H(1BD)	156.7(8)	C(4)-Dy(1)-H(1BD)	114.5(4)
C(5)-Dy(1)-H(1BD)	126.5(7)	C(2)-Dy(1)-H(1BD)	158.1(6)
C(3)-Dy(1)-H(1BD)	127.7(5)	H(1BA)-Dy(1)-H(1BD)	44.0(4)
H(1BB)-Dy(1)-H(1BD)	44.4(5)	B(2)-Dy(2)-Cl(3)	100.3(3)
B(2)-Dy(2)-Cl(4A)	103.2(3)	Cl(3)-Dy(2)-Cl(4A)	98.9(3)
B(2)-Dy(2)-Cl(4B)	70.2(8)	Cl(3)-Dy(2)-Cl(4B)	132.6(8)
Cl(4A)-Dy(2)-Cl(4B)	44.3(8)	B(2)-Dy(2)-C(30)	94.0(3)
Cl(3)-Dy(2)-C(30)	115.7(2)	Cl(4A)-Dy(2)-C(30)	137.8(3)
Cl(4B)-Dy(2)-C(30)	111.3(8)	B(2)-Dy(2)-C(33)	124.3(3)
Cl(3)-Dy(2)-C(33)	131.8(2)	Cl(4A)-Dy(2)-C(33)	88.6(3)
Cl(4B)-Dy(2)-C(33)	83.9(8)	C(30)-Dy(2)-C(33)	50.6(2)
B(2)-Dy(2)-C(34)	95.7(3)	Cl(3)-Dy(2)-C(34)	144.3(2)
Cl(4A)-Dy(2)-C(34)	108.3(3)	Cl(4B)-Dy(2)-C(34)	82.9(8)
C(30)-Dy(2)-C(34)	30.8(2)	C(33)-Dy(2)-C(34)	31.0(2)
B(2)-Dy(2)-C(32)	144.7(3)	Cl(3)-Dy(2)-C(32)	101.1(2)
Cl(4A)-Dy(2)-C(32)	100.8(3)	Cl(4B)-Dy(2)-C(32)	112.8(8)
C(30)-Dy(2)-C(32)	51.3(2)	C(33)-Dy(2)-C(32)	31.3(2)
C(34)-Dy(2)-C(32)	52.0(2)	B(2)-Dy(2)-C(31)	120.3(3)
Cl(3)-Dy(2)-C(31)	92.7(2)	Cl(4A)-Dy(2)-C(31)	132.0(3)
Cl(4B)-Dy(2)-C(31)	133.0(8)	C(30)-Dy(2)-C(31)	31.2(2)
C(33)-Dy(2)-C(31)	51.3(2)	C(34)-Dy(2)-C(31)	51.9(2)
C(32)-Dy(2)-C(31)	31.2(2)	B(2)-Dy(2)-H(2BA)	26.0(2)
Cl(3)-Dy(2)-H(2BA)	80.0(7)	Cl(4A)-Dy(2)-H(2BA)	91(1)
Cl(4B)-Dy(2)-H(2BA)	73(1)	C(30)-Dy(2)-H(2BA)	117.5(6)
C(33)-Dy(2)-H(2BA)	147.9(6)	C(34)-Dy(2)-H(2BA)	121.4(3)
C(32)-Dy(2)-H(2BA)	168.2(8)	C(31)-Dy(2)-H(2BA)	137(1)
B(2)-Dy(2)-H(2BB)	26.2(1)	Cl(3)-Dy(2)-H(2BB)	96(1)
Cl(4A)-Dy(2)-H(2BB)	129.3(4)	Cl(4B)-Dy(2)-H(2BB)	92(1)
C(30)-Dy(2)-H(2BB)	72.7(7)	C(33)-Dy(2)-H(2BB)	116(1)
C(34)-Dy(2)-H(2BB)	85(1)	C(32)-Dy(2)-H(2BB)	123.4(6)
C(31)-Dy(2)-H(2BB)	95.1(4)	H(2BA)-Dy(2)-H(2BB)	45.0(5)
B(2)-Dy(2)-H(2BD)	26.0(2)	Cl(3)-Dy(2)-H(2BD)	123.9(6)
Cl(4A)-Dy(2)-H(2BD)	88(1)	Cl(4B)-Dy(2)-H(2BD)	47(1)
C(30)-Dy(2)-H(2BD)	92(1)	C(33)-Dy(2)-H(2BD)	103.7(7)
C(34)-Dy(2)-H(2BD)	81(1)	C(32)-Dy(2)-H(2BD)	132.4(8)
C(31)-Dy(2)-H(2BD)	123(1)	H(2BA)-Dy(2)-H(2BD)	44.1(5)
H(2BB)-Dy(2)-H(2BD)	45.0(5)	Dy(1)-B(1)-H(1BA)	70(2)
Dy(1)-B(1)-H(1BB)	68(2)	H(1BA)-B(1)-H(1BB)	109.5(2)
Dy(1)-B(1)-H(1BC)	176(2)	H(1BA)-B(1)-H(1BC)	109.5(2)
H(1BB)-B(1)-H(1BC)	109.5(2)	Dy(1)-B(1)-H(1BD)	74(2)
H(1BA)-B(1)-H(1BD)	109.5(2)	H(1BB)-B(1)-H(1BD)	109.5(2)
H(1BC)-B(1)-H(1BD)	109.5(2)	Dy(2)-B(2)-H(2BA)	72(2)
Dy(2)-B(2)-H(2BB)	67(2)	H(2BA)-B(2)-H(2BB)	109.5(2)
Dy(2)-B(2)-H(2BC)	177(2)	H(2BA)-B(2)-H(2BC)	109.5(2)
H(2BB)-B(2)-H(2BC)	109.5(2)	Dy(2)-B(2)-H(2BD)	72(2)
H(2BA)-B(2)-H(2BD)	109.5(2)	H(2BB)-B(2)-H(2BD)	109.5(2)
H(2BC)-B(2)-H(2BD)	109.5(2)	O(5)-K(1)-O(6)	58.2(2)
O(5)-K(1)-O(1)	112.9(2)	O(6)-K(1)-O(1)	59.0(2)
O(5)-K(1)-O(2)	152.2(2)	O(6)-K(1)-O(2)	117.8(2)
O(1)-K(1)-O(2)	59.2(2)	O(5)-K(1)-O(3)	109.2(2)
O(6)-K(1)-O(3)	148.8(2)	O(1)-K(1)-O(3)	111.8(2)
O(2)-K(1)-O(3)	58.4(2)	O(5)-K(1)-O(4)	58.3(2)
O(6)-K(1)-O(4)	116.5(2)	O(1)-K(1)-O(4)	156.0(2)
O(2)-K(1)-O(4)	116.7(2)	O(3)-K(1)-O(4)	58.3(2)

O(5)-K(1)-Cl(2)#2	106.0(2)	O(6)-K(1)-Cl(2)#2	76.5(2)
O(1)-K(1)-Cl(2)#2	79.9(2)	O(2)-K(1)-Cl(2)#2	98.8(2)
O(3)-K(1)-Cl(2)#2	133.7(2)	O(4)-K(1)-Cl(2)#2	123.3(2)
O(5)-K(1)-C(41)#4	72.7(2)	O(6)-K(1)-C(41)#4	73.8(2)
O(1)-K(1)-C(41)#4	69.7(2)	O(2)-K(1)-C(41)#4	79.9(2)
O(3)-K(1)-C(41)#4	75.2(2)	O(4)-K(1)-C(41)#4	86.4(2)
Cl(2)#2-K(1)-C(41)#4	145.3(2)	O(10)-K(2)-O(8)	119.0(2)
O(10)-K(2)-O(12)	120.1(2)	O(8)-K(2)-O(12)	119.8(2)
O(10)-K(2)-O(7)	164.1(2)	O(8)-K(2)-O(7)	60.6(2)
O(12)-K(2)-O(7)	59.5(2)	O(10)-K(2)-O(11)	59.8(2)
O(8)-K(2)-O(11)	169.4(2)	O(12)-K(2)-O(11)	60.3(2)
O(7)-K(2)-O(11)	117.2(2)	O(10)-K(2)-O(9)	59.4(2)
O(8)-K(2)-O(9)	60.0(2)	O(12)-K(2)-O(9)	164.1(2)
O(7)-K(2)-O(9)	116.0(2)	O(11)-K(2)-O(9)	116.6(2)
O(10)-K(2)-Cl(4A)#3	104.5(2)	O(8)-K(2)-Cl(4A)#3	87.1(2)
O(12)-K(2)-Cl(4A)#3	88.6(2)	O(7)-K(2)-Cl(4A)#3	91.5(2)
O(11)-K(2)-Cl(4A)#3	103.4(2)	O(9)-K(2)-Cl(4A)#3	107.1(2)
O(10)-K(2)-C(12)	99.4(2)	O(8)-K(2)-C(12)	76.2(2)
O(12)-K(2)-C(12)	84.3(2)	O(7)-K(2)-C(12)	64.7(2)
O(11)-K(2)-C(12)	93.4(2)	O(9)-K(2)-C(12)	80.2(1)
Cl(4A)#3-K(2)-C(12)	155.4(2)	O(10)-K(2)-Cl(4B)#3	83.2(6)
O(8)-K(2)-Cl(4B)#3	119.3(6)	O(12)-K(2)-Cl(4B)#3	78.0(6)
O(7)-K(2)-Cl(4B)#3	111.3(6)	O(11)-K(2)-Cl(4B)#3	71.3(6)
O(9)-K(2)-Cl(4B)#3	116.7(6)	Cl(4A)#3-K(2)-Cl(4B)#3	32.7(6)
C(12)-K(2)-Cl(4B)#3	160.8(6)	O(10)-K(2)-H(12B)	107.6(3)
O(8)-K(2)-H(12B)	83.2(4)	O(12)-K(2)-H(12B)	69.7(4)
O(7)-K(2)-H(12B)	56.6(3)	O(11)-K(2)-H(12B)	87.2(4)
O(9)-K(2)-H(12B)	94.9(4)	Cl(4A)#3-K(2)-H(12B)	147.2(3)
C(12)-K(2)-H(12B)	14.7(3)	Cl(4B)#3-K(2)-H(12B)	147.2(7)
O(10)-K(2)-H(12C)	90(1)	O(8)-K(2)-H(12C)	69(2)
O(12)-K(2)-H(12C)	100.6(6)	O(7)-K(2)-H(12C)	75(1)
O(11)-K(2)-H(12C)	100(2)	O(9)-K(2)-H(12C)	63.9(6)
Cl(4A)#3-K(2)-H(12C)	156(2)	C(12)-K(2)-H(12C)	16.3(5)
Cl(4B)#3-K(2)-H(12C)	171(2)	H(12B)-K(2)-H(12C)	31.0(4)
C(18)-O(1)-C(29)	112.4(7)	C(18)-O(1)-K(1)	109.3(5)
C(29)-O(1)-K(1)	109.9(5)	C(20)-O(2)-C(19)	111.7(7)
C(20)-O(2)-K(1)	118.4(5)	C(19)-O(2)-K(1)	117.2(5)
C(21)-O(3)-C(22)	111.7(7)	C(21)-O(3)-K(1)	111.0(5)
C(22)-O(3)-K(1)	111.8(6)	C(24)-O(4)-C(23)	111.0(8)
C(24)-O(4)-K(1)	116.7(5)	C(23)-O(4)-K(1)	117.1(5)
C(25)-O(5)-C(26)	111.9(8)	C(25)-O(5)-K(1)	112.8(6)
C(26)-O(5)-K(1)	117.0(5)	C(28)-O(6)-C(27)	111.7(8)
C(28)-O(6)-K(1)	118.5(6)	C(27)-O(6)-K(1)	118.5(5)
C(58)-O(7)-C(47)	113.2(8)	C(58)-O(7)-K(2)	115.1(6)
C(47)-O(7)-K(2)	110.2(5)	C(49)-O(8)-C(48)	111.4(7)
C(49)-O(8)-K(2)	117.4(5)	C(48)-O(8)-K(2)	117.4(6)
C(50)-O(9)-C(51)	111.3(7)	C(50)-O(9)-K(2)	111.3(5)
C(51)-O(9)-K(2)	112.0(5)	C(52)-O(10)-C(53)	112.7(7)
C(52)-O(10)-K(2)	120.2(5)	C(53)-O(10)-K(2)	119.1(5)
C(54)-O(11)-C(55)	112.0(8)	C(54)-O(11)-K(2)	110.4(5)
C(55)-O(11)-K(2)	111.2(6)	C(56)-O(12)-C(57)	113(1)
C(56)-O(12)-K(2)	116.4(6)	C(57)-O(12)-K(2)	116.0(6)
Dy(1)-Cl(2)-K(1)#2	107.5(1)	Dy(2)-Cl(4A)-K(2)#3	116.5(3)
Dy(2)-Cl(4B)-K(2)#3	105(1)	C(5)-C(1)-C(2)	110.2(7)
C(5)-C(1)-Dy(1)	75.1(4)	C(2)-C(1)-Dy(1)	75.9(4)
C(5)-C(1)-H(1)	124.9	C(2)-C(1)-H(1)	124.9
Dy(1)-C(1)-H(1)	115.9	C(1)-C(2)-C(3)	107.1(6)
C(1)-C(2)-C(14)	118.8(7)	C(3)-C(2)-C(14)	133.0(7)
C(1)-C(2)-Dy(1)	73.0(4)	C(3)-C(2)-Dy(1)	75.1(4)
C(14)-C(2)-Dy(1)	126.0(5)	C(4)-C(3)-C(2)	106.0(6)
C(4)-C(3)-C(10)	119.9(7)	C(2)-C(3)-C(10)	133.7(7)
C(4)-C(3)-Dy(1)	72.4(4)	C(2)-C(3)-Dy(1)	73.9(4)
C(10)-C(3)-Dy(1)	123.6(5)	C(5)-C(4)-C(3)	110.6(7)
C(5)-C(4)-Dy(1)	75.1(4)	C(3)-C(4)-Dy(1)	76.5(4)
C(5)-C(4)-H(4)	124.7	C(3)-C(4)-H(4)	124.7
Dy(1)-C(4)-H(4)	115.6	C(4)-C(5)-C(1)	106.1(7)
C(4)-C(5)-C(6)	125.8(7)	C(1)-C(5)-C(6)	127.3(7)
C(4)-C(5)-Dy(1)	74.1(4)	C(1)-C(5)-Dy(1)	74.0(4)

C(6)-C(5)-Dy(1)	125.2(5)	C(7)-C(6)-C(8)	109.4(7)
C(7)-C(6)-C(9)	108.5(7)	C(8)-C(6)-C(9)	109.1(7)
C(7)-C(6)-C(5)	110.6(7)	C(8)-C(6)-C(5)	112.7(7)
C(9)-C(6)-C(5)	106.3(6)	C(6)-C(7)-H(7A)	109.5
C(6)-C(7)-H(7B)	109.5	H(7A)-C(7)-H(7B)	109.5
C(6)-C(7)-H(7C)	109.5	H(7A)-C(7)-H(7C)	109.5
H(7B)-C(7)-H(7C)	109.5	C(6)-C(8)-H(8A)	109.5
C(6)-C(8)-H(8B)	109.5	H(8A)-C(8)-H(8B)	109.5
C(6)-C(8)-H(8C)	109.5	H(8A)-C(8)-H(8C)	109.5
H(8B)-C(8)-H(8C)	109.5	C(6)-C(9)-H(9A)	109.5
C(6)-C(9)-H(9B)	109.5	H(9A)-C(9)-H(9B)	109.5
C(6)-C(9)-H(9C)	109.5	H(9A)-C(9)-H(9C)	109.5
H(9B)-C(9)-H(9C)	109.5	C(12)-C(10)-C(11)	109.4(6)
C(12)-C(10)-C(13)	105.7(6)	C(11)-C(10)-C(13)	106.0(7)
C(12)-C(10)-C(3)	110.7(6)	C(11)-C(10)-C(3)	115.0(6)
C(13)-C(10)-C(3)	109.5(6)	C(10)-C(11)-H(11A)	109.5
C(10)-C(11)-H(11B)	109.5	H(11A)-C(11)-H(11B)	109.5
C(10)-C(11)-H(11C)	109.5	H(11A)-C(11)-H(11C)	109.5
H(11B)-C(11)-H(11C)	109.5	C(10)-C(12)-K(2)	124.2(4)
C(10)-C(12)-H(12A)	110(1)	K(2)-C(12)-H(12A)	125(1)
C(10)-C(12)-H(12B)	112(2)	K(2)-C(12)-H(12B)	47(2)
H(12A)-C(12)-H(12B)	109.44(2)	C(10)-C(12)-H(12C)	107(5)
K(2)-C(12)-H(12C)	62(3)	H(12A)-C(12)-H(12C)	109(3)
H(12B)-C(12)-H(12C)	109(3)	C(10)-C(13)-H(13A)	109.5
C(10)-C(13)-H(13B)	109.5	H(13A)-C(13)-H(13B)	109.5
C(10)-C(13)-H(13C)	109.5	H(13A)-C(13)-H(13C)	109.5
H(13B)-C(13)-H(13C)	109.5	C(16)-C(14)-C(15)	106.8(7)
C(16)-C(14)-C(2)	115.3(7)	C(15)-C(14)-C(2)	110.4(7)
C(16)-C(14)-C(17)	109.7(7)	C(15)-C(14)-C(17)	106.4(7)
C(2)-C(14)-C(17)	107.9(7)	C(14)-C(15)-H(15A)	109.5
C(14)-C(15)-H(15B)	109.5	H(15A)-C(15)-H(15B)	109.5
C(14)-C(15)-H(15C)	109.5	H(15A)-C(15)-H(15C)	109.5
H(15B)-C(15)-H(15C)	109.5	C(14)-C(16)-H(16A)	109.5
C(14)-C(16)-H(16B)	109.5	H(16A)-C(16)-H(16B)	109.5
C(14)-C(16)-H(16C)	109.5	H(16A)-C(16)-H(16C)	109.5
H(16B)-C(16)-H(16C)	109.5	C(14)-C(17)-H(17A)	109.5
C(14)-C(17)-H(17B)	109.5	H(17A)-C(17)-H(17B)	109.5
C(14)-C(17)-H(17C)	109.5	H(17A)-C(17)-H(17C)	109.5
H(17B)-C(17)-H(17C)	109.5	O(1)-C(18)-C(19)	107.8(7)
O(1)-C(18)-H(18A)	110.2	C(19)-C(18)-H(18A)	110.2
O(1)-C(18)-H(18B)	110.2	C(19)-C(18)-H(18B)	110.2
H(18A)-C(18)-H(18B)	108.5	O(2)-C(19)-C(18)	108.4(7)
O(2)-C(19)-H(19A)	110.0	C(18)-C(19)-H(19A)	110.0
O(2)-C(19)-H(19B)	110.0	C(18)-C(19)-H(19B)	110.0
H(19A)-C(19)-H(19B)	108.4	O(2)-C(20)-C(21)	108.7(7)
O(2)-C(20)-H(20A)	109.9	C(21)-C(20)-H(20A)	109.9
O(2)-C(20)-H(20B)	109.9	C(21)-C(20)-H(20B)	109.9
H(20A)-C(20)-H(20B)	108.3	O(3)-C(21)-C(20)	108.7(8)
O(3)-C(21)-H(21A)	109.9	C(20)-C(21)-H(21A)	109.9
O(3)-C(21)-H(21B)	109.9	C(20)-C(21)-H(21B)	109.9
H(21A)-C(21)-H(21B)	108.3	O(3)-C(22)-C(23)	108.9(8)
O(3)-C(22)-H(22A)	109.9	C(23)-C(22)-H(22A)	109.9
O(3)-C(22)-H(22B)	109.9	C(23)-C(22)-H(22B)	109.9
H(22A)-C(22)-H(22B)	108.3	O(4)-C(23)-C(22)	108.8(8)
O(4)-C(23)-H(23A)	109.9	C(22)-C(23)-H(23A)	109.9
O(4)-C(23)-H(23B)	109.9	C(22)-C(23)-H(23B)	109.9
H(23A)-C(23)-H(23B)	108.3	O(4)-C(24)-C(25)	110.0(8)
O(4)-C(24)-H(24A)	109.7	C(25)-C(24)-H(24A)	109.7
O(4)-C(24)-H(24B)	109.7	C(25)-C(24)-H(24B)	109.7
H(24A)-C(24)-H(24B)	108.2	O(5)-C(25)-C(24)	108.6(8)
O(5)-C(25)-H(25A)	110.0	C(24)-C(25)-H(25A)	110.0
O(5)-C(25)-H(25B)	110.0	C(24)-C(25)-H(25B)	110.0
H(25A)-C(25)-H(25B)	108.4	O(5)-C(26)-C(27)	108.0(8)
O(5)-C(26)-H(26A)	110.1	C(27)-C(26)-H(26A)	110.1
O(5)-C(26)-H(26B)	110.1	C(27)-C(26)-H(26B)	110.1
H(26A)-C(26)-H(26B)	108.4	O(6)-C(27)-C(26)	110(1)
O(6)-C(27)-H(27A)	109.8	C(26)-C(27)-H(27A)	109.8
O(6)-C(27)-H(27B)	109.8	C(26)-C(27)-H(27B)	109.8
H(27A)-C(27)-H(27B)	108.2	O(6)-C(28)-C(29)	108.6(8)
O(6)-C(28)-H(28A)	110.0	C(29)-C(28)-H(28A)	110.0

O(6)-C(28)-H(28B)	110.0	C(29)-C(28)-H(28B)	110.0
H(28A)-C(28)-H(28B)	108.4	O(1)-C(29)-C(28)	107.6(7)
O(1)-C(29)-H(29A)	110.2	C(28)-C(29)-H(29A)	110.2
O(1)-C(29)-H(29B)	110.2	C(28)-C(29)-H(29B)	110.2
H(29A)-C(29)-H(29B)	108.5	C(34)-C(30)-C(31)	110.7(7)
C(34)-C(30)-Dy(2)	75.6(4)	C(31)-C(30)-Dy(2)	75.8(4)
C(34)-C(30)-H(30)	124.7	C(31)-C(30)-H(30)	124.7
Dy(2)-C(30)-H(30)	115.8	C(30)-C(31)-C(32)	106.6(6)
C(30)-C(31)-C(39)	117.8(7)	C(32)-C(31)-C(39)	134.8(7)
C(30)-C(31)-Dy(2)	73.0(4)	C(32)-C(31)-Dy(2)	74.3(4)
C(39)-C(31)-Dy(2)	125.5(5)	C(33)-C(32)-C(31)	106.5(6)
C(33)-C(32)-C(43)	119.1(6)	C(31)-C(32)-C(43)	133.6(7)
C(33)-C(32)-Dy(2)	73.1(4)	C(31)-C(32)-Dy(2)	74.5(4)
C(43)-C(32)-Dy(2)	125.4(5)	C(34)-C(33)-C(32)	110.3(7)
C(34)-C(33)-Dy(2)	75.4(4)	C(32)-C(33)-Dy(2)	75.6(4)
C(34)-C(33)-H(33)	124.9	C(32)-C(33)-H(33)	124.9
Dy(2)-C(33)-H(33)	116.0	C(30)-C(34)-C(33)	106.0(7)
C(30)-C(34)-C(35)	126.9(7)	C(33)-C(34)-C(35)	125.7(7)
C(30)-C(34)-Dy(2)	73.6(4)	C(33)-C(34)-Dy(2)	73.6(4)
C(35)-C(34)-Dy(2)	128.5(5)	C(34)-C(35)-C(37)	112.3(7)
C(34)-C(35)-C(36)	111.4(7)	C(37)-C(35)-C(36)	108.9(8)
C(34)-C(35)-C(38)	106.8(7)	C(37)-C(35)-C(38)	107.5(8)
C(36)-C(35)-C(38)	110.0(8)	C(35)-C(36)-H(36A)	109.5
C(35)-C(36)-H(36B)	109.5	H(36A)-C(36)-H(36B)	109.5
C(35)-C(36)-H(36C)	109.5	H(36A)-C(36)-H(36C)	109.5
H(36B)-C(36)-H(36C)	109.5	C(35)-C(37)-H(37A)	109.5
C(35)-C(37)-H(37B)	109.5	H(37A)-C(37)-H(37B)	109.5
C(35)-C(37)-H(37C)	109.5	H(37A)-C(37)-H(37C)	109.5
H(37B)-C(37)-H(37C)	109.5	C(35)-C(38)-H(38A)	109.5
C(35)-C(38)-H(38B)	109.5	H(38A)-C(38)-H(38B)	109.5
C(35)-C(38)-H(38C)	109.5	H(38A)-C(38)-H(38C)	109.5
H(38B)-C(38)-H(38C)	109.5	C(42)-C(39)-C(40)	106.8(7)
C(42)-C(39)-C(31)	115.9(7)	C(40)-C(39)-C(31)	111.8(7)
C(42)-C(39)-C(41)	108.3(7)	C(40)-C(39)-C(41)	106.4(6)
C(31)-C(39)-C(41)	107.2(6)	C(39)-C(40)-H(40A)	109.5
C(39)-C(40)-H(40B)	109.5	H(40A)-C(40)-H(40B)	109.5
C(39)-C(40)-H(40C)	109.5	H(40A)-C(40)-H(40C)	109.5
H(40B)-C(40)-H(40C)	109.5	C(39)-C(41)-K(1)#4	159.8(5)
C(39)-C(41)-H(41A)	113(2)	K(1)#4-C(41)-H(41A)	69(2)
C(39)-C(41)-H(41B)	112(2)	K(1)#4-C(41)-H(41B)	52(2)
H(41A)-C(41)-H(41B)	109.44(2)	C(39)-C(41)-H(41C)	109(6)
K(1)#4-C(41)-H(41C)	89(6)	H(41A)-C(41)-H(41C)	106(3)
H(41B)-C(41)-H(41C)	106(3)	C(39)-C(42)-H(42A)	109.5
C(39)-C(42)-H(42B)	109.5	H(42A)-C(42)-H(42B)	109.5
C(39)-C(42)-H(42C)	109.5	H(42A)-C(42)-H(42C)	109.5
H(42B)-C(42)-H(42C)	109.5	C(46)-C(43)-C(45)	110.7(7)
C(46)-C(43)-C(44)	105.3(7)	C(45)-C(43)-C(44)	106.1(7)
C(46)-C(43)-C(32)	114.5(6)	C(45)-C(43)-C(32)	109.8(7)
C(44)-C(43)-C(32)	110.1(7)	C(43)-C(44)-H(44A)	109.5
C(43)-C(44)-H(44B)	109.5	H(44A)-C(44)-H(44B)	109.5
C(43)-C(44)-H(44C)	109.5	H(44A)-C(44)-H(44C)	109.5
H(44B)-C(44)-H(44C)	109.5	C(43)-C(45)-H(45A)	109.5
C(43)-C(45)-H(45B)	109.5	H(45A)-C(45)-H(45B)	109.5
C(43)-C(45)-H(45C)	109.5	H(45A)-C(45)-H(45C)	109.5
H(45B)-C(45)-H(45C)	109.5	C(43)-C(46)-H(46A)	109.5
C(43)-C(46)-H(46B)	109.5	H(46A)-C(46)-H(46B)	109.5
C(43)-C(46)-H(46C)	109.5	H(46A)-C(46)-H(46C)	109.5
H(46B)-C(46)-H(46C)	109.5	O(7)-C(47)-C(48)	109.5(8)
O(7)-C(47)-H(47A)	109.8	C(48)-C(47)-H(47A)	109.8
O(7)-C(47)-H(47B)	109.8	C(48)-C(47)-H(47B)	109.8
H(47A)-C(47)-H(47B)	108.2	O(8)-C(48)-C(47)	108.8(8)
O(8)-C(48)-H(48A)	109.9	C(47)-C(48)-H(48A)	109.9
O(8)-C(48)-H(48B)	109.9	C(47)-C(48)-H(48B)	109.9
H(48A)-C(48)-H(48B)	108.3	O(8)-C(49)-C(50)	108.7(7)
O(8)-C(49)-H(49A)	110.0	C(50)-C(49)-H(49A)	110.0
O(8)-C(49)-H(49B)	110.0	C(50)-C(49)-H(49B)	110.0
H(49A)-C(49)-H(49B)	108.3	O(9)-C(50)-C(49)	108.5(8)
O(9)-C(50)-H(50A)	110.0	C(49)-C(50)-H(50A)	110.0

O(9)-C(50)-H(50B)	110.0	C(49)-C(50)-H(50B)	110.0
H(50A)-C(50)-H(50B)	108.4	O(9)-C(51)-C(52)	108.4(7)
O(9)-C(51)-H(51A)	110.0	C(52)-C(51)-H(51A)	110.0
O(9)-C(51)-H(51B)	110.0	C(52)-C(51)-H(51B)	110.0
H(51A)-C(51)-H(51B)	108.4	O(10)-C(52)-C(51)	108.9(7)
O(10)-C(52)-H(52A)	109.9	C(51)-C(52)-H(52A)	109.9
O(10)-C(52)-H(52B)	109.9	C(51)-C(52)-H(52B)	109.9
H(52A)-C(52)-H(52B)	108.3	O(10)-C(53)-C(54)	108.9(8)
O(10)-C(53)-H(53A)	109.9	C(54)-C(53)-H(53A)	109.9
O(10)-C(53)-H(53B)	109.9	C(54)-C(53)-H(53B)	109.9
H(53A)-C(53)-H(53B)	108.3	O(11)-C(54)-C(53)	108.1(8)
O(11)-C(54)-H(54A)	110.1	C(53)-C(54)-H(54A)	110.1
O(11)-C(54)-H(54B)	110.1	C(53)-C(54)-H(54B)	110.1
H(54A)-C(54)-H(54B)	108.4	O(11)-C(55)-C(56)	108(1)
O(11)-C(55)-H(55A)	110.2	C(56)-C(55)-H(55A)	110.2
O(11)-C(55)-H(55B)	110.2	C(56)-C(55)-H(55B)	110.2
H(55A)-C(55)-H(55B)	108.5	O(12)-C(56)-C(55)	110(1)
O(12)-C(56)-H(56A)	109.7	C(55)-C(56)-H(56A)	109.7
O(12)-C(56)-H(56B)	109.7	C(55)-C(56)-H(56B)	109.7
H(56A)-C(56)-H(56B)	108.2	O(12)-C(57)-C(58)	109(1)
O(12)-C(57)-H(57A)	109.9	C(58)-C(57)-H(57A)	109.9
O(12)-C(57)-H(57B)	109.9	C(58)-C(57)-H(57B)	109.9
H(57A)-C(57)-H(57B)	108.3	O(7)-C(58)-C(57)	110(1)
O(7)-C(58)-H(58A)	109.6	C(57)-C(58)-H(58A)	109.6
O(7)-C(58)-H(58B)	109.6	C(57)-C(58)-H(58B)	109.6
H(58A)-C(58)-H(58B)	108.1		

Estimated standard deviations are given in the parenthesis.

Symmetry operators ::

1: x, y, z 2: -x+1/2, y+1/2, -z 3: -x, -y, -z

4: x-1/2, -y-1/2, z

[{K([18]crown-6)}{(Cp^{ttt})$_2$DyBr($OC_{13}H_8$)}] (39)

Compound	fj220
Molecular formula	$C_{47}H_{66}BrDyO,C_{12}H_{24}KO_6,C_7H_8$
Molecular weight	1284.95
Crystal habit	Needle
Crystal dimensions(mm)	0.20x0.08x0.06
Crystal system	monoclinic
Space group	$P2_1/c$
a(≈)	12.633(1)
b(≈)	30.385(1)
c(≈)	18.870(1)
α(∞)	90.00
β(∞)	116.352(1)
γ(∞)	90.00
V(≈^{3})	6490.6(7)
Z	4
d(g-cm^{-3})	1.315
F(000)	2680
μ(cm^{-1})	1.879
Absorption corrections	multi-scan ; 0.7050 min, 0.8956 max
Diffractometer	KappaCCD
X-ray source	MoKα
λ(≈)	0.71069

Monochromator	graphite
T (K)	150.0(1)
Scan mode	phi and omega scans
Maximum θ	23.25
HKL ranges	-14 12 ; -32 33 ; -16 20
Reflections measured	30127
Unique data	9247
Rint	0.1036
Reflections used	4598
Criterion	I > 2σ(I)
Refinement type	Fsqd
Hydrogen atoms	constr
Parameters refined	640
Reflections / parameter	7
wR2	0.1617
R1	0.0615
Weights a, b	0.0759 ; 0.0000
GoF	0.898
difference peak / hole (e ≈$^{-3}$)	0.713(0.115) / -0.573(0.115)

Table. Bond lengths (A) and angles (deg) for fj220

Dy(1)-O(1)	2.133(7)	Dy(1)-C(2)	2.72(1)
Dy(1)-C(20)	2.72(1)	Dy(1)-C(1)	2.72(1)
Dy(1)-C(19)	2.73(1)	Dy(1)-C(3)	2.74(1)
Dy(1)-C(18)	2.77(1)	Dy(1)-Br(1)	2.806(1)
Dy(1)-C(21)	2.81(1)	Dy(1)-C(5)	2.81(1)
Dy(1)-C(4)	2.85(1)	Dy(1)-C(22)	2.846(8)
O(1)-C(35)	1.32(1)	C(1)-C(2)	1.38(1)
C(1)-C(5)	1.40(1)	C(1)-H(1)	0.9499
C(2)-C(3)	1.40(1)	C(2)-C(14)	1.51(1)
C(3)-C(4)	1.46(1)	C(3)-H(3)	0.9499
C(4)-C(5)	1.40(1)	C(4)-C(10)	1.58(1)
C(5)-C(6)	1.56(1)	C(6)-C(9)	1.50(1)
C(6)-C(7)	1.54(1)	C(6)-C(8)	1.57(1)
C(7)-H(7A)	0.9800	C(7)-H(7B)	0.9800
C(7)-H(7C)	0.9800	C(8)-H(8A)	0.9800
C(8)-H(8B)	0.9800	C(8)-H(8C)	0.9800
C(9)-H(9A)	0.9800	C(9)-H(9B)	0.9800
C(9)-H(9C)	0.9800	C(10)-C(11)	1.49(1)
C(10)-C(13)	1.50(1)	C(10)-C(12)	1.55(1)
C(11)-H(11A)	0.9800	C(11)-H(11B)	0.9800
C(11)-H(11C)	0.9800	C(12)-H(12A)	0.9800
C(12)-H(12B)	0.9800	C(12)-H(12C)	0.9800
C(13)-H(13A)	0.9800	C(13)-H(13B)	0.9800
C(13)-H(13C)	0.9800	C(14)-C(15)	1.53(1)
C(14)-C(17)	1.55(1)	C(14)-C(16)	1.57(1)
C(15)-H(15A)	0.9800	C(15)-H(15B)	0.9800
C(15)-H(15C)	0.9800	C(16)-H(16A)	0.9800
C(16)-H(16B)	0.9800	C(16)-H(16C)	0.9800
C(17)-H(17A)	0.9800	C(17)-H(17B)	0.9800
C(17)-H(17C)	0.9800	C(18)-C(22)	1.37(1)
C(18)-C(19)	1.43(1)	C(18)-H(18)	0.9500
C(19)-C(20)	1.41(1)	C(19)-C(31)	1.57(1)
C(20)-C(21)	1.41(1)	C(20)-H(20)	0.9499
C(21)-C(22)	1.43(1)	C(21)-C(27)	1.51(1)
C(22)-C(23)	1.52(1)	C(23)-C(25)	1.53(1)
C(23)-C(26)	1.55(1)	C(23)-C(24)	1.57(1)
C(24)-H(24A)	0.9800	C(24)-H(24B)	0.9800

C(24)-H(24C)	0.9800	C(25)-H(25A)	0.9800
C(25)-H(25B)	0.9800	C(25)-H(25C)	0.9800
C(26)-H(26A)	0.9800	C(26)-H(26B)	0.9800
C(26)-H(26C)	0.9800	C(27)-C(29)	1.50(1)
C(27)-C(28)	1.55(1)	C(27)-C(30)	1.55(1)
C(28)-H(28A)	0.9800	C(28)-H(28B)	0.9800
C(28)-H(28C)	0.9800	C(29)-H(29A)	0.9800
C(29)-H(29B)	0.9800	C(29)-H(29C)	0.9800
C(30)-H(30A)	0.9800	C(30)-H(30B)	0.9800
C(30)-H(30C)	0.9800	C(31)-C(32)	1.56(1)
C(31)-C(34)	1.57(1)	C(31)-C(33)	1.58(1)
C(32)-H(32A)	0.9800	C(32)-H(32B)	0.9800
C(32)-H(32C)	0.9800	C(33)-H(33A)	0.9800
C(33)-H(33B)	0.9800	C(33)-H(33C)	0.9800
C(34)-H(34A)	0.9800	C(34)-H(34B)	0.9800
C(34)-H(34C)	0.9800	C(35)-C(36)	1.43(1)
C(35)-C(47)	1.45(1)	C(36)-C(37)	1.40(1)
C(36)-C(41)	1.44(1)	C(37)-C(38)	1.40(1)
C(37)-H(37)	0.9500	C(38)-C(39)	1.39(1)
C(38)-H(38)	0.9500	C(39)-C(40)	1.43(1)
C(39)-H(39)	0.9500	C(40)-C(41)	1.42(1)
C(40)-H(40)	0.9500	C(41)-C(42)	1.50(1)
C(42)-C(43)	1.37(1)	C(42)-C(47)	1.43(1)
C(43)-C(44)	1.35(1)	C(43)-H(43)	0.9500
C(44)-C(45)	1.40(2)	C(44)-H(44)	0.9500
C(45)-C(46)	1.43(1)	C(45)-H(45)	0.9500
C(46)-C(47)	1.40(1)	C(46)-H(46)	0.9500
K(1)-O(7)	2.681(7)	K(1)-O(3)	2.768(7)
K(1)-O(4)	2.791(7)	K(1)-O(2)	2.798(7)
K(1)-O(5)	2.830(7)	K(1)-O(6)	2.868(7)
K(1)-C(29)#4	3.52(1)	O(2)-C(48)	1.42(1)
O(2)-C(59)	1.43(1)	O(3)-C(49)	1.38(1)
O(3)-C(50)	1.40(1)	O(4)-C(52)	1.43(1)
O(4)-C(51)	1.49(1)	O(5)-C(54)	1.41(1)
O(5)-C(53)	1.44(1)	O(6)-C(55)	1.43(1)
O(6)-C(56)	1.45(1)	O(7)-C(58)	1.46(1)
O(7)-C(57)	1.47(1)	C(48)-C(49)	1.48(1)
C(48)-H(48A)	0.9900	C(48)-H(48B)	0.9900
C(49)-H(49A)	0.9900	C(49)-H(49B)	0.9900
C(50)-C(51)	1.45(2)	C(50)-H(50A)	0.9900
C(50)-H(50B)	0.9900	C(51)-H(51A)	0.9900
C(51)-H(51B)	0.9900	C(52)-C(53)	1.46(1)
C(52)-H(52A)	0.9900	C(52)-H(52B)	0.9900
C(53)-H(53A)	0.9900	C(53)-H(53B)	0.9900
C(54)-C(55)	1.52(1)	C(54)-H(54A)	0.9900
C(54)-H(54B)	0.9900	C(55)-H(55A)	0.9900
C(55)-H(55B)	0.9900	C(56)-C(57)	1.50(1)
C(56)-H(56A)	0.9900	C(56)-H(56B)	0.9900
C(57)-H(57A)	0.9900	C(57)-H(57B)	0.9900
C(58)-C(59)	1.44(1)	C(58)-H(58A)	0.9900
C(58)-H(58B)	0.9900	C(59)-H(59A)	0.9900
C(59)-H(59B)	0.9900		

O(1)-Dy(1)-C(2)	106.5(3)	O(1)-Dy(1)-C(20)	107.9(3)
C(2)-Dy(1)-C(20)	134.6(3)	O(1)-Dy(1)-C(1)	80.7(3)
C(2)-Dy(1)-C(1)	29.4(3)	C(20)-Dy(1)-C(1)	162.5(3)
O(1)-Dy(1)-C(19)	132.4(3)	C(2)-Dy(1)-C(19)	105.2(3)
C(20)-Dy(1)-C(19)	29.9(3)	C(1)-Dy(1)-C(19)	134.4(4)
O(1)-Dy(1)-C(3)	128.0(3)	C(2)-Dy(1)-C(3)	29.8(3)
C(20)-Dy(1)-C(3)	123.8(3)	C(1)-Dy(1)-C(3)	48.1(3)
C(19)-Dy(1)-C(3)	96.1(3)	O(1)-Dy(1)-C(18)	116.5(3)
C(2)-Dy(1)-C(18)	89.9(3)	C(20)-Dy(1)-C(18)	48.2(3)
C(1)-Dy(1)-C(18)	114.4(3)	C(19)-Dy(1)-C(18)	30.1(3)
C(3)-Dy(1)-C(18)	95.7(3)	O(1)-Dy(1)-Br(1)	93.1(2)
C(2)-Dy(1)-Br(1)	130.0(2)	C(20)-Dy(1)-Br(1)	76.3(2)
C(1)-Dy(1)-Br(1)	119.3(2)	C(19)-Dy(1)-Br(1)	92.8(2)
C(3)-Dy(1)-Br(1)	103.5(2)	C(18)-Dy(1)-Br(1)	121.8(2)
O(1)-Dy(1)-C(21)	83.3(3)	C(2)-Dy(1)-C(21)	133.6(3)
C(20)-Dy(1)-C(21)	29.5(3)	C(1)-Dy(1)-C(21)	144.2(3)

C(19)-Dy(1)-C(21)	49.3(3)	C(3)-Dy(1)-C(21)	142.5(3)
C(18)-Dy(1)-C(21)	47.6(3)	Br(1)-Dy(1)-C(21)	93.3(2)
O(1)-Dy(1)-C(5)	83.5(3)	C(2)-Dy(1)-C(5)	48.9(3)
C(20)-Dy(1)-C(5)	162.6(3)	C(1)-Dy(1)-C(5)	29.1(3)
C(19)-Dy(1)-C(5)	143.7(3)	C(3)-Dy(1)-C(5)	48.2(3)
C(18)-Dy(1)-C(5)	138.7(3)	Br(1)-Dy(1)-C(5)	90.2(2)
C(21)-Dy(1)-C(5)	166.4(3)	O(1)-Dy(1)-C(4)	110.8(3)
C(2)-Dy(1)-C(4)	49.7(3)	C(20)-Dy(1)-C(4)	135.5(3)
C(1)-Dy(1)-C(4)	48.1(3)	C(19)-Dy(1)-C(4)	116.8(3)
C(3)-Dy(1)-C(4)	30.3(3)	C(18)-Dy(1)-C(4)	125.0(3)
Br(1)-Dy(1)-C(4)	80.5(2)	C(21)-Dy(1)-C(4)	164.8(3)
C(5)-Dy(1)-C(4)	28.7(3)	O(1)-Dy(1)-C(22)	88.9(3)
C(2)-Dy(1)-C(22)	104.4(3)	C(20)-Dy(1)-C(22)	48.5(3)
C(1)-Dy(1)-C(22)	118.3(3)	C(19)-Dy(1)-C(22)	49.1(3)
C(3)-Dy(1)-C(22)	120.0(3)	C(18)-Dy(1)-C(22)	28.2(3)
Br(1)-Dy(1)-C(22)	121.9(2)	C(21)-Dy(1)-C(22)	29.4(3)
C(5)-Dy(1)-C(22)	147.4(3)	C(4)-Dy(1)-C(22)	150.2(3)
C(35)-O(1)-Dy(1)	172.9(6)	C(2)-C(1)-C(5)	111(1)
C(2)-C(1)-Dy(1)	75.1(5)	C(5)-C(1)-Dy(1)	78.9(6)
C(2)-C(1)-H(1)	124.5	C(5)-C(1)-H(1)	124.5
Dy(1)-C(1)-H(1)	113.4	C(1)-C(2)-C(3)	106(1)
C(1)-C(2)-C(14)	126(1)	C(3)-C(2)-C(14)	122(1)
C(1)-C(2)-Dy(1)	75.5(6)	C(3)-C(2)-Dy(1)	75.8(6)
C(14)-C(2)-Dy(1)	134.7(6)	C(2)-C(3)-C(4)	110(1)
C(2)-C(3)-Dy(1)	74.3(6)	C(4)-C(3)-Dy(1)	79.0(6)
C(2)-C(3)-H(3)	125.6	C(4)-C(3)-H(3)	124.9
Dy(1)-C(3)-H(3)	113.3	C(5)-C(4)-C(3)	105(1)
C(5)-C(4)-C(10)	136(1)	C(3)-C(4)-C(10)	117(1)
C(5)-C(4)-Dy(1)	74.4(5)	C(3)-C(4)-Dy(1)	70.8(5)
C(10)-C(4)-Dy(1)	128.1(7)	C(1)-C(5)-C(4)	109(1)
C(1)-C(5)-C(6)	119(1)	C(4)-C(5)-C(6)	130(1)
C(1)-C(5)-Dy(1)	71.9(5)	C(4)-C(5)-Dy(1)	77.0(5)
C(6)-C(5)-Dy(1)	127.9(6)	C(9)-C(6)-C(7)	103.3(8)
C(9)-C(6)-C(5)	110(1)	C(7)-C(6)-C(5)	110.0(8)
C(9)-C(6)-C(8)	113(1)	C(7)-C(6)-C(8)	108(1)
C(5)-C(6)-C(8)	112.2(8)	C(6)-C(7)-H(7A)	109.5
C(6)-C(7)-H(7B)	109.5	H(7A)-C(7)-H(7B)	109.5
C(6)-C(7)-H(7C)	109.5	H(7A)-C(7)-H(7C)	109.5
H(7B)-C(7)-H(7C)	109.5	C(6)-C(8)-H(8A)	109.5
C(6)-C(8)-H(8B)	109.5	H(8A)-C(8)-H(8B)	109.5
C(6)-C(8)-H(8C)	109.5	H(8A)-C(8)-H(8C)	109.5
H(8B)-C(8)-H(8C)	109.5	C(6)-C(9)-H(9A)	109.5
C(6)-C(9)-H(9B)	109.5	H(9A)-C(9)-H(9B)	109.5
C(6)-C(9)-H(9C)	109.5	H(9A)-C(9)-H(9C)	109.5
H(9B)-C(9)-H(9C)	109.5	C(11)-C(10)-C(13)	106(1)
C(11)-C(10)-C(12)	107.6(8)	C(13)-C(10)-C(12)	105(1)
C(11)-C(10)-C(4)	118(1)	C(13)-C(10)-C(4)	113.9(8)
C(12)-C(10)-C(4)	106(1)	C(10)-C(11)-H(11A)	109.5
C(10)-C(11)-H(11B)	109.5	H(11A)-C(11)-H(11B)	109.5
C(10)-C(11)-H(11C)	109.5	H(11A)-C(11)-H(11C)	109.5
H(11B)-C(11)-H(11C)	109.5	C(10)-C(12)-H(12A)	109.5
C(10)-C(12)-H(12B)	109.5	H(12A)-C(12)-H(12B)	109.5
C(10)-C(12)-H(12C)	109.5	H(12A)-C(12)-H(12C)	109.5
H(12B)-C(12)-H(12C)	109.5	C(10)-C(13)-H(13A)	109.5
C(10)-C(13)-H(13B)	109.5	H(13A)-C(13)-H(13B)	109.5
C(10)-C(13)-H(13C)	109.5	H(13A)-C(13)-H(13C)	109.5
H(13B)-C(13)-H(13C)	109.5	C(2)-C(14)-C(15)	107.4(8)
C(2)-C(14)-C(17)	111(1)	C(15)-C(14)-C(17)	110(1)
C(2)-C(14)-C(16)	115(1)	C(15)-C(14)-C(16)	104(1)
C(17)-C(14)-C(16)	110(1)	C(14)-C(15)-H(15A)	109.5
C(14)-C(15)-H(15B)	109.5	H(15A)-C(15)-H(15B)	109.5
C(14)-C(15)-H(15C)	109.5	H(15A)-C(15)-H(15C)	109.5
H(15B)-C(15)-H(15C)	109.5	C(14)-C(16)-H(16A)	109.5
C(14)-C(16)-H(16B)	109.5	H(16A)-C(16)-H(16B)	109.5
C(14)-C(16)-H(16C)	109.5	H(16A)-C(16)-H(16C)	109.5
H(16B)-C(16)-H(16C)	109.5	C(14)-C(17)-H(17A)	109.5
C(14)-C(17)-H(17B)	109.5	H(17A)-C(17)-H(17B)	109.5
C(14)-C(17)-H(17C)	109.5	H(17A)-C(17)-H(17C)	109.5

H(17B)-C(17)-H(17C)	109.5	C(22)-C(18)-C(19)	112(1)
C(22)-C(18)-Dy(1)	79.0(5)	C(19)-C(18)-Dy(1)	73.4(5)
C(22)-C(18)-H(18)	124.2	C(19)-C(18)-H(18)	124.2
Dy(1)-C(18)-H(18)	115.0	C(20)-C(19)-C(18)	105(1)
C(20)-C(19)-C(31)	127(1)	C(18)-C(19)-C(31)	126(1)
C(20)-C(19)-Dy(1)	74.8(6)	C(18)-C(19)-Dy(1)	76.5(5)
C(31)-C(19)-Dy(1)	128.3(6)	C(19)-C(20)-C(21)	110(1)
C(19)-C(20)-Dy(1)	75.3(6)	C(21)-C(20)-Dy(1)	78.6(6)
C(19)-C(20)-H(20)	125.0	C(21)-C(20)-H(20)	124.9
Dy(1)-C(20)-H(20)	113.2	C(20)-C(21)-C(22)	107(1)
C(20)-C(21)-C(27)	117(1)	C(22)-C(21)-C(27)	135(1)
C(20)-C(21)-Dy(1)	71.9(5)	C(22)-C(21)-Dy(1)	76.8(5)
C(27)-C(21)-Dy(1)	125.5(6)	C(18)-C(22)-C(21)	107(1)
C(18)-C(22)-C(23)	121(1)	C(21)-C(22)-C(23)	130(1)
C(18)-C(22)-Dy(1)	72.7(5)	C(21)-C(22)-Dy(1)	73.8(5)
C(23)-C(22)-Dy(1)	129.8(6)	C(22)-C(23)-C(25)	112.8(8)
C(22)-C(23)-C(26)	111.4(8)	C(25)-C(23)-C(26)	111(1)
C(22)-C(23)-C(24)	110(1)	C(25)-C(23)-C(24)	103.9(8)
C(26)-C(23)-C(24)	108(1)	C(23)-C(24)-H(24A)	109.5
C(23)-C(24)-H(24B)	109.5	H(24A)-C(24)-H(24B)	109.5
C(23)-C(24)-H(24C)	109.5	H(24A)-C(24)-H(24C)	109.5
H(24B)-C(24)-H(24C)	109.5	C(23)-C(25)-H(25A)	109.5
C(23)-C(25)-H(25B)	109.5	H(25A)-C(25)-H(25B)	109.5
C(23)-C(25)-H(25C)	109.5	H(25A)-C(25)-H(25C)	109.5
H(25B)-C(25)-H(25C)	109.5	C(23)-C(26)-H(26A)	109.5
C(23)-C(26)-H(26B)	109.5	H(26A)-C(26)-H(26B)	109.5
C(23)-C(26)-H(26C)	109.5	H(26A)-C(26)-H(26C)	109.5
H(26B)-C(26)-H(26C)	109.5	C(29)-C(27)-C(21)	116(1)
C(29)-C(27)-C(28)	108.6(8)	C(21)-C(27)-C(28)	109(1)
C(29)-C(27)-C(30)	107(1)	C(21)-C(27)-C(30)	109.7(8)
C(28)-C(27)-C(30)	107(1)	C(27)-C(28)-H(28A)	109.5
C(27)-C(28)-H(28B)	109.5	H(28A)-C(28)-H(28B)	109.5
C(27)-C(28)-H(28C)	109.5	H(28A)-C(28)-H(28C)	109.5
H(28B)-C(28)-H(28C)	109.5	C(27)-C(29)-H(29A)	109.5
C(27)-C(29)-H(29B)	109.5	H(29A)-C(29)-H(29B)	109.5
C(27)-C(29)-H(29C)	109.5	H(29A)-C(29)-H(29C)	109.5
H(29B)-C(29)-H(29C)	109.5	C(27)-C(30)-H(30A)	109.5
C(27)-C(30)-H(30B)	109.5	H(30A)-C(30)-H(30B)	109.5
C(27)-C(30)-H(30C)	109.5	H(30A)-C(30)-H(30C)	109.5
H(30B)-C(30)-H(30C)	109.5	C(32)-C(31)-C(34)	108(1)
C(32)-C(31)-C(19)	112(1)	C(34)-C(31)-C(19)	105(1)
C(32)-C(31)-C(33)	112(1)	C(34)-C(31)-C(33)	106(1)
C(19)-C(31)-C(33)	114(1)	C(31)-C(32)-H(32A)	109.5
C(31)-C(32)-H(32B)	109.5	H(32A)-C(32)-H(32B)	109.5
C(31)-C(32)-H(32C)	109.5	H(32A)-C(32)-H(32C)	109.5
H(32B)-C(32)-H(32C)	109.5	C(31)-C(33)-H(33A)	109.5
C(31)-C(33)-H(33B)	109.5	H(33A)-C(33)-H(33B)	109.5
C(31)-C(33)-H(33C)	109.5	H(33A)-C(33)-H(33C)	109.5
H(33B)-C(33)-H(33C)	109.5	C(31)-C(34)-H(34A)	109.5
C(31)-C(34)-H(34B)	109.5	H(34A)-C(34)-H(34B)	109.5
C(31)-C(34)-H(34C)	109.5	H(34A)-C(34)-H(34C)	109.5
H(34B)-C(34)-H(34C)	109.5	O(1)-C(35)-C(36)	127(1)
O(1)-C(35)-C(47)	125(1)	C(36)-C(35)-C(47)	108(1)
C(37)-C(36)-C(35)	132(1)	C(37)-C(36)-C(41)	119(1)
C(35)-C(36)-C(41)	109(1)	C(36)-C(37)-C(38)	118(1)
C(36)-C(37)-H(37)	121.1	C(38)-C(37)-H(37)	121.1
C(39)-C(38)-C(37)	124(1)	C(39)-C(38)-H(38)	118.0
C(37)-C(38)-H(38)	118.0	C(38)-C(39)-C(40)	120(1)
C(38)-C(39)-H(39)	120.1	C(40)-C(39)-H(39)	120.1
C(41)-C(40)-C(39)	117(1)	C(41)-C(40)-H(40)	121.6
C(39)-C(40)-H(40)	121.6	C(40)-C(41)-C(36)	122(1)
C(40)-C(41)-C(42)	130(1)	C(36)-C(41)-C(42)	108(1)
C(43)-C(42)-C(47)	124(1)	C(43)-C(42)-C(41)	130(1)
C(47)-C(42)-C(41)	106(1)	C(44)-C(43)-C(42)	118(1)
C(44)-C(43)-H(43)	121.0	C(42)-C(43)-H(43)	121.0
C(43)-C(44)-C(45)	122(1)	C(43)-C(44)-H(44)	118.9
C(45)-C(44)-H(44)	118.9	C(44)-C(45)-C(46)	120(1)
C(44)-C(45)-H(45)	120.2	C(46)-C(45)-H(45)	120.2
C(47)-C(46)-C(45)	119(1)	C(47)-C(46)-H(46)	120.5
C(45)-C(46)-H(46)	120.5	C(46)-C(47)-C(42)	117(1)

C(46)-C(47)-C(35)	133(1)	C(42)-C(47)-C(35)	110(1)
O(7)-K(1)-O(3)	120.5(2)	O(7)-K(1)-O(4)	168.8(2)
O(3)-K(1)-O(4)	61.0(2)	O(7)-K(1)-O(2)	61.0(2)
O(3)-K(1)-O(2)	59.6(2)	O(4)-K(1)-O(2)	118.3(2)
O(7)-K(1)-O(5)	119.4(2)	O(3)-K(1)-O(5)	119.8(2)
O(4)-K(1)-O(5)	58.9(2)	O(2)-K(1)-O(5)	169.0(2)
O(7)-K(1)-O(6)	61.1(2)	O(3)-K(1)-O(6)	170.8(2)
O(4)-K(1)-O(6)	115.4(2)	O(2)-K(1)-O(6)	120.3(2)
O(5)-K(1)-O(6)	58.3(2)	O(7)-K(1)-C(29)#4	97.4(2)
O(3)-K(1)-C(29)#4	75.5(2)	O(4)-K(1)-C(29)#4	71.8(2)
O(2)-K(1)-C(29)#4	78.5(2)	O(5)-K(1)-C(29)#4	90.7(2)
O(6)-K(1)-C(29)#4	95.4(2)	C(48)-O(2)-C(59)	113.7(8)
C(48)-O(2)-K(1)	114.2(6)	C(59)-O(2)-K(1)	110.5(6)
C(49)-O(3)-C(50)	112(1)	C(49)-O(3)-K(1)	116.7(6)
C(50)-O(3)-K(1)	116.2(6)	C(52)-O(4)-C(51)	117(1)
C(52)-O(4)-K(1)	116.1(6)	C(51)-O(4)-K(1)	111.7(6)
C(54)-O(5)-C(53)	111.7(7)	C(54)-O(5)-K(1)	119.0(6)
C(53)-O(5)-K(1)	117.9(6)	C(55)-O(6)-C(56)	112(1)
C(55)-O(6)-K(1)	113.4(6)	C(56)-O(6)-K(1)	107.4(6)
C(58)-O(7)-C(57)	114.5(8)	C(58)-O(7)-K(1)	117.0(6)
C(57)-O(7)-K(1)	119.0(6)	O(2)-C(48)-C(49)	107(1)
O(2)-C(48)-H(48A)	110.4	C(49)-C(48)-H(48A)	110.4
O(2)-C(48)-H(48B)	110.4	C(49)-C(48)-H(48B)	110.4
H(48A)-C(48)-H(48B)	108.6	O(3)-C(49)-C(48)	112(1)
O(3)-C(49)-H(49A)	109.1	C(48)-C(49)-H(49A)	109.1
O(3)-C(49)-H(49B)	109.1	C(48)-C(49)-H(49B)	109.1
H(49A)-C(49)-H(49B)	107.9	O(3)-C(50)-C(51)	109(1)
O(3)-C(50)-H(50A)	110.0	C(51)-C(50)-H(50A)	110.0
O(3)-C(50)-H(50B)	110.0	C(51)-C(50)-H(50B)	110.0
H(50A)-C(50)-H(50B)	108.3	C(50)-C(51)-O(4)	110(1)
C(50)-C(51)-H(51A)	109.7	O(4)-C(51)-H(51A)	109.7
C(50)-C(51)-H(51B)	109.7	O(4)-C(51)-H(51B)	109.7
H(51A)-C(51)-H(51B)	108.2	O(4)-C(52)-C(53)	111(1)
O(4)-C(52)-H(52A)	109.5	C(53)-C(52)-H(52A)	109.5
O(4)-C(52)-H(52B)	109.5	C(53)-C(52)-H(52B)	109.5
H(52A)-C(52)-H(52B)	108.1	O(5)-C(53)-C(52)	108.4(8)
O(5)-C(53)-H(53A)	110.0	C(52)-C(53)-H(53A)	110.0
O(5)-C(53)-H(53B)	110.0	C(52)-C(53)-H(53B)	110.0
H(53A)-C(53)-H(53B)	108.4	O(5)-C(54)-C(55)	107.5(8)
O(5)-C(54)-H(54A)	110.2	C(55)-C(54)-H(54A)	110.2
O(5)-C(54)-H(54B)	110.2	C(55)-C(54)-H(54B)	110.2
H(54A)-C(54)-H(54B)	108.5	O(6)-C(55)-C(54)	107(1)
O(6)-C(55)-H(55A)	110.4	C(54)-C(55)-H(55A)	110.4
O(6)-C(55)-H(55B)	110.4	C(54)-C(55)-H(55B)	110.4
H(55A)-C(55)-H(55B)	108.6	O(6)-C(56)-C(57)	107(1)
O(6)-C(56)-H(56A)	110.3	C(57)-C(56)-H(56A)	110.3
O(6)-C(56)-H(56B)	110.3	C(57)-C(56)-H(56B)	110.3
H(56A)-C(56)-H(56B)	108.6	O(7)-C(57)-C(56)	107(1)
O(7)-C(57)-H(57A)	110.3	C(56)-C(57)-H(57A)	110.3
O(7)-C(57)-H(57B)	110.3	C(56)-C(57)-H(57B)	110.3
H(57A)-C(57)-H(57B)	108.5	C(59)-C(58)-O(7)	108(1)
C(59)-C(58)-H(58A)	110.2	O(7)-C(58)-H(58A)	110.2
C(59)-C(58)-H(58B)	110.2	O(7)-C(58)-H(58B)	110.2
H(58A)-C(58)-H(58B)	108.5	O(2)-C(59)-C(58)	108.5(8)
O(2)-C(59)-H(59A)	110.0	C(58)-C(59)-H(59A)	110.0
O(2)-C(59)-H(59B)	110.0	C(58)-C(59)-H(59B)	110.0
H(59A)-C(59)-H(59B)	108.4		

Estimated standard deviations are given in the parenthesis.

Symmetry operators ::

1: x, y, z 2: -x, y+1/2, -z+1/2 3: -x, -y, -z

4: x, -y-1/2, z-1/2

[(Cp^{ttt})$_2$Nd(BH$_4$)] (40-BH$_4$)

Compound	fj204
Molecular formula	$C_{34}H_{62}BNd$
Molecular weight	625.89
Crystal habit	pale blue plate
Crystal dimensions(mm)	0.22x0.18x0.12
Crystal system	monoclinic
Space group	$P2_1/c$
a(Å)	10.3570(10)
b(Å)	15.5890(10)
c(Å)	20.6360(10)
α(°)	90.00
β(°)	98.6940(10)
γ(°)	90.00
V(Å^3)	3293.5(4)
Z	4
d(g-cm^{-3})	1.262
F(000)	1324
μ(cm^{-1})	1.595
Absorption corrections	multi-scan ; 0.7204 min, 0.8316 max
Diffractometer	KappaCCD
X-ray source	MoKα
λ(Å)	0.71069
Monochromator	graphite
T (K)	150.0(1)
Scan mode	phi and omega scans
Maximum θ	30.01
HKL ranges	-14 13 ; -21 21 ; -29 28
Reflections measured	23612
Unique data	9077
Rint	0.0235
Reflections used	6290
Criterion	I > 2σI)
Refinement type	Fsqd
Hydrogen atoms	mixed
Parameters refined	350
Reflections / parameter	17
wR2	0.1172
R1	0.0416
Weights a, b	0.0716 ; 1.5553
GoF	1.052
difference peak / hole (e Å^{-3})	7.385(0.158) / -0.747(0.158)

Table. Bond lengths (A) and angles (deg) for fj204

Nd(1)-B(1)	2.634(4)	Nd(1)-C(4)	2.725(3)
Nd(1)-C(21)	2.736(3)	Nd(1)-C(20)	2.737(3)
Nd(1)-C(3)	2.740(3)	Nd(1)-C(22)	2.749(3)
Nd(1)-C(5)	2.752(3)	Nd(1)-H(3B1)	2.76(3)
Nd(1)-C(19)	2.858(3)	Nd(1)-C(2)	2.864(3)
Nd(1)-C(18)	2.864(3)	Nd(1)-C(1)	2.867(3)
Nd(1)-H(2B1)	2.33(3)	Nd(1)-H(4B1)	2.45(3)
C(1)-C(5)	1.426(4)	C(1)-C(2)	1.445(4)
C(1)-C(6)	1.544(4)	C(2)-C(3)	1.430(4)

C(2)-C(10)	1.547(4)	C(3)-C(4)	1.402(4)
C(3)-H(3)	0.9500	C(4)-C(5)	1.410(4)
C(4)-C(14)	1.529(4)	C(5)-H(5)	0.9500
C(6)-C(7)	1.534(5)	C(6)-C(8)	1.542(5)
C(6)-C(9)	1.551(4)	C(7)-H(7A)	0.9800
C(7)-H(7B)	0.9800	C(7)-H(7C)	0.9800
C(8)-H(8A)	0.9800	C(8)-H(8B)	0.9800
C(8)-H(8C)	0.9800	C(9)-H(9A)	0.9800
C(9)-H(9B)	0.9800	C(9)-H(9C)	0.9800
C(10)-C(12)	1.528(5)	C(10)-C(13)	1.538(5)
C(10)-C(11)	1.551(5)	C(11)-H(11A)	0.9800
C(11)-H(11B)	0.9800	C(11)-H(11C)	0.9800
C(12)-H(12A)	0.9800	C(12)-H(12B)	0.9800
C(12)-H(12C)	0.9800	C(13)-H(13A)	0.9800
C(13)-H(13B)	0.9800	C(13)-H(13C)	0.9800
C(14)-C(17)	1.521(5)	C(14)-C(16)	1.523(5)
C(14)-C(15)	1.529(5)	C(15)-H(15A)	0.9800
C(15)-H(15B)	0.9800	C(15)-H(15C)	0.9800
C(16)-H(16A)	0.9800	C(16)-H(16B)	0.9800
C(16)-H(16C)	0.9800	C(17)-H(17A)	0.9800
C(17)-H(17B)	0.9800	C(17)-H(17C)	0.9800
C(18)-C(22)	1.435(4)	C(18)-C(19)	1.455(4)
C(18)-C(23)	1.538(4)	C(19)-C(20)	1.430(4)
C(19)-C(26)	1.544(4)	C(20)-C(21)	1.404(4)
C(20)-H(20)	0.9500	C(21)-C(22)	1.405(4)
C(21)-C(31)	1.522(4)	C(22)-H(22)	0.9500
C(23)-C(29)	1.529(5)	C(23)-C(25)	1.533(4)
C(23)-C(24)	1.546(5)	C(24)-H(24A)	0.9800
C(24)-H(24B)	0.9800	C(24)-H(24C)	0.9800
C(25)-H(25A)	0.9800	C(25)-H(25B)	0.9800
C(25)-H(25C)	0.9800	C(26)-C(30)	1.528(4)
C(26)-C(27)	1.537(5)	C(26)-C(28)	1.541(5)
C(27)-H(27A)	0.9800	C(27)-H(27B)	0.9800
C(27)-H(27C)	0.9800	C(28)-H(28A)	0.9800
C(28)-H(28B)	0.9800	C(28)-H(28C)	0.9800
C(29)-H(29A)	0.9800	C(29)-H(29B)	0.9800
C(29)-H(29C)	0.9800	C(30)-H(30A)	0.9800
C(30)-H(30B)	0.9800	C(30)-H(30C)	0.9800
C(31)-C(33)	1.531(5)	C(31)-C(32)	1.531(5)
C(31)-C(34)	1.532(5)	C(32)-H(32A)	0.9800
C(32)-H(32B)	0.9800	C(32)-H(32C)	0.9800
C(33)-H(33A)	0.9800	C(33)-H(33B)	0.9800
C(33)-H(33C)	0.9800	C(34)-H(34A)	0.9800
C(34)-H(34B)	0.9800	C(34)-H(34C)	0.9800
B(1)-H(1B1)	1.22(3)	B(1)-H(2B1)	1.07(3)
B(1)-H(3B1)	1.25(3)	B(1)-H(4B1)	1.09(3)

B(1)-Nd(1)-C(4)	107.8(1)	B(1)-Nd(1)-C(21)	105.0(1)
C(4)-Nd(1)-C(21)	147.2(1)	B(1)-Nd(1)-C(20)	82.9(1)
C(4)-Nd(1)-C(20)	157.8(1)	C(21)-Nd(1)-C(20)	29.7(1)
B(1)-Nd(1)-C(3)	133.9(1)	C(4)-Nd(1)-C(3)	29.7(1)
C(21)-Nd(1)-C(3)	119.1(1)	C(20)-Nd(1)-C(3)	143.1(1)
B(1)-Nd(1)-C(22)	131.2(1)	C(4)-Nd(1)-C(22)	119.2(1)
C(21)-Nd(1)-C(22)	29.7(1)	C(20)-Nd(1)-C(22)	48.4(1)
C(3)-Nd(1)-C(22)	94.9(1)	B(1)-Nd(1)-C(5)	85.6(1)
C(4)-Nd(1)-C(5)	29.8(1)	C(21)-Nd(1)-C(5)	157.4(1)
C(20)-Nd(1)-C(5)	168.4(1)	C(3)-Nd(1)-C(5)	48.4(1)
C(22)-Nd(1)-C(5)	143.1(1)	B(1)-Nd(1)-H(3B1)	26.6(6)
C(4)-Nd(1)-H(3B1)	83.8(6)	C(21)-Nd(1)-H(3B1)	128.1(6)
C(20)-Nd(1)-H(3B1)	109.3(6)	C(3)-Nd(1)-H(3B1)	107.6(6)
C(22)-Nd(1)-H(3B1)	156.9(6)	C(5)-Nd(1)-H(3B1)	59.1(6)
B(1)-Nd(1)-C(19)	92.1(1)	C(4)-Nd(1)-C(19)	128.7(1)
C(21)-Nd(1)-C(19)	49.2(1)	C(20)-Nd(1)-C(19)	29.51(8)
C(3)-Nd(1)-C(19)	126.3(1)	C(22)-Nd(1)-C(19)	48.6(1)
C(5)-Nd(1)-C(19)	152.1(1)	H(3B1)-Nd(1)-C(19)	116.6(6)
B(1)-Nd(1)-C(2)	123.1(1)	C(4)-Nd(1)-C(2)	49.1(1)
C(21)-Nd(1)-C(2)	110.6(1)	C(20)-Nd(1)-C(2)	140.3(1)

C(3)-Nd(1)-C(2)	29.5(1)	C(22)-Nd(1)-C(2)	98.6(1)
C(5)-Nd(1)-C(2)	48.3(1)	H(3B1)-Nd(1)-C(2)	98.6(6)
C(19)-Nd(1)-C(2)	144.6(1)	B(1)-Nd(1)-C(18)	121.4(1)
C(4)-Nd(1)-C(18)	110.7(1)	C(21)-Nd(1)-C(18)	49.2(1)
C(20)-Nd(1)-C(18)	48.5(1)	C(3)-Nd(1)-C(18)	98.6(1)
C(22)-Nd(1)-C(18)	29.5(1)	C(5)-Nd(1)-C(18)	140.6(1)
H(3B1)-Nd(1)-C(18)	144.5(6)	C(19)-Nd(1)-C(18)	29.5(1)
C(2)-Nd(1)-C(18)	115.5(1)	B(1)-Nd(1)-C(1)	94.1(1)
C(4)-Nd(1)-C(1)	49.1(1)	C(21)-Nd(1)-C(1)	128.4(1)
C(20)-Nd(1)-C(1)	151.7(1)	C(3)-Nd(1)-C(1)	48.4(1)
C(22)-Nd(1)-C(1)	126.0(1)	C(5)-Nd(1)-C(1)	29.31(8)
H(3B1)-Nd(1)-C(1)	69.5(6)	C(19)-Nd(1)-C(1)	173.8(1)
C(2)-Nd(1)-C(1)	29.2(1)	C(18)-Nd(1)-C(1)	144.4(1)
B(1)-Nd(1)-H(2B1)	24.0(6)	C(4)-Nd(1)-H(2B1)	102.2(8)
C(21)-Nd(1)-H(2B1)	108(1)	C(20)-Nd(1)-H(2B1)	79.5(8)
C(3)-Nd(1)-H(2B1)	131.9(8)	C(22)-Nd(1)-H(2B1)	124.8(8)
C(5)-Nd(1)-H(2B1)	90.0(8)	H(3B1)-Nd(1)-H(2B1)	40.1(8)
C(19)-Nd(1)-H(2B1)	77.5(8)	C(2)-Nd(1)-H(2B1)	136.7(8)
C(18)-Nd(1)-H(2B1)	104.4(7)	C(1)-Nd(1)-H(2B1)	108.4(8)
B(1)-Nd(1)-H(4B1)	24.4(6)	C(4)-Nd(1)-H(4B1)	121.6(7)
C(21)-Nd(1)-H(4B1)	89.1(7)	C(20)-Nd(1)-H(4B1)	75.8(8)
C(3)-Nd(1)-H(4B1)	137.9(8)	C(22)-Nd(1)-H(4B1)	118.6(7)
C(5)-Nd(1)-H(4B1)	93.5(8)	H(3B1)-Nd(1)-H(4B1)	39.2(8)
C(19)-Nd(1)-H(4B1)	95.7(8)	C(2)-Nd(1)-H(4B1)	114.6(8)
C(18)-Nd(1)-H(4B1)	123.3(8)	C(1)-Nd(1)-H(4B1)	89.8(8)
H(2B1)-Nd(1)-H(4B1)	46.8(8)	C(5)-C(1)-C(2)	106.5(3)
C(5)-C(1)-C(6)	119.8(3)	C(2)-C(1)-C(6)	133.0(3)
C(5)-C(1)-Nd(1)	70.9(2)	C(2)-C(1)-Nd(1)	75.3(2)
C(6)-C(1)-Nd(1)	125.4(2)	C(3)-C(2)-C(1)	106.3(3)
C(3)-C(2)-C(10)	117.6(3)	C(1)-C(2)-C(10)	133.8(3)
C(3)-C(2)-Nd(1)	70.5(2)	C(1)-C(2)-Nd(1)	75.5(2)
C(10)-C(2)-Nd(1)	131.2(2)	C(4)-C(3)-C(2)	110.4(3)
C(4)-C(3)-Nd(1)	74.5(2)	C(2)-C(3)-Nd(1)	80.1(2)
C(4)-C(3)-H(3)	124.8	C(2)-C(3)-H(3)	124.8
Nd(1)-C(3)-H(3)	112.6	C(3)-C(4)-C(5)	106.4(3)
C(3)-C(4)-C(14)	127.7(3)	C(5)-C(4)-C(14)	125.8(3)
C(3)-C(4)-Nd(1)	75.7(2)	C(5)-C(4)-Nd(1)	76.2(2)
C(14)-C(4)-Nd(1)	112.4(2)	C(4)-C(5)-C(1)	110.3(3)
C(4)-C(5)-Nd(1)	74.0(2)	C(1)-C(5)-Nd(1)	79.8(2)
C(4)-C(5)-H(5)	124.9	C(1)-C(5)-H(5)	124.9
Nd(1)-C(5)-H(5)	113.3	C(7)-C(6)-C(8)	105.7(3)
C(7)-C(6)-C(1)	110.0(2)	C(8)-C(6)-C(1)	111.1(3)
C(7)-C(6)-C(9)	105.9(3)	C(8)-C(6)-C(9)	110.1(3)
C(1)-C(6)-C(9)	113.6(3)	C(6)-C(7)-H(7A)	109.5
C(6)-C(7)-H(7B)	109.5	H(7A)-C(7)-H(7B)	109.5
C(6)-C(7)-H(7C)	109.5	H(7A)-C(7)-H(7C)	109.5
H(7B)-C(7)-H(7C)	109.5	C(6)-C(8)-H(8A)	109.5
C(6)-C(8)-H(8B)	109.5	H(8A)-C(8)-H(8B)	109.5
C(6)-C(8)-H(8C)	109.5	H(8A)-C(8)-H(8C)	109.5
H(8B)-C(8)-H(8C)	109.5	C(6)-C(9)-H(9A)	109.5
C(6)-C(9)-H(9B)	109.5	H(9A)-C(9)-H(9B)	109.5
C(6)-C(9)-H(9C)	109.5	H(9A)-C(9)-H(9C)	109.5
H(9B)-C(9)-H(9C)	109.5	C(12)-C(10)-C(13)	106.3(3)
C(12)-C(10)-C(2)	116.5(3)	C(13)-C(10)-C(2)	110.7(3)
C(12)-C(10)-C(11)	108.9(3)	C(13)-C(10)-C(11)	106.2(3)
C(2)-C(10)-C(11)	107.7(3)	C(10)-C(11)-H(11A)	109.5
C(10)-C(11)-H(11B)	109.5	H(11A)-C(11)-H(11B)	109.5
C(10)-C(11)-H(11C)	109.5	H(11A)-C(11)-H(11C)	109.5
H(11B)-C(11)-H(11C)	109.5	C(10)-C(12)-H(12A)	109.5
C(10)-C(12)-H(12B)	109.5	H(12A)-C(12)-H(12B)	109.5
C(10)-C(12)-H(12C)	109.5	H(12A)-C(12)-H(12C)	109.5
H(12B)-C(12)-H(12C)	109.5	C(10)-C(13)-H(13A)	109.5
C(10)-C(13)-H(13B)	109.5	H(13A)-C(13)-H(13B)	109.5
C(10)-C(13)-H(13C)	109.5	H(13A)-C(13)-H(13C)	109.5
H(13B)-C(13)-H(13C)	109.5	C(17)-C(14)-C(16)	109.1(3)
C(17)-C(14)-C(4)	111.2(3)	C(16)-C(14)-C(4)	111.1(3)
C(17)-C(14)-C(15)	108.1(3)	C(16)-C(14)-C(15)	109.7(3)
C(4)-C(14)-C(15)	107.6(3)	C(14)-C(15)-H(15A)	109.5
C(14)-C(15)-H(15B)	109.5	H(15A)-C(15)-H(15B)	109.5
C(14)-C(15)-H(15C)	109.5	H(15A)-C(15)-H(15C)	109.5

H(15B)-C(15)-H(15C)	109.5	C(14)-C(16)-H(16A)	109.5
C(14)-C(16)-H(16B)	109.5	H(16A)-C(16)-H(16B)	109.5
C(14)-C(16)-H(16C)	109.5	H(16A)-C(16)-H(16C)	109.5
H(16B)-C(16)-H(16C)	109.5	C(14)-C(17)-H(17A)	109.5
C(14)-C(17)-H(17B)	109.5	H(17A)-C(17)-H(17B)	109.5
C(14)-C(17)-H(17C)	109.5	H(17A)-C(17)-H(17C)	109.5
H(17B)-C(17)-H(17C)	109.5	C(22)-C(18)-C(19)	106.1(3)
C(22)-C(18)-C(23)	117.7(3)	C(19)-C(18)-C(23)	133.5(3)
C(22)-C(18)-Nd(1)	70.8(2)	C(19)-C(18)-Nd(1)	75.1(2)
C(23)-C(18)-Nd(1)	132.5(2)	C(20)-C(19)-C(18)	106.0(3)
C(20)-C(19)-C(26)	119.9(3)	C(18)-C(19)-C(26)	133.6(3)
C(20)-C(19)-Nd(1)	70.5(2)	C(18)-C(19)-Nd(1)	75.5(2)
C(26)-C(19)-Nd(1)	124.2(2)	C(21)-C(20)-C(19)	110.8(3)
C(21)-C(20)-Nd(1)	75.1(2)	C(19)-C(20)-Nd(1)	80.0(2)
C(21)-C(20)-H(20)	124.6	C(19)-C(20)-H(20)	124.6
Nd(1)-C(20)-H(20)	112.3	C(20)-C(21)-C(22)	106.4(3)
C(20)-C(21)-C(31)	125.7(3)	C(22)-C(21)-C(31)	127.8(3)
C(20)-C(21)-Nd(1)	75.2(2)	C(22)-C(21)-Nd(1)	75.7(2)
C(31)-C(21)-Nd(1)	114.3(2)	C(21)-C(22)-C(18)	110.5(3)
C(21)-C(22)-Nd(1)	74.7(2)	C(18)-C(22)-Nd(1)	79.7(2)
C(21)-C(22)-H(22)	124.8	C(18)-C(22)-H(22)	124.8
Nd(1)-C(22)-H(22)	112.9	C(29)-C(23)-C(25)	106.1(3)
C(29)-C(23)-C(18)	110.5(3)	C(25)-C(23)-C(18)	116.7(3)
C(29)-C(23)-C(24)	107.1(3)	C(25)-C(23)-C(24)	108.6(3)
C(18)-C(23)-C(24)	107.5(3)	C(23)-C(24)-H(24A)	109.5
C(23)-C(24)-H(24B)	109.5	H(24A)-C(24)-H(24B)	109.5
C(23)-C(24)-H(24C)	109.5	H(24A)-C(24)-H(24C)	109.5
H(24B)-C(24)-H(24C)	109.5	C(23)-C(25)-H(25A)	109.5
C(23)-C(25)-H(25B)	109.5	H(25A)-C(25)-H(25B)	109.5
C(23)-C(25)-H(25C)	109.5	H(25A)-C(25)-H(25C)	109.5
H(25B)-C(25)-H(25C)	109.5	C(30)-C(26)-C(27)	106.4(3)
C(30)-C(26)-C(28)	109.4(3)	C(27)-C(26)-C(28)	105.3(3)
C(30)-C(26)-C(19)	115.0(3)	C(27)-C(26)-C(19)	110.4(3)
C(28)-C(26)-C(19)	109.9(3)	C(26)-C(27)-H(27A)	109.5
C(26)-C(27)-H(27B)	109.5	H(27A)-C(27)-H(27B)	109.5
C(26)-C(27)-H(27C)	109.5	H(27A)-C(27)-H(27C)	109.5
H(27B)-C(27)-H(27C)	109.5	C(26)-C(28)-H(28A)	109.5
C(26)-C(28)-H(28B)	109.5	H(28A)-C(28)-H(28B)	109.5
C(26)-C(28)-H(28C)	109.5	H(28A)-C(28)-H(28C)	109.5
H(28B)-C(28)-H(28C)	109.5	C(23)-C(29)-H(29A)	109.5
C(23)-C(29)-H(29B)	109.5	H(29A)-C(29)-H(29B)	109.5
C(23)-C(29)-H(29C)	109.5	H(29A)-C(29)-H(29C)	109.5
H(29B)-C(29)-H(29C)	109.5	C(26)-C(30)-H(30A)	109.5
C(26)-C(30)-H(30B)	109.5	H(30A)-C(30)-H(30B)	109.5
C(26)-C(30)-H(30C)	109.5	H(30A)-C(30)-H(30C)	109.5
H(30B)-C(30)-H(30C)	109.5	C(21)-C(31)-C(33)	111.4(3)
C(21)-C(31)-C(32)	108.6(3)	C(33)-C(31)-C(32)	108.9(3)
C(21)-C(31)-C(34)	110.3(3)	C(33)-C(31)-C(34)	108.6(3)
C(32)-C(31)-C(34)	109.0(3)	C(31)-C(32)-H(32A)	109.5
C(31)-C(32)-H(32B)	109.5	H(32A)-C(32)-H(32B)	109.5
C(31)-C(32)-H(32C)	109.5	H(32A)-C(32)-H(32C)	109.5
H(32B)-C(32)-H(32C)	109.5	C(31)-C(33)-H(33A)	109.5
C(31)-C(33)-H(33B)	109.5	H(33A)-C(33)-H(33B)	109.5
C(31)-C(33)-H(33C)	109.5	H(33A)-C(33)-H(33C)	109.5
H(33B)-C(33)-H(33C)	109.5	C(31)-C(34)-H(34A)	109.5
C(31)-C(34)-H(34B)	109.5	H(34A)-C(34)-H(34B)	109.5
C(31)-C(34)-H(34C)	109.5	H(34A)-C(34)-H(34C)	109.5
H(34B)-C(34)-H(34C)	109.5	Nd(1)-B(1)-H(1B1)	175(2)
Nd(1)-B(1)-H(2B1)	62(2)	H(1B1)-B(1)-H(2B1)	115(2)
Nd(1)-B(1)-H(3B1)	82(2)	H(1B1)-B(1)-H(3B1)	103(2)
H(2B1)-B(1)-H(3B1)	101(2)	Nd(1)-B(1)-H(4B1)	69(2)
H(1B1)-B(1)-H(4B1)	111(2)	H(2B1)-B(1)-H(4B1)	123(3)
H(3B1)-B(1)-H(4B1)	98(2)		

[(Cp^{ttt})$_2$Nd(μ-I)K([18]crown-6)] (41)

Compound	fj230
Molecular formula	$C_{46}H_{82}IKNdO_6$,C_6H_{12}
Molecular weight	2251.02
Crystal habit	Dark Red Plate
Crystal dimensions(mm)	0.12x0.10x0.04
Crystal system	triclinic
Space group	Pbar1
a(≈)	13.593(1)
b(≈)	14.136(1)
c(≈)	16.101(1)
α(∞)	81.546(1)
β(∞)	74.412(1)
γ(∞)	70.613(1)
V(≈^{3})	2805.4(3)
Z	1
d(g-cm^{-3})	1.332
F(000)	1172
μ(cm^{-1})	1.592
Absorption corrections	multi-scan ; 0.8319 min, 0.9391 max
Diffractometer	KappaCCD
X-ray source	MoKα
λ(≈)	0.71069
Monochromator	graphite
T (K)	150.0(1)
Scan mode	phi and omega scans
Maximum θ	25.35
HKL ranges	-16 16 ; -17 16 ; -18 19
Reflections measured	23274
Unique data	10106
Rint	0.0497
Reflections used	7008
Criterion	I > 2σ(I)
Refinement type	Fsqd
Hydrogen atoms	constr
Parameters refined	568
Reflections / parameter	12
wR2	0.1587
R1	0.0607
Weights a, b	0.0580 ; 9.9887
GoF	1.025
difference peak / hole (e ≈$^{-3}$)	2.015(0.096) / -1.694(0.096)

Table. Bond lengths (A) and angles (deg) for fj230

Nd(1)-C(1)	2.742(7)	Nd(1)-C(5)	2.747(6)
Nd(1)-C(18)	2.756(7)	Nd(1)-C(4)	2.771(7)
Nd(1)-C(19)	2.776(7)	Nd(1)-C(20)	2.798(7)
Nd(1)-C(22)	2.824(7)	Nd(1)-C(2)	2.856(7)
Nd(1)-C(21)	2.869(7)	Nd(1)-C(3)	2.888(7)
Nd(1)-I(1A)	3.1565(6	I(1A)-K(1)	3.408(2)
K(1)-O(1)	2.755(5)	K(1)-O(5)	2.759(6)

K(1)-O(4)	2.769(6)	K(1)-O(2)	2.800(6)
K(1)-O(3)	2.808(5)	K(1)-O(6)	2.895(6)
K(1)-C(36)	3.49(1)	K(1)-C(41)	3.52(1)
O(1)-C(46)	1.42(1)	O(1)-C(35)	1.43(1)
O(2)-C(36)	1.40(1)	O(2)-C(37)	1.42(1)
O(3)-C(38)	1.41(1)	O(3)-C(39)	1.42(1)
O(4)-C(41)	1.37(1)	O(4)-C(40)	1.43(1)
O(5)-C(43)	1.41(1)	O(5)-C(42)	1.42(1)
O(6)-C(44)	1.36(1)	O(6)-C(45)	1.43(1)
C(1)-C(5)	1.40(1)	C(1)-C(2)	1.43(1)
C(1)-H(1)	0.9500	C(2)-C(3)	1.44(1)
C(2)-C(14)	1.53(1)	C(3)-C(4)	1.41(1)
C(3)-C(10)	1.55(1)	C(4)-C(5)	1.40(1)
C(4)-H(4)	0.9500	C(5)-C(6)	1.52(1)
C(6)-C(8)	1.49(1)	C(6)-C(7)	1.52(1)
C(6)-C(9)	1.61(1)	C(7)-H(7A)	0.9800
C(7)-H(7B)	0.9800	C(7)-H(7C)	0.9800
C(8)-H(8A)	0.9800	C(8)-H(8B)	0.9800
C(8)-H(8C)	0.9800	C(9)-H(9A)	0.9800
C(9)-H(9B)	0.9800	C(9)-H(9C)	0.9800
C(10)-C(12)	1.52(1)	C(10)-C(13)	1.53(1)
C(10)-C(11)	1.54(1)	C(11)-H(11A)	0.9800
C(11)-H(11B)	0.9800	C(11)-H(11C)	0.9800
C(12)-H(12A)	0.9800	C(12)-H(12B)	0.9800
C(12)-H(12C)	0.9800	C(13)-H(13A)	0.9800
C(13)-H(13B)	0.9800	C(13)-H(13C)	0.9800
C(14)-C(15)	1.53(1)	C(14)-C(17)	1.53(1)
C(14)-C(16)	1.54(1)	C(15)-H(15A)	0.9800
C(15)-H(15B)	0.9800	C(15)-H(15C)	0.9800
C(16)-H(16A)	0.9800	C(16)-H(16B)	0.9800
C(16)-H(16C)	0.9800	C(17)-H(17A)	0.9800
C(17)-H(17B)	0.9800	C(17)-H(17C)	0.9800
C(18)-C(19)	1.39(1)	C(18)-C(22)	1.43(1)
C(18)-H(18)	0.9500	C(19)-C(20)	1.41(1)
C(19)-C(31)	1.53(1)	C(20)-C(21)	1.45(1)
C(20)-H(20)	0.9500	C(21)-C(22)	1.42(1)
C(21)-C(27)	1.55(1)	C(22)-C(23)	1.54(1)
C(23)-C(25)	1.49(1)	C(23)-C(24)	1.51(1)
C(23)-C(26)	1.56(1)	C(24)-H(24A)	0.9800
C(24)-H(24B)	0.9800	C(24)-H(24C)	0.9800
C(25)-H(25A)	0.9800	C(25)-H(25B)	0.9800
C(25)-H(25C)	0.9800	C(26)-H(26A)	0.9800
C(26)-H(26B)	0.9800	C(26)-H(26C)	0.9800
C(27)-C(29)	1.50(1)	C(27)-C(28)	1.51(1)
C(27)-C(30)	1.51(1)	C(28)-H(28A)	0.9800
C(28)-H(28B)	0.9800	C(28)-H(28C)	0.9800
C(29)-H(29A)	0.9800	C(29)-H(29B)	0.9800
C(29)-H(29C)	0.9800	C(30)-H(30A)	0.9800
C(30)-H(30B)	0.9800	C(30)-H(30C)	0.9800
C(31)-C(32)	1.51(1)	C(31)-C(33)	1.52(1)
C(31)-C(34)	1.54(1)	C(32)-H(32A)	0.9800
C(32)-H(32B)	0.9800	C(32)-H(32C)	0.9800
C(33)-H(33A)	0.9800	C(33)-H(33B)	0.9800
C(33)-H(33C)	0.9800	C(34)-H(34A)	0.9800
C(34)-H(34B)	0.9800	C(34)-H(34C)	0.9800
C(35)-C(36)	1.49(1)	C(35)-H(35A)	0.9900
C(35)-H(35B)	0.9900	C(36)-H(36A)	0.9900
C(36)-H(36B)	0.9900	C(37)-C(38)	1.47(1)
C(37)-H(37A)	0.9900	C(37)-H(37B)	0.9900
C(38)-H(38A)	0.9900	C(38)-H(38B)	0.9900
C(39)-C(40)	1.50(1)	C(39)-H(39A)	0.9900
C(39)-H(39B)	0.9900	C(40)-H(40A)	0.9900
C(40)-H(40B)	0.9900	C(41)-C(42)	1.49(1)
C(41)-H(41A)	0.9900	C(41)-H(41B)	0.9900
C(42)-H(42A)	0.9900	C(42)-H(42B)	0.9900
C(43)-C(44)	1.51(1)	C(43)-H(43A)	0.9900
C(43)-H(43B)	0.9900	C(44)-H(44A)	0.9900
C(44)-H(44B)	0.9900	C(45)-C(46)	1.48(1)

C(45)-H(45A)	0.9900	C(45)-H(45B)	0.9900
C(46)-H(46A)	0.9900	C(46)-H(46B)	0.9900
C(47)-C(48)	1.35(3)	C(47)-C(52)	1.47(2)
C(47)-H(47A)	0.9900	C(47)-H(47B)	0.9900
C(48)-C(49)	1.40(2)	C(48)-H(48A)	0.9900
C(48)-H(48B)	0.9900	C(49)-C(50)	1.53(2)
C(49)-H(49A)	0.9900	C(49)-H(49B)	0.9900
C(50)-C(51)	1.35(2)	C(50)-H(50A)	0.9900
C(50)-H(50B)	0.9900	C(51)-C(52)	1.32(2)
C(51)-H(51A)	0.9900	C(51)-H(51B)	0.9900
C(52)-H(52A)	0.9900	C(52)-H(52B)	0.9900

C(1)-Nd(1)-C(5)	29.6(2)	C(1)-Nd(1)-C(18)	151.3(2)
C(5)-Nd(1)-C(18)	158.1(2)	C(1)-Nd(1)-C(4)	47.4(2)
C(5)-Nd(1)-C(4)	29.3(2)	C(18)-Nd(1)-C(4)	160.8(2)
C(1)-Nd(1)-C(19)	132.9(2)	C(5)-Nd(1)-C(19)	161.9(2)
C(18)-Nd(1)-C(19)	29.1(2)	C(4)-Nd(1)-C(19)	157.3(2)
C(1)-Nd(1)-C(20)	106.5(2)	C(5)-Nd(1)-C(20)	133.1(2)
C(18)-Nd(1)-C(20)	47.7(2)	C(4)-Nd(1)-C(20)	150.6(2)
C(19)-Nd(1)-C(20)	29.4(2)	C(1)-Nd(1)-C(22)	126.8(2)
C(5)-Nd(1)-C(22)	129.6(2)	C(18)-Nd(1)-C(22)	29.7(2)
C(4)-Nd(1)-C(22)	153.4(2)	C(19)-Nd(1)-C(22)	49.1(2)
C(20)-Nd(1)-C(22)	48.4(2)	C(1)-Nd(1)-C(2)	29.5(2)
C(5)-Nd(1)-C(2)	49.2(2)	C(18)-Nd(1)-C(2)	147.9(2)
C(4)-Nd(1)-C(2)	47.7(2)	C(19)-Nd(1)-C(2)	118.9(2)
C(20)-Nd(1)-C(2)	103.2(2)	C(22)-Nd(1)-C(2)	144.4(2)
C(1)-Nd(1)-C(21)	103.7(2)	C(5)-Nd(1)-C(21)	119.5(2)
C(18)-Nd(1)-C(21)	47.9(2)	C(4)-Nd(1)-C(21)	148.5(2)
C(19)-Nd(1)-C(21)	48.8(2)	C(20)-Nd(1)-C(21)	29.5(2)
C(22)-Nd(1)-C(21)	29.0(2)	C(2)-Nd(1)-C(21)	115.6(2)
C(1)-Nd(1)-C(3)	48.0(2)	C(5)-Nd(1)-C(3)	48.9(2)
C(18)-Nd(1)-C(3)	152.8(2)	C(4)-Nd(1)-C(3)	28.8(2)
C(19)-Nd(1)-C(3)	129.7(2)	C(20)-Nd(1)-C(3)	126.7(2)
C(22)-Nd(1)-C(3)	173.5(2)	C(2)-Nd(1)-C(3)	29.1(2)
C(21)-Nd(1)-C(3)	144.5(2)	C(1)-Nd(1)-I(1A)	129.4(2)
C(5)-Nd(1)-I(1A)	104.2(2)	C(18)-Nd(1)-I(1A)	79.0(2)
C(4)-Nd(1)-I(1A)	81.9(2)	C(19)-Nd(1)-I(1A)	93.7(2)
C(20)-Nd(1)-I(1A)	122.7(2)	C(22)-Nd(1)-I(1A)	96.9(2)
C(2)-Nd(1)-I(1A)	118.4(2)	C(21)-Nd(1)-I(1A)	124.7(2)
C(3)-Nd(1)-I(1A)	89.6(1)	Nd(1)-I(1A)-K(1)	132.89(3)
O(1)-K(1)-O(5)	107.4(2)	O(1)-K(1)-O(4)	164.3(2)
O(5)-K(1)-O(4)	60.0(2)	O(1)-K(1)-O(2)	61.1(2)
O(5)-K(1)-O(2)	129.0(2)	O(4)-K(1)-O(2)	117.7(2)
O(1)-K(1)-O(3)	120.5(2)	O(5)-K(1)-O(3)	108.3(2)
O(4)-K(1)-O(3)	60.5(2)	O(2)-K(1)-O(3)	59.4(2)
O(1)-K(1)-O(6)	59.4(2)	O(5)-K(1)-O(6)	59.0(2)
O(4)-K(1)-O(6)	114.5(2)	O(2)-K(1)-O(6)	117.8(2)
O(3)-K(1)-O(6)	162.9(2)	O(1)-K(1)-I(1A)	92.6(1)
O(5)-K(1)-I(1A)	145.7(2)	O(4)-K(1)-I(1A)	103.1(1)
O(2)-K(1)-I(1A)	85.1(1)	O(3)-K(1)-I(1A)	83.3(1)
O(6)-K(1)-I(1A)	113.7(1)	O(1)-K(1)-C(36)	42.7(2)
O(5)-K(1)-C(36)	136.9(2)	O(4)-K(1)-C(36)	139.4(2)
O(2)-K(1)-C(36)	22.4(2)	O(3)-K(1)-C(36)	79.3(2)
O(6)-K(1)-C(36)	102.1(2)	I(1A)-K(1)-C(36)	76.2(2)
O(1)-K(1)-C(41)	143.5(2)	O(5)-K(1)-C(41)	42.2(2)
O(4)-K(1)-C(41)	21.0(2)	O(2)-K(1)-C(41)	116.9(2)
O(3)-K(1)-C(41)	69.4(2)	O(6)-K(1)-C(41)	100.6(2)
I(1A)-K(1)-C(41)	124.0(2)	C(36)-K(1)-C(41)	138.8(3)
C(46)-O(1)-C(35)	112.3(6)	C(46)-O(1)-K(1)	121.6(5)
C(35)-O(1)-K(1)	116.8(5)	C(36)-O(2)-C(37)	112.7(7)
C(36)-O(2)-K(1)	107.7(5)	C(37)-O(2)-K(1)	111.7(5)
C(38)-O(3)-C(39)	114.5(6)	C(38)-O(3)-K(1)	117.4(5)
C(39)-O(3)-K(1)	118.4(5)	C(41)-O(4)-C(40)	113.7(7)
C(41)-O(4)-K(1)	112.5(5)	C(40)-O(4)-K(1)	113.8(5)
C(43)-O(5)-C(42)	112.6(7)	C(43)-O(5)-K(1)	119.8(5)
C(42)-O(5)-K(1)	117.7(5)	C(44)-O(6)-C(45)	113.0(7)
C(44)-O(6)-K(1)	109.2(5)	C(45)-O(6)-K(1)	113.2(5)
C(5)-C(1)-C(2)	111.1(6)	C(5)-C(1)-Nd(1)	75.4(4)
C(2)-C(1)-Nd(1)	79.6(4)	C(5)-C(1)-H(1)	124.4

C(2)-C(1)-H(1)	124.4	Nd(1)-C(1)-H(1)	112.5
C(1)-C(2)-C(3)	105.9(6)	C(1)-C(2)-C(14)	119.5(7)
C(3)-C(2)-C(14)	133.2(7)	C(1)-C(2)-Nd(1)	70.8(4)
C(3)-C(2)-Nd(1)	76.7(4)	C(14)-C(2)-Nd(1)	126.8(5)
C(4)-C(3)-C(2)	105.7(6)	C(4)-C(3)-C(10)	120.9(6)
C(2)-C(3)-C(10)	133.1(7)	C(4)-C(3)-Nd(1)	71.0(4)
C(2)-C(3)-Nd(1)	74.2(4)	C(10)-C(3)-Nd(1)	124.7(4)
C(5)-C(4)-C(3)	112.4(7)	C(5)-C(4)-Nd(1)	74.3(4)
C(3)-C(4)-Nd(1)	80.2(4)	C(5)-C(4)-H(4)	123.8
C(3)-C(4)-H(4)	123.8	Nd(1)-C(4)-H(4)	113.3
C(4)-C(5)-C(1)	104.8(6)	C(4)-C(5)-C(6)	125.5(7)
C(1)-C(5)-C(6)	129.6(7)	C(4)-C(5)-Nd(1)	76.3(4)
C(1)-C(5)-Nd(1)	75.0(4)	C(6)-C(5)-Nd(1)	115.9(5)
C(8)-C(6)-C(5)	116.2(7)	C(8)-C(6)-C(7)	114(1)
C(5)-C(6)-C(7)	112.4(7)	C(8)-C(6)-C(9)	102(1)
C(5)-C(6)-C(9)	106.9(7)	C(7)-C(6)-C(9)	103.3(7)
C(6)-C(7)-H(7A)	109.5	C(6)-C(7)-H(7B)	109.5
H(7A)-C(7)-H(7B)	109.5	C(6)-C(7)-H(7C)	109.5
H(7A)-C(7)-H(7C)	109.5	H(7B)-C(7)-H(7C)	109.5
C(6)-C(8)-H(8A)	109.5	C(6)-C(8)-H(8B)	109.5
H(8A)-C(8)-H(8B)	109.5	C(6)-C(8)-H(8C)	109.5
H(8A)-C(8)-H(8C)	109.5	H(8B)-C(8)-H(8C)	109.5
C(6)-C(9)-H(9A)	109.5	C(6)-C(9)-H(9B)	109.5
H(9A)-C(9)-H(9B)	109.5	C(6)-C(9)-H(9C)	109.5
H(9A)-C(9)-H(9C)	109.5	H(9B)-C(9)-H(9C)	109.5
C(12)-C(10)-C(13)	106.8(7)	C(12)-C(10)-C(11)	105.4(6)
C(13)-C(10)-C(11)	109.8(7)	C(12)-C(10)-C(3)	110.6(6)
C(13)-C(10)-C(3)	110.8(6)	C(11)-C(10)-C(3)	113.2(6)
C(10)-C(11)-H(11A)	109.5	C(10)-C(11)-H(11B)	109.5
H(11A)-C(11)-H(11B)	109.5	C(10)-C(11)-H(11C)	109.5
H(11A)-C(11)-H(11C)	109.5	H(11B)-C(11)-H(11C)	109.5
C(10)-C(12)-H(12A)	109.5	C(10)-C(12)-H(12B)	109.5
H(12A)-C(12)-H(12B)	109.5	C(10)-C(12)-H(12C)	109.5
H(12A)-C(12)-H(12C)	109.5	H(12B)-C(12)-H(12C)	109.5
C(10)-C(13)-H(13A)	109.5	C(10)-C(13)-H(13B)	109.5
H(13A)-C(13)-H(13B)	109.5	C(10)-C(13)-H(13C)	109.5
H(13A)-C(13)-H(13C)	109.5	H(13B)-C(13)-H(13C)	109.5
C(15)-C(14)-C(2)	116.5(7)	C(15)-C(14)-C(17)	104.5(8)
C(2)-C(14)-C(17)	110.6(7)	C(15)-C(14)-C(16)	107.8(7)
C(2)-C(14)-C(16)	108.4(6)	C(17)-C(14)-C(16)	108.7(7)
C(14)-C(15)-H(15A)	109.5	C(14)-C(15)-H(15B)	109.5
H(15A)-C(15)-H(15B)	109.5	C(14)-C(15)-H(15C)	109.5
H(15A)-C(15)-H(15C)	109.5	H(15B)-C(15)-H(15C)	109.5
C(14)-C(16)-H(16A)	109.5	C(14)-C(16)-H(16B)	109.5
H(16A)-C(16)-H(16B)	109.5	C(14)-C(16)-H(16C)	109.5
H(16A)-C(16)-H(16C)	109.5	H(16B)-C(16)-H(16C)	109.5
C(14)-C(17)-H(17A)	109.5	C(14)-C(17)-H(17B)	109.5
H(17A)-C(17)-H(17B)	109.5	C(14)-C(17)-H(17C)	109.5
H(17A)-C(17)-H(17C)	109.5	H(17B)-C(17)-H(17C)	109.5
C(19)-C(18)-C(22)	110.9(6)	C(19)-C(18)-Nd(1)	76.2(4)
C(22)-C(18)-Nd(1)	77.7(4)	C(19)-C(18)-H(18)	124.5
C(22)-C(18)-H(18)	124.5	Nd(1)-C(18)-H(18)	113.4
C(18)-C(19)-C(20)	106.5(7)	C(18)-C(19)-C(31)	127.2(7)
C(20)-C(19)-C(31)	125.4(7)	C(18)-C(19)-Nd(1)	74.6(4)
C(20)-C(19)-Nd(1)	76.1(4)	C(31)-C(19)-Nd(1)	123.7(5)
C(19)-C(20)-C(21)	109.3(7)	C(19)-C(20)-Nd(1)	74.4(4)
C(21)-C(20)-Nd(1)	77.9(4)	C(19)-C(20)-H(20)	125.4
C(21)-C(20)-H(20)	125.4	Nd(1)-C(20)-H(20)	114.3
C(22)-C(21)-C(20)	106.9(6)	C(22)-C(21)-C(27)	133.5(7)
C(20)-C(21)-C(27)	118.5(7)	C(22)-C(21)-Nd(1)	73.8(4)
C(20)-C(21)-Nd(1)	72.5(4)	C(27)-C(21)-Nd(1)	128.0(5)
C(21)-C(22)-C(18)	106.4(7)	C(21)-C(22)-C(23)	134.2(8)
C(18)-C(22)-C(23)	118.8(7)	C(21)-C(22)-Nd(1)	77.3(4)
C(18)-C(22)-Nd(1)	72.5(4)	C(23)-C(22)-Nd(1)	121.7(5)
C(25)-C(23)-C(24)	111(1)	C(25)-C(23)-C(22)	110.0(8)
C(24)-C(23)-C(22)	112.8(8)	C(25)-C(23)-C(26)	106(1)
C(24)-C(23)-C(26)	100(1)	C(22)-C(23)-C(26)	116.9(8)
C(23)-C(24)-H(24A)	109.5	C(23)-C(24)-H(24B)	109.5

H(24A)-C(24)-H(24B)	109.5	C(23)-C(24)-H(24C)	109.5
H(24A)-C(24)-H(24C)	109.5	H(24B)-C(24)-H(24C)	109.5
C(23)-C(25)-H(25A)	109.5	C(23)-C(25)-H(25B)	109.5
H(25A)-C(25)-H(25B)	109.5	C(23)-C(25)-H(25C)	109.5
H(25A)-C(25)-H(25C)	109.5	H(25B)-C(25)-H(25C)	109.5
C(23)-C(26)-H(26A)	109.5	C(23)-C(26)-H(26B)	109.5
H(26A)-C(26)-H(26B)	109.5	C(23)-C(26)-H(26C)	109.5
H(26A)-C(26)-H(26C)	109.5	H(26B)-C(26)-H(26C)	109.5
C(29)-C(27)-C(28)	107(1)	C(29)-C(27)-C(30)	105(1)
C(28)-C(27)-C(30)	109(1)	C(29)-C(27)-C(21)	112.2(7)
C(28)-C(27)-C(21)	113.2(7)	C(30)-C(27)-C(21)	110.2(7)
C(27)-C(28)-H(28A)	109.5	C(27)-C(28)-H(28B)	109.5
H(28A)-C(28)-H(28B)	109.5	C(27)-C(28)-H(28C)	109.5
H(28A)-C(28)-H(28C)	109.5	H(28B)-C(28)-H(28C)	109.5
C(27)-C(29)-H(29A)	109.5	C(27)-C(29)-H(29B)	109.5
H(29A)-C(29)-H(29B)	109.5	C(27)-C(29)-H(29C)	109.5
H(29A)-C(29)-H(29C)	109.5	H(29B)-C(29)-H(29C)	109.5
C(27)-C(30)-H(30A)	109.5	C(27)-C(30)-H(30B)	109.5
H(30A)-C(30)-H(30B)	109.5	C(27)-C(30)-H(30C)	109.5
H(30A)-C(30)-H(30C)	109.5	H(30B)-C(30)-H(30C)	109.5
C(32)-C(31)-C(33)	109.2(8)	C(32)-C(31)-C(19)	110.6(7)
C(33)-C(31)-C(19)	111.0(6)	C(32)-C(31)-C(34)	110.3(7)
C(33)-C(31)-C(34)	107.9(7)	C(19)-C(31)-C(34)	107.7(7)
C(31)-C(32)-H(32A)	109.5	C(31)-C(32)-H(32B)	109.5
H(32A)-C(32)-H(32B)	109.5	C(31)-C(32)-H(32C)	109.5
H(32A)-C(32)-H(32C)	109.5	H(32B)-C(32)-H(32C)	109.5
C(31)-C(33)-H(33A)	109.5	C(31)-C(33)-H(33B)	109.5
H(33A)-C(33)-H(33B)	109.5	C(31)-C(33)-H(33C)	109.5
H(33A)-C(33)-H(33C)	109.5	H(33B)-C(33)-H(33C)	109.5
C(31)-C(34)-H(34A)	109.5	C(31)-C(34)-H(34B)	109.5
H(34A)-C(34)-H(34B)	109.5	C(31)-C(34)-H(34C)	109.5
H(34A)-C(34)-H(34C)	109.5	H(34B)-C(34)-H(34C)	109.5
O(1)-C(35)-C(36)	108.8(7)	O(1)-C(35)-H(35A)	109.9
C(36)-C(35)-H(35A)	109.9	O(1)-C(35)-H(35B)	109.9
C(36)-C(35)-H(35B)	109.9	H(35A)-C(35)-H(35B)	108.3
O(2)-C(36)-C(35)	109.7(8)	O(2)-C(36)-K(1)	49.9(4)
C(35)-C(36)-K(1)	83.3(5)	O(2)-C(36)-H(36A)	109.7
C(35)-C(36)-H(36A)	109.7	K(1)-C(36)-H(36A)	159.5
O(2)-C(36)-H(36B)	109.7	C(35)-C(36)-H(36B)	109.7
K(1)-C(36)-H(36B)	80.7	H(36A)-C(36)-H(36B)	108.2
O(2)-C(37)-C(38)	108.6(7)	O(2)-C(37)-H(37A)	110.0
C(38)-C(37)-H(37A)	110.0	O(2)-C(37)-H(37B)	110.0
C(38)-C(37)-H(37B)	110.0	H(37A)-C(37)-H(37B)	108.3
O(3)-C(38)-C(37)	108.3(7)	O(3)-C(38)-H(38A)	110.0
C(37)-C(38)-H(38A)	110.0	O(3)-C(38)-H(38B)	110.0
C(37)-C(38)-H(38B)	110.0	H(38A)-C(38)-H(38B)	108.4
O(3)-C(39)-C(40)	107.4(7)	O(3)-C(39)-H(39A)	110.2
C(40)-C(39)-H(39A)	110.2	O(3)-C(39)-H(39B)	110.2
C(40)-C(39)-H(39B)	110.2	H(39A)-C(39)-H(39B)	108.5
O(4)-C(40)-C(39)	112.6(7)	O(4)-C(40)-H(40A)	109.1
C(39)-C(40)-H(40A)	109.1	O(4)-C(40)-H(40B)	109.1
C(39)-C(40)-H(40B)	109.1	H(40A)-C(40)-H(40B)	107.8
O(4)-C(41)-C(42)	109.7(8)	O(4)-C(41)-K(1)	46.5(4)
C(42)-C(41)-K(1)	82.6(5)	O(4)-C(41)-H(41A)	109.7
C(42)-C(41)-H(41A)	109.7	K(1)-C(41)-H(41A)	156.3
O(4)-C(41)-H(41B)	109.7	C(42)-C(41)-H(41B)	109.7
K(1)-C(41)-H(41B)	85.2	H(41A)-C(41)-H(41B)	108.2
O(5)-C(42)-C(41)	108.7(7)	O(5)-C(42)-H(42A)	110.0
C(41)-C(42)-H(42A)	110.0	O(5)-C(42)-H(42B)	110.0
C(41)-C(42)-H(42B)	110.0	H(42A)-C(42)-H(42B)	108.3
O(5)-C(43)-C(44)	108.1(8)	O(5)-C(43)-H(43A)	110.1
C(44)-C(43)-H(43A)	110.1	O(5)-C(43)-H(43B)	110.1
C(44)-C(43)-H(43B)	110.1	H(43A)-C(43)-H(43B)	108.4
O(6)-C(44)-C(43)	109.0(8)	O(6)-C(44)-H(44A)	109.9
C(43)-C(44)-H(44A)	109.9	O(6)-C(44)-H(44B)	109.9
C(43)-C(44)-H(44B)	109.9	H(44A)-C(44)-H(44B)	108.3
O(6)-C(45)-C(46)	113.5(7)	O(6)-C(45)-H(45A)	108.9
C(46)-C(45)-H(45A)	108.9	O(6)-C(45)-H(45B)	108.9
C(46)-C(45)-H(45B)	108.9	H(45A)-C(45)-H(45B)	107.7
O(1)-C(46)-C(45)	108.6(7)	O(1)-C(46)-H(46A)	110.0

C(45)-C(46)-H(46A)	110.0	O(1)-C(46)-H(46B)	110.0
C(45)-C(46)-H(46B)	110.0	H(46A)-C(46)-H(46B)	108.3
C(48)-C(47)-C(52)	114(2)	C(48)-C(47)-H(47A)	108.8
C(52)-C(47)-H(47A)	108.8	C(48)-C(47)-H(47B)	108.8
C(52)-C(47)-H(47B)	108.8	H(47A)-C(47)-H(47B)	107.7
C(47)-C(48)-C(49)	115(2)	C(47)-C(48)-H(48A)	108.6
C(49)-C(48)-H(48A)	108.6	C(47)-C(48)-H(48B)	108.6
C(49)-C(48)-H(48B)	108.6	H(48A)-C(48)-H(48B)	107.6
C(48)-C(49)-C(50)	112(1)	C(48)-C(49)-H(49A)	109.2
C(50)-C(49)-H(49A)	109.2	C(48)-C(49)-H(49B)	109.2
C(50)-C(49)-H(49B)	109.2	H(49A)-C(49)-H(49B)	107.9
C(51)-C(50)-C(49)	114(1)	C(51)-C(50)-H(50A)	108.7
C(49)-C(50)-H(50A)	108.7	C(51)-C(50)-H(50B)	108.7
C(49)-C(50)-H(50B)	108.7	H(50A)-C(50)-H(50B)	107.6
C(52)-C(51)-C(50)	121(2)	C(52)-C(51)-H(51A)	107.2
C(50)-C(51)-H(51A)	107.2	C(52)-C(51)-H(51B)	107.2
C(50)-C(51)-H(51B)	107.2	H(51A)-C(51)-H(51B)	106.8
C(51)-C(52)-C(47)	113(2)	C(51)-C(52)-H(52A)	109.0
C(47)-C(52)-H(52A)	109.0	C(51)-C(52)-H(52B)	109.0
C(47)-C(52)-H(52B)	109.0	H(52A)-C(52)-H(52B)	107.8

Part III

[{Li(THF)$_4$}{(SPCPS)$_2$Sm}] (4b) (230K)

Compound	smbiscarb_230
Molecular formula	$C_{50}H_{40}P_4S_4Sm$,$C_{16}H_{32}LiO_4$
Molecular weight	1338.65
Crystal habit	
Crystal dimensions(mm)	0.20x0.20x0.12
Crystal system	
Space group	C2/c
a(Å)	26.7970(10)
b(Å)	14.5650(10)
c(Å)	16.9830(10)
α(°)	90.00
β(°)	98.5700(10)
γ(°)	90.00
V(Å^3)	6554.4(6)
Z	4
d(g-cm^{-3})	1.357
F(000)	2756
μ(cm^{-1})	1.166
Absorption corrections	multi-scan ; 0.8003 min, 0.8728 max
Diffractometer	KappaCCD
X-ray source	MoKα
λ(Å)	0.71069
Monochromator	graphite
T (K)	230.0(2)
Scan mode	phi and omega scans
Maximum θ	22.98
HKL ranges	-29 29 ; -15 16 ; -18 18
Reflections measured	6516

Unique data	4165
Rint	0.0321
Reflections used	3983
Criterion	I > 2σI)
Refinement type	Fsqd
Hydrogen atoms	mixed
Parameters refined	348
Reflections / parameter	11
wR2	0.1666
R1	0.0593
Weights a, b	0.0651 ; 83.188
GoF	1.133
difference peak / hole (e Å^{-3})	0.799(0.092) / -1.003(0.092)

Table. Bond lengths (A) and angles (deg) for smbiscarb_230

Sm(1)-C(1)	2.448(8)	Sm(1)-C(1)#2	2.448(8)
Sm(1)-S(1)#2	2.833(2)	Sm(1)-S(1)	2.833(2)
Sm(1)-S(2)	2.835(2)	Sm(1)-S(2)#2	2.835(2)
Sm(1)-P(1)#2	3.188(2)	Sm(1)-P(1)	3.188(2)
Sm(1)-P(2)	3.199(2)	Sm(1)-P(2)#2	3.199(2)
S(1)-P(1)	2.023(3)	S(2)-P(2)	2.029(3)
P(1)-C(1)	1.645(8)	P(1)-C(8)	1.811(5)
P(1)-C(2)	1.822(9)	P(2)-C(1)	1.632(8)
P(2)-C(14)	1.810(9)	P(2)-C(20)	1.821(8)
O(1)-C(26)	1.41(1)	O(1)-C(29)	1.45(1)
O(1)-Li(1)	1.92(2)	O(2)-C(33)	1.30(2)
O(2)-C(30)	1.41(2)	O(2)-Li(1)	1.95(2)
C(2)-C(7)	1.34(1)	C(2)-C(3)	1.43(1)
C(3)-C(4)	1.3900	C(4)-C(5)	1.3900
C(5)-C(6)	1.3900	C(6)-C(7)	1.3900
C(8)-C(13)	1.38(1)	C(8)-C(9)	1.3857
C(9)-C(10)	1.39(1)	C(10)-C(11)	1.37(2)
C(11)-C(12)	1.34(2)	C(12)-C(13)	1.37(1)
C(14)-C(15)	1.36(1)	C(14)-C(19)	1.39(1)
C(15)-C(16)	1.39(1)	C(16)-C(17)	1.34(2)
C(17)-C(18)	1.37(2)	C(18)-C(19)	1.37(2)
C(20)-C(21)	1.37(1)	C(20)-C(25)	1.38(1)
C(21)-C(22)	1.39(1)	C(22)-C(23)	1.38(2)
C(23)-C(24)	1.36(2)	C(24)-C(25)	1.38(2)
C(26)-C(27)	1.44(2)	C(27)-C(28)	1.43(2)
C(28)-C(29)	1.50(2)	C(30)-C(31)	1.44(2)
C(31)-C(32)	1.38(2)	C(32)-C(33)	1.46(2)
Li(1)-O(1)#2	1.92(2)	Li(1)-O(2)#2	1.95(2)

C(1)-Sm(1)-C(1)#2	161.7(4)	C(1)-Sm(1)-S(1)#2	125.2(2)
C(1)#2-Sm(1)-S(1)#2	69.1(2)	C(1)-Sm(1)-S(1)	69.1(2)
C(1)#2-Sm(1)-S(1)	125.2(2)	S(1)#2-Sm(1)-S(1)	91.8(1)
C(1)-Sm(1)-S(2)	68.6(2)	C(1)#2-Sm(1)-S(2)	99.9(2)
S(1)#2-Sm(1)-S(2)	98.59(7)	S(1)-Sm(1)-S(2)	134.35(6)
C(1)-Sm(1)-S(2)#2	99.9(2)	C(1)#2-Sm(1)-S(2)#2	68.6(2)
S(1)#2-Sm(1)-S(2)#2	134.35(6)	S(1)-Sm(1)-S(2)#2	98.59(7)
S(2)-Sm(1)-S(2)#2	104.8(1)	C(1)-Sm(1)-P(1)#2	160.6(2)
C(1)#2-Sm(1)-P(1)#2	30.5(2)	S(1)#2-Sm(1)-P(1)#2	38.69(6)
S(1)-Sm(1)-P(1)#2	114.98(6)	S(2)-Sm(1)-P(1)#2	99.89(6)
S(2)#2-Sm(1)-P(1)#2	98.18(6)	C(1)-Sm(1)-P(1)	30.5(2)
C(1)#2-Sm(1)-P(1)	160.6(2)	S(1)#2-Sm(1)-P(1)	114.98(6)
S(1)-Sm(1)-P(1)	38.69(6)	S(2)-Sm(1)-P(1)	98.18(6)
S(2)#2-Sm(1)-P(1)	99.89(6)	P(1)#2-Sm(1)-P(1)	150.16(8)
C(1)-Sm(1)-P(2)	30.0(2)	C(1)#2-Sm(1)-P(2)	137.5(2)
S(1)#2-Sm(1)-P(2)	116.02(6)	S(1)-Sm(1)-P(2)	97.23(6)
S(2)-Sm(1)-P(2)	38.72(6)	S(2)#2-Sm(1)-P(2)	106.58(6)
P(1)#2-Sm(1)-P(2)	135.65(5)	P(1)-Sm(1)-P(2)	59.59(5)

C(1)-Sm(1)-P(2)#2	137.5(2)	C(1)#2-Sm(1)-P(2)#2	30.0(2)
S(1)#2-Sm(1)-P(2)#2	97.23(6)	S(1)-Sm(1)-P(2)#2	116.02(6)
S(2)-Sm(1)-P(2)#2	106.58(6)	S(2)#2-Sm(1)-P(2)#2	38.72(6)
P(1)#2-Sm(1)-P(2)#2	59.59(5)	P(1)-Sm(1)-P(2)#2	135.65(5)
P(2)-Sm(1)-P(2)#2	132.12(8)	P(1)-S(1)-Sm(1)	80.2(1)
P(2)-S(2)-Sm(1)	80.4(1)	C(1)-P(1)-C(8)	112.6(4)
C(1)-P(1)-C(2)	116.6(4)	C(8)-P(1)-C(2)	102.9(3)
C(1)-P(1)-S(1)	110.1(3)	C(8)-P(1)-S(1)	104.8(2)
C(2)-P(1)-S(1)	109.1(4)	C(1)-P(1)-Sm(1)	49.0(3)
C(8)-P(1)-Sm(1)	121.3(2)	C(2)-P(1)-Sm(1)	135.7(3)
S(1)-P(1)-Sm(1)	61.12(8)	C(1)-P(2)-C(14)	114.6(5)
C(1)-P(2)-C(20)	113.0(4)	C(14)-P(2)-C(20)	103.3(4)
C(1)-P(2)-S(2)	109.3(3)	C(14)-P(2)-S(2)	107.4(3)
C(20)-P(2)-S(2)	108.8(3)	C(1)-P(2)-Sm(1)	48.6(3)
C(14)-P(2)-Sm(1)	124.4(3)	C(20)-P(2)-Sm(1)	132.3(3)
S(2)-P(2)-Sm(1)	60.91(8)	C(26)-O(1)-C(29)	108(1)
C(26)-O(1)-Li(1)	121(1)	C(29)-O(1)-Li(1)	128(1)
C(33)-O(2)-C(30)	106(1)	C(33)-O(2)-Li(1)	125(1)
C(30)-O(2)-Li(1)	128(1)	P(2)-C(1)-P(1)	151.2(6)
P(2)-C(1)-Sm(1)	101.4(4)	P(1)-C(1)-Sm(1)	100.5(4)
C(7)-C(2)-C(3)	120.9(7)	C(7)-C(2)-P(1)	124.6(7)
C(3)-C(2)-P(1)	114.5(7)	C(4)-C(3)-C(2)	118.4(4)
C(5)-C(4)-C(3)	120.0	C(4)-C(5)-C(6)	120.0
C(7)-C(6)-C(5)	120.0	C(2)-C(7)-C(6)	120.7(4)
C(13)-C(8)-C(9)	118.0(4)	C(13)-C(8)-P(1)	119.0(5)
C(9)-C(8)-P(1)	122.9(2)	C(8)-C(9)-C(10)	119.7(5)
C(11)-C(10)-C(9)	120(1)	C(12)-C(11)-C(10)	121(1)
C(11)-C(12)-C(13)	120(1)	C(12)-C(13)-C(8)	122(1)
C(15)-C(14)-C(19)	118(1)	C(15)-C(14)-P(2)	123.9(7)
C(19)-C(14)-P(2)	118.1(7)	C(14)-C(15)-C(16)	121(1)
C(17)-C(16)-C(15)	120(1)	C(16)-C(17)-C(18)	121(1)
C(19)-C(18)-C(17)	120(1)	C(18)-C(19)-C(14)	121(1)
C(21)-C(20)-C(25)	118(1)	C(21)-C(20)-P(2)	119.9(7)
C(25)-C(20)-P(2)	122.4(7)	C(20)-C(21)-C(22)	122(1)
C(23)-C(22)-C(21)	118(1)	C(24)-C(23)-C(22)	121(1)
C(23)-C(24)-C(25)	120(1)	C(24)-C(25)-C(20)	121(1)
O(1)-C(26)-C(27)	109(1)	C(28)-C(27)-C(26)	105(1)
C(27)-C(28)-C(29)	108(1)	O(1)-C(29)-C(28)	105(1)
O(2)-C(30)-C(31)	108(1)	C(32)-C(31)-C(30)	109(1)
C(31)-C(32)-C(33)	102(1)	O(2)-C(33)-C(32)	113(2)
O(1)#2-Li(1)-O(1)	112(1)	O(1)#2-Li(1)-O(2)#2	103.5(3)
O(1)-Li(1)-O(2)#2	114.8(3)	O(1)#2-Li(1)-O(2)	114.8(3)
O(1)-Li(1)-O(2)	103.5(3)	O(2)#2-Li(1)-O(2)	109(1)

Estimated standard deviations are given in the parenthesis.

Symmetry operators ::

1: x, y, z; 2: -x, y, -z+1/2; 3: x+1/2, y+1/2, z

4: -x+1/2, y+1/2, -z+1/; 5: -x, -y, -z; 6: x, -y, z-1/2

7: -x+1/2, -y+1/2, -z; 8: x+1/2, -y+1/2, z-1/2

[{Na(THF)$_3$}{(SPCPS)Sm(Cp*)$_2$}] (11)

Compound	smcps2carbna
Molecular formula	$C_{57}H_{74}NaO_3P_2S_2Sm$
Molecular weight	1106.56
Crystal habit	lemon yellow plate
Crystal dimensions(mm)	0.22x0.20x0.16
Crystal system	triclinic
Space group	Pbar1
a(Å)	12.1460(10)
b(Å)	13.3710(10)
c(Å)	17.5810(10)

α(°)	83.5000(10)
β(°)	79.4400(10)
γ(°)	75.8600(10)
V(Å^3)	2714.8(3)
Z	2
d(g-cm^{-3})	1.354
F(000)	1150
μ(cm^{-1})	1.267
Absorption corrections	multi-scan ; 0.7679 min, 0.8230 max
Diffractometer	KappaCCD
X-ray source	MoKα
λ(Å)	0.71069
Monochromator	graphite
T (K)	150.0(1)
Scan mode	phi and omega scans
Maximum θ	30.03
HKL ranges	-17 17 ; -18 18 ; -24 23
Reflections measured	22817
Unique data	15599
Rint	0.0223
Reflections used	13424
Criterion	I > 2σI)
Refinement type	Fsqd
Hydrogen atoms	mixed
Parameters refined	625
Reflections / parameter	21
wR2	0.0945
R1	0.0345
Weights a, b	0.0535 ; 0.0290
GoF	1.072
difference peak / hole (e Å^{-3})	1.686(0.088) / -1.006(0.088)

Table. Bond lengths (A) and angles (deg) for smcps2carbna

Sm(1)-C(1)	2.527(2)	Sm(1)-C(30)	2.753(2)
Sm(1)-C(36)	2.777(2)	Sm(1)-C(26)	2.788(2)
Sm(1)-C(40)	2.788(2)	Sm(1)-C(29)	2.798(2)
Sm(1)-C(27)	2.800(2)	Sm(1)-C(37)	2.809(2)
Sm(1)-C(28)	2.816(2)	Sm(1)-C(39)	2.821(2)
Sm(1)-C(38)	2.868(2)	Sm(1)-S(2)	2.9561(6)
S(1)-P(1)	2.0398(7	S(1)-Na(1)	2.717(1)
S(2)-P(2)	2.0250(7	P(1)-C(1)	1.646(2)
P(1)-C(2)	1.832(2)	P(1)-C(8)	1.839(2)
P(2)-C(1)	1.664(2)	P(2)-C(14)	1.836(2)
P(2)-C(20)	1.838(2)	Na(1)-O(2)	2.223(3)
Na(1)-O(3)	2.240(3)	Na(1)-O(1)	2.294(2)
Na(1)-C(7)	3.071(3)	O(1)-C(46)	1.424(4)
O(1)-C(49)	1.437(4)	O(2)-C(53)	1.428(4)
O(2)-C(50)	1.436(4)	O(3)-C(57)	1.397(4)
O(3)-C(54)	1.423(5)	C(2)-C(3)	1.396(3)
C(2)-C(7)	1.397(3)	C(3)-C(4)	1.381(3)
C(4)-C(5)	1.387(4)	C(5)-C(6)	1.373(4)
C(6)-C(7)	1.380(3)	C(8)-C(13)	1.390(3)
C(8)-C(9)	1.392(3)	C(9)-C(10)	1.387(3)
C(10)-C(11)	1.378(4)	C(11)-C(12)	1.387(4)
C(12)-C(13)	1.388(3)	C(14)-C(15)	1.389(3)
C(14)-C(19)	1.398(3)	C(15)-C(16)	1.386(3)

C(16)-C(17)	1.387(4)	C(17)-C(18)	1.386(4)
C(18)-C(19)	1.386(3)	C(20)-C(21)	1.384(3)
C(20)-C(25)	1.394(4)	C(21)-C(22)	1.383(4)
C(22)-C(23)	1.370(6)	C(23)-C(24)	1.363(5)
C(24)-C(25)	1.404(3)	C(26)-C(30)	1.406(4)
C(26)-C(27)	1.415(3)	C(26)-C(31)	1.506(3)
C(27)-C(28)	1.411(4)	C(27)-C(32)	1.513(4)
C(28)-C(29)	1.425(4)	C(28)-C(33)	1.500(3)
C(29)-C(30)	1.420(3)	C(29)-C(34)	1.493(4)
C(30)-C(35)	1.508(3)	C(36)-C(37)	1.418(3)
C(36)-C(40)	1.420(3)	C(36)-C(41)	1.494(3)
C(37)-C(38)	1.414(3)	C(37)-C(42)	1.490(3)
C(38)-C(39)	1.410(3)	C(38)-C(43)	1.506(3)
C(39)-C(40)	1.414(3)	C(39)-C(44)	1.502(3)
C(40)-C(45)	1.502(3)	C(46)-C(47A)	1.503(9)
C(46)-C(47)	1.514(8)	C(47)-C(48)	1.504(9)
C(47A)-C(48)	1.57(1)	C(48)-C(49)	1.487(5)
C(50)-C(51)	1.461(5)	C(51)-C(52)	1.531(4)
C(52)-C(53)	1.507(4)	C(54)-C(55)	1.440(7)
C(55)-C(56)	1.389(8)	C(55)-C(56A)	1.60(2)
C(56)-C(57)	1.471(8)	C(56A)-C(57)	1.63(2)

C(1)-Sm(1)-C(30)	127.99(7)	C(1)-Sm(1)-C(36)	91.58(6)
C(30)-Sm(1)-C(36)	127.05(7)	C(1)-Sm(1)-C(26)	141.63(7)
C(30)-Sm(1)-C(26)	29.39(7)	C(36)-Sm(1)-C(26)	126.79(7)
C(1)-Sm(1)-C(40)	96.58(7)	C(30)-Sm(1)-C(40)	134.66(7)
C(36)-Sm(1)-C(40)	29.56(7)	C(26)-Sm(1)-C(40)	116.89(7)
C(1)-Sm(1)-C(29)	99.30(7)	C(30)-Sm(1)-C(29)	29.64(7)
C(36)-Sm(1)-C(29)	148.32(7)	C(26)-Sm(1)-C(29)	48.55(7)
C(40)-Sm(1)-C(29)	164.10(7)	C(1)-Sm(1)-C(27)	116.03(7)
C(30)-Sm(1)-C(27)	48.46(7)	C(36)-Sm(1)-C(27)	147.29(7)
C(26)-Sm(1)-C(27)	29.33(7)	C(40)-Sm(1)-C(27)	123.66(7)
C(29)-Sm(1)-C(27)	48.38(7)	C(1)-Sm(1)-C(37)	115.74(6)
C(30)-Sm(1)-C(37)	97.72(7)	C(36)-Sm(1)-C(37)	29.40(7)
C(26)-Sm(1)-C(37)	101.00(7)	C(40)-Sm(1)-C(37)	48.36(7)
C(29)-Sm(1)-C(37)	122.21(7)	C(27)-Sm(1)-C(37)	128.22(7)
C(1)-Sm(1)-C(28)	93.35(7)	C(30)-Sm(1)-C(28)	48.54(7)
C(36)-Sm(1)-C(28)	174.99(6)	C(26)-Sm(1)-C(28)	48.27(7)
C(40)-Sm(1)-C(28)	150.01(7)	C(29)-Sm(1)-C(28)	29.41(7)
C(27)-Sm(1)-C(28)	29.10(7)	C(37)-Sm(1)-C(28)	145.94(7)
C(1)-Sm(1)-C(39)	124.62(7)	C(30)-Sm(1)-C(39)	107.40(7)
C(36)-Sm(1)-C(39)	48.40(6)	C(26)-Sm(1)-C(39)	87.78(7)
C(40)-Sm(1)-C(39)	29.18(7)	C(29)-Sm(1)-C(39)	135.41(7)
C(27)-Sm(1)-C(39)	99.36(7)	C(37)-Sm(1)-C(39)	48.11(7)
C(28)-Sm(1)-C(39)	128.44(7)	C(1)-Sm(1)-C(38)	139.17(7)
C(30)-Sm(1)-C(38)	87.83(7)	C(36)-Sm(1)-C(38)	47.73(6)
C(26)-Sm(1)-C(38)	79.16(7)	C(40)-Sm(1)-C(38)	47.50(7)
C(29)-Sm(1)-C(38)	117.36(7)	C(27)-Sm(1)-C(38)	102.19(7)
C(37)-Sm(1)-C(38)	28.83(6)	C(28)-Sm(1)-C(38)	127.40(7)
C(39)-Sm(1)-C(38)	28.69(7)	C(1)-Sm(1)-S(2)	65.58(5)
C(30)-Sm(1)-S(2)	87.02(5)	C(36)-Sm(1)-S(2)	78.97(5)
C(26)-Sm(1)-S(2)	116.28(6)	C(40)-Sm(1)-S(2)	107.58(5)
C(29)-Sm(1)-S(2)	78.71(5)	C(27)-Sm(1)-S(2)	127.09(6)
C(37)-Sm(1)-S(2)	76.48(5)	C(28)-Sm(1)-S(2)	102.31(6)
C(39)-Sm(1)-S(2)	123.58(5)	C(38)-Sm(1)-S(2)	102.92(5)
P(1)-S(1)-Na(1)	101.31(4)	P(1)-S(1)-Sm(1)	81.82(2)
Na(1)-S(1)-Sm(1)	147.42(3)	P(2)-S(2)-Sm(1)	82.23(2)
C(1)-P(1)-C(2)	116.9(1)	C(1)-P(1)-C(8)	117.1(1)
C(2)-P(1)-C(8)	100.3(1)	C(1)-P(1)-S(1)	107.55(8)
C(2)-P(1)-S(1)	106.43(7)	C(8)-P(1)-S(1)	107.71(7)
C(1)-P(1)-Sm(1)	46.19(7)	C(2)-P(1)-Sm(1)	130.15(7)
C(8)-P(1)-Sm(1)	129.50(7)	S(1)-P(1)-Sm(1)	61.37(2)
C(1)-P(2)-C(14)	116.3(1)	C(1)-P(2)-C(20)	115.9(1)
C(14)-P(2)-C(20)	99.4(1)	C(1)-P(2)-S(2)	107.96(8)
C(14)-P(2)-S(2)	108.79(7)	C(20)-P(2)-S(2)	107.94(8)
C(1)-P(2)-Sm(1)	46.99(7)	C(14)-P(2)-Sm(1)	131.18(6)
C(20)-P(2)-Sm(1)	129.45(8)	S(2)-P(2)-Sm(1)	60.97(2)

O(2)-Na(1)-O(3)	107.1(1)	O(2)-Na(1)-O(1)	95.2(1)
O(3)-Na(1)-O(1)	95.9(1)	O(2)-Na(1)-S(1)	139.13(8)
O(3)-Na(1)-S(1)	109.9(1)	O(1)-Na(1)-S(1)	97.82(7)
O(2)-Na(1)-C(7)	83.86(8)	O(3)-Na(1)-C(7)	87.4(1)
O(1)-Na(1)-C(7)	176.6(1)	S(1)-Na(1)-C(7)	80.94(5)
C(46)-O(1)-C(49)	108.5(3)	C(46)-O(1)-Na(1)	125.6(2)
C(49)-O(1)-Na(1)	123.6(2)	C(53)-O(2)-C(50)	105.0(3)
C(53)-O(2)-Na(1)	126.5(2)	C(50)-O(2)-Na(1)	127.7(2)
C(57)-O(3)-C(54)	108.7(3)	C(57)-O(3)-Na(1)	133.1(2)
C(54)-O(3)-Na(1)	117.9(3)	P(1)-C(1)-P(2)	149.9(1)
P(1)-C(1)-Sm(1)	105.8(1)	P(2)-C(1)-Sm(1)	104.2(1)
C(3)-C(2)-C(7)	117.8(2)	C(3)-C(2)-P(1)	120.0(2)
C(7)-C(2)-P(1)	122.1(2)	C(4)-C(3)-C(2)	120.4(2)
C(3)-C(4)-C(5)	120.8(2)	C(6)-C(5)-C(4)	119.4(2)
C(5)-C(6)-C(7)	120.2(2)	C(6)-C(7)-C(2)	121.4(2)
C(6)-C(7)-Na(1)	106.4(2)	C(2)-C(7)-Na(1)	87.0(1)
C(13)-C(8)-C(9)	118.6(2)	C(13)-C(8)-P(1)	118.8(2)
C(9)-C(8)-P(1)	122.6(2)	C(10)-C(9)-C(8)	120.4(2)
C(11)-C(10)-C(9)	120.5(2)	C(10)-C(11)-C(12)	119.8(2)
C(11)-C(12)-C(13)	119.7(2)	C(12)-C(13)-C(8)	121.0(2)
C(15)-C(14)-C(19)	118.8(2)	C(15)-C(14)-P(2)	122.0(2)
C(19)-C(14)-P(2)	119.1(2)	C(16)-C(15)-C(14)	120.7(2)
C(15)-C(16)-C(17)	120.2(2)	C(18)-C(17)-C(16)	119.5(2)
C(17)-C(18)-C(19)	120.4(2)	C(18)-C(19)-C(14)	120.4(2)
C(21)-C(20)-C(25)	119.0(2)	C(21)-C(20)-P(2)	119.7(2)
C(25)-C(20)-P(2)	121.4(2)	C(22)-C(21)-C(20)	120.6(3)
C(23)-C(22)-C(21)	120.4(3)	C(24)-C(23)-C(22)	120.2(3)
C(23)-C(24)-C(25)	120.4(3)	C(20)-C(25)-C(24)	119.5(3)
C(30)-C(26)-C(27)	107.8(2)	C(30)-C(26)-C(31)	127.8(2)
C(27)-C(26)-C(31)	123.1(2)	C(30)-C(26)-Sm(1)	73.9(1)
C(27)-C(26)-Sm(1)	75.8(1)	C(31)-C(26)-Sm(1)	126.7(2)
C(28)-C(27)-C(26)	108.4(2)	C(28)-C(27)-C(32)	125.9(2)
C(26)-C(27)-C(32)	125.0(2)	C(28)-C(27)-Sm(1)	76.1(1)
C(26)-C(27)-Sm(1)	74.9(1)	C(32)-C(27)-Sm(1)	123.1(2)
C(27)-C(28)-C(29)	107.9(2)	C(27)-C(28)-C(33)	125.9(2)
C(29)-C(28)-C(33)	125.8(2)	C(27)-C(28)-Sm(1)	74.8(1)
C(29)-C(28)-Sm(1)	74.6(1)	C(33)-C(28)-Sm(1)	122.4(2)
C(30)-C(29)-C(28)	107.2(2)	C(30)-C(29)-C(34)	126.1(2)
C(28)-C(29)-C(34)	126.1(2)	C(30)-C(29)-Sm(1)	73.4(1)
C(28)-C(29)-Sm(1)	76.0(1)	C(34)-C(29)-Sm(1)	123.4(2)
C(26)-C(30)-C(29)	108.7(2)	C(26)-C(30)-C(35)	127.3(2)
C(29)-C(30)-C(35)	123.6(2)	C(26)-C(30)-Sm(1)	76.7(1)
C(29)-C(30)-Sm(1)	76.9(1)	C(35)-C(30)-Sm(1)	118.3(2)
C(37)-C(36)-C(40)	107.8(2)	C(37)-C(36)-C(41)	125.5(2)
C(40)-C(36)-C(41)	126.1(2)	C(37)-C(36)-Sm(1)	76.6(1)
C(40)-C(36)-Sm(1)	75.7(1)	C(41)-C(36)-Sm(1)	120.9(1)
C(38)-C(37)-C(36)	107.6(2)	C(38)-C(37)-C(42)	124.7(2)
C(36)-C(37)-C(42)	126.8(2)	C(38)-C(37)-Sm(1)	77.9(1)
C(36)-C(37)-Sm(1)	74.1(1)	C(42)-C(37)-Sm(1)	122.8(2)
C(39)-C(38)-C(37)	108.7(2)	C(39)-C(38)-C(43)	126.9(2)
C(37)-C(38)-C(43)	122.4(2)	C(39)-C(38)-Sm(1)	73.8(1)
C(37)-C(38)-Sm(1)	73.3(1)	C(43)-C(38)-Sm(1)	131.9(2)
C(38)-C(39)-C(40)	107.6(2)	C(38)-C(39)-C(44)	127.4(2)
C(40)-C(39)-C(44)	124.4(2)	C(38)-C(39)-Sm(1)	77.5(1)
C(40)-C(39)-Sm(1)	74.1(1)	C(44)-C(39)-Sm(1)	121.2(2)
C(39)-C(40)-C(36)	108.2(2)	C(39)-C(40)-C(45)	125.8(2)
C(36)-C(40)-C(45)	125.2(2)	C(39)-C(40)-Sm(1)	76.7(1)
C(36)-C(40)-Sm(1)	74.8(1)	C(45)-C(40)-Sm(1)	122.8(1)
O(1)-C(46)-C(47A)	106.8(5)	O(1)-C(46)-C(47)	102.3(4)
C(47A)-C(46)-C(47)	46.2(4)	C(48)-C(47)-C(46)	102.3(4)
C(46)-C(47A)-C(48)	99.7(6)	C(49)-C(48)-C(47)	104.3(3)
C(49)-C(48)-C(47A)	99.7(4)	C(47)-C(48)-C(47A)	45.2(5)
O(1)-C(49)-C(48)	106.8(3)	O(2)-C(50)-C(51)	107.0(3)
C(50)-C(51)-C(52)	103.7(3)	C(53)-C(52)-C(51)	105.1(2)
O(2)-C(53)-C(52)	105.2(2)	O(3)-C(54)-C(55)	105.5(4)
C(56)-C(55)-C(54)	106.8(4)	C(56)-C(55)-C(56A)	31.3(5)
C(54)-C(55)-C(56A)	111.6(8)	C(55)-C(56)-C(57)	107.3(5)
C(55)-C(56A)-C(57)	91(1)	O(3)-C(57)-C(56)	106.2(4)
O(3)-C(57)-C(56A)	105.9(7)	C(56)-C(57)-C(56A)	30.6(5)